HIGH RESOLUTION NUCLEAR MAGNETIC RESONANCE STUDIES OF KRINGLE CONTAINING PROTEINS

A thesis submitted in partial fulfilment of the requirements for the degree of Doctor of Philosophy

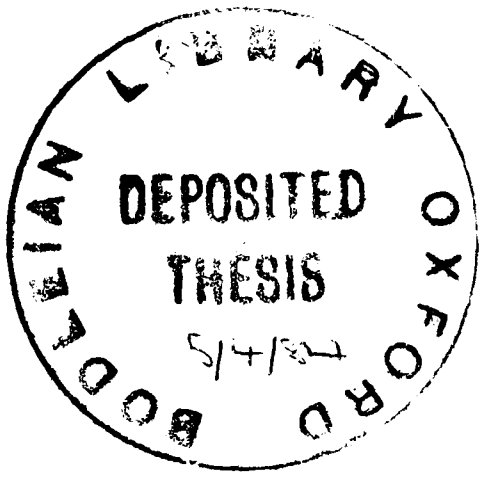

N.D. Pluck

Wadham College

1983

ABSTRACT

HIGH RESOLUTION NUCLEAR MAGNETIC RESONANCE STUDIES OF KRINGLE CONTAINING PROTEINS

Nigel David Pluck, Wadham College, Oxford.
Submitted for the degree of Doctor of Philosophy.
Michaelmas Term, 1983.

The kringle is a name given to a sequence of seventy nine residues linked by three disulphide bridges, multiple copies of which have been found in a number of proteins involved in haemostasis. Kringles from plasminogen and prothrombin have been studied using high resolution nuclear magnetic resonance (NMR) spectroscopy.

Preliminary experiments demonstrated the kringles to be globular proteins in aqueous solution having well defined tertiary folds. Resonances have been assigned in the NMR spectrum to all but two of the aromatic residues of kringle 4 of human plasminogen and in addition a number of aliphatic residues have also been assigned. The majority of these assignments have been made to specific protons in the protein with the aid of chemically modified kringle 4 derivatives and comparison with other kringle protein spectra. Nuclear Overhauser enhancement studies have demonstrated a number of structurally significant side chain interactions. The lysine binding site of kringle 4 has been explored using two ω-aminocarboxylic acids as ligands. Further structural probes have included copper and lanthanide ions as well as chemically modified kringle 4 species. Combining all the data has allowed a preliminary molecular model to be built of part of kringle 4 incorporating all the residues between the second and third disulphide bridges. Preliminary studies demonstrate the possibility of being able to refine parts of this structure to an accuracy approaching that of X-ray crystallographic studies.

A similar number of assignments have been made in the spectrum of bovine prothrombin fragment 2. Comparison of the data on the kringles of both fragment 2 and kringle 4 shows the two proteins to have preserved structural elements, and in particular one of these involves the conserved residues Trp 25, Leu 45 and Trp 61. Furthermore, the two tryptophan residues have been shown to have quite unique spectral charateristics. Brief studies of human prothrombin fragment 2 reveals similar findings.

The results discussed indicate that the kringle sequence gives rise to a well defined fold. In kringle 4 of human plasminogen this is seen to provide a highly specific binding site for certain ω-aminocarboxylic acids. The data is all in accord with kringles being autonomous units within the non protease portion of zymogen molecules and which are ideally suited to include the mediation of protein-protein interactions amongst their biological functions.

Timor Domini Initium Sapientiae

Psalm 111.10

Acknowledgements

I should like to thank

Professor R.J.P. Williams, F.R.S. my supervisor, whose knowledge, enthusiasm and support have been very much appreciated over the years and from whom I have learnt a great deal.

Dr. Peter Esnouf for his consistent interest and endless supply of protein.

Dr. László Patthy for the ready supply of many proteins and lively correspondence.

Dr. Barry Levine for his constant help, encouragement and discussion at all times of the day and night.

Dr. Antonio Aguiar for his painstaking example and interest.

Dr. Robin Leatherbarrow for collaboration with ring current calculations.

All members of the R.J.P.W group past and present and the many other NMR machine users with whom I have had much profitable conversation.

Mrs Julie Edwards who has typed part of this thesis.

CONTENTS

CHAPTER 1 INTRODUCTION

1.1 Definition and Occurrence of Kringles 1
1.2 Haemostasis - An Overview 2
1.3 Kringle Homology 4
1.4 Kringle Function 8
1.5 Protein Structure Determination by NMR 9
1.6 Outline of the Thesis 12

CHAPTER 2 MATERIALS AND METHODS

2.1 Materials 17
2.1.1 Proteins 17
2.1.2 Other Materials 18
2.2 Methods 19
2.2.1 Sample Handling 19
2.2.2 NMR Methods 19
2.2.2.1 Multiplet Selection Spectra 20
2.2.2.2 NOE Difference Spectra 20
2.2.2.3 Two Dimensional Correlated Spectroscopy 21
2.2.3 Lanthanide Reagents 21

CHAPTER 3 ASSIGNMENTS IN THE NMR SPECTRUM OF KRINGLE 4

3.1 Introduction to the NMR Spectrum 23
3.2 Aromatic Region of the Spectrum 26
3.2.1 Tryptophans 26
3.2.2 Histidines 36
3.2.3 Tyrosines 41
3.2.4 Phenylalanine 41
3.2.5 Spectral Simulation 44
3.3 Aliphatic Region of the Spectrum 45
3.3.1 Extra-kringle Residues 48
3.3.2 Methionines 49
3.3.3 Leucines 49
3.3.4 Valines 52
3.3.5 Threonines 53
3.3.6 Alanines 55
3.3.7 Glutamates 59
3.3.8 Lysines 60

3.4 NOE Experiments 61
3.4.1 Aliphatics 61
3.4.2 Aromatics 64
3.5 Labile Proton Resonances 72
3.6 Temperature Dependence 73
3.7 Summary 76

CHAPTER 4 PROBE AND LIGAND BINDING STUDIES OF KRINGLE 4

4.1 Introduction 78
4.2 pH Dependence 79
4.2.1 Histidines 84
4.2.2 Tyrosines 86
4.2.3 Tryptophans 88
4.2.4 Terminal Residues 90
4.2.5 Methyl Proton Resonances 90
4.2.6 Glutamates 93
4.2.7 Lysine ε Protons 93
4.2.8 α CH Proton Resonances 94
4.2.9 Protein Unfolding 94
4.2.10 Tyrosine and Histidine Assignments 95
4.2.11 Preliminary Structural Model 102
4.3 Copper II Ion Binding 106
4.4 Ligand Binding 110
4.4.1 Introduction 110
4.4.2 Spectral Effects of 6 Aminohexanoic Acid Binding 114
4.4.2.1 Aromatic Region 114
4.4.2.2 NH and Aromatic Assignments 116
4.4.2.3 Unassigned Aromatic Residues 120
4.4.2.4 Temperature Dependence 124
4.4.2.5 Labile Proton Resonances 127
4.4.2.6 Aliphatic Region 128
4.4.2.7 pH Dependence 130
4.4.2.8 Aliphatic Temperature Dependence 138
4.4.2.9 Summary 138
4.4.3 AMBOC 141
4.4.3.1 Aromatic Region 141
4.4.3.2 Aliphatic Region 146
4.4.3.3 Temperature Dependence 149
4.4.3.4 Summary 151

4.5 Lanthanide Ion Binding to Kringle 4 153
4.5.1 Lanthanum 153
4.5.2 Praseodymium 159
4.5.2.1 Resonance Shifts 159
4.5.2.2 6 Aminohexanoic Acid 167
4.5.2.3 Subsequent Addition of Gadolinium Ions 169
4.5.3 Europium 171
4.5.4 Shift Ratios 175
4.5.5 Gadolinium 178
4.5.6 Lanthanide Ion Binding Sites 182
4.6 Summary 186

CHAPTER 5 CHEMICAL MODIFICATIONS OF KRINGLE 4

5.1 Introduction 188
5.2 Results of Other Studies 191
5.3 Tyrosine Modifications 195
5.3.1 Nitrated Tyrosine 40 198
5.3.2 Nitrated Tyrosines 40 and 49 205
5.3.3 Tyrosine 40 - Lysine 35 Crosslinked 209
5.3.4 Summary 216
5.4 Tryptophan 71, Methionines 27 and 48 Oxidised 217
5.5 Arginine Modifications 222
5.5.1 Arginine 32 Modified 223
5.5.2 Arginines 32 and 70 Modified 231
5.6 Met 47 - Asn 48 Cleavage 233
5.7 Cys 1 - Cys 79 Disulphide Bond Cleavage 236
5.8 Model Building 243
5.9 Structural Refinement 251

CHAPTER 6 NMR STUDIES OF PROTHROMBIN FRAGMENT 2

6.1 Introduction 256
6.2 Aromatic Region of the Spectrum 262
6.2.1 Phenylalanines 264
6.2.2 Tryptophans 270
6.2.3 Tyrosines 277
6.2.4 Spectral Simulation 279
6.3 NOE Experiments 279
6.4 Temperature Dependence 284
6.5 pH Dependence 286

6.6 Human Prothrombin Fragment 2 290
6.6.1 pH Dependence 290
6.6.2 Temperature Dependence 295
6.6.3 Comparison of the Human and Bovine Spectra 297
6.7 Summary 298

CHAPTER 7 BIOLOGICAL SIGNIFICANCE OF THE KRINGLE STRUCTURE

7.1 Introduction 301
7.2 Prothrombin 301
7.2.1 Prothrombin Fragment 1 302
7.2.2 Prothrombin Fragment 2 307
7.3 Plasminogen 308
7.4 Plasminogen Activators 315
7.5 Conclusions and Prospects for Future Study 317

APPENDIX I The Sequences of Twelve Kringles 319
APPENDIX II Parameters used in Spectral Simulations 322
APPENDIX III Amino Acid Sequence of Human Prothrombin Fragment 2 324

REFERENCES 325

CHAPTER 1

INTRODUCTION

1.1 Definition and Occurrence of Kringles

In Denmark "Kringle" means a cake or more precisely a cake of very characteristic shape, so much so that it is used as a sign outside a shop to denote a baker in the way a striped pole in this country indicates a barber. Thus, Magnusson and co-workers (1975), working in Denmark, gave the name kringle to a portion of the primary sequence (demarcated by three disulphide bridges), of the proenzyme prothrombin. Indeed, it was a noticeable feature on the elucidation of the amino acid sequence of this protein that it contained two such regions of seventy-nine residues with three interlinking disulphide bridges. Figure 1.1 shows the position of the cysteine residues forming the bridges within the kringle and the imagination of the Danish workers can be guaged by comparison with the photograph opposite!

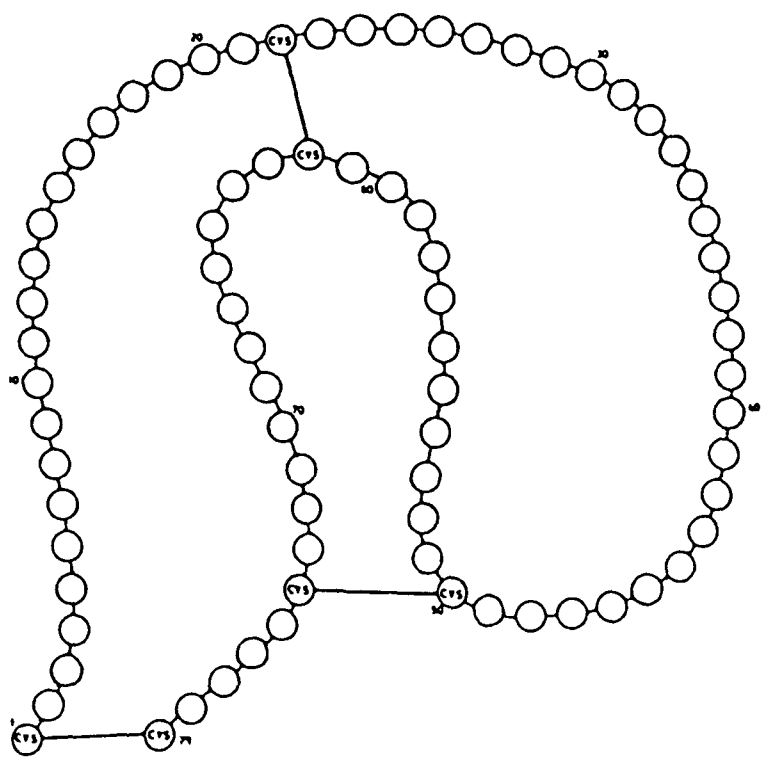

Fig.1.1 Outline of the seventy nine residues comprising a kringle showing the three disulphide links.

Subsequent protein sequence determinations have revealed five such kringles in another proenzyme - plasminogen (Sottrup-Jensen et al., 1982), two more in a plasminogen activator protein (Pennica et al., 1983) and one reported in a further plasminogen activator - urokinase (Günzler et al., 1982). It is remarkable that all the proteins so far shown to contain an intact kringle are intimately involved in the formation and destruction of blood clots and a brief overview of their roles will now be considered.

1.2 Haemostasis - an Overview

Figure 1.2 attempts to provide a simple summary of an extremely complex process, for which many details are still to be discovered. However, in essence, damaged endothelial lining of a blood vessel leads to aggregation of platelets as well as vascoconstriction to stem the flow of blood. The platelet plug, as initially formed, is unstable and various mechanisms activate a cascade of zymogen to enzyme conversions culminating in the release of the final protease - thrombin. Thrombin cleaves soluble fibrinogen monomers that aggregate and are subsequently covalently crosslinked forming a fibrin meshwork around the platelet plug and so rapidly reinforcing it as a mechanical barrier. Blood cells and plasma proteins are also inevitably entrapped and a thrombus is formed.

However, typical of a biological process, a clot once formed does not remain unchanged. The processes of recanalisation, resolution and healing, require that the thrombus be broken down and the fibrin mesh disrupted. The details of fibrinolysis are possibly even less clear than those of thrombosis but it seems likely that during thrombus formation, plasminogen and plasminogen activators are incorporated into the clot and intimately associated with the fibrin mesh. Thus, the means of destruction is inserted during the formation, allowing constant regulation of a potential disaster should thrombosis go out of control. Indeed, it is interesting that fibrin degradation products released by the action

HAEMOSTASIS

THROMBOSIS

Damaged blood vessel

↓

Platelet plug formation

↓

Clotting enzymes activated

↓

Prothrombin → Thrombin

↓

Fibrinogen → Fibrin → Fibrin degradation

↓

Platelet Plug Stabilised

FIBRINOLYSIS

Tissue activators

(Urokinase)

Plasminogen activators

↓

Plasmin ← Plasminogen

↓

Platelet Plug Destabilised

Fig. 1.2 A simplified overview of haemostasis showing the importance of the kringle containing proteins (underlined).

of plasmin inhibit thrombin activity, although this negative feedback loop is thought probably not quantitatively significant. However, many inhibitors and other means of control are being elucidated that check these processes driven by positive feedback loops.

Plasminogen activators are found in most organs of the body and strongly concentrated in the walls of blood vessels, particularly veins where blood flow is most sluggish. Plasma normally has a low level of activator activity which is markedly increased by exercise, stress and venous occlusion. Differences in immunological properties have resulted in plasminogen activators being classified into two major groups, tissue-type and urokinase-type plasminogen activators. Urokinase, itself, is synthesised by kidney cells, excreted in the urine and presumed to be concerned with the maintenance of ureteric patency. However, both tissue-type plasminogen activator and more frequently, urokinase have been used clinically with success as thrombolytic agents in patients with thrombus occluded blood vessels.

Thus, it is seen that kringle containing proteins have important and central roles in haemostasis and we need to consider their individual similarities.

1.3 Kringle Homology

We note that all of these kringle containing proteins are enzymes or proenzymes, and indeed more specifically contain serine proteases with a high degree of homology to the classical serine proteases such as trypsin and chymotrypsin. (Kurosky et al., 1980; Pennica et al., 1983). At this point it is extremely interesting to mention a very intriguing plasma protein - haptoglobin. This is a glycoprotein that has an extremely high affinity for the haemoglobin molecule.

The protein consists essentially of two αβ subunits, each chain linked by a single disulphide bridge as are the two subunits across the two chains. However, sequence analysis (Kurosky, et al., 1980) has revealed the β chain to have a reasonable degree of homology to the serine proteases mentioned above although haptoglobin itself has no protease activity; the β chain being thought to bear the haemoglobin binding site. Furthermore, the α chain has been shown to have some 25% homology to a plasminogen kringle with probability of less than 0.014 that the similarity was due to chance. However, it must be noted that the triple disulphide links that characterise the kringle sequence are absent from haptoglobin which lacks the first cysteine residue completely and uses another for the cross link between the α chains. But, haptoglobin does demonstrate a feature of kringle containing proteins in that the "kringle" region is separate from the protease-like part. Table 1.1 shows the position of the kringles within the complete zymogen sequences. It can be seen that the kringles are all found in the N terminal region of the proteins and the protease portion lies in the C terminal half.

Gene duplication obviously accounts for multiple proteins containing similar sequences and multiple copies of the kringle structure within the molecules. However, the degree of homology within the kringles is not very high. Appendix I lists the sequences of a representative twelve kringles and Fig. 1.3 shows the kringle outline with the invariant residues marked and the number of different residues found at each other site in these twelve kringles. Some positions show only two different types of side chain and perhaps the most significant is at position 49 which is always either phenylalanine or tyrosine and position 59 which is either glycine or a deletion. Position 63 is also either phenylalanine or tyrosine and one sequence where it is histidine. Other places, however, show great variety such as position 71 which ranges from serine and

Table 1.1 Positions of the kringles within the entire molecule. (Residues numbered from the N terminus). See Appendix I for references.

	Bovine Prothrombin	Human Plasminogen	Human Tissue Type Plasminogen Activator	Human Urokinase
Total number of residues	582	790	562	410
Kringle Positions in the Sequence	65-143 170-248	83-161 165-242 255-332 357-434 461-540	92-173 180-261	50-131

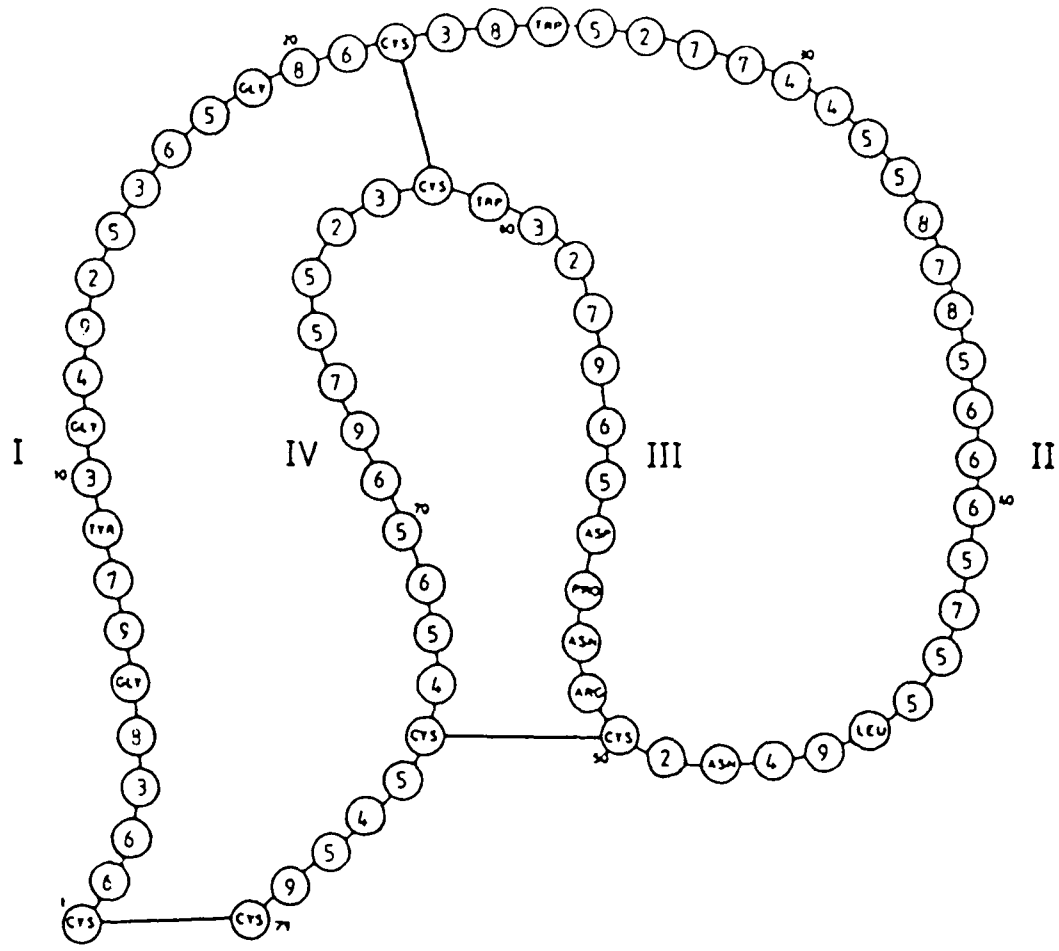

Fig. 1.3 Kringle outline showing conserved residues in twelve kringles (see Appendix I). The numbers of different residues at other sites are indicated.

arginine to tyrosine or tryptophan. However, despite the differences, studies of the amino acid changes in the prothrombin and plasminogen kringles have indicated that the sequences have been linked genetically for an extended period of their evolutionary history (Kurosky et al., 1980). This suggests, as would be expected teleologically that the processes of thrombosis and fibrinolysis have developed concurrently.

We note that eighteen of the seventy-nine residues are conserved in all the twelve sequences, and this of course includes the six cysteine residues. Dayhoff et al., (1972) have constructed a table of relative mutabilities of each amino acid reflecting the ratio of its changes to its occurrence in particular sequences. Cysteine and tryptophan are both at the bottom of the table. This is also borne out in Fig. 1.3 and is understandable in that cysteine is a unique amino acid with no alternative in its ability to form cross links. The reasoning for tryptophan is that such a bulky side chain is not often incorporated in a sequence but that when it is, it cannot be suitably replaced by another capable of performing the same structural role. Phenylalanine and tyrosine are also fairly low in the table presumably for similar reasons to tryptophan. Interestingly, glycine is also of the same order and this is explained on the reverse principle that being the smallest residue, it can not be satisfactorily replaced. The amino acids mentioned so far account for twelve of the eighteen conserved residues suggesting that the kringle sequence gives rise to a three dimensional structure that has some definite conserved structural elements that are always present and necessarily so. The elucidation of the position and nature of these features will concern us in what follows, but it is also appropriate to consider what function the kringle may perform in the various proteins.

1.4 Kringle Function

It is apparent from cursory glance at Fig.1.2 that the kringle containg proteins are all intimately involved in protein - protein interactions and this will be emphasised further when the biological significance of the kringle structure is considered in more detail in Chapter 7. However, it is clear that the protease part of the molecule is less likely to contain the basic site of protein interaction being more adapted to recognition of the particular site for its enzymatic activity. Indeed, this conclusion has been borne out by studies of plasminogen for instance. This protein binds to fibrin via sites localised to the kringle containing portion of the molecule and referred to as lysine binding sites from their ability to also mediate binding to lysine-Sepharose columns (Wiman et al., 1979; Thorsen et al., 1981). Two such specific sites have been localised to kringles 1 and 4 of human plasminogen and are not present on the other three kringles (Váli and Patthy, 1982). In addition to binding to lysine-Sepharose these protein fragments of plasminogen will also bind ω-aminocarboxylic acids. However, as will be discussed in Chapter 7 and indicated by the difference in binding capability of the five plasminogen kringles already referred to, the kringle structure in general does not appear simply to exist to provide lysine binding sites and indeed, their various functions have not yet been fully elucidated.

It is clear, though, that knowledge of the three dimensional structure of the kringles is vital to understanding their biological roles and two groups are currently involved in determining the X-ray crystal structure of bovine prothrombin fragment 1 which contains a kringle. (Aschaffenburg et al., 1977; Olsson et al., 1982). However, although it seems likely that there is a basic structure conserved in all kringles, parts of the sequences are extremely variable and as demonstrated by the plasminogen

kringles, each one has very different detailed behaviour that is presumably reflected in its structure. In particular much needs to be known of the protein fold that leads to formation of the lysine binding sites. With these ends in mind this thesis is concerned with the application of nuclear magnetic resonance spectroscopy as a technique for elucidating protein structure in solution and it behoves us briefly to consider the eminent suitability of this approach.

1.5 Protein Strucure Determination by NMR

The application of NMR spectroscopy to biological problems is well established (Dwek, 1973; Wüthrich, 1976; Jardetzky and Roberts, 1981). The method is well able to give information about spatial relationships, relative mobility and local energetic effects and of the spectroscopic techniques, is inherently the most powerful because of its ability to study virtually all the atoms of the system (Campbell, 1977). From the last remark it is an ultimate goal to be able to translate the complex spectrum of resonances resulting from a proton magnetic resonance study of a protein into a three dimensional structure in much the same way as X-ray diffraction patterns of protein crystals are. However, up to recent times, attempts to achieve the former aim have been very much dependent on the latter having been completed. The most extensive NMR studies of proteins have been carried out on proteins for which high resolution crystal structures are available and exemplified, for instance, by studies of lysozyme (Blake et al,. 1978); cytochrome c (Moore, 1978); snake venom toxins (Inagaki et al., 1981); trypsin inhibitor (Wüthrich and Wagner,1979); superoxide dismutase (Cass et al., 1977); Azurin (Canters et al., 1983) to name but a few. The reason for this is not difficult to see. Even at high magnetic field strengths the proton magnetic resonance spectrum of a protein contains hundreds of

resonances and to make much progress it is clearly essential to know which proton in the protein gives rise to which resonance in the spectrum - the problem of assignment. The application of probe studies and nuclear Overhauser enhancement experiments in conjunction with a good crystal structure can lead to considerable advances in the matter of spectral assignment as demonstrated in studies of some calcium binding proteins (Dalgarno, 1983) and cytochrome c (Williams, 1983) for instance. Indeed, on occassions NMR studies have been used to complement and refine the X-ray structure as demonstrated by studies of antibody combining sites (Dower et al., 1977).

However, with the advent and application of two dimensional NMR spectroscopy with suitable proteins under study, the problems of spectral assignment have been considerably simplified and for some proteins almost the entire spectrum has been accounted for. This has been demonstrated so far, for example, for the basic pancreatic trypsin inhibitor (Wagner and Wüthrich, 1982) albeit making use of data derived with benefit of the crystal structure and for the 29 amino acid peptide hormone glucagon, bound to perdeuterated dodecylphosphocholine micelles (Wider et al., 1982), without the aid of a crystal structure. The procedure involved in this process has been outlined by Wüthrich et al., (1982). First of all, J-connectivity maps are constructed via 2 dimensional J and spin echo correlated spectroscopy (Wagner et al., 1981) allowing the spin systems to be identified and so assigning resonances to different types of amino acid residues. Then, NOE connectivity maps are constructed using 2 dimensional NOE spectroscopy which provides semi quantitative distance measurements in the range 2 to 5 $\mathring{A}$ (Kumar et al., 1981). The two types of map are then combined and sequential resonance assignments can be made via connectivities between neighbouring residues, established

using the amide protons, necessitating the maps also being constucted from spectra of samples in H_2O. This assumes one set of resonances can be unambiguously assigned to a particular residue - often, for instance, because it is the only one of that type in the molecule. Thus, large numbers of resonances can be completely assigned to precise protons within the protein. In addition, β sheet structures give rise to charateristic NOE connectivities between resonances arising from residues on the antiparallel strands and these can also be recognised in the NOESY map as, of course, can data indicative of supersecondary structure such as the combination of extended polypeptide segments into β sheets (Wagner et al., 1981). Finally, NOE's arising solely from close proximity of residues through the tertiary fold can be identified and described in terms of specific residues and individual protons. In suitable circumstances the semi-quantitative distance constraints derived from the NOESY experiment can be used to considerably limit the number of possible conformations a computer simulation of the molecule needs to take account of in arriving at the most likely solution conformation. Indeed, using smaller sets of assigned resonances the latter technique has been applied to predict the solution conformation of glucagon bound to lipid micelles and of the anticancer drug, bleomycin (Braun et al., 1981; Crippen et al., 1981). Thus, the goal mentioned above of arriving at a three dimensional structure entirely from the known amino acid sequence and a suitable set of NMR data is not so far off.

The problems of the task multiply, of course, as the size of the protein considered increases, and further data is required to provide many more constraints in order to limit still further the number of possible conformations to be considered, and to arrive at a unique structure. More "conventional" NMR experiments can provide this data through for

example, studies of pH dependence effects between different groups, use of paramagnetic shift and relaxation probes and various other structural probes including any natural ligands and so on. Many of these experiments have been performed on lysozyme for instance (Blake et al., 1978) and have on their own provided much structural information about the molecule in solution. In conclusion, it can be seen that NMR is ideally suited to gaining knowledge of protein structure and rapidly approaching X-ray crystallography in this field, but with further advantages, not the least of which is the ability to readily monitor perturbations to the structure resulting from changes in the solution conditions and in due course, to provide descriptions of any conformational changes produced. We now consider the strategy employed in this thesis to the use of NMR to study some kringle containing proteins.

1.6 Outline of the Thesis

The initial intention had been to study the effects of calcium binding by the γ-carboxyglutamic acid residues of fragment 1 of the vitamin K dependent protein, prothrombin using high resolution NMR to monitor the solution structure. Some progress was made in this direction (Esnouf et al.,1979, 1980a, 1980b), and our work was amply confirmed by another group (Pletcher et al., 1981). However, it soon became apparent that we required more information on the overall structure of fragment 1 to be able to fully interpret our observations. With regard to this objective we shifted our attention to the smaller protein prothrombin fragment 2 in order to study the solution conformation of the kringle. However, this fragment of 118 residues is still a little large for satisfactory initial NMR studies of the kringle structure and so we concentrated our interest on the 88 residue fragment of plasminogen, containing kringle 4 (and

referred to in the rest of the text as "kringle 4" containing only ten residues additional to those comprising the kringle). This protein has the additional advantage of a well defined ligand binding site and a variety of small ligands with which to probe the structure that are not available for the kringles of prothrombin fragments 1 and 2.

Thus, in Chapter 3 we begin the task, vital to our aims, of assigning the NMR spectrum of krinlge 4. The whole range of techniques discussed above to simplify this process have not been available to us so far, in the course of this work. However, we have been able to perform COSY experiments on samples in D_2O and as will be seen this has been of great benefit. The majority of experiments therefore have been one dimensional but as will be discussed these are nevertheless invaluable as part of the assignment process.

Chapter 4 describes the application of a number of structural probes including some ligands specific for the lysine-binding site of kringle 4 and the data interpreted in terms of the structural perturbations indicated by the spectral changes.

Chapter 5 considers the NMR spectra of various chemically modified kringle 4 species which serve to aid the assignment process but also throw light on the molecular structure and the effects on it of specific chemical changes to various residues. The chapter ends by collecting all the information gathered on kringle 4 into a description of building a molecular model for part of the structure and considering the possibilities for refining it.

Chapter 6 discusses some aspects of NMR studies of prothrombin fragment 2 and provides information on the structure of another kringle, this allows comparisons to be made and features common to kringles to be elucidated.

Finally, in chapter 7 we consider other information relevant to the biological role of kringles and relate it to the data presented in the previous chapters ending with a discussion of prospects for further work.

Overall the aim has been to arrive at some notion of the solution structure of the kringle entity. The task is somewhat akin to doing a jig-saw puzzle except that the pieces have to be found and fitted together to try and produce an overall picture - the structure - which has not been seen. Unfortunately, the result of describing the constituent pieces gives the impression of much disparate information, the relevance of which is only completely assimilated when all of it is brought together. Some attempt has been made to try and construct rough outlines of the structure before more detailed model building of part of the structure of kringle 4 is considered near the end of chapter 5. However, in order to facilitate the reading of the preceeding material figures 1.4 and 1.5 show photographs of the model structure described in section 5.8.

It must be emphasised that this model has not attained the status of a definitive structure for kringle 4 in solution. It depicts the backbone of the kringle loops labelled II, III and IV in Fig. 1.3 including the second and third disulphide links. Only side chains of particular interest have been added to the backbone and these are indicated, using one letter amino acid codes with their positions in the sequence, around the edge of the photographs. The relative dispositions of these side chains have been arranged in order to account for as much of the data accumulated from the NMR studies of chapters 3, 4 and 5 as possible, although it is conceivable that other configurations would be equally as acceptable. Further discussion of this must obviously be delayed until section 5.8. However, reference to these and the additional photographs of chapter 5 may help in reading the description of the various pieces of an incomplete jig-saw, presented with a possible picture.

Key to the colours of the model atoms

White - peptide backbone

Purple - aromatic residues

Yellow - sulphur atoms

Red - carboxyl groups, hydroxyl groups

Blue - amino groups

Grey - methyl groups

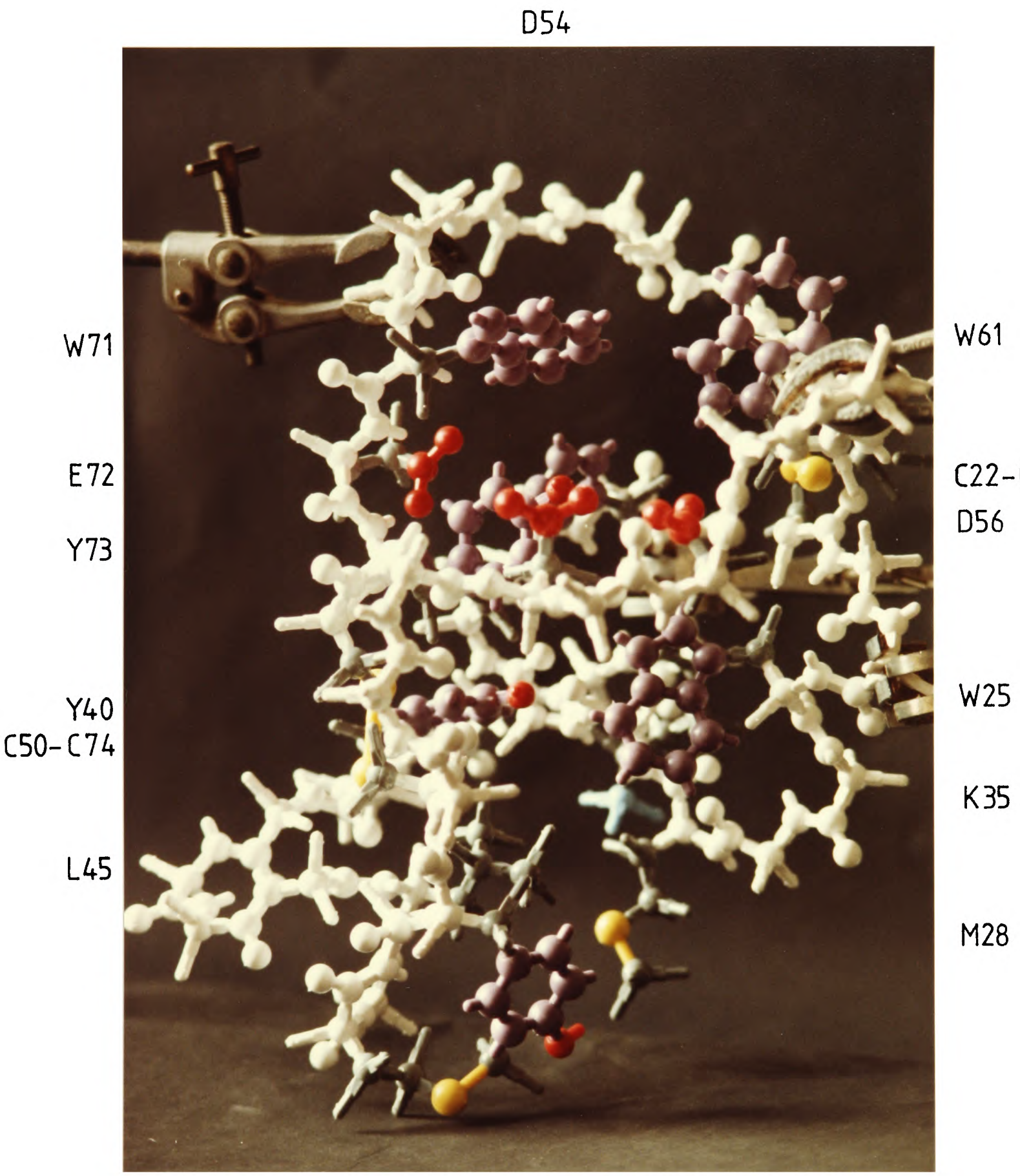

Fig. 1.4 Photograph of what is arbitrarily taken as the "front" of the molecule for reference of the other photographs.

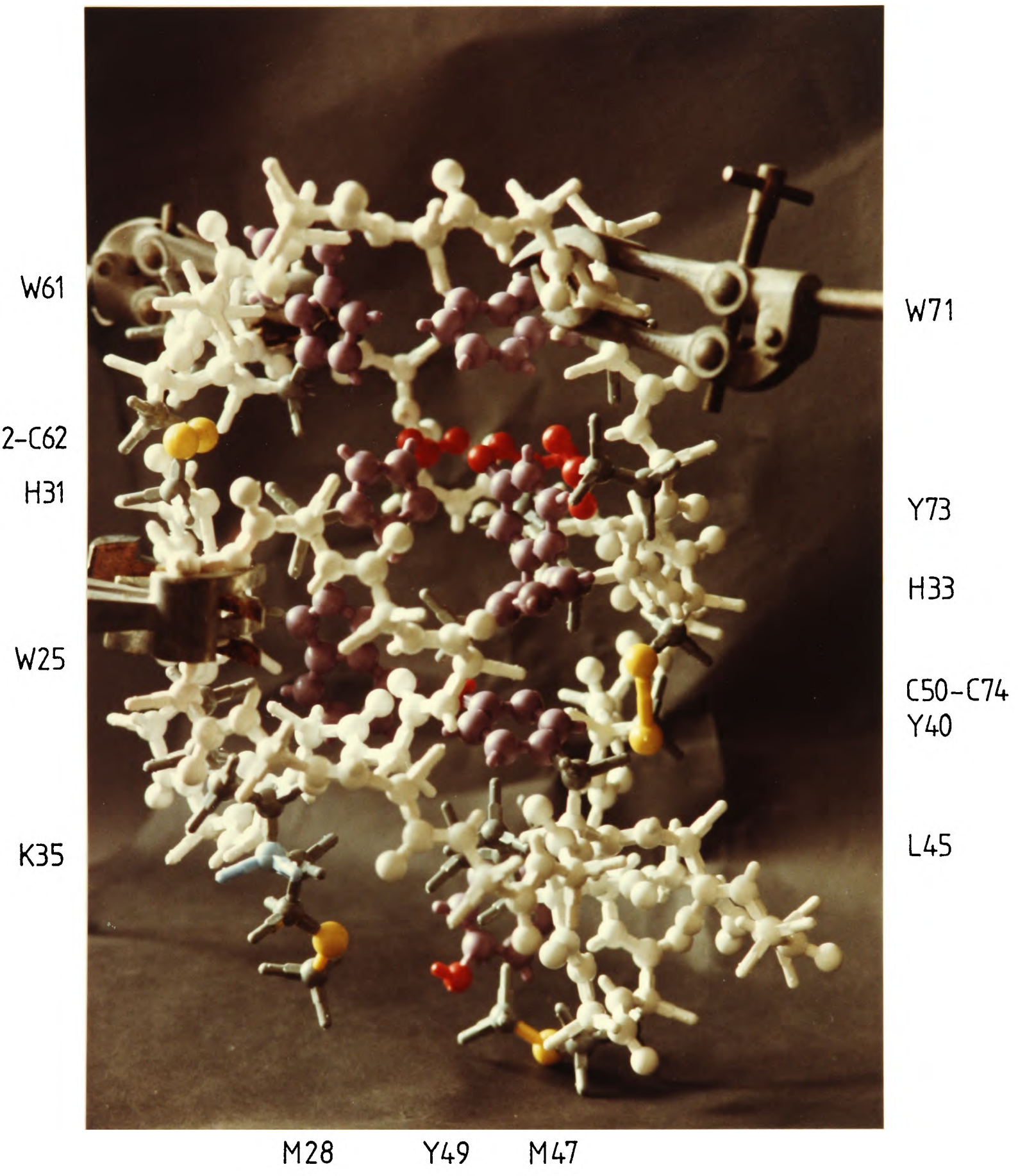

Fig. 1.5 The back of the molecule.

CHAPTER 2

MATERIALS AND METHODS

2.1 Materials

2.1.1 Proteins

Native kringle 4 of human plasminogen and the modified kringle 4 species were all supplied in lyophilised form by Dr.L. Patthy and his coworkers. Precise details of the preparations are not given here but the essential features are summarised. Thus, plasminogen was prepared from fresh citrated plasma by affinity chromatography on lysine-Sepharose as described by Deutsch and Mertz (1970). Kringle 4 is then obtained by limited proteolysis of plasminogen with porcine pancreatic elastase followed by separation of the resulting fragments with gel filtration on Sephadex G-75 and affinity chromatography on lysine-Sepharose essentially as described by Sottrup-Jensen et al., (1978).*

Full details of the modification procedures and in particular, of the characterisation of the modified proteins will be published shortly by Patthy et al. However, the nitration of the tyrosine residues 40 and 49 of kringle 4 was carried out using tetranitromethane at pH 8, 25°C for one hour, according to the method of Sokolovsky et al., (1966). The protein containing Tyr 40 - Lys 35 crosslinked was prepared by reaction of plasminogen with 1,3-difluoro-4,6-dinitrobenzene, pH 8, 25°C and subsequent elastase digestion of the modified plasminogen. Oxidation of Trp 71 and methionines 28 and 47 of kringle 4 was performed by reaction with hydrogen peroxide in dioxan, pH 8, 25°C (Matsushima et al., 1980).

Complete details of the arginine modified species have been published already (Trexler et al., 1982) and involved the reaction of kringle 4 with

* The kringle 4 produced is actually a mixture of two forms having the same N terminus but different C terminal residues, namely Ala 84 or Val 86 (Hochschwender et al., 1983).

1,2-cyclohexanedione in borate buffer at pH 8, 37°C for 30 min. The kringle 4 cleaved at Met 47-Asn 48 was prepared by reaction with cyanogen bromide and the Cys 1-Cys 79 cleaved protein by selective reduction and carboxymethylation.

All prothrombin fragments were supplied by Dr.M.P. Esnouf and his coworkers. Bovine prothrombin was obtained by adsorption of the protein from serum on to barium citrate and then fragment 1 was cleaved off by incubating the purified prothrombin at pH 8, 25°C in the presence of 5mM calcium chloride (Aschaffenburg et al., 1977). Bovine and human fragment 2 proteins were prepared by passing the respective molecule in 5 mM $CaCl_2$, pH 7.5 through a Factor Xa-Sepharose column (Esnouf et al., 1980b).

2.1.2 Other Materials

Lanthanide solutions were made from the oxides obtained from Koch-Light and dissolved in deuterium chloride. 500mM stock solutions were standardised using EDTA and acetate buffer with xylenol orange as the indicator. They were diluted for use with D_2O.

Solutions of NaOD (40% in D_2O, isotopic purity 99%) and DCl (35% in D_2O, isotopic purity 99.6%) were obtained from CIBA. D_2O of isotopic purity, 99.8% from Merck, Sharpe and Dohme was used for all one dimensional NMR experiments, but D_2O of isotopic purity 99.996% from the Aldrich Chemical Company was procured for the two dimensional experiments in order to improve the signal to noise ratio. Wilmad 507-PP NMR tubes were always used.

6 aminohexanoic acid was puchased from the Sigma Chemical Company while the ligand 4-aminomethyl-bicyclo[2,2,2]-octane-1-carboxylic acid (AMBOC) was a gift from Dr.S.A. Cederholm-Williams.

Nicholson molecular models, 1cm to 1Å were bought from Labquip.

2.2 Methods

2.2.1 Sample Handling

All proteins were used as lyophilised powders and concentration determined solely by calculation from the dry weight. Sample volumes were between 0.4 and 0.45 cm^3 and protein concentrations of about 1mM were used for one dimensional experiments and 5mM for 2 dimensional ones. Nearly all solutions were made up in 100 mM NaCl and 3mM Tris-(hydroxy-methyl)aminomethane. pH measurements were made using Pye Ingold combination microelectrodes with a Radiometer pH Meter and the pH was adjusted using very small amounts of 1M and 0.1M stock DCl and NaOD solutions. Where possible pH dependent resonances of the protein were used to indicate the pH in order to save further loss of protein on the electrode. All pH values quoted are meter readings without correction for isotope effects.

One practical procedure of note was that in all external pH measurements and additions of reagents in titrations, the sample volume was transferred to a small glass sample tube using a drawn Pasteur pipette. This facilitated mixing in the solution and avoided spreading the sample down the walls of the NMR tube.

Dioxan was used as an internal reference with chemical shifts related to its resonance at 3.741 ppm (Dobson, 1975).

2.2.2 NMR Methods

The majority of spectra were recorded using a Bruker WH300 spectrometer incorporating an Aspect 2000 computer, Diablo series 30 disc system and an Oxford Instruments narrow bore magnet. The two dimensional experiments were carried out using a 470MHz spectrometer developed by the Oxford Enzyme Group. This machine includes a Nicolet 1180 computer, and 293B pulse

controller with a Data Recording Equipment disc system and an Oxford Instruments narrow bore magnet. Probe temperatures were calibrated when necessary using an ethylene glycol sample according to the method of Van Geet, (1968).

Resolution enhanced spectra were obtained through Gaussian multiplication of the free induction decay prior to Fourier transformation.

2.2.2.1 Multiplet Selection Spectra

Concurrent acquisition using the pulse sequences $90^{o}-\tau_1-180^{o}-\tau_1$ and $90^{o}-\tau_2-(180^{o}-2\tau_2)_n-180^{o}-\tau_2$ produces two spectra modulated by spin coupling (J) effects. In actual fact, in the experiments described τ_1 was always 60 msec but τ_2, taken as 1 msec, was too short for any J modulation. This results in two spectra which can be added or subtracted to produce further spectra; one containing odd multiplet resonances (singlets, triplets) and the other only even multiplets (doublets) respectively (Campbell et al., 1975). This provides a very useful simplification of some complex areas of the spectrum as will be seen. The τ values chosen were such that the time, T between the 90^{o} pulse and the data acquisition was 120 msec, which is ideal for the modulation of resonances of coupling constant, J of about 8.5Hz (T=1/2J) as occur for aromatic ring proton resonances.

2.2.2.2 NOE Difference Spectra

Driven nuclear Overhauser enhancements (Dubs et al., 1979) were obtained as difference spectra by automatic subtraction of concurrently acquired spectra where the resonance is saturated in one and the pre-saturation pulse moved to an empty region of the spectrum in the other. In the majority of experiments a presaturation pulse length of 1sec was employed. The irradiated resonance is shown in the figures in the text by an arrowhead. The same symbol is used to denote the position of spin decoupling pulses,

with filled circles over decoupled resonances. The latter effects are marked when a spin decoupling pulse is combined with an NOE experiment, the resonance saturated being indicated in the text.

NOE data is used in the text to provide qualitative distance data for the spatial separation of protons. Despite mechanisms of spin relaxation other than proton-proton dipolar coupling affecting the system, it is generally taken that NOE effects are seen between protons of 5Å separation or less (Dubs et al., 1979 ; Wüthrich et al., 1982). NMR studies of cytochrome c for which a well resolved crystal structure is available show that this is true in most cases for the type of NOE experiments carried out in this work (G.R. Moore, G. Williams, personal communication).

2.2.2.3 Two Dimensional Correlated Spectroscopy

The use of two dimensional spectroscopy - COSY - in protein NMR studies has been well demonstrated as for instance by Wagner et al., 1981. A similar method was used in this work to obtain COSY spectra. The data was accumulated such that the digital resolution was 5.8 Hz/point (the digital resolution was 0.99 Hz/point in the one dimensional experiments). The free induction decays were multiplied by a shifted sine-bell routine applied in both dimensions and the final set of data was subject to a symmetrisation procedure removing all intensity not symmetric about the diagonal. The latter effect is not always apparent in the contour plots shown, due to the limitations of the contour plotting routine.

2.2.3 Lanthanide Reagents

The theory and use of lanthanide ion reagents is well known in NMR studies (Dwek, 1973; Dobson and Levine, 1975). The general equation for a dipolar shift of a nuclear magnetic resonance line due to perturbation by a paramagnetic ion at a distance, r, from the given nucleus is

$$\Delta p = D\left\langle \frac{3\cos^2\theta - 1}{r^3} \right\rangle - D'\left\langle \frac{\sin^2\theta\cos 2\psi}{r^3} \right\rangle$$

where θ defines the angle between the principle axis and the vector joining the paramagnetic probe and the nucleus under study, ψ is the angular position in the plane around the symmetry axis, and D and D' are ligand field parameters (Bleaney, 1972). In certain circumstances the above equation reduces to the form

$$\Delta p = D\left\langle \frac{3\cos^2\theta - 1}{r^3} \right\rangle$$

when either D' = 0; true axial symmetry, or through some averaging process in solution such that $\langle \cos 2\psi \rangle = 0$; effective axial symmetry. However, in these cases the shift, Δp is found to depend on only two parameters θ and r, for any given metal ion.

A paramagnetic ion affects the rate of relaxation of an excited nucleus. In the absence of contact contributions, if the relaxation rate of the paramagnetic ion is slow then the relaxation of the nucleus due to the presence of the ion is given by

$$\frac{1}{T_i} \alpha \frac{1}{r^6} \quad \text{where } i = 1 \text{ or } 2$$

Thus, the relaxation times of the proton resonances in the presence of gadolinium ions are inversely proportioned to the sixth power of the distance separating the proton from the metal ion.

CHAPTER 3

ASSIGNMENTS IN THE NMR SPECTRUM OF KRINGLE 4

3.1 Introduction to the NMR spectrum

Figure 3.1(a) shows the 300 MHz spectrum of the kringle 4 fragment of human plasminogen at 27°C and pH 8.3, immediately on dissolving in D_2O.

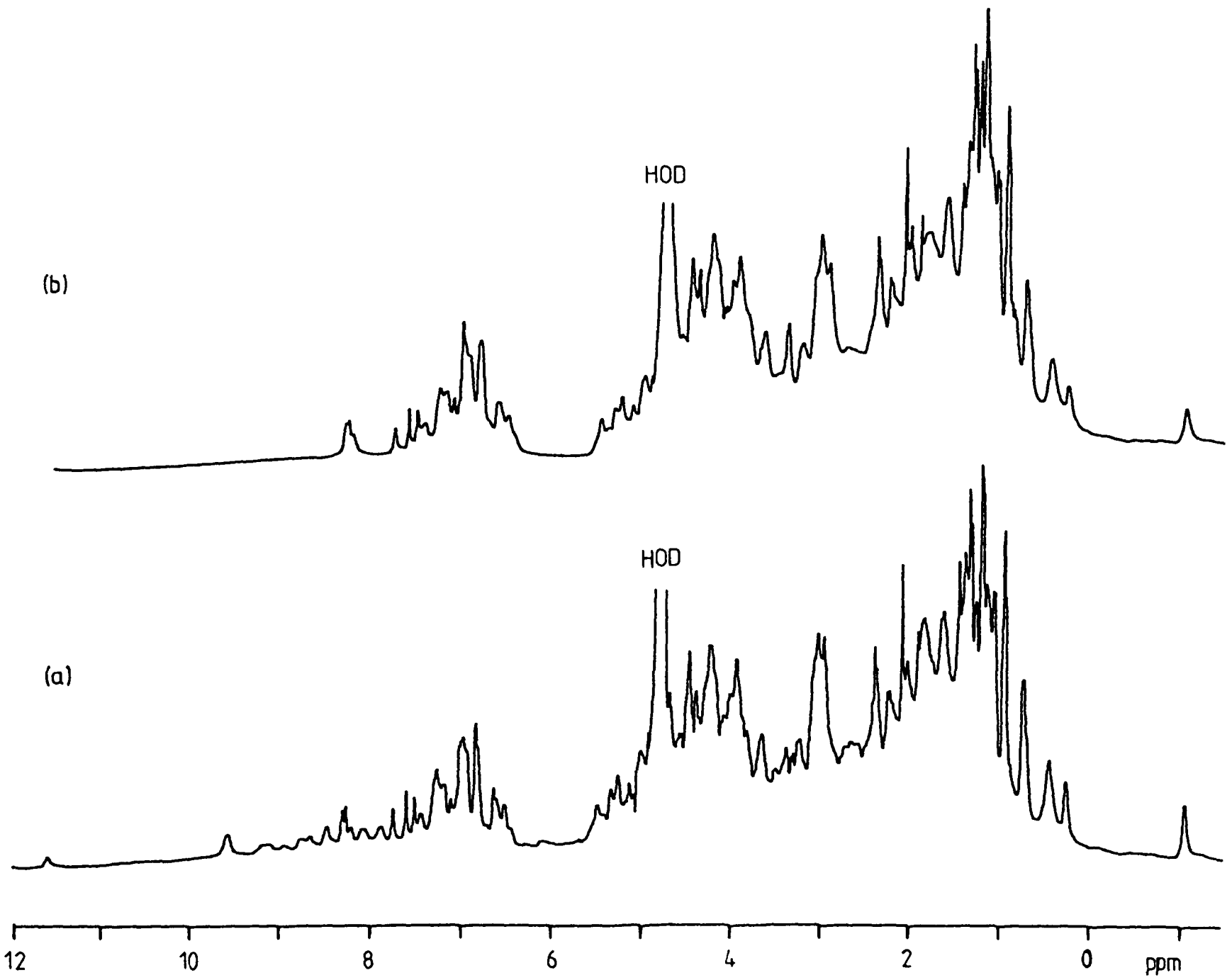

Fig. 3.1 300 MHz spectrum of kringle 4 at 27°C, pH 8.3 (a) within 15 minutes of dissolving the protein in D_2O (b) similar sample some hours later.

Figure 3.1(b) shows the spectrum of a similar sample some hours after dissolving in D_2O and clearly shows the loss of a number of resonances between 6 and 11.6 ppm. These peaks arise from labile protons attached to nitrogen and oxygen atoms of the backbone and certain side chains, and which exchange with deuterons in the solvent at varying rates to be lost from the proton spectrum. Dissolving single amino acids and oligopeptides in D_2O rarely results in such resonances ever being observed, as the rate of exchange of such protons, freely accessible to the solvent, is extremely rapid. Indeed, this can be the case for proteins as demonstrated by our studies of bovine parathyroid hormone - a protein consisting of 83 residues with no disulphide bridges (Brewer and Ronan, 1970), (kringle 4 having 88 residues and 3 disulphide links) -- in the NMR spectrum of which no such exchanging resonances have been observed (Pluck and Williams, unpublished results). For this and other reasons we believe that this hormone molecule has little or no tertiary structure in solution and all the constituent protons have ready access to the solvent. However, typical globular proteins, such as lysozyme and cytochrome c, do produce NMR spectra containing these characteristic resonances and X-ray studies on crystals confirm that some internal regions of the molecule are well shielded from the surrounding solvent, in accord with greatly reduced labile proton exchange rates. Thus, the presence of these resonances in the spectrum of kringle 4 indicates that the molecule has a tertiary fold resulting in some region or regions of relative solvent inaccessibility.

That the protein is folded in solution is further indicated by the considerable spread of resonances clearly seen in Fig. 3.1 and, as will be shown in what follows, it differs markedly from the spectrum expected for a random coil structure in which all the side chains are intimately associated with solvent molecules (see sections 3.6 and 4.2, for example). In particular studies on tetrapeptides show that aliphatic side chains

produce resonances between 0.8 and 4.3 ppm, αCH resonances between 3.9 and 4.8 ppm and aromatic side chain peaks (not including histidines) between 6.85 and 7.65 ppm (Bundi and Wüthrich, 1979. All random coil chemical shifts quoted herein are from this reference). Numerous resonances are seen to be outside these limits in the spectra in Fig. 3.1. These so called "secondary shifts" of resonances from their random coil positions arise from protons lying in environments provided by close proximity to other parts of the molecule, as opposed to solvent molecules which surround the residues of the reference tetrapeptides quoted above. For instance, it has been shown that the peaks between 5 and 5.5 ppm can arise from αCH backbone protons which are shifted downfield through being involved in β sheet structure in the protein (Dalgarno et al. 1983). Similarly, methyl group resonances of various side chains have been found to be shifted upfield beyond 0.8 ppm through being in very close proximity to aromatic rings contained in the molecule and receiving "ring current shifts" (Wüthrich, 1976). These and other features characteristic of the NMR spectrum of a globular protein are seen to be present in the spectrum of kringle 4.

Thus, preliminary observation of the kringle 4 NMR spectrum demonstrates that in solution the molecule has a definite tertiary fold resulting in considerable perturbation of resonances from random coil positions. In order to define the nature and extent of this folding and to characterise the structural changes induced by altering the solution conditions, it is clearly necessary to assign the peaks and especially the perturbed resonances in the spectrum to particular types of amino acid side chain and then to correlate the residues with their position in the primary amino acid sequence of the protein. This is conventionally known as the first and the second stages of the assignment process respectively and is the method adopted below. We begin this task with the aromatic region of the spectrum.

3.2 Aromatic Region of the Spectrum

Figure 3.2 shows the position of the aromatic residues within the kringle primary sequence, and Table 3.1 gives the number and type of multiplets expected in the aromatic region of the spectrum assuming that the phenylalanine and tyrosine rings are free to rotate about the Cβ-Cγ bond. Figure 3.3(a) shows the aromatic region of the kringle 4 spectrum with peaks numbered for reference and where necessary will be referred to in the text with the prefix "R" to indicate aromatic resonances. (Some of the downfield shifted αCH proton resonances are also numbered in Fig. 3.3(d) with the prefix "A"). Multiplet selection spectra are shown in Fig. 3.3(b) and (c) and the reference numbers more clearly related to resonances. Figure 3.3(b) shows the expected nine singlet resonances (the very sharp peak at 8.4 ppm is very variable in intensity and due to an impurity) but no clear triplet resonances beyond 5.5 ppm. However, resonance R1 is seen to be a one proton triplet from (a) and (d) and R22 is implicated as the same by its absence from spectrum (c). Four one proton doublets are seen at R23, R11, R15, and R19 and most likely attributable to tryptophans, the complete assignment of which we now consider.

3.2.1 Tryptophans

Figure 3.4 demonstrates that (b) R19, R1, (c) R11, R4 and (d) RX, R22 are coupled pairs of doublet and triplet resonances confirmed by irradiating the other partner of the pair except in the case of RX, R22 where RX represents an unspecified resonance in the region of R8. With the exception of RX these resonances are all seen from Fig. 3.3 to be of one proton intensity and Fig. 3.5 indicates that six pairs of doublet-triplet and three triplet-triplet couplings are expected in all for the three tryptophans of kringle 4. However, countless spin decoupling

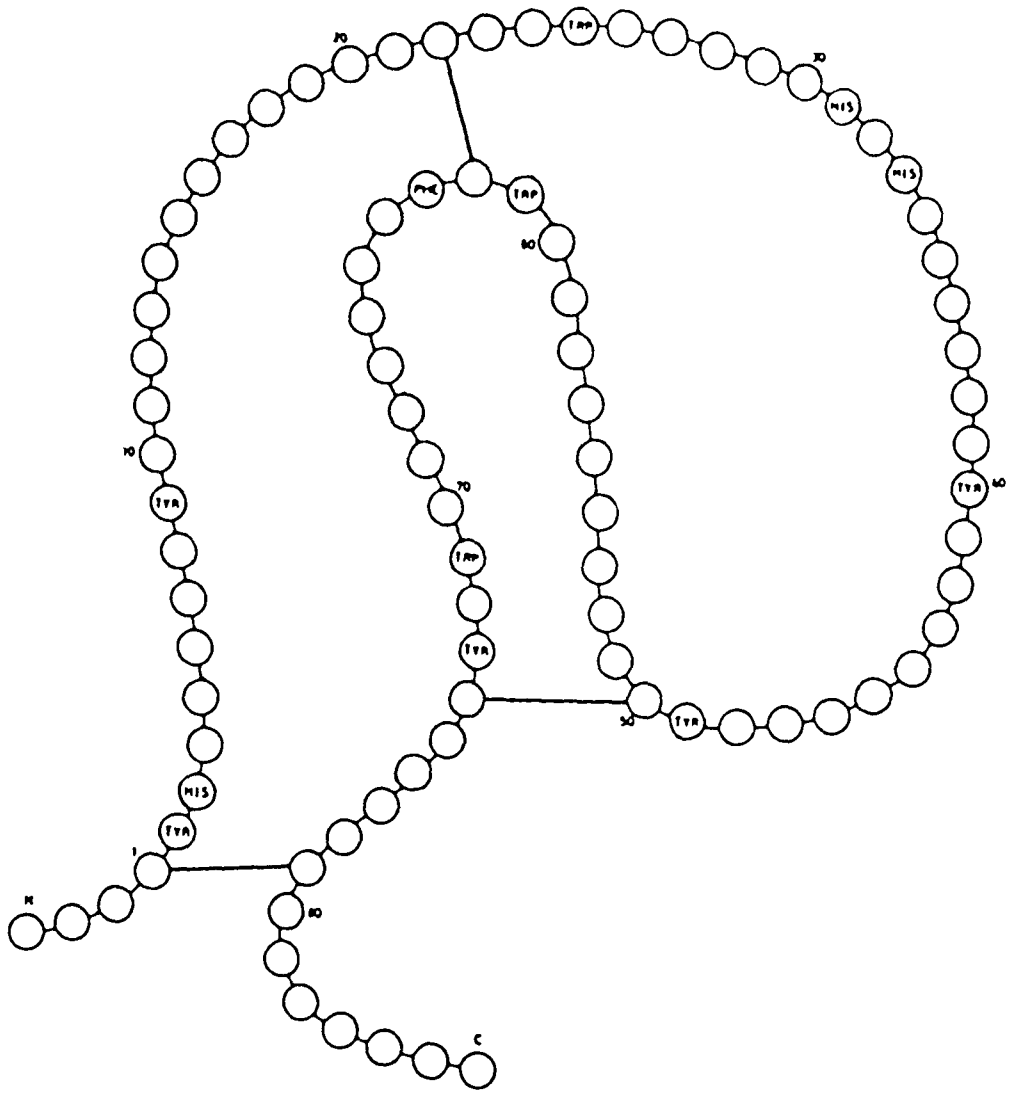

Fig. 3.2 Positions of the aromatic side chains in the primary sequence of human plasminogen kringle 4.

Table 3.1 Origin of the Expected Multiplets in the Aromatic Region of the NMR Spectrum of Kringle 4.

RESIDUE	SINGLETS	DOUBLETS		TRIPLETS	
		One Proton	Two Proton	One Proton	Two Proton
3 Histidines	6				
1 Phenylalanine			1	1	1
5 Tyrosines			10		
3 Tryptophans	3	6		6	
TOTAL	9	6	11	7	1

Total Number of Protons is 46.

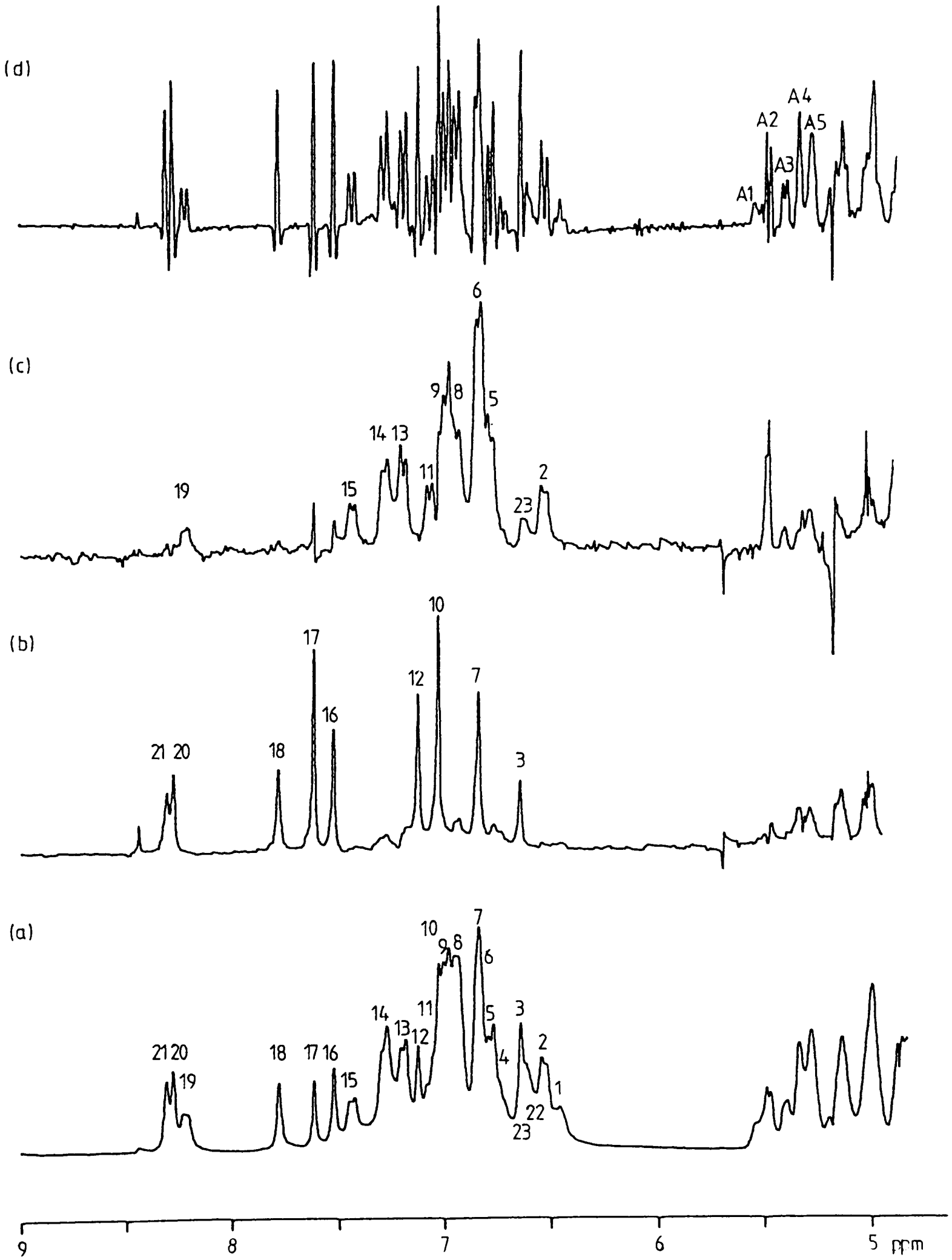

Fig. 3.3 Aromatic region of the spectrum; 47°C, pH 8.6. (a) Normal spectrum. (b) Odd multiplet selection. (c) Even multiplet selection. (d) Resolution enhanced form of (a).

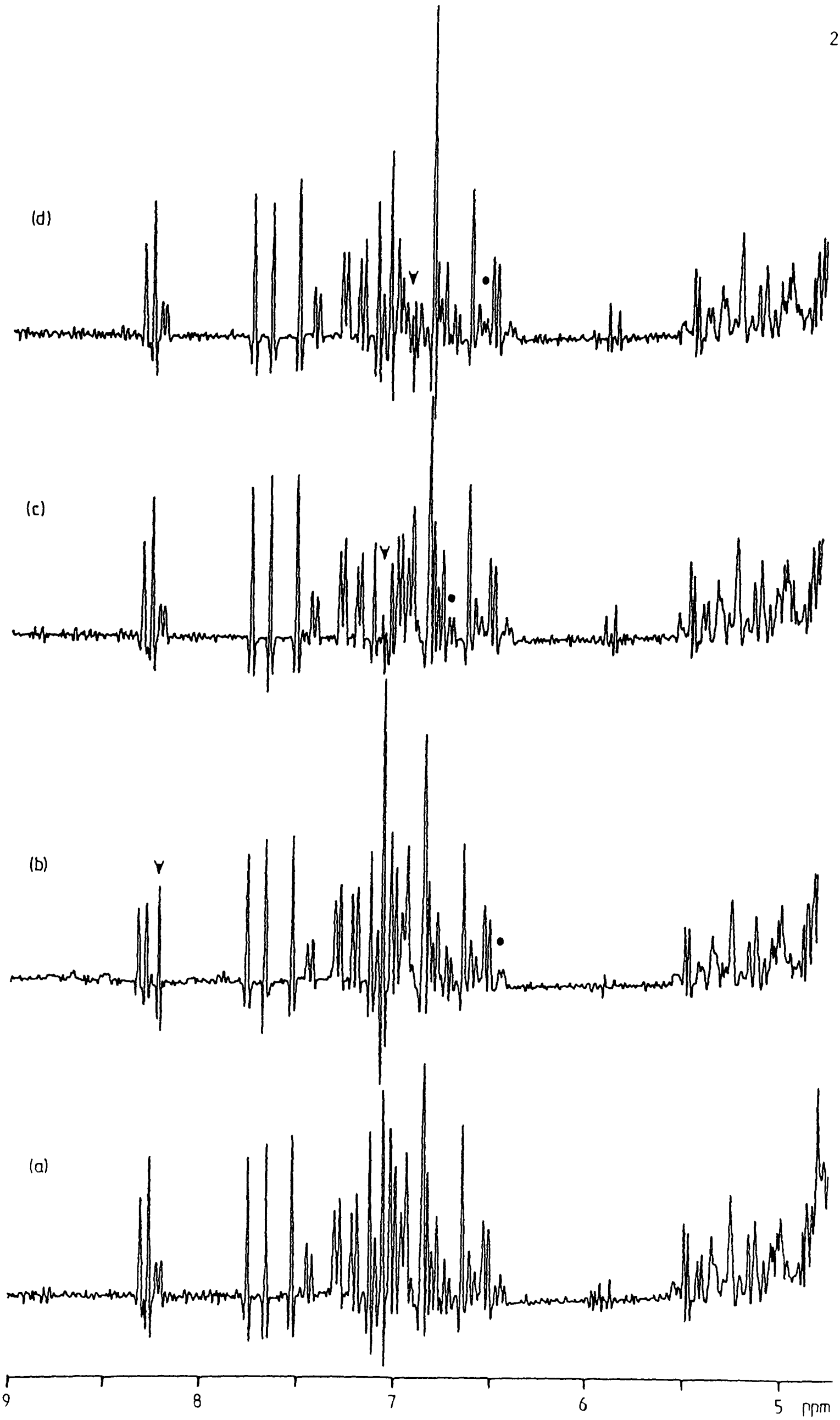

Fig. 3.4 Resolution enhanced spectra; 37°C, pH 7.6. (a) Normal, (b) - (d) spin decoupling experiments.

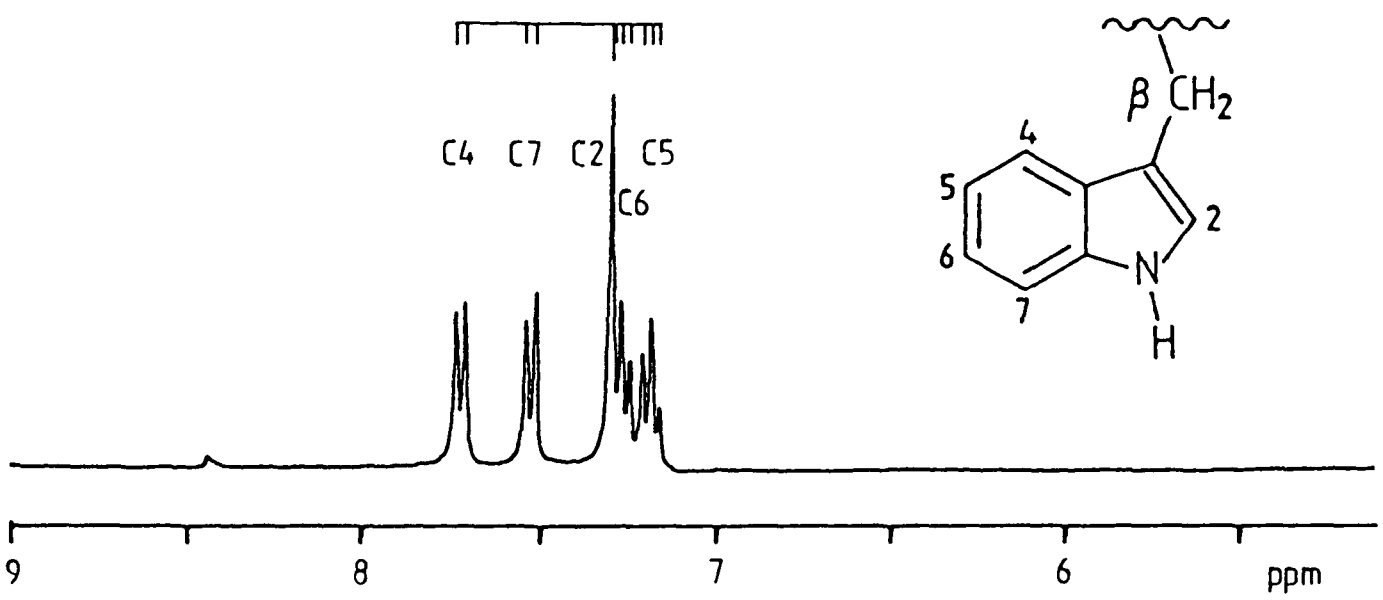

Fig. 3.5 Aromatic region of the 300 MHz spectrum of the amino acid tryptophan in solution; assigned from Bundi and Wüthrich, 1979.

experiments were performed between 6.4 and 7.4 ppm without decoupling R1, which as a triplet coupled to a doublet seen by irradiating R19, must be coupled to another resonance. Furthermore, the clear one proton doublets R23 and R15 were also never decoupled in this search. Numerous NOE experiments also failed to resolve the problem except that the Overhauser enhancement on irradiating the labile proton resonance at 11.6 ppm was very informative. This is shown in Fig. 3.6 and demonstrates proximity of the exchangeable resonance to a singlet, R12 and the one proton doublet, R15. This result is typical of irradiating the NH proton of a tryptophan and observing enhancements on the C2 and C7 proton resonances and it is noteworthy that this indole NH is further downfield than any of those arising from the six tryptophan rings of lysozyme (Poulsen et al., 1980). Thus, R12 and R15 are assigned, but the rest of the coupling scheme of this and the other tryptophans remained elusive until it was possible to perform a COSY experiment. This is shown in Fig. 3.7 where the off diagonal cross peaks manifest proton-proton J connectivities. The surprising feature of this experiment was the presence of three pairs of cross peaks between the typical aromatic region of the spectrum for a

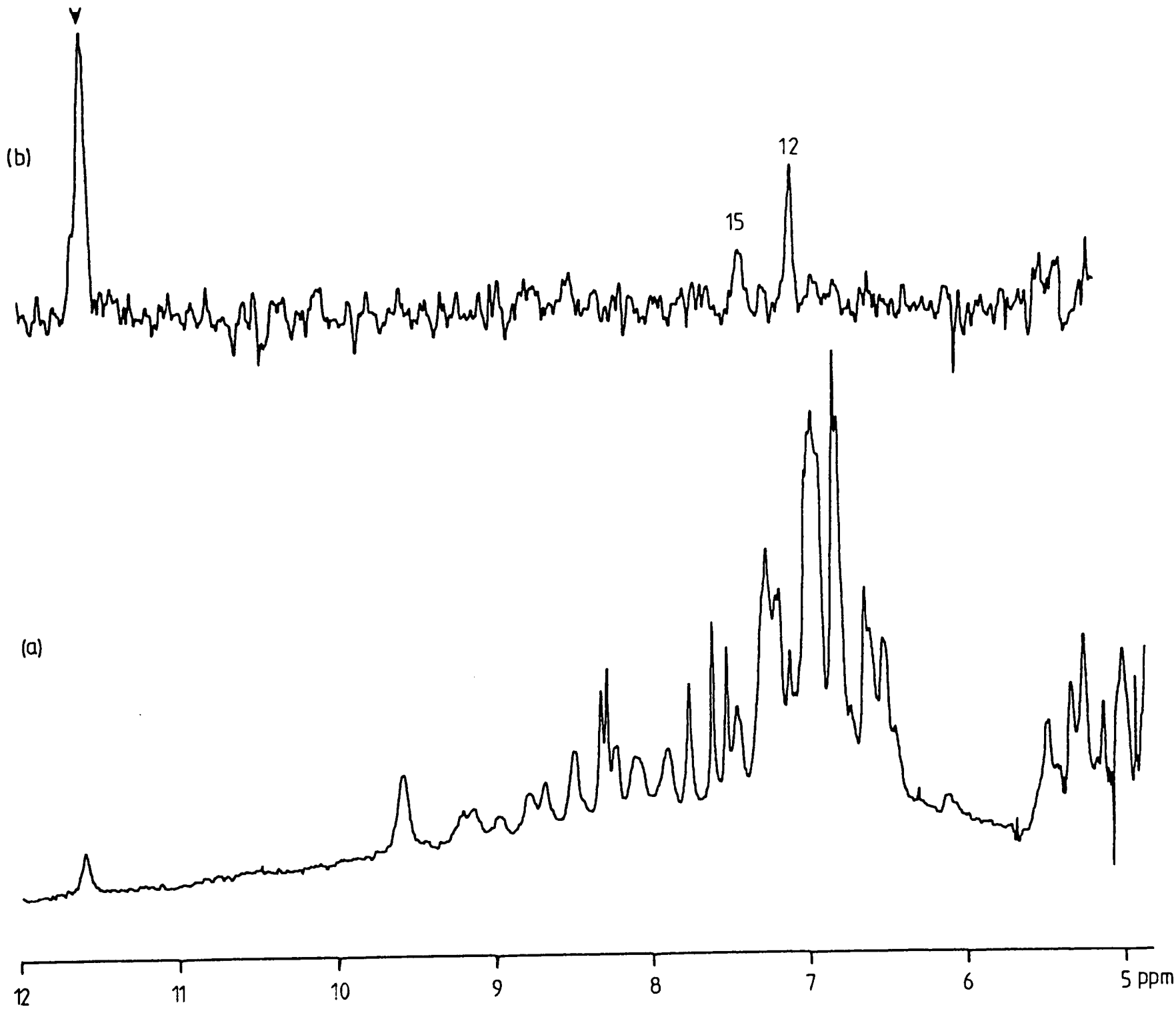

Fig. 3.6 27°C, pH 8.3 (a) Normal spectrum (b) NOE difference spectrum.

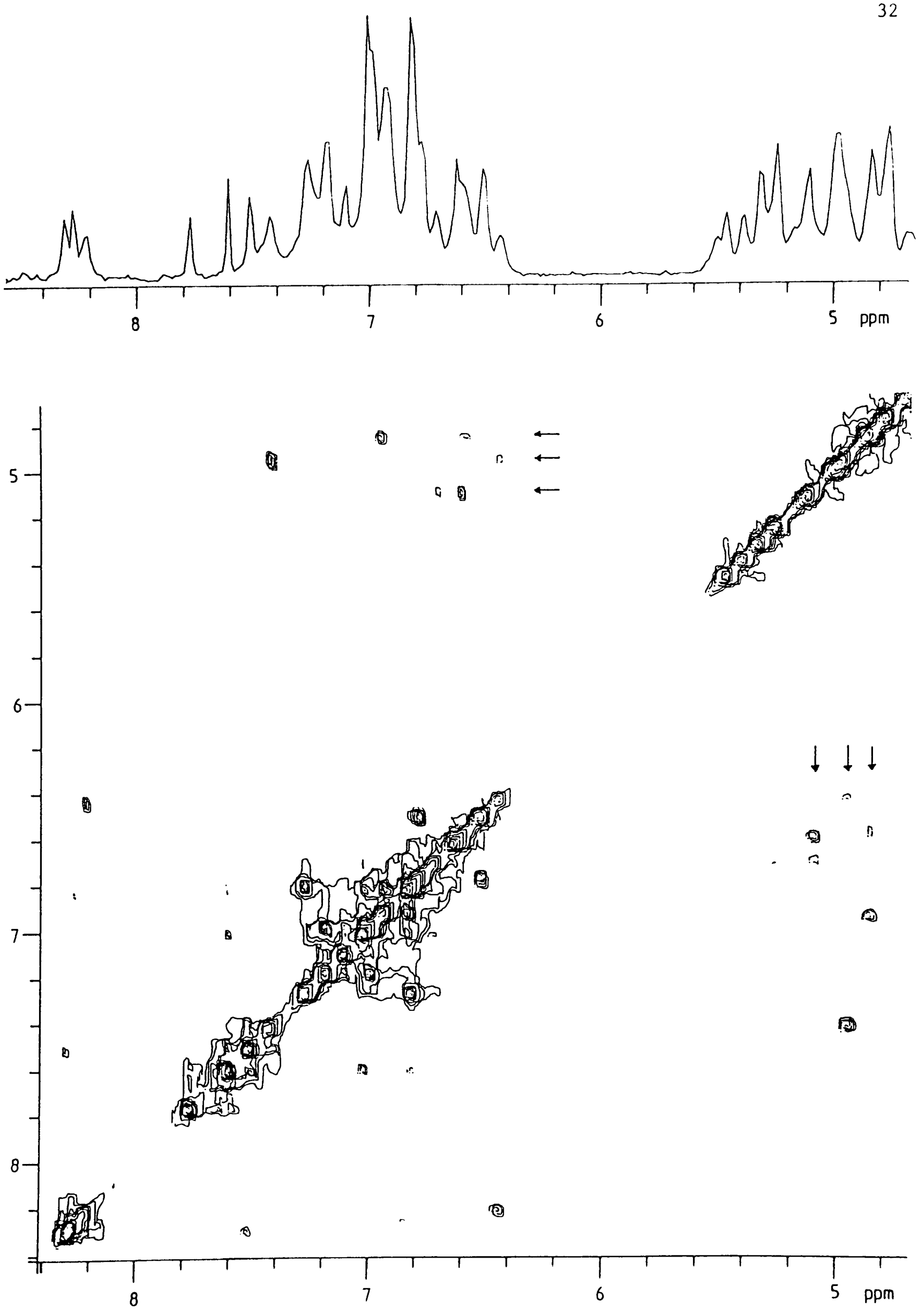

Fig. 3.7 Aromatic region of the 470MHz COSY experiment; 37°C, pH 8.3.

non-heme containing protein i.e. beyond 6 ppm, and the downfield shifted αCH region of the spectrum (5-5.5 ppm). This result was thus confirmed by one dimensional spin decoupling experiments as seen in Fig. 3.8. (This sample contained some 6 aminohexanoic acid which results in two of the triplets at around 4.9 ppm being coincident as will be shown in section 4.4. Some slow exchanging labile resonances are also present beyond 7.7 ppm). Thus, the coupling schemes of the indole ring protons for the three tryptophan residues were derived and are as shown in Fig. 3.9.

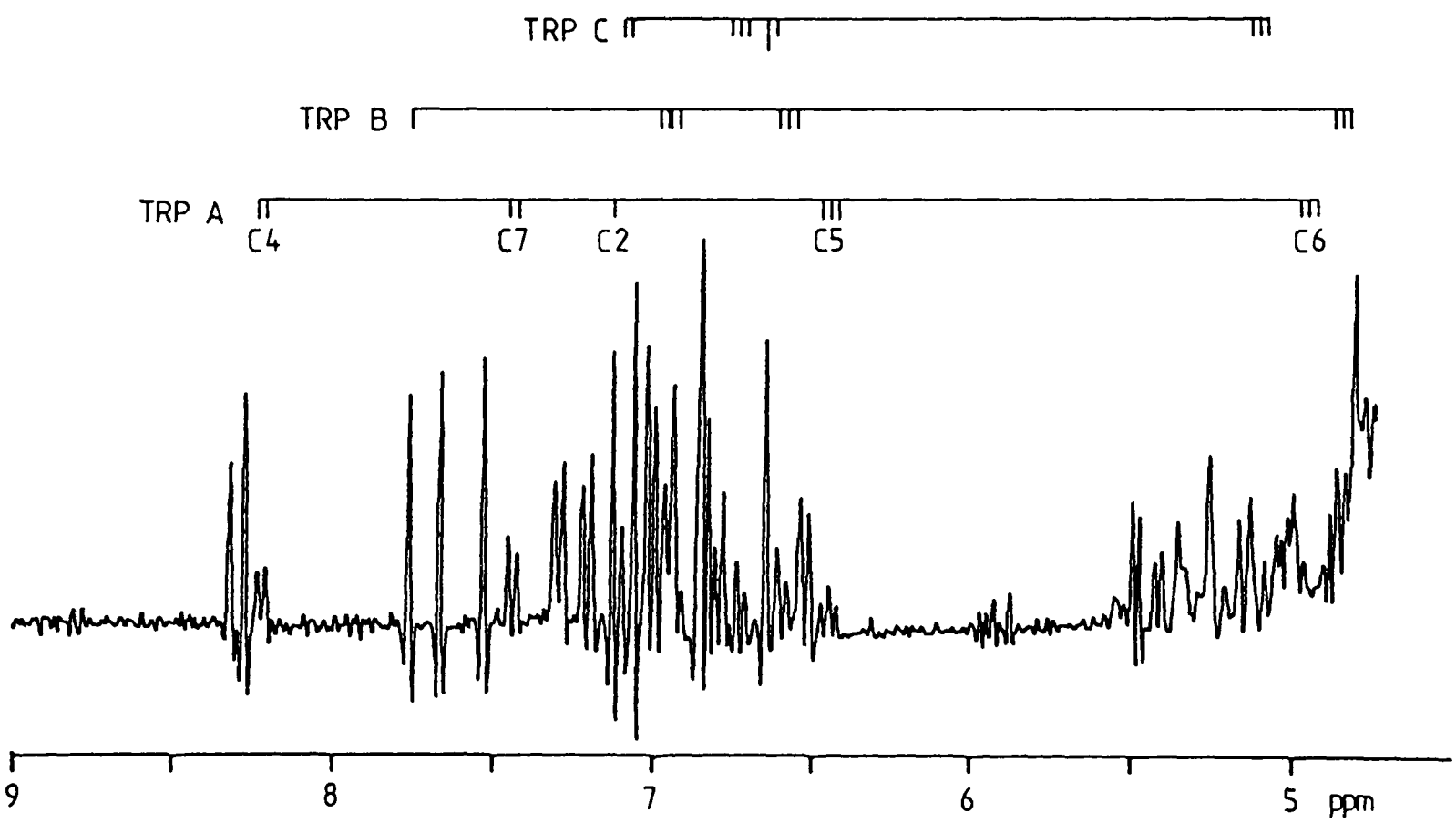

Fig. 3.9 Summary of the coupling patterns for the three tryptophan residues of kringle 4.

We note that three of the four multiplets of the Trp A ring are clearly resolved in the normal spectrum and from this we can see in Fig. 3.7 that the intensity (indicated by the number of contours) of cross peaks in the COSY spectrum between doublets and triplets is greater than that of triplet-triplet cross peaks. This independently confirms R22 as a triplet

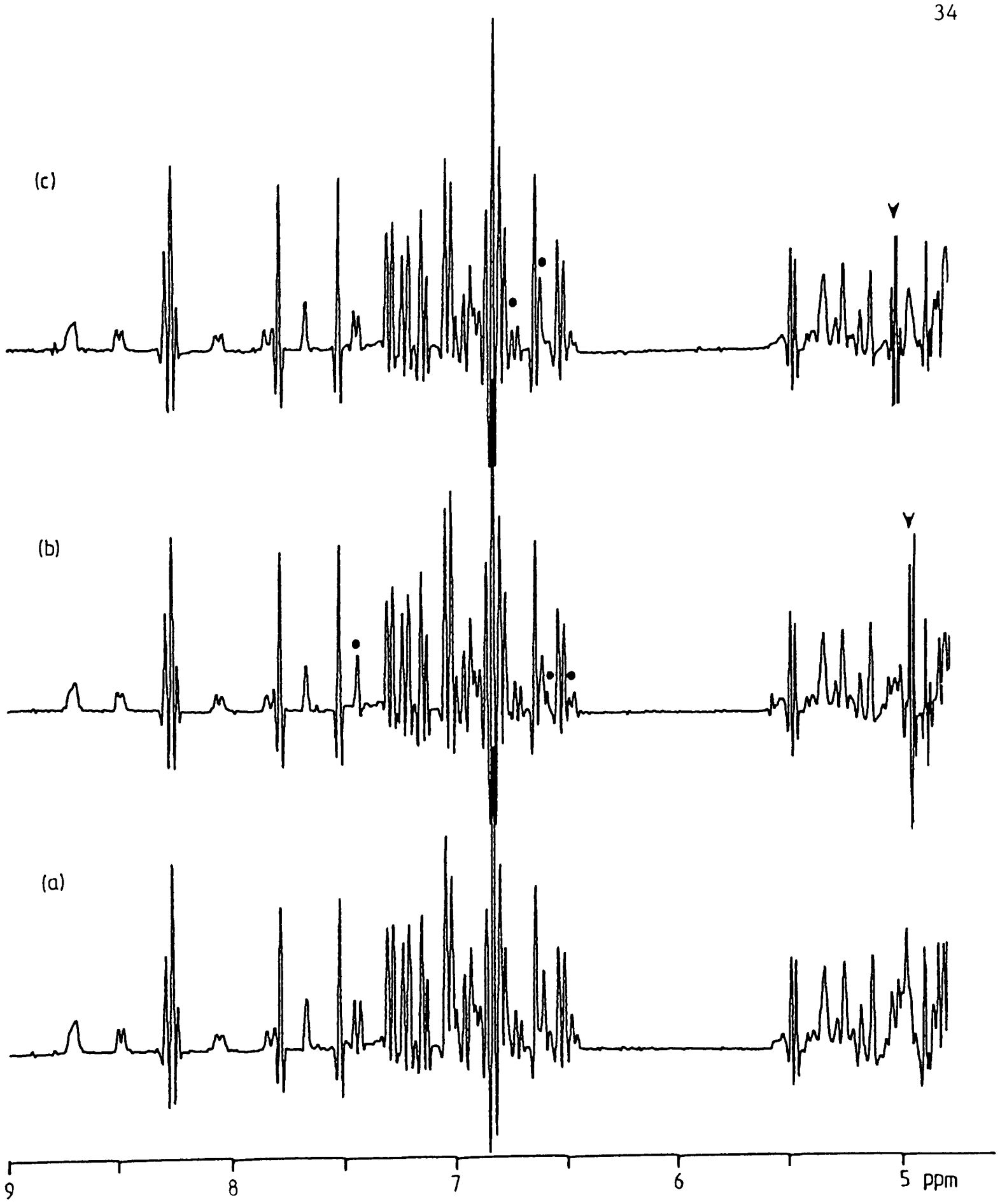

Fig. 3.8 Resolution enhanced spectra; 47°C, pH 7.7. (a) Normal (b), (c) spin decoupling experiments. (The sample contains the ligand 6 aminohexanoic acid. Some slow exchanging labile proton resonances are also present).

and shows R4 to be one also as seen in the one dimensional spin decoupling experiments shown in Fig. 3.4(c) and Fig. 3.8(c), when it collapses to a doublet. The C2 of Trp B was so assigned by default in that all the other singlets in the spectrum were accounted for, as will be seen. However, in the presence of 6 aminohexanoic acid it was possible to assign it in the same manner as the C2 assignment of Trp A was made above (see section 4.4) and it also has a very similar pH dependence as shown by a tryptophan C2 proton in the spectrum of bovine prothrombin fragment 2 (see sections 4.2 and 6.2). Indeed, it will be seen that the resonances of Trps A and B in kringle 4 are very similar to those of the two tryptophans in fragment 2 and the latter only contains the two tryptophans conserved in all the kringle sequences shown in Appendix I - tryptophans 25 and 61 clustered around the second disulphide bridge. Thus, this gives the second stage assignment of Trp C to tryptophan 71 in the kringle 4 sequence. The C2 of Trp C was assigned by the simultaneous and similar effects of lanthanide ion binding on the chemical shifts of R3 and R22, R4 and R11 (section 4.5).

As much evidence as possible has been presented here that led to the coupling patterns of these three tryptophans being elucidated to be as shown in Fig. 3.9, for they are very remarkable in protein NMR spectroscopy. Table 3.2 quantifies the large secondary shifts experienced, by some of the resonances of Trp A, and indeed, we know of no other protein in which the indole ring resonances of a tryptophan are spread over such a wide range of chemical shift. The C2 proton of Trp B experiences a downfield shift of 0.52 ppm and one of its triplet protons like another of Trp C is shifted upfield by some 2 ppm. The magnitude of these shifts suggests very close proximity of the affected protons to at least one other aromatic ring, and in the case of the upfield shifted triplets this means close approach above or below the plane of the ring because of the geometrical dependence of the secondary shifts induced by aromatic ring

Table 3.2 Chemical Shifts of Trp A in Kringle 4 at 37°C, pH 7.5 Compared with Random Coil Values to give Secondary Shift Values.

	Chemical Shifts - ppm				
	C2	C4	C5	C6	C7
Tryptophan in a tetrapeptide	7.24	7.65	7.17	7.24	7.50
Trp A in kringle 4	7.12	8.22	6.44	4.95	7.43
Secondary shifts on Trp A	-0.12	+0.57	-0.73	-2.29	-0.07

currents (Johnson and Bovey, 1958). It is also very curious that all three tryptophan side chains should have one proton triplet with such a large upfield secondary shift. Further consideration and information on their local environments will emerge in what follows, but we need to pursue the assignment of the other aromatic proton resonances.

3.2.2 Histidines

Histidine side chains give rise to two one proton singlet resonances in the aromatic range of chemical shifts and show marked pH dependences reflecting the imidazole ionisation. Indeed, the pH dependences of the histidine resonances in the spectrum of kringle 4 will be described in section 4.2 and clearly show one side chain to give rise to peaks R10 and R17 with pH dependent shifts consistent with their assignment to the C4 and C2 resonances respectively of the histidine designated His B. This was confirmed by an exchange experiment performed in an attempt to identify the other two C2 proton resonances. Figure 3.10 shows the effect of incubating the protein at 40°C for 90 hours at pH 8.6. Resonance R17 has diminished considerably owing to exchange with deuterium atoms. However, no other singlet resonance has markedly lost intensity even though both

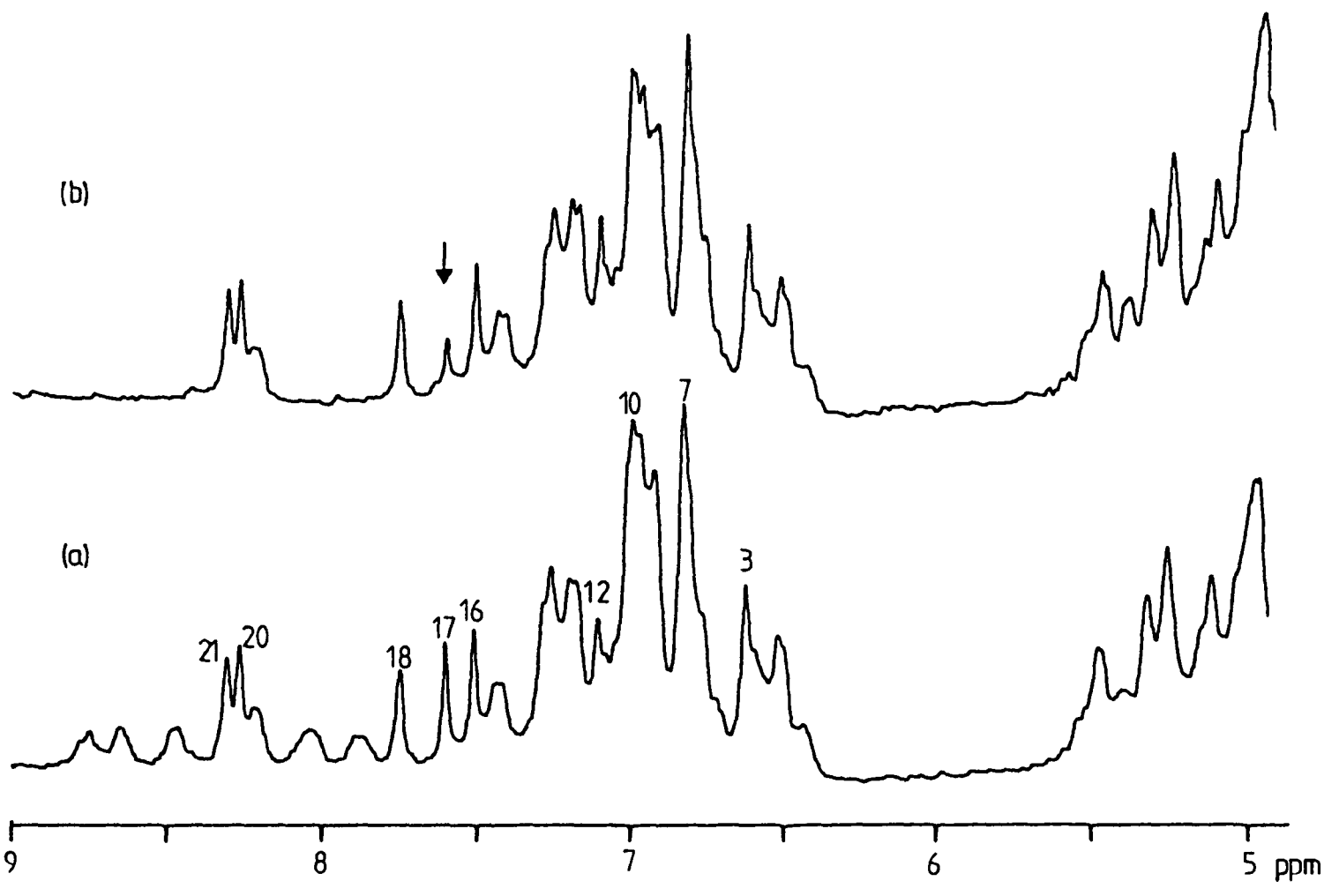

Fig. 3.10 Aromatic region of the spectrum, 37°C, pH 8.6
(a) immediately on dissolving the protein in D_2O
(b) after 90 hours at 40°C.

theory and experiment predict the rate of exchange to be near a maximum at pH 8 and above (Vaughan et al. 1970; Taylor, 1982). Thus, we note that the C2 protons of the other two histidines are very resistent under these somewhat gentle conditions to exchange for deuterium atoms indicative of either a solvent restricted environment or close proximity to an unfavourable electrostatic environment or both. Consequently, two sets of histidine resonances need to be assigned.

Histidine ring resonances are normally referred to and behave as singlets - the C2, C4 coupling constant being too small to be readily detected. However, a COSY experiment with an additional delay selects for smaller coupling constants (King and Wright, 1982) and such an experiment

was performed on a kringle sample in the presence of the ligand AMBOC and is shown in Fig. 3.11. The effect on the singlet chemical shifts of adding the ligand is shown in Fig. 4.24 and they are labelled in Fig. 3.11. It can be seen clearly that there is a cross peak between R20 and R7 and probably between R21 and R16. This is confirmed in Fig. 3.12 which shows the relevant cross sections and also demonstrates a cross peak beween R17 and R10 despite R17 being more than 50% deuterated as a result of the high temperature of the experiment. In actual fact close inspection of Fig. 3.7 shows all these cross peaks are present in an ordinary COSY experiment with no additional delay. Thus, these cross peaks between "singlet" resonances conclusively assign the three histidine side chain protons to be as shown in Fig. 3.13. It is clear that the three histidine side chains are in very

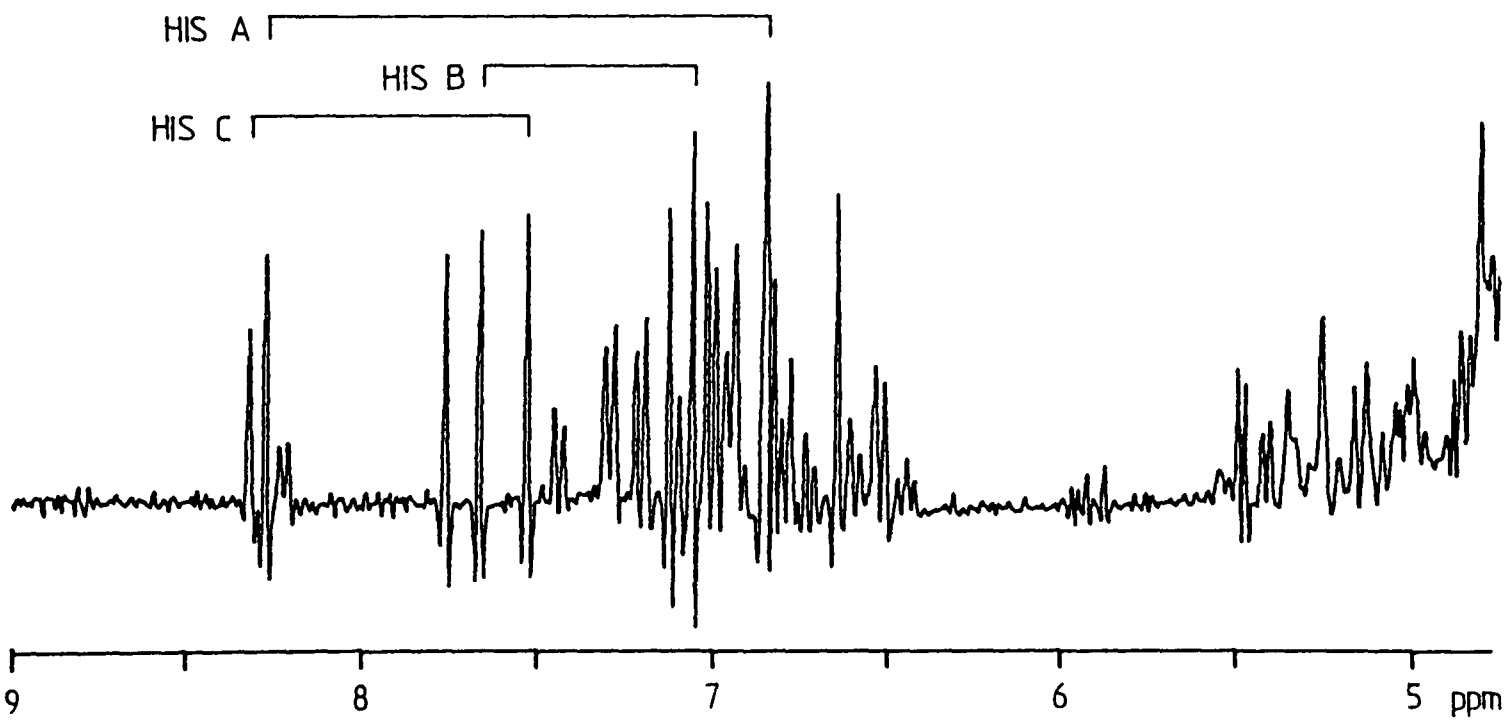

Fig. 3.13 Summary of the aromatic resonance assignments of the three histidine residues of kringle 4.

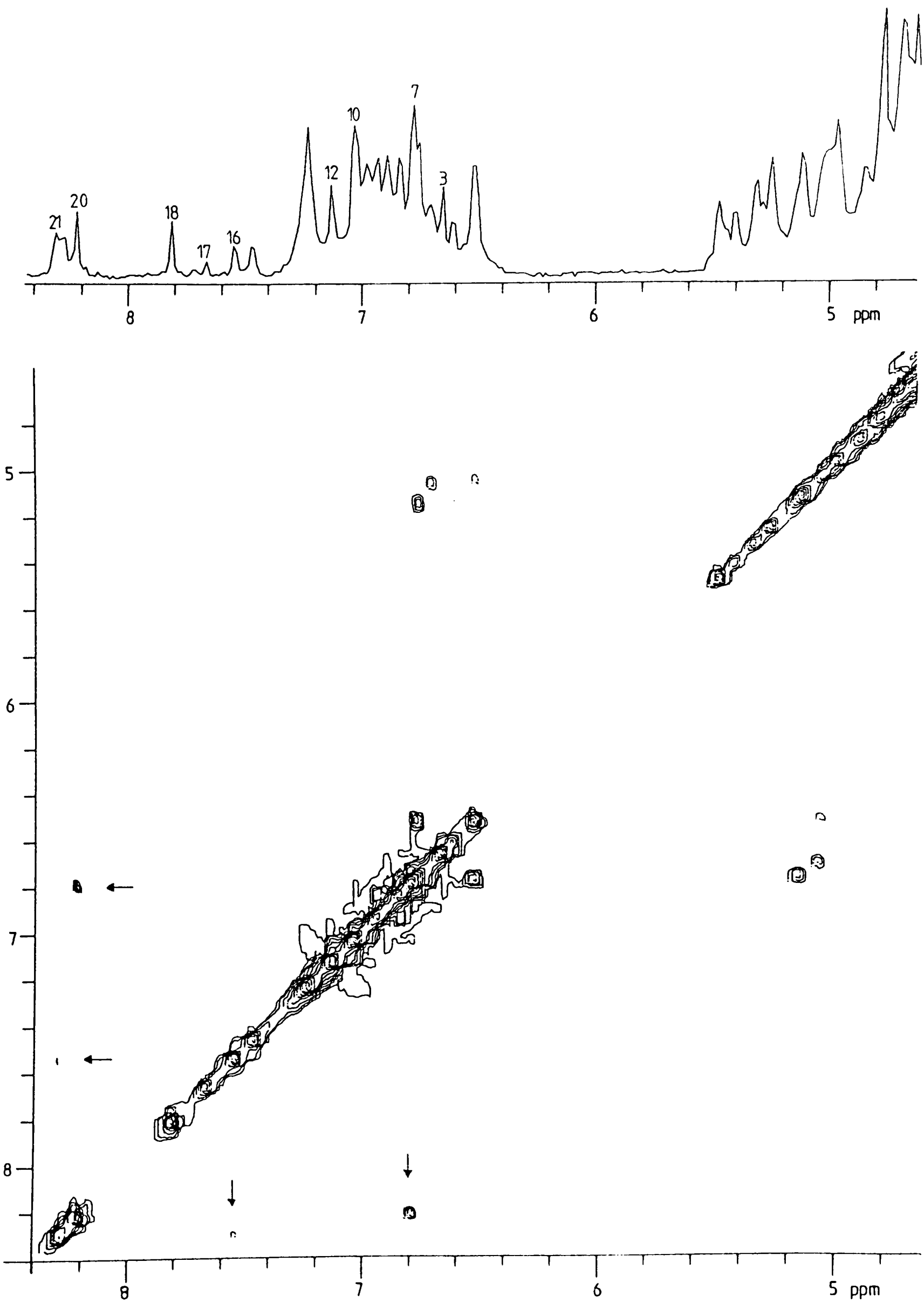

Fig. 3.11 Aromatic region of the 470 MHz COSY experiment using an additional delay of 50msecs; 57°C, pH 7.8. The sample contained the ligand AMBOC.

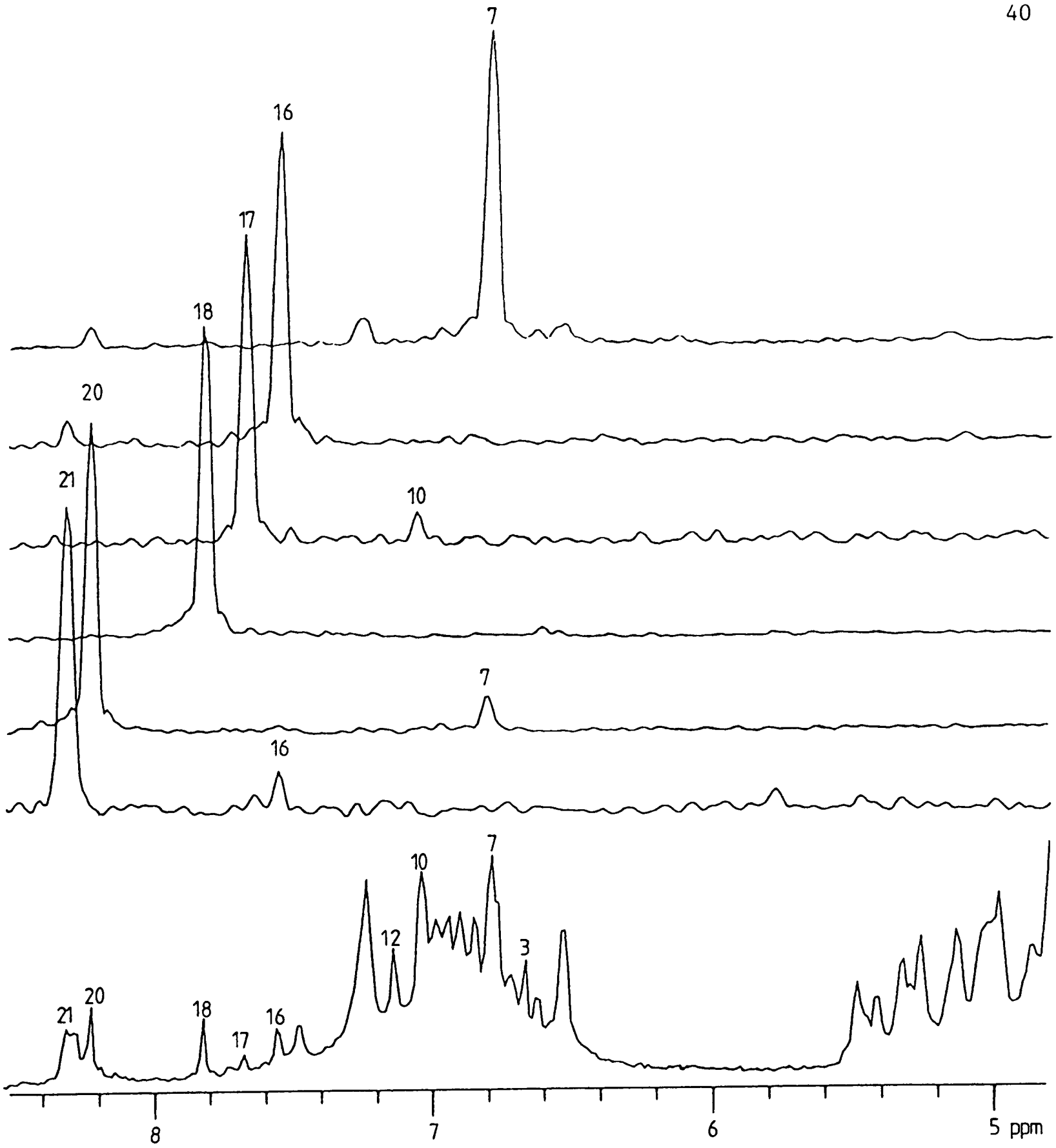

Fig. 3.12 Cross sections taken from the COSY experiment data that gave the contour plot of Fig. 3.11. The largest peak in each cross section represents the intensity along the diagonal in the latter figure.

different environments. Only the resonance positions of His B are similar to those expected of a side chain freely accessible to the solvent at the same pH, but further discussion will be delayed until the pH dependences of the resonances have been detailed in section 4.2. It can also be seen in Fig. 3.11 by comparison with Fig. 4.25 that with the additional delay the triplet-triplet cross peaks of the tryptophans are enhanced and the double-triplet cross peaks diminished.

3.2.3 Tyrosines

Tyrosine aromatic rings that are free to rotate about the Cβ-Cγ axis give rise to two 2 proton doublets in the spectrum. Figure 3.14(a) shows the assignment of four of the five tyrosines of kringle 4. Figures 3.14(b)-(e) are NOE difference spectra using a 0.5 sec irradiation pulse that only strongly enhances intra-residue near protons, and thus irradiating a phenylalanine resonance usually results in two peaks appearing in the difference spectrum unless there is a fortuitous coincidence of chemical shifts. The assignments shown in Fig. 3.14 were confirmed by one dimensional decoupling and indeed cross peaks can be seen in Fig. 3.7 between these four pairs of resonances. The even multiplet selection spectrum of Fig. 3.3(c) is consistent with the positions of the two proton intensity peaks but the most reliable data for tyrosine assignment is provided by a pH dependence of the resonances with pKa around 10.2 This will be considered in section 4.2 and data from other sections will also confirm these assignments. However, the resonances from one tyrosine remain elusive.

3.2.4 Phenylalanine

Kringle 4 contains only one phenylalanine but the complete assignment of its aromatic protons so far eludes us. Table 3.1 indicates that only phenylalanine and tryptophan residues give rise to triplet resonances

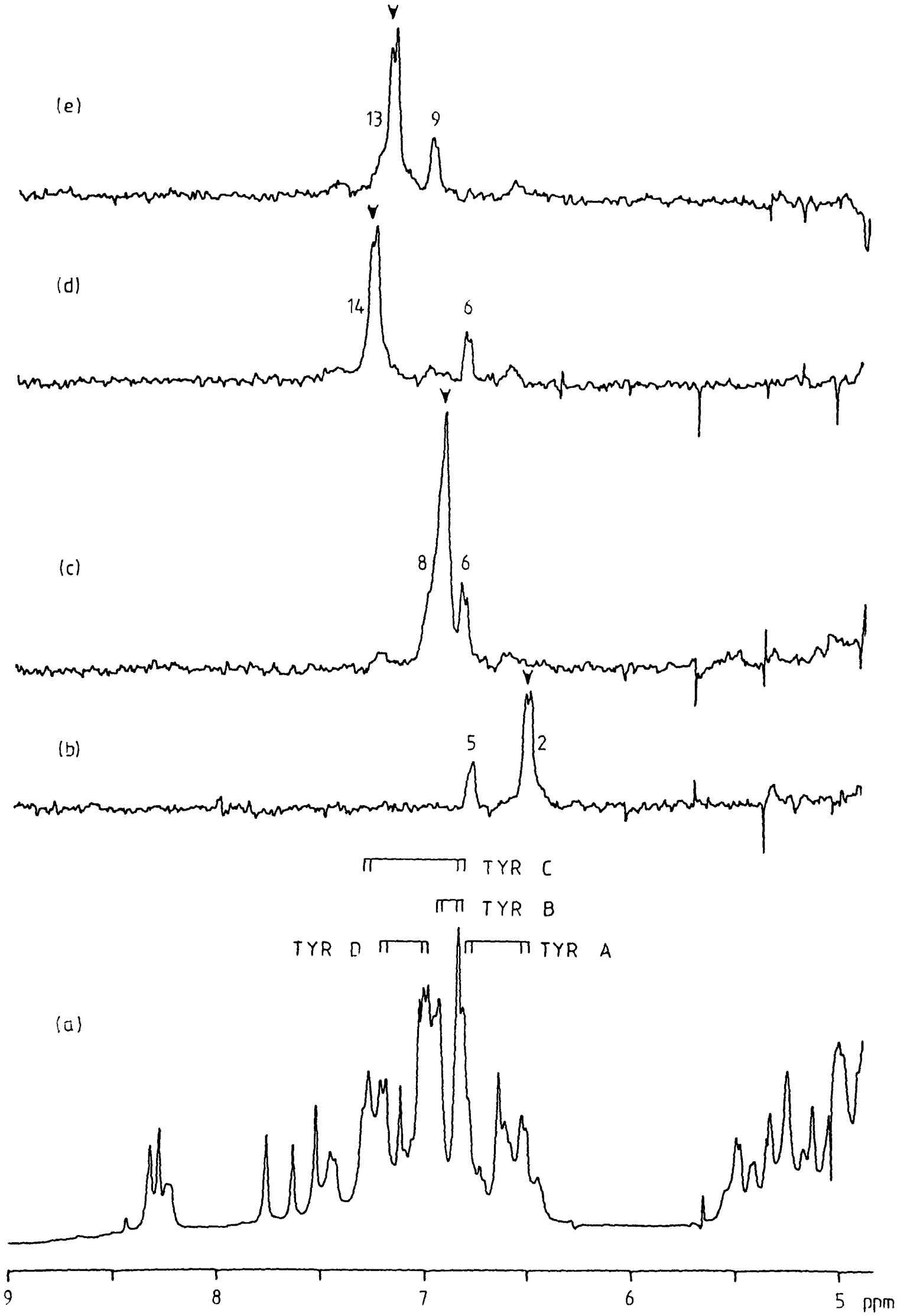

Fig. 3.14 27°C, pH 7.5 (a) Summary of the assigned tyrosine resonances. (b) - (e) NOE difference spectra from 0.5 sec pre-irradiation of selected tyrosine resonances.

in the aromatic region of the spectrum and all the tryptophan triplets have been assigned. However, Fig. 3.15 shows a 470 MHz spectrum in which an additional one proton triplet resonance appears at 7.25 ppm. and must therefore arise from Phe 63. If the ring is free to rotate then this

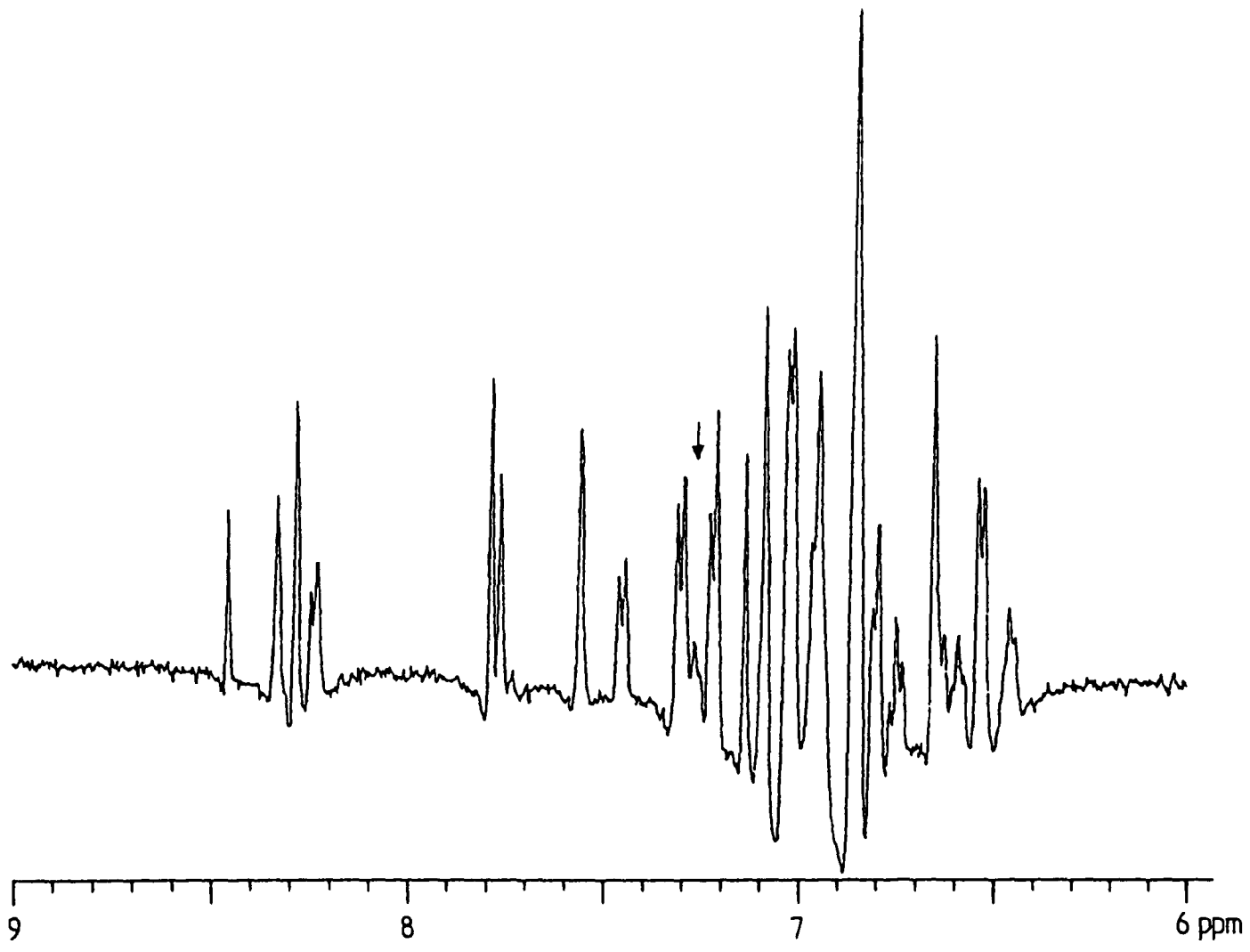

Fig. 3.15 Aromatic region of the 470 MHz spectrum of kringle 4, 37°C, pH 7.2.

resonance would be from the para proton and NOE and spin decoupling experiments would be expected to reveal a two proton triplet resonance from the meta protons. However, this has not been detected. Alternatively, if the aromatic ring is not free to rotate then three one proton triplets and two one proton doublets would be expected in the spectrum.

However, this possible coupling scheme is more difficult to demonstrate and has not been achieved so far. In order to define the aromatic region of the spectrum more clearly a simulated spectrum was produced.

3.2.5 Spectral Simulation

Figure 3.16(b) shows the simulated spectrum produced using the data in Appendix II and comprising all the histidine, tryptophan and four tyrosine aromatic resonances and can be compared with the real spectrum in Fig. 3.16(a). The two spectra are seen to be remarkably similar despite

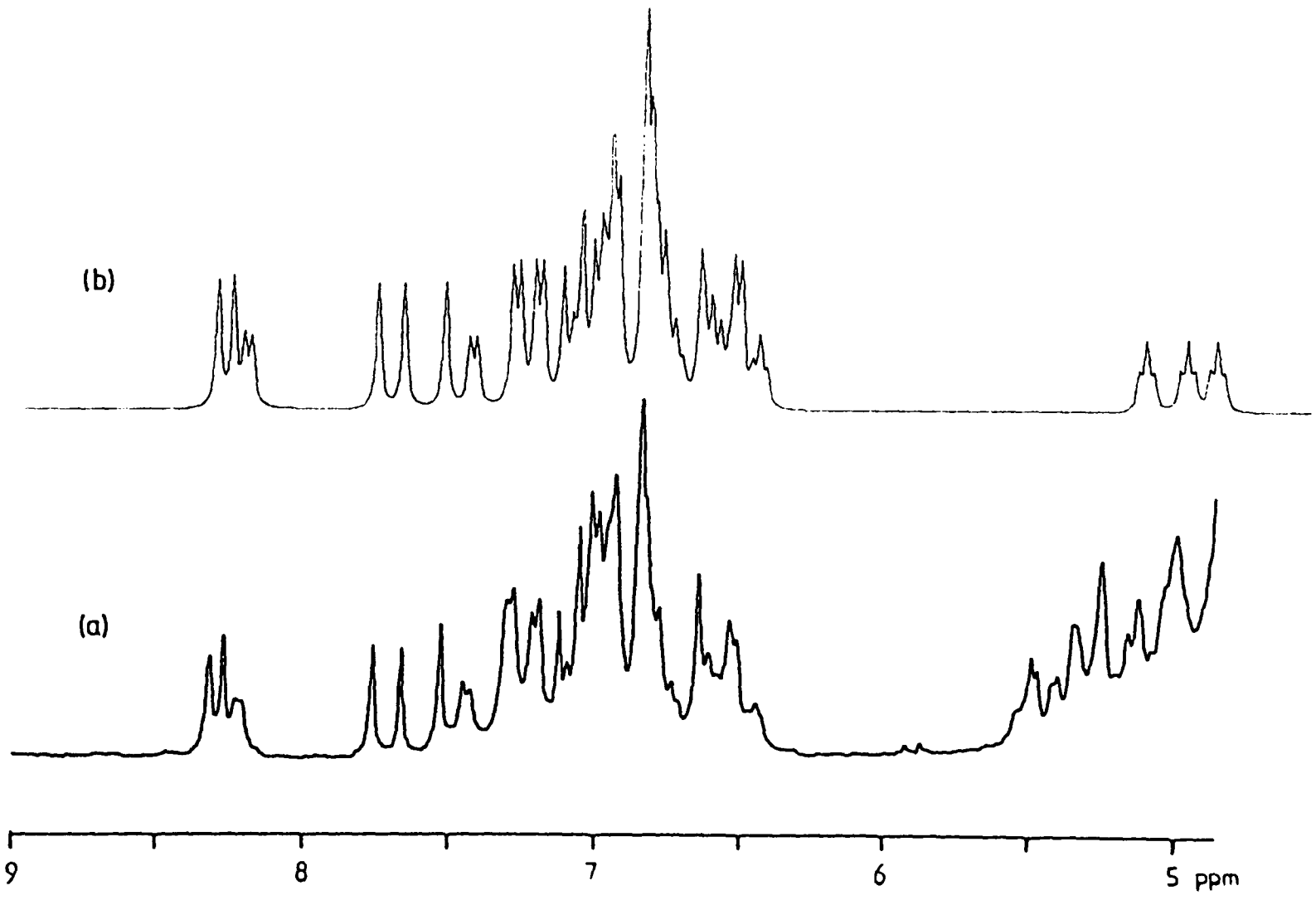

Fig. 3.16 (a) The real spectrum 37°C, pH 7.5 (b) Computer simulation of the aromatic region of the spectrum of kringle 4 (see text).

the fact that only 34 protons are present in the simulation between 6 and 9 ppm whereas an extra nine protons from the unidentified tyrosine and

phenylalanine side chain resonances should be present in this region of the real spectrum. The most obvious difference in intensity between the real and simulated spectrum is seen around 7.0 ppm which could account for two protons but the remaining seven proton intensity is not obvious and it would seem unlikely that any more two proton resonances could be present but unaccounted for. A possible explanation for the lack of intensity is that the aromatic ring does not freely rotate but rather the motion is such that the resonances are exchanged broadened and so not seen in the spectrum. This phenomenon is well recognised, there being a tyrosine and a phenylalanine in bovine colostrum trypsin inhibitor (a glycoprotein of 64 residues and 3 disulphide bridges) exhibiting just these characteristics in its NMR spectrum and indeed some resonances are never clearly resolved under a wide range of temperatures and solution conditions (Wagner et al., 1978). This problem of the missing assignments will be raised in other sections. However, we now move on to consider the aliphatic region of NMR spectrum of kringle 4.

3.3 Aliphatic Region of the Spectrum

Figure 3.17 gives the complete sequence of the kringle 4 containing fragment of human plasminogen and Table 3.3 gives the amino acid compositions. Figure 3.18 shows the aliphatic region of the NMR spectrum and Fig. 3.18(c) is the multiplet selection spectrum with the odd multiplets above the baseline, and the even ones below. (The spectrum exhibits two common impurities that give rise to sharp peaks at 0.24 ppm, presumed to arise from silicon grease, and a small amount of acetate at 1.9 ppm. The other small peak at 0.05 ppm is also due to an impurity from its variable occurrence. The origin of the small "bumps" that are often seen between 0 and -1 ppm is completely unknown). As with the aromatic region the resonances are somewhat arbitrarily numbered and will be

Fig. 3.17 Primary structure of kringle 4 of human plasminogen. (Sottrup-Jensen et al., 1978)

Table 3.3 Amino Acid Composition of the Kringle 4 containing Fragment of Human Plasminogen.

Ala 3	Glu 3	Phe 1	Val 3
Arg 4	Gly 7	Pro 6	
Asn 5	His 3	Ser 9	
Asp 5	Leu 2	Thr 11	
Cys 6	Lys 6	Trp 3	
Gln 4	Met 2	Tyr 5	

Total Number of Residues is 88.

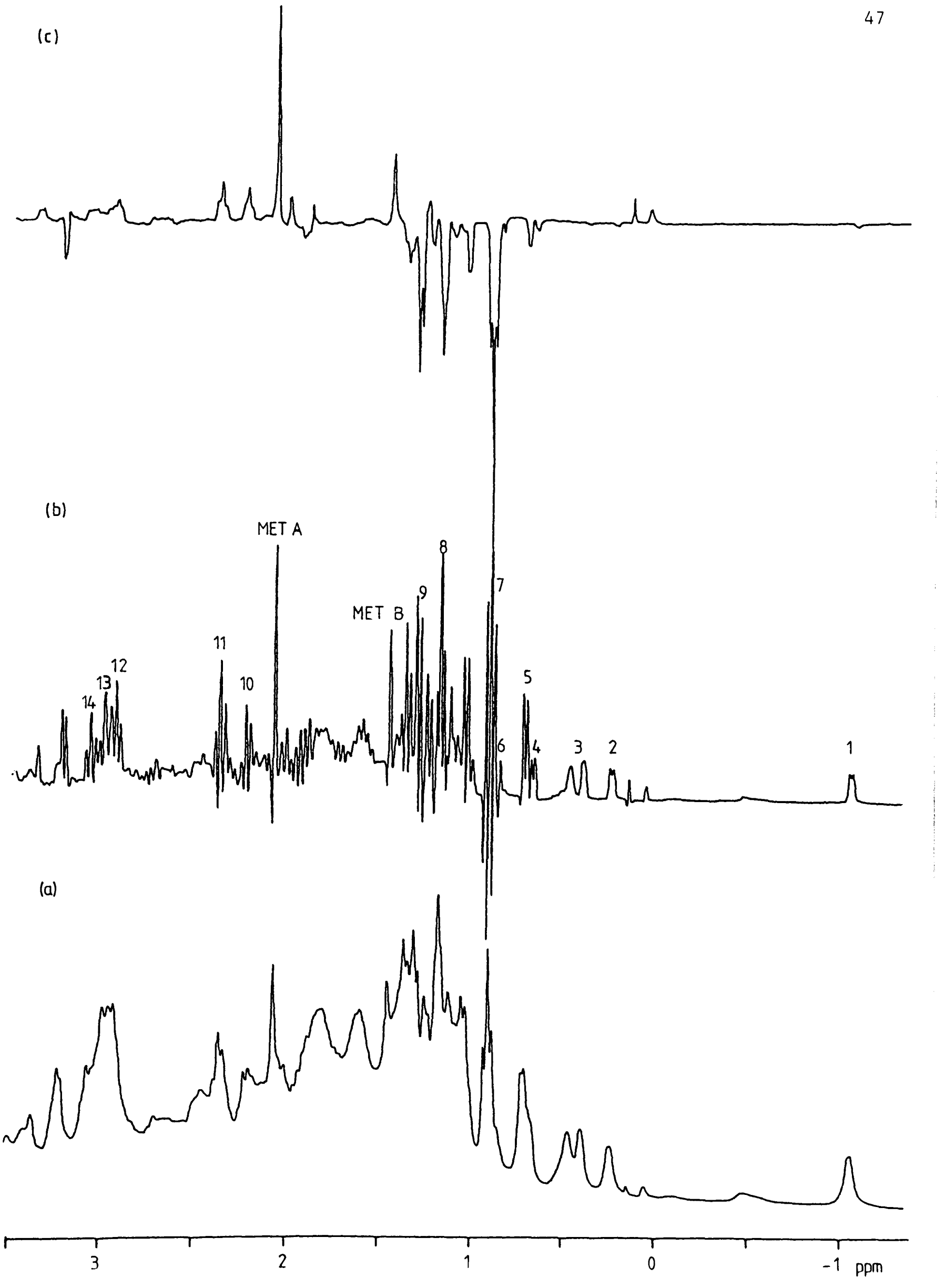

Fig. 3.18 Aliphatic region of the spectrum of kringle 4 at 47°C, pH 8.8. (a) Normal spectrum (b) Resolution enhanced (c) Multiplet selection spectrum.

referred to by the prefix "L" for aliphatic. Obviously, by comparison of the relative intensity of the two regions of the complete spectrum shown in Fig. 3.1 there are many more resonances producing a complex envelope in the aliphatic region of the spectrum and considerably fewer isolated resonances than in the aromatic part. However, it is also clear that the spectrum is far from a superposition of resonances of the amino acid composition at their random coil values (see sections 3.6 and 4.2), and the resonances well shifted to 0.7 ppm and further upfield, especially need to be assigned as they are highly indicative of a defined tertiary fold (see section 3.1).

3.3.1 Extra-kringle Residues

It is noticeable in the normal spectrum of Fig. 3.18(a) that there are some resonances of narrower linewidth than the majority, and in particular L7, L8 and L9 which perhaps more convincingly are seen to be especially intense compared to the rest of the spectrum in the multiplet selection spectrum. The linewidths of the majority of resonances are determined by the overall tumbling time of the molecule in solution and are all therefore fairly similar. However, residues near to the N and C termini are capable of further types of motion not being as constrained as residues in the bulk of the protein and this results in their narrower linewidths, and increased intensity in the multiplet selection spectrum.

Thus, the pH dependence (section 4.2) and chemical shift of the peaks at L7 assign them to the six protons of the two methyl groups of the N terminal valine. Similarly, the sharp doublet in Fig. 3.18(c) numbered as L9 at 1.31 ppm is taken to be the methyl group of alanine 84. This is only very slightly shifted upfield from the random coil position of an alanine (1.39 ppm) that would be expected for this residue so close to the C terminus. But as pointed out in section 2.1 the samples of kringle 4

used in this study are not homogeneous at the C terminus and are a mixture of Ala 84 and Val 86 as C termini. Indeed, as mentioned in section 4.2 the resonance L9 is seen to titrate at pH below 4 as would be expected of a C-terminal carboxyl containing residue. Likewise resonances at L6, seen more clearly at lower pH's when the N terminal valine methyl peaks are further downfield, are very sharp and also titrate below pH 4 and are assigned to the lesser amount, in the sample of Fig. 3.18, of valine 86 (C terminal) methyl proton resonances. Other resonances are not so readily assigned to the remaining extra kringle side chains, although it is tempting to consider L8, a prominent even multiplet in Fig. 3.18(c), as arising from the methyl protons of Thr 82. However, the chemical shift is not precisely the same as that for the random coil side chain and we have no other evidence to make this assignment. The possibilities for Glu 83 will be considered below.

3.3.2 Methionines

Methionine methyl proton resonances are readily assigned from the multiplet selection spectrum since they give rise to the only singlets in the methyl proton region. Thus, two methionines A and B are labelled in Fig. 3.18(b). We note that Met A at 2.07 ppm is close to the random coil chemical shift for this resonance but that Met B at 1.44 ppm is far from this position, although this does not allow us, as yet, to make a second stage assignment of Met 28 or Met 47 in the sequence.

3.3.3 Leucines

Irradiation of either of the two most upfield shifted 3 proton resonances L1 or L2 always produces an Overhauser enhancement of the other. Furthermore, a spin decoupling experiment with the decoupling pulse at 1.05 ppm simultaneously results in both doublets collapsing to singlets. Thus, L1 and L2 arise from the two methyl groups of an isopropyl moiety

of either a leucine or a valine, with the former being more likely from the position of the CH proton resonance, since in a tetrapeptide the CH proton resonates at 1.65 ppm and 2.13 ppm in a leucine and valine side chain respectively. From Fig. 3.19 it can be seen that a three proton resonance at around -1.0 ppm is a conspicuous feature of the NMR spectra of kringles and comparison of the primary sequences of these proteins (Appendix I; Fig. 1.3) reveals that of the leucines and valines, only one leucine is conserved throughout, at position 45, and so the assignment of L1 and L2 is made. We note that the secondary shift on resonance L1 in kringle 4 is some 1.9 ppm upfield and is of a similar order of magnitude to some of the shifts of the tryptophan resonances from random coil positions, as discussed above. This shows that one of the methyl groups of leucine 45 is lying in close proximity to an aromatic ring within the molecule and from the direction of the secondary shift is orientated above or below the ring plane. In addition, from the assignment argument presented above the aromatic side chain leading to this secondary shift must also be conserved in all the sequences of the kringles shown in Fig. 3.19 or at the very least an aromatic side chain of some description must be present at the same position in the sequence - the possibilities for this were considered in section 1.3. Finally, the three dimensional folding of each kringle must be such that the structural element incorporating Leu 45 and the aromatic side chain is fairly precisely conserved. These considerations immediately impose some constraints on possible tertiary folds than could be envisaged for a kringle and will be referred to in succeeding sections.

Two other three proton doublets are labelled together as L3 in Fig. 3.18(b) where the resonances are seen to be somewhat less well resolved as doublets, compared to L1 and L2 for instance. However, their identical temperature dependence (section 3.6) indicates that these two resonances arise from the same side chain and are again assigned to the

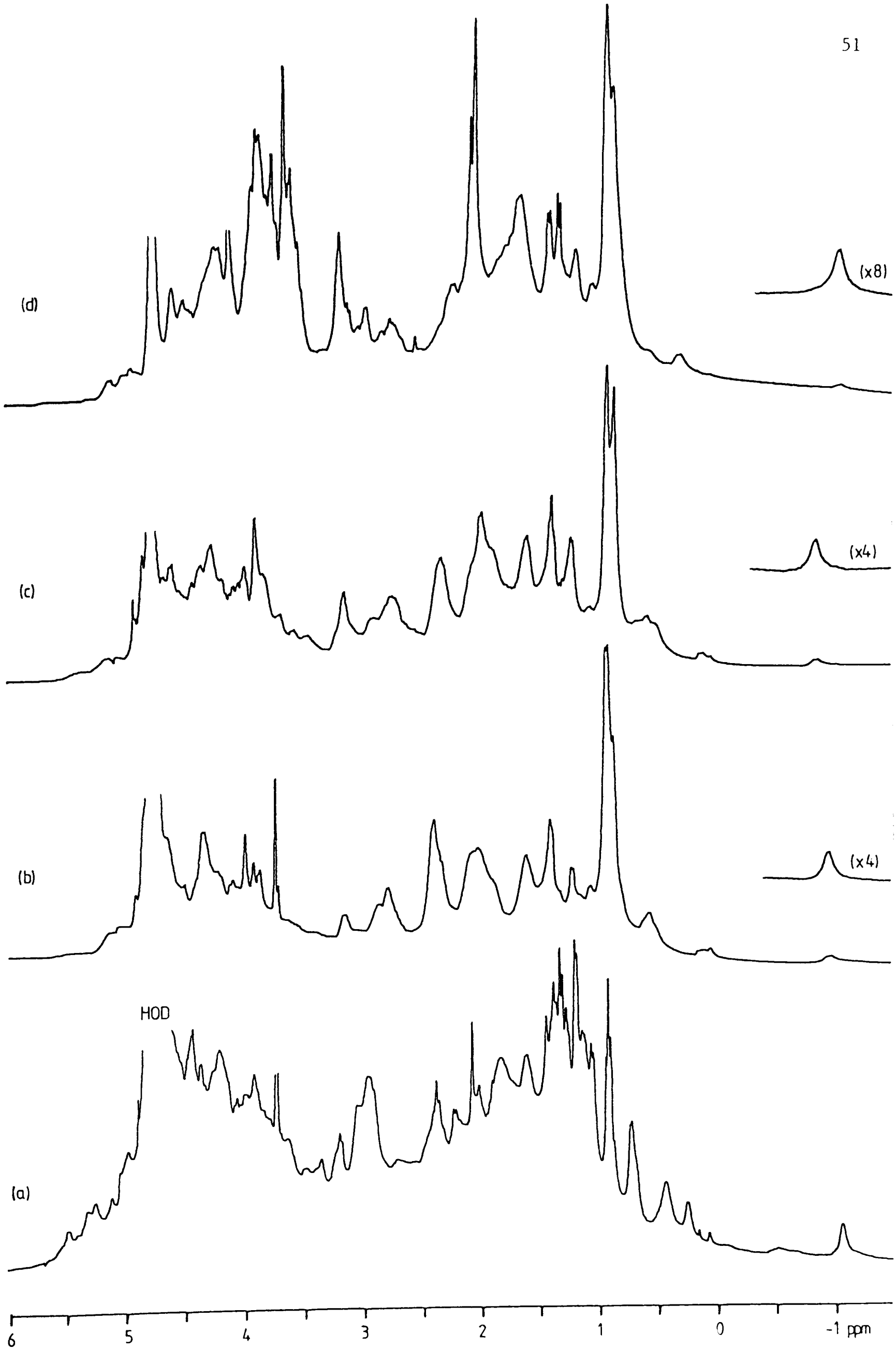

Fig.3.19 Comparisons of the aliphatic regions of the spectra of four kringle containing proteins (a) Human plasminogen kringle 4 (b) Human prothrombin fragment 2 (c) Bovine prothrombin fragment 2 (d) Bovine prothrombin fragment 1.

isopropyl methyl protons of a leucine or valine. Nuclear Overhauser enhancements and sections from COSY experiments strongly indicate that the CH proton to which they are coupled resonates at 1.45 ppm and, as above, this again favours their assignment to a leucine side chain. Since kringle 4 contains only two leucine residues we can make the second stage assignment of the peaks at L3 to the methyl protons of Leu 76. Further, independent evidence to support this will be presented in later sections. We note that the resonances have secondary shifts of about 0.45 ppm upfield.

3.3.4 Valines

The resonance L5 has been seen from many experiments to be composed of two three proton doublets that are coincident under the conditions in which the spectrum of Fig. 3.18(a) was obtained. One of the doublets is decoupled by irradiating at 4.22 ppm, while irradiation at 1.79 ppm resulted in both the other doublet at L5 and the three proton doublet labelled L4, simultaneously collapsing to singlets. Indeed, other results have confirmed the presence of two three proton doublets with very similar behaviour - see section 4.5 for example - and so are assigned to a third isopropyl gouping which must be that of a valine, since both leucines in the sequence have been accounted for above. This assignment is also in agreement with the position of the βCH resonance when compared to the random coil position, bearing in mind, as in the previous section, that the methyl proton resonances are shifted upfield from their random coil chemical shifts. The kringle 4 fragment contains three valine residues, two of which are the N and C termini assigned above, and so the two resonances at L4 and L5 are assigned to the methyl protons of valine 69. The secondary shift on these peaks is only about 0.2 ppm.

3.3.5 Threonines

The kringle 4 fragment contains eleven threonine residues, the methyl group of which has a chemical shift of 1.23 ppm in a tetrapeptide. Resonance L8, while of sizeable intensity cannot account for thirty three protons. It was suggested above that the single threonine outside the disulphide linked region at the C terminal end contributed to L8, but it is clear that the majority of the threonine methyl protons are not in equivalent environments. Obviously this poses considerable problems in assignment.

Figure 3.20 shows the aliphatic region of the COSY experiment of which the aromatic region was shown in Fig.3.7. As expected the contour plot is considerably more complicated. However, at least ten cross peaks can be discerned in the group between 1.0 and 1.4 ppm on one axis and from 3.5 to 4.5 ppm on the other. Random coil chemical shifts (Bundi and Wüthrich, 1979) are given:

Threonine	αCH 4.34	βCH 4.2	γCH_3 1.23
Alanine	αCH 4.35	βCH_3 1.39	

Thus, the group of cross peaks referred to above will also contain alanine α-β connectivities as well as threonine β-γ and so to differentiate the two requires a threonine α-β connecting cross peak to be demonstrated. However, as can be appreciated these latter cross peaks being so close to the diagonal would not be easily detected in a simple COSY experiment. Two strong cross peaks are seen between 3.9 and 4.3 ppm on one axis and 5.4 to 5.5 ppm on the other and these could arise from threonine α-β couplings where the αCH proton resonance has been downfield shifted through incorporation in a β-structural element for instance (section 3.1), but other residues such as serine could also give rise to the same resonances. Thus, the problem now arises - of matching the putative β proton resonance suggested by the α-β cross peak with that of one

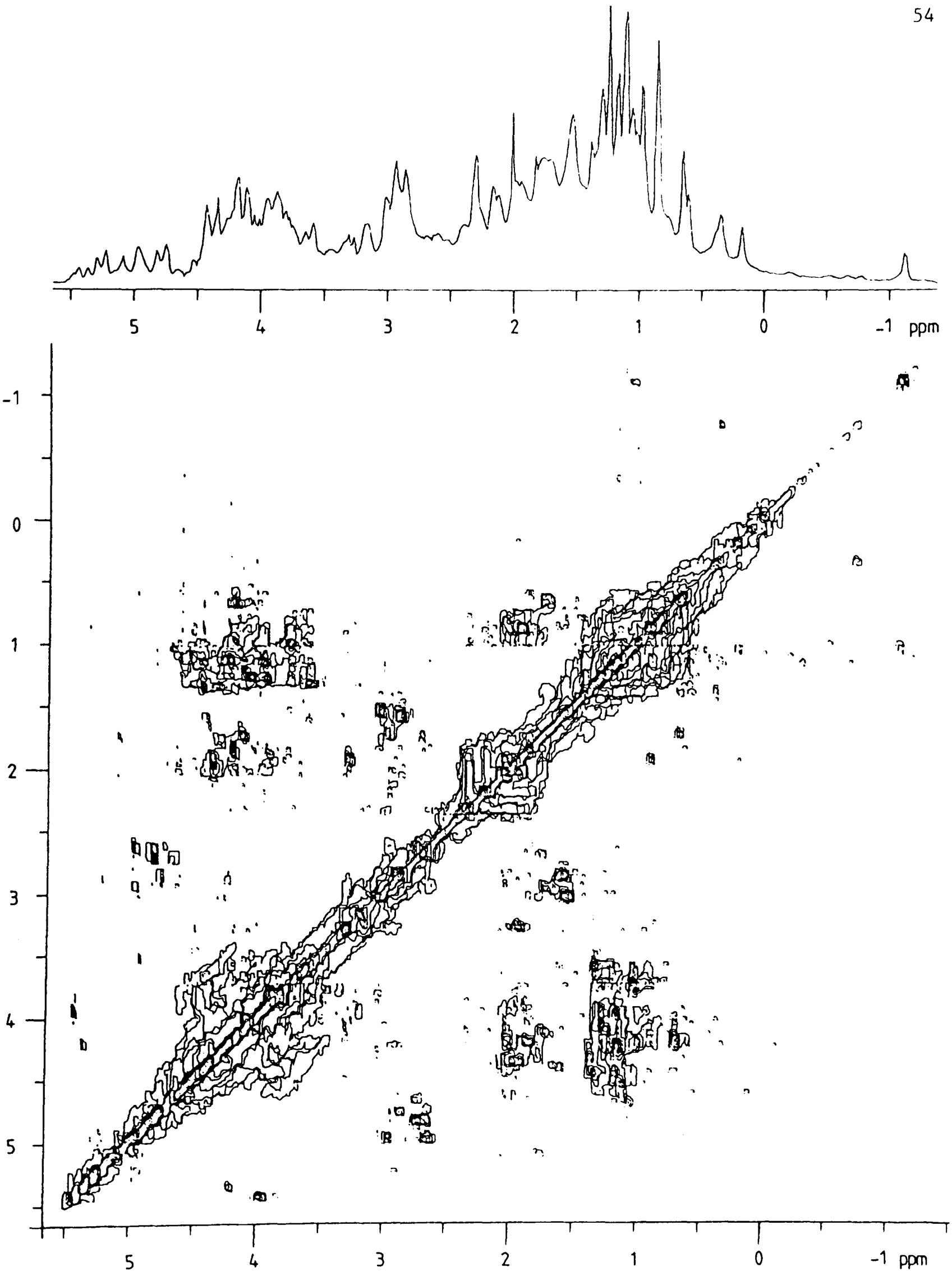

Fig. 3.20 Aliphatic region of the 470MHz COSY experiment; 37°C, pH 8.3.

indicated by the β-γ cross peak and avoiding fortuitous coincidence of resonance positions in a very crowded region of the spectrum. This is especially difficult even using cross sections from a COSY experiment because of poor digital resolution and the possibility that the coincidence of chemical shifts of the β proton(s) is exact. The results of an experiment to resolve this problem in one case is shown in Fig. 3.21 showing NOE difference spectra irradiating at the αCH position and simultaneous J decoupling. The "blank" reveals the putative β resonance to have the multiplet structure expected for a threonine side chain conformation resulting in similar α-β and β-γ coupling constants. The coupling pattern is confirmed be decoupling the methyl proton resonance leading to a reasonable doublet at the β proton in Fig. 3.21(b) and a quartet on decoupling the α proton in (c). Thus, the complete pattern of a threonine residue is assigned but the experiments are time consuming, and results as convincing as those shown in Fig. 3.21 rarely achieved. Furthermore, the most useful aspect of the above is the assignment of the α proton at an unusual chemical shift rather than the methyl and β proton resonances which are not clearly resolved in the complete spectrum and would require a similar treatment to be demonstrated each time under a new set of solution conditions. Similar consideration and worse apply to the remaining threonine side chain resonances and they will not be discussed further.

3.3.6 Alanines

As mentioned in the previous section COSY spectra alone cannot be used to assign resonances from alanine residues because of confusion with peaks from threonines. Kringle 4 contains three alanine residues and the C terminal one has been assigned in section 3.3.1. It would be extremely useful to assign the other two in the sequence but if the methyl protons resonate between 1.0 and 1.4 ppm then similar problems arise as mentioned

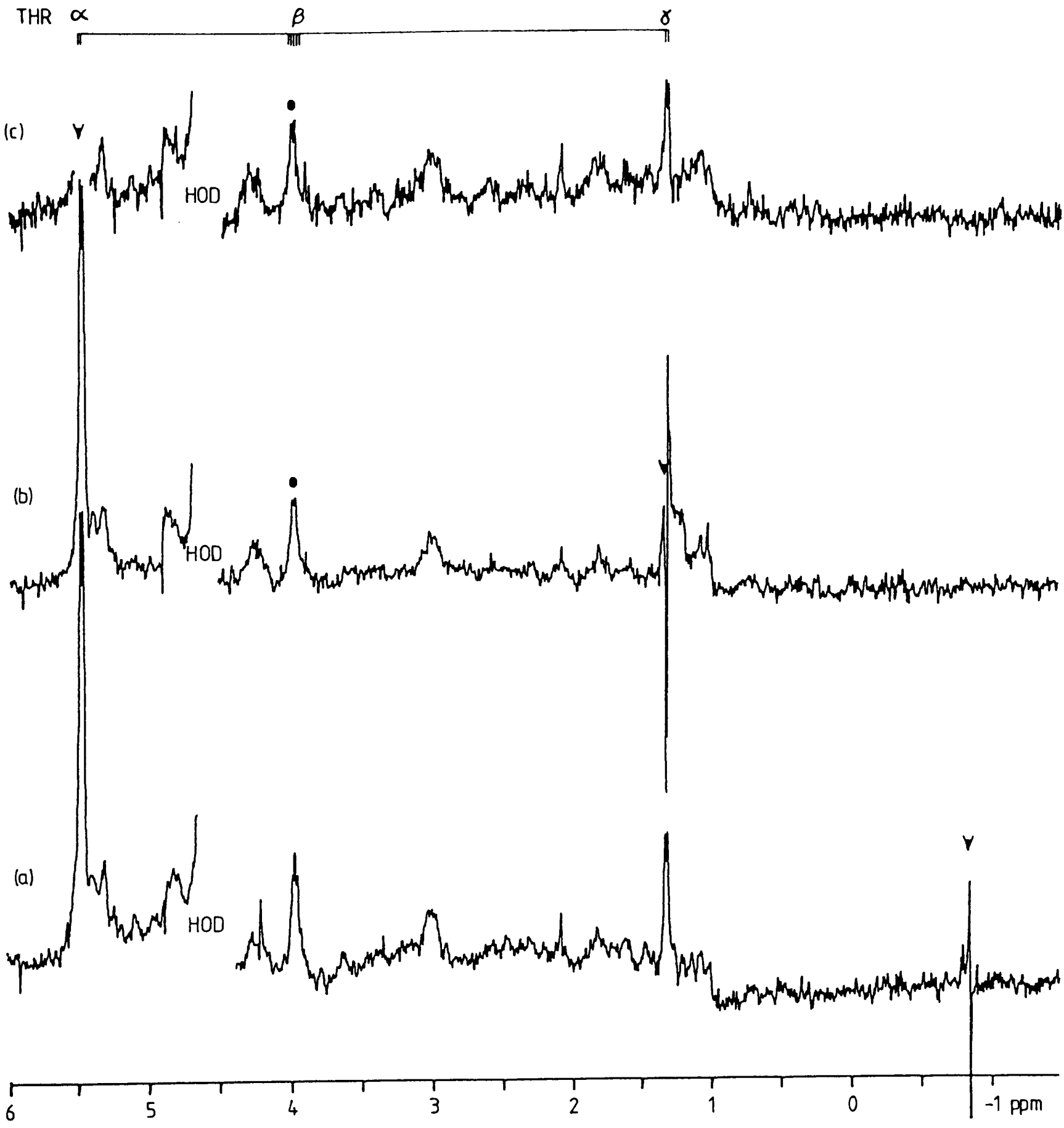

Fig. 3.21 NOE difference spectra with the presaturation pulse at 5.47ppm (resonance A2 in Fig. 3.3(d)); 47°C, pH8.8. Simultaneous spin decoupling pulse at (a) -0.8ppm to serve as a control (b) 1.31ppm (c) 5.47ppm.

above, in trying to follow the peaks under differing solution conditions. However, the additional three proton doublet at L5 is eminently discernable in the majority of spectra. Figure 3.22 shows the results of NOE difference spectra irradiating L5 with simultaneous spin decoupling, on a sample containing the ligand AMBOC. (The presence of the ligand makes a negligble difference to the results). Comparison of the blank (a) and the decoupling pulse at L5, (b) shows the collapse of a quartet to a singlet completely in accord with an alanine coupling pattern. For completeness a strong doublet is also seen in the difference spectrum centered at 4.17 ppm with a coupling constant of about 11 Hz. Figure 3.22(c) shows that a spin decoupling pulse at 1.79 ppm simultaneously collapses the doublet to a singlet and the two doublets at L4 and L5 to singlets confirming the coupling pattern discussed above in the assignment of valine 69 and showing the doublet at 4.17 ppm to be from the α proton of this residue.

However, returning to the tentative assignment of an alanine coupling pattern there remains a further problem; it has been found that some threonine α-β coupling constants are sufficiently small so as not to be seen in ordinary spectra with the α proton behaving as a singlet and the β proton apparently only coupled to the methyl proton resonance (Delepierre et al., 1982; Williams, 1983). The upshot of this is that the results shown in Fig. 3.22, while certainly suggestive of an alanine coupling pattern, do not prove this irrefutably. The αCH proton of a threonine is usually seen in a NOE difference spectrum on irradiating the methyl resonance but could be absent from the spectrum if it was "underneath" the HOD resonance which necessitates repeating the experiment at another temperature which may not be favourable for an Overhauser enhancement. We do note though, that a strong resonance at 3.37 ppm is also seen in the NOE difference spectrum of Fig. 3.22 and this looks very much like a singlet although it is not clearly seen as such in the multiplet

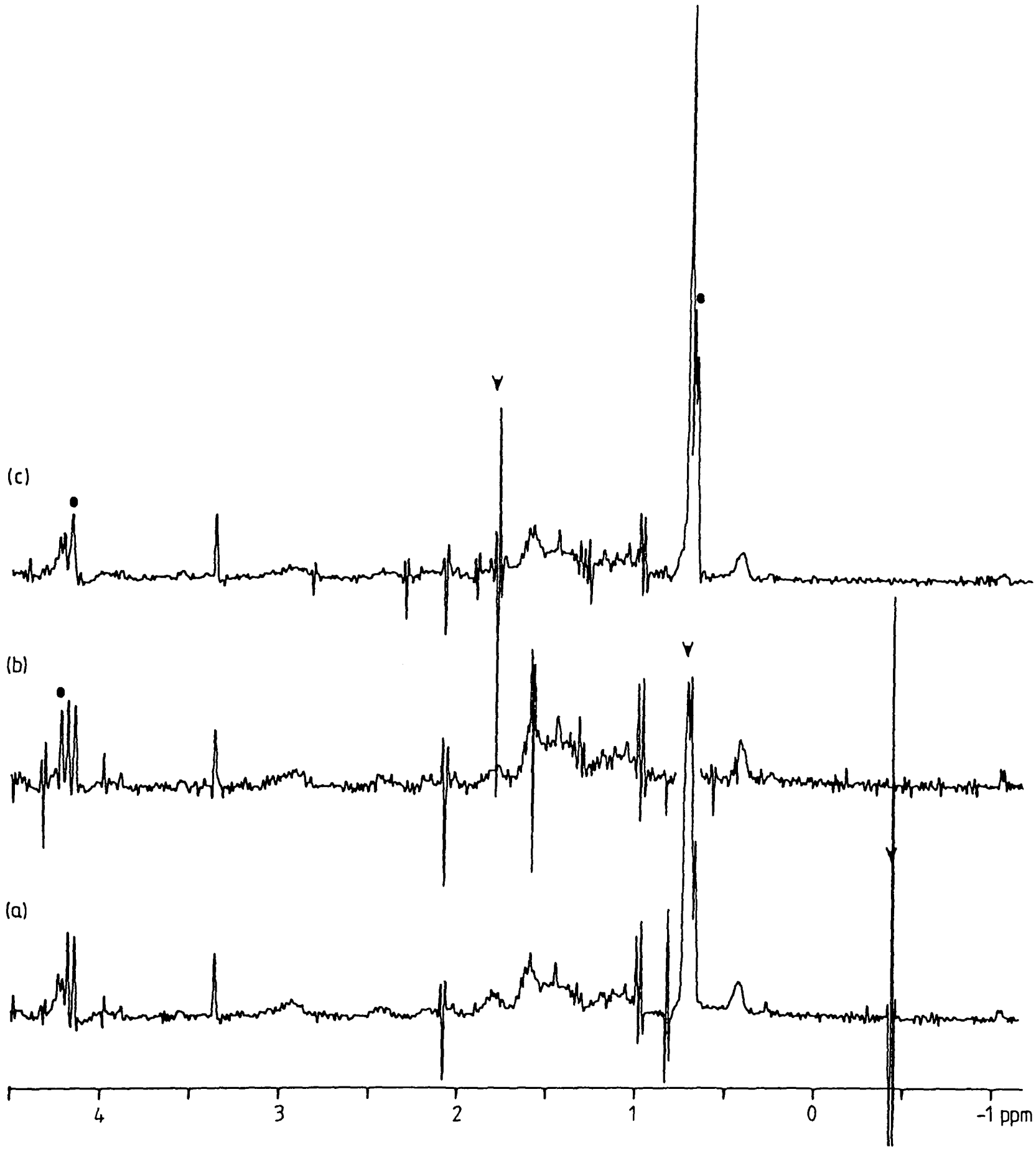

Fig. 3.22 Resolution enhanced NOE difference spectra with the presaturation pulse at 0.70ppm (L5); 37°C, pH 8.5. Simultaneous spin decoupling pulse at (a) 0.45ppm for the blank (b) 0.70ppm, L5 (c) 1.79ppm.

selection spectrum shown in Fig. 3.18(c). The possibility arises then, that it is from the αCH proton of a threonine residue of which L5 comes from the methyl resonance, and where the α-β coupling constant is about 4 Hz or less. If this is the case, then the α proton is shifted about 1 ppm upfield from its random coil, the β proton is unshifted and the secondary shift on L5, assuming it is from threonine methyl protons, is 0.5 ppm upfield. While not impossible, such shifts are certainly remarkable if true. While writing this we have been fortunate to see a preprint from Llinás et al.,(1983). In this paper the authors assign L5 to a threonine methyl resonance, largely through homology arguments as there is a very similar resonance in the NMR spectrum of kringle 1, but no alanines are conserved in the two sequences. The possible threonines in the sequence are at positions 12, 16, 64, 65. Thus, the resonance at L5 may be tentatively assigned to a threonine methyl group rather than an alanine. This resonance will also be discussed in a number of sections to come. The resonances arising clearly from any other alanine residue have not been identified largely for the reasons outlined above.

3.3.7 Glutamates

The γCH_2 protons of glutamate side chians characteristically give rise to 2 proton triplets at around 2.3 ppm, and two such possible resonances can be seen at L10, L11, in Fig. 3.18. Although cross peaks are not clearly seen in Fig. 3.20, one dimensional spin decoupling experiments shows the coupled protons to be at about 2.0 ppm which is consistent with the expected position of glutamate protons. However, glutamine side chains have very similar chemical shifts and a pH dependence study is therefore required to differentiate the two. This will be considered briefly in section 4.2.

3.3.8 Lysines

Lysine εCH_2 protons commonly give rise to two proton triplets around 3.0 ppm. At least three such overlapping multiplets can be seen in Fig. 3.18 as L12, 13, 14, although at the temperature of the multiplet selection experiment they do not show clearly in Fig. 3.18(c). However, three cross peaks are seen from these resonances to peaks at 1.55 to 1.70 ppm in Fig. 3.20 entirely consistent with the expected resonance position of lysine δCH_2 protons. There are six lysines in this protein and from the sequence (Fig. 3.17) one might suggest two pairs to have similar chemical shifts as they are adjacent residues, and indeed the resonances are sufficiently intense at L12, L13 for this to be possible, although, as yet, little effort has been expended in investigating this.

Most of the assignments in the aliphatic region of the spectrum discussed above have been summarised in Fig. 3.23. The rest of this chapter, while not

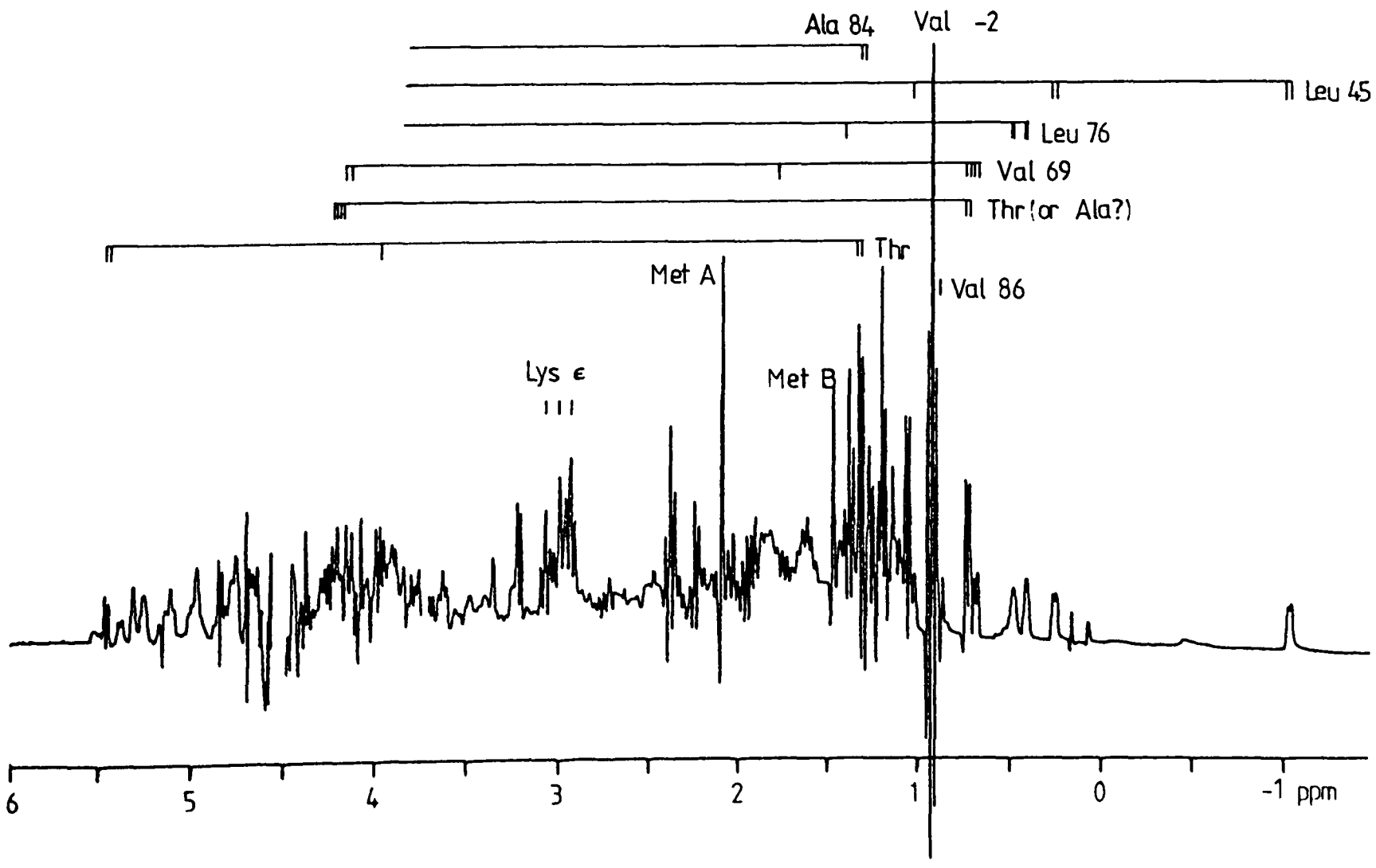

Fig. 3.23 Summary of a number of resonance assignments made in the aliphatic region of the kringle 4 spectrum.

strictly directed to assigning resonances, provides much supportive evidence and is included here because the experiments described do not involve changing the solution conditions of the protein.

3.4 NOE Experiments

The structural implications of the Nuclear Overhauser Enhancements were discussed in section 2.2 and are taken to signify a proximity of the protons involved of about 5Å or less. Very many Nuclear Overhauser experiments have been carried out on kringle 4 samples at various solution temperatures and pH using different spectrometer settings. Some of these are discussed below and we begin with the irradiation of aliphatic resonances.

3.4.1 Aliphatics

Figure 3.24 shows the results of irradiating the upfield methyl resonances, all experiments being carried out under the same conditions. Figure 3.24(b) with the irradiation of L1 shows enhancements in the aromatic region of R12 and R15 both assigned above to Trp A. In support of this, irradiation of the other methyl group protons of Leu 45 at L2 is seen to give enhancements to R12 and R19 in Fig. 3.24 and each show intensity at R9 and R13, indicating proximity to Tyr D. Both Leu 45 and Trp A - one of Trps 25, 61 - are conserved residues in the kringle sequences, and as suggested in section 3.3.3, from the common resonance around -1.0 ppm in the spectra of a number of kringles, Leu 45 must be part of a conserved structural element and this data indicates that Trp A is involved in it also. Similar data for bovine prothrombin fragment 2 (section 6.3) will corroborate this. In the primary sequence Leu 45 and Trp A are seen to be some distance apart being close to the second and third disulphide links respectively, but in three dimensions, these two regions of the molecule must therefore be in close proximity.

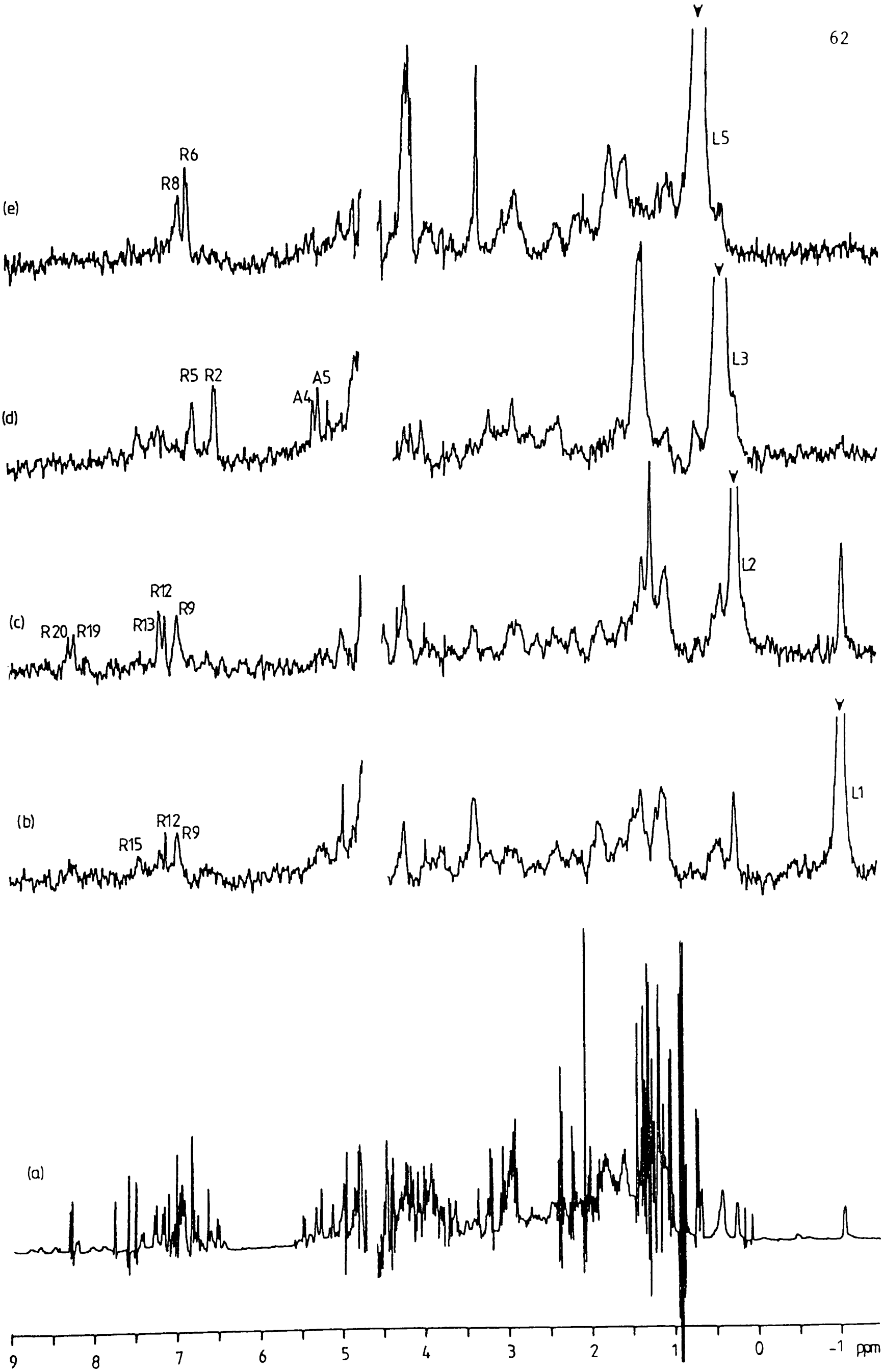

Fig. 3.24 NOE difference spectra from presaturation of upfield shifted methyl proton resonances; 37°C, pH 8.8.

Moving on to the pre-irradiation of L3 assigned to the methyl protons of Leu 76, we see a clear enhancement of the resonances of Tyr A in Fig. 3.24(d), but we have yet to discuss the second stage assignment of Tyr A to a particular tyrosine in the sequence; this will be done in the next chapter. Similarly the resonances of Tyr B are selectively enhanced through pre-irradiation of L5 in Fig. 3.24(e). However, the peak L4 is also within the irradiation pulse width, and indeed, L5 was seen above to be a composite resonance. To try and resolve the resonances involved in the enhancement of those of Tyr B, the pre-irradiation pulse was set precisely on L4 under otherwise the same conditions. The intensity of the Tyr B peaks and the resonances at 4.22 and 3.37 ppm (the former of which and perhaps the latter, are associated with the methyl protons of an alanine or threonine residue with methly proton intensity at L5, see section 3.3.6) were noted to diminish in intensity, while the enhanced peaks at 4.17 and 1.79 ppm assigned to Val 69 were unchanged compared to Fig. 3.24(e) as expected with the methyl protons of Val 69 assigned to L4 and L5. Further experiments included pre-irradiation of the Tyr B resonances at R6 and R8. One of these is shown below in Fig. 3.26(c) and as can be seen the peak at L5 was always clearly enhanced, but any enhancement of L4, if present, was only weak. It must be borne in mind though, that the L5 resonance has a much larger secondary shift than the methyl proton resonances of Val 69 indicating that it is closer to an aromatic ring than the methyl protons of the valine residue and would therefore be expected to give more intense Nuclear Overhauser Enhancements. Nevertheless, all this data strongly suggests that it is the methyl group whose protons resonate at L5 that is in close proximity to Tyr B rather than those of Val 69.

The above problems of interpretation when irradiating overlapping resonances highlights the difficulties encountered in performing such

experiments within the main envelope of aliphatic resonances. However, Fig. 3.25 shows the result of pre-irradiating the two methionine singlet resonances under the same conditions. It is seen that each peak gives an enhancement to the other but further discussion of the aromatic resonance enhancements from these irradiations is continued in the next section.

3.4.2 Aromatics

It is obvious from the wide dispersion of resonances in the aromatic region of the spectrum described above that many of the aromatic rings are in close proximity producing the secondary shifts, and it is desirable to detail these interactions from Nuclear Overhauser Enhancments. However, it was noted in the previous section that unequivocal results of such experiments are only readily obtainable through irradiating individual resonances well separated from others and such as seen in Fig. 3.26(b). This shows that the C2 proton of Trp B (R18) is close in space to the ring of Tyr C (R14, R6) and because of the downfield secondary shift is most likely to be lying in the plane of the Tyr C ring. On the other hand irradiating in a crowded part of the aromatic region such as R6 seen in Fig. 3.26(c) demonstrates the plethora of enhancements obtained. In view of the appreciable bandwidth of the pre-irradiation pulse and the number of overlapping resonances arising from disparate protons it is not possible to immediately extract the required information. Furthermore, it is unsatisfactory to use resolution enhancement as a technique for filtering out weak NOE effects as higher multiplets will be reduced in the process more significantly than the smaller ones, especially singlets. But to try and extract some information, a method was introduced for analysing the data of numerous NOE experiments. We have since noted Braun et al., (1981) to have used a very similar approach but applied to a much smaller system

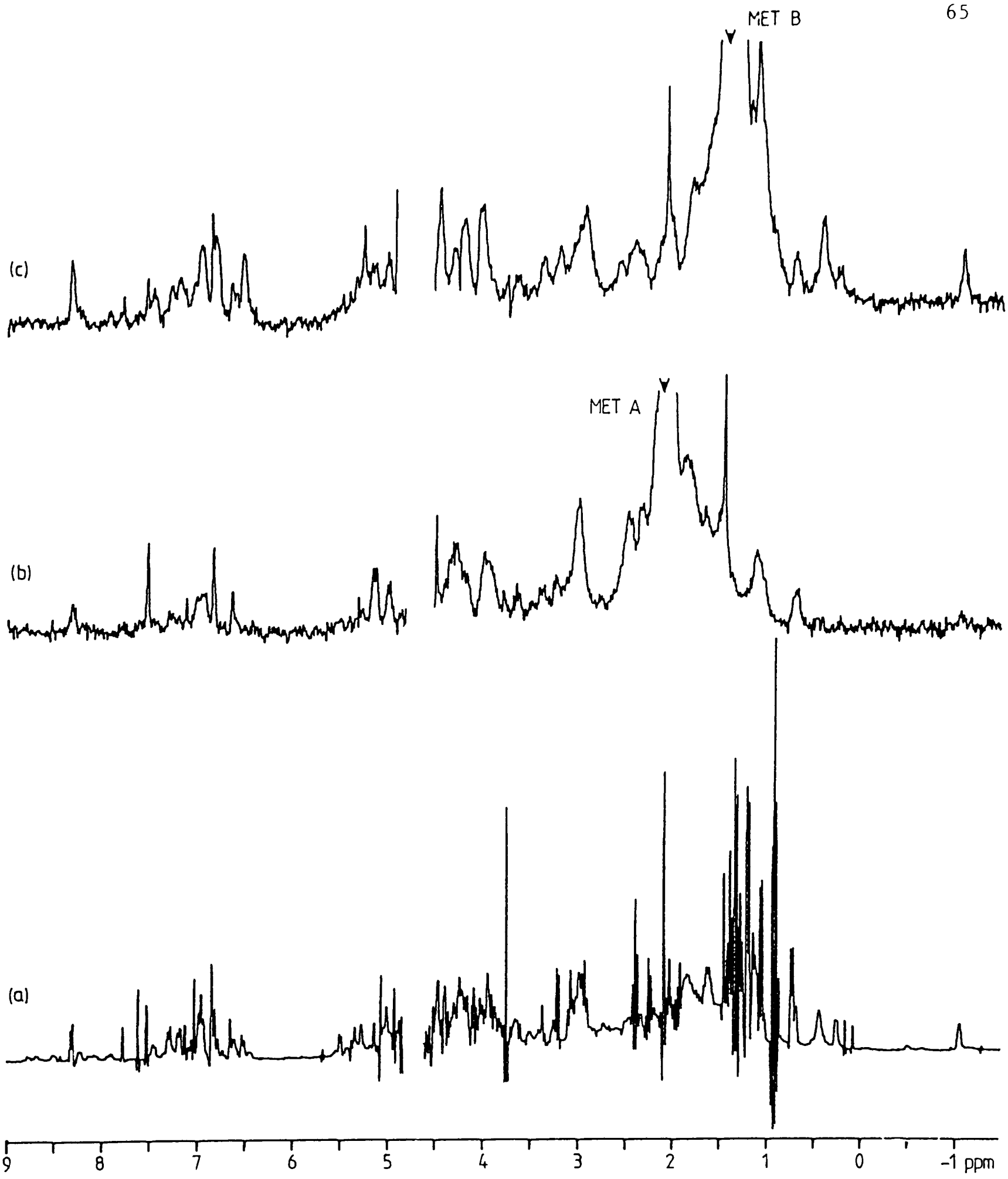

Fig. 3.25 NOE difference spectra from presaturation of the two methionine methyl proton resonances; 37°C, pH 8.8.

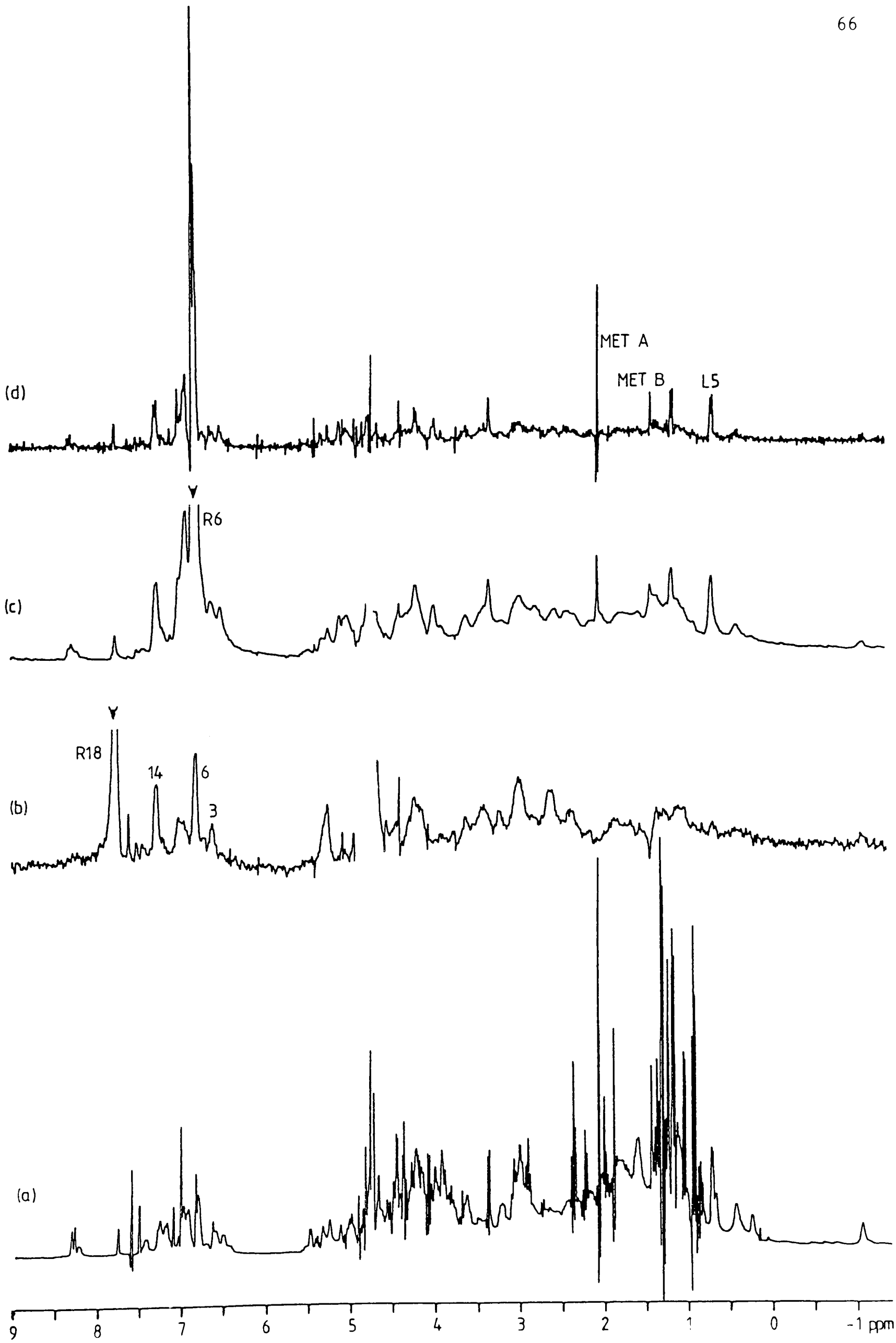

Fig. 3.26 NOE difference spectra resulting from presaturation in the aromatic region of the spectrum; 37°C, pH 8.8. (d) is the resolution enhanced form of (c).

in terms of the number of proton resonances. In essence all enhancements are noted for each pre-irradiation position but only effects noted to be reciprocal are taken to be significant. This will take account, to a large extent, of the sizeable bandwidth of the irradiating pulse but confusion can still arise from precisely overlapping resonances. One further consideration arises in that the aromatic region of the spectrum of kringle 4 contains some unassigned intensity as discussed and this too may also serve as a source of confusion in data interpretation. However, the accumulated results of many experiments subjected to the analysis outlined above are displayed in Fig. 3.27 and because of the reciprocal requirement it is of necessity symmetrical about the diagonal.

Only selected resonances have been considered for simplicity and from difficulties in resolving individual resonances in NOE difference spectra when the intensities are low. For instance R23 could not be clearly resolved from R3 in the spectra and they may well occur together as they both arise from the same Trp C ring. Intensity from the one proton triplet R22 was also very difficult to be certain of and so it is omitted. Very strong enhancements were obtained between some coupled resonances and could be selected for as shown in Fig. 3.14, and as indicated in Fig. 3.27. The number of peaks giving enhancements to R8,R9 is quite high and while this is a crowded part of the spectrum it may reflect the difficulty in resolving individual resonances and the question of unassigned intensity. Thus, the data is far from complete and beset with problems. The representation in Fig. 3.27 reminiscent of a 2 dimensional contour plot, indicates the more satisfactory data to come from the NOESY experiment, but at the time of writing it is not an experiment routinely performed in Oxford. However we will discuss the findings of Fig. 3.27.

Consider resonance R15 enhanced from both R9 and R13, consistent with Tyr D, and corroborated by enhancements from L1 and L2 discussed above,

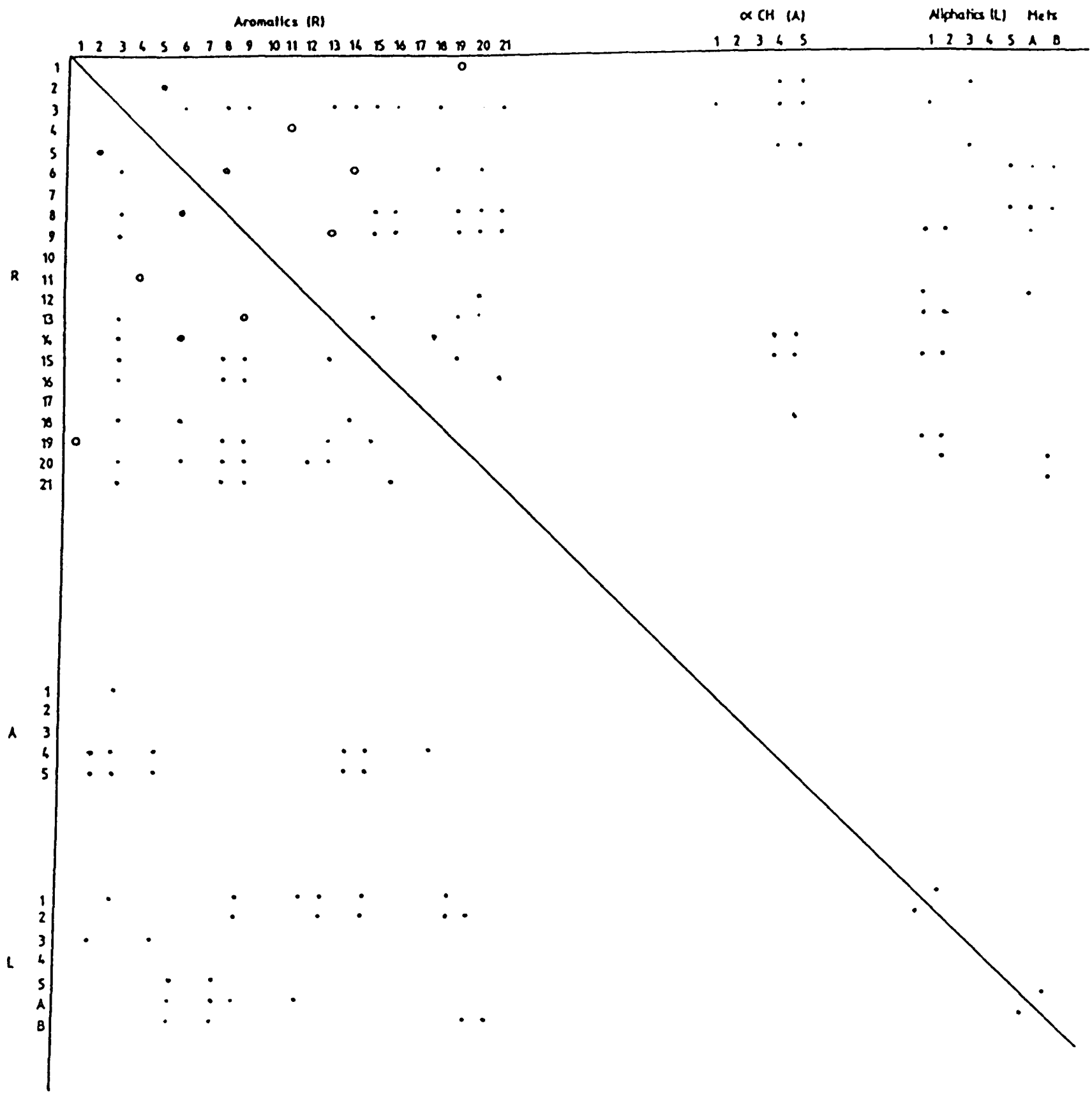

Fig. 3.27 Synopsis of numerous NOE experiments on kringle 4 indicating reciprocal enhancements between recognised resonances (see text). The open circles show directly coupled resonances.

showing Leu 45, Tyr D and part of Trp A to be close in space. The C2 of Trp B (R18) is the only clearly resolved resonance from this ring and was seen from Fig. 3.26 to be near to the ring of Tyr C. But it is also involved in a reciprocal enhancement with R3, the C2 of Trp C (Trp 71). Furthermore, resonances R6 and R14 of Tyr C also show this arrangement indicative of another group of residues initmately associated consisting of Tyr C and parts of Trps B and C. The grouping of Tyr A (R2,R5) and the methyls of Leu 77 (L3) is confirmed but with no further associations discovered. Liekwise the proximity of the L5 methyl group and Tyr B (R6,R8) is indicated, but in addition both methionine methyl groups are suggested to be closely related to this region in space as seen from Fig. 3.26(c) for instance. Thus, despite their separation in the sequence (28 and 47) the two methionine residues appear to be near each other and Tyr B in the folded protein. There are no reciprocal enhancements noted for His B resonances R10 and R17 although in fact a mutual one between themselves was seen. Liekwise, weak enhancements between the C2 and C4 resonances of the other two histidines were noted and that between R16 and R21 is recorded. Intensity attributable solely to R7 could not be distinguished from that of R6 and so was ignored. However, consider R16, R21 and R20 which are seen to give very similar enhancements, but R20 gives enhancements to both R9 and R13 suggestive of Tyr D and R12 of Trp A which His C does not. Further, all give enhancements to R3 indicative of proximity to the C2 of Trp 71.

The findings discussed above are summarised in Fig. 3.28, but it must be emphasised that some of the interactions indicated must be regarded as tentative.

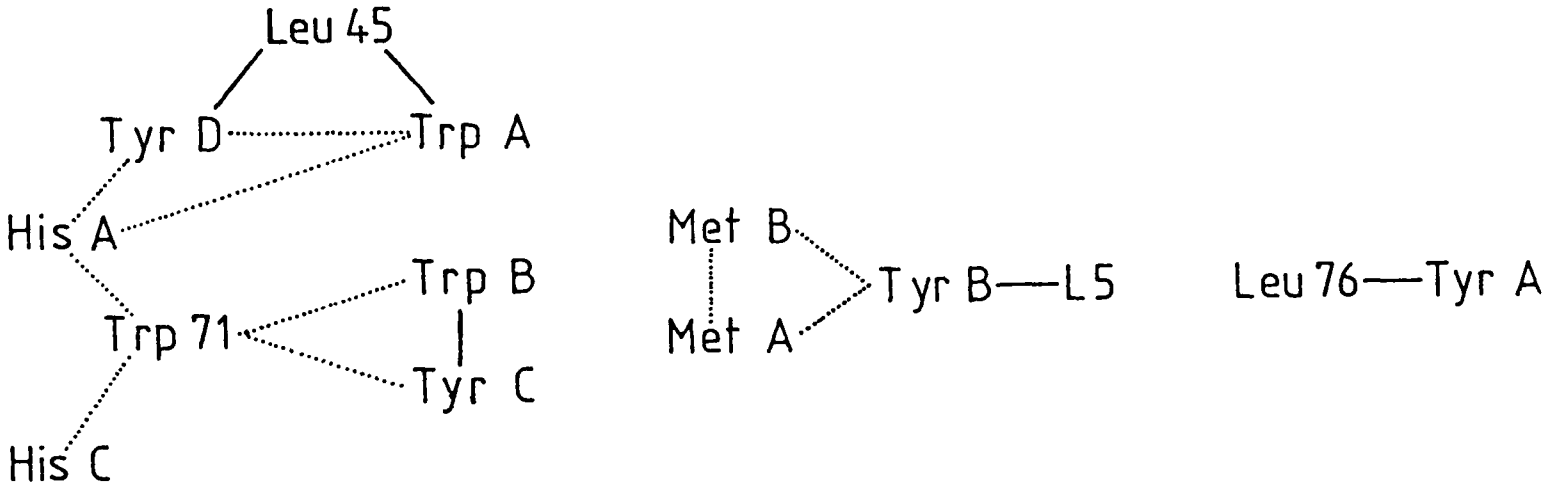

Fig. 3.28 Summary of the ——— and ····· (more tentative) spatial proximities indicated by NOE experiments

Figure 3.27 included some data on the downfield shifted αCH proton resonances. Little progress has been made on the assignment of these resonances although A2 arises from a threonine resonance as shown in section 3.3.5. But enhancements from these peaks should be consistent with the above, bearing in mind the problem of overlapping resonances. Figure 3.29 shows the enhancements obtained on the pre-irradiation of three such resonances. Figure 3.29(b) supports the proximity of Trp C (R3) and His C (R21) and Fig. 3.29(c) that of Trp B (R18) and Tyr C (R14,R6) as well as Leu 76 (L3) and Tyr A (R2,,R5). Finally, Fig. 3.29(d) is more complex as the irradiation is in the region of the upfield shifted triplet resonance of Trp A giving rise in the difference spectrum to L1, L2, R1, R12, R15 and R19 as well as perhaps R9, R13 of Tyr D. Although R20 of His A is enhanced selectively from R21, its neighbour, this is consistent with the presence of the Tyr D and Trp A resonances in the spectrum. In addition, resonances R6, R8 of Tyr B are also present as is L5 and selectively Met B. Thus, some corroboration of the

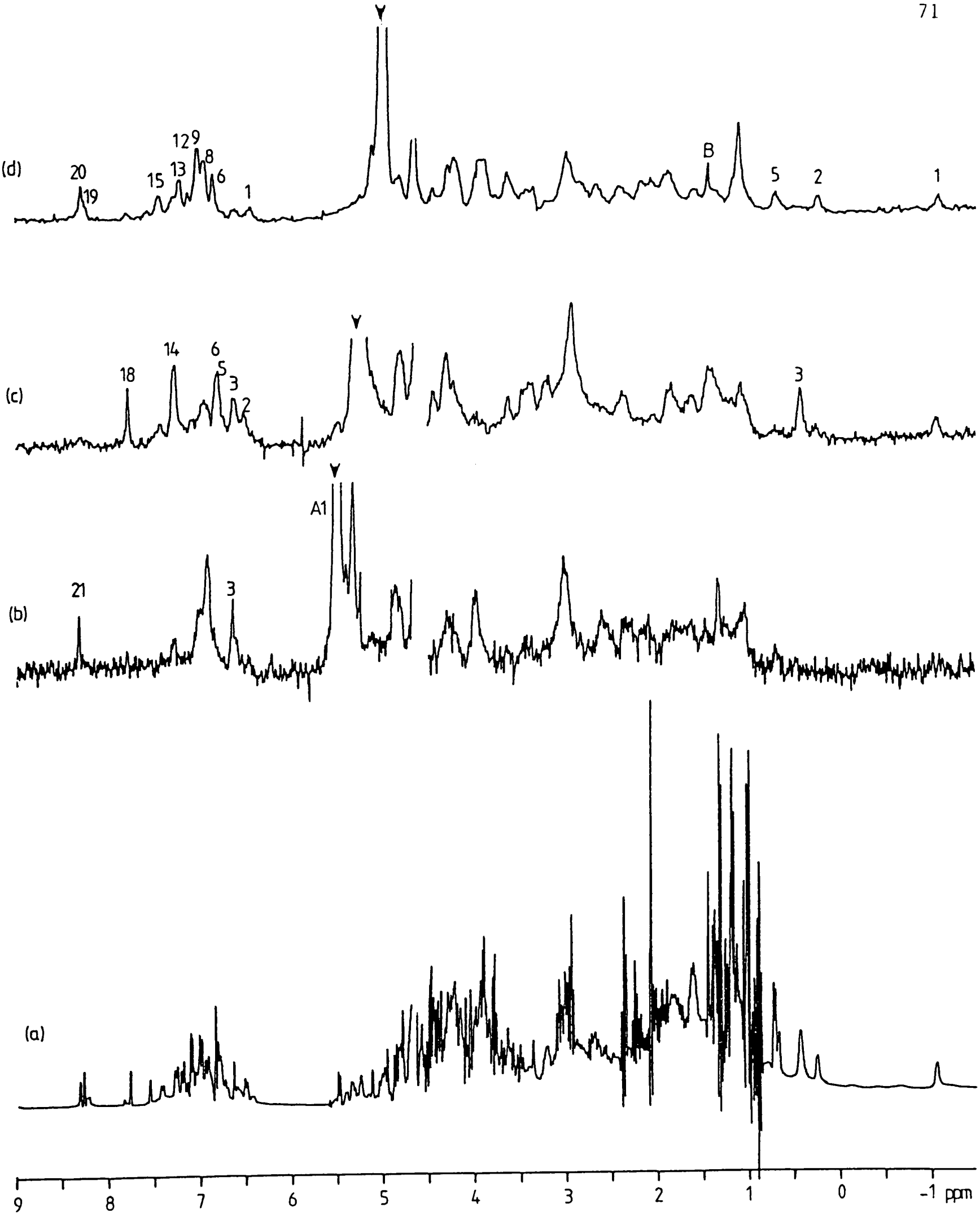

Fig. 3.29 NOE difference spectra resulting from presaturation of downfield shifted αCH proton resonances; 37°C, pH 6.8.

interactions shown in Fig. 3.28 is provided, but it is far from conclusive. It was also noteworthy that not all the data has been included in the discussion above. For instance the Lys ε proton peaks showed enhancements in a number of experiments, but for simplicity consideration has only been given to the more significant results.

3.5 Labile proton resonances

The significance of these resonances was commented on in section 3.1. No formal studies of their rate of exchange for solvent deuterons have been made, but Fig. 3.30 shows the persistent peaks after five hours at 27°C. From past experience they would all have exchanged in a similar time

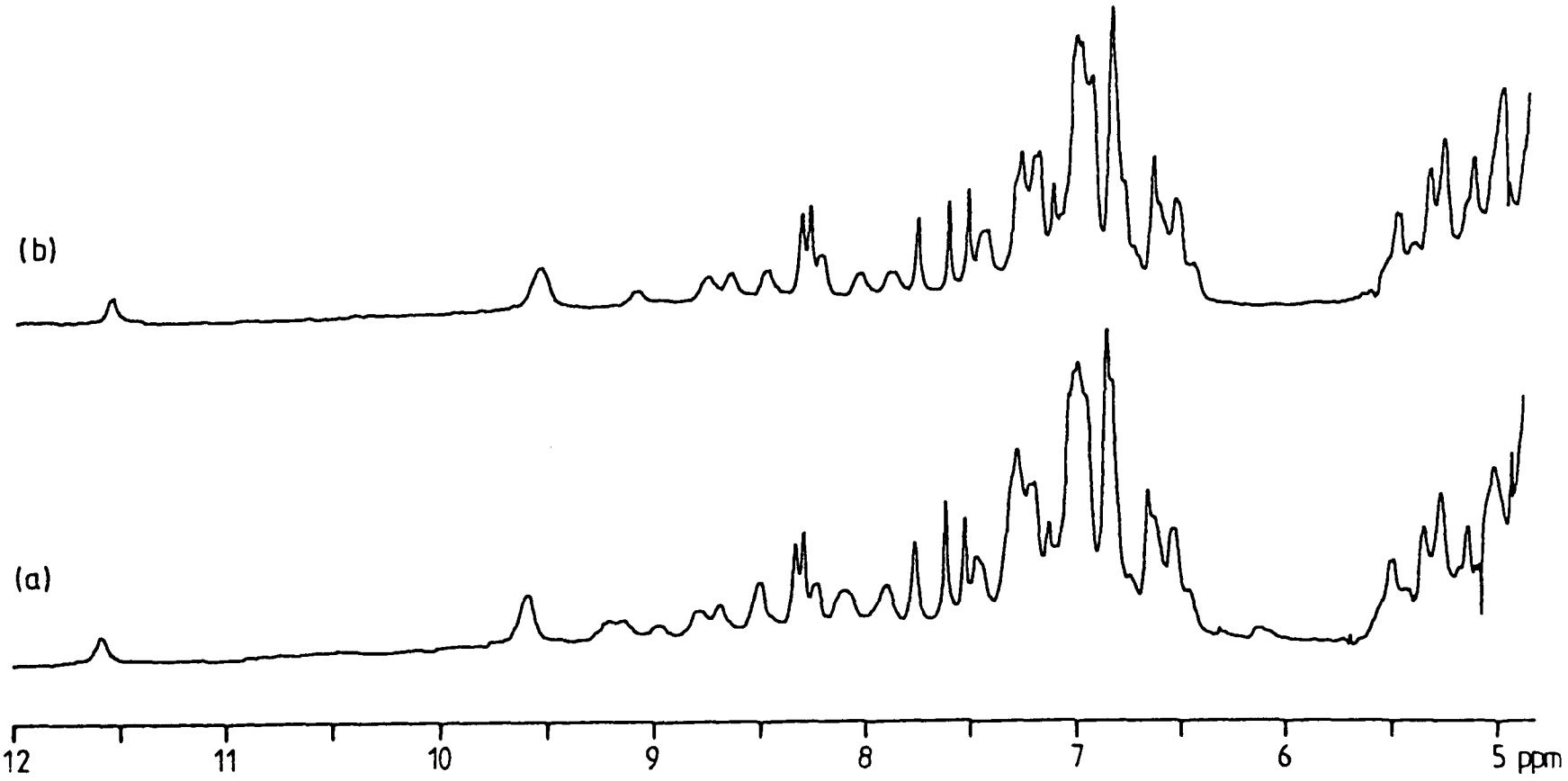

Fig. 3.30 pH 8.3, 27°C (a) Spectrum obtained just after dissolving the protein in D_2O (b) Same sample after 5 hours at 27°C

period at 37°C. This is in reasonable agreement with the results of Hochschwender et al., (1983) who found almost complete exchange some 16 hours after dissolving at pH 6.5 and 25°C. The resonance at 11.56 ppm has already been assigned to the indole NH of Trp A, but no other labile

proton resonances have been assigned so far. The Trp NH is shifted some 1.3 ppm downfield of its random coil position. Another noteworthy resonance, having a fairly rapid exchange rate, appears at 6.2 ppm. The well studied bovine pancreatic trypsin inhibitor protein has no labile protons below 6.6 ppm despite having labile protons with much slower exchange rates than those present in kringle 4 (Wüthrich and Wagner, 1979). However, we have not yet assigned the resonance and although a series of NOE experiments have been performed on these resonances, they will not be discussed here.

3.6 Temperature dependence

This is shown in Fig. 3.31. It can be seen that at 77°C all signs of a globular protein have been lost from the spectrum which is approaching that expected for a random coil protein, with all the residues of a particular type giving rise to spectral intensity at the same chemical shift values. We note the intense peak at 1.2 ppm comprising the eleven threonine methyl proton resonances, and the superposition of the six lysine εCH_2 protons at 3 ppm and so on. In particular, we note that the two methionine methyl resonances overlap at 1.99 ppm in the unfolded protein spectrum and so Met A is slightly downfield and Met B well upfield shifted in the spectrum of the intact folded structure. So the protein is seen to be thermally denatured and indeed this was irreversible for on withdrawing the sample from the probe the solution was opaque and gelatinous. Castellino et al., (1981) using the technique of differential scanning calorimetry showed the maximum change in the thermogram for kringle 4 to occur at 58°C and the thermal induced changes of denaturation took place over the range of about 50-70°C, in reasonable agreement with our NMR findings.

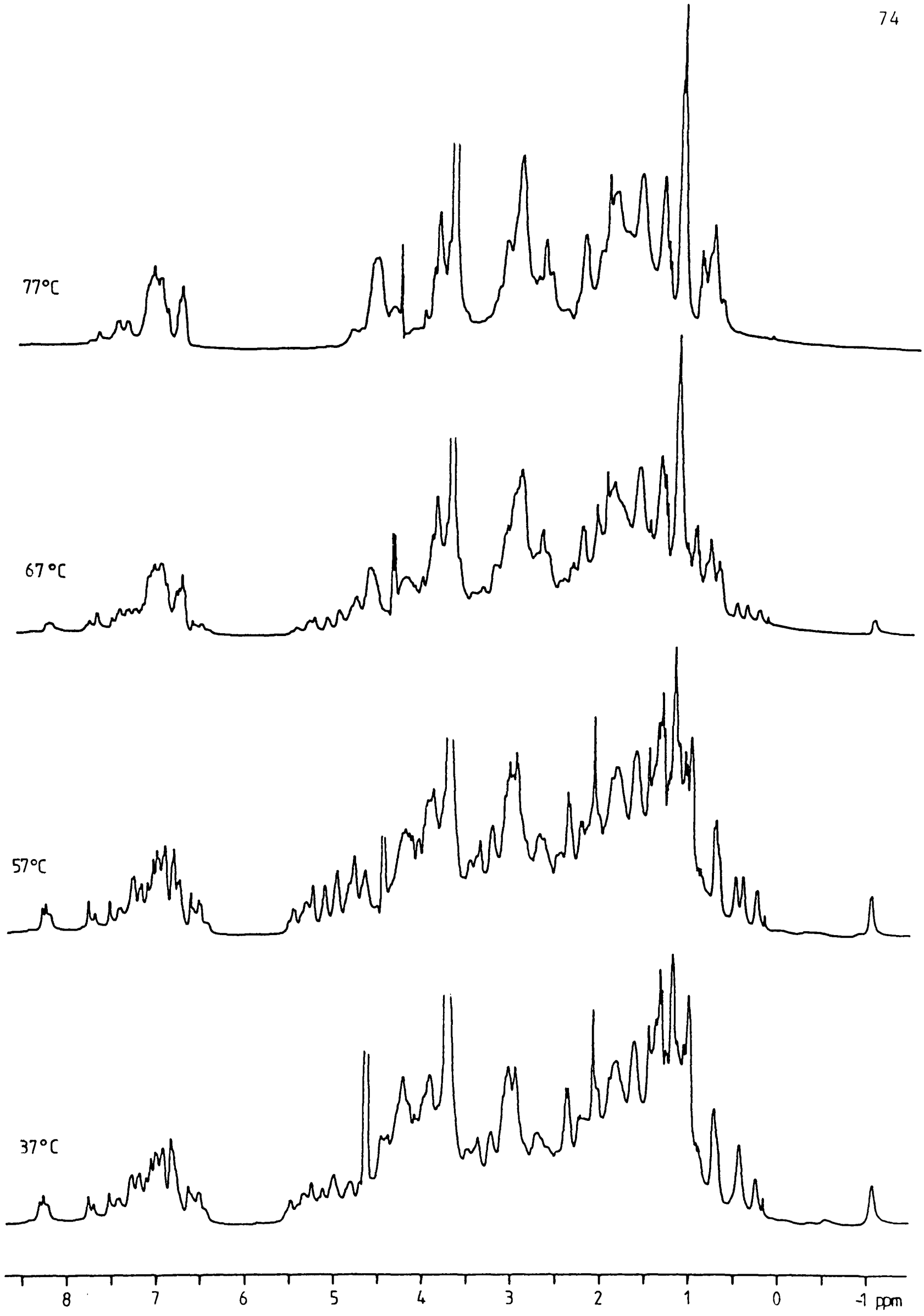

Fig. 3.31 Temperature dependence of the spectrum of kringle 4; pH 7.4.

It is seen from Fig. 3.31 that between 57°C and 67°C the changes are manifest by a slow exchange process and it was thus not possible to follow resonances through to their random coil positions as can be done with other proteins, such as phosphilipase A2 for instance. (Aguiar, 1980). However, between 37°C and 57°C while the protein structure is intact some noteworthy changes do occur. The most noticeable of these is the separation of the resonances L3 into two distinct resonances at chemical shifts either side of the low temperature position. At the same time and completely in accord with NOE data presented above, resonance R5 of Tyr A sharpens and moves upfield very slightly while R2 moves downfield by only about 0.02 ppm. This is understood as an increase in local motion in the structural element incorporating Tyr A and Leu 77 and in all spectra below 40°C, resonance L3 arising from the methyl protons of Leu 77, is broad with no resolved multiplet structure. The only other temperature dependent resonance of note is that of Met B which between 37°C and 57°C moves downfield by only about 0.03 ppm, but the implication of this is not clear.

We note that before the protein denatures there are no dramatic intensity changes, especially in the aromatic region, that would indicate other resonances, exchange broadened at low temperature, but brought back into the spectrum by raised temperature leading to a process in fast exchange. The lack of this behaviour does not however, preclude the possibility of some of the unassigned tyrosine and phenylalanine resonances being too broad to be observed at any temperature until after denaturation has occurred, which is the case, as mentioned above, for some resonances in the glycoprotein, cow-colostrum trypsin inhibitor (Wagner et al., 1978)

The large difference between the folded and unfolded structure clearly demonstrates that the great majority of the residues of the protein are incorporated into non random coil environments for both the aliphatic and aromatic side chains, or in other words, kringle 4 is a globular protein.

3.7 Summary

The chapter began and ended through consideration of the general spectrum and its temperature dependence with the conclusion that the kringle 4 fragment of human plasminogen has a well defined tertiary fold typical of a classical globular protein. Many resonances were noted to be secondarily shifted through close proximity to other side chains and not solvent molecules and the vital task of assigning the peaks to particular protons in order to try and define the structure was considered in detail. All, but two, of the aromatic ring side chains were assigned and a second stage assignment of resonances to Trp 71 in the sequence was made from homology arguments and data on another kringle to be presented in chapter 6. In addition, all three tryptophan side chains gave rise to triplet resonances at a novel chemical shift. Two of the three histidine side chains were noted to give resonances at positions very different from those expected for residues freely accessible to the solvent. In the aliphatic region of the spectrum a number of assignments were made to the second stage and in particular a feature common to a number of kringle structures was found to involve the conserved residue, leucine 45. Nuclear Overhauser experiments contributed greatly to defining the structure in terms of the proximity of various defined resonances. Of particular note was the finding that Leu 45 and Trp A - one of the tryptophans 25 or 61 in the sequence - both conserved in all kringles sequenced so far, are close in space, strongly suggesting at least one structural element is also conserved by the primary sequence of the kringle. Brief discussion of the labile proton resonances served again to emphasise the tight fold of the kringle in solution.

Thus, having considered the NMR spectrum of kringle 4 in great detail we are now in a position to add probe substances to the protein solution

to observe the spectral effects and gather further information on the structure. Furthermore, we can add various ligands that bind kringle 4 and attempt explanations of the observed changes in terms of the structural information acquired.

CHAPTER 4

PROBE AND LIGAND BINDING STUDIES OF KRINGLE 4

4.1 Introduction

Probe experiments are very much part of protein NMR studies and demonstrate the power of the technique for monitoring the structure under an infinite variety of solution conditions, see for instance Dwek (1973), Wüthrich (1976). The most commonly used probe is the hydrogen ion and is the first one considered below. However, with all probe studies it is necessary to constantly differentiate between effects in the spectrum arising genuinely from the reagent probing the structure and effects due to the added substance changing the structure. For instance, pH studies of lysozyme have revealed the individual pK_a of the Glu 35 residue, but at the same time marked effects are noted on the resonances of Trp 108 and some other residues in the hydrophobic groove (Campbell et al., 1975). This, and other data, is taken to imply that Glu 35 moves away from Trp 108 as the former ionises (Blake et al., 1978). Less subtle examples occur when pH titration reveal pK_a's of surface histidine residues that may ionise without causing a conformational change for example, but at extremes of pH disruption of salt bridges can cause profound structural alteration and concomitant large effects in the NMR spectrum. Obviously, probe studies using more highly charged species require similar care in differentiating the spectral changes induced by the same processes. Adding calcium to a calcium protein is often done to monitor induced structural changes, see for example, Levine et al., (1977) for a NMR study of the calcium binding muscle protein, troponin C. On the other hand, paramagnetic lanthanide ions can be used to map out metal binding sites as for instance for lysozyme (Campbell et al., 1975), with the added advantage of the iso-

morphous diamagnetic ions, lanthanum and lutetium with which to study solely the effects of metal binding on the protein spectrum.

For those proteins which bind ligands, NMR studies using a variety of ligands and analogues can provide information not only on the effects of the ligand on the protein structure and vice versa, but also on the binding site itself, as demonstrated for instance by studies of inhibitor binding to lysozyme (McDonald and Phillips, 1970) and spin-labelled ligands combining with the Fv fragment of an immunoglobulin (Dwek et al., 1975). In addition, combination of probes provides further scope for structural studies, although competitive interactions must also be considered then. Many of the structural probes mentioned above are discussed below. Following on from pH dependence studies, we consider the effects of adding copper(II) ions to the protein; the ω-amino carboxylic acid binding of kringle 4 is then discussed and seen to be complimented by results of lanthanide ion binding experiments.

4.2 pH Dependence

Figures 4.1A and B show the spectral changes resulting from altering the pH of the protein solution over the range from 2.8 to about 10.75. It is clear from the changes in the form of the spectrum at very low pH that a profound effect has occurred on the protein structure under these conditions. Indeed, the spectrum at pH 2.81 is very similar to that expected for a random coil protein - the upfield methyl resonances have all but disappeared as have the αCH proton resonances beyond 5 ppm and the aliphatic and aromatic region envelopes are comprised of peaks arising from the almost coincident resonances of each type of amino acid. The intensity between 0.8 and 1 ppm is compatible with that expected from two leucine and one valine residues, the methyl proton resonances of the N and the variable amount of the C terminal valines occurring just beyond 1 ppm at this pH.

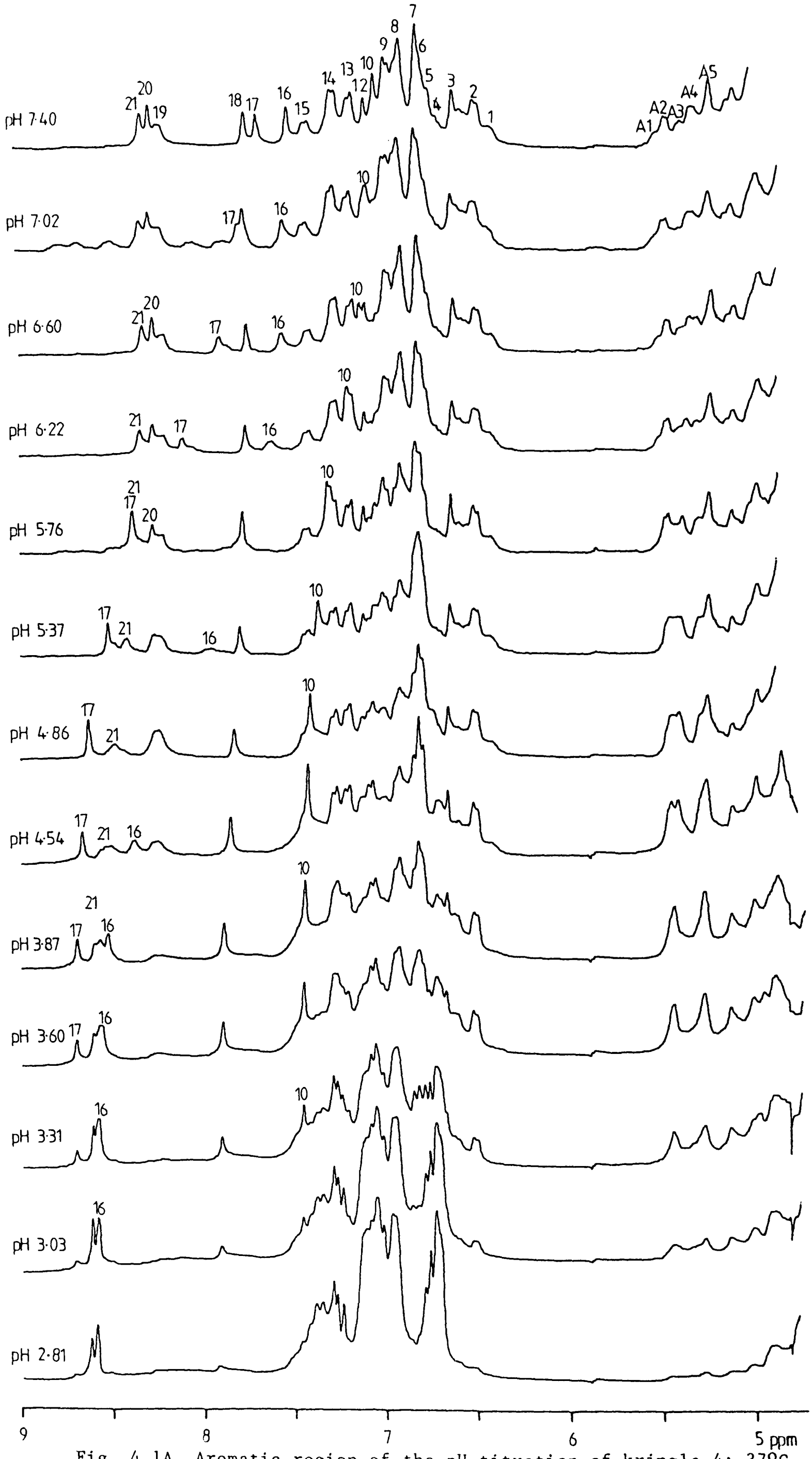

Fig. 4.1A Aromatic region of the pH titration of kringle 4; 37°C, 100mM NaCl.

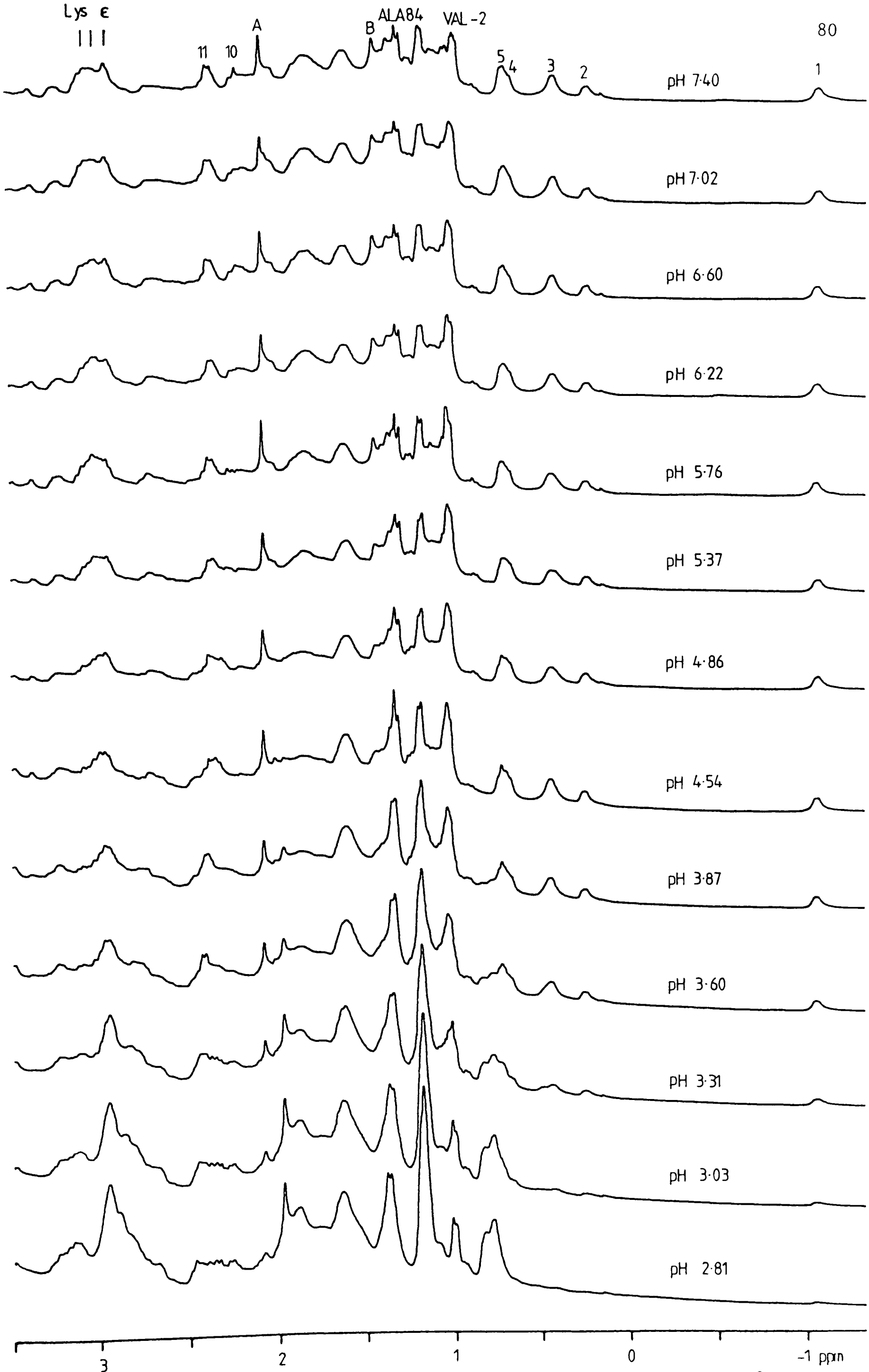

Fig. 4.1B Aliphatic region of the pH titration of kringle 4; 37°C, 100mM NaCl.

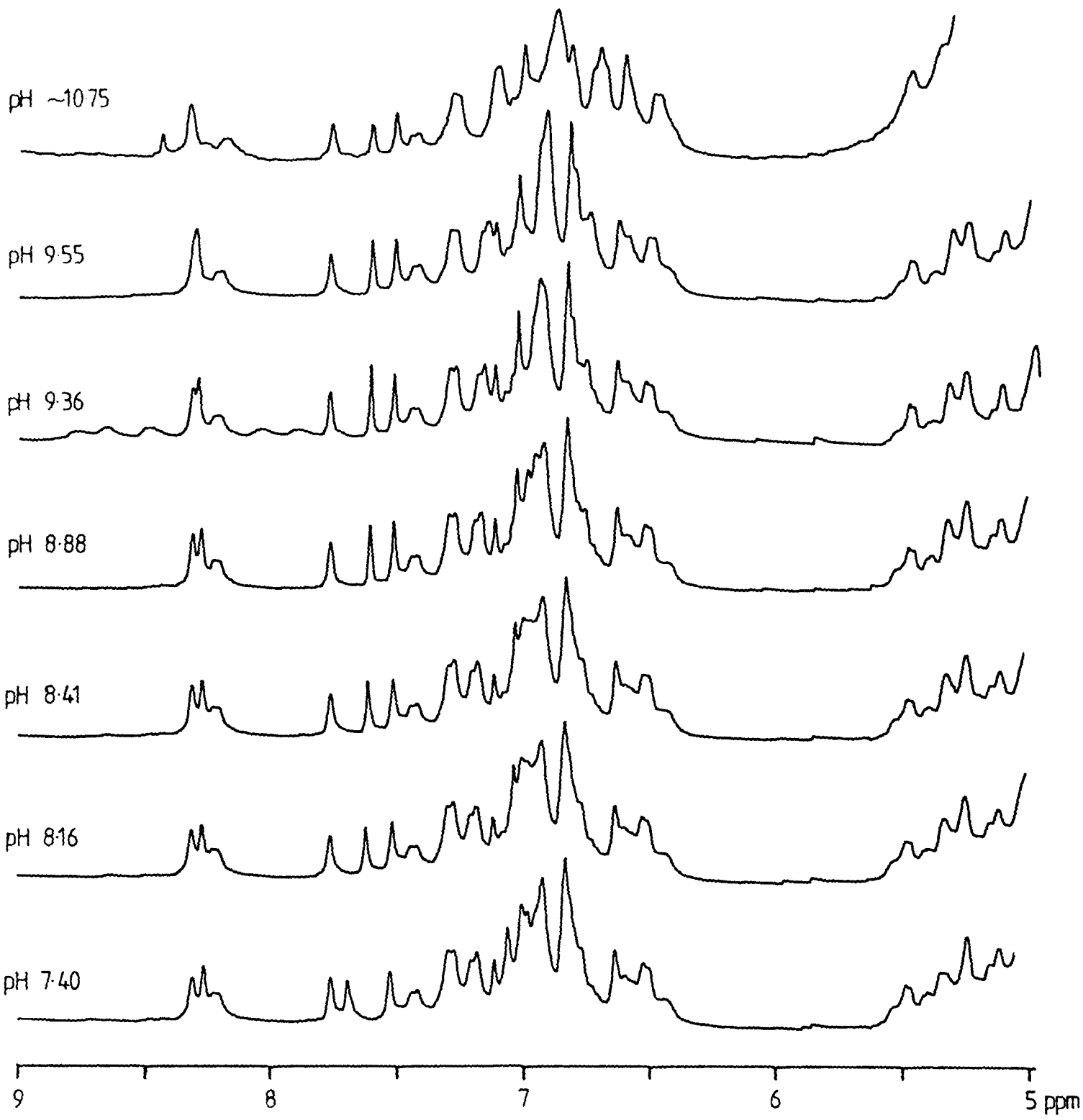

Fig. 4.1A Continued.

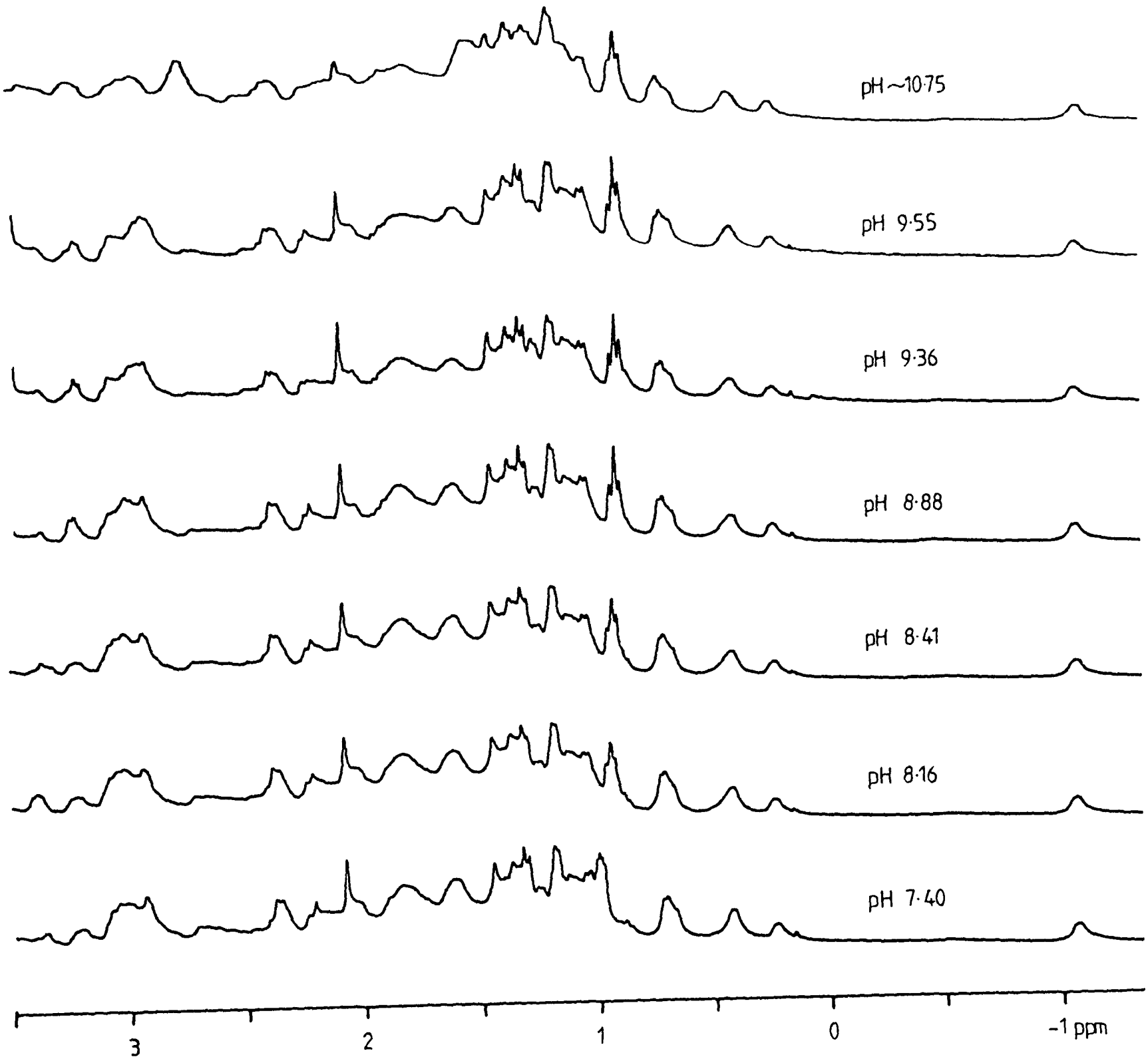

Fig. 4.1B Continued.

The intensity at 1.18 ppm is reasonably consistent with that expected from eleven threonine methyl group protons. The resonances from the two methionine methyl protons are coincident at 1.97 ppm, and the lysine εCH_2 intensity is amassed around 2.95 ppm. Similarly the aromatic region has lost all indications of spectral features associated with a globular protein.

Denaturation under very acidic conditions is a well recognised phenomenon shown by a number of globular proteins (Tanford, 1968). As mentioned above, it may occur through the disruption of structurally vital salt bridges or alternatively the changed state of molecular ionisation at low pH may lead to unfavourable protein-solvent interactions leading to denaturation and sometimes aggregation and precipitation. However, it is not inevitable, lysozyme, for instance, being entirely unaffected in its general structure in very acidic solution (Tanford, 1968; Dobson, 1975).

Denaturation at very high pH is also a common occurrence especially in proteins containing disulphide bridges due to nucleophilic attack by hydroxyl ions on the disulphide bonds. This was found to be the case for kringle 4 and the sample from which the pH 10.75 spectrum was obtained was irreversibly denatured at higher pH.

We now consider more detailed aspects of the pH dependence of the spectrum, beginning with the aromatic region of the spectrum. Figure 4.2 shows the chemical shift versus pH curves for some of the resonances. It will be noticed that many of the points are not continued through to the lower pH values. Reference to Fig. 4.1A shows that it is not possible to follow all resonances throughout the titration as the protein unfolds. In addition, as will be discovered on looking in more detail, some resonances broaden and disappear from the spectrum before denaturation of the whole protein begins. The points of Fig. 4.2 were obtained from resolution enhanced spectra corresponding to those of Fig. 4.1A and so only resonances clearly visible in that form of the spectrum are plotted.

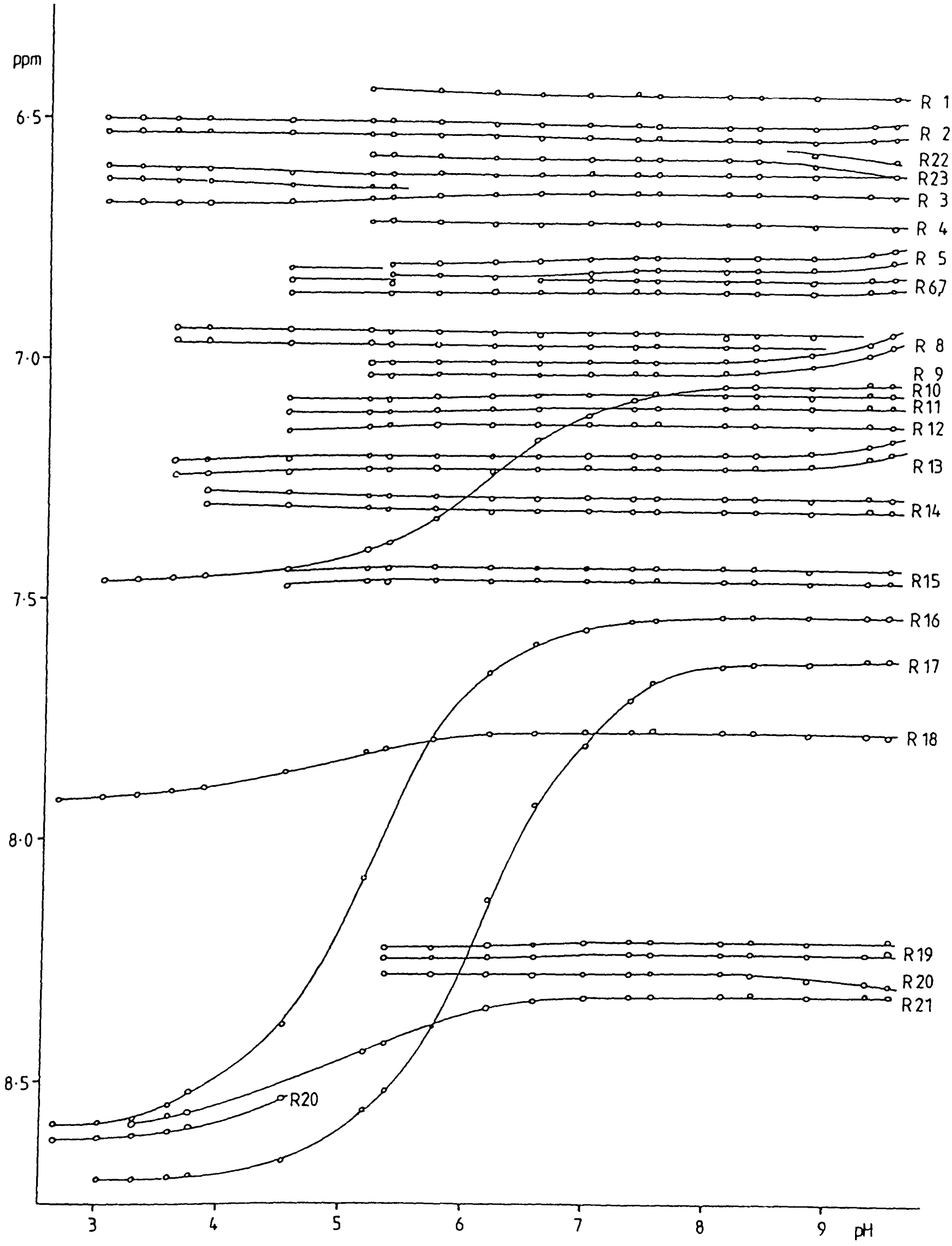

Fig. 4.2 Plots of chemical shift versus pH for aromatic resonances of kringle 4; 37°C, 100mM NaCl (see text).

Points from the pH ∿10.75 spectrum are not included because of poor resolution and uncertainty in the pH measurement. We now consider resonances arising from the various types of aromatic side chain.

4.1.2 Histidines

Observation of the pH behaviour of histidine resonances as an aid to assignment and to determine individual pKa's is a well established procedure (Markely, 1975).

In section 3.2.2 we made the following assignments:

His A	R20, R7
His B	R17, R10
His C	R21, R16

From Fig. 4.2 we see that R17 and R10 both show the same pK_a of ∿6.2 and furthermore both show chemical shift changes - 1.1 ppm and 0.4 ppm - in reasonable agreement with those shown by histidine in a random coil peptide (Bundi and Wüthrich, 1979) (0.86 ppm and 0.38 ppm) for the C2 and C4 protons respectively. The broadening of the resonance R17 seen in Fig. 4.1A as the residue passes through its pK_a is a common occurrence in histidine pH titrations (see Sudmeier et al., 1980 for a discussion). Thus, this data amply confirms the assignment of section 3.2.2 for His B and specifically R17 as the C2 proton resonance. Bundi and Wüthrich (1979) give the random coil histidine pK_a as 7.0 at 35°C with 50 mM tetrapeptide in 100 mM NaCl. Thus, the His pK_a quoted above, also for a solution in 100 mM NaCl at 37°C, is seen to be lower, presumably as a result of its local environment causing some stabilisation of the unprotonated form, suggesting that the side chain is folded into the protein structure to some extent. Indeed, it can be seen in Fig. 4.1A that as the pH is lowered below 3.87 both resonances R17 and R10 gradually disappear from the spectrum as the protein denatures. Finally, their chemical shifts are not quite those of a histidine side chain in a random coil environment which are given:

	δ_{HA}(ppm)	δ_{A^-}(ppm)
C2H	8.61	7.75
C4H	7.35	6.97

and thus it is concluded that the imidazole ring of His B is not entirely surrounded by solvent molecules.

Similarly,resonance R16 is seen to titrate over a chemical shift range typical for a C2 proton and is assigned as such for His C, and in the protonated form this resonance has a chemical shift very close to the random coil value. However, this is far from the case for R21, the C4 proton resonance where although the chemical shift range (0.26 ppm) is consistent with a C4 proton,the chemical shift is some 1.35 ppm upfield from the random coil position in the unprotonated species. This may be partly explained by proximity of the protons of His C to the C2 proton of Trp 71 as was suggested from NOE experiments described in section 3.4. Indeed, close inspection of Fig. 4.2 reveals that the C2 proton resonance of Trp 71 (R3) has a slight inflection with pH over this range as do R11 and R23 also arising from the Trp 71 ring, although the triplet resonance R4 does not appear to be affected. However, the shifts on the tryptophan resonances are so small that an accurate pK_a cannot be obtained to demonstrate it to be precisely the same as that of His C. But, in addition we note that R16 and R21 show smooth, continuous curves down to very low pH, suggesting that they are all, together, part of a structural element that denatures only below pH 3. (It must be stated though, that there is a possibility of some confusion of the curve of R21 and the continuation of that of R20 at low pH since both resonances broaden as the pH is raised, but Fig. 4.2 shows what is thought most likely. The spectrum at pH 3.87 clearly shows four resonances beyond 8.5 ppm indicating the presence of four singlets including R21 - a very unusual C4 proton peak and the

expected three histidine C2 proton resonances. However, at pH 2.81 it seems probable that there is only three proton intensity beyond 8.5 ppm with the C4 proton resonance of His C having broadened to reappear in the random coil position around 7.35 ppm).

The third histidine, His A is assigned to R20 and R7 which are seen from Fig. 4.2 to behave in an even more atypical fashion with pH. The resonance R20 at low pH begins to show promise of a normal titration curve for a C2 proton as deprotonation of the histidine ring begins. However, barely has this begun than the resonance disappears completely and a histidine singlet resonance appears at 8.27 ppm (it is of course possible that the latter resonance is the C4 proton peak and the C2 is at R7 but this is much less likely and is assumed not to be the case). The R7 resonance is much harder to follow but certainly shows no tendency toward a normal histidine C4 proton peak behaviour, being like R20, unaffected by pH above about pH 5.0. The inflection above pH 8.5 in the curve of R20 will be discussed below. Thus, the histidine C residue appears to get locked into its protonated form above pH 4.5 presumably through interaction with an aspartate or glutamate residue carboxyl group which ionises over this pH. Non titrating histidines are a feature of metallo-proteins in which the histidine acts as a metal ligand, but the significance of the behaviour of His A to the kringle structure and function is far from clear as yet.

4.2.2 Tyrosines

The resonances of Tyr A were assigned to R2 and R5 and in accord with this it can be seen that these peaks begin to titrate upfield with pH above about 9.1. From the spectrum at pH 10.75 the R5 resonance is noted to have moved more than the R2, indicating that it is from the meta protons. The random coil values are given:

	δ_{HA}(ppm)	δ_{A^-}(ppm)
ortho	7.149	6.981
meta	6.857	6.573

and thus for Tyr A the ortho protons at R2 have a much larger secondary shift than the meta which are close to the random coil values. However, it is noticeable that the peak comprising R5, R6 and R7 changes shape between pH 5 and pH 7 and this is attributed in Fig. 4.2 to movement in R5 although R2 appears unshifted. This pH dependence reflects the pK_a of His B and although no clear spacial proximity between Tyr A and His B was indicated from NOE experiments, their proximity will be seen to be borne out by the copper ion probe studies. We also note that as discussed above for Trp 71 and His C, the resonances from Tyr A and His B show very similar pH dependence at very low pH in that below pH 3, R2, R10 and R17 disappear in unison from the spectrum much as would be expected if they occupy positions close in space.

The resonances R6,R8 of Tyr B are less clearly visualised than those of Tyr A but R6 is seen to begin titrating just above pH 9 and R9 obscures the R8 peak so that it is not possible to be sure which resonance arises from the ortho protons. This will be discussed again in section 5.3 but the pH dependence of R6 does at least confirm their assignment to a tyrosine side chain.

Tyr C assigned to R14, R6 shows no sign of titrating with pH up to 9.6 as judged by R14 and indeed by pH 10.75, R14 is showing only the very smallest of shifts. (Hence the movement at R6 could be attributed to Tyr B and not Tyr C). The normal tyrosine pK_a is around 10.3 and so that of Tyr C is seen to be considerably elevated. However, the assignment to a tyrosine is justified by the small pH dependence and from the NOE on irradiating R18 showing R6 and R14 clearly in the difference spectrum of Fig. 3.26(b).

Finally, Tyr D giving rise to resonances R9, R13 clearly shows the lowest pK_a of all the assigned tyrosines and again from the magnitude of the shifts, R9 is seen to be from the meta protons. We also note that R20 shows a pH dependent shift coincident with the ionisation of Tyr D and this is entirely consistent with the proximity of His A to Tyr D indicated from the NOE experiments. However, in addition resonance R22 of Trp B also moves over this pH range suggesting that Trp B may also be close to Tyr D and senses the ionisation, although this relationship was not obvious from the NOE data and it must be borne in mind that the lysine residues also begin to titrate around this pH (see below). Furthermore, R18 the only other clearly resolved resonance of Trp B at this pH is not similarly affected. At low pH, R13 shows a further pH dependent shift but it is too small to obtain a pK_a and correlate with any other titrating groups. But, very curiously below pH 5 resonance R9, which at a higher pH is a clearly resolved doublet in the resolution enhanced spectrum, begins to broaden and disappear although R13 appears to remain well defined down to pH 3.5. At the same time R12, the singlet resonance of the indole ring of Trp A shows a very similar behaviour, and so we now consider the tryptophan pH dependence in more detail.

4.2.3 Tryptophans

As well as broadening and disappearing from the spectrum around pH 4.5, R12 also shows a small shift around this pH as was seen for R13. Resonances R19 and R1 from Trp A show very similar behaviour in broadening out. R15 is more difficult to follow due to the overlying R10 resonance at this pH, but of all the Trp A resonances it is the one of chemical shift nearest to that of a random coil side chain (Table 3.2) and so may not be exchange broadened to the same extent as the other resonances should Trp A be moving to a random coil environment over this pH range. Unfortunately, it is not

possible as yet to detect where the Trp A resonances reappear in the spectrum. Accompanying these changes of the Trp A (and Tyr D) resonances it is very noticeable in Fig. 4.1A that R20 (His A) shows synchronous behaviour. The proximity in space of His A to Tyr D has already been commented on above and in turn Tyr D was seen from the NOE results to be close to Trp A. Leu 45 was also part of this structural unit as depicted in Fig. 3.28, but yet Fig. 4.1B shows that they do not begin to disappear from the spectrum until the pH drops below 3.87 as was the case for R13 of Tyr D. The interpretation of these observations is not entirely clear as yet in terms of the protein structure. It could be tentatively suggested that as the carboxyl group presumed to be associated with His A is protonated, part of the structure involving His A and Trp A loosens and even unfolds causing some resonances such as R9 to be exchange broadened in the process but it is curious that L1, L2 and R13 are so little affected. As will be remarked below L2 does show a slight shift analagous to that of R13 with pH over the range in question. In addition R22, a one proton triplet resonance of Trp B also broadens from the resolution enhanced spectrum at the same time although the singlet R20 of Trp B, like L1 and L2 is only broadened at much lower pH's.

It is seen, however, from Fig. 4.2 that R18 shows a pronounced pH dependence between pH 4 and 6. This pH range is too narrow for a true pK_a and indicates some degree of cooperativity. The midpoint of the shift versus pH curve occurs around pH 4.7 whereas that for His C occurs at about pH 5.3. Thus, the pH dependence of R18 is presumed to reflect a carboxyl group ionisation and this process may also account for the broadening noticed on R22, but it is not clear whether it is the same carboxyl group that when ionised also holds His A in its protonated form.

The pH dependent behaviour of Trp C resonances was considered above and related to the ionisation of His C, partly as prompted by an association

indicated from NOE experiments, but it is clear by now that more than one titrating group affects aromatic resonances below pH 6 and discrimination between them is not unequivocal. Thus, some of the additional interactions between residues that have been suggested above need further supporting evidence to be made conclusive.

We now go on to consider the chemical shift versus pH curves for resonances in the aliphatic region of the spectrum as shown in Fig. 4.3. As for Fig. 4.2 this was compiled using data from resolution enhanced spectra and the curves continued for as long as the peaks were clearly defined but they were interrupted on occasions by significant changes in the multiplet structure.

4.2.4 Terminal Residues

The ionisation of the N terminal valine and the two C terminal residues Ala 84 and Val 86 can be seen reflected in the shifts of their methyl group resonances (only one peak of the valine methyl multiplets is plotted). The pH was not taken sufficiently low to measure the pK_a of the C terminal residues but it is seen to be around 3.5 which is characteristic of a C terminal carboxyl group. The N terminal valine has a pK_a about 8.0, which is also a satisfactory value for the terminal NH_3^+ group, and the αCH resonance of this residue was also identified, as shown, from its large pH dependent shift. These findings confirm the assignments made in section 3.3.

4.2.5 Methyl Proton Resonances

It was remarked above that L1 and L2 from Leu 45 do not begin to broaden from the spectrum until below pH 3.8 despite most of the resonances of Trp A, to which they give strong Overhauser enhancements, having completely disappeared by then. L2 does show a slight inflection in its pH versus chemical shift curve which may reflect the Trp A changes, but it

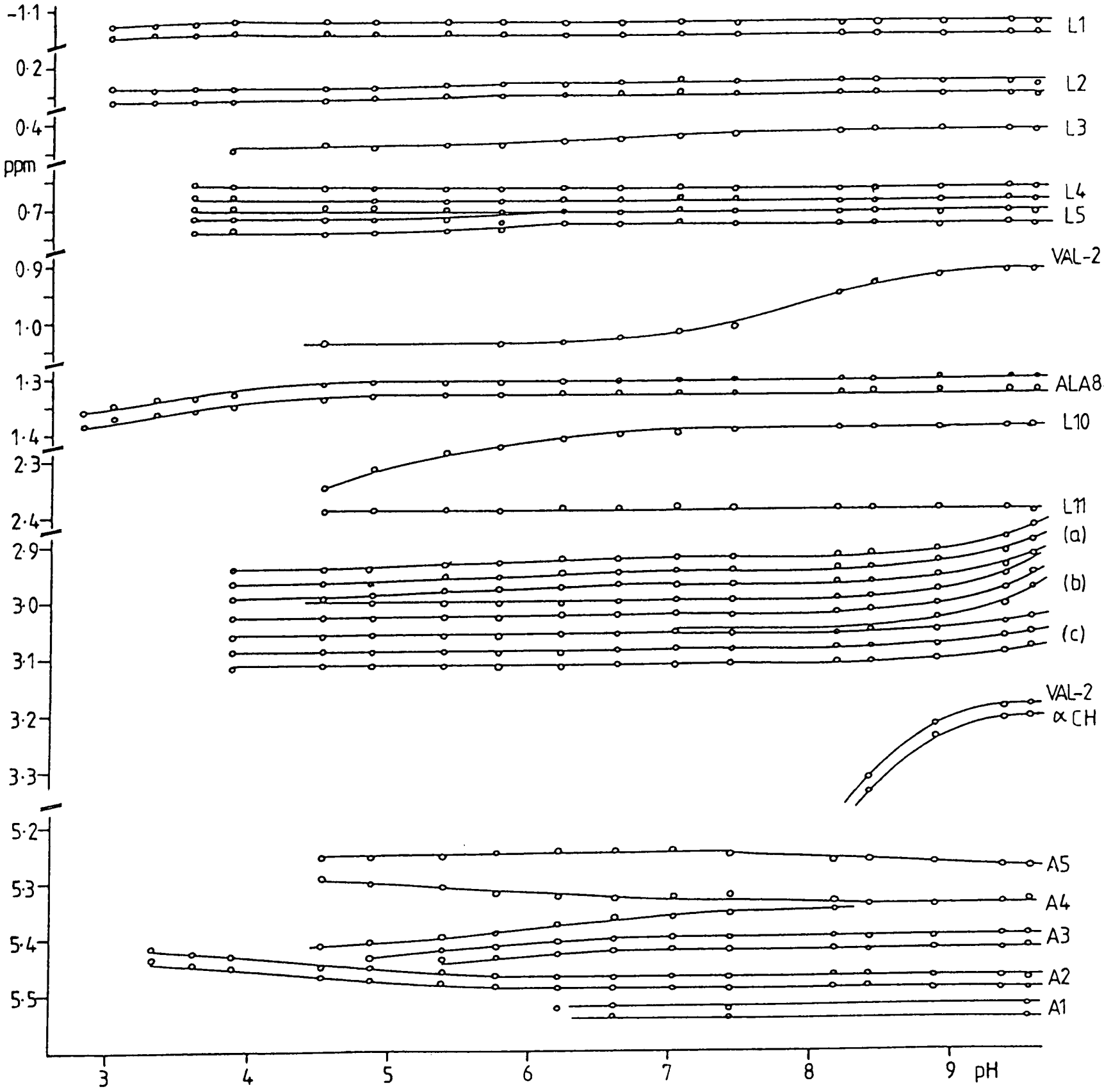

Fig. 4.3 Plots of chemical shift versus pH for aliphatic resonances of kringle 4; 37°C, 100mM NaCl (see text).

is a very small effect. As the protein denatures L1 also shows a very small shift in the direction of the random coil position but the resonance disappears essentially via a slow exchange process.

L3, the broad peak from the two methyl groups of Leu 77, shows some pH dependent changes with a midpoint about pH 6.5, which within the accuracy attainable, is a fair reflection of the pK_a of His B. We noted above that one of the resonances assigned to Tyr A (R5) also showed a pH dependence in accord with the His B ionisation and the NOE experiments of section 3.4 demonstrated spacial proximity of Leu 77 to Tyr A. This structural element including His B will be confirmed in the copper ion studies discussed in the next main section of this chapter, and as expected L3 broadens out at low pH in unison with the resonances of His B and Tyr A.

The methyl proton resonances of Val 69, L4 and L5 show no pH dependence until they return to their random coil chemical shifts at low pH. However, the other methyl proton doublet that overlaps L5 at pH's above 6.5 does show a smooth curve downfield at lower pH values but again it is not clear which pK_a it is sensing. NOE results indicated proximity of this resonance to Tyr B but Fig. 4.2 shows no pH dependence for resonances R6 and R8 as drawn over this pH range. However close inspection of Fig. 4.1A shows intensity just downfield of R3 at pH 4.54 moving into R6 as the pH is raised. Over the same range the intensity at R8 is augmented. Unfortunately these effects are not followed readily in the resolution enhanced spectra and so do not appear in Fig. 4.2. The significance of these changes - whether they represent unassigned tyrosine intensity for instance or movement of Tyr B resonances - has not yet been elucidated. However, we note that these changes also accompany the appearance in the spectrum of the Trp A and His A resonances into their intact protein positions and thus it could also be speculated that all the changes are part of the same process.

In addition, it is seen from Fig. 4.1B that the Met B methyl proton peak also goes into slow/intermediate exchange below pH 5.76 to reappear at its random coil position in unison with the behaviour of the Trp A and His A resonances again suggesting the unfolding involving the latter residues is more widespread and that Met B is incorporated in the structural element concerned. On the other hand the Met A methyl proton only returns to the random coil position below pH 3.87, although NOE data suggested both methionine methyl resonances were 5Å or less apart. This is curious but no more so than the apparently analagous behaviour, as discussed above, of resonances R9 and R13 although they belong to the same residue, Tyr D.

4.2.6 Glutamates

There are three glumatic acid residues in the kringle 4 fragment, but pH studies only clearly indicate L10 to show a pKa suitable for assignment to the γCH_2 protons of a glutamic side chain. Furthermore, for the deprotonated form the chemical shift is near to that expected for a random coil peptide and this is confirmed by the intensity in the spectrum of the thermally denatured protein and so L10 is tentatively assigned to the extra-kringle residue, Glu 83. This assignment will be considered again in the discussion of the lanthanide ion probe experiments. Below pH 4.5 the spectral changes in the 2.3 to 2.5 ppm region of the spectrum are too confused to be certain of the pH behaviour of resonances comprising L11.

4.2.7 Lysine εProtons

The resonances of these protons were considered generally in section 3.3, and Fig. 4.3 shows that they all begin to titrate upfield at around pH9 as expected for lysine residues which in a random coil peptide show a pKa of about 11. We do note though that the most upfield of the three

triplets (a) in Fig. 4.1B shows a small inflection in its pH curve between about pH 4 and 7, but this will not be commented on here.

4.2.8 αCH Proton Resonances

The pH versus shift curves for some of the downfield shifted resonances have been included in Fig. 4.3 to show that some are quite markedly affected and reflect ionisations discussed above although no detailed correlations have been made as yet. αCH proton resonances are strong indicators of the peptide backbone status and it is not surprising that these resonances do show pronounced changes as parts of the molecule unfold and a brief summary of this is now considered.

4.2.9 Protein Unfolding

We began this section by observing that kringle 4 on going to very low pH underwent a reversible denaturation, but we have seen that this is by no means a continuous process. The resonances of Trp A, His A and Met B, for instance, have all disappeared from the spectrum on reducing the pH to 4.5 with His A and Met B peaks clearly reappearing in their random coil shift positions indicative of these side chains having unfolded. However, there are many resonances completely unaffected by this process and which do not broaden out till well below pH 3.8 with the whole protein being unfolded below pH 2.8. However, the precise nature and extent of these separate stages is not clear and indeed the pH dependence of the NMR spectrum is seen to be somewhat complex.

The pH titration as a whole serves once again to demonstrate that the kringle 4 structure is a tightly folded one with many side chains in close proximity to each other. Some of the additional side chain interactions suggested by the results of the pH titration but which must be regarded as tentative are incorporated into Fig. 3.28 and shown in Fig. 4.4. Furthermore, the pH dependence of certain resonances has confirmed a number

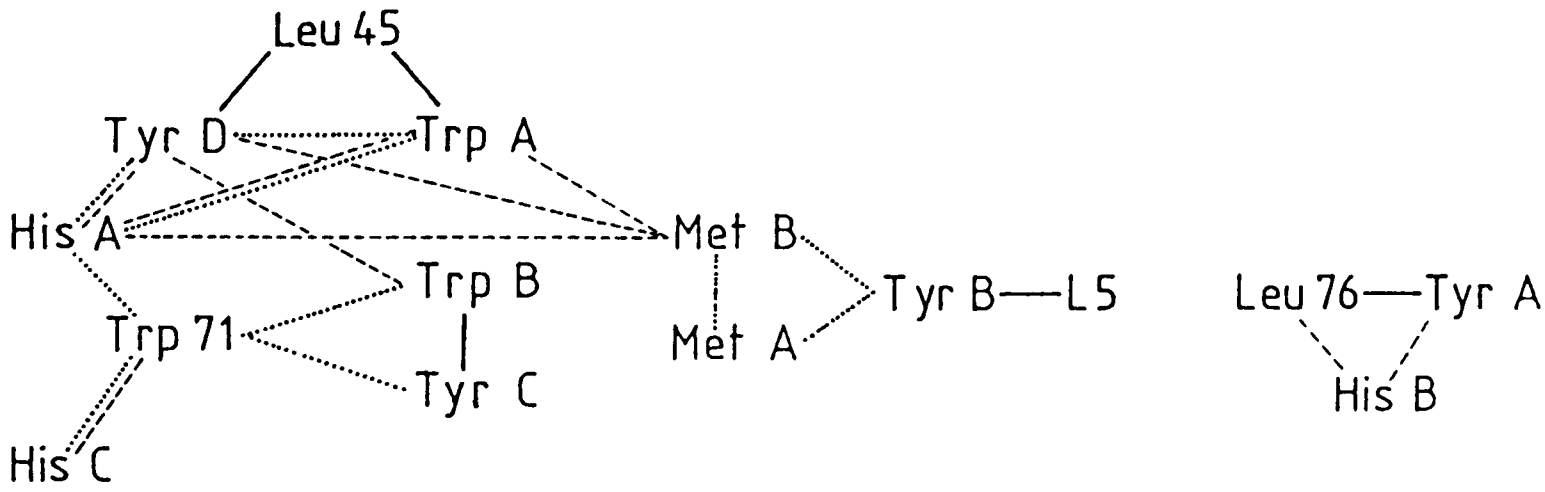

Fig. 4.4 — and .... (more tentative) proximities indicated by NOE experiments (Fig. 3.28)
- - - proximity indicated by the results of the pH titration.

of assignments which were made in the previous chapter, such as the lysine εCH_2 protons, for instance, and in particular some of the tyrosine peaks. With regard to the latter it is convenient at this point to briefly consider the second stage assignment of the tyrosine residues as this will aid considerably the discussion in succeeding sections. In addition the histidine residues can also be assigned at the same time.

4.2.10 Tyrosine and Histidine Assignments

It has been possible to make these assignments largely through the use of chemically modified kringle 4 samples. The NMR spectra of these proteins will be discussed in detail in chapter 5, but selected spectra are shown here to support the statements made. Thus, Fig. 4.5(b) shows the aromatic region of the spectrum of kringle 4 in which tyrosine 40 in the sequence has been nitrated. This can be compared to that of the native protein under similar conditions in Fig. 4.5(a) and it is seen that the two spectra are very similar. However, the most significant difference is the absence of peaks R9 and R13, assigned to Tyr D, from the spectrum of the modified protein. Hence, we can immediately assign Tyr D to Tyr 40 in the sequence. Closer inspection of Fig. 4.5(b) shows some additional peaks which arise from the nitrated Tyr 40 side chain and these will be discussed in Chapter 5.

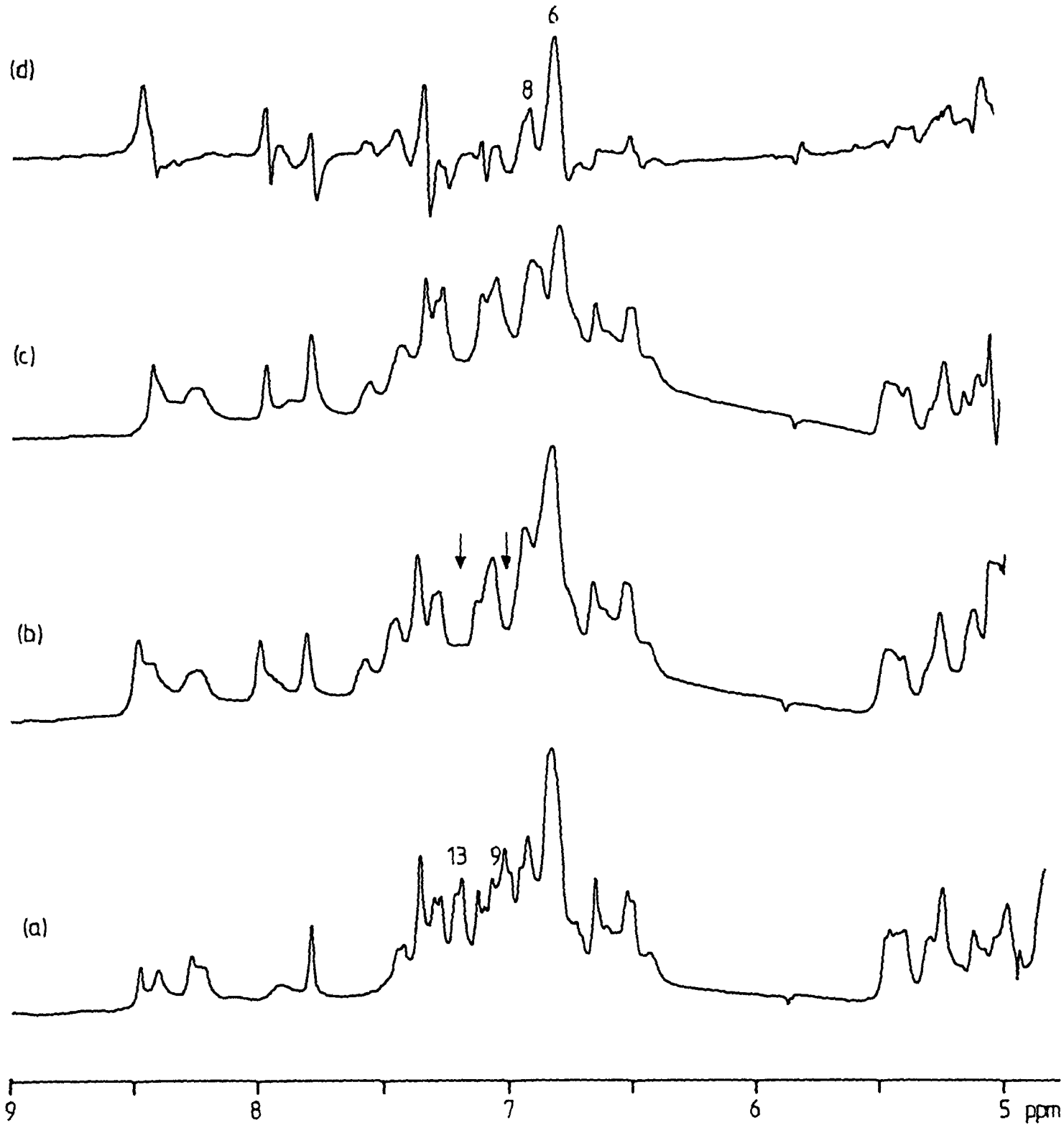

Fig. 4.5 Aromatic region of the spectra; 37°C, pH 5.5. (a) Native kringle 4 (b) Nitrated tyrosine 40 kringle 4 (c) Nitrated tyrosines 40 and 49 kringle 4 (d) Difference spectrum of (b)-(c).

Figure 4.5(c) shows the aromatic region of the spectrum of kringle 4 containing both nitrated tyrosine 40 and tyrosine 49. Comparison with Fig. 4.5(b) shows very little difference and as expected peaks R9 and R13 are again absent and the new resonances of the modified Tyr 40 are present. However, additional resonances from the nitrated Tyr 49 are not readily apparent. Fig. 4.5(d) shows the result of subtracting the double tyrosine nitrated protein spectrum from that of the mono, and most noticeable is the appearance in the difference spectrum of resonances R6 and R8 previously assigned to Tyr B. In actual fact, close comparison of the relative intensities of these peaks in the spectra of Fig. 4.5 demonstrated this without recourse to a difference spectrum which is somewhat confused by the presence of "dispersion mode" peaks due to a slight mismatch of sample pH between the two constituent spectra. Nevertheless, Tyr B is assigned with reasonable confidence to Tyr 49 in the sequence. The additional resonances of the nitrated Tyr 49 residue remain elusive in the difference spectrum and this matter will be considered in more detail in the next chapter.

Figure 4.6A and B compares the spectrum of the modified protein in which the first disulphide bridge between Cys 1 and Cys 79 has been broken, with that of the native protein (incidentally both samples contain bound 6 aminohexanoic acid, which as will be shown subsequently for both proteins, has only small effects on the NMR spectrum relative to that of the native sample). In the aromatic region of the spectrum the most obvious difference is the complete absence of R2 from the spectrum of the modified protein. Reference to Fig. 3.2 or Fig. 3.17 shows that tyrosine 2 is likely to be most affected by the disruption of the first disulphide link, and so Tyr A is assigned to Tyr 2 in the sequence. It is not possible to confirm that the meta proton resonance, R5, of this residue has been similarly affected, but this is presumed to be the case.

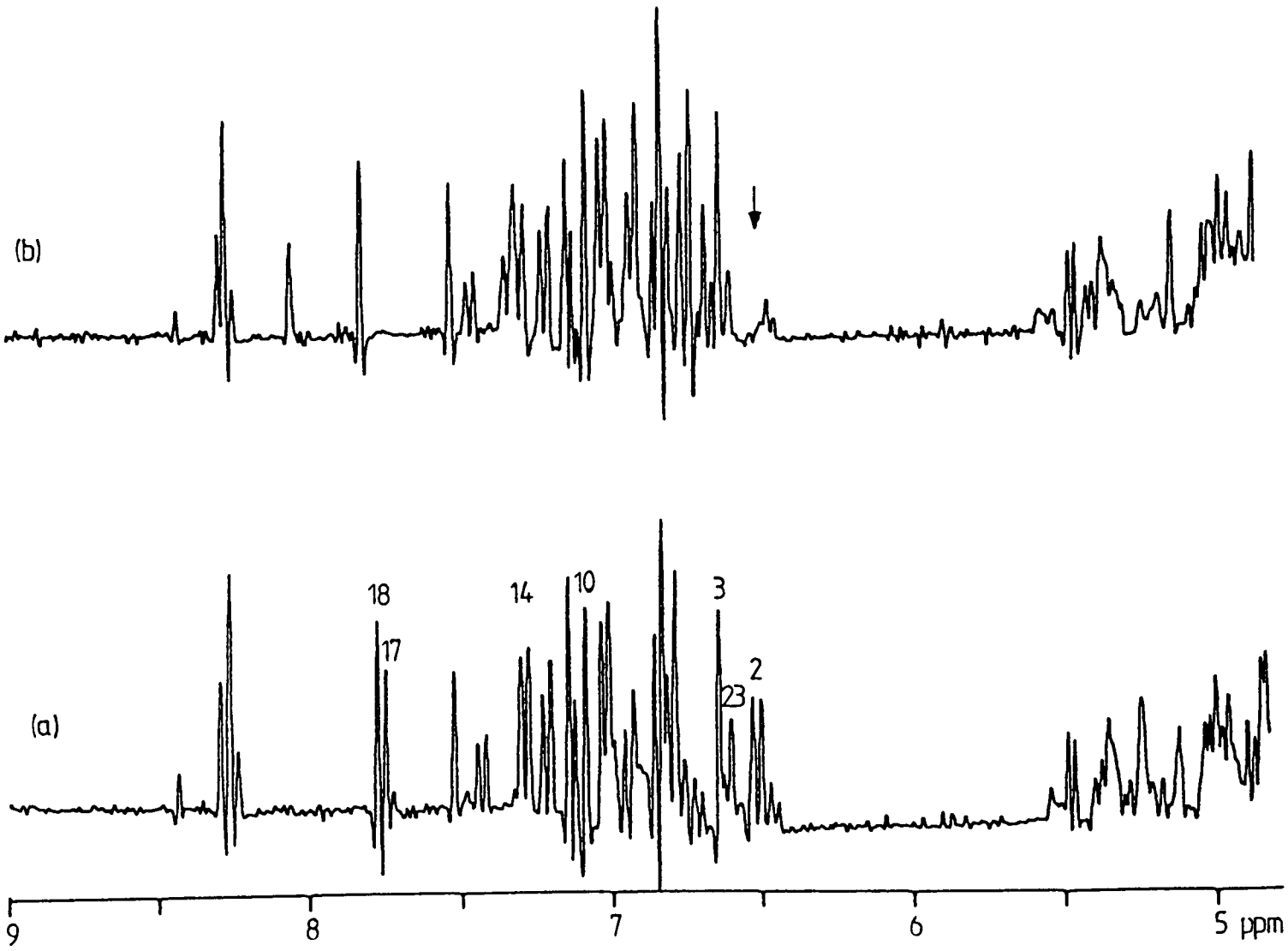

Fig. 4.6A Aromatic region of the spectra of samples containing 6 amino-hexanoic acid; 37°C. (a) Native kringle 4, pH 7.2 (b) Cys 1-Cys 79 cleaved kringle 4, pH 7.4. Resolution enhanced spectra.

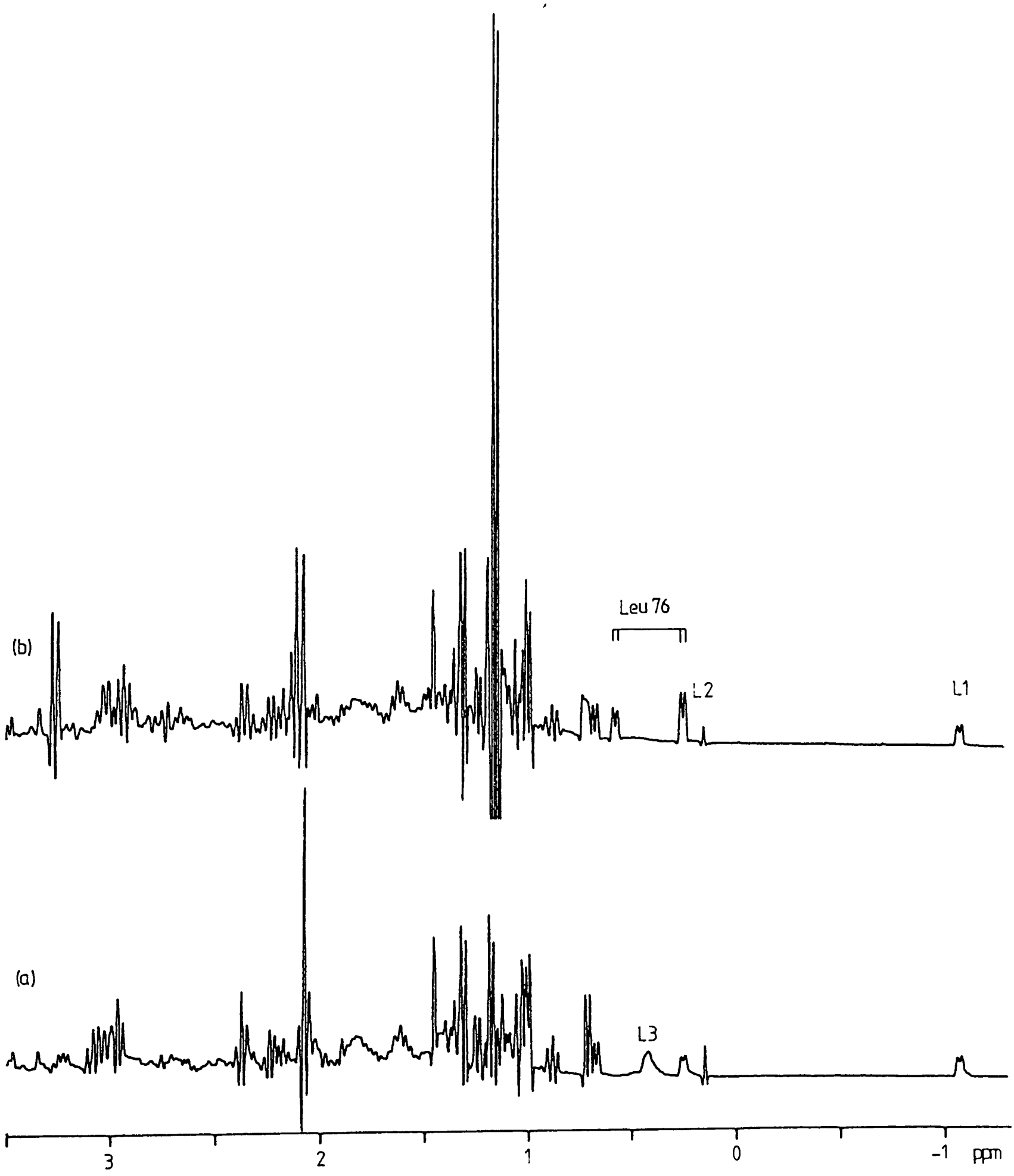

Fig. 4.6B Aliphatic region of the spectra of samples containing 6 amino-hexanoic acid; 37°C. (a) Native kringle 4, pH 7.2 (b) Cys 1-Cys 79 cleaved kringle 4, pH 7.4. Resolution enhanced spectra.

However, the assignment is amply confirmed by the effect on the methyl resonances of Leu 76 (L3 in the native protein) of the modification. Fig. 3.24(d) demonstrated a strong Overhauser enhancement of the resonances of Tyr 2 (A) on preirradiation of L3 and Fig. 4.6B(b) shows that the modification also results in substantial alteration in the methyl proton resonances of Leu 76 (the upfield doublet is coincident in chemical shift under these conditions with the L2 doublet of Leu 45). This is also in full agreement with its proximity to the site of chemical modification in terms of the primary sequence. Finally, His B was indicated from the results of the pH titration to be close in space to both Leu 76 and Tyr A (2) and indeed, His 3 in the sequence would similarly be expected to be affected by a modification that destroys the nearby internal bridge. Fig. 4.6A shows that R17 of His B is altered in resonance position by the modification although the C4 proton resonance, R10, appears unaffected. Moreover, the resonances of His A and His C are practically identical in both spectra and so the assignment of His B to His 3 is made. This in turn means that His A and His C arise from the two histidines either side of arginine 32. Llinás et al., (1983) have made the assignment of His C to His 31 from the similarity in resonance positions between the spectra of kringle 1 and kringle 4, with His 31 being the only conserved histidine residue in the two sequences. Thus, His A is then assigned to His 33 in the sequence. We note from these assignments that the most unusual histidines in terms of their pH dependence and proton chemical shifts are found to be the two very close in the sequence, while His 3 (B) which shows behaviour closest to that of a random coil residue is near to the N terminal end of the protein. However, we reiterate the findings of the pH titration that His 3 (B) is nevertheless not freely accessible to the solvent as it was

shown to unfold with Tyr 2 (A) and Leu 76 along with the rest of the protein below pH 3. Thus, we have seen that these three residues clustered around the first disulphide bridge in kringle 4 are profoundly altered by its cleavage. This grouping of residues will be independently confirmed by the results of adding copper II ions to the native protein as will be discussed in section 4.3 below.

Three out of four sets of recognised tyrosine resonances have now been assigned to residues in the sequence and the resonances of one tyrosine ring have not been identified in the spectrum. The two remaining tyrosines are at positions 9 and 73 in the sequence and to one of these Tyr C must be assigned. Considering the effects of breaking the first disulphide bridge would have on the two possible tyrosine residues, suggests that Tyr 9 would be much more affected than Tyr 73 as in principle the chain containing Tyr 9 would now be completely free, only eight residues away, whereas the region around Tyr 73 would be expected to be considerably less altered. Indeed, we see from the spectra of Fig. 4.6 that resonances R3 and R23 of Trp 71 and L4, L5 of Val 69 are almost the same for the modified protein as for the native one, strongly indicating the modification to have very little effect on the residues around Tyr 73, before the third disulphide bridge. Now it is also seen from Fig. 4.6A that resonance R14 assigned to Tyr C is unchanged in the spectrum of the modified protein. In addition R18 is only marginally altered in chemical shift and, as was shown in section 3.4, R18 and the resonances of Tyr C (R14, R6) are connected in the native protein via a strong Overhauser enhancement. This will be demonstrated to be the case also for the modified protein in Chapter 5. Thus, the fact that the resonances of Tyr C are unchanged by the breakage of the first disulphide bridge leads us to the assignment of the Tyr C to Tyr 73 in the sequence. In support of the proposed large conformational change of the loop of the protein chain

bearing Tyr 9, on removing the link to the remainder of the protein provided by the Cys 1 residue, we note the substantial intensity at 1.15 ppm in the modified protein spectrum (Fig. 4.6B). From the composition of the protein and the chemical shift, this peak is most likely to arise from threonine methyl protons and looking at the sequence reveals five of the eleven such residues in the protein are contained in the same loop of the chain bearing Tyr 9. Thus, the assignment of Tyr C to Tyr 73 is strengthened and it is rather unlikely that the assignment should have been made to Tyr 9. However, this does mean that the resonances of Tyr 9 are either too broad to be observed in the spectrum of the native protein perhaps through some exchange process if part of the chain on which it lies is relatively flexible or that the resonances are of complex form maybe arising from an immobilised ring and/or lie in a crowded part of the spectrum and so have not been clearly distinguished. In either case we have no indication from the spectrum of the behaviour of Tyr 9 on perturbing the protein with various probes and ligands, indicentally, such is the situation also for phenylalanine 63. In various sections to come additional resonances will be identified in the aromatic region of the spectrum assumed to arise from protons of these residues but so far complete coupling patterns for either of them have not been conclusively demonstrated. This is unfortunate, especially in the case of Tyr 9 as it would form a useful reporter group for a part of the molecule for which at present we have none. However, the residues so far assigned enable us to monitor much of the protein and combined with the NOE and pH data summarised in Fig. 4.4 allows us to propose a preliminary structure for a good part of the protein.

4.2.11 Preliminary Structural Model

Table 4.1 lists the resonances to the completely assigned residues in the sequence within the kringle structure, and thus Fig. 4.7 has been compiled showing the sequence with lines joining residues that have been shown to be closely related in space from either NOE or pH experiments and summarised in Fig. 4.4. By "closely related" is meant some 5Å or less in many cases. No attempt has been made in Fig. 4.7 to differentiate between more tentative and well defined data that was indicated in Fig. 4.4 and discussed in the text. However, with the additional second stage assignments having been made it can be seen that many of the inter residue relations are consistent with their positions within the sequence. Further corroboration of many of the structural elements proposed in Fig. 4.7 will be provided by experiments described in what follows.

As yet it has not proved possible to unequivocally assign Trps A and B specifically to each of Trps 25 and 61. Similarly, the two methionine methyl resonances have not been conclusively attributed to Mets 28 and 47 in the sequence. It is tempting to consider Trp A as Trp 25 and Met B as Met 28, just three residues away in the sequence, to explain the simultaneous broadening of the resonances of Trp A, Met B, His A and R9 of Tyr 40 (D) as the pH is lowered towards pH 4.5. It could then be proposed that part of the loop containing Trp 25 and Met 28 is destabilised on lowering the pH and unfolds leaving the remainder of that loop and the two inner ones intact to denature at much lower pH. However, this is conjecture and as yet we have no other data to confirm this.

Unfortunately, we have not yet made a second stage assignment of the methyl doublet at L5 tentatively assigned to a threonine side chain in

Table 4.1 Listing of Resonances to Assigned Residues in the Kringle 4 Spectrum.

AROMATIC RESIDUES			
	His A	His 33	R20, R7
	His B	His 3	R17, R10
	His C	His 31	R16, R21
	Trp A	Trps 25, 61	R1, R12, R15, R19
	Trp B		R18, R22
	Trp C	Trp 71	R3, R4, R11, R23
	Tyr A	Tyr 2	R2, R5
	Tyr B	Tyr 49	R6, R8
	Tyr C	Tyr 73	R6, R14
	Tyr D	Tyr 40	R9, R13
ALIPHATIC RESIDUES			
		Leu 45	L1, L2
		Leu 76	L3
		Val 69	L4, L5
	Met A	Mets 28, 47	A
	Met B		B

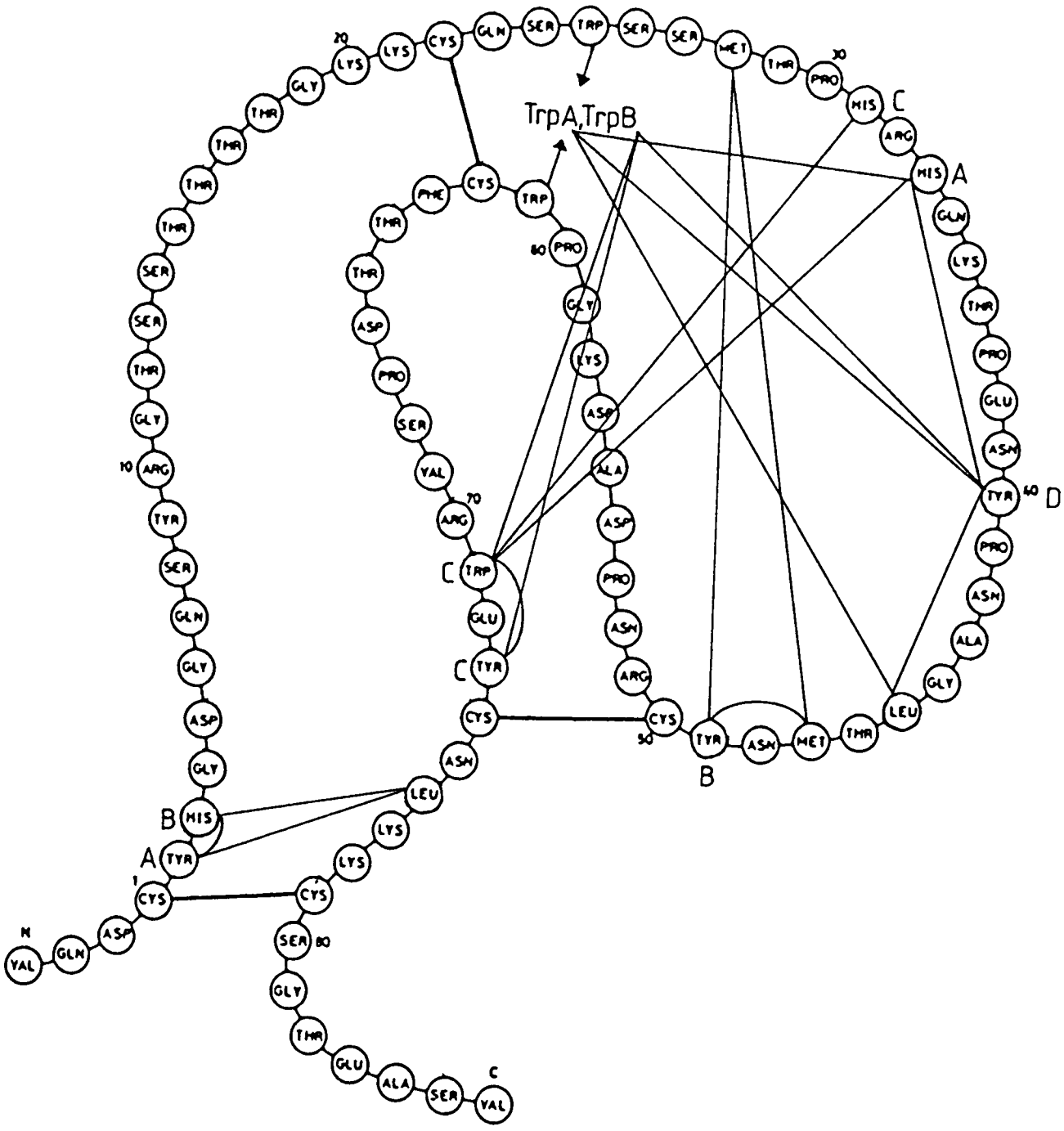

Fig. 4.7 Primary structure of kringle 4. Lines connect residues found to be close in space within the three dimensional structure (see text).

section 3.3 As mentioned Llinás et al., (1983) from homology with the spectrum and sequence of kringle 1, have suggested possible residues to include threonines at positions 12, 16, 64, and 65. However, the data shown in Fig. 4.7 does not favour one particular residue over the other three. In addition, the coincidence of chemical shifts of the L5 doublet with one of the methyl doublets of Val 69 has masked NOE data for the latter residue as discussed in section 3.4. Consequently, data on the spatial relations of Val 69 has been sought from other experiments described below.

One feature is particularly noticeable in Fig. 4.7 and that is the proximity of residues around the second disulphide bridge to those near to the third. For instance Trp A being close to Leu 45 and Trp B close to Tyr 73 and Trp 71. Thus, it would be predicted that these two disulphide bridges themselves are not very far apart in the three dimensional structure. We have been in communication with the Swedish group working on the crystal structure of bovine prothrombin fragment 1 which contains a kringle structure. Although their electron density maps go to a nominal resolution of 2.8Å, they are apparently of poor quality. Nevertheless, disulphide bridges appear more strongly and they have confirmed that the second disulphide bridge is relatively close to the third (Sjölin, 1983, personal communication). This presupposes that the kringles of different proteins maintain a similar structure, but as we saw in Fig. 3.19 the upfield shifted methyl resonances of the conserved Leu 45 was at very similar chemical shift in both the spectrum of bovine prothrombin fragment 1 and that of human plasminogen kringle 4. Further discussion along these lines will be continued in Chapter 7, but we note the information that is beginning to accrue on the solution structure of kringle 4. Further progress and refinement is provided through metal ion probe and ligand binding experiments discussed in the remainder of this

chapter.

4.3 Copper II Ion Binding

Copper II ions have a particular affinity for imidazole rings and in particular histidine side chains are frequent ligands to copper in copper containing proteins. (Martell, 1958: Cass and Hill, 1980). Thus, initially copper II ions were added to kringle 4 in order to demonstrate corresponding C2, C4 proton resonances of the same histidine side chain at a time before the 2 dimensional J correlated spectra of figure 3.7 and 3.11 could be obtained. The results of one such experiment are shown in Fig. 4.8. Unfortunately the protein sample had been dissolved in D_2O for some time and R17 from the C2 proton of His 3 (B) had almost completely disappeared due to the exchange with solvent deuterium atoms. However, previous experiments had shown initial addition of Cu^{2+} ions rapidly broadened resonances R17 and R10 from the spectrum and the disappearance of R10 ion can still be readily seen in Fig. 4.8. At the same time but not quite so rapidly the methyl proton resonance (L3) of Leu 76 also broadens and eventually disappears along with both of the resonances of Tyr 2 (R2, and R5 on the upfield edge of the composite peak R6), by a molar Cu^{2+} to protein ratio of about 1.2:1. This is interpreted as the Cu^{2+} ions binding in fast exchange to the imidazole ring of His 3 leading to the resonances R17, R10 being broadened. As the concentration is increased resonances in the immediate vicinity of the binding site, namely those arising from Tyr 2 and Leu 76 are also broadened. These three residues are all clustered in the sequence around the first disulphide bridge and this data fully vindicates the assignments and spatial grouping of these side chains as discussed in the previous section. We note further that the resonance from the N-terminal valine methyl groups also disappears from the spectrum at a still slower rate and

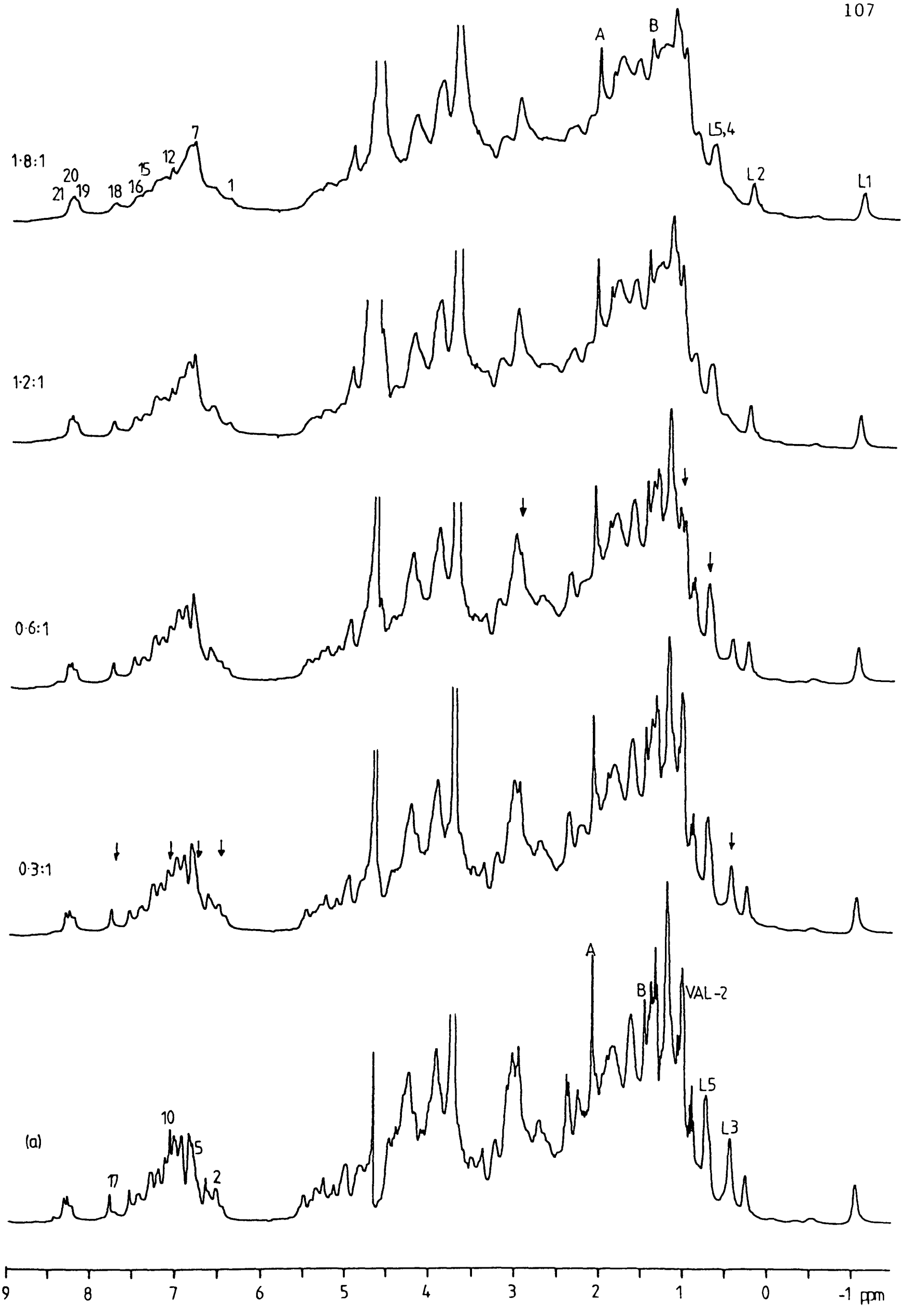

Fig. 4.8 Addition of Cu^{2+} ions to kringle 4; 37°C, pH 7.4. (a) Native protein with no added metal ions. Approximate values of the metal ion to protein concentration ratios are given for the other spectra.

during the titration the protein solution turned from colourless to mauve, typical of the biuret reaction. As seen with polypeptides (Sigel and Martin, 1982) this is taken to mean that the Cu^{2+} coordinates not only with His 3 but also with the amino group of the N-terminus.

It can also be discerned from Fig. 4.8 and was obvious from resolution enhanced spectra that the L5 doublet also broadened out from the spectrum over a similar copper concentration range as the effects already mentioned. This suggests that it is reasonably close to the main copper binding site. However, curiously the tyrosine residue to which it gives a strong Overhauser enhancement, Tyr 49 (B) appears unaffected by the metal ion binding as judged by the little change in intensity at R6, R8 even at the highest metal to protein ratio. The reason for this is not clear but it maybe simply that the methyl group, giving rise to L5 comes between the metal atom and the tyrosine ring and the latter is then too far away to be affected by the presence of the metal ion. We also note that the most upfield of the lysine ε CH_2 proton resonances also broadens out over the same range and the significance of this is also not clear although it is noted that there are two lysine side chains between Leu 76 and the cysteine of the first disulphide bridge.

At the highest metal to protein ratio non-specific broadening of many resonances in the spectrum is occurring and further metal ion additions were of no use. However, some resonances are noticeably unaffected and included among these are L1 and L2 of Leu 45 and the resonances of Trp A; R1, R12, R15, R19. Both residues are known to be close in space from NOE experiments and the slow exchange of the NH proton of Trp A suggests that it is well shielded from the solvent, being within the molecule and so inaccesible to non specific binding of copper ions. Similarly we note that both methionine methyl proton resonances and those of Val 69 (L4, L5) along with the peaks from Tyr 49(B)

mentioned above are also noticeably unaffected. But more curious is the lack of any marked effect on the resonances of the other two histidine residues His 31 (R21, R16) and His 33 (R20, R7). The situation with respect to the latter is perhaps understandable in that from the pH dependence of its resonances the side chain appears to get folded into the structure in its protonated form and so would be unfavourable for binding a positive metal ion. However, this is not the case for His 31 and indeed its pKa is lower than that of His 3 which would be expected to facilitate binding of the Cu^{2+} ion. A number of suggestions can be made to explain this but the precise reason is not known as yet.

Thus, in summary, it is seen that there is one principle binding site for Cu^{2+} ions on kringle 4 at the N terminal end of the molecule around the first disulphide bridge and His 3 in the sequence. Before considering the effects of adding tripositive lanthanide ions to the protein, the spectral changes induced by ligand binding will be discussed. In connection with this, though, a similar copper II ion titration was carried out in the presence of added ligand (6 aminohexanoic acid) and the results were essentially identical, especially with regard to the immediate broadening of the resonances of His 3 and the very selective effects on Tyr 2 and Leu 76. This strongly suggests that not only does ligand binding not compete with that of Cu^{2+} ions (and vice versa was also seen to be true) but that the region around the first disulphide bridge incorporating these residues is not affected by the ligand binding. It will be seen in the next section that the ligand binding studies amply confirm the latter conclusion, but we begin with a more general discussion of some results of other ligand binding studies.

4.4 Ligand Binding

4.4.1 Introduction

Intact plasminogen and the products of elastase digestion containing separately kringles 1+2+3 and kringle 4, all bind to lysine-Sepharose and therefore are said to have lysine binding sites. There have been a number of studies of these sites, using various ω-aminocarboxylic acids as lysine analogues (see for instance, Markus et al., 1978; 1979). However, we will consider here the results of Winn et al., (1980) who determined the concentration of various analogues required to displace 50% of the bound protein from lysine-Sepharose. Some of their results are shown in Table 4.2. (Lys-plasminogen is readily obtained from the native Glu-plasminogen with the loss of the first seventy-six residues from the N terminus. The prefix denotes the N terminal residue). The values for the range of ω-aminocarboxylic acids studied demonstrate a stringent requirement for optimal binding on the chain length. For all the proteins, the eluting efficiency of the amino acid was found to be optimal when the calculated position between nitrogen atom and carboxylic carbon in the fully extended chain was 6.8Å - a length exactly met in tranexamic acid. The ligand AMBOC was not considered by these workers but it is known to bind to plasminogen with greater affinity than tranexamic acid (Dr. S.A. Cederholm-Williams, personal communication).

It can be seen from Table 4.2 that binding to the protein is primarily mediated through the amino terminal end of the ligand. This is supported by the data for arginine analogues for instance, despite the additional chain length and confirmed in practice by the following experiment. In Fig. 4.9(a) the aliphatic region of the spectrum is shown for kringle 4 saturated with the ligand, 6 aminohexanoic acid. To this sample was added approximately the same amount again of ligand and from the resulting spectrum the original was subtracted to give the difference

Table 4.2 Displacement of Plasminogen and Plasminogen Fragments from Lysine-Sepharose by Lysine Analogues. c_{50} is the Concentration of Analogue Required to Displace 50% of the Protein from Lysine-Sepharose. Data from Winn et al., 1980.

	c_{50} (mM)	Plasminogen		Kringle	
		Glu-	Lys-	1+2+3	4
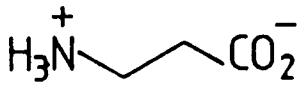		500	>1000	320	340
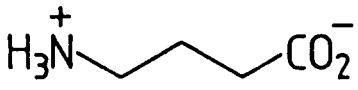		37	29	12	8·5
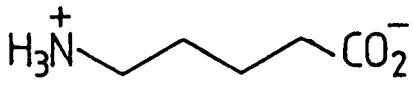		3·0	2·7	0·7	1·1
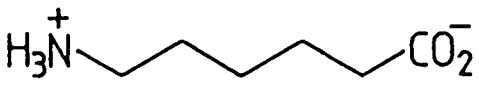	(6 Aminohexanoic acid)	2·0	3·1	0·9	1·0
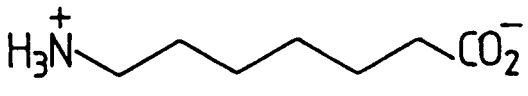		20	18	6·2	36
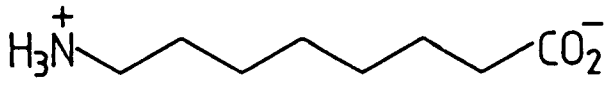		46	190	31	90
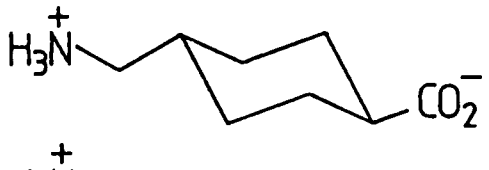	(Tranexamic acid)	0·35	0·46	0·11	0·23
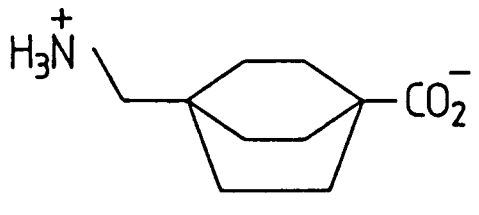	(AMBOC)		<0·46		
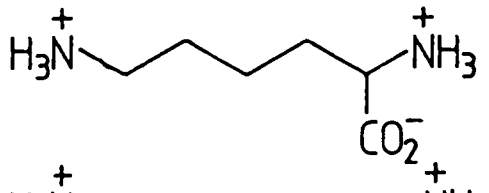	(L-Lysine)		29		
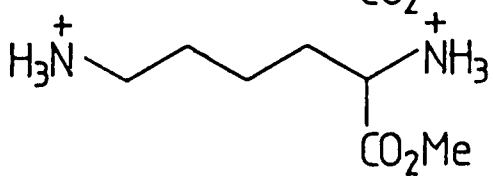			200		
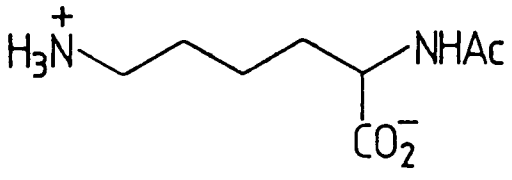			4·7		
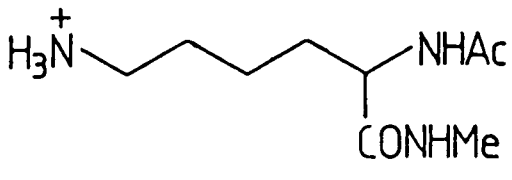			48		
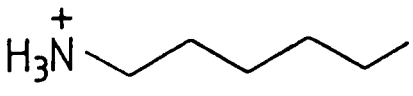			48		
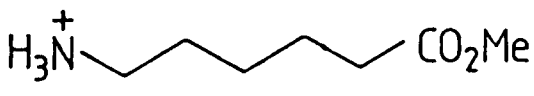			92		
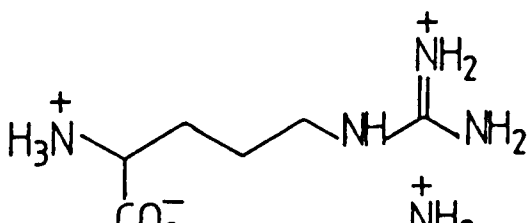	(L-Arginine)		390		
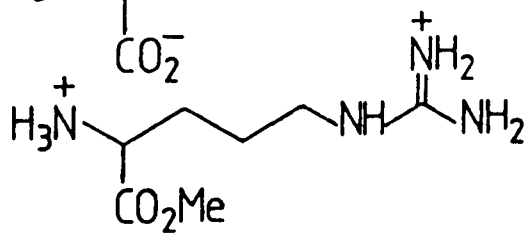			380		

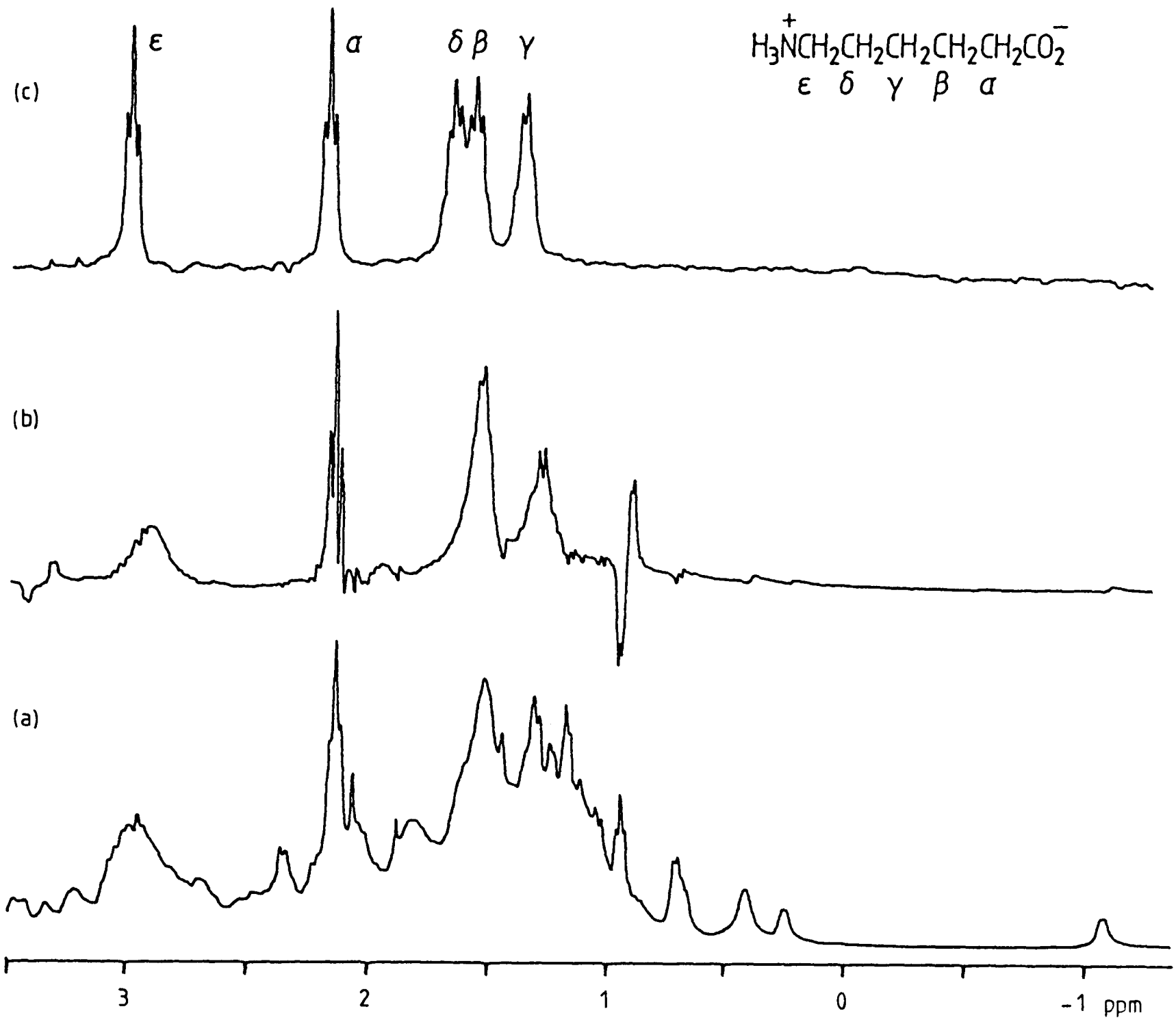

$H_3\overset{+}{N}CH_2CH_2CH_2CH_2CH_2CO_2^-$
ε δ γ β α

Fig. 4.9 37°C, pH 8.3 (a) Kringle 4 saturated with the ligand 6 amino-hexanoic acid.(b) Difference spectrum obtained from subtracting (a) from that acquired on adding more ligand to the sample of spectrum (a) (see text). (c) Assigned spectrum of the ligand.

spectrum of Fig. 4.9(b). Because the protein binding site is saturated with the ligand there should be no further change in the protein resonances on adding additional ligand to the sample and so the only resonances in the difference spectrum should be from the ligand. (In actual fact, the addition caused a slight change in the pH of the solution as demonstrated by the appearance in the difference spectrum of resonances from the N terminal valine methyl protons and confirmed by similar small shifts on the resonance of His 3(B) in the aromatic region). Fig 4.9(c) shows the spectrum of free 6 aminohexanoic acid (the assignments shown were confirmed by a pH titration) and comparison with Fig. 4.9(b) demonstrates the ε and δ peaks of the ligand to be considerably more affected by the binding than the α and β proton resonances with the γ peak in between. The greater broadening and shift of the ε CH_2 proton peak compared to that of the α protons is entirely consistent with the amino end of the molecule being more firmly bound than the carboxylic. This result is, of course what would be expected if a lysine residue within a protein is the natural ligand of this binding site. However, we note that the α and β CH_2 proton resonances are not immune to the binding process and indeed, the data on the ligands based on lysine and for the methyl ester of 6 aminohexanoic acid in Table 4.2, confirm that some of the binding is mediated by the carboxylic group but indicates a much weaker association. The value for Nα-acetyl-L-lysine-N-methylamide, simulating a lysine side chain within a protein, also confirms that a free carboxyl group or a terminal polar group capable of forming hydrogen bonds, such as that present on the latter ligand or on 5-aminopentanol, improves the ligand affinity considerably. These data suggest that more than a specific lysine residue may be involved in mediating the binding of the natural molecule to plasminogen in vivo. We now go on to consider in detail the effects of the binding of 6 aminohexanoic acid to kringle 4.

4.4.2 Spectral effects of 6 Aminohexanoic Acid Binding

4.4.2.1 Aromatic Region

Fig. 4.10 shows the effects on the aromatic region of the spectrum of adding 6 aminohexanoic acid to kringle 4 in solution. Cursory inspection reveals that the changes induced are not large and the majority of resonances show effects of fast exchange on the NMR time scale between their perturbed chemical shifts. The spectrum in Fig. 4.10 (d) is very close to that of the protein saturated with ligand, but no attempt has been made to derive a value for the binding constant because the shifts are all too small for any reasonable accuracy to be achieved.

Closer scrutiny of Fig. 4.10 reveals significant downfield shifts of R1 and R19 each by about 0.03 ppm, R12 moves in the same direction by 0.02 ppm but R15 is untouched - all resonances assigned to Trp A. Of the resonances of Trp B, R18 and R22 both shift slightly downfield by about 0.01 ppm but as will be seen below other resonances assigned to this residue are more significantly shifted. R3, R4 and R23 of Trp 71(C) are all unmoved through the titration but R11 has a notable downfield shift of 0.06 ppm. Thus, resonances of all three tryptophan residues are affected by the binding of 6 aminohexanoic acid to kringle 4.

R7 and R20 of His 33(A) show very small upfield shifts of about 0.01 ppm as do almost exactly the resonances of His 31(C), but the peaks assigned to His 3(B), R17 and R10, are completely unchanged. Although the effects of ligand binding are very subtle it is noteworthy that two histidines are affected while the third is not and this data in conjunction with the results of their pH dependence and the data of Fig. 4.4 again support their second stage assignments made above.

Considering the resonances of the assigned tyrosine residues reveals no change in those of Tyr 2(A) or Tyr 73(C). R9 and R13 of Tyr 40(D) both move downfield by 0.02 ppm. R8 assigned to Tyr 49(B) appears unmoved but

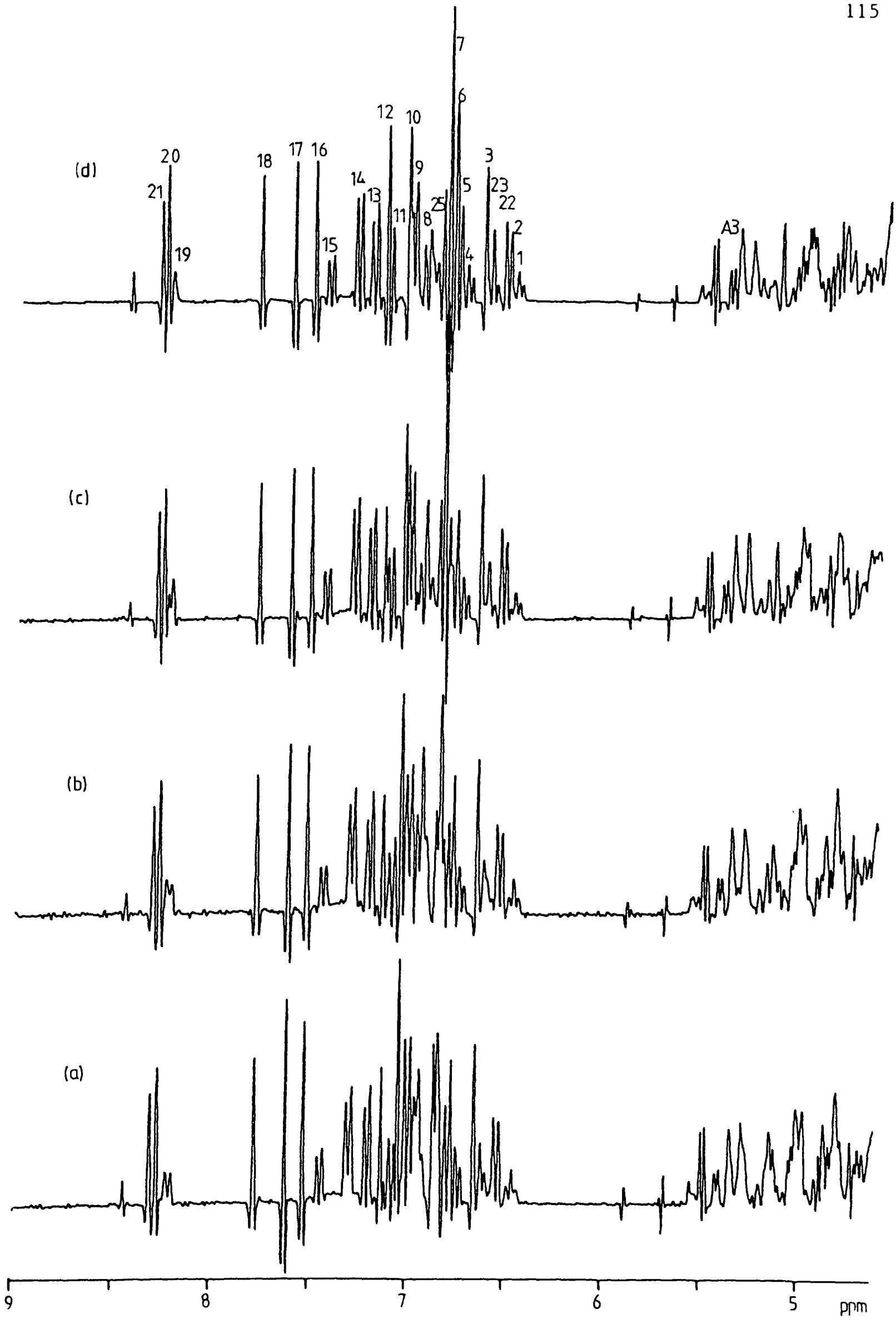

Fig. 4.10 Aromatic region of the resolution enhanced spectrum; 47°C, pH 8.4 showing the effects of adding 6 aminohexanoic acid to kringle 4. (a) Native protein (b) 0.2:1 (c) 0.5:1 (d) 1.1:1 approximate molar, ligand to protein concentration ratios.

R6 is not so easily resolved. Indeed, the non resolution enhanced spectra show very noticeable changes in the intensity of peaks R6 and R8 through the titration and these are reflected in Fig. 4.10. Some of these changes are accounted for by movements of two Trp B resonances from underneath R8 as will be described below. A new resolved peak is labelled R25 in Fig. 4.10(d). This and other features of the aromatic region of the spectrum will be considered in greater detail in the following subsection. A summary of the assigned aromatic residues that are affected or not by the binding of 6 aminohexanoic acid is given in table 4.3A. It is noteworthy that the grouping of the residues given in this table is in very good agreement with the groups of residues that have been shown to be close in space within the protein as summarised in Fig. 4.7.

Table 4.3A Lists the Aromatic Residues that are affected or not by the Binding of 6 Aminohexanoic Acid.

ALTERED	UNALTERED
Trp A	
Trp B	
Trp 71	
His 31	His 3
His 33	
Tyr 40	Tyr 2
	Tyr 49
	Tyr 73

4.4.2.2 NH and Aromatic Assignments

Fig. 4.11(a) shows the spectrum obtained immediately on dissolving a sample of kringle 4 fully bound with 6 aminohexanoic acid in D_2O. Comparison with Fig. 3.6(a) shows that there are changes in some of the labile proton resonances as well as more such resonances being

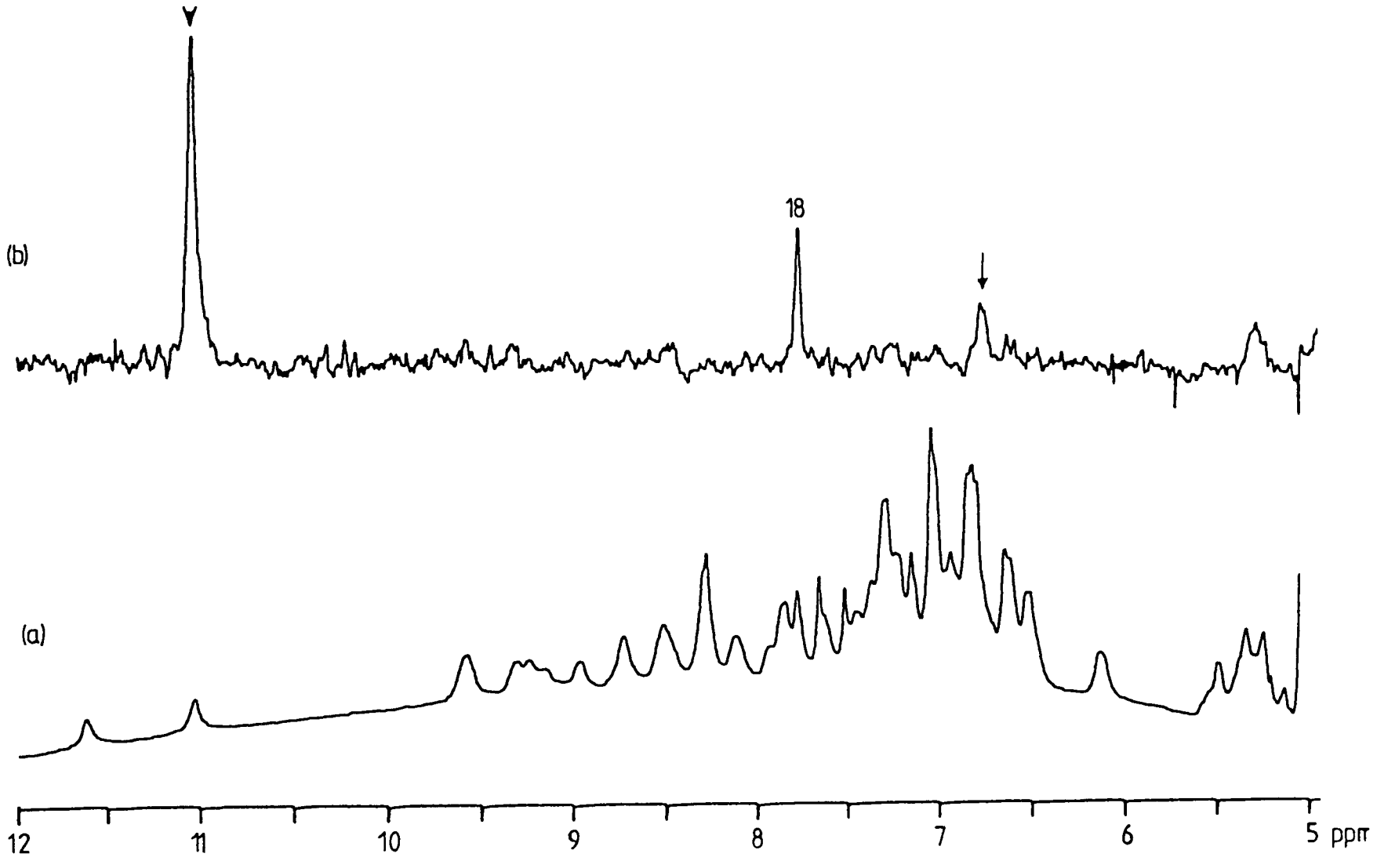

Fig. 4.11 30°C, pH 7.8 (a) Kringle 4 with added 6 aminohexanoic acid (b) NOE difference spectrum.

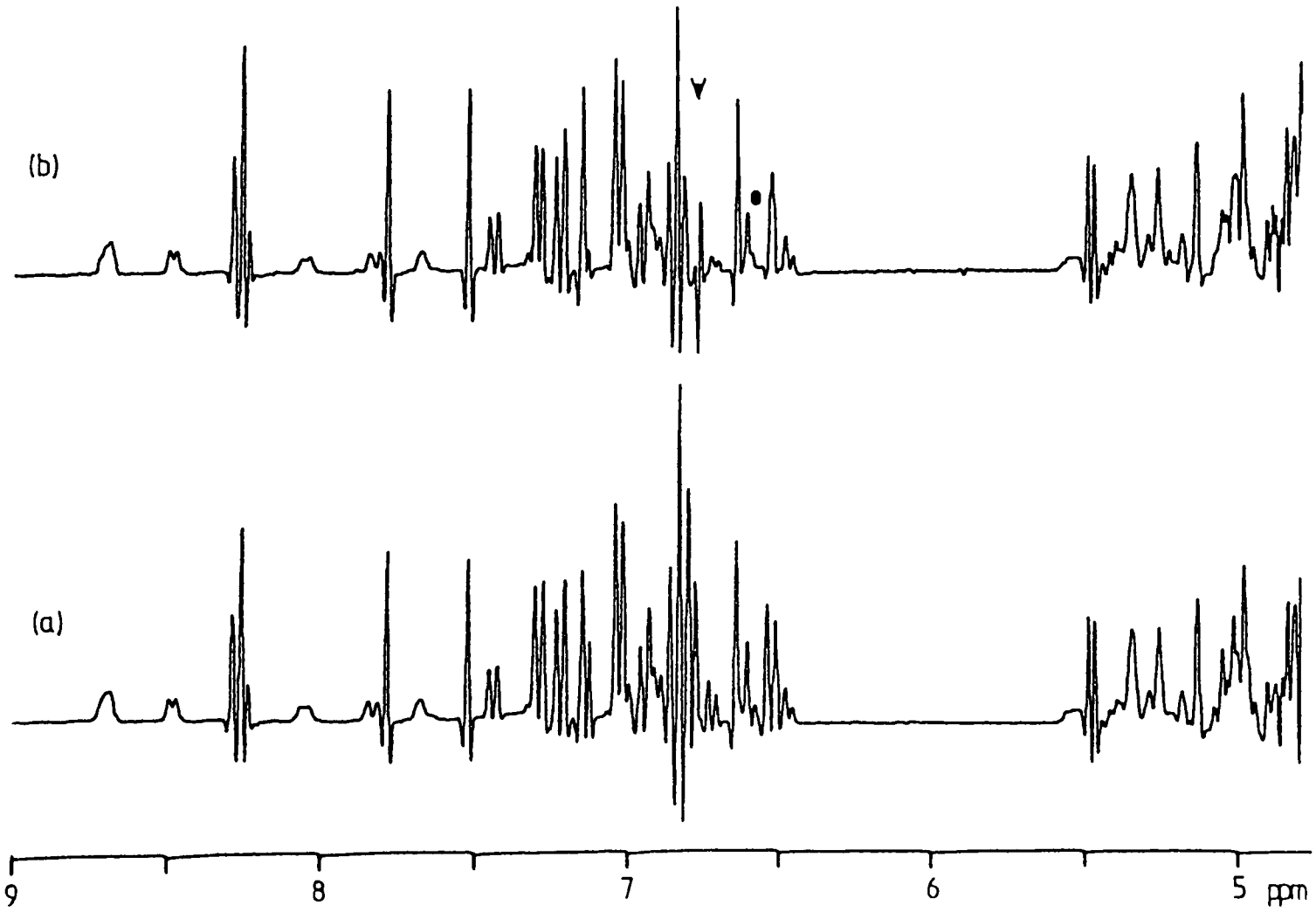

Fig. 4.12 47°C, pH 7.8 (a) Kringle 4 with added 6 aminohexanoic acid (some labile proton resonances are present). (b) Spin decoupling experiment. Resolution enhanced spectra.

present. Again no formal studies of exchange rates for these peaks have yet been undertaken nor have the number of such resonances been quantified, but the more persistent peaks will be briefly discussed below. However, the resonance at 11.05 ppm is a notable addition to the spectrum compared to that of the kringle without the ligand added. As with the Trp A NH seen again at 11.6 ppm, the chemical shift alone is very indicative of this resonance arising from an indole NH proton, and this is confirmed by the Overhauser enhancements resulting from the pre-irradiation of this peak as shown in Fig. 4.11(b). A singlet, R18 is clearly visible in the difference spectrum and another peak corresponding to the C7 proton of a tryptophan ring is present at 6.77 ppm. A spin decoupling experiment irradiating this resonance results in the triplet, R22 (moved downfield by the added ligand) collapsing to a doublet as seen in Fig. 4.12(b). Thus, the assignment of R18 as the C2 resonance of Trp B in section 3.2 is completely vindicated. We note that the C7 proton resonance is upfield shifted by at least 0.17 ppm by the added ω-aminocarboxylic acid ligand. A COSY experiment was required to determine the positions of the other resonances of Trp B and the contour plot is shown in Fig. 4.13. The same six cross peaks to the upfield triplets of each tryptophan are visible. As mentioned when discussing Fig. 3.8 the presence of bound ligand results in the C6 proton resonance of Trp A and the C4 proton peak of Trp B being almost coincident either side of 4.93 ppm - the Trp B resonance being moved 0.08 ppm downfield by the acid binding while the Trp C peak has been moved 0.07 ppm upfield, and the Trp A triplet being unchanged. The changes in the resonance positions of the indole protons of each tryptophan residue on saturating the ligand binding sites with 6 aminohexanoic acid at 47^{o}C are summarised in Fig. 4.14. (Note that in Fig. 4.14, the C4 and C5 assignments of Trp C have not been demonstrated so far and may actually be the C 7 and C6 and vice versa).

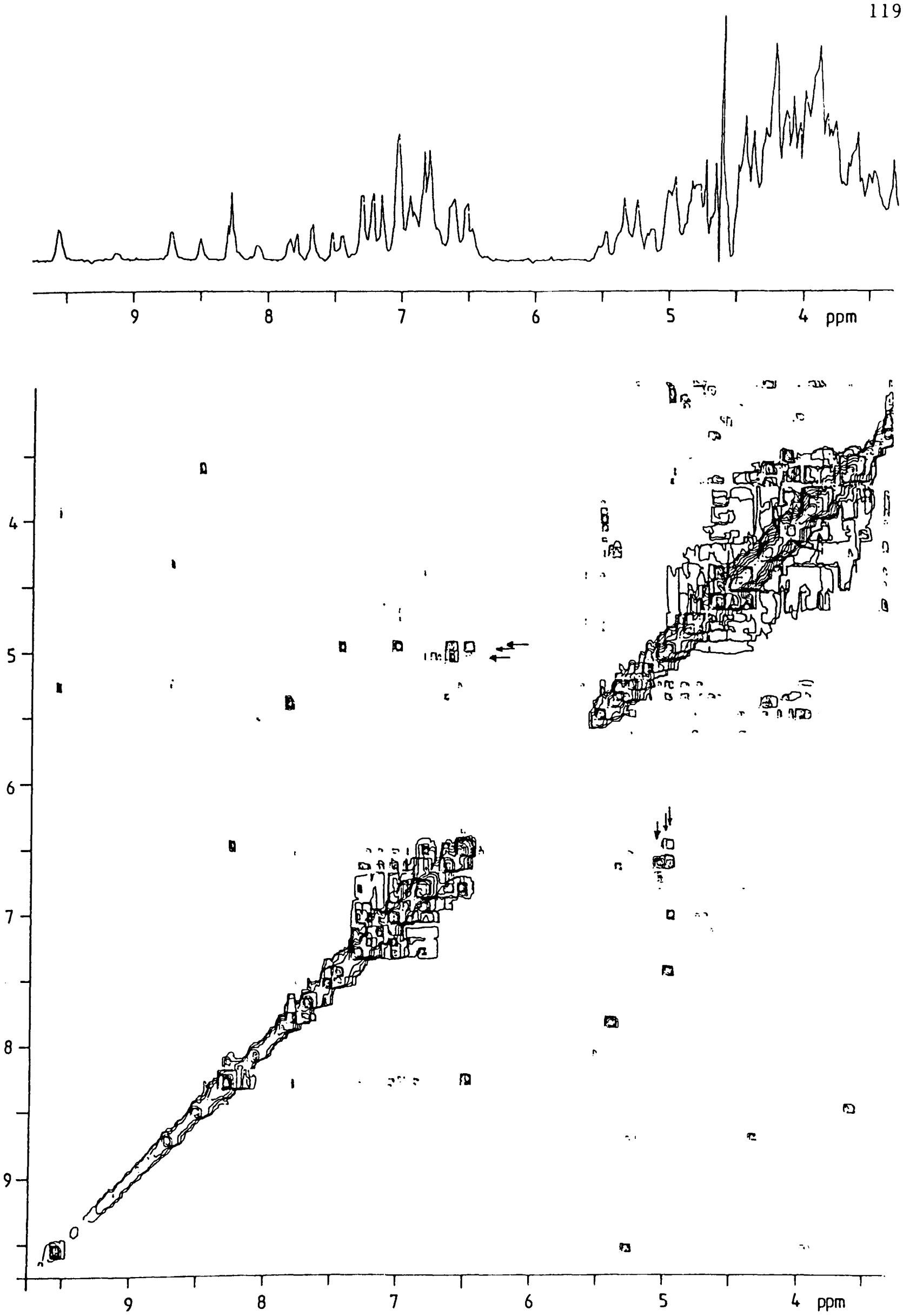

Fig. 4.13 Part of the 470MHz COSY spectrum at 37°C, pH 7.8 of kringle 4 saturated with the ligand 6 aminohexanoic acid.

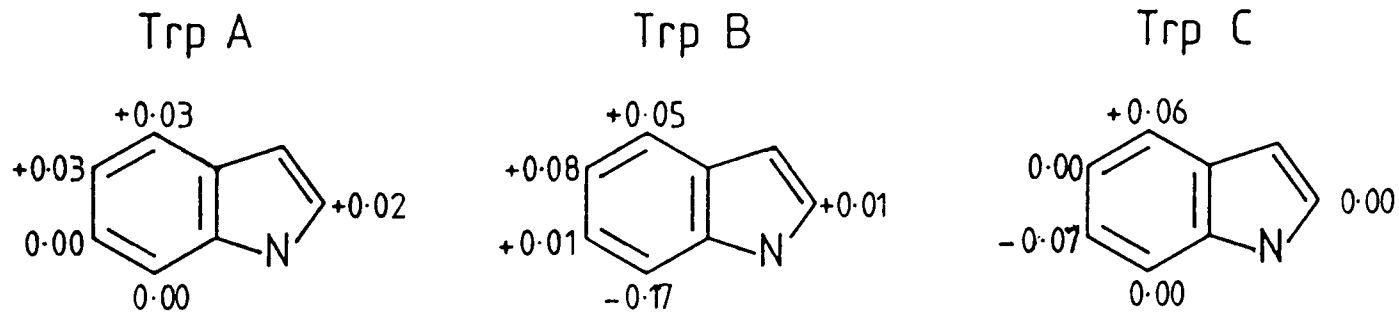

Fig. 4.14 Shifts (ppm) induced on the indole ring protons of kringle 4 on binding 6 aminohexanoic acid. (+ve sign indicates downfield, -ve sign upfield).

4.4.2.3 Unassigned aromatic residues

In this and the previous section all the assigned aromatic resonances have been accounted for and Fig 4.15 compares the real and simulated spectrum of the acid bound kringle 4. Only the assigned protons have been included in the simulation accounting for 37 of the 46 expected aromatic proton resonances. (The data used is given in Appendix II). Intensity from the tyrosine 9 and phenylalanine 63 has still not been identified in the spectrum and this matter is raised again as the presence of bound ligand provides a new set of conditions under which these resonances might be more readily identified.

As was found for the native protein spectrum in Fig. 3.16, the similarity between the real and simulated spectrum is quite good. Again there is a significant difference in intensity around 7.0 ppm with approximately two protons unaccounted for in the simulation and the possibility of one proton each at positions R13 and R14, otherwise the peak intensities are very similar between the two spectra. In particular, the changes in the region of peaks R5, R6, R7 and R8 remarked on in the previous section resulting from the ligand binding have been well accounted for. Only the new, unassigned resonance R25 of Fig. 4.10(d) on the edge of R8 is not included. Fig. 4.16 shows that a spin decoupling

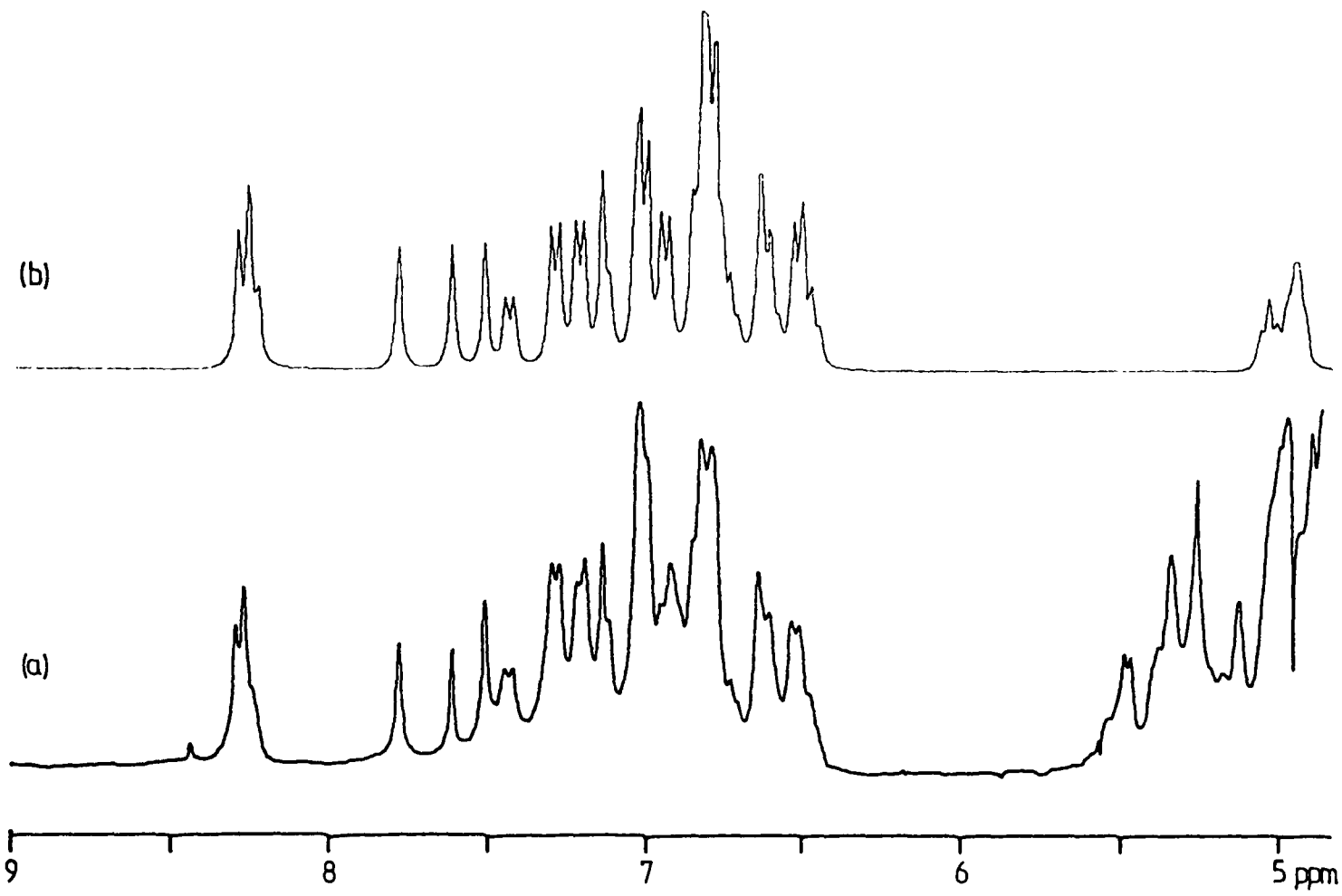

Fig. 4.15 (a) Real (b) Computer simulated spectrum of the aromatic region of kringle 4 in the presence of the ligand 6 amino-hexanoic acid (see text).

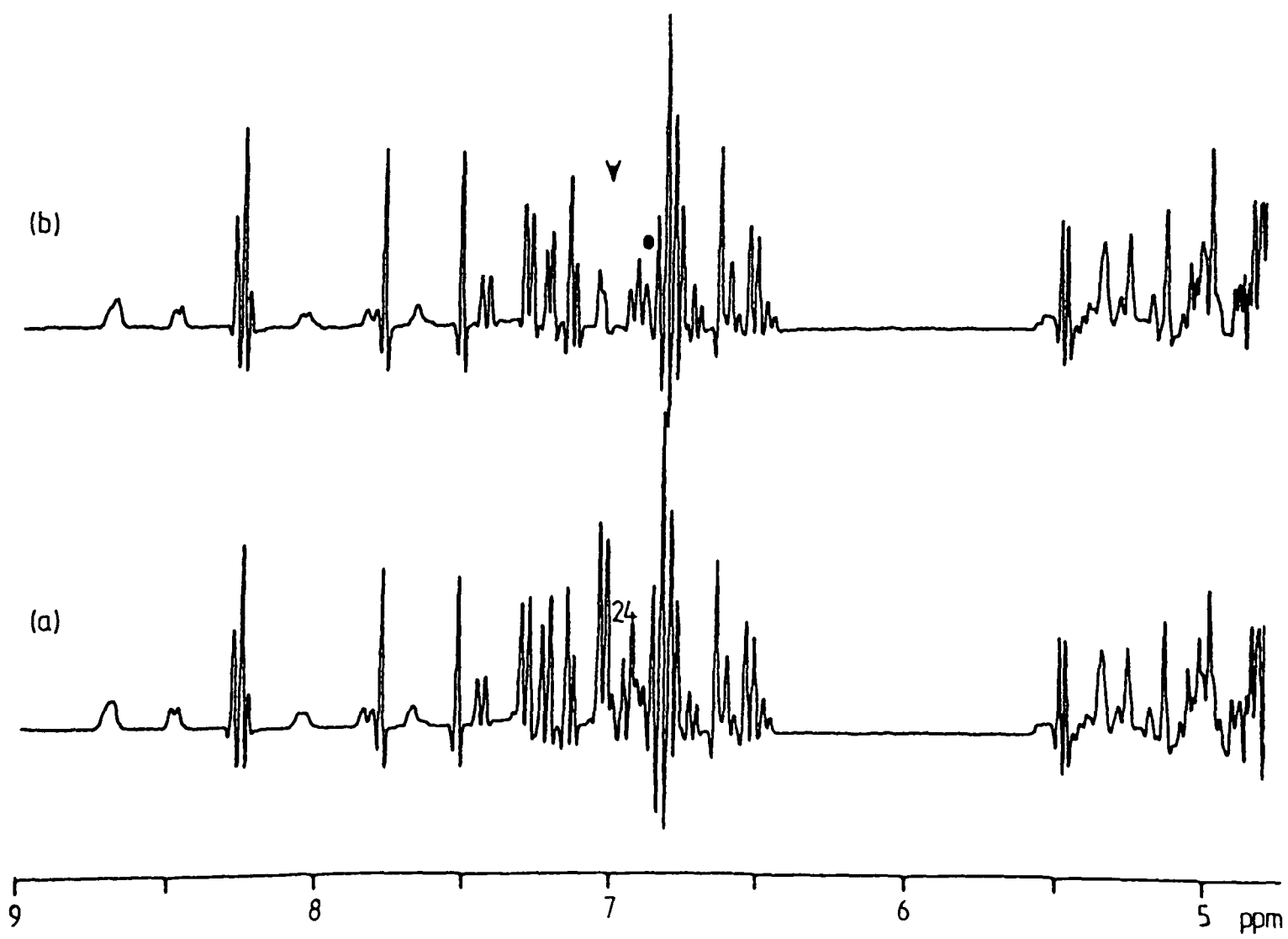

Fig. 4.16 47°C, pH 7.8 (a) Native protein in the presence of 6 amino-hexanoic acid (some labile proton resonances are present).

pulse on the upfield side of R9 results in R25 being decoupled, and indeed a shoulder can be seen on the edge of R9 in Fig. 4.16(a), and is labelled R24.

Now R25 appears in the normal spectrum to be of one proton intensity and in Fig. 4.16 as a doublet decoupling to a singlet. Only the resonances of one tyrosine and one phenylalanine side chain are unaccounted for, and in either case, the presence of a one proton doublet indicates at least one aromatic ring to be immobilised. If R24 is also a doublet then one set of ortho and meta protons of the tyrosine residue have been revealed. Another similar set would then be expected or a more complex peak if the two resonances had very similar chemical shifts or finally a two proton singlet resonance if they were coincident. The latter possibility can be ruled out as no such resonance is present and the former is less likely unless both one proton doublets are exactly coincident with familiar peaks in the spectrum, thus the second possibility of a more complex two proton resonance remains a distinct possibility. Alternatively, if R24 is a triplet then one set of ortho and meta proton resonances of the phenylalanine residue have been assigned and the remaining three one proton peaks of the immobilised ring remain undetected. Whichever case pertains not only is the remaining intensity arising from that ring not obvious, but the five or four proton intensity of the other ring is completely unaccounted for.

In an attempt to resolve this issue, multiplet selection spectra were obtained and are shown in Fig. 4.17. However, far from resolution, the problem is only complicated. Observing the odd multiplet selection in Fig. 4.17(b), intensity is seen in the regions of R1, R22 and R4 corresponding to the three tryptophan triplet peaks in this part of the spectrum, but then there are at least four clear peaks between 7 and 7.5 ppm indicative of triplet resonances, which is too many for any simple

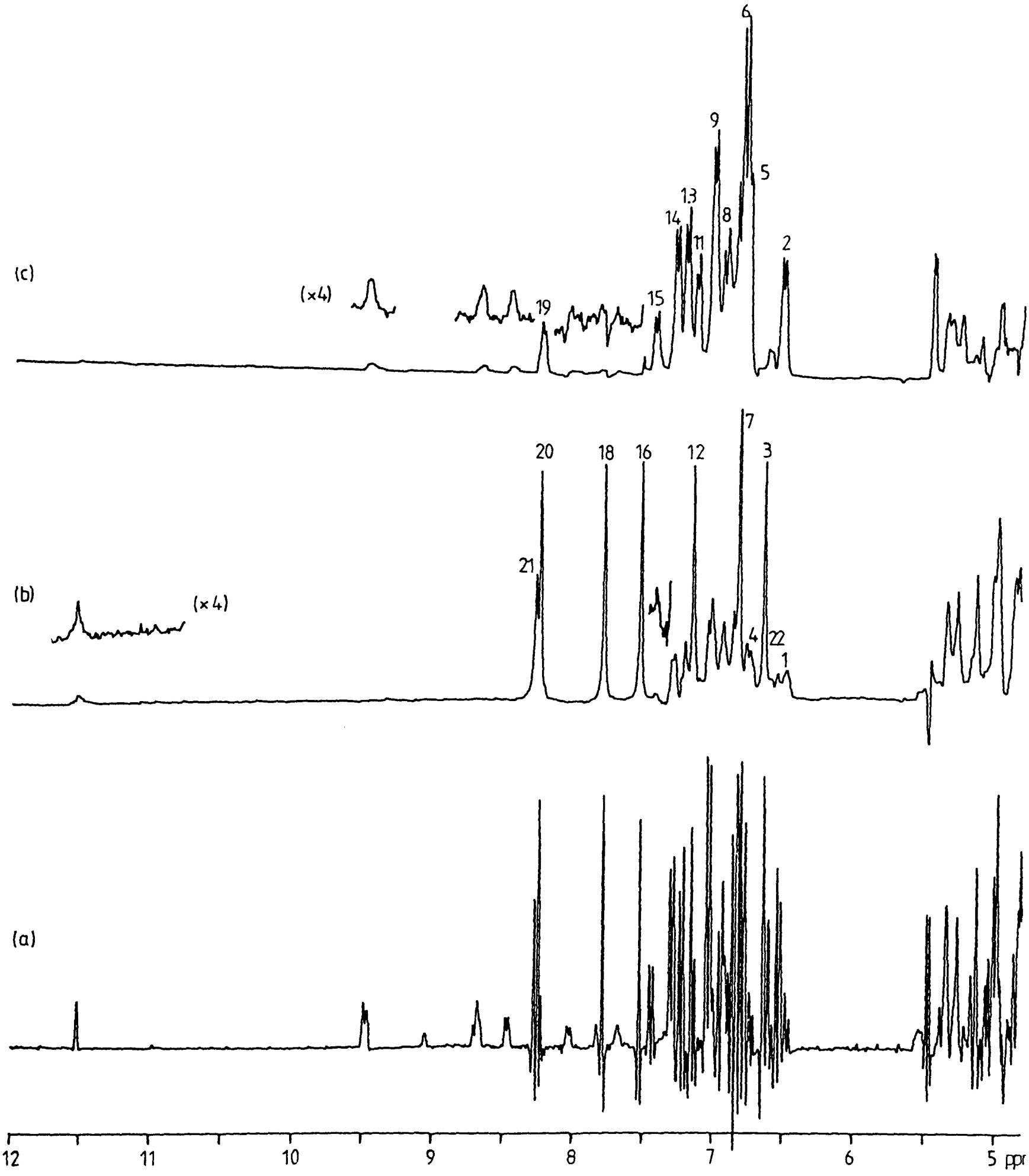

Fig. 4.17 Kringle 4 with added 6 aminohexanoic acid; 57°C, pH 7.8. (a) Resolution enhanced spectrum (b) Odd multiplet spectrum (c) Even multiplet spectrum. (Note the intensity of the labile proton resonances is low in the multiplet selection spectra).

scheme of resonances from immobilised tyrosine and phenylalanine side chains. As these spectra are produced by taking differences between two spectra accumulated simultaneously (section 2.2) the possibility arises of inaccuracy in the amount of one spectrum subtracted from the other, but this is an unlikely explanation of intensity in Fig. 4.17(b) as can be seen from the negligible intensity at R15 and R2 for instance. Thus, R24 and R25 remain unassigned as do the remaining resonances of the phenylalanine 63 and tyrosine 9 side chains. We note, furthermore, that the intensity in Fig. 4.17 (b) that is unaccounted for is all at resonance positions already with peaks of two or more proton intensity that will mask the underlying peaks of interest. Finally, 57^{o}C the temperature at which Fig. 4.17 was obtained is quite high for aromatic side chains to be immobilised as compared with other proteins such as the isoinhibitor K (snail inhibitor) for instance, studied by Wagner et al., (1978). Thus, the temperature dependence of the spectrum was investigated.

4.4.2.4 Temperature dependence

This is shown for the aromatic region in Fig 4.18. The sample was cooled to 7^{o}C in order to slow internal motions and bring any resonances, broadened by intermediate exchange, into the spectrum in slow exchange. Unfortunately, the reduced rate of molecular tumbling at lower temperatures results in increased linewidth and poorer spectral resolution. Nevertheless, at 27^{o}C and below, the doublet R15 has some intensity on its high field edge. This does not represent intensity from a labile proton resonance moving out from underneath R15 as it is also seen in spectra from samples where the labile protons have all exchanged and indeed, published spectra at 600 MHz clearly show an additional peak in this position (Hochschwender et al., 1983). Apart from perhaps a shoulder on the high field edge of R14 there is no other discernable change

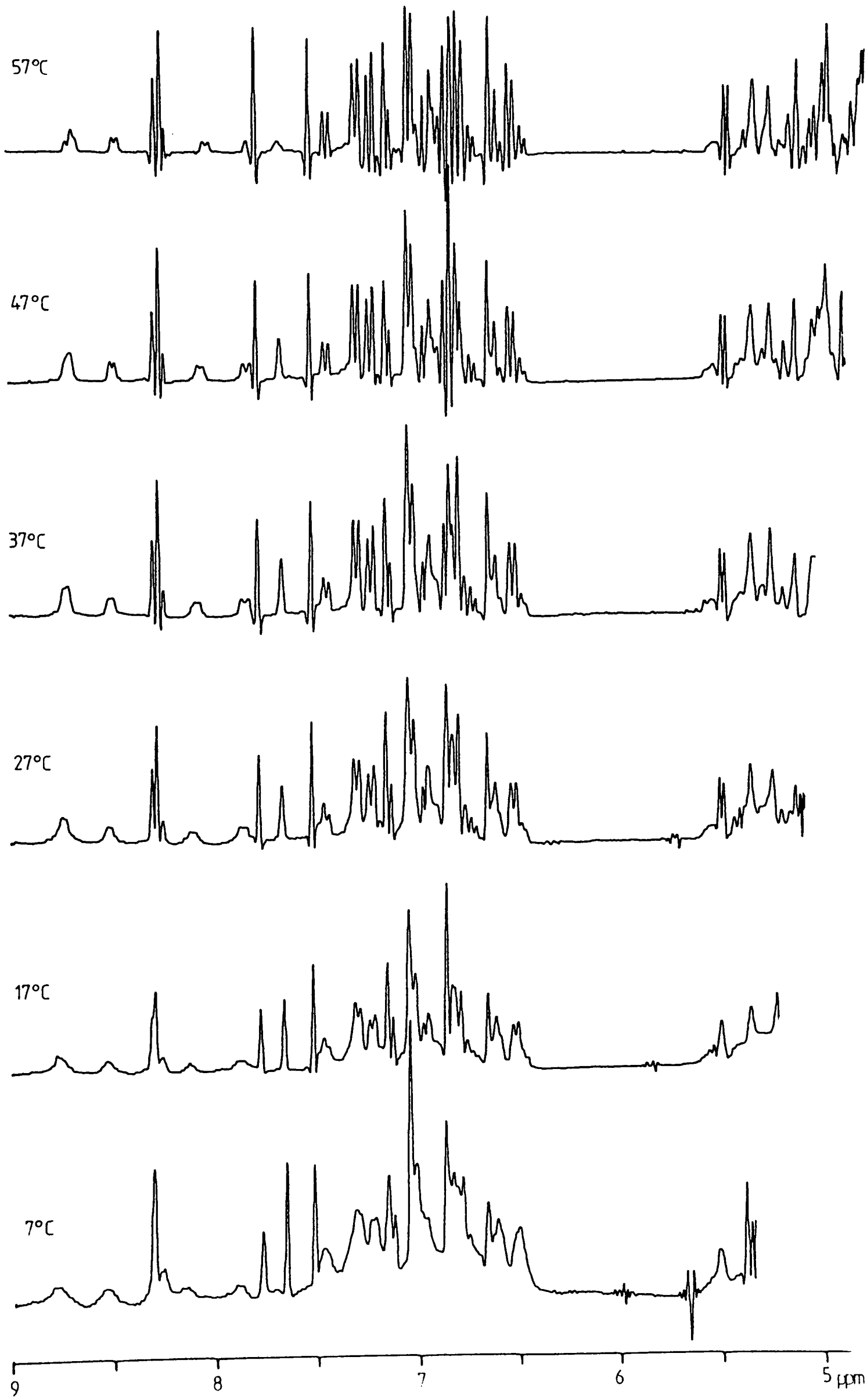

Fig. 4.18 Temperature dependence of the aromatic region of the spectrum of kringle 4 in the presence of 6 aminohexanoic acid, pH 7.8. Resolution enhanced spectra.

in intensity suggestive of resonances appearing in slow exchange at low temperature, although it is noticeable that R25 diminishes in height being lost from the spectrum at the lowest temperature. Thus, the possibility of some of the missing aromatic intensity being exchange broadened at room temperature remains and that even at 57°C this is not a sufficiently high temperature for it to be brought into fast exchange. This is by no means an unfamiliar occurrence, the phenomenon being encountered for instance in the spectrum of cytochrome c (Moore, 1978) and as referred to previously for cow-colostrum inhibitor (Wagner et al., 1978). Indeed, changes in the rate of chemical exchange generally extend over larger temperature ranges than studied here as can be seen in the aliphatic region of the spectrum for example (Fig. 4.23) where the methyl resonances of Leu 76 (L3) broaden in intermediate exchange as the temperature is reduced. We note that at the pH of the sample of Fig. 4.18, His 3 (R17,R10) is beginning to be protonated and both its resonances gradually disappear with increasing temperature. The majority of resonances show small temperature dependences over the range studied and in particular, the region of R5, R6 and R7 shows a number of changes, but as yet a sample containing ligand has not been thermally denatured. Castellino et al., (1981) have reported the thermal transition point of kringle 4 to be raised some 13°C by the presence of 6 aminohexanoic acid and certainly practical experience shows the ligand bound protein to be more stable at higher temperature than the native form, but no formal studies of this and its pH dependence have been performed so far. However, we note that labile proton resonances are still present at 57°C which has certainly not been observed for any sample of the native protein, and these peaks are now considered.

4.4.2.5 Labile Proton Resonances

At least eight proton resonances including that of the indole ring NH of Trp A are found to be considerably more resistant to exchange with solvent deuterons when the protein has bound 6 aminohexanoic acid. Some measure of their persistence is provided by the observation that the C2 proton of His 3 was fully deuterated after some hours at 47°C with negligible loss of intensity of some of the labile proton resonances. They were all finally exchanged after three to four hours at 57°C. It is obviously desirable to assign these resonances and so determine which parts of the protein are shielded so effectively from solvent access through the ligand binding. A number of nuclear Overhauser experiments were carried out when the sample was initially dissolved and subsequently, but as yet no firm assignments have been made, except for the Trps A and B NH resonances, and the data is not presented here. Part of the difficulty lies in the observation that many enhancements originating from pre-irradiation of NH resonances are to protons not directly coupled to the peak under consideration. This is particularly the case for NH protons incorporated into β sheet structures (see Dalagrno, 1983; Wagner et al., 1981) and this considerably complicates the assignment process especially when incomplete data is obtained from one dimensional experiments rather than the more comprehensive information provided by two dimensional procedures in both D_2O and H_2O. Nevertheless, it was a noticeable finding that Overhauser enhancements from the most persistent resonances all included several different aromatic peaks. It can also be seen from Fig. 4.13 that the positions of J coupled peaks have been determined for some of the most persistent resonances. For two such peaks, a pair of cross peaks can be discerned and are more readily seen in the individual cross sections. This was very suggestive of two glycine NH resonances having been detected giving J connectivities to the two αCH

protons. However, this possibility was not corroborated by cross sections which showed no connectivity between the two putative αCH resonances, and so this occurrence must be attributed to two sets of coincident pairs of NH resonances. In addition, Fig. 4.17(c) shows these two peaksto consist of doublets and not triplet resonances as is often seen for glycine NH proton peaks, and these peaks too remain unassigned. We now go on to discuss the effects on the aliphatic region of the ligand binding.

4.4.2.6 Aliphatic Region

This spectrum is shown with and without added 6 aminohexanoic acid in Fig. 4.19. As with the aromatic region the changes induced are very small, but on closer inspection there are seen to be very few differences between the two spectra compared to the situation in the aromatic region. Of the resonances of interest only L2 shows a slight shift of 0.01 ppm downfield and the L3 peak at 0.47 ppm moves a similar amount upfield, otherwise resonances L1, L4, L5 and Mets A and B are completely unchanged. The most upfield lysine εCH_2 peak (a) is moved slightly downfield by the ligand binding, as is the middle one (b) by an even smaller amount. From the discussion in section 4.4.1 it would be expected that the amino group of the ligand would be involved in an electrostatic interaction with at least one carboxyl group that is part of either an aspartate or glutamate residue. L10, assigned to the γCH_2 protons of the glumatic acid residue outside the kringle part of the molecule, Glu 83, is unaffected as would be anticipated. As discussed previously resonances from the two glutamate side chains within the kringle have not been identified and so we have no information on their possible involvement in the ligand binding. Aspartate β protons resonate at 2.75 and 2.83 ppm in random coil peptides and we note that there are changes

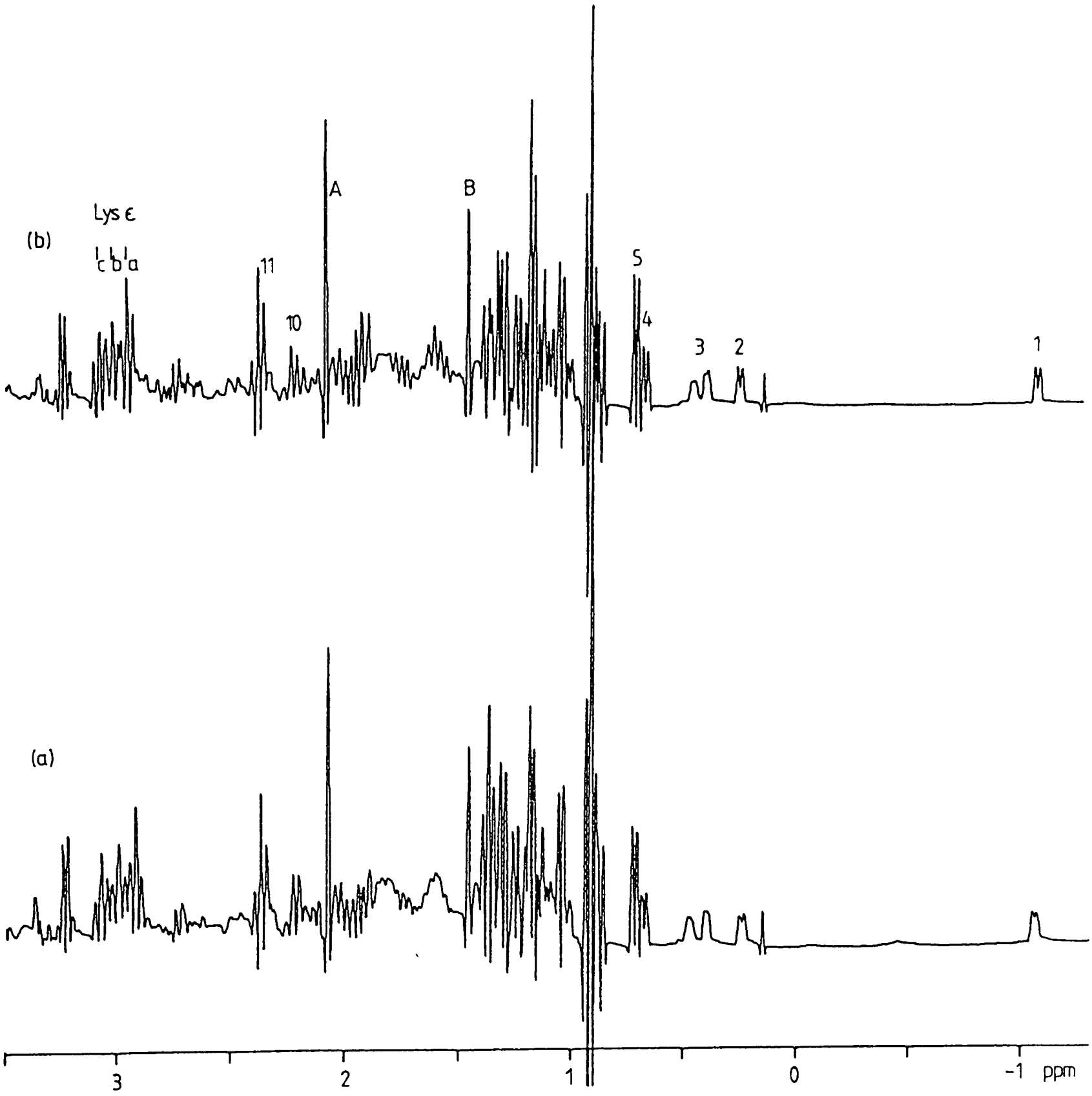

Fig. 4.19 Aliphatic region of the resolution enhanced spectra; 47°C, pH 8.4. (a) Native protein (b) Approximately 1.1:1 6 aminohexanoic acid to kringle 4, molar concentration ratio.

in resonances around these chemical shifts, although very small, as seen in Fig. 4.19. In fact, these changes are more noticeable in the non resolution enhanced spectra, but with four aspartate residues and five asparagines, which have very similar chemical shifts at pH 7.0, in the kringle sequence, we can say no more than the data is compatible with aspartate involvement in the ligand binding, but this is far from defining the precise residue involved. Further information on this question was sought through investigation of the pH dependence of the spectrum.

4.4.2.7 pH Dependence

A complete and detailed titration of the kringle saturated with 6 aminohexanoic acid was carried out over the pH range 2.7 to 9.7 under the same conditions as that for the native protein described in section 4.2. As would be anticipated from the foregoing the results of this experiment were extremely similar to those presented in section 4.2 and noticeably agreeing in a number of details that added confidence to some of the more subtle findings. However, there were some significant differences and these are now discussed.

Figure 4.20 shows some chemical shift versus pH curves for the acid bound kringle superimposed on the corresponding curves obtained for the native protein. The largest difference is clearly seen in that for the Trp B, C2 proton resonance, R18. As before, the curve proceeds too rapidly for a simple pKa but has been moved towards more acidic pH and is also altered in form. The pKa's of His 3 (B) (R17, R10) and 31(C) (R16, R21) are seen to be essentially unaltered by the presence of the ligand and the pH dependence of His 33(A) (R20, R7) is very similar in both samples. This supports the notion that R18 reflects a carboxylic acid group ionisation and not a histidine pKa and from the direction of the

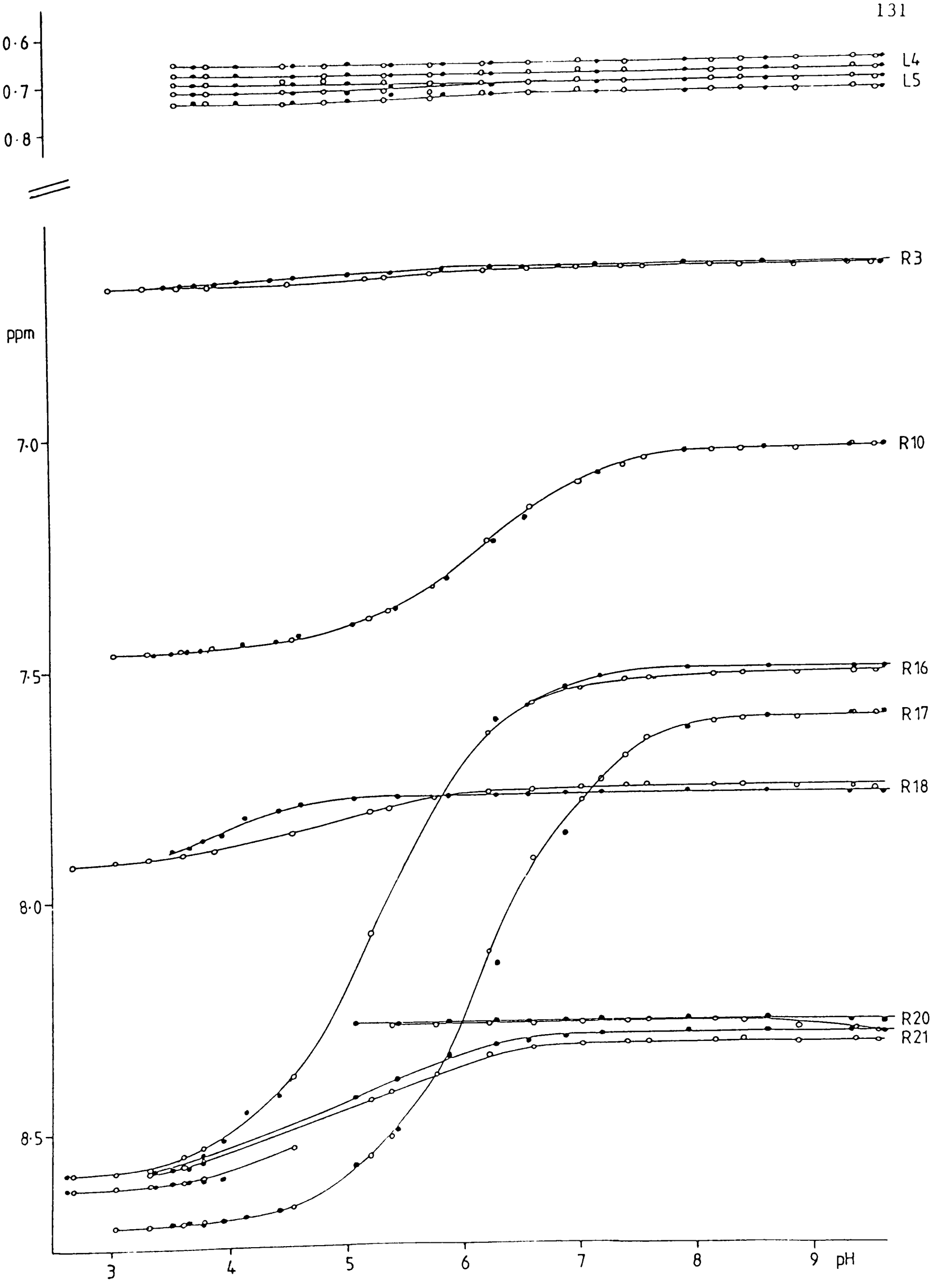

Fig. 4.20 Plots of chemical shift versus pH for resonances of kringle 4; 37°C, 100mM NaCl (see text).

- ∘ Native protein
- • Kringle 4 with bound 6 aminohexanoic acid

change it is clear that the added ligand results in some stabilisation of the deprotonated form of the carboxyl group which may well mediate the binding of the amino group of the ligand. Furthermore, such a strong pH dependence shown by R18 to the carboxyl ionisation indicates very close proximity in space of these two side chains - much as the relationship between Glu 35 and Trp 108 in the lysozyme molecule (Dobson and Williams, 1977). NOE and pH data has indicated that Trp B is also in close proximity to a number of aromatic side chains and therefore suggests that the carboxyl group, and the amino group of the ligand, may lie in a hydrophobic environment within the protein. This is in accord with the slower exchange of labile proton resonances noted above as the presence of the ligand further blocks access of solvent molecules to the interior of the molecule, and in particular accounts for the persistence of the indole NH proton resonance of Trp B. In addition, the greater perturbation of the aromatic rather than the aliphatic region of the spectrum by the binding is then explained.

However, returning to the discussion of the pH dependence of the spectrum in the presence of added ligand, it was again not possible to detect whether the one proton triplet resonance, R22 of Trp B reflected the same change as R18 as it still broadened and disappeared from the spectrum around pH 4.5. But it did show a slight downfield shift above pH9 attributed, above in the native protein, to a reflection of the ionisation of the Tyr 40(D), which is unaltered, as are the early portions of the Tyr 2(A) and 49 (B) ionisations. R20 from His 33, though, is seen from Fig. 4.20 to be less influenced by the Tyr 40 ionisation than without ligand present. This raises the possibility of the ligand causing a slight separation between these two side chains, but it must be remembered that the changes in chemical shift are small.

In the native protein small pH dependences of some of the Trp 71(C)

resonances were correlated with the His 31(C) ionisation, although it was pointed out that the evidence for this was lacking as clearly similar pKa's could not be obtained from the very small shifts on the tryptophan resonances. This remains the case when the ligand is present, but as shown for R3 in Fig. 4.20 the presence of bound ligand makes little difference to the pH dependence of this resonance or indeed that of other resonances of Trp 71, R23 and R11. This does tend to dismiss the possibility, though, that R3 reflects the same pKa as R18, which is so dramatically altered by the ligand binding. Furthermore, the pH behaviour of the His 33(A), Trp A, R9 and Met B resonances disappearing from the spectrum around pH5 is unaffected as far as can be ascertained by the presence of 6 aminohexanoic acid. In return, the lack of an effect on the curve of R18 when the ligand is bound suggests that whatever structural alteration the broadening of those resonances signifies, it has little or no effect on the ligand binding as monitored by R18. This conclusion will be considered again below for the carboxyl terminal region of the ligand, but before considering the pH dependence of the ligand resonances we will briefly discuss the aliphatic resonances.

As for the native protein the pH dependence of resonances from non titrating aliphatic side chains are all small but L2, for instance, does not show the slight inflection around pH 5 just detected in the sample without ligand. The L3 resonances show a more complex pH dependence manifest in broader, ill-defined peaks at 37^{o}C, more widely separated than in the native protein and a pKa that is not readily measured. The doublet overlying the valine 69 resonance at L5 shows a small difference in behaviour from the titration in the absence of ligand as seen in Fig. 4.20, in that on reducing the pH it does not begin to move until 0.5 pH lower. This would not have been mentioned except that careful scrutiny of some further diagrams would have revealed this effect and it will be

referred to again then. All three lysine peaks indicated in Fig. 4.3 show a slightly diminished response in chemical shift change above pH 9, but much more noticeable is that the most upfield, Lys ε CH_2 (a) resonance no longer shows any pH dependence between pH 4 and 7 being at the low pH chemical shift until pH 9. This again suggests that it has been moved slightly apart from the ionising group that perturbed it in the absence of the ω-aminocarboxylic acid. Of the side chains that do titrate other than the termini, only the resonance L10 assigned to Glu 83 has been identified and its pH behaviour was found to be independent of the ligand. Thus, the pH dependence of aliphatic resonances is relatively uninformative, but we now consider the ligand resonances themselves.

Figure 4.21 shows the chemical shift versus pH curves for two resonances of 6 aminohexanoic acid under the same conditions and at the same concentration in the presence and absence of kringle 4, and some of the protein spectra are shown in Fig. 4.22. It can be seen that at the lowest pH, all the ligand resonances are visible as sharp peaks at unshifted positions in the resolution enhanced spectra. However, as the pH is raised Fig. 4.21 shows the α and β CH_2 ligand resonances are shifted upfield in the presence of the protein and in Fig. 4.22 the ligand resonances are seen to broaden and disappear from the spectrum in order, from the NH_3^+ end, until by pH 5.06 only the α CH_2 proton resonance remains clearly visible. This is totally in accord with the findings shown in Fig. 4.9, and interpreted as the amino end being bound within the protein. But as commented above, the carboxyl end does demonstrate some effects of binding as seen from the titration curves in Fig. 4.21. On reducing the pH below 6, the α CH_2 proton curve moves parallel to that for the free ligand until about pH 4.6 when it becomes much steeper to end at the same chemical shift as the unbound ligand at pH3. In a similar vein, the β CH_2 proton curve starting at pH 4.6 when the

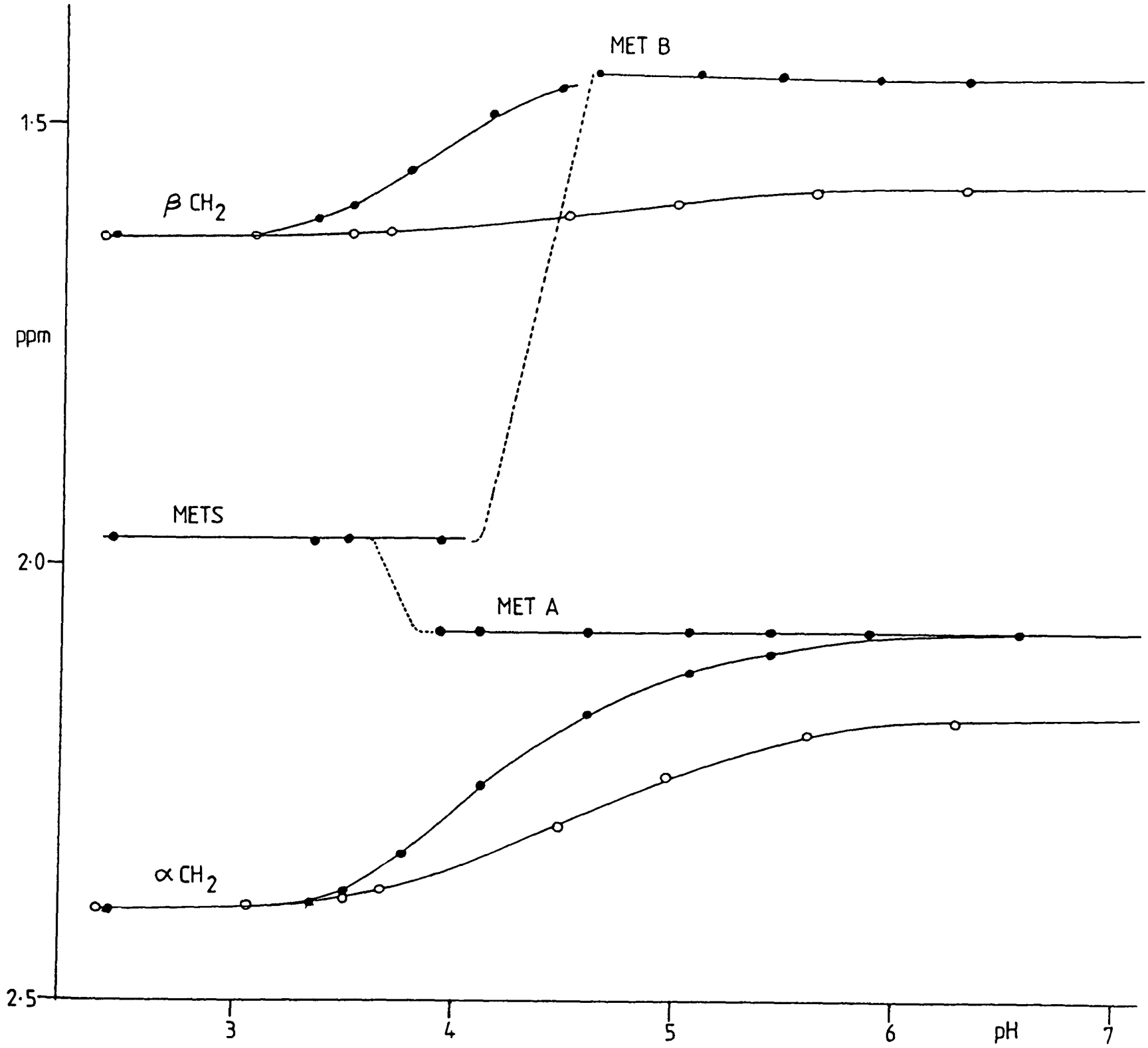

Fig. 4.21 Plots of chemical shift versus pH; 37°C, 100mM NaCl (see text).

o Free 6 aminohexanoic acid

• Protein bound 6 aminohexanoic acid

(The dotted lines connect the methionine resonances to the random coil position over the pH range that they are in intermediate exchange and at which they reappear at low pH).

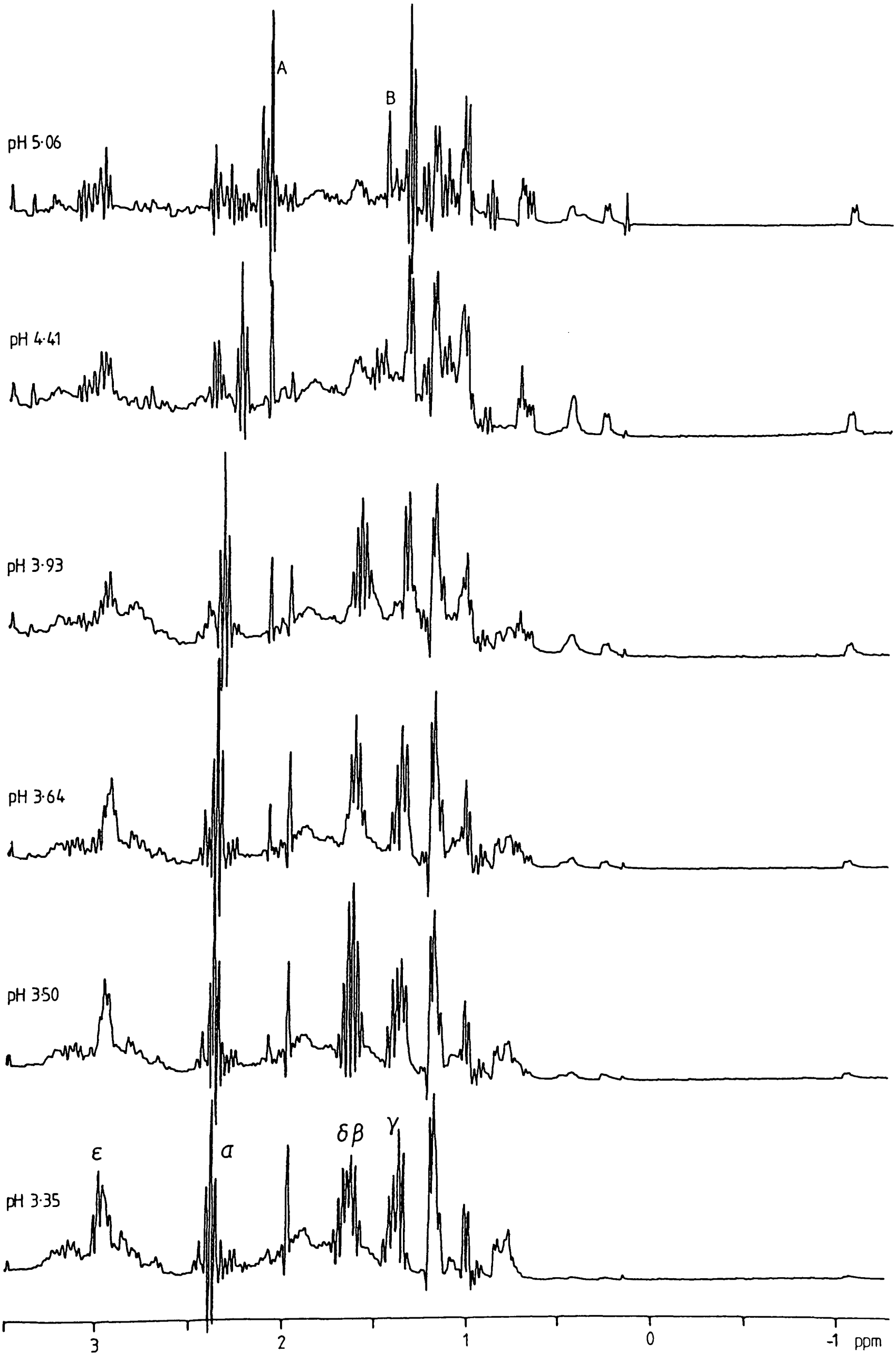

Fig. 4.22 Resolution enhanced spectra of the aliphatic region of kringle 4 in the presence of 6 aminohexanoic acid at various pH values; 37°C, 100mM NaCl.

resonances become visible in the spectrum moves steeply to join the free ligand curve at low pH. We note that the quite sizeable shifts on these resonances through binding may indicate interaction with an unidentified aromatic side chain, but the initial effects of protonation of the ligand carboxyl group on lowering the pH are seen to be unaltered. Regarding the protein resonances we see that from the upfield methyl proton peaks and that of Met A, the protein itself begins to denature below about pH 4 and is almost totally unfolded by pH 3.35 when the ligand is also no longer bound. Thus, it is seen that the ligand binding site is clearly formed by the specific protein fold. We also note that the form of the α CH_2 proton curve differs from that of the unbound ligand between pH 4.6 and 3.35 which is just the range over which the protein resonance R18 moves in the presence of the ligand. Careful comparison of the protein pH titrations with and without added 6 aminohexanoic acid demonstrate no distinct difference in the pH dependence of the denaturation process. This implies that the carboxyl ionisation which the Trp B resonance, R18, reflects and which is taken to mediate the ligand amino group binding is not responsible for maintaining the protein structure and is not directly involved in the denaturation mechanism, which is unaffected by the presence of the ligand. Thus, again it is emphasised that the ligand binding site has been shown to be constructed only as a result of the protein adopting a specific tertiary fold, as would indeed be expected. In addition, we again note that the changes resulting in the methionine methyl resonance, Met B and the Trp A, His 33(A) and R9 peaks disappearing from the spectrum have no effect on the α CH_2 proton shift against pH curve of the ligand, suggesting that they are not directly involved in forming the ligand binding site.

4.4.2.8 Aliphatic Temperature Dependence

This is shown in Fig. 4.23 being the aliphatic region of the spectra shown in Fig. 4.18, and the sample contains a considerable excess of 6 aminohexanoic acid compared to the sample used for the spectra shown in Fig. 4.22, as demonstrated by the presence of the ligand βCH_2 proton resonance at all temperatures. It can be seen that at the lowest temperatures the rate of chemical exchange has been reduced such that all the ligand resonances are clearly visible but broaden out from the amino end and sharpen at the carboxylic terminus as the temperature is raised. The protein resonances show identical behaviour to those of the native kringle at higher temperature, and at low temperatures we note that the methyl proton peaks of Leu 76 broaden out almost completely from the spectrum.

4.4.2.9 Summary

A summary of some of the assigned aliphatic resonances and residues that are affected or not by the binding of 6 aminohexanoic acid to kringle 4 is given in table 4.3B. (Table 4.3A for the aromatic resonances is reproduced for easier reference).

Although a number of resonances are altered by the binding of 6 aminohexanoic acid especially in the aromatic region, the changes induced are all small with many resonances being completely unaffected. A series of NOE experiments have also been performed which all produced very similar results to those discussed in section 3.4 for the protein without bound ligand. This all indicates that the overall structure of the protein is very little perturbed by the binding and indeed, it has been seen that the protein fold forms the ligand binding site. Certainly, the data shown completely excludes the possibility of any gross conformational change in the kringle structure being induced by the

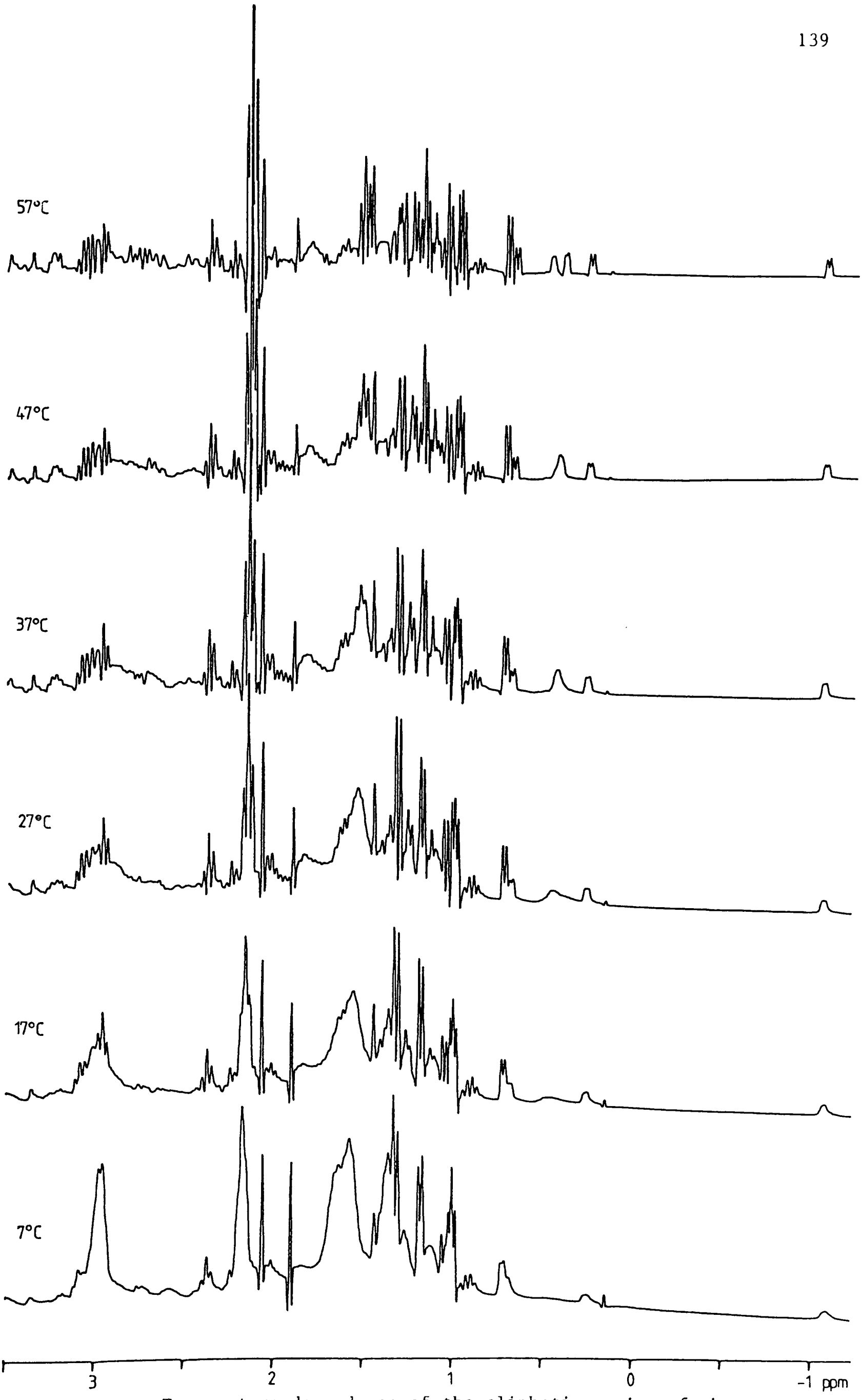

Fig. 4.23 Temperature dependence of the aliphatic region of the spectrum of kringle 4 with added 6 aminohexanoic acid, pH 7.8. Resolution enhanced spectra.

Table 4.3 Summary of the Assigned Resonances and Residues that are affected or not by the Binding of 6 Aminohexanoic Acid.

	ALTERED	UNALTERED
A.AROMATICS	Trp A	
	Trp B	
	Trp 71	
	His 31	His 3
	His 33	
	Tyr 40	Tyr 2
		Tyr 49
		Tyr 73
B.ALIPHATICS	L1	L2
		Leu 76
	L5*	Val 69
	Lys ε CH_2 (a),(b)	Met A
		Met B

* Only below pH 6.0.

binding of 6 aminohexanoic acid. On the contrary, the perturbation of many hydrophobic residues and prominent involvement of an unassigned carboxyl group inferred from the effects of its ionisation on an aromatic proton resonance strongly suggest, that the amino terminal end of the ligand penetrated to the hydrophobic core of the molecule. Indeed, this is supported by the much slower exchange of a number of labile proton resonances that are either indole NH proton peaks or give Overhauser enhancements to aromatic protons indicating that the presence of the ligand further blocks access of solvent molecules to the centre of the protein. In addition, it is very noticeable that all the side chains seen to be affected by the ligand binding, listed in Table 4.3, have previously independently been shown to be close in space as was summarised in Fig. 4.7. The inference from these two sets of data is that these residues surround the ligand binding site. That this is indeed the case will be shown by the lanthanide ion probe studies, but before discussing them we now consider the spectral effects of the binding of another ω-amino-carboxylic acid, AMBOC, to kringle 4.

4.4.3 AMBOC

The binding of this ligand has been less thoroughly investigated than that of 6 aminohexanoic acid discussed above, but the preliminary findings provide a valuable comparison.

4.4.3.1 Aromatic Region

This is shown in Fig. 4.24 for the addition of AMBOC and can be compared with the analogous figure (Fig. 4.10) for the 6 aminohexanoic acid above, although the pH and temperature of the two experiments were not the same. At first glance it is seen that changes induced are larger than with 6 aminohexanoic acid although, as before, many

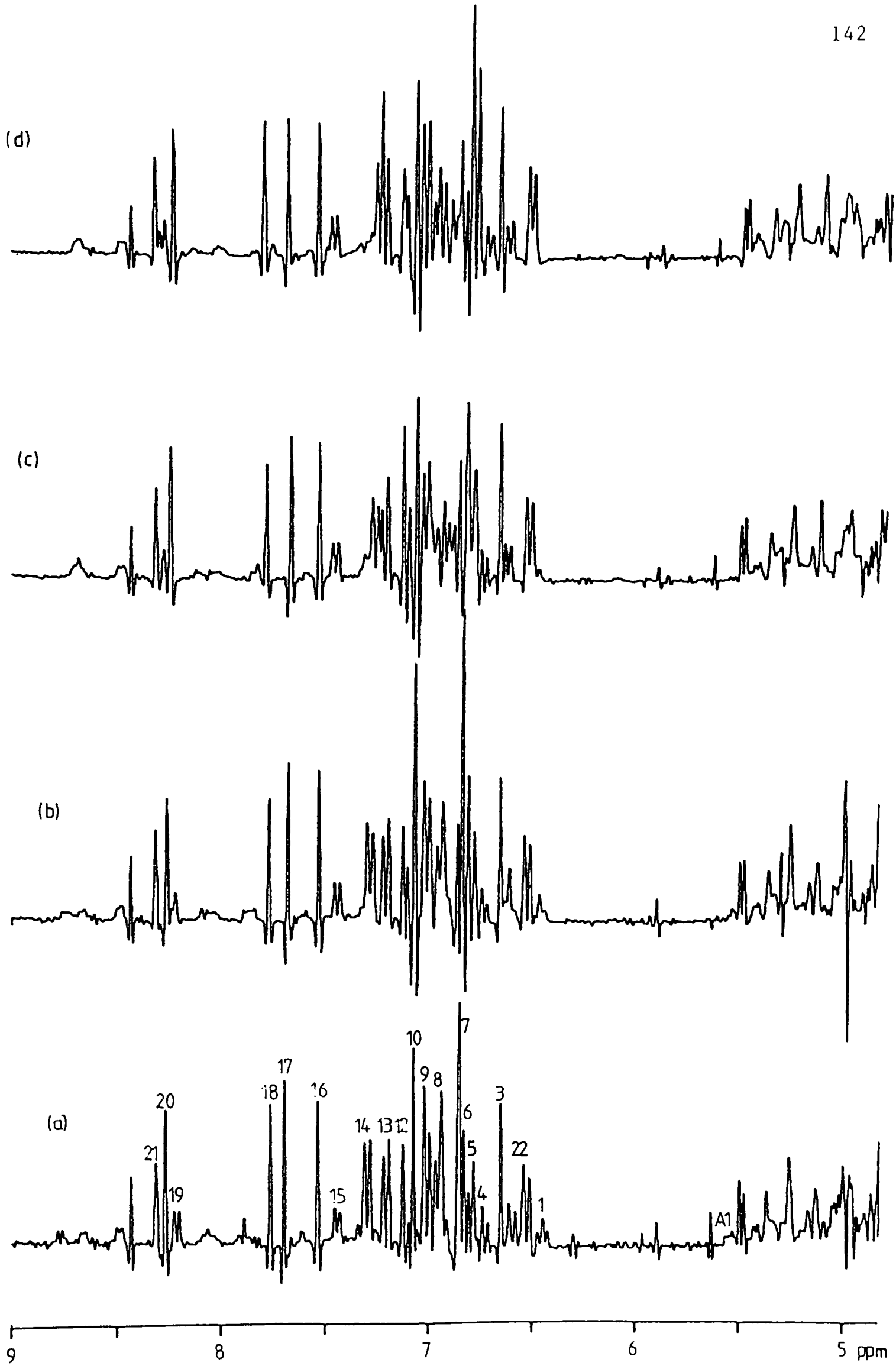

Fig. 4.24 Aromatic region of the resolution enhanced spectrum; 37°C, pH 7.4 showing the effects of adding AMBOC to kringle 4. (a) Native protein (b) 0.2:1 (c) 0.6:1 (d) 1.2:1 approximate molar ligand to protein concentration ratios.

resonances remain unpeturbed by the ligand binding. For instance a number of the downfield shifted αCH resonances are seen to be completely unaffected by the binding process which again precludes the possibility of the ligand being responsible for any gross conformational change of the protein. But there are some changes in this region, such as the broad resonance A1 moving upfield, and these are unaccounted for at present. (Note the sharp peak at 8.44 ppm is the impurity mentioned in section 3.2).

Considering the tryptophan side chain resonances, quite marked downfield shifts are seen on R1, R15, and R19 of Trp A with little if any change on R12 or, incidentally, the NH resonance at 11.56 ppm. A COSY experiment, shown in Fig. 4.25, was carried out to determine the positions of the upfield shifted tryptophan triplet resonances and that of Trp A is now seen to be shifted downfield by the addition of AMBOC to the protein. The effects are qualitatively similar to those on 6 aminohexanoic acid binding but of larger magnitude. R18 and R22 of Trp B again show movement to larger chemical shift values as do the C4 doublet and C5 triplet resonances the positions of which were detected from COSY data. As yet the C7 doublet resonance has not been identified but is presumed from the intensity changes to have been moved upfield in analogy to the change occurring on 6 aminohexanoic acid binding. Finally, the C2 proton resonance of Trp 71, R3, now shows a small downfield shift with ligand binding while R11 shows a very similar movement with both ligands. R4 is also affected and the upfield triplet is now shifted downfield and R23 again unchanged. These shifts have been summarised in Fig. 4.26 which can be compared with Fig. 4.14 compiled for the 6 aminohexanoic acid binding. (Note as before the C4, C5 and C7, C6 resonances pairs of Trp C have not been conclusively assigned and

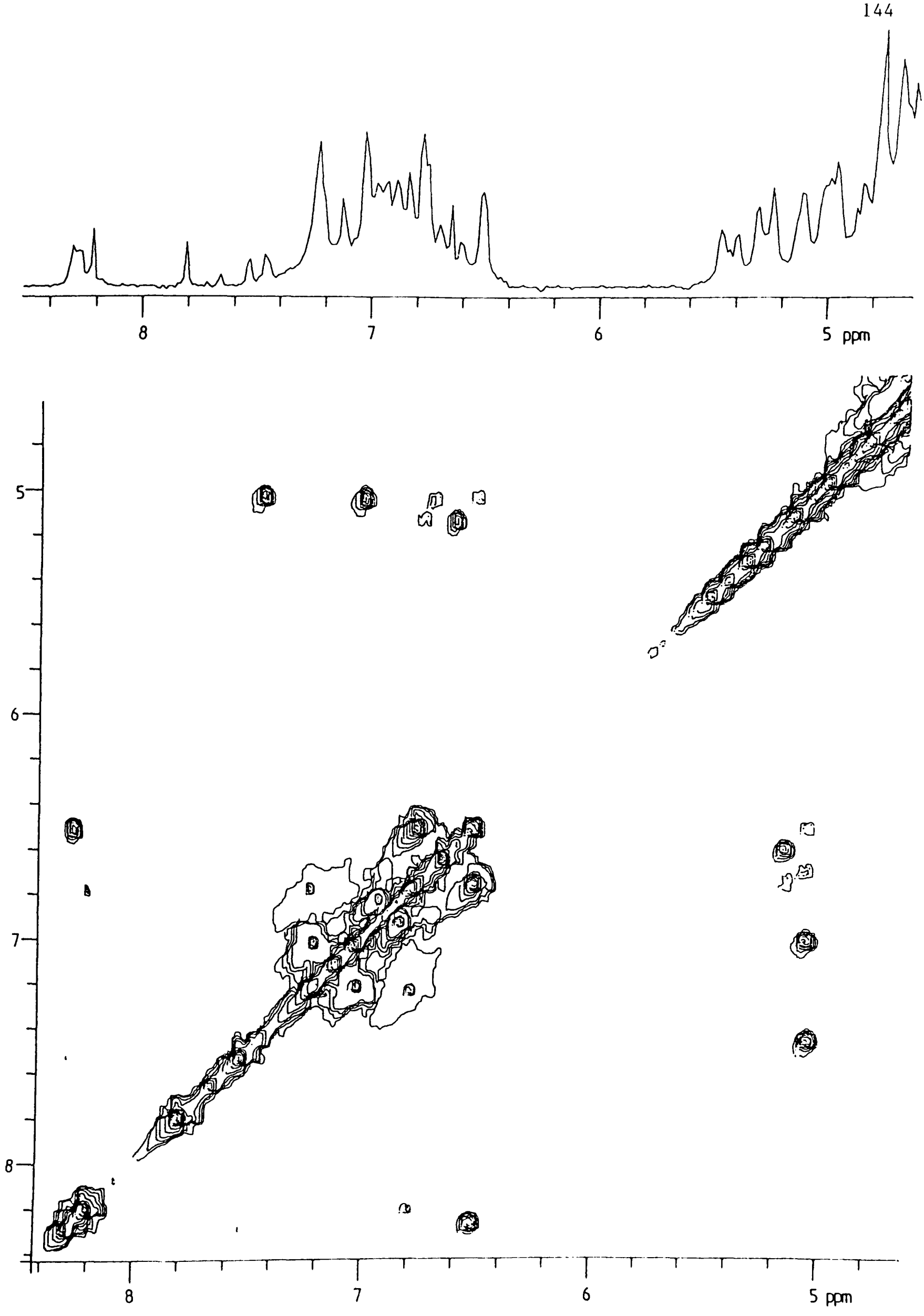

Fig. 4.25 Aromatic region of the 470MHz COSY spectrum 57°C, pH 7.8 of kringle 4 with added ligand AMBOC.

maybe reversed.

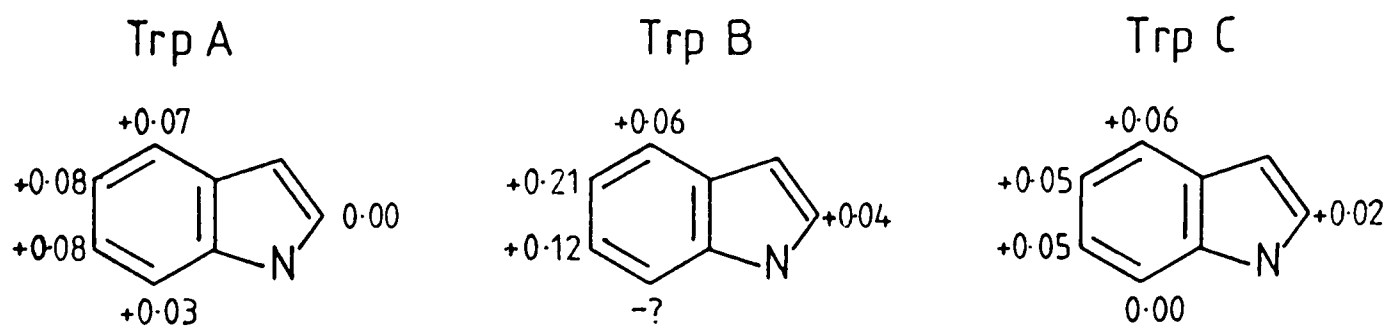

Fig. 4.26 Shifts (ppm) induced on the indole ring protons of kringle 4 on binding AMBOC. (+ve sign indicates downfield, -ve sign upfield)

As before all three tryptophans show changes in resonance positions, but those of Trps A and B while similar in direction are generally much larger in magnitude with the ligand AMBOC. With regard to this it must be borne in mind that, while the ligand AMBOC binds more tightly to kringle 4 than 6 aminohexanoic acid, it is also a more bulky molecule.

R7 and R20 of His 33 are again both upfield shifted but by the larger amount of 0.04 ppm. As before, the His 3 peaks R17 and R10 are completely unchanged. This fact also negates any possibility of small shifts on any resonances arising from small pH changes as the His 3 peaks, especially the C2 resonance, R17 are very sensitive to pH at that chosen for the experiment. In contrast to the effects of 6 aminohexanoic acid, AMBOC binding causes the His 31 (R21, R16) resonances to move downfield by about 0.01 ppm.

Finally, we consider the assigned tyrosine peaks and note once more that Tyr 2 (R2, R5) is unaffected by ligand binding. As before the resonances of Tyr 49 (R6, R8) are not readily distinguished lying in spectral regions of much change, but R8 appears unaffected. This was confirmed by pre-irradiation of the aliphatic peak; L5 which was seen in the native protein to result in strong enhancements to two aromatic peaks, R6 and R8 assigned to Tyr 49(B) (Fig. 3.24(e)). The results for

the identical experiment but in the presence of ligand are shown in Fig. 4.27 and seen to be extremely similar in the aromatic region to the spectrum of Fig. 3.24(e). (The differences in the aliphatic region will be discussed below). R14 of Tyr 73 (R6, R14) is shifted upfield by 0.04 ppm and the COSY data in Fig. 4.25 shows a smaller downfield shift on the R6 doublet from this residue. This finding is in marked contrast to the effects of 6 aminohexanoic acid binding when the resonances of Tyr 73 were unaffected. In addition, the C2 proton resonance of Trp B, R18 is moved more by AMBOC, in complete accord with the effects on Tyr 73 (R14, R6) of ligand binding and the strong NOE between R18 and R14, R6 (section 3.4). Finally, resonances R9 and R13 of Tyr 40 again move downfield both by about 0.03 ppm. Thus, overall the spectral effects of the binding of each ligand are similar, but generally more pronounced for the more tightly bound, larger ligand, AMBOC and do differ in some details. We now go on to consider the aliphatic region of the spectrum.

4.4.3.2 Aliphatic Region

This is shown in Fig. 4.28 which also shows the AMBOC spectrum. As with 6 aminohexanoic acid binding the changes caused by the addition of AMBOC to kringle 4 are few and small in magnitude. However, again in contrast, L2 and now L1, arising from the methyl groups of Leu 45, move downfield some 0.02 ppm. L3 (Leu 76) shows a negligible change in resolution but no shift and is again considered unaffected. The methyl proton resonances of Val 69 (L4, L5) now move 0.01 ppm downfield while the L5 doublet is unchanged. (We note that L5 was also unchanged at pH's above 6 on binding 6 aminohexanoic acid, but no pH dependence study has yet been performed on the AMBOC bound protein). Both methionine resonances are untouched, but like before the Lys ε CH_2 (a) resonance is downfield shifted as is the (b) resonance again by a lesser amount.

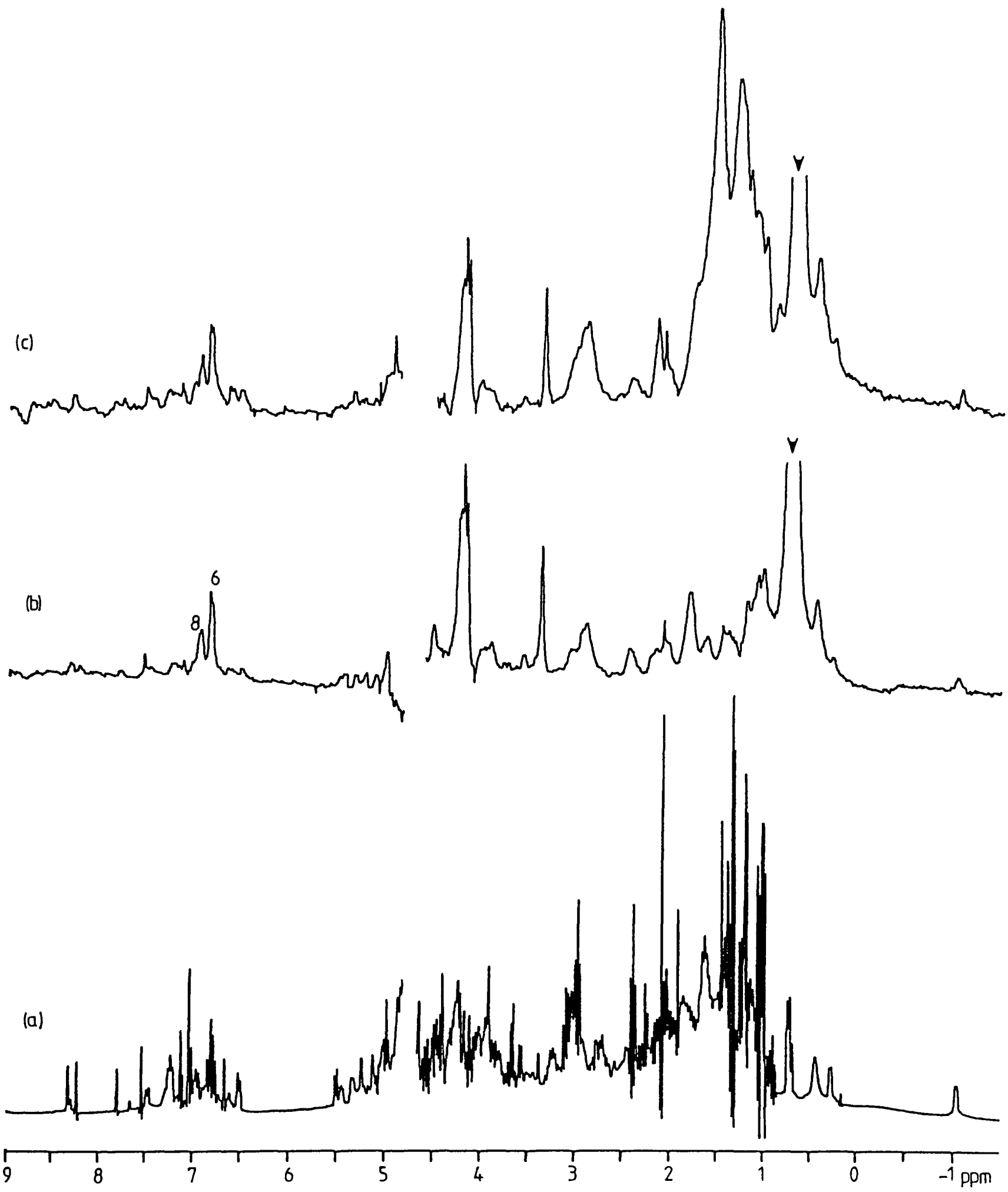

Fig. 4.27 27°C (a) Resolution enhanced spectrum of kringle 4 in the presence of the ligand AMBOC. NOE difference spectra for (b) kringle 4 with added AMBOC (c) kringle 4 with added 6 aminohexanoic acid.

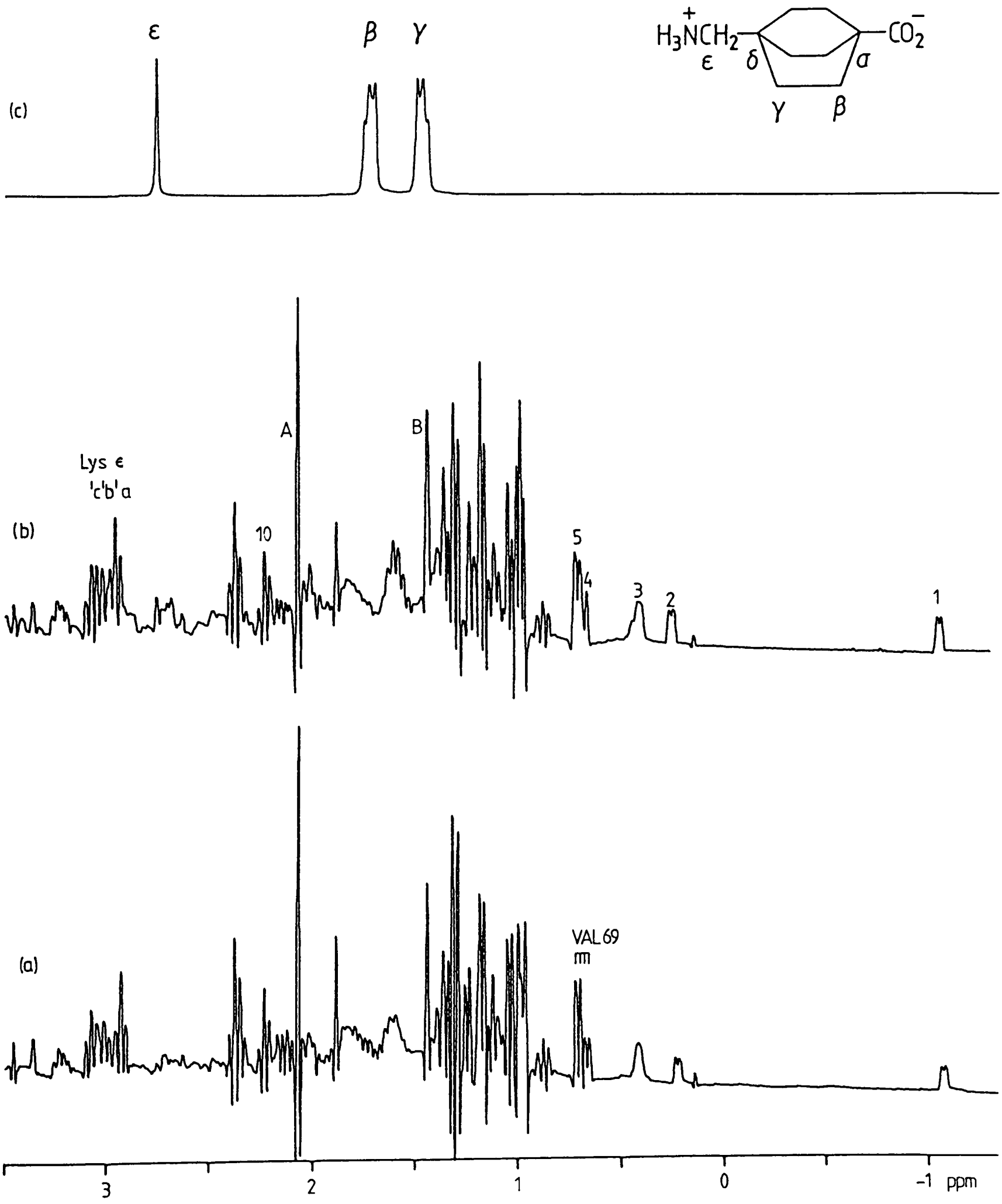

Fig. 4.28 Aliphatic region of the resolution enhanced spectra, 37°C pH 7.4. (a) Native protein (b) Approximately 1.2:1 AMBOC: kringle 4 molar concentration ratio (c) Assigned spectrum of the ligand AMBOC.

Likewise, L10 (Glu 83) is not altered, and the non resolution enhanced spectra again clearly show intensity changes in the asparate β CH_2 proton resonance region, compatible, as discussed above with aspartate involvement in ligand binding.

These results are very similar to those for the less tightly bound ligand and serve to highlight the small effect that ligand binding has on the aliphatic side chains of the protein, which from X-ray crystallographic studies of globular proteins tend to be more peripheral, with the aromatic residues more centrally placed. Before summarising the effects of AMBOC binding, we will briefly consider the temperature dependence of the ligand bound spectrum.

4.4.3.3 Temperature Dependence

This is shown in Fig. 4.29 for the aromatic region (The His 3 C2 proton (R17) had already been substantially exchanged for solvent deuterium atoms). Comparison with the data for the 6 aminohexanoic acid bound protein (Fig 4.18) shows very similar effects. The changes on the high field edge of R15 at lowest temperatures suggesting additional intensity are perhaps not so clear, while evidence for an additional peak on the edge of R14 is perhaps better. A number of one dimensional spin decoupling experiments have been performed irradiating these and other positions as indicated but no definite extra coupling schemes have been elucidated and the preliminary findings will not be discussed further. Suffice is to say that the possiblity of an immobilised tyrosine and/or phenylalanine side chain has by no means been discounted. Furthermore, the multiplet selection spectra again produced more triplet resonances than are assigned or expected for simple coupling schemes for the two unassigned aromatic rings. As expected the AMBOC bound protein sample was stable at high temperature remaining at 57°C

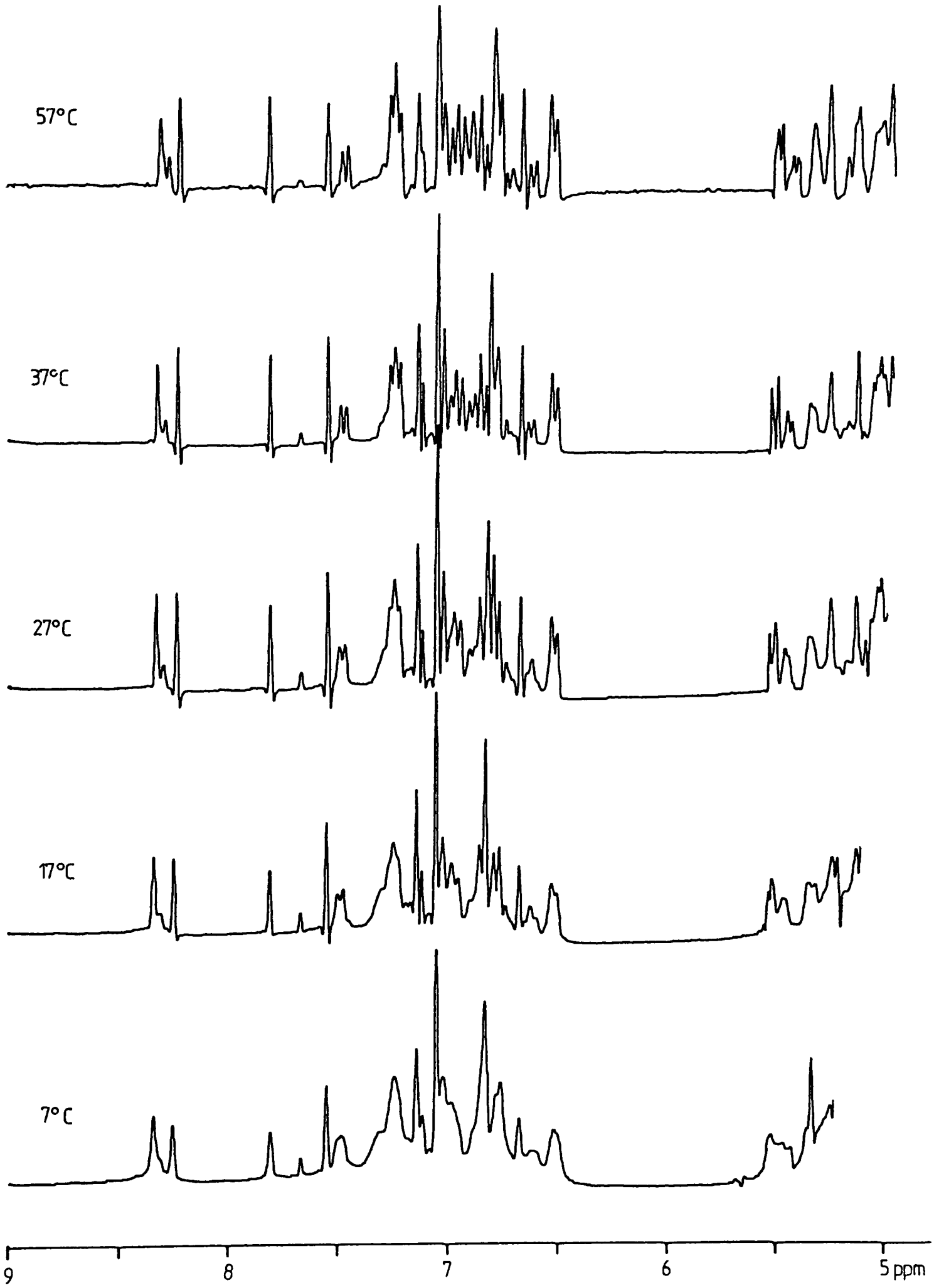

Fig. 4.29 Temperature dependence of the aromatic region of the spectrum of kringle 4 in the presence of AMBOC, pH 7.8. Resolution enhanced spectra.

for more than 24 hours, for instance, with little protein degradation occurring. The temperature dependence of the aliphatic region of the spectrum was very comparable to that of the 6 aminohexanoic acid bound protein (Fig. 4.23); although the ligand was at much lower concentration and its resonances considerably less prominent in the spectrum at low temperature.

4.4.3.4 Summary

Table 4.4 lists the assigned resonances and residues that are affected or not by the binding of AMBOC to kringle 4 and this can be compared directly with Table 4.3.

The conclusions to be drawn from the less extensive study of AMBOC binding to kringle 4 are very similar to those discussed above for the 6 aminohexanoic acid binding, and indeed the small differences are in one accord with the different nature of the two ligands. Discussion of the nature of the ω-aminocarboxylic acid binding site has already suggested that the amino group of the ligand penetrated to the hydrophobic core of the globular protein. This in turn indicates that part of the ligand chain at least may be in close proximity to protein side chains lining the "cleft" or "well" into the core. As yet little work has been directed towards exploring this possibility. However, referring to the NOE experiments shown in Fig. 4.27 on irradiating L5 in the ligand bound samples and comparing them with the same experiment for the native protein (Fig. 3.24(e)), is very interesting. While the aromatic regions of the difference spectra are very similar as pointed out above, the aliphatic regions have noticeable differences. In particular, Fig. 4.27(c) shows strong intensity at positions consistent with the ligand β and γ CH_2 proton resonances and to a lesser extent the α proton peak. The ligand concentration in the sample of Fig. 4.27(b) is much

Table 4.4 Summary of the Assigned Resonances and Residues that are affected or not by the Binding of the ligand AMBOC to Kringle 4.

	ALTERED	UNALTERED
AROMATICS	Trp A	
	Trp B	
	Trp 71	
	His 31	His 3
	His 33	
	Tyr 40	Tyr 2
	Tyr 73	Tyr 49
ALIPHATICS	L1, L2	
		Leu 76
	Val 69	L5
	Lys ε CH_2 (a),(b)	Met A
		Met B

less than that of (c) but yet there is intensity consistent with the βCH_2 resonance position of AMBOC. Now it must be emphasised that these findings are preliminary and as yet unsubstantiated but, they do raise the possibility that either Val 69 or the methyl group giving rise to L5 are in spatial proximity to the β and γ methylene groups of the ligand. This possibility is certainly not inconsistent with all the data presented above, and will be considered further in section 4.5.

The notion, then, of a "well" into the centre of the molecule with a carboxyl group lying amongst a cluster of hydrophobic residues at the bottom to attract the amino group of the ligand, suggested the possibility of probing this part of the lysine binding site using lanthanide ions and these studies are now described.

4.5 Lanthanide Ion Binding To Kringle 4

As mentioned in section 4.1 lanthanide ion binding studies are particularly useful in that the effects arising from binding the paramagnetic ions can be differentiated from the effects on the spectrum of simple metal binding by the use of a diamagnetic tripositive lanthanide ion. Thus, we begin this study by considering the addition of lanthanum ions to the native protein.

4.5.1 Lanthanum

The spectra at various metal ion to protein molar concentration ratios are shown in Fig. 4.30 and it can be seen that the additions are not without effect on a number of resonance positions. This is not only indicative of the metal ions binding to the protein but also of actually perturbing the structure in such a way as to cause these changes in the spectrum. Thus, adding these metal ions provides a probe for the structure while at the same time altering it in some way and it is obviously essential to separate the two features. It must be emphasised that this

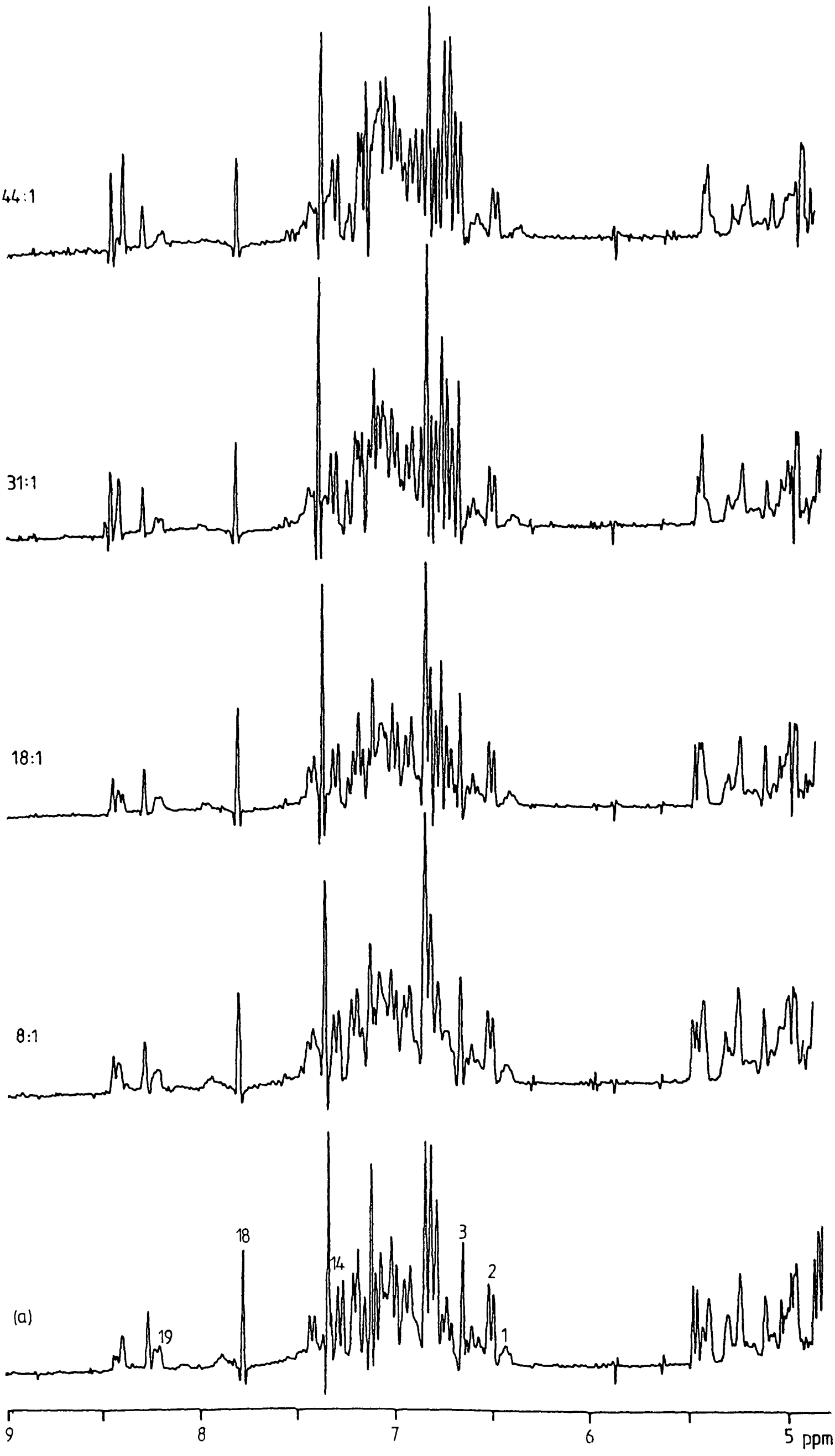

Fig. 4.30A Aromatic region of the lanthanum ion titration of kringle 4; 37°C, pH 5.5. Resolution enhanced spectra. (a) Native protein. Approximate molar concentration ratios of metal ions to protein are indicated.

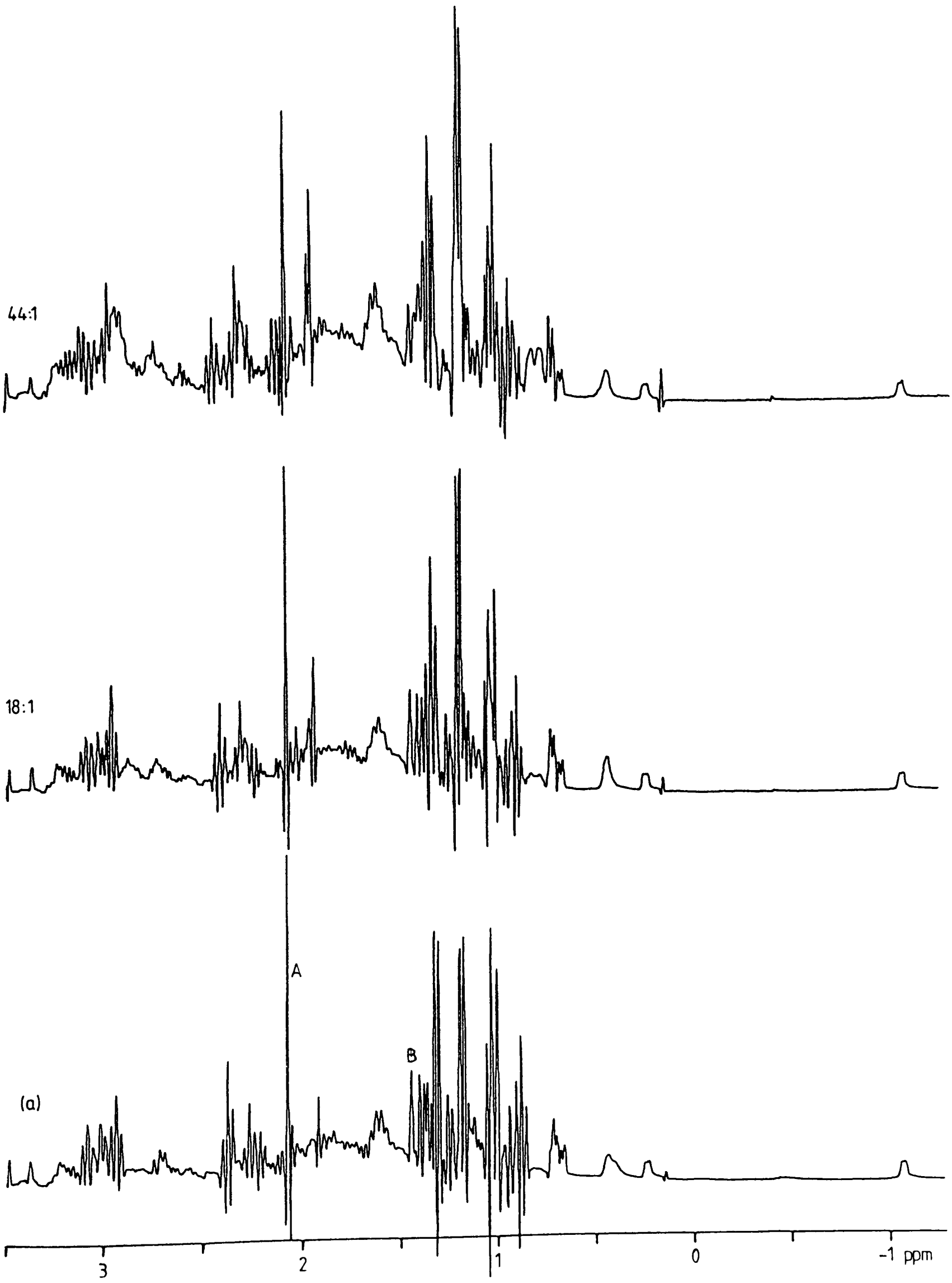

Fig. 4.30B Aliphatic region of the lanthanum ion titration of kringle 4; 37°C, pH 5.5. Resolution enhanced spectra. (a) Native protein. Approximate molar concentration ratios of metal ions to protein are indicated.

titration, and indeed all the lanthanide experiments discussed here, were carried out at a constant pH of 5.5 and that spectral changes are not attributable to changes in the pH of the solution.

Looking more closely at Fig.4.30B we note the appearance of peaks at about 0.8 ppm particularly prominent in the spectrum at the highest metal ion to protein ratio. Furthermore, the Met B resonance loses intensity through the titration while a peak appears at 1.95 ppm (just downfield of the acetate impurity peak) which is the random coil position for the methionine methyl protons. In addition, the peak at the threonine methyl proton random coil position becomes more intense. These changes are all consistent with the metal ion binding destablising the protein structure leading to denaturation. The aromatic region of the spectrum also shows changes indicative of this process. Intensity can be seen to gradually amass at random coil values, while other resonances broaden out, exemplified for instance, by the peaks R1, R12, R15, and R19 of Trp. A. Resonance R2 of Tyr 2(A) is also seen to lose intensity as the metal ion concentration is increased. The temperature dependence of the spectrum for the sample at the highest metal ion concentration is shown in Fig. 4.31. The spectrum obtained at $47^{o}C$ is essentially that expected of a random coil structure being extremely similar to that of the native protein thermally denatured at $77^{o}C$ (Fig. 3.31). Comparison of figures 4.30 and 4.31 then does show that many of the changes induced by metal ion binding are leading to denaturation of the protein. A direct contrast between the widely differing transition points for the thermal denaturation of the protein with and without added lanthanum ions cannot be drawn because the two samples were not at the same pH and no formal pH studies of this have been made. However, extrapolation of the changes shown in Fig. 4.30 strongly suggests that the spectrum of the denatured protein would have

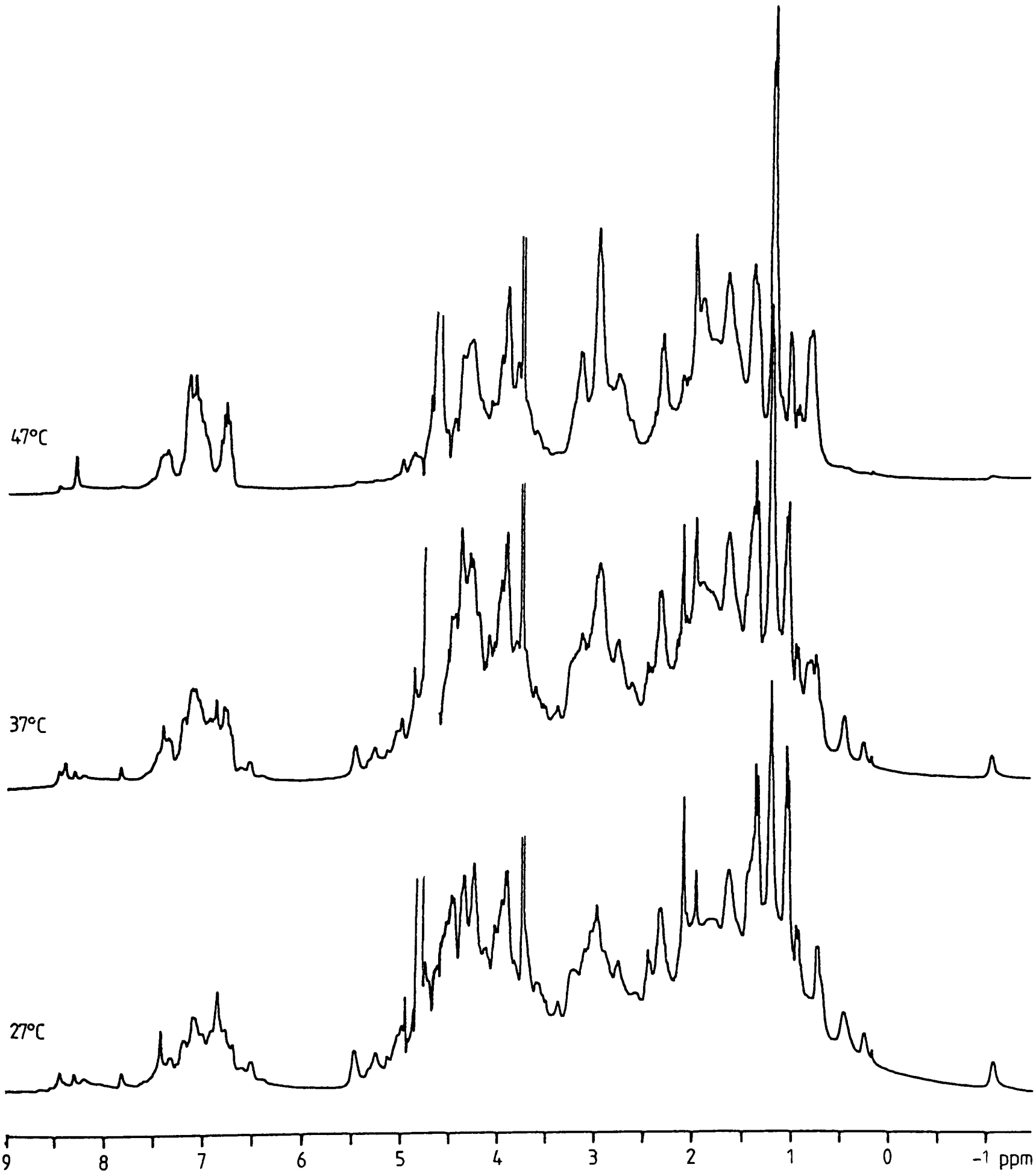

Fig. 4.31 Temperature dependence of the lanthanum ion bound sample (~44:1) of kringle 4, pH 5.5 (see text).

been obtained at 37°C if the metal ion concentration had been raised sufficiently high. This would also keep increasing the ionic strength of the solution and the possibility arises that it is this effect which leads to the denaturation. However, even at the highest metal ion to protein ratio shown in Fig. 4.30 the ionic strength has only been increased some two and a half fold. Again no formal studies of the spectral dependence on the ionic strength of the solution have been performed as yet, but no significant changes are seen between spectra from samples in D_2O and 100 mM NaCl solution, at the same pH and temperature. Furthermore, the spectral changes begin with and continue smoothly from the first addition of lanthanum mitigating, in view of the previous remark, against a simple ionic strength effect. Another possibility is that simple association of the tripositive ions with surface carboxyl groups leads to an unfavourable surface charge promoting denaturation, and indeed this factor may well make a contribution to the observed effects. However, as the titration proceeded, the changes induced were reminiscent of the denaturation at low pH produced by the presence of excess hydrogen ions described in section 4.2. The changes mentioned specifically above support this notion, but the lanthanum ion titration was of course performed at a constant pH. A further possible explanation then of the denaturation is that the metal ions are preferentially bound by a carboxyl group or groups involved in the native protein in forming salt bridges essential for stabilising the structure. Thus, a precise description of the unfolding produced by the addition of lanthanum ions, like that arising from added protons, is unclear.

As well as the spectral changes specifically attributed to the denaturation, many resonances show smooth linear shifts in their resonance positions when plotted against the added metal ion concentration. These plots are not shown as the induced shifts are very

small, but their form indicates the metal ion to be binding in fast exchange. As with the ligand binding described in the previous section, the changes are much more pronounced in the aromatic region of the spectrum as can be seen in Fig. 4.30A, the final spectrum being very different from the first. A number of well resolved resonances can be followed throughout and of these R1, R3, R14, R18 and R19 show the largest shifts of around 0.03 ppm, at the most over, the whole range of the titration. It is interesting to note that in this list, resonances from the indole rings of all three tryptophans are included and R14, assigned to Tyr 73 which was seen above to have a considerably elevated pKa indicative of an environment involving other parts of the protein molecule. The NOE and ligand binding studies have all indicated these side chains to be closely related and to lie within the core of the molecule. Thus, it appears that the lanthanide binding specifically affects side chains in the hydrophobic core of the molecule. This could be the result of conformational changes as the protein unfolds, but it is unlikely as not all residues shown to be intimately related are similarly affected. For instance, the resonances of Leu 45 (L1, L2) and of Tyr (R9, R13) seen in Fig. 4.7 to be close in space to Trps 25 and 61 are not shifted to the same extent as some of the tryptophan peaks. Consequently, a lanthanide ion binding site may well be located close to the hydrophobic interior of the protein and as suggested at the end of the last main section could serve as a probe of the amino site of the ω-amino carboxylic acid ligands. Further evidence that this is indeed the case will be shown below in the section on praseodymium ion binding.

One common use of lanthanide shift reagents in NMR studies is to simplify spectra by spreading resonances over a larger chemical shift range as an aid to assignment. Although lanthanum is not a shift reagent, we have remarked on the changes its addition to the protein makes on the

aromatic region of the spectrum, and while not leading to a simpler spectrum does provide yet another opportunity to try and recognise the intensity from the unassigned phenylalanine and tyrosine side chains. A number of spin decoupling experiments were performed on samples containing metal ions. Again no clear new assignments were elucidated but as demonstrated by previous sections much more intensive investigation of each spectrum is required to make substantial progress in this direction. It is clear that these lanthanide ion binding studies could be of considerable benefit in completing the assignment of the aromatic region of the spectrum but as yet this has not been a dominant aim and no further reference to this will be made in what follows. Only resonances that are clearly visible and assigned will be commented on in discussions of these metal ion titrations. The fact that high lanthanum ion concentrations lead to unfolding of the protein means that useful information from the lanthanide ion acting solely as a structural probe can only come from data at low metal ion concentrations. In the praseodymium and europium additions considered below the metal ion to protein concentration did not exceed 18:1 and the gadolinium ion concentrations are an order of magnitude smaller. The shifts produced by the addition of lanthanum at the same concentration provide a diamagnetic blank which can be subtracted from the shifts produced by the other ions to give the value of the paramagnetic contribution to the total. We now consider the addition of praseodymium ions to kringle 4.

4.5.2 Praseodymium

4.5.2.1 Resonance Shifts

Spectra at increasing metal ion to protein concentration ratios are shown in Fig. 4.32. As expected from a shift reagent the spectra are

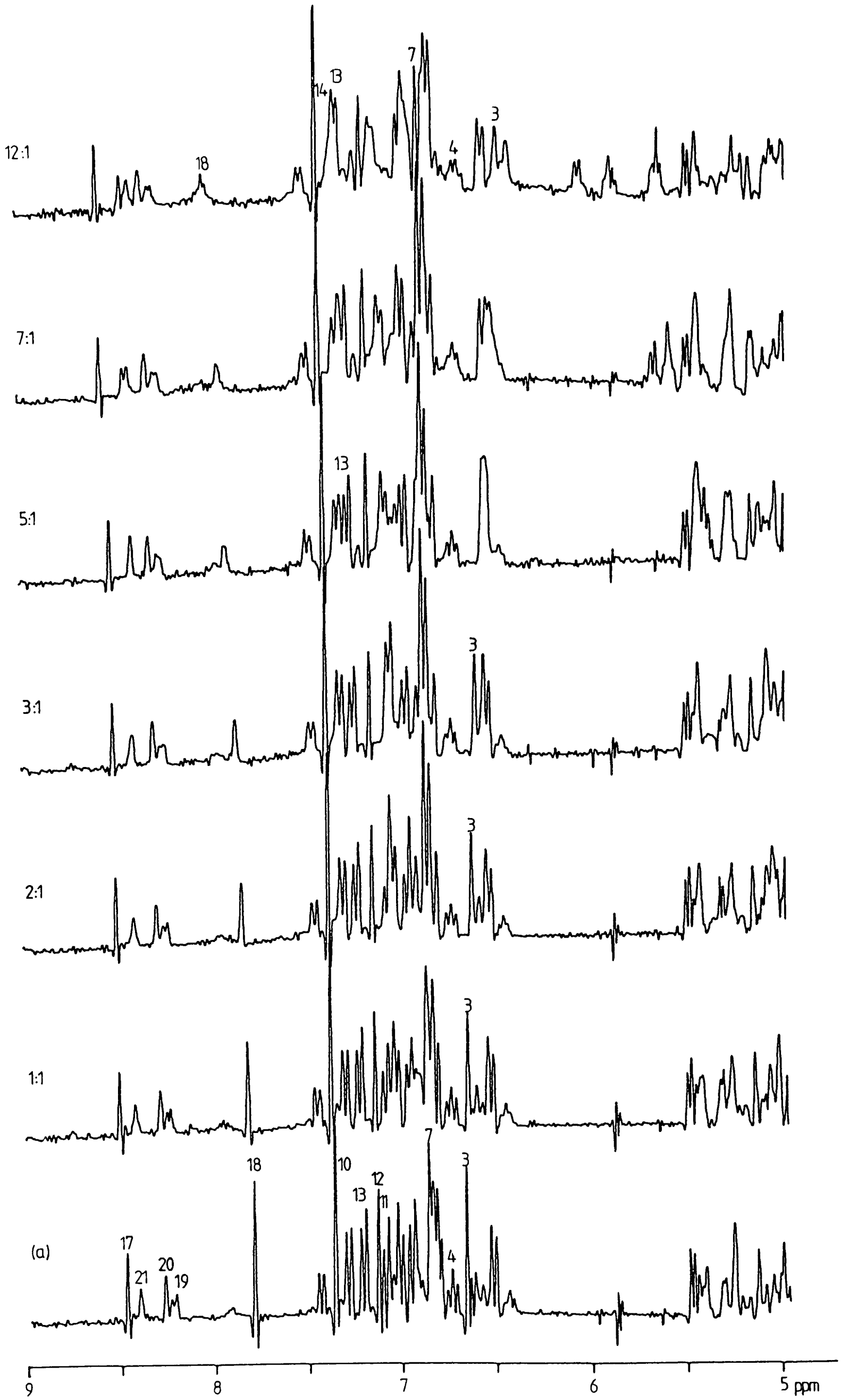

Fig. 4.32A Aromatic region of the praseodymium ion titration of kringle 4; 37°C, pH 5.5. Resolution enhanced spectra. Approximate molar concentration ratios of metal ion to protein are indicated.

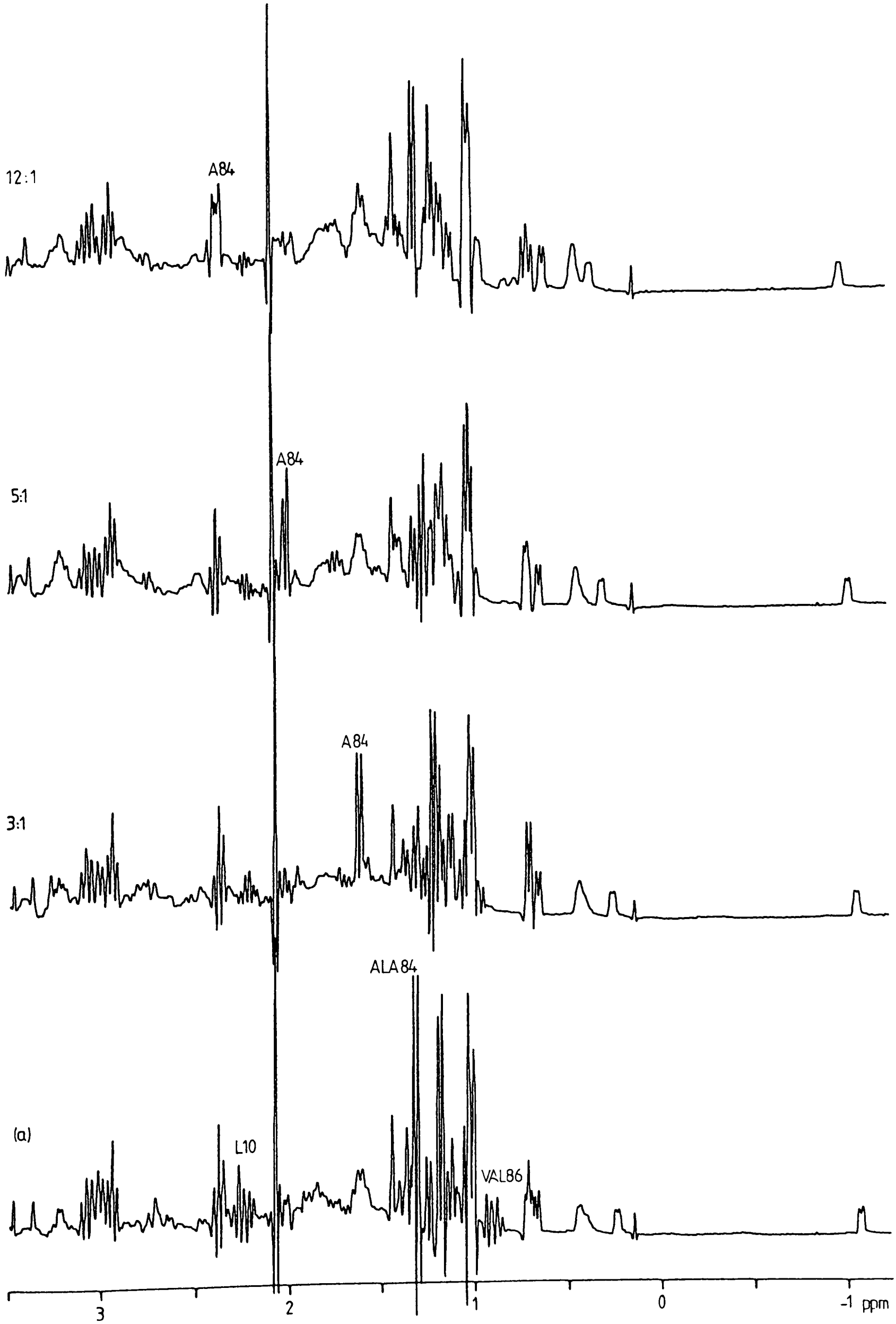

Fig. 4.32B Aliphatic region of the praseodymium ion titration of kringle 4 37°C, pH 5.5. Resolution enhanced spectra. Approximate molar concentration ratios of metal ion to protein are indicated.

considerably more perturbed by praseodymium ion binding than with lanthanum, but once again the changes in the aromatic region of the spectrum are on the whole more widespread and extensive than in the aliphatic. The plots of chemical shift versus metal ion to protein concentration ratios for some of the resonances are shown for the two regions in Fig. 4.33 and Fig 4.34 respectively. The metal ion binding is again seen to be in fast exchange with only slight broadening of resonances occurring at the higher metal ion concentrations due to the additional relaxation induced by the parmagnetic ion. This is most noticeable on the resonances that receive the largest shifts, for example R3, R18 and Ala 84 and is a direct reflection of the proximity of the proton to the metal ion.

Praseodymium commonly causes downfield shifts of resonance positions (Bleaney et al., 1972) as is the case for the majority of resonances shown in the plots. However, R3, R23, R4 and R11 all assigned to Trp 71 are moved upfield by the added metal ions as are the methyl proton resonances of Val 69. (R21 assigned to His 31 may also move in the same direction but Fig. 4.32A shows the difficulty in following this resonance. Unfortunately, the C2 proton resonances, R16 of this residue is exchange broadened at the pH of this experiment and so cannot be followed either). This is a reflection of the geometric distribution of these side chains about the metal ion binding site as discussed in section 2.2 and indicated in Fig. 4.35.

It is very interesting that Val 69 and Trp 71 both close in the primary sequence should be linked in this way and in particular that the Val 69 resonances are separated from the L5 methyl proton resonance. This data strongly suggests that Val 69 and Trp 71 lie in similar regions of the molecule. Both side chains were affected by AMBOC binding

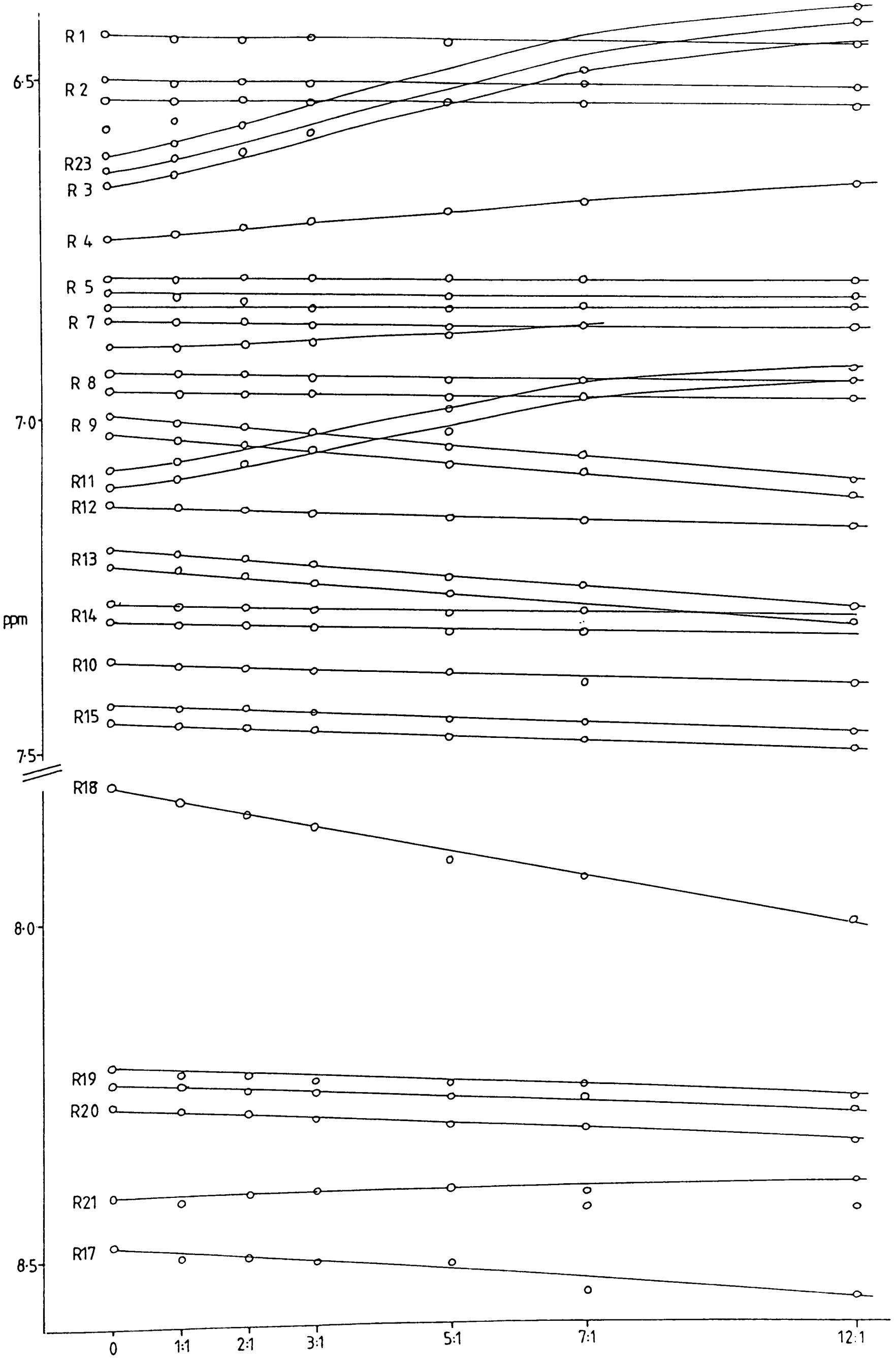

Fig. 4.33 Plots of chemical shift of aromatic resonances versus metal ion to protein concentration ratio for the praseodymium ion titration of kringle 4; 37°C, pH 5.5.

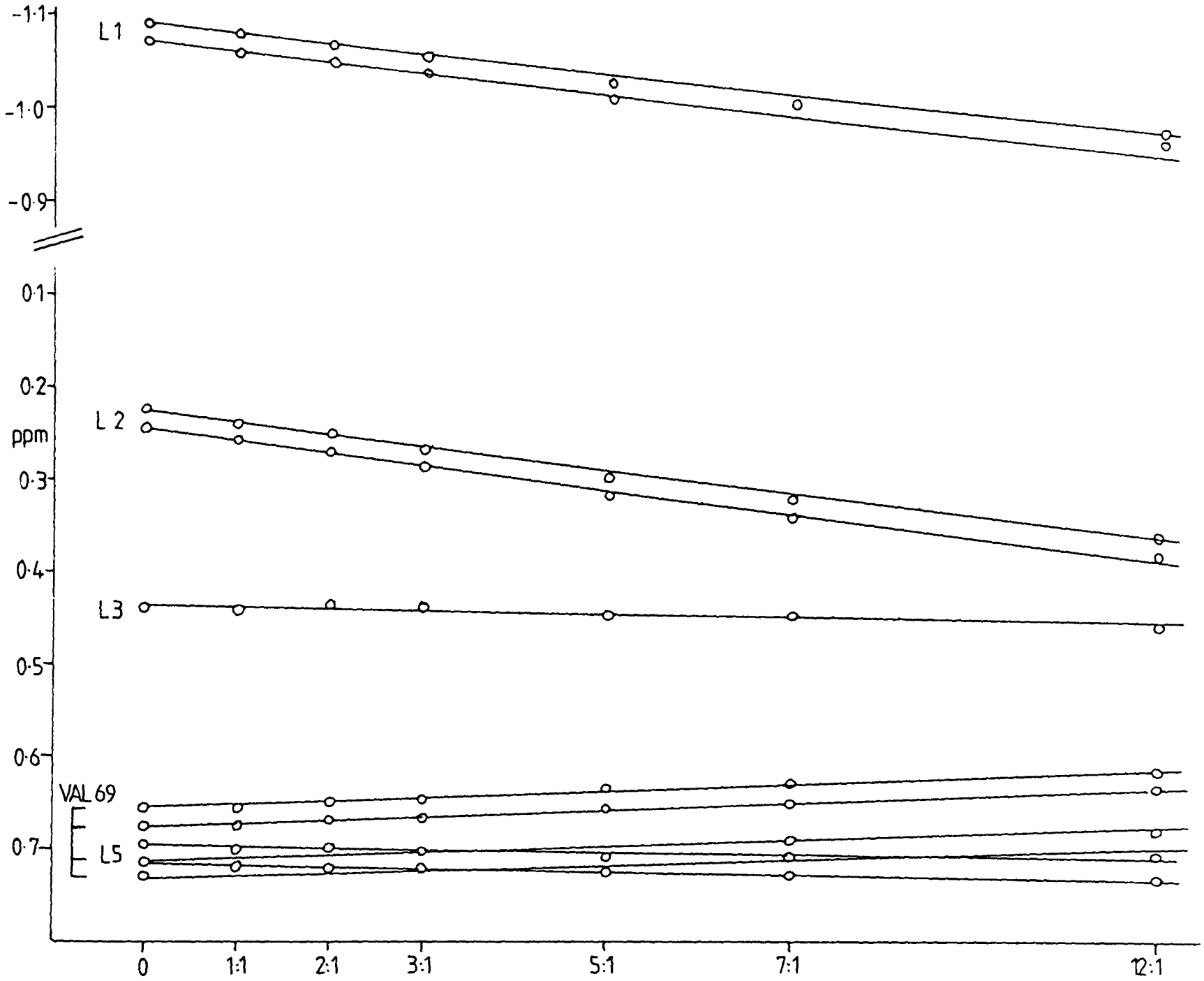

Fig. 4.34 Plots of chemical shift of aliphatic resonances versus metal ion to protein concentration ratio for the praseodymium ion titration of kringle 4; 37°C, pH 5.5.

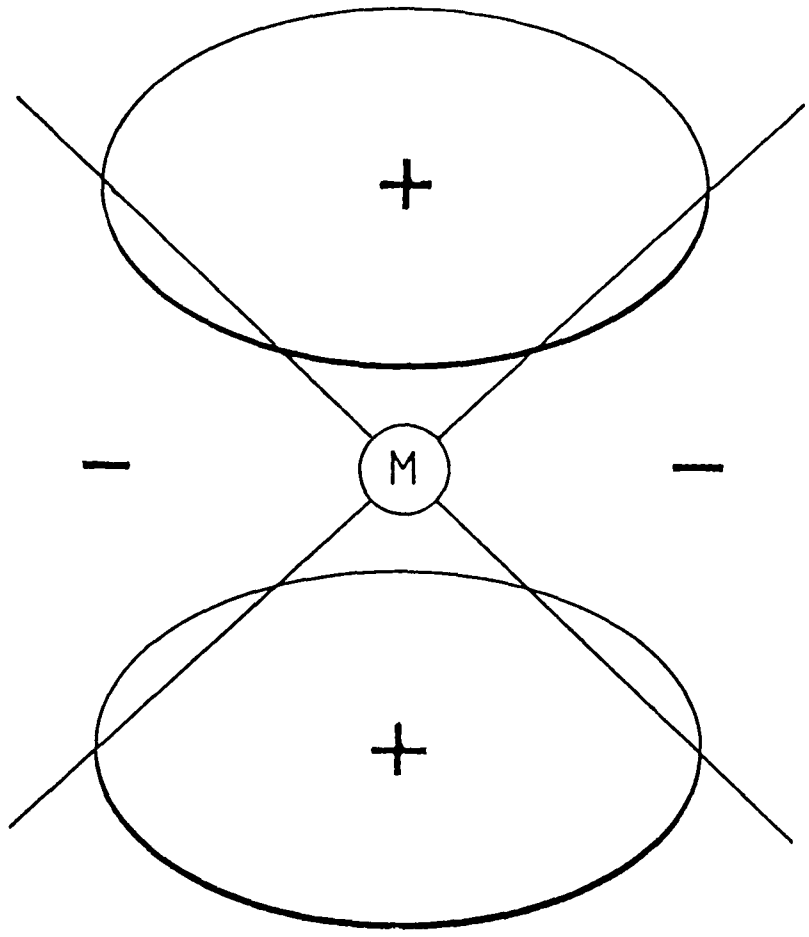

Fig. 4.35 Geometric dependence of the induced shift about the praseodymium ion. The signs indicate the direction of the shift: +ve is downfield, -ve upfield.

although Val 69 appeared to be unaffected by 6 aminohexanoic acid binding. In connection with this, ligand binding studies of kringle 4 carried out by Hochschwender et al., (1983) using the ligand p-benzylaminesulphonic acid are of interest. In common with our results they found the aliphatic region of the spectrum markedly unperturbed by the addition of the ligand, except for the methyl proton resonances of Val 69 which showed a marked upfield shift. The ligand they used contains an aromatic ring and it is conceivable that it is a ring current shift that accounts for this effect on the Val 69 peaks. Incidentally R3 in their spectra was quite dramatically affected by the ligand binding . Thus, although the NOE data may not have been conclusive for reasons mentioned before, it seems very probable that Val 69 lies near in space to Trp 71 and to the bound ligand. The latter conclusion though was suggested by the results of the NOE experiment shown in Fig. 4.27 for the ligand bound proteins and discussed in section 4.4.3.4.

We note from Fig. 4.33 that the largest shifts in the aromatic region are shown by the resonances of Trp 71 and the C2 proton resonance of Trp B (R18). The intimate relation of the Trp B resonance to the site of the amino group binding was noted from the difference in its pH dependence in the presence of bound ligand. These data again suggest that the lanthanide ion is binding to the same carboxyl group or groups that form the amino binding site of the ligand. We note the different shifts induced on the doublet resonances of Trp 71 (R23, R11) compared to that of the triplet (R4). These well characterised shifts could form valuable data in future computation involved in specifying precise distances and orientations about the metal ion, as will be considered further below.

In accord with the effects on the resonances of Trp 71 and Trp B other side chains affected by ligand binding would similarly be expected to be altered by the presence of the paramagnetic ion. Indeed, it is seen

that resonances of Trp A (R1, R12, R15 and R19), Tyr 40 (R9, R13), His 31 (R21), His 33 (R20, R7) are all affected to varying extents. Noticeably, R14 of Tyr 73 is barely altered but was only affected by AMBOC binding and not by 6 aminohexanoic acid. In the aliphatic region L1 and L2 of Leu 45 are markedly shifted. This is all in complete agreement with the ligand binding data and the proposed site of metal ion binding. In addition Tyr 49 (R6, R8) and the L5 resonance, little affected by ligand, are only marginally altered by praseodymium binding. The Met A resonance is unaffected but very curiously the Met B peak shows a very small upfield shift, the significance of which is unexplained. However, we note that although Tyr 2 and His 3 are conspicuously untouched by ligand binding, their resonances (R2, R5 and R10, R17) do show some metal ion induced changes but the methyl proton resonances of Leu 76 (L3) are relatively unaffected, all three residues being closely related in space around the first disulphide bridge. It is not surprising to see that the methyl proton resonance of the C terminal Ala 84 shows a marked shift, as do the methyl proton resonances of the other C terminal residue Val 86. The γ CH_2 proton resonance, L10 assigned to Glu 83 disappears from the spectrum. These findings suggest the presence of another metal ion binding site formed by the carboxyl groups of the extra-kringle residues and perhaps accounts for the small shifts on the peaks of Tyr 2 and His 3. Once again the involvement of any aspartate side chains in the binding can only be said to be supported by changes in intensity at the random coil chemical shift values of their β CH_2 protons. It is noticeable that some intensity is shifted well downfield of the aliphatic region to almost 6 ppm at the highest metal ion concentration and it is postulated to arise from protons closest to the metal ion most likely those adjacent to the carboxylic acid groups directly involved. Unfortunately, though they remain unassigned as yet.

Having considered the more significant effects of the addition of praseodymium ions we now go on to discuss the effects of adding 6 aminohexanoic acid to the protein sample containing metal ions at a concentration ratio of 12:1.

4.5.2.2 6 Aminohexanoic Acid Addition

Figure 4.36(a) shows again the spectrum at 12:1 metal ion to protein from Fig. 4.32. Figure 4.36(b) shows the spectrum of the same sample which now also contained 6aminohexanoic acid at a ligand to protein concentration ratio of 4:1. Figure 4.36(c) shows the spectrum of 6 aminohexanoic acid bound protein at a similar pH for comparison. It is seen that the effects of adding the ligand to the metal bound protein are dramatic with much of the resulting spectrum being identical to that of the protein with no praseodymium ions present. In particular, resonances substantially moved by the addition of the metal ions such as R3 and R18 from Trp 71 and Trp B respectively are completely restored to their unshifted positions. Furthermore, resonances such as R1, R11, R19, R22 which are markedly affected in the native protein on adding 6 aminohexanoic acid are found at positions indicative of the ligand also binding to the protein in the presence of the praseodymium ions. This is supported by the comparison of the exact overlap of the L5 methyl resonance with the downfield methyl proton doublet of Val 69 in Fig. 4.36 B (b) and (c) with the difference in the native protein, Fig. 4.32 B (a). This curious feature of ligand binding was commented on in section 4.4. The implication of these observations are important for they remove all possibility that the spectral effects of adding the ligand are due to it chelating the metal ions more firmly than the protein. Rather the protein is seen to have a higher affinity for the ligand and the bound metal ions are displaced by the ligand. Thus, the praseodymium is indeed

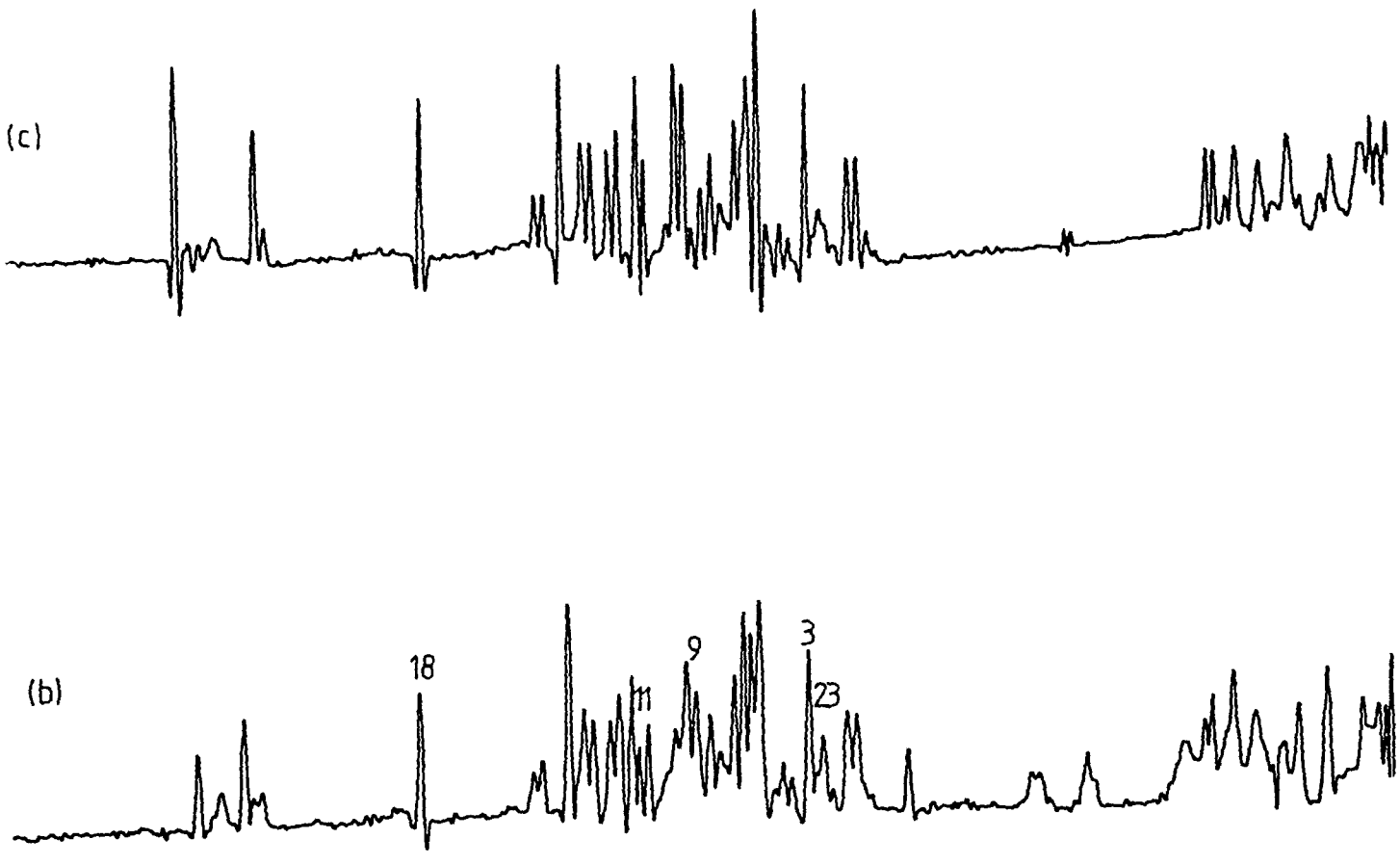

Fig. 4.36A Resolution enhanced spectra of the aromatic region of the spectrum; 37°C, pH 5.5. (a) Praseodymium ion to protein ratio of ~12:1 (b) 6 aminohexanoic acid addition to the sample of (a) ligand:protein concentration ratio of 4:1 (c) Native protein with added 6 aminohexanoic acid.

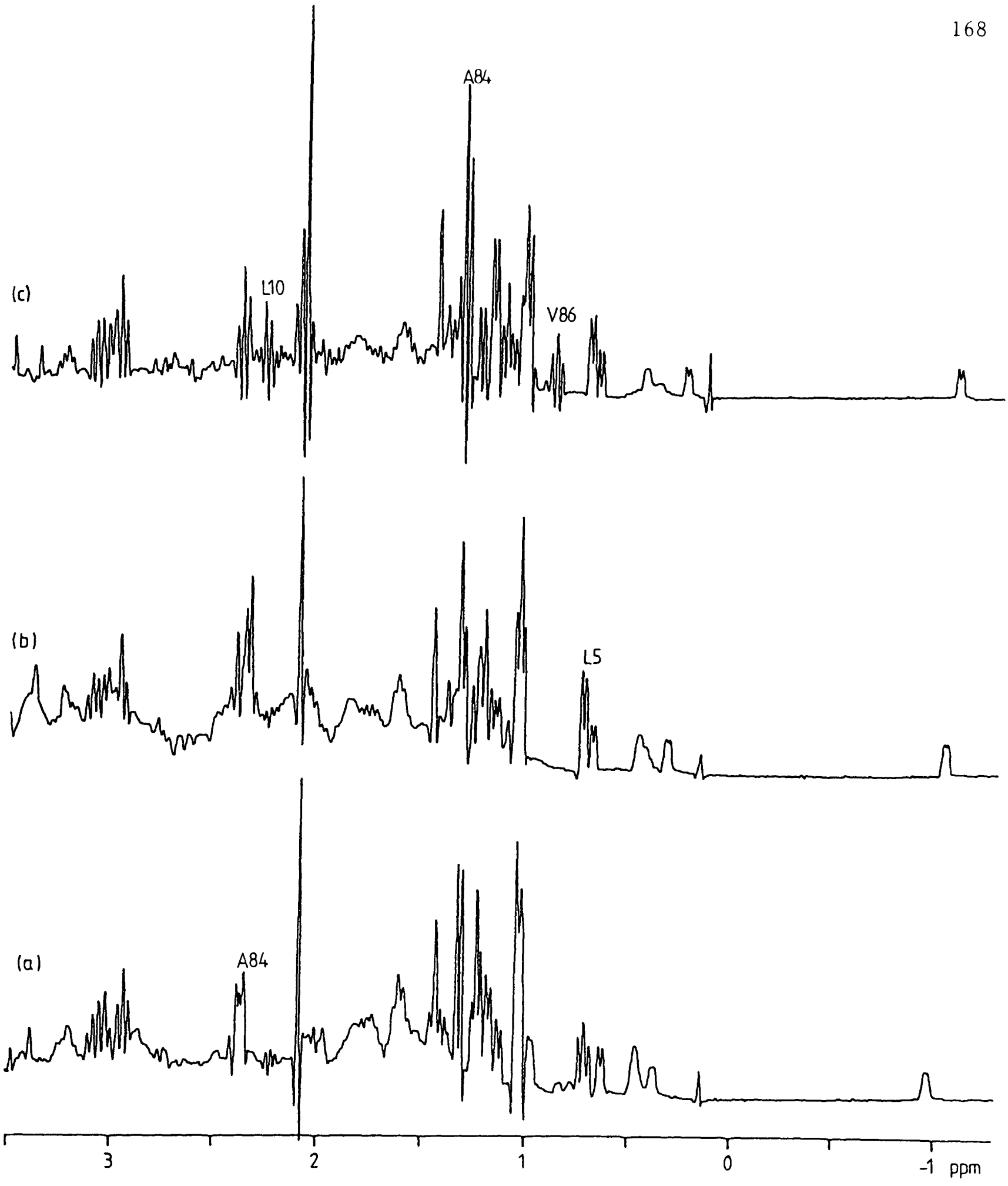

Fig. 4.36B Resolution enhanced spectra of the aliphatic region of the spectrum; 37°C, pH 5.5. (a) Praseodymium ion to protein ratio of ~12:1 (b) 6 aminohexanoic acid addition to the sample of (a) ligand:protein concentration ratio of 4:1 (c) Native protein with added 6 aminohexanoic acid.

actingas a probe of the ligand amino acid group binding site, and confirms what was suggested by the lanthanum ion binding. However, the data described above indicated the presence of two main metal ion binding sites, the second being located around the first disulphide bridge and the C terminal carboxyl groups. This is fully vindicated by the data in Fig. 4.36, for it is seen that the resonances assigned to Glu 83 (L10), Ala 84 and Val 86 are not restored to their unshifted positions by the addition of ligand and are still affected by the bound metal ions. The effects of the metal binding at this other site on aromatic resonances was generally small, and unfortunately the pH was slightly altered by adding the ligand so that any effects on the His 3 resonances are therefore obscured. However, it is clear that not all the bound metal has been displaced by the ligand binding for the resonances around 6 ppm in Fig. 4.36 A (a) remain in the spectrum with added ligand Fig. 4.36 A (b). To further characterise these other metal binding sites another addition of ligand was made to the sample of Fig. 4.36(b) and gadolinium ions added to the solution.

4.5.2.3 Subsequent Addition of Gadolinium Ions

The results are shown in Fig. 4.37. Gadolinium ions cause increased relaxtion of nearby protons and so broaden resonances but do not lead to any shifts. Thus, as expected, the unassigned resonances around 6 ppm disappear from the spectrum on the first addition. Similarly, the methyl proton resonance of Ala 84 is broadened (as is the adjacent resonance from the α $C\dot{H}_2$ protons of the ligand, labelled "α" in Fig. 4.37 B (a)). This is in accord with the proposed metal binding site around the C terminal residues and supported by the disappearance of the His 3 resonances (R17, R10), although the resonances of Tyr 2 (R2, R5) appear little, if at all affected. We note that most of the resonances affected

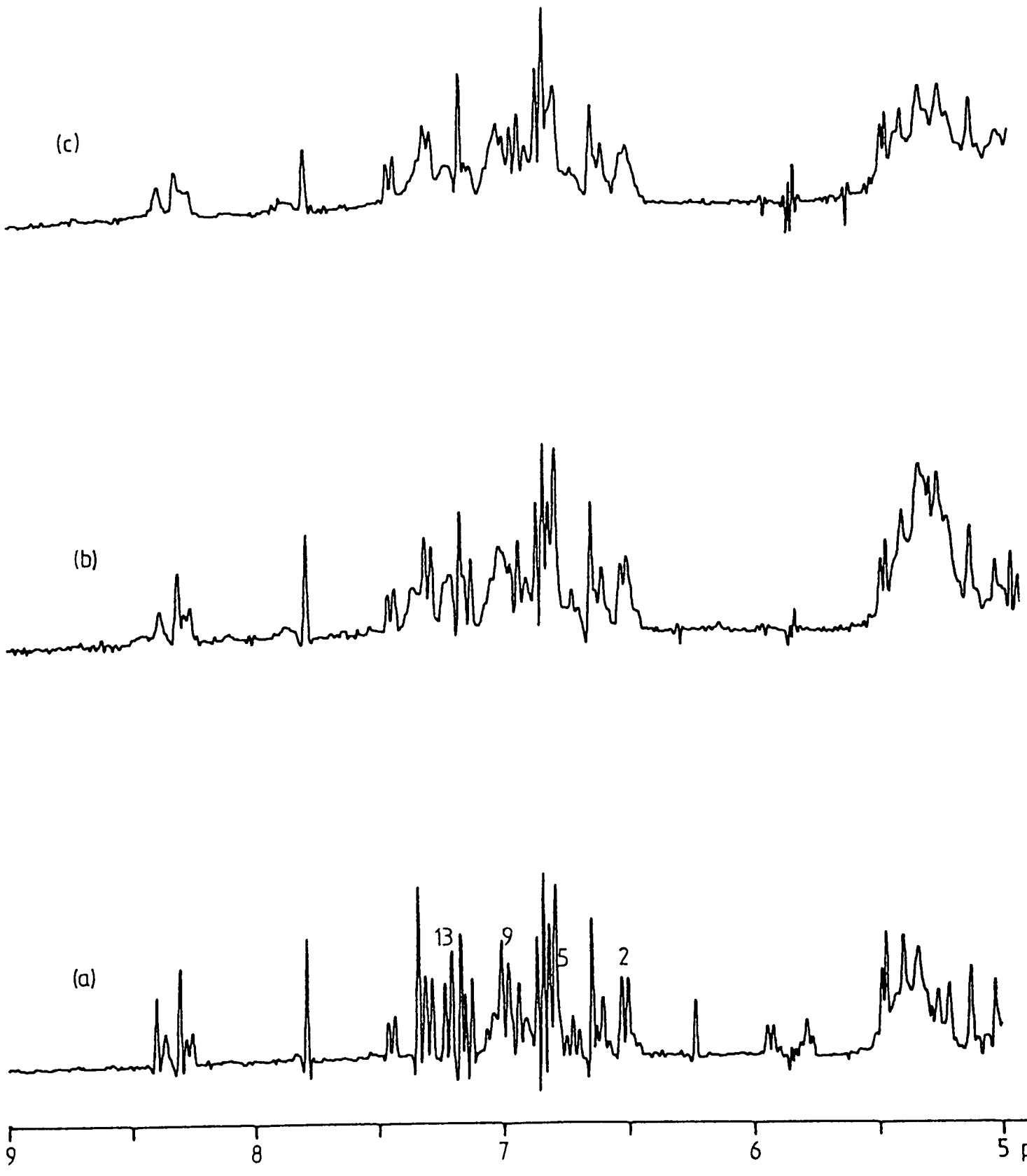

Fig. 4.37A Resolution enhanced spectra of the aromatic region; 37°C, pH 5.5. (a) Sample of Fig. 4.36(b) with additional 6 amino-hexanoic acid (~6:1 ligand to protein) (b) and (c) are successive additions of gadolinium ions.

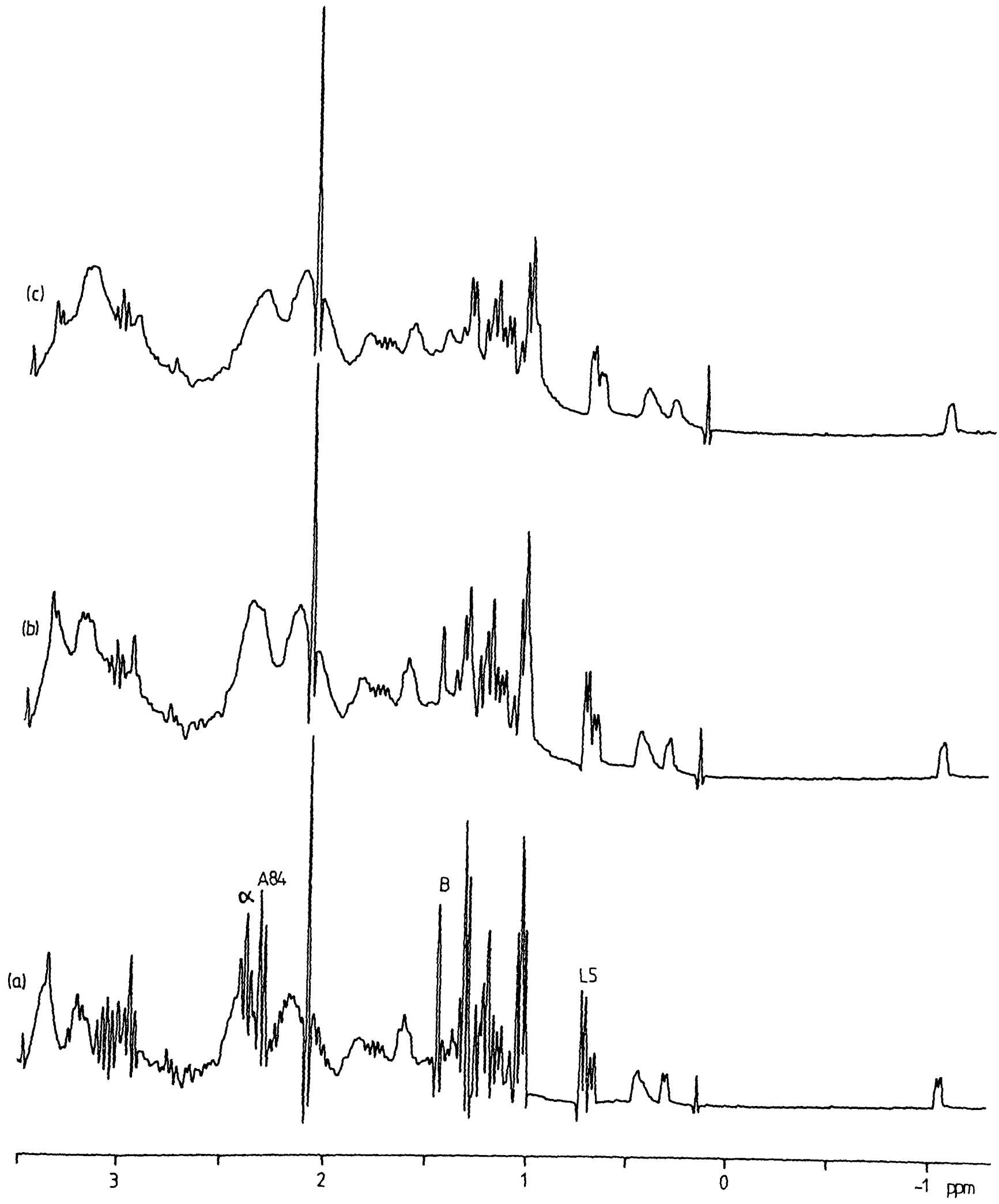

Fig. 4.37B Resolution enhanced spectra of the aliphatic region; 37°C, pH 5.5. (a) Sample of Fig. 4.36(b) with additional 6 amino-hexanoic acid (~6:1 ligand to protein) (b) and (c) are successive additions of gadolinium ions.

by ligand and praseodymium ion binding are protected from the effects of gadolinium ions by the presence of the bound ligand. However, there is one noticeable exception to this statement. The resonances of Tyr 40 (R9, R13) are quite noticeably broadened by the added gadolinium ions, suggesting that of the residues lying around the lysine binding site, this side chain is more superficial and accessible to the solvent. This notion is corroborated by the normal tyrosine pKa exhibited by this residue and will be further supported by data from chemical modification studies. Interestingly, we note that the methyl proton doublet L5 and the Met B peak (which is incidentally returned to its unshifted position on adding the ligand) are also affected by the gadolinium additions. Both these residues have been related to Tyr 49 (B) in space (Fig. 4.4) although the latter (peaks R6, R8) appears untouched by the gadolinium additions and these effects are unexplained.

Thus, these experiments using praseodymium have established lanthanide ions as valuable probes of the ligand binding site and we now briefly consider the effects of adding a different lanthanide shift reagent.

4.5.3 Europium

As would be expected the spectral effects of adding europium ions to kringle 4 are qualitatively similar to those arising from the praseodymium ion titration, with the difference that europium causes slightly more broadening of resonances. This is seen in Fig. 4.38 which can be compared with Fig. 4.32 A. R3 and R18 are again markedly shifted, but R18 and probably R3 is almost completely broadened from the spectrum at the highest metal ion concentration. Plots of the shift versus metal ion to protein concentration ratio are given in Figs. 4.39 and 4.40. (The curves for resonances R17, R10 of His 3 have been omitted as the pH was not absolutely constant over the intial additions of europium). In

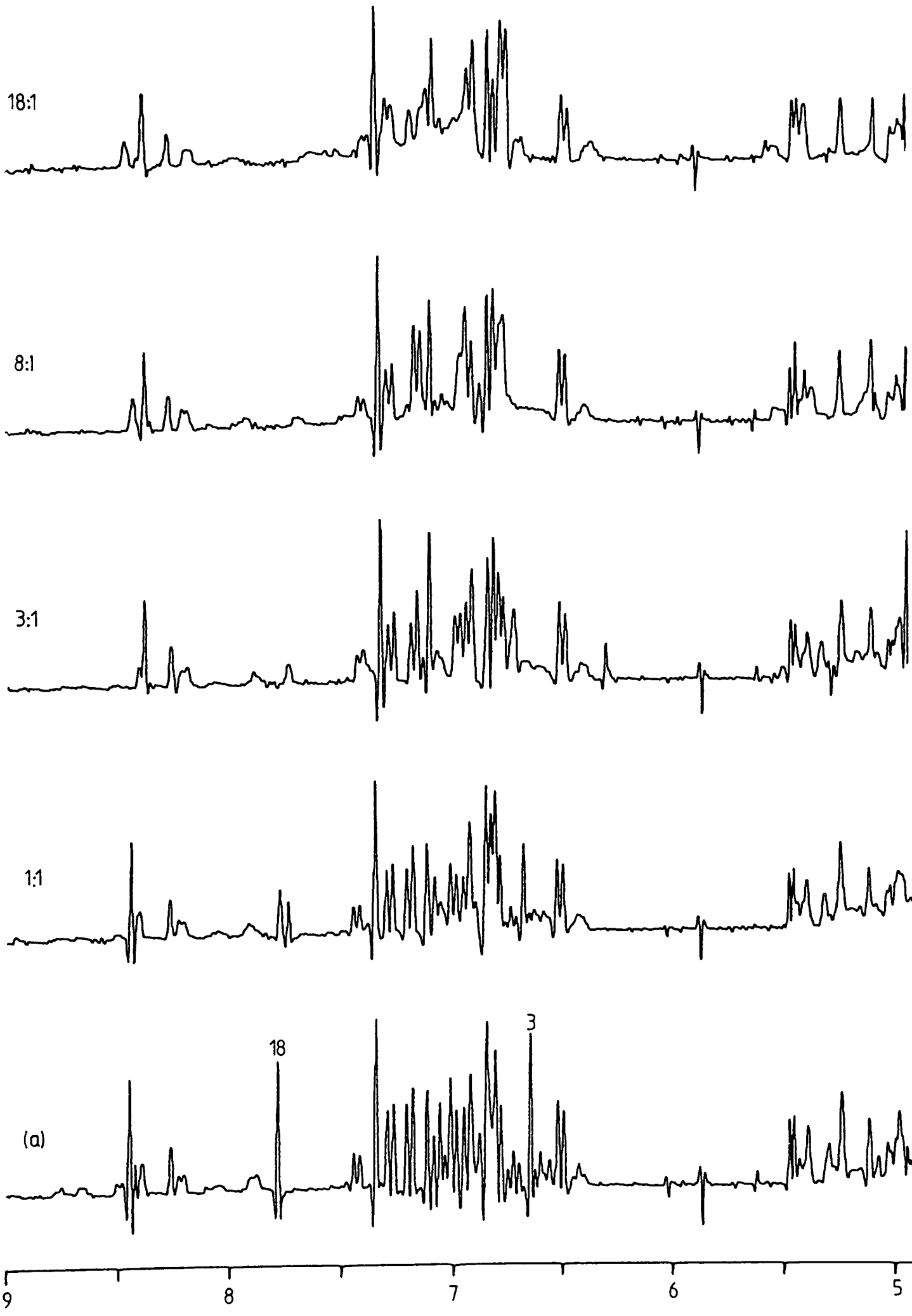

Fig. 4.38 Aromatic region of the europium ion titration of kringle 4; 37°C, pH 5.5. Resolution enhanced spectra. Approximate molar concentration ratios of metal ions to protein are indicated.

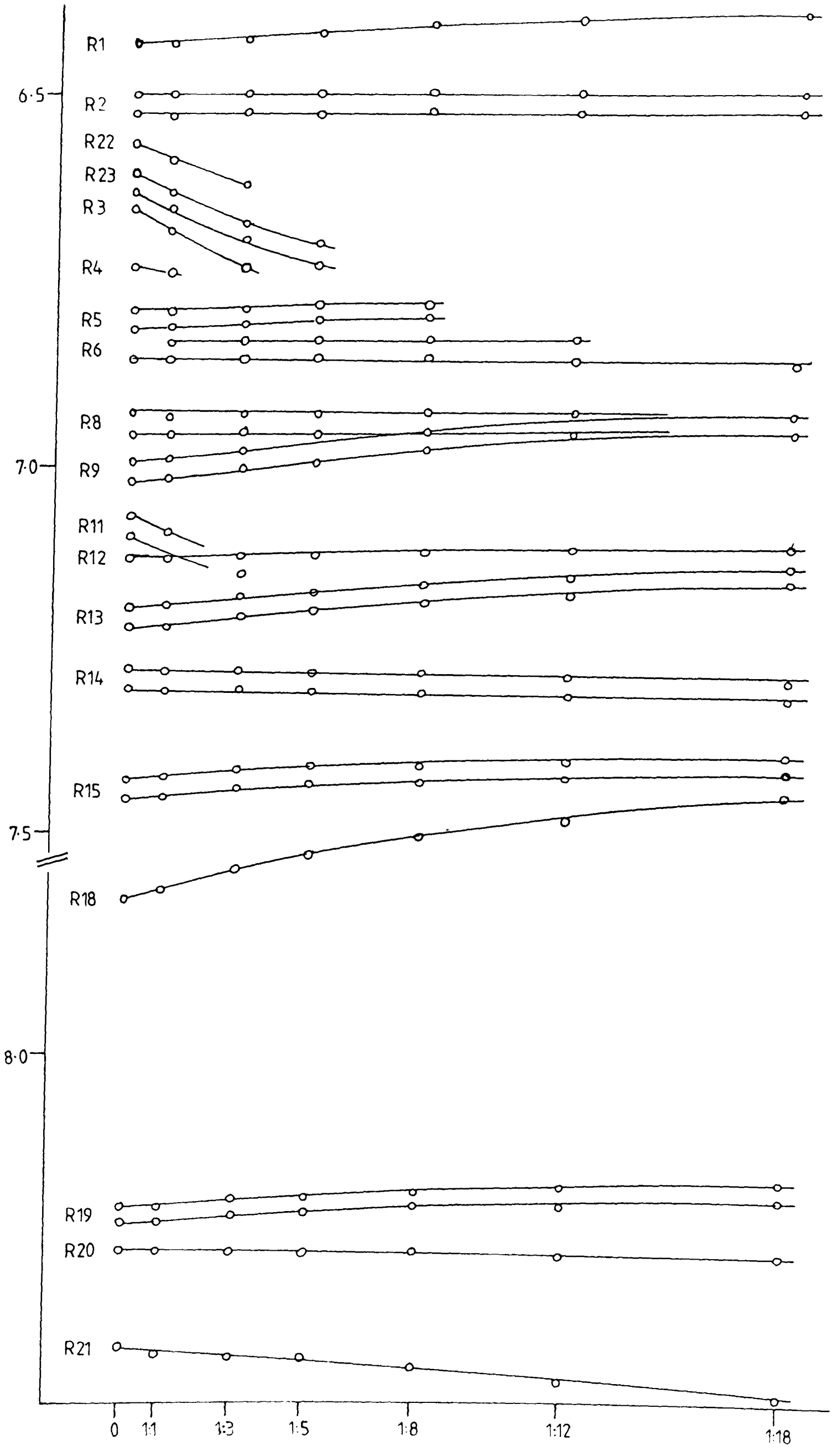

Fig. 4.39 Plots of chemical shift of aromatic resonances versus metal ion to protein concentration ratio for the titration of kringle 4 by europium ions; 37°C, pH 5.5.

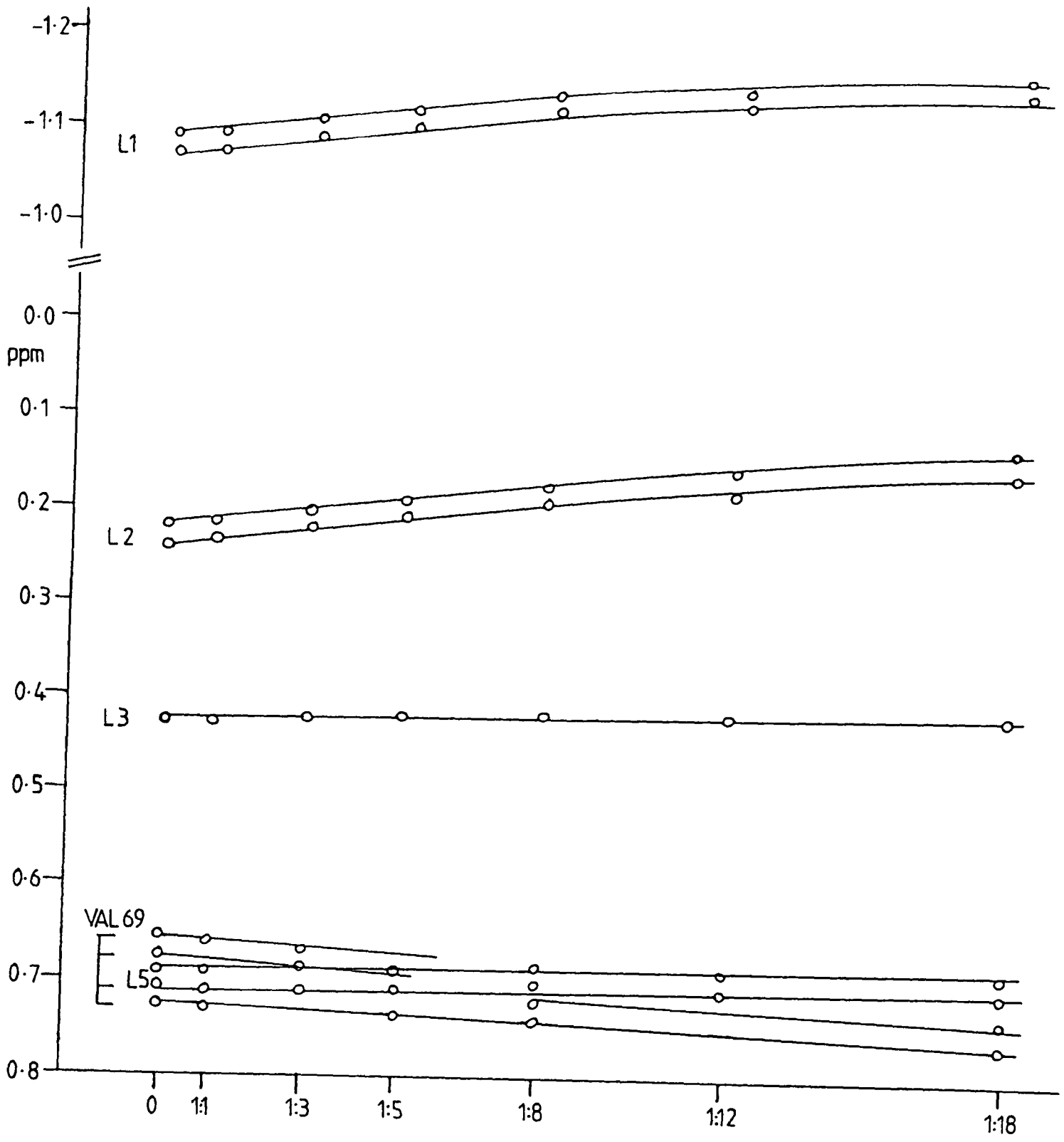

Fig. 4.40 Plots of chemical shift of aliphatic resonances versus metal ion to protein concentration ratio for the titration of kringle 4 by europium ions; 37^{o}C, pH 5.5.

contrast to praseodymium, europium characteristically leads to upfield shifts of resonances as are clearly seen in the plots. But in excellent agreement with the results shown in Figs. 4.33 and 4.34, resonances R3, R23, R11 from Trp 71, R21 from His 31 and the methyl proton peaks of Val 69 are all moved in the opposite direction. In addition, although R18 from Trp B is moved upfield it appears that the triplet resonance R22 from the same resonance may be moved downfield, but the data is not clear and needs to be confirmed as this resonance was obscured by the Trp 71 peaks in the praseodymium titration.

Adding 6 aminohexanoic acid to the europium bound protein again caused the majority of shifted resonances to return to their unperturbed positions and in general, the relative magnitude of the effects arising with the two shift reagents was found to be extremely similar. This latter remark raises the possibility that the lanthanide ions may be binding with effective axial symmetry. As described in section 2.2 this is extremely important, for if this condition does indeed pertain then detailed distances and angles of specific protons in the protein may be obtained relative to the metal ion. To test the hypothesis of axial symmetry the ratios of the shifts relative to a given resonance must be compared for each reagent.

4.5.4 Shift Ratios

Table 4.5 lists the shifts and shift ratios for a number of assigned resonances at the highest metal ion concentrations reached (The value for L5 refers to the unassigned methyl proton doublet and not the resonance of Val 69 which is considered by the L4 peak). The shifts have been corrected for the diamagnetic contribution using the data from the lanthanum titration. R12 was arbitrarily used for a reference resonance as it receives a moderate shift and is well defined in the spectra. The

Table 4.5 Shifts and shift ratios for selected resonances produced by Europium and Praseodymium ion binding to kringle 4. The shift ratios are referenced on that of resonance R12. +ve indicates downfield shift, -ve upfield.

RESONANCE	SHIFTS		SHIFT RATIOS	
	Eu^{3+}	Pr^{3+}	Eu^{3+}	Pr^{3+}
L1	-0.084	+0.100	3.23	2.33
L2	-0.092	+0.135	3.54	3.14
L3	-0.018	+0.020	0.69	0.47
L4	+0.033	-0.042	-1.27	-0.98
L5	0.000	+0.017	0.00	0.40
R1	-0.036	+0.039	1.38	0.91
R2	-0.015	+0.023	0.58	0.53
R3	+	-0.205	-	-4.77
R4	+	-0.071	-	-1.65
R9	-0.069	+0.110	2.65	2.56
R11	+	-0.142	-	-3.30
R12	-0.026	+0.043	1.00	1.00
R13	-0.068	+0.092	2.62	2.14
R14	-0.006	+0.032	0.23	0.74
R15	-0.042	+0.048	1.62	1.12
R18	-0.158	+0.193	6.08	4.49
R19	-0.015	+0.057	0.58	1.33
R20	0.000	+0.053	0.00	1.23
R21	+0.066	-0.010	-2.54	-0.23

magnitude of the shifts are generally not large and the ratios therefore subject to reasonable error, but the similarity in the values for the two reagents is generally very good indeed. There are one or two discrepancies such as R20 and R21 but overall the case for effective axial symmetry is very good. Obviously, data for further shift reagents is required to strengthen this conclusion and indeed titrations using metals causing larger shifts such as dysprosium are desirable to identify resonances marginally affected by the less potent reagents.

However, one very important conclusion can be drawn from the data. The similarity in shift ratios means that the protons affected lie in the sphere of influence of the metal atom, the magnitude of the effect depending on r^{-3} for any given angular distribution where r is the distance separating the metal and proton (section 2.2). On the other hand, shifts arising in the proton spectrum on binding ligand molecules do not have this simple interpretation. The majority of such changes result from alterations in the "secondary shifts" of resonances often as a result of the relative movement of the aromatic residue, for instance, occurring on ligand binding and can result in a change in chemical shift of a proton at quite some distance from the ligand binding site. The lanthanide ion probe data is therefore of considerable value in interpretating the results of the ligand binding. For example, it was seen that the methyl proton resonances of Val 69 were unaffected by 6 aminohexanoic acid binding but were moved by the addition of AMBOC to the protein. This difference could have been interpreted as due to a conformational change produced by the more bulky and tighter binding AMBOC ligand, with the effect transmitted over quite some distance from the binding site. However, lanthanide binding by two different shift reagents show very similar and significant shift ratios for these resonances (given as L4 in Table 4.5), and furthermore the peaks return

to their unshifted positions on adding ligand to the metal bound protein. Thus, the metal ion probe experiments demonstrate that Val 69 is actually in very close proximity to the ligand binding site.

As yet no attempt has been made to fit the observed proton shifts to precise distances and angles from the metal atom, but if the case for axial symmetry holds then this procedure offers a real prospect of refining the structure around the metal ion binding sites to an accuracy approaching that of X-ray crystallographic analysis.

We note that although large shifts have been specifically commented on in previous dicussions, Fig. 4.35 clearly shows that because of the geometrical dependence of the shift, its magnitude cannot be directly correlated with the proximity of the particular proton to the metal atom. However, as considered above and discussed in section 2.2 the effects of adding gadolinium ions are directly proportional to the inverse of the sixth power of the distance between the proton and metal atom with no angular dependence. The effects of adding gadolinium ions to native kringle 4 were therefore investigated in order to provide qualitative data on the relative distances of specific protons from the metal binding site.

4.5.5 Gadolinium

Spectra of kringle 4 at increasing concentrations of gadolinium ions are shown in Fig. 4.41 with the final spectrum being the same sample as that of Fig. 4.41(e) but with added 6 aminohexanoic acid. Table 4.6 provides a rough summary of the order in which the resonances from the residues listed are broadened. It must be borne in mind that all the resonances of each residue are not monitored and different parts of the same residue can obviously receive different degrees of broadening. For instance the C2 proton resonance of Trp A is remarkably resistant to the broadening probe whereas the C4 and C7 doublets (R19, R15) of the

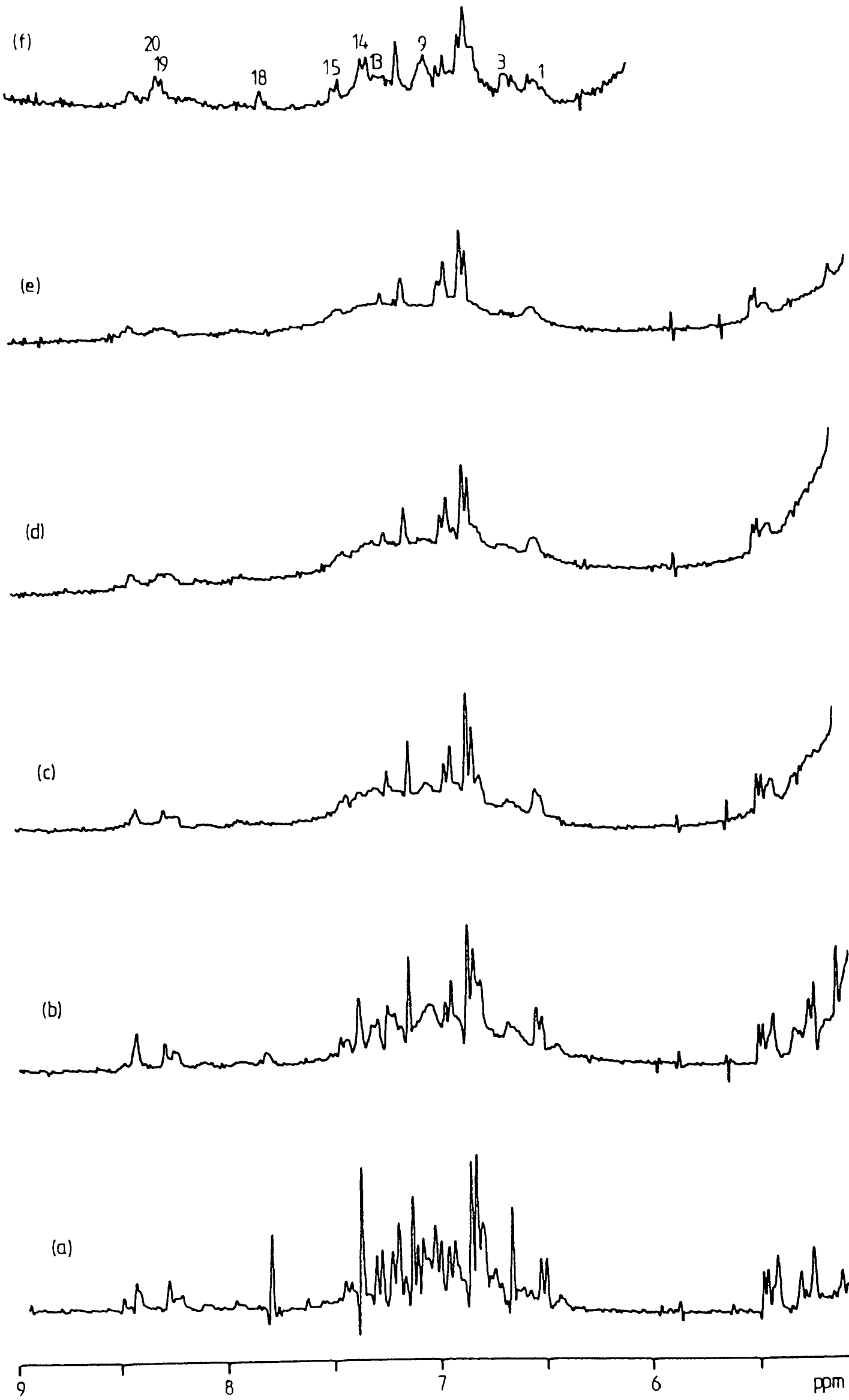

Fig. 4.41A Aromatic region of the gadolinium ion titration of kringle 4; 37°C, pH 5.5. Resolution enhanced spectra. (a) Native protein (b)-(e) increasing metal ion concentration (f) 6 amino-hexanoic acid added to the sample of (e).

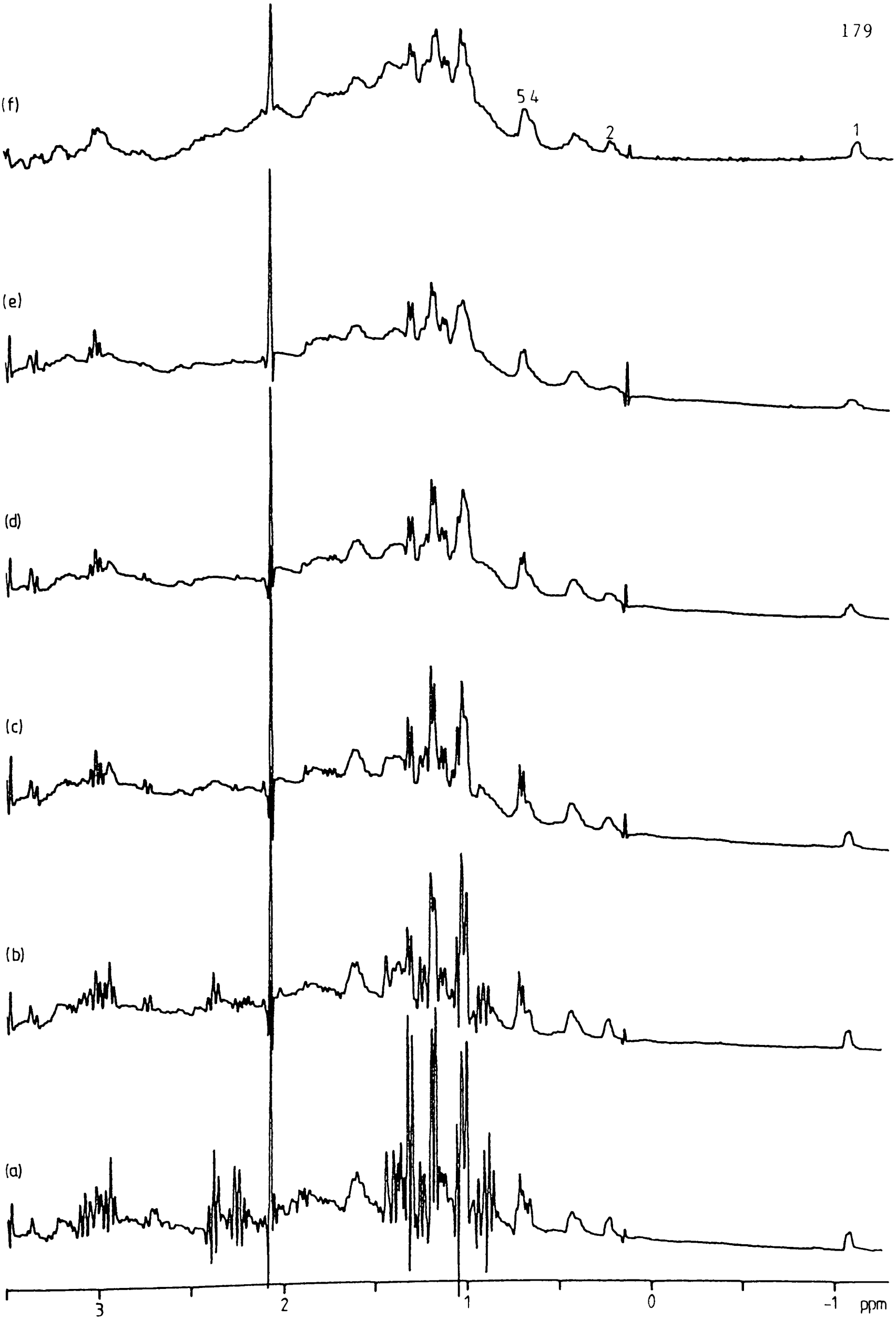

Fig. 4.41B Aliphatic region of the gadolinium ion titration of kringle 4; 37°C, pH 5.5. Resolution enhanced spectra. (a) Native protein (b)-(e) increasing metal ion concentration (f) 6 aminohexanoic acid added to the sample of (e).

Table 4.6 Summary of the effects of Gadolinium ion binding to kringle 4. (see text)

DEGREE OF BROADENING	AROMATIC	ALIPHATIC
SEVERE	Trp B, Trp 71, His 3	Met B, Glu 83, Ala 84, Val 86
MODERATE	Trp A, Tyr 40, Tyr 73, Tyr 2, His 31, His 33	Leu 45, Val 69, Leu 76, Val -2, Lys ε CH_2 (a), (c)
MINIMAL	Tyr 49, Trp A C2 Resonance (R12)	Met A, L5, Lys ε CH_2 (b)

same indole ring are much more susceptible. This can in turn be interpretated to indicate that the latter protons are closer to a gadolinium ion than the former.

The arbitrary categorisation of the effects into three degrees of broadening from severe to minimal can be looked upon as three increasingly large spheres of influence radiating from the metal ions as centres, and from previous sections, two such main centres are envisaged. The large effects again on R3 and R18 confirm that these tryptophan C2 protons are indeed close to a gadolinium ion and from the discussion above this is the metal atom probing the ligand amino terminal binding site. In addition, the other resonances of Trp 71 that are readily distinguished R23, R4 and R11 are also strongly affected indicating that the whole of the indole ring is close to the amino group binding site. Other resonances of Trp B are not so clearly recognised for this statement to be made about that residue also. Gadolinium binding to the second main site is well represented by the effects on the assigned extra kringle residues and His 3. Which site is responsible for the rapid broadening of the Met B resonance is not clear, but the minimal shift that it received with both europium and praseodymium ion binding strongly suggests that its methyl group lies on the edge of the shift cone of the metal ion to which it is close.

Resonances showing more moderate degrees of broadening again fall into two groups based on the two sites as expected. Tyr 40, Trp A, Tyr 73, His 33 and Leu 45 being clustered around the ligand binding site while Tyr 2, Val -2, and Leu 76 midly affected, are situated around the first disulphide bridge. The effects on the lysine ε protons are curious as these side chains are positively charged at the pH of this titration. Furthermore, X-ray crystal structures of proteins usually show lysine side chains extending into the solvent as a consequence of their

hydrophilicity. However, as mentioned before, when discussing the copper ion titration, it is possible that some of the intensity affected may arise from the two lysine residues lying between Leu 76 and the first disulphide bridge in the sequence. Alternatively it was noted from pH dependence studies that the most upfield lysine ε CH_2 peak was affected subtly by ligand binding and so is perhaps influenced by the metal ion bound at the ligand site. Again the degree of broadening is larger than might be expected from the minimal effects that shift reagents had on them, but this only serves to emphasise the angular dependence of the effects from such probes.

Finally we note the residues barely, if at all, influenced by the gadolinium ion binding to include Tyr 49 (B), Met A and L5. These three sets of resonances had all been previously linked from the results of NOE experiments. It is most likely that they are all clustered on a side of the molecule away from the first disulphide bridge and more superficially situated as the interior of the molecule is well perturbed by the metal ion probing the ligand binding site.

The spectrum obtained on adding the 6 aminohexanoic acid Fig. 4.4.1(f) is not particularly well resolved, but nevertheless, R1, R3, R9, R13, R14, R15, R18, R19, R20, L1, L2, L4, L5 all gain noticeably in intensity. These resonances arise from the following residues Trp A, Trp 71, Trp B, Val 69, Tyr 73, His 33, Tyr 40 and Leu 45 which by now have come to be recognised as intimately related to the ligand site and which were previously independently interrelated in space as shown in Fig. 4.7.

4.5.6 Lanthanide Ion Binding Sites

Two main sites of lanthanide ion binding have been proposed in the discussion above and some of the residues in the immediate vicinity of the bound metal atoms have been listed in Table 4.7. The residues

Table 4.7 Summary of the residues in the vicinity of the two main lanthanide ion binding sites (see text).

	PROTEIN RESIDUES	
SITE 1	Trp A, Trp B, His 31, His 33, Tyr 40, Leu 45, Val 69, Trp 71, Tyr 73	Ligand amino group binding site
SITE 2	Val -2, Tyr 2, His 3, Leu 76, Glu 83, Ala 84 Val 86	Vicinity of first disulphide bridge

underlined are known from gadolinium data to be particularly close to the metal atom. Some assigned resonances such as the Lys ε peaks, have been omitted because it is not clear to which site they do belong or the data is equivocal. The distinction between the two groups in Table 4.7 being drawn largely from the effects of adding ligand to the metal bound protein and the known spatial clustering of side chains summarised in Fig. 4.7 with some additional data provided by the results of the copper ion titration regarding site 2. One notable omission from the table, though, is Met B. It was noted in section 4.5.2.3 that this resonance which was only slightly affected by the shift reagents (incidentally in the same direction as the effects on Trp 71 and Val 69) was nevertheless restored to its unshifted position by the addition of ligand. This would strongly suggest that it is very much a part of site 1, and although the presence of bound ligand did not prevent the further addition of gadolinium ions from broadening the resonance, this behaviour was also shown by the resonances of Tyr 40 which is much more firmly assigned to the ligand binding site. Another possibility though is that this residue is affected by more than one lanthanide ion. As yet no attempt has been made to define the stoichiometry of the metal ion binding. It has been tacitly assumed that one atom binds to each site but it is conceivable for instance that more than one atom is responsible for the effects ascribed to site 2. However, the NOE and copper titration data have already indicated the majority of site 2 residues to be close in space in any case. Certainly, if more than two metal atoms do bind specifically then they have comparable binding constants. This can be extended to include the possibility that a metal binding site consists of the rapid exchange of the metal atom between two (or more parts) of the site spreading its influence therefore over a larger region of the molecule.

These conjectures obviously require further investigation. In addition, we have not paid much attention to the number of carboxyl groups involved in these two sites. Obviously those of the C terminus and Glu 83 will contribute to site 2, but the possibilities for site 1 will be considered in the next chapter.

Site 1 has been seen to be equivalent to the amino group binding site of the ligand and whereas Fig. 4.7 shows the residues of site 1 to be interrelated, the lanthanide probe data indicates them to be intimately distributed around the metal ion - the difference in the direction of the induced shifts for different residues making this abundantly clear. This has resulted in Val 69 being included in this group as discussed in section 4.5.4, although this was not obvious previously. However, the NOE data discussed in section 4.4.3.4 is now explained in that it is Val 69 and not the methyl group giving rise to the L5 peak, which is close in space to the ligand. This conclusion is supported by the minimal effect of gadolinium binding on L5 compared to the resonances of Val 69. Finally, the selective effects of binding the ligand p-benzylamine-sulphonic acid on the Val 69 methyl peaks, described by Hochschwender et al., (1983) and discussed in section 4.5.2, are therefore understood. Following on from this, the marked effects of the latter ligand and lanthanide ions on the C2 proton resonance of Trp 71 (R3) contrasts significantly with the minor effects induced by binding 6 aminohexanoic acid or AMBOC to the protein (see Figs. 4.14 and 4.26). This discussion raises the possibility for site 1 that the lanthanide ion actually probes a larger volume of space around the binding site than the ligand amino group occupies. This matter will be raised again in the next chapter and it will be apparant again there, that as accurate a model as possible of the ligand binding site is required for a full understanding of all the data.

Likewise, the characterisation of the site 2 lanthanide ion binding site is serving to define more clearly the structure of another part of the molecule. In addition, by exclusion, the lack of effects on resonance L5, Tyr 49 and Met A by metal ion binding provides good supporting evidence for these resonances being grouped in space as indicated in Fig. 4.4.

4.6 Summary

This chapter has been concerned with the addition of various probes and ligands to kringle 4. The pH titration confirmed a number of assignments and spatial relationships as well as providing information on the stability of part of, as well as the whole structure, to increasing proton concentrations. Along with the results of a copper II ion titration, data from the following chapter allowed second stage assignments of all three histidine residues and four of the five tyrosine side chains to be made. This resulted in considerable simplification of further discussion, as data accumulated so far led to a preliminary structural model being proposed incorporating a number of well defined structural elements consisting of clusters of various assigned side chains in the sequence. With this background, studies of the effects of the binding of two ligands to the protein were discussed in terms of the spectral perturbations produced and interpreted with reference to the structure. It was concluded that the protein is folded in such a way that the lysine binding site is precisely formed and that the binding of the ligand causes little structural perturbation. Finally, lanthanide ion binding studies were discussed and the metals were seen to be ideal probes of the ligand binding site. Along with the ligand binding studies, the amino end of the ligand was seen to be bound within the hydrophobic core of the molecule, many aromatic residues being intimately related to the

binding site. Lanthanide ions were also seen to probe the region of the molecule around the first disulphide bridge and the extra-kringle residues. The prospects of defining various parts of the structure to a considerable extent (from more extensive lanthanide ion studies) were seen to be extremely promising. Incidentally we note that no anionic probe studies have been discussed. Some preliminary experiments have been performed but the results as yet have not been particularly informative and so these probes have been omitted from this chapter.

We now go on, in the next chapter, to consider the effects on the spectrum of various chemical modifications to the protein. These have already been seen, in section 4.2, to provide valuable information towards the assignment process.

CHAPTER 5

Chemical Modifications of Kringle 4

5.1 Introduction

Chemical modification is a widely used technique in the study of proteins and enzymes and very many modifications of varying specificity can be performed (Means and Feeney, 1971; Spande et al., 1970). Modified proteins can be of great value in the assignment of NMR spectra, especially when the modifcation is well characterised and very selective. This was of considerable benefit in the assignment of the tryptophan residues of lysozyme (Cassels et al., 1978) and it was seen in Section 4.2 that nitration of some tyrosine side chains in kringle 4 enabled the second stage assignment of resonances to tyrosine 40 and 49 in the sequence to be made. The latter was possible because the spectral changes were discrete. As with probe studies, chemical modifications may cause changes confined to their immediate vicinity or the effects may be more widespread due to a change in conformation resulting from the alteration. Obviously some modifications such as reduction and carboxymethylation of disulphide bridges are designed to demonstrate structural effects and one such modification was also briefly considered,in section 4.2. Thus, again, it is necessary to differentiate between spectral changes resulting from changed environments of protons surrounding the modified group, from those occurring as a result of changed conformations more distant from the site of modification. However, in this process information is thereby gathered on the integrity of the protein structure from the effects produced on it by any given modification and NMR spectroscopy is an ideal method to investigate this, especially as the new protein can be studied under an infinite variety of solution conditions. Some modifications are such, though, that the protein structure

is radically altered and essentially a new protein is generated. In these circumstances the NMR spectrum requires assigning once more. Investigation of some modifications then becomes a lengthy task and is often hampered by lack of material as protein modifications consume considerable amounts of the native protein both in the preparation and purification processes. Thus, a number of the modified proteins considered below have not been studied in so much detail as desired. The amounts obtained of each have permitted only at most two suitable samples to be prepared at concentrations required for an adequate spectrum and this has resulted in considerable curtailment in the extent of the experiments that could be carried out on them. Unfortunately, this has meant no COSY experiments have been performed although this would be of great benefit in a number of cases, for instance. Nevertheless, although the investigations are far from complete, useful data has been obtained as will be discussed below.

Chemical modification of proteins and enzymes has also proved of great value in identifying side chains essential for ligand binding or enzyme activity, for example. A number of such studies have been published for kringle 4 with the aim of defining the specific residues in the sequence involved in ligand binding. These will be considered first as they provide background information against which our data can be compared. In addition Dr. Patthy and his coworkers, who have supplied all the modified proteins, have informed us of a number, of as yet unpublished results, referring to further modifications. The primary sequence of kringle 4 is shown again in Fig. 5.1 for easier reference and copies of fig. 4.7 have also been included in the text. Table 5.1 lists the modified proteins that we have studied.

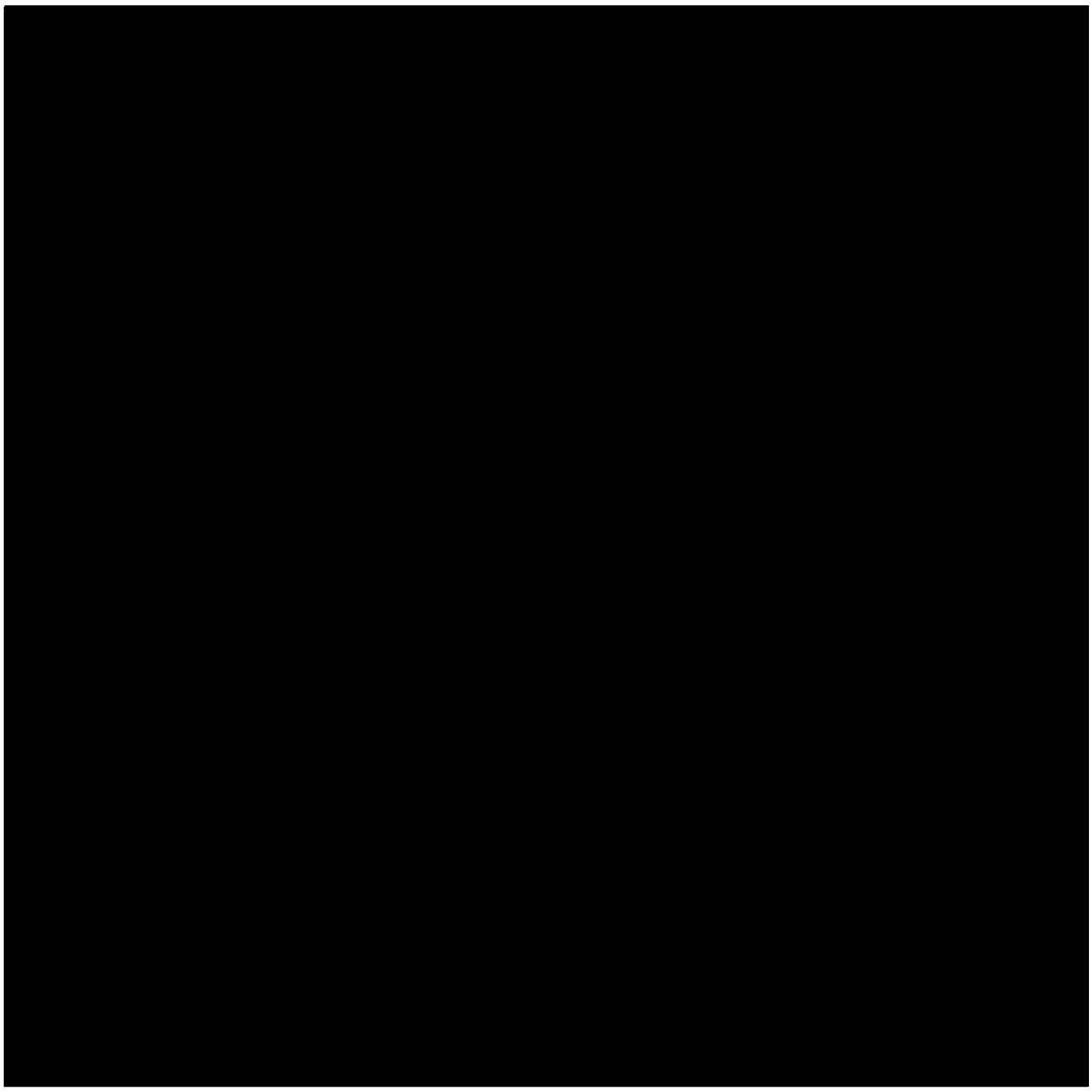

Fig. 5.1 Primary structure of kringle 4 of human plasminogen. (Sottrup-Jensen et al., 1978)

Table 5.1 List of the modified proteins discussed in this chapter.

TYROSINE	Tyrosine 40	Nitrated
	Tyrosine 40,49	
	Tyr 40 - Lys 35	Crosslinked
TRYPTOPHAN METHIONINE	Trp 71, Mets 28,47	Oxidised
ARGININE	Arginine 32	Reaction with cyclohexanedione
	Arginine 32,70	
CLEAVAGES	Met 47 - Asn 48	Cyanogen bromide
	Cys 1 - Cys 79	Selective reduction and carboxymethylation

5.2 Results of Other Studies

Lerch and Rickli (1980) have published data on the greatest variety of modifications and we begin by considering some of their results. Reduction and carboxymethylation of all three disulphide bridges together was found to destroy all affinity of the protein for a lysine-Sepharose column. This is not unexpected in that we have found that the same modification to the kringles of bovine prothrombin fragments one and two removes all suggestion of a globular protein fold from the NMR spectrum, (Esnouf, Pluck and Williams; unpublished results) and we saw in the last chapter how the presence of a lysine binding site is dependent on the protein having a definite tertiary fold. However, as will be seen below, selective disruption of the first disulphide bridge does not destroy the ligand binding properties and the spectrum still shows considerable evidence for folded regions of the molecule. On the other hand cleavage of the peptide chain between methionine 47 and asparagine 48 resulted in complete loss of the binding capacity. This result was confirmed by Patthy and coworkers and the spectrum discussed below reveals that much if not all the native protein fold is lost in this modification. Thus, it is clear that in Fig. 5.1 the integrity of the right outer loop is essential for ligand binding whereas that of the left outer is not. This conclusion is admirably supported by the data for kringle 1 of human plasminogen which also has a lysine binding site. Cyanogen bromide cleavage between methionine 13 and serine 14 on the left hand outer loop of this protein was found to cause no change in its lysine binding capacity. In addition, it was also demonstrated in the previous chapter that the residues most affected by ligand binding were on the right outer and the two inner loops but that residues on the left hand loop such as Tyr 2 and His 3 and others associated with them, such as Leu 76, were noticeably unaffected. Indeed, data summarised in Fig. 4.7 demonstrated clear structural relations

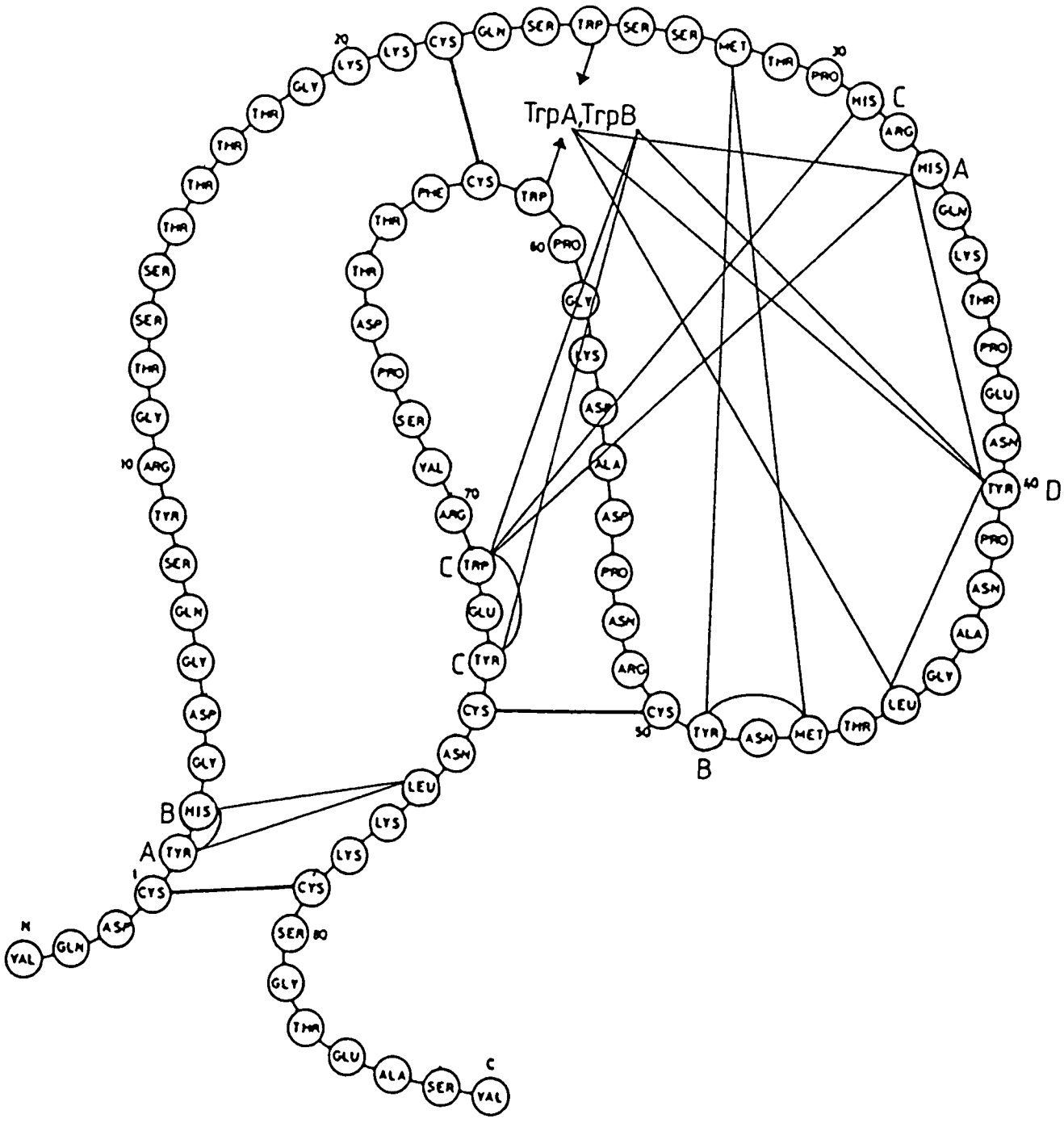

Fig. 4.7 Primary structure of kringle 4. Lines connect residues found to be close in space within the three dimensional structure (see text).

between residues on the three loops to the right and thus disruption of any one of them might well be expected to affect ligand binding.

Much data in the last chapter indicated a carboxyl group to play a crucial role in mediating the binding of the ligand amino group. This was supported by the finding that preparations of the methyl esters of all susceptible carboxyl groups of the protein destroyed the ligand binding but this was partially restored by saponification. Trexler et al., (1982) have investigated the carboxyl group requirement much more thoroughly. They showed that formation of an N-acylurea derivative of Asp 56 eliminated the affinity of kringle 4 for lysine-Sepharose. Furthermore, the presence of 6 aminohexanoic acid in the reaction medium containing the carbodiimide modification reagent led to a much reduced rate of loss of affinity. Control experiments showed that this was not due to consumption of the reagent by the ligand carboxyl group but rather reflected Asp 56 to be directly involved in ligand binding. This conclusion was promulgated, as opposed to the ligand protection resulting from an induced conformational change, by reasoning from data indicating that the peptide backbone of kringle structures was remarkably insensitive to saturation of ω-amino-carboxylic acid binding sites. This matter will be discussed further in chapter 7 but again the ligand binding studies of the previous chapter give good support to this notion. Thus, Asp 56 is postulated to mediate the binding of the positively charged end of the ligand, which has been seen to be more important than that of the carboxyl end to overall ligand binding. The position of this residue in the sequence fits in extremely well with our data, being surrounded by residues known to be affected by both ligand and lanthanide ion binding. In addition, it is possible that other nearby carboxyl group containing residues such as Asp 54 and Glu 72 may also contribute to the ligand and metal atom binding site but are not modified under the conditions in which Asp 56 is. Unfortunately as was

mentioned in the previous chapters, as yet there are no definite assignments of carboxyl containing side chains within the kringle in the spectrum and specifically our data could only be reckoned compatible with the involvement of aspartate residues in ligand and lanthanide ion binidng.

Further specific probes of the ligand binding site have been provided by selective modification of tryptophan 71. Hochschwender and Laursen (1981) introduced the 2-hydroxy-5-nitrobenzyl group to this residue and found the ligand binding capacity to be lost. This was confirmed by Patthy's group, which made a similar finding on oxidation of this residue, along with both methionine residues. This latter protein is considered below, but previously it was seen that Trp 71 was affected by ligand binding and extremely susceptible to the presence of lanthanide ions with the resonances being restored to unshifted positions by competitive ligand binding. Thus, the presence of a bulky group on this residue may well interfere with ligand binding either by direct steric interference or by distortion of the geometry of the site which was indicated to be crucial by the data given in table 4.2.

Section 4.4 also indicated that the carboxyl group of the ligand did play some part in the binding. Trexler et al., (1982) again using well characterised derivatives demonstrated that reaction of Arginine 70 with cyclohexanedione eliminated ligand binding capacity and again the presence of bound ligand was found to protect this residue from modification. It was therefore suggested that Arg 70 provides the complimentary binding site for the negatively charged end of the ligand and so assumed to be separated from Asp 56 by some 6.8Å. This modified protein is also discussed below but unfortunately as yet the data does not confirm this conclusion. For instance, it is possible that like the modification to Trp 71, that to Arg 70 simply results in steric hindrance to the ligand entering the binding site. In connection with this it is worthy of note that all these

modified proteins are tested for their ligand binding capability by their affinity for lysine-Sepharose columns. Now the 2-hydroxy-5-nitrobenzyl derivative of Trp 71 was found not to bind to the column, but NMR studies of this derivative by Llinás et al., (1983) showed that there remained some weak ligand binding in fact. Thus, although the L-lysine is bound to Sepharose through its α amino group (Deutsch and Metz, 1970) it is obviously not as accessible to the protein as a free ligand in solution. Nevertheless, a critical role for Arg 70 in ligand binding is also in accord with our data lying as it does beside Trp 71 in the sequence.

Trexler et al., (1982) also modified Arg 32 specifically in the same manner and this was found to be without affect on the ligand binding as will be demonstrated below. We note that Arg 32 is sandwiched between two histidine residues both of which have been implicated by our results to be affected by the presence of the ligand. Rickli and Lerch (1980) showed that photo oxidation of histidine resulted in considerable loss of the binding capacity for both kringles 1 and 4 (kringle 1 has the homologous His 31 and a second histidine at position 41). Once again bound 6 aminohexanoic acid exerted a protective effect. Amino acid analysis suggested one residue only was involved and they decided on His 31 by homology. While involvement of His 31 is in accord with our data, the evidence from chemical modification studies is not firm and so far we have not been able to study any proteins with specifically modified histidine residues. However, they concluded that His 31 and Asp 54 were the two residues either end of the site responsible for ligand binding. Asp 54 was chosen as the esterification mentioned above implicated a carboxyl group and these two residues are conserved in all five kringles of human plasminogen. But, as will be discussed in chapter 7, it is known that all five do not contain lysine binding sites and in fact these residues are also present in bovine and human prothrombin fragment 1 which also do not bind lysine. Thus,

Trexler et al., suggest the effects of histidine modification are, like those of the tryptophan modification, to affect the binding site indirectly. In addition, our determination of the pK_a for His 31 as discussed in the previous chapter, shows the side chain to be deprotonated at pH values when the ligand is bound and the pH dependence of its resonances are little perturbed by ligand binding. Thus, the His 31 side chain cannot be acting as the binding site for the carboxyl group end of the ligand.

It is clear that much work needs to be done with chemically modified proteins to be sure of the precise residues responsible for ω-aminocarboxylic acid binding. The data described in the two previous chapters strongly indicates involvement of a carboxyl group buried in the hydrophobic core of the molecule being responsible for the ω-amino group binding, and this may well be that of Asp 56 with the possible involvement of other nearby carboxyl groups. The situation at the other end of the ligand is not so clear without adequate supporting evidence from anionic probe experiments, for instance. The modification of Arg 70 alone is not conclusive proof of it specifically binding the ligand carboxyl group.

Patthy and his coworkers report that all three modifications involving tyrosine residues that we have studied do not disrupt ligand binding. This has been confirmed by Hochschwender and Laursen (1981) for nitrated tyrosine proteins, and the discussion of the NMR spectra is begun with these modifications.

5.3 Tyrosine Modifications

Three separate proteins incorporating modified tyrosine residues have been studied and their spectra are shown in Fig. 5.2 compared to that of the native protein at a similar pH and temperature. Patthy and coworkers have found that only Tyr 40 and Tyr 49 are susceptible in the native protein to modification by reaction with tetranitromethane. Hochschwender

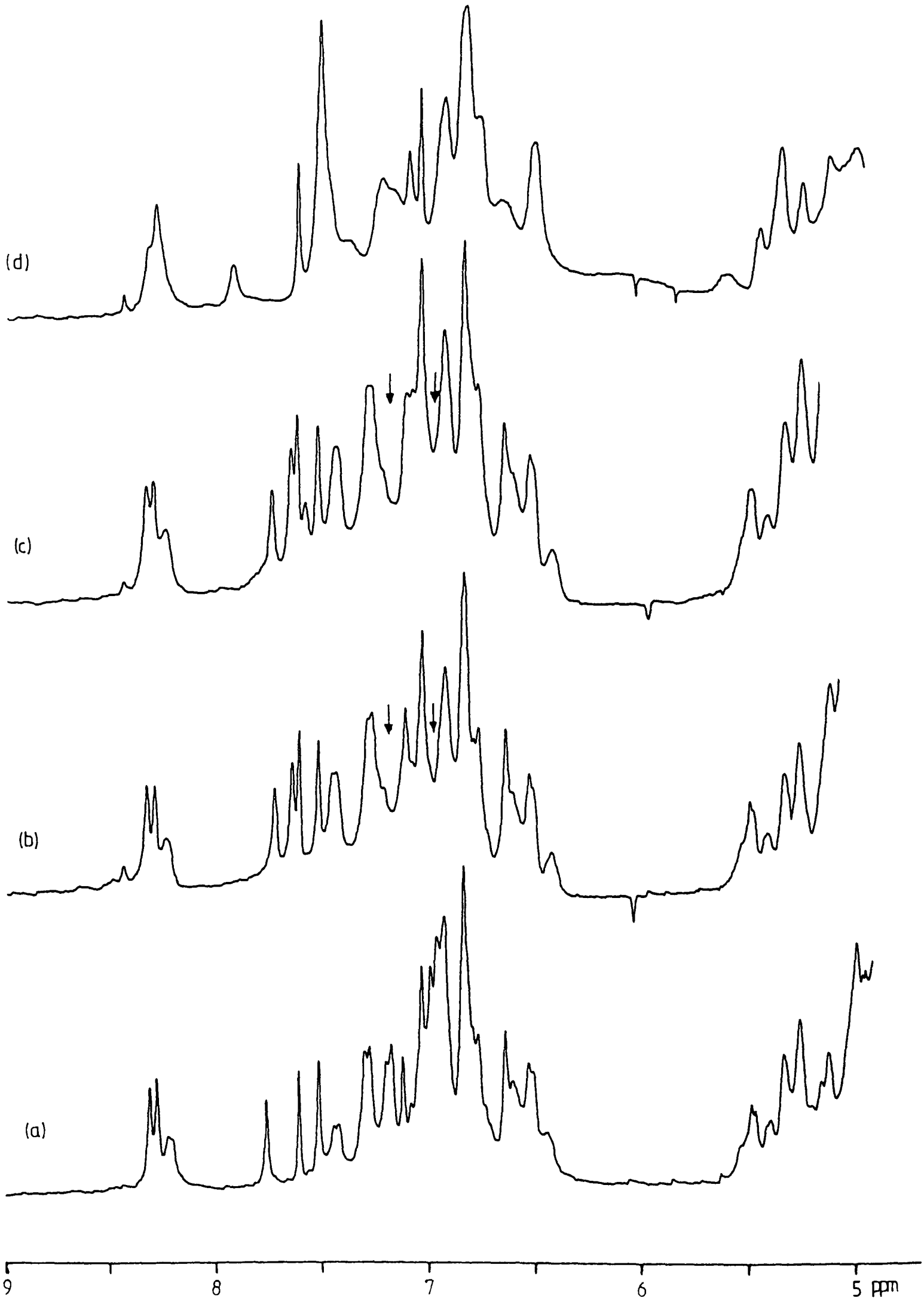

Fig. 5.2A Aromatic region of the spectrum; 37°C. (a) Native protein, pH 8.9 (b) Tyr 40 nitrated; pH 8.8 (c) Tyr 40, Tyr 49 nitrated pH 8.5 (d) Tyr 40-Lys 35 crosslinked, pH 8.8.

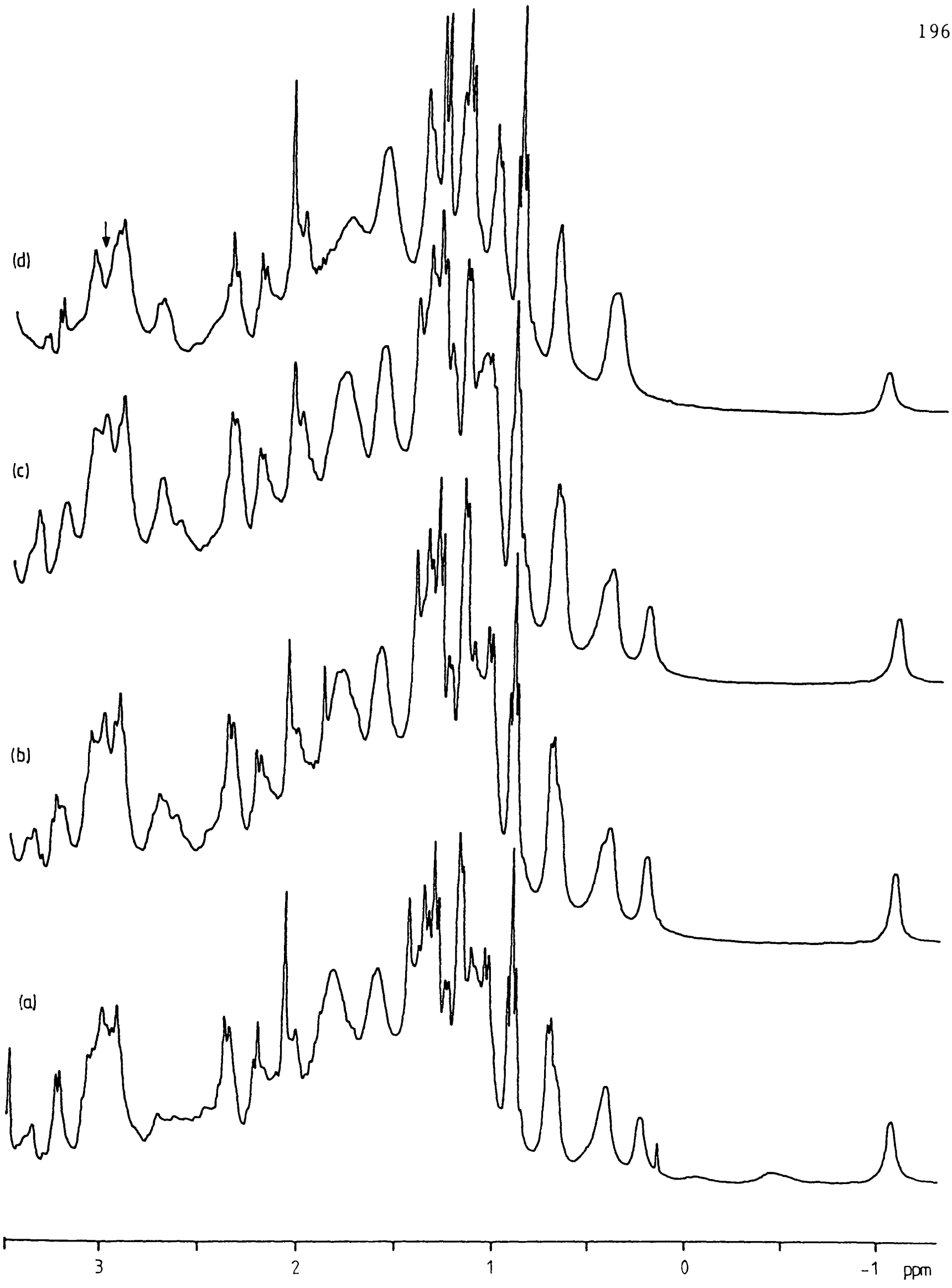

Fig. 5.2B Aliphatic region of the spectrum; 37°C. (a) Native protein, pH 8.9 (b) Tyr 40 nitrated; pH 8.8 (c) Tyr 40, Tyr 49 nitrated pH 8.5 (d) Tyr 40-Lys 35 crosslinked, pH 8.8.

and Laursen (1981) also found only two tyrosines were modified by the same reagent. From the assignments made in section 4.2 of these modified side chains to Tyr D (R9,R13) and Tyr B (R6,R8) in the spectrum we see that these residues have the lowest pK_a's of the four assigned tyrosine residues and this most likely accounts for their reactivity and in particular for the ability to selectively modify Tyr 40 alone. Tyr 73 was shown to have a considerably elevated pK_a but that of Tyr 2 (A) was found, from the pH dependence of its resonances, to be not too dissimilar from that of Tyr 49 (B) as will be shown below. Thus, the reason for the lack of susceptibility to modification shown by Tyr 2 is not so clear but it may be related to an environment preventing satisfactory access to the modifying reagent. Indeed, the secondary shifts on its resonances and the results of denaturation experiments have shown this residue to be intimately related to other parts of the protein, whereas the peaks of Tyr 49 are much closer to the chemical shifts of a random coil side chain perhaps suggesting Tyr 49 is in a more hydrophilic environment, for instance, amenable to the approach of tetranitromethane. We note also that the tyrosine residue, the resonances of which have not been assigned, Tyr 9 is not modified. This is not unexpected since the resonances of a tyrosine side chain freely accessible to the solvent and having a normal pK_a would be expected to be readily recognised in the spectrum (and the side chain readily modified). In previous discussion this has been shown not to be the case for Tyr 9 and furthermore the possibility that it may have restricted side chain mobility strongly indicates an environment with closely related residues from other parts of the molecule, which is very likely to inhibit modification.

The protein with the cross link between Tyr 40 and Lys 35 was made by reaction with 1,3-difluoro-4,6-dinitrobenzene and the nature of the link is shown in Fig.5.3. The fact that such a link is formed suggests that Tyr 40 is relatively close to the surface of the protein since positively

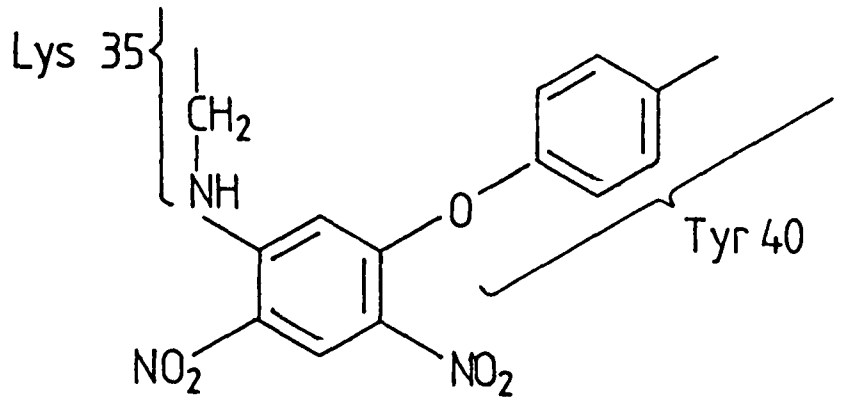

Fig. 5.3 Chemical structure of the linking group between Tyr 40 and Lys 35 in the modified protein.

charged lysine side chains, unless involved in salt bridges, are consistently seen to be extended into the solvent from X-ray crystallography studies of proteins. The more superficial position of Tyr 40 had been previously suggested by the lanthanide ion probe experiments. It is, of course, taken as axiomatic that Tyr 40 and Lys 35 are fairly close in space in the native protein, although some degree of conformational adjustment may well have occurred in the process of chemical modification and this will be considered below, but the simplest tyrosine modified protein is discussed first.

5.3.1 Nitrated Tyrosine 40

As mentioned in section 4.2, it can be seen in Fig. 5.2(b) that the spectrum of the modified protein is very similar to that of the native sample, the most noticeable difference being the loss of resonances R9 and R13 which consequently gave the assignment. That nitration of Tyr 40 does make little difference to the overall structure of the protein is further indicated by the similarity of the labile proton resonaces on initial dissolution of the protein in D_2O to those of the unmodified protein as shown in Fig. 5.4. The resonance at 10.3 ppm in the modified protein is a

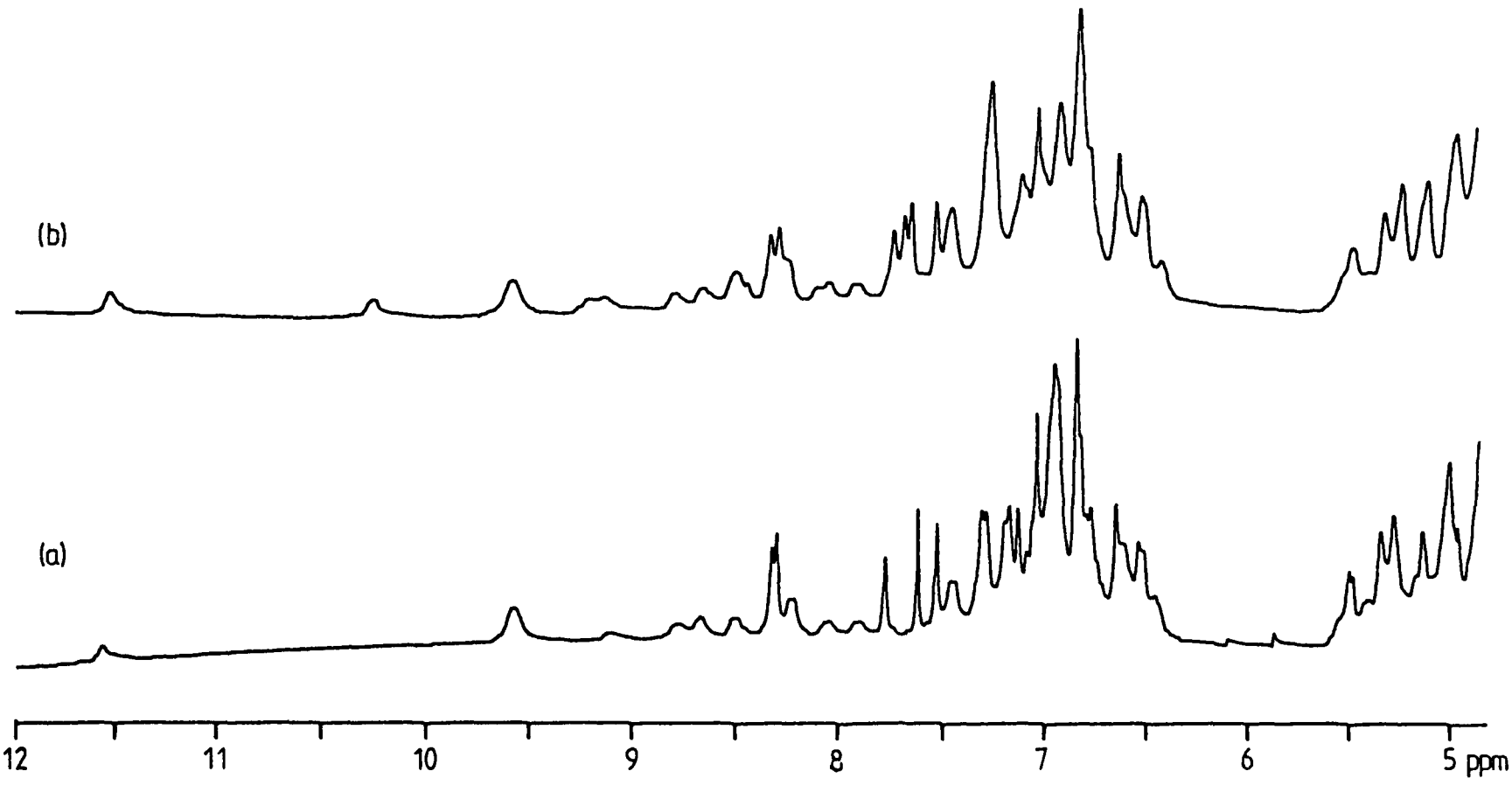

Fig. 5.4 Spectra obtained immediately on dissolving proteins in D_2O; 37°C. (a) Native protein, pH 9.4 (b) Tyr 40 nitrated kringle 4, pH 7.6

noteworthy addition though. The chemical shift is suggestive of an indole NH proton resonance and unless addition of 6 aminohexanoic acid causes a large downfield shift of that of Trp B (section 4.4) then this one may arise from Trp 71. Unfortunately, the half life of solvent deuteration of this proton has been too fast, under conditions tried so far, for an Overhauser enhancement to be performed to confirm this assignment. This resonance is not peculiar to the spectrum of the modified protein for it is seen in a published spectrum of kringle 4 (Hochschwender, et al., 1983).

The loss of the two proton doublets from the normal spectrum has been remarked upon, but a nitrated tyrosine side chain will still give rise to two one proton doublets and a one proton singlet in the aromatic region of the spectrum. In Fig. 5.2A(b) additional intensity is seen on the upfield edge of R14 and overlying R15, consistent with two one proton peaks.

Spin decoupling experiments confirmed that they were coupled and this was substantiated by the Nuclear Overhauser Enhancement between them and seen in the difference spectra of Fig. 5.5. An additional singlet resonance is seen between R17 and R18 and thus the resonances of the modified residue have been identified and will be referred to using the prefix "M". We note in Fig. 5.5(c) that R14 is inevitably included in the presaturation pulse bandwidth with the consequent enhancement of resonances R6 (to which it is coupled), R3 from Trp 71 and R18 from Trp B. This confirms the structural unit incorporating Trp B, Trp 71(C) and Tyr 73(C) indicated for the native protein in Fig. 3.28 is preserved in the modified protein.

Closer inspection of the spectrum of the modified and unmodified protein in Fig. 5.2 does reveal small shifts on a number of resonances, one of the largest being that of R18 from Trp B, moved upfield by 0.03 ppm. As just remarked this peak still received an Overhauser enhancement from Tyr 73 and so there is no gross relative displacement of these two residues on modifying tyrosine 40. Thus, the interpretation of small changes in chemical shift position due to the alteration are not immediately apparent and further progress is made through use of probe experiments. Unfortunately, these have not been extensive as yet being hampered through lack of the protein but some of the results of a limited pH dependence are shown for the aromatic region in Fig. 5.6. This is a rather complicated diagram incorporating results from all three tyrosine modified proteins and relating them to curves discussed previously for the native protein.

The resonances M1 to M3 assigned to nitrated Tyr 40 all show a pK_a for the residue of about 7.0, consistent with the presence of the nitro group substituted on the aromatic ring. (The titration through the pK_a could also be followed visually as the protein solution went from yellow to colourless as the nitrated tyrosine residue was protonated.) However, there are more subtle changes in the pH dependences of other resonances

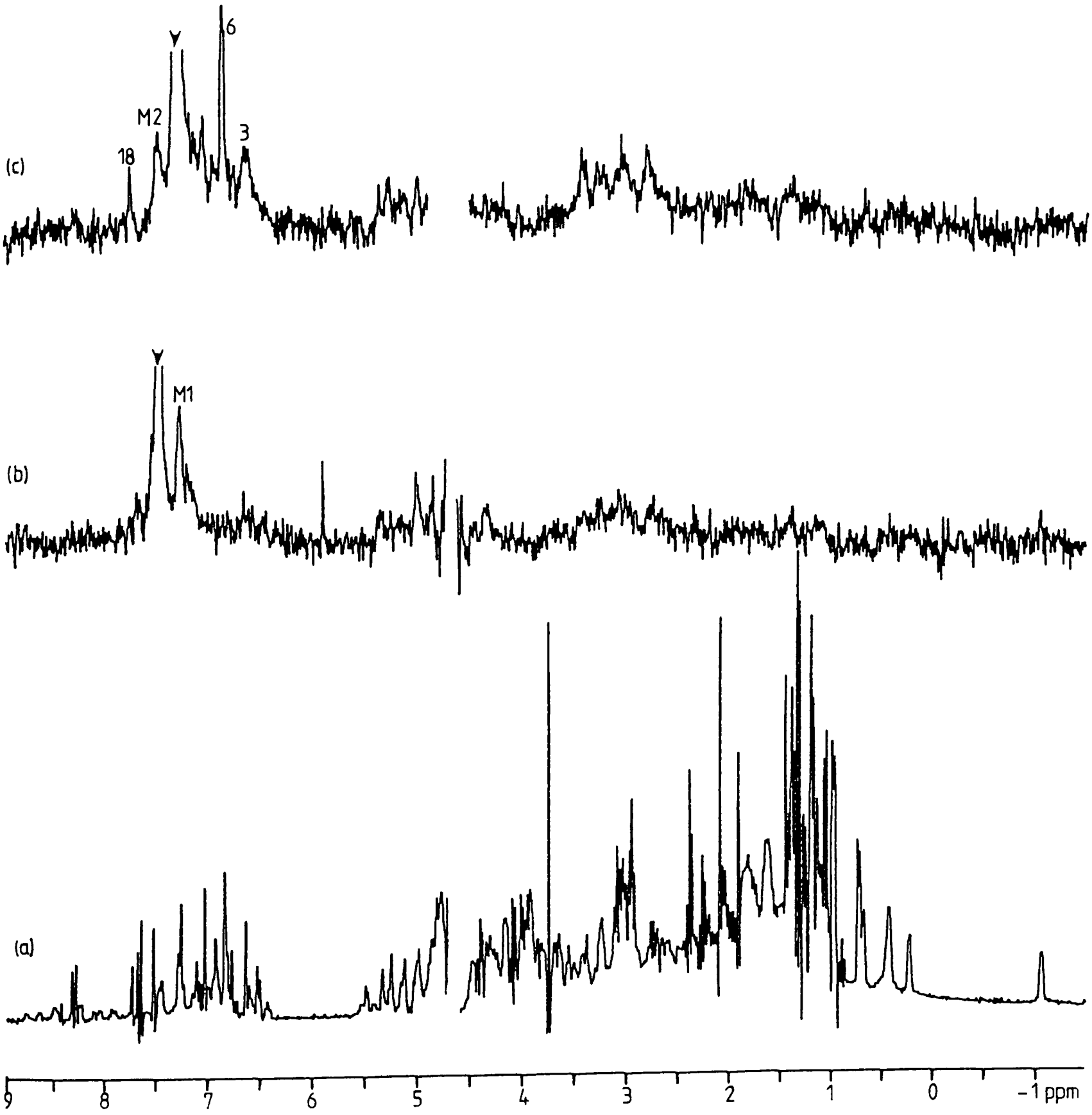

Fig. 5.5 NOE difference spectra of Tyr 40 nitrated kringle 4; 37°C, pH 7.8. (a) Resolution enhanced spectrum.

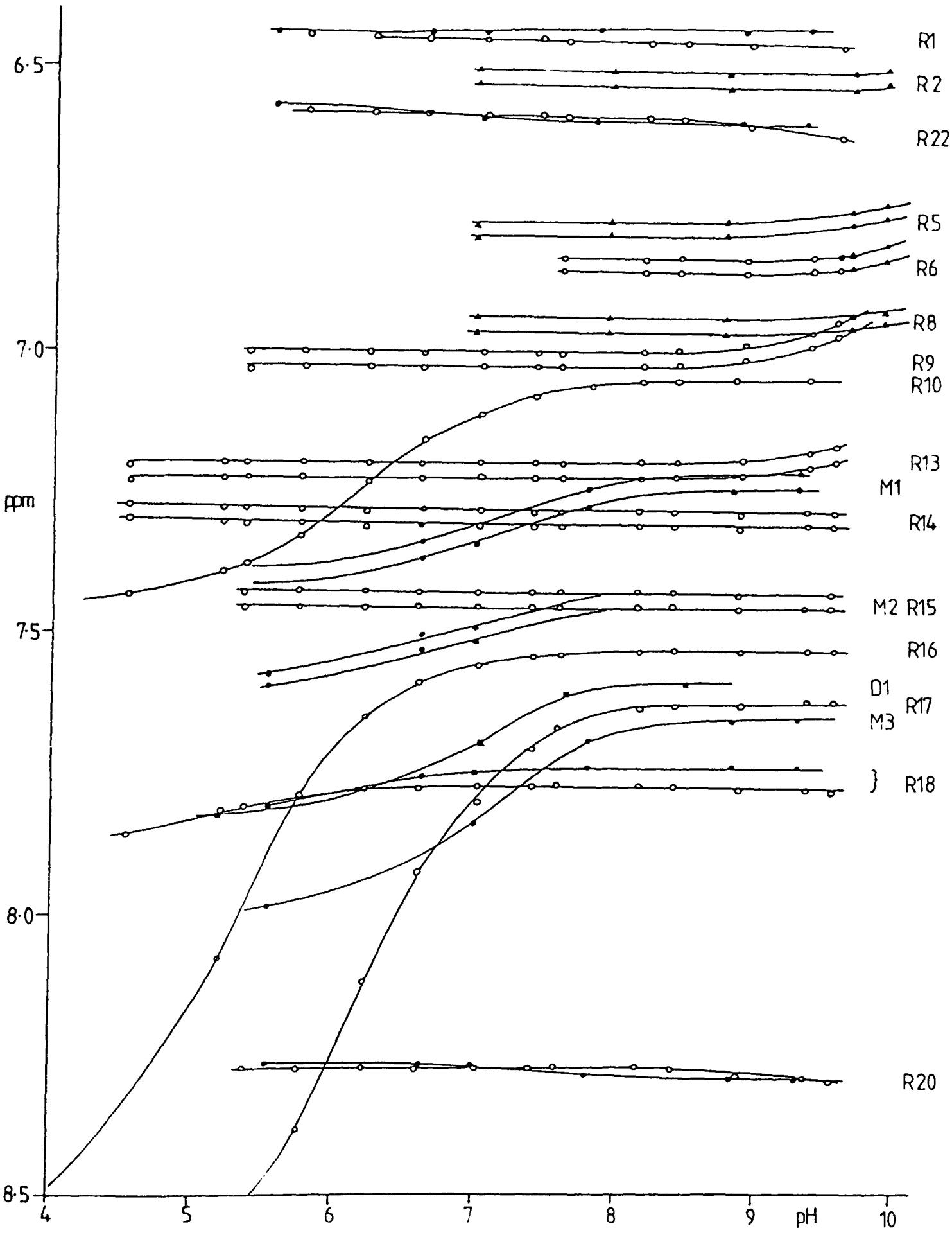

Fig. 5.6 Chemical shift versus pH curves for a number of aromatic resonances; 37°C, 100 mM NaCl.

- ∘ Native kringle 4
- • Tyr 40 nitrated
- ▪ Tyr 40, 49 nitrated
- ▲ Tyr 40-Lys 35 crosslinked

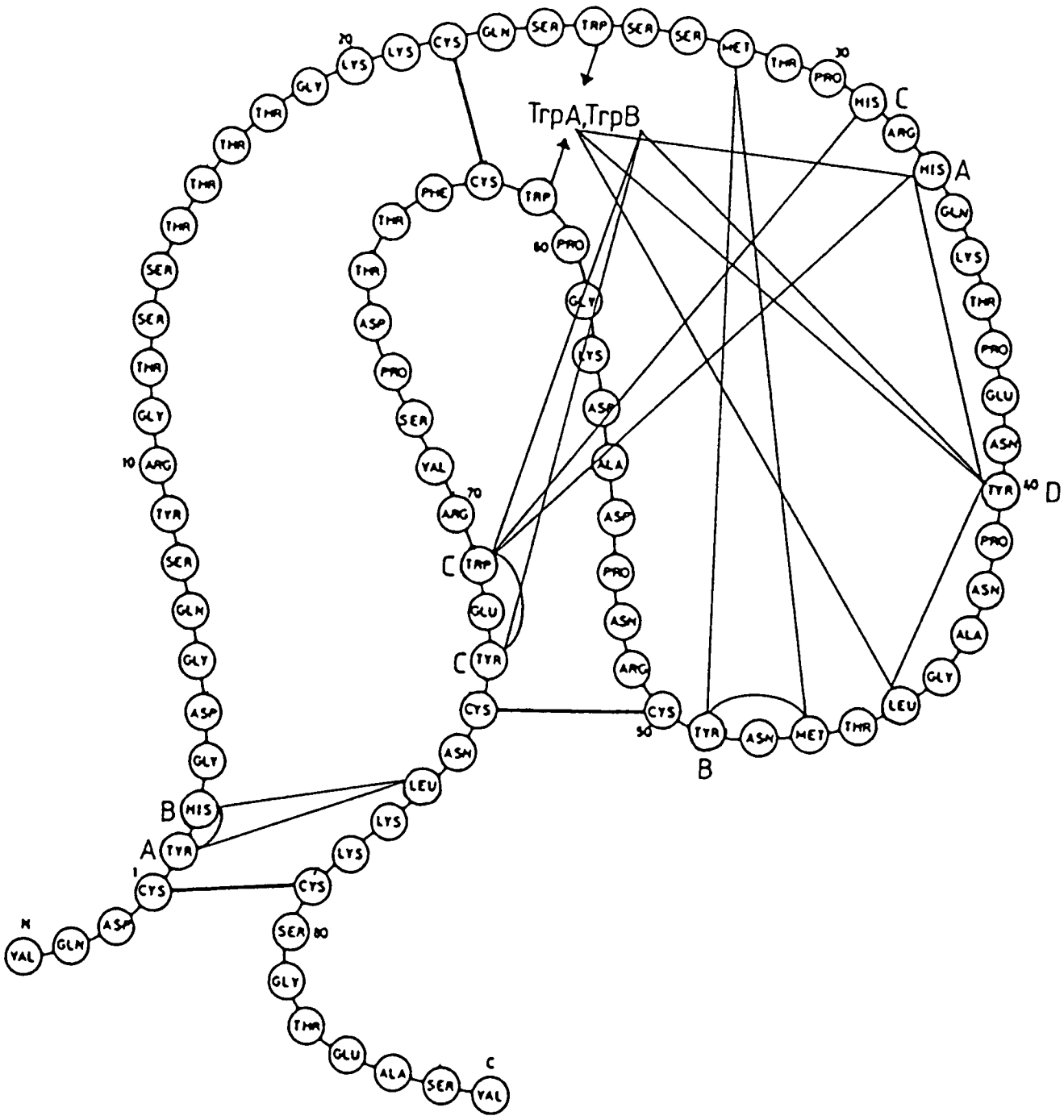

Fig. 4.7 Primary structure of kringle 4. Lines connect residues found to be close in space within the three dimensional structure (see text).

in the spectrum. R20 arising from His 33 is seen to reflect the same pK_a as the modified residue and it will be recalled as shown in Fig.5.6 that this was thought to be the case for the native protein reflecting the ionisation of Tyr 40. Likewise, R22 the C6 proton triplet of Trp B shows a corresponding change in the position of the inflection in its chemical shift versus pH curve. R18, from the C2 proton of Trp B has been seen to be shifted by the modification and does show a slightly different pH dependence, although this was only followed to pH 5.5. These data add support to that for the native protein and indicate as before, that parts of Trp B and His 33 are in the immediate environment of the ionising nitrated tyrosine side chain. In the native protein R18 did not show any appreciable change as Tyr 40 began to be deprotonated as the pH was raised. Neither did R1 of Trp A or L2 of Leu 45. However, Fig. 5.6 shows that R1 now also has a small inflection in its curve over the same range as the modified residue peaks. Figure 5.7 showing data for the aliphatic region of the spectrum shows a similar but more pronounced inflection in the curve of L2. This suggests that Trp A and one methyl group of Leu 45 are closer in space to the nitro Tyr 40 than to the unmodified residue in the native protein. The change in conformation leading to this is undoubtedly small since these residues are known to be clustered in space in the native protein (fig. 4.7). In particular, the data carries much detail in that irradiating L2 in the native protein was noted to give a much stronger NOE to the resonances of Tyr 40 than presaturation of L1 (the other methyl resonance of Leu 45) while in the modified protein, L1 is not affected by the tyrosine modification and does not show any pH dependence. This confirms that the same methyl group of Leu 45 remains closer to nitro-Tyr 40 that the other. The only other remaining resonance of note to reflect the new pK_a, which it did not in the unmodified protein, is that of Met B. Again this is in complete accord with the results of the pH dependence

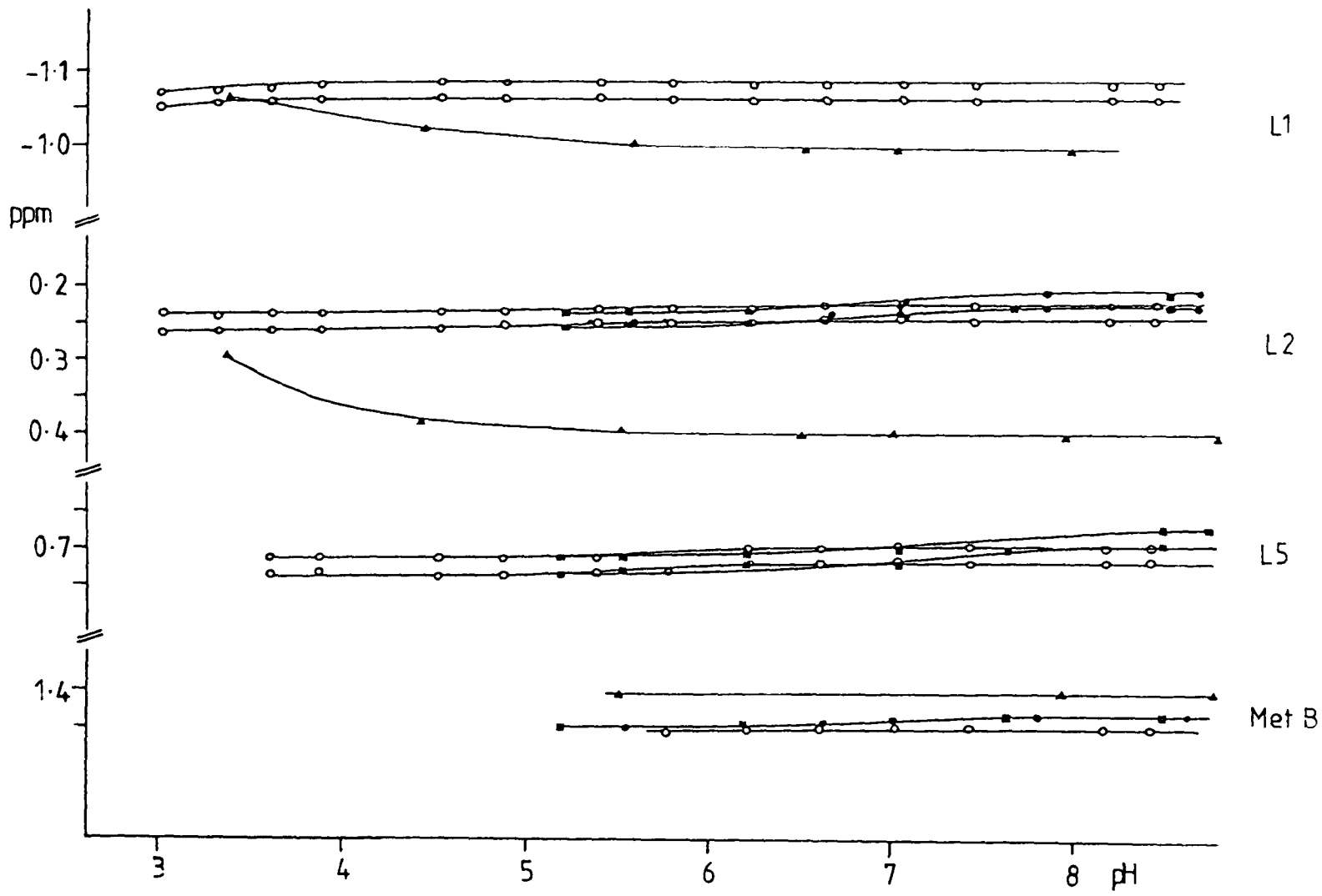

Fig. 5.7 Chemical shift versus pH curves for some aliphatic resonances 37°C, 100 mM NaCl.

- ∘ Native kringle 4
- • Tyr 40 nitrated
- ▪ Tyr 40, 49 nitrated
- ▲ Tyr 40-Lys 35 crosslinked

studies in the native protein in that Met B, His 33 and Tyr 40 were all linked by simultaneous broadening of their resonances from the spectrum below about pH 5.5. It would obviously be of interest to observe the effects of the modification on that process but this has not yet been carried out.

In summary, the resonances of the modified side chain have been identified, and the spectral effects of the nitration are seen to be minimal. Limited pH dependence and NOE experiments all indicate that any conformational changes resulting from the modification are very small and essentially localised to the immediate environment of the modified residue. The protein in which Tyr 49 is also nitrated is now considered.

5.3.2 Nitrated Tyrosines 40 and 49

From the previous discussion it would be expected that substitution of a nitro group into the ring of a further tyrsoine residue would likewise cause little structural perturbation reflected in only minor spectral changes. Such is indeed the case as can be seen by comparing Figs. 5.2(c) and (b). As with the mono nitro sample, resonances R9 and R13 have disappeared and resonances M1 to M3 are present. However, the loss of resonances assigned to Tyr 49 and the new peaks of the nitro substituted ring are not as obvious. In section 4.2. the assignment of resonances R6 and R8 to Tyr 49 was made and the spectrum in Fig. 4.5 at a lower pH than that of Fig. 5.2, showed a reasonable difference in intensity at these chemical shift values compared to the mono nitro and native spectra. However, such a difference is not very obvious in the spectrum of Fig. 5.2 and alternative ways of confirming the assignment were sought.

For the native protein it was shown that presaturation of L5 gave rise to enhancements of resonances R6, R8 of Tyr B in the difference spectrum (section 3.4) and it was concluded that the enhancement was actually

between Tyr B and the methyl proton resonance designated as L5 rather than between the methyl proton peaks of Val 69 which it partially overlaps. This conclusion was supported by the results of the copper II ion titration (section 4.3). The difference spectrum resulting from irradiating L5 in the dinitro protein is shown in Fig. 5.8 as are the spectra for the same experiment run under identical conditions for the two other tyrosine modified proteins. It is readily seen that R6 and R8 are well resolved in the spectra of the latter two samples and the aromatic region of the spectrum is extremely similar to those of analogous experiments shown in Figures 4.27 and 3.24(e). However, such clearly defined peaks are not seen for the dinitro protein. It could be suggested that the assignment is wrong and that the loss of peaks in the NOE difference spectrum is due to a conformational change involving Tyr B (R6,R8) resulting from the modification. This is very unlikely. The great similarity in the spectra of the di and mono nitro proteins to that of the native sample and, as shown above for the mono nitro protein, tyrosine nitration can occur with only minimal conformational changes occurring, all mitigates against the possibility of any significant conformational change. Indeed, this will be confirmed below and it is seen in Fig. 5.8 that the aliphatic region of the difference spectra are all very comparable, especially for the two nitrated proteins. Furthermore, R2 of Tyr 2 and R14 of Tyr 73 are both present and unchanged in the spectrum of the dinitro tyrosine modified protein (Fig. 5.8(a)) and so the only other possibility is that tyrosine 49 is the residue for which no resonances have been assigned, but then the resonances of Tyr B would be expected to be readily demonstrated in the spectrum of the modified protein. Additional evidence that Tyr B is correctly assigned to Tyr 49 is supplied by the results of a pH dependence study, the pertinent results of which are seen in Figures 5.6 and 5.7.

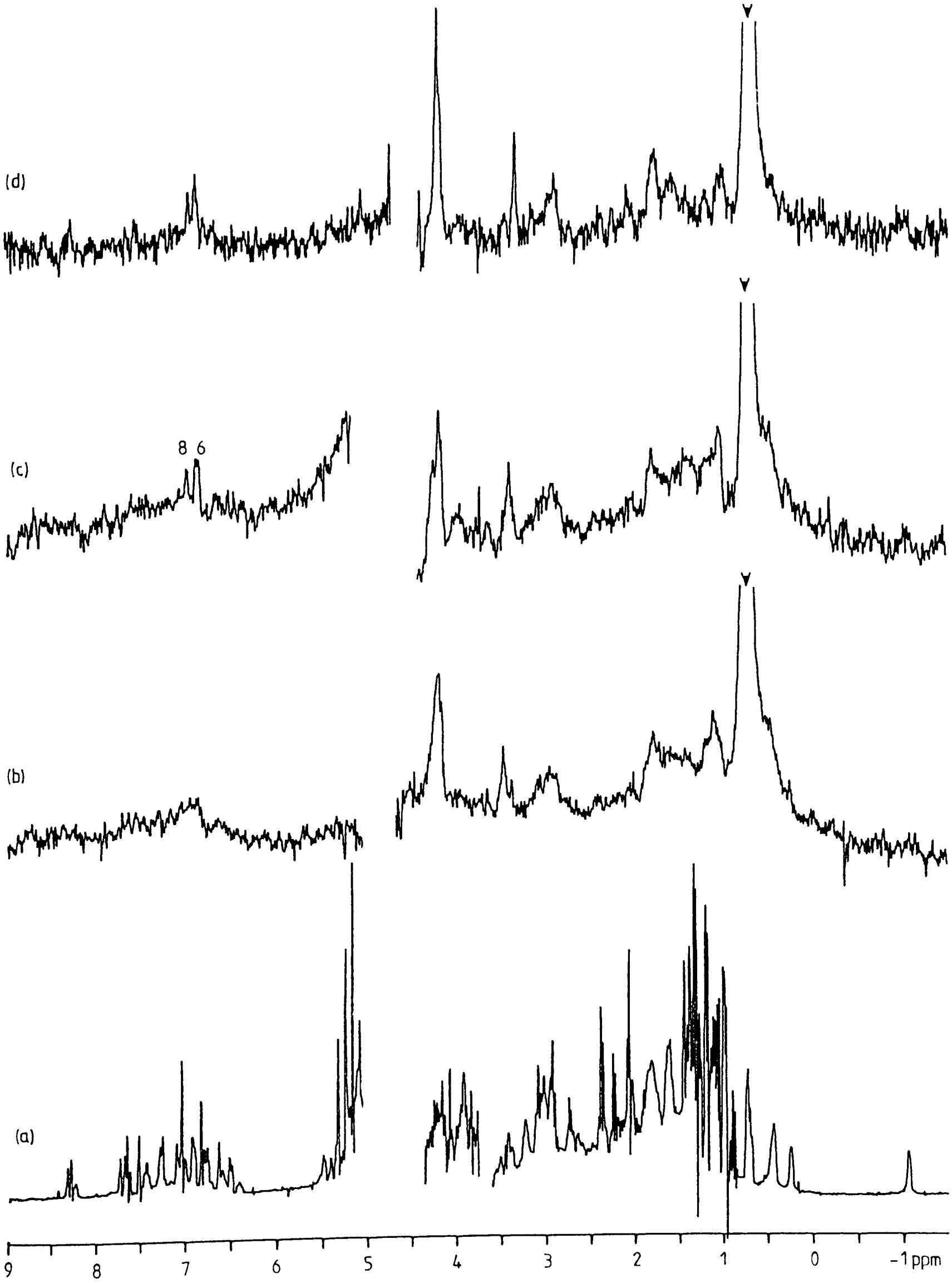

Fig. 5.8 NOE difference spectra of tyrosine modified proteins; 37°C
(a) Resolution enhanced spectrum of Tyr 40, 49 nitrated kringle 4 (b) Nitrated Tyr 40, 49 (c) Nitrated Tyr 40 (d) Tyr 40-Lys 35 crosslinked.

An extra one proton singlet resonance, designated D1, was seen to titrate over a similar chemical shift and pH range as M3 and so is assigned to the singlet resonance of the nitrated Tyr 49 ring, but the two one proton doublet peaks of the ring have not been clearly identified. We note that as for the corresponding resonances of the two residues in the native protein, the singlet resonance of nitro Tyr 49 is upfield relative to that of the nitrated Tyr 40. This suggests such is also the case for the two doublet peaks and overlap with other resonances may well account for their elusiveness. The broad "bump" in the aromatic region of the spectrum of Fig. 5.8(b) intimates this may well be the case and it may also be the reason the difference in peak intensity at position R6 and R8 is more noticeable at low pH when these resonances have moved downfield over the range of their pH dependence. Otherwise the aromatic region of the spectrum demonstrated all the effects described above for the mono nitrated protein on changing the pH. This was also the case for the aliphatic region as shown in Fig. 5.7 even to the subtle changes in the curves of L2 and Met B. However, one noteable exception was the behaviour of L5. This resonance was unaffected by nitration of Tyr 40 but as can be seen in Fig. 5.7 shows a small inflection in its chemical shift versus pH curve over the pH range of the pK_a indicated by resonance D1. This is in complete agreement with the discussion above and confirms the proximity of the methyl group, giving rise to L5, to tyrosine 49. The observed change in the pH dependence of the resonance is exactly analogous to that of L2 due to the modification of Tyr 40 and may well indicate that nitro Tyr 49 lies marginally closer to the unassigned methyl group of L5. Alternatively these effects could be accounted for by larger changes in induced ring current shifts resulting from altering the ionisation state of the aromatic ring substituents.

Final conformation of the assignment was sought by raising the pH to 10.4. In the native protein and more clearly for the Tyr 40-Lys 35 cross-

linked protein described below, the resonances of Tyr 49(B) are seen to be shifted upfield above pH 9. This is shown in Fig. 5.6. Thus, if the assignment was wrong, peaks would be expected to move out from positions R6 and R8. This was not found and the only tyrosine resonances found to be moving at this pH were those of Tyr 2.

In summary, the assignment of Tyr 49 to the resonances of Tyr B has been well substantiated. The specific effects of modifying tyrosine 40 alone were all seen to be reproduced in the doubly modified protein and for both, nitration of tyrosines is seen to have minimal if any effect on the gross conformation of the protein and at most only extremely subtle changes in the immediate environment of the modified residue. Thus, tyrosine nitration with tetranitromethane is confirmed as an extremely valuable tool to aid spectral assignment via minimal structural and spectral perturbation.

5.3.3 Tyrosine 40-Lysine 35 Cross Linked

The nature of the cross linking group was shown in Fig. 5.3 and the protein spectrum in Fig. 5.2(d). From the latter it is seen that this modification causes more spectral perturbations than observed for the tyrosine nitrations. As might be anticipated, the differences compared to the spectrum of the native protein are more pronounced in the aromatic region, but there is a noticeable absence of intensity in the lysine εCH_2 proton region of the aliphatics that may well reflect on the new environment of Lys 35. This assignment remains to be confirmed. The peaks from the methyl groups of Leu 45 (L1,L2) are also appreciably moved downfield. In the aromatic region the resonances of Tyr 40 (R9,R13) are no longer present at the native protein positions in accord with the modification. There are a number of other differences in the aromatic region of the spectrum and notably the resonances appear somewhat broader, except for

the two singlet peaks of His 3, when compared with the other spectra shown in Fig. 5.2. Thus, the temperature was raised to try and improve the spectral resolution and the spectrum of a sample recently dissolved in D_2O is shown in Fig. 5.9 at 47°C. The change in linewidth was not dramatic

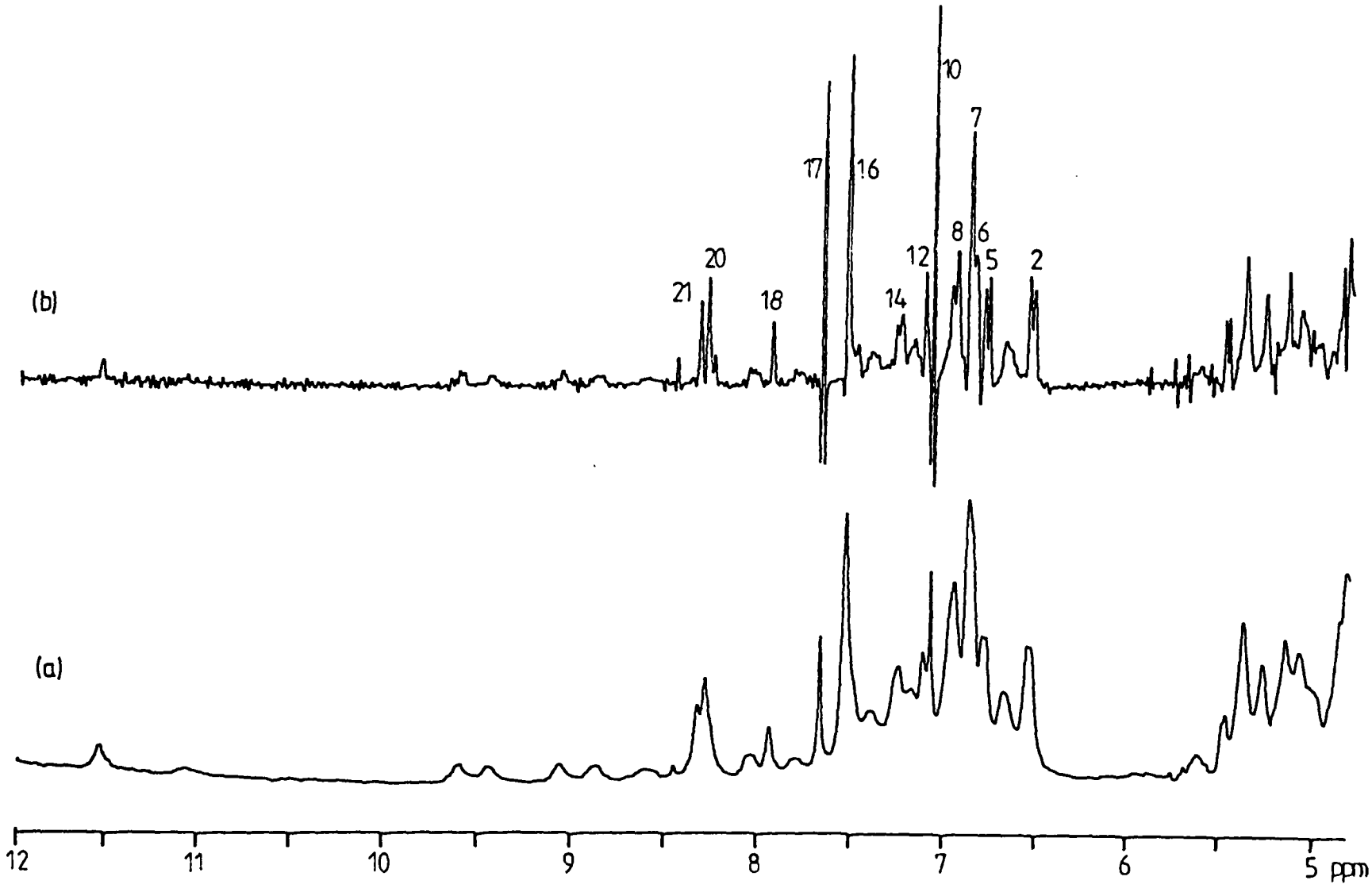

Fig. 5.9 Tyr 40-Lys 35 crosslinked kringle 4; 47°C, pH 7.9
(a) Ordinary (b) Resolution enhanced spectrum.

and all subsequent spectra were obtained at 37°C. Thus, it can be proposed that the chemical modification has introduced some restriction in the mobility of a number of aromatic side chains leading to an exchange broadening of their resonances. This will be considered further below. We note the presence of a number of labile proton NH's in the spectrum of Fig. 5.9 which were slightly more persistent than those seen in native protein samples. For instance an additional peak is just visible at

11.1 ppm at a chemical shift position almost identical to the indole NH proton resonance of Trp B as discussed in section 4.4. This peak has only been seen in spectra of samples containing bound 6 aminohexanoic acid when dissolved in D_2O and certainly not for native protein samples at 47°C. This suggests the modification may lead to additional protection of the interior of the protein from access of solvent molecules.

In Figures 5.2(d) and 5.9 a number of resonances can be readily identified from similarity to the native protein spectrum. All the histidine peaks are present at expected positions although R16 appears too intense when compared with R21. It is possible that it overlaps a singlet resonance from the aromatic ring introduced by the modification and this was supported by pH dependence studies which showed a peak move downfield from this position on lowering the pH from 8 to 7 after which it broadened from the spectrum, typical for R16. However, the two singlets expected to be introduced into the aromatic spectrum by the additional ring have not been clearly identified and neither have the peaks of Tyr 40 been discerned in the modified protein spectrum. The resonances of Tyr 2 (R2,R5) are clearly seen as are those of Tyr 49 (R6,R8) and which were demonstrated by NOE from irradiating L5 as shown in Fig. 5.8(d). R14 of Tyr 73 is less intense than usually observed but confirmed by NOE below. R12 of Trp A is present in its usual position as is R19 although overlapped by a slightly upfield shifted R20. However, R1 and R15 are not clearly seen but their presence is indicated by NOE experiments as to be shown in Fig. 5.10. The C2 proton of Trp B appears shifted downfield by 0.16 ppm and the other resonance used to monitor this residue, R22 is not identified. Finally, the Trp 71 resonances appear particularly poorly resolved in that the intensity at the position of R3, the C2 proton resonance in the native protein, only a broad, ill-defined peak is present. In the aliphatic region of the spectrum the most notable feature is the downfield shift on the two Leu 45 resonances and the Met B methyl proton resonance is moved 0.04 ppm towards higher field.

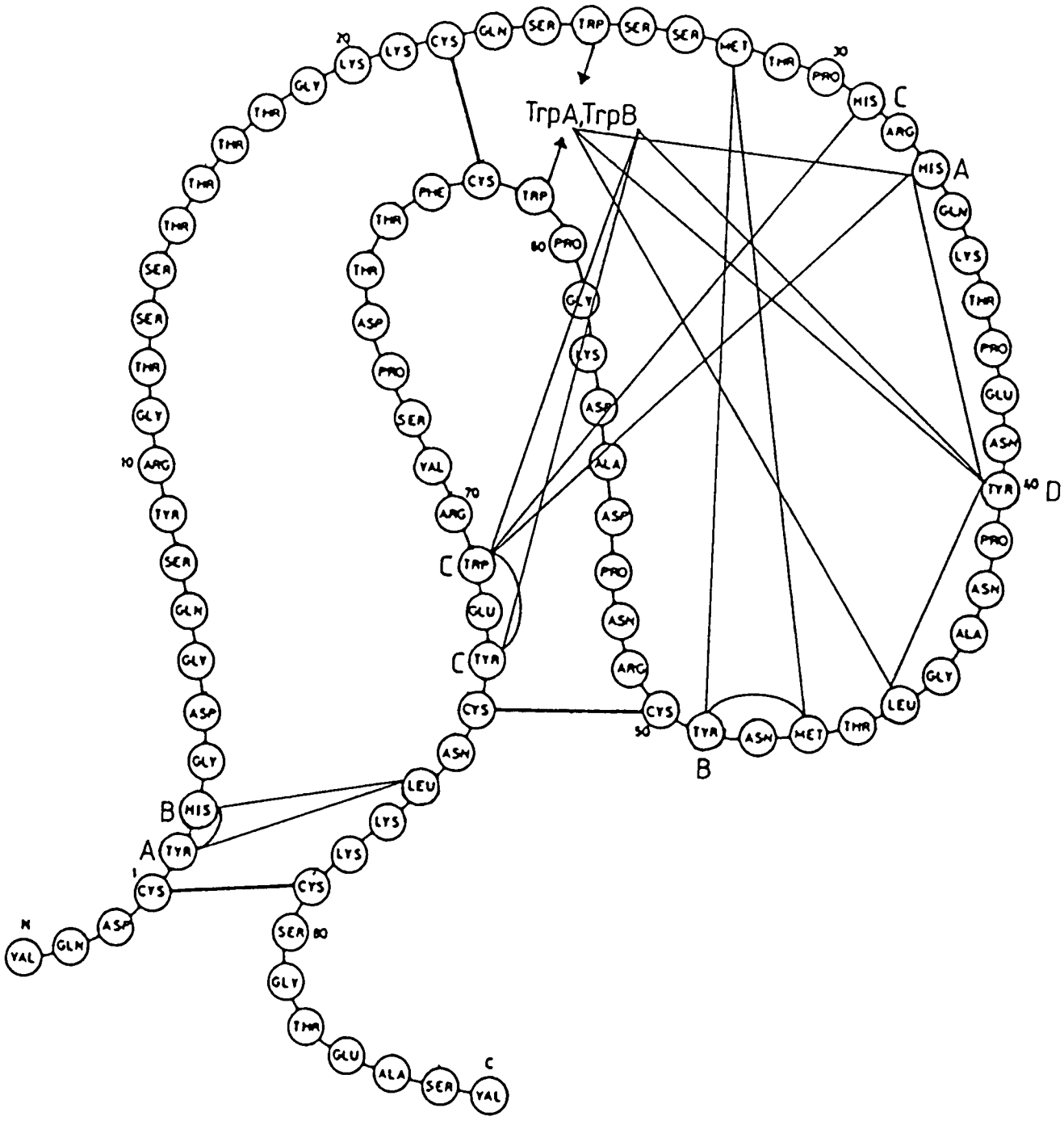

Fig. 4.7 Primary structure of kringle 4. Lines connect residues found to be close in space within the three dimensional structure (see text).

Further aid in resolving the spectrum was provided through NOE experiments which also probe the spatial proximities in the new protein. Some of the results are shown in Fig. 5.10. Irradiation of L1 gives clear peaks in the difference spectrum analogous to the results in the native protein shown in Fig. 3.24(b) with the exception that no enhancement of a Tyr 40 resonance is recognised. This confirms that the spatial proximity of the methyl group of Leu 45 to the C2 and C7 protons of Trp A is maintained in the modified protein. Likewise irradiation of L3, asssigned to the methyl protons of Leu 76 gives a strong enhancement of the Tyr 2 aromatic resonances indicating the spatial proximity of these two residues is also retained. Presaturation of R19 shows R1, to which it is coupled, in the difference spectrum to be at a chemical shift overlapping with R2 of Tyr 2 and hence not discerned in the ordinary spectrum. Finally, irradiation of R14 demonstrates R6 in the difference confirming Tyr 73 resonances at the usual chemical shift positions and supported by enhancement of R18 of Trp B as seen for the native protein. In addition, there is also a suspicion of intensity at R3 in the difference spectrum which would be in full agreement with results on the native protein and demonstrates integrity of the spatial unit incorporating Trp 71, Tyr 73 and Trp B.

Further investigation of the protein included a limited pH dependence study with some of the spectra being shown in Fig. 5.11, and data included in Figures 5.6 and 5.7. In the aromatic region of the spectrum the resonances of Tyr 49 (R6,R8) could be followed more easily at high pH than in the native protein as, in particular, R8 was not obscured now by the meta proton peak, R9 of Tyr 40. The size of the shifts shown in Fig. 5.6 demonstrate R6 to be from the meta protons of Tyr 49. However, of more interest is the behaviour of R3 with pH. The singlet resonance can be clearly seen (Fig. 5.11A) in the spectrum at pH 3.36 but broadens considerably as the pH is raised. Very similar effects are seen at the positions of

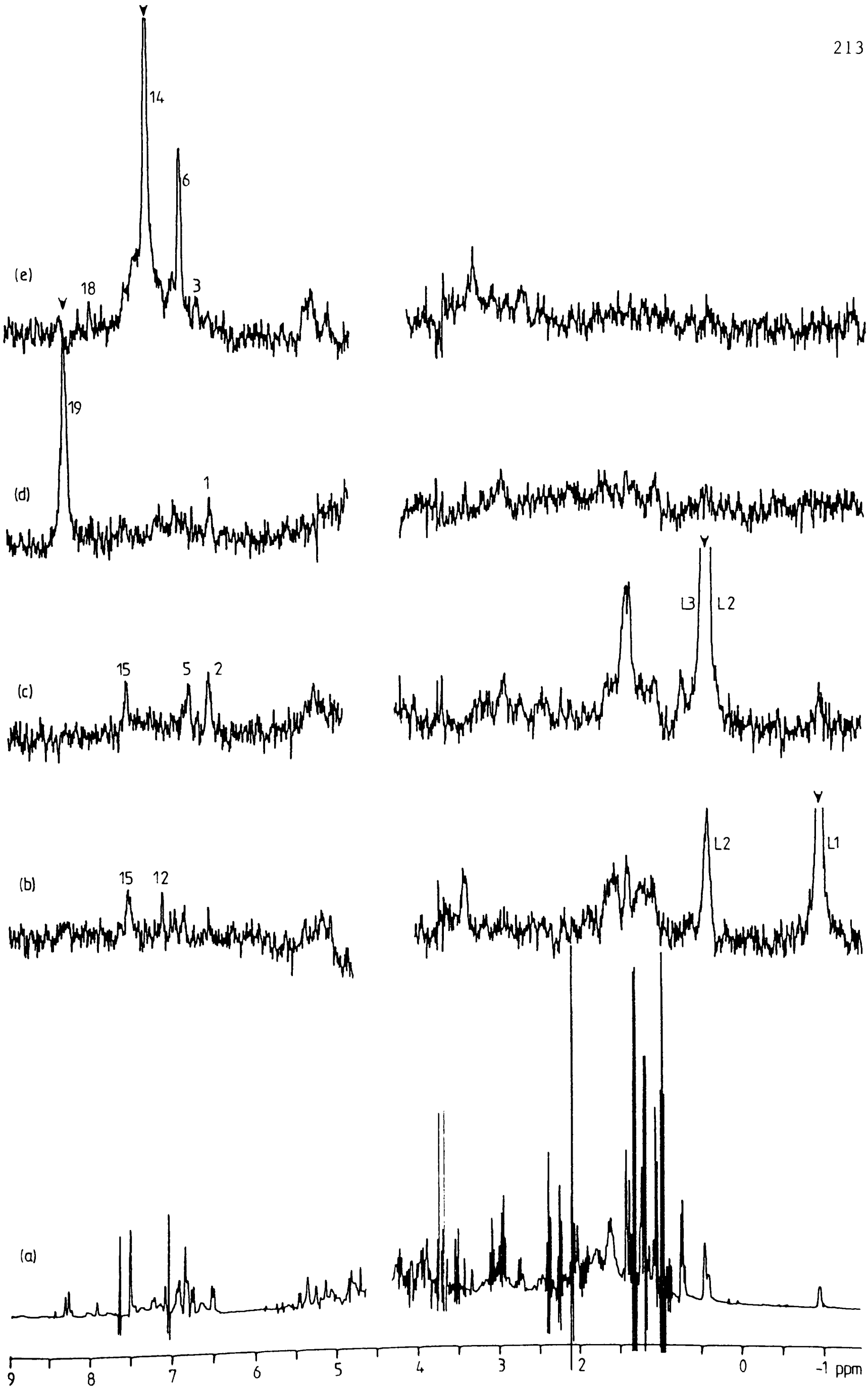

Fig. 5.10 NOE difference spectra of Tyr 40-Lys 35 crosslinked kringle 4; 37°C, [illegible] 7.0. (a) Resolution enhanced spectrum.

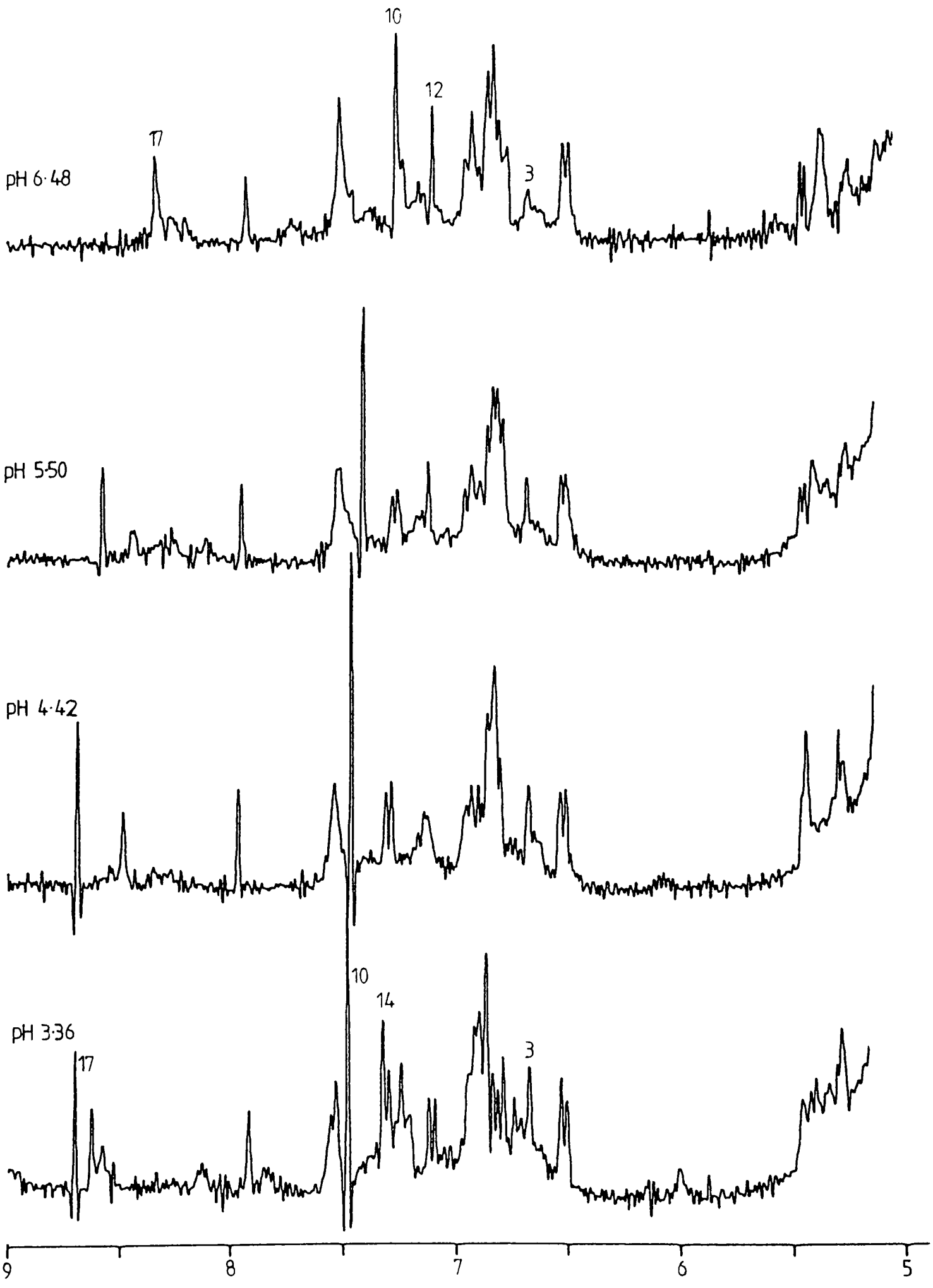

Fig. 5.11A Aromatic region of the spectrum of Tyr 40–Lys 35 cross-linked kringle 4; 37°C. Resolution enhanced spectra.

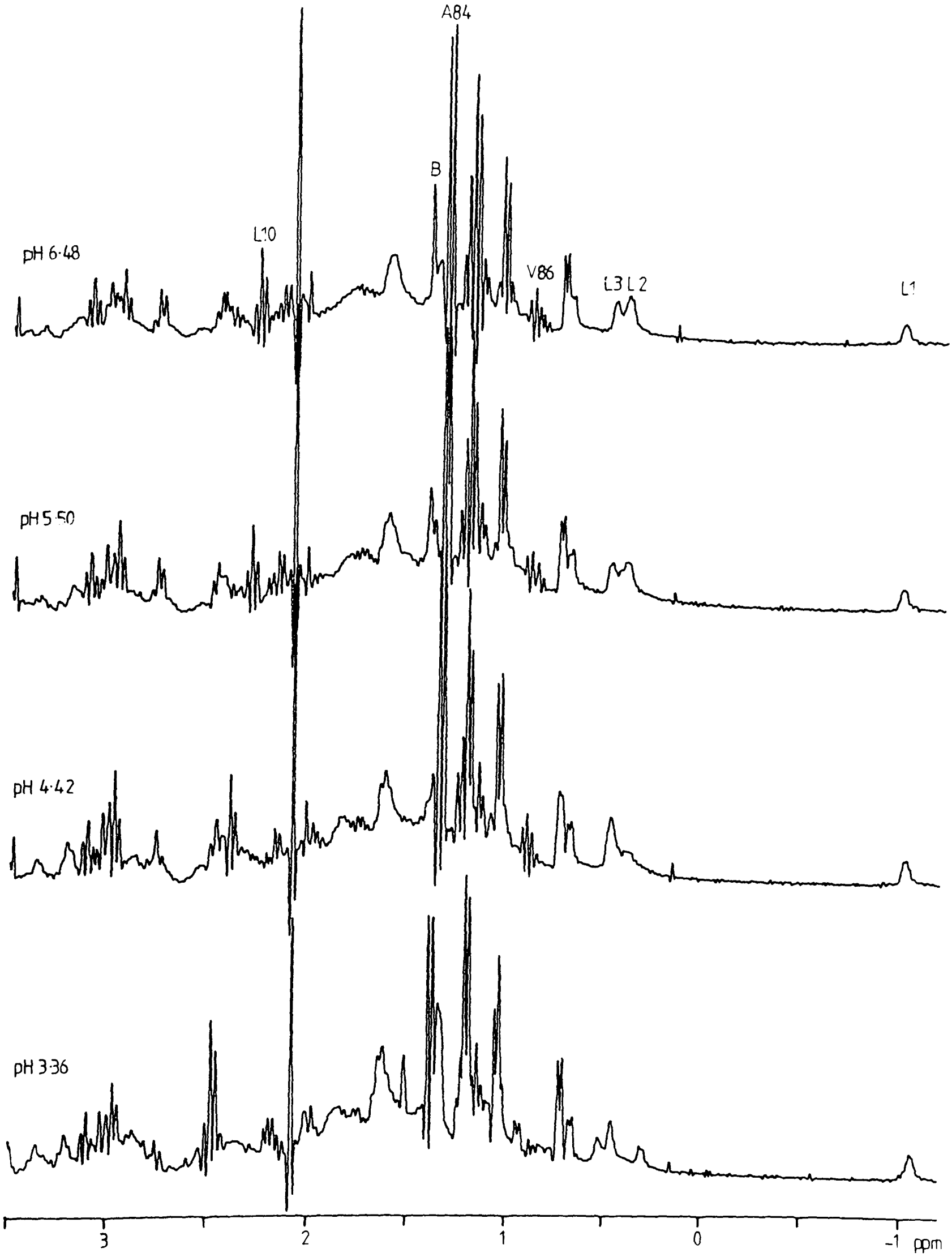

Fig. 5.11B Aliphatic region of the spectrum of Tyr 40-Lys 35 cross-linked kringle 4; 37^{o}C. Resolution enhanced spectra.

other resonances arising from Trp 71 - R23, R4 and R11. Over the same pH range R12 broadens as the pH is lowered in much the same way as occurs in the native protein, when it will be recalled R3 showed a slight pH dependent shift but no intensity change until denaturation occurred below pH 3.5. R14 of Tyr 73, too shows similar behaviour to R3 of Trp 71 and it was remarked above, from Fig. 5.9 at higher pH, that R14 was less intense than normally observed. R18 shows some pH dependent movements over this pH range but they are much less pronounced than those observed for the native protein. In the aliphatic region of the spectrum the most noticeable feature of the pH dependence study is the marked shift of the Leu 45 methyl proton resonances L1 and L2 as the pH is dropped below pH 5.5. As can be seen in Fig. 5.7 they move towards the native protein positions at low pH values. The methyl group resonance of Ala 84 reflects the terminal carboxyl group ionisation (Fig. 5.11B) as does the lesser fraction of Val 86, and the peak L10 moves with the protonation of Glu 83, as seen for the native protein. But, in particular the methyl proton peak of Met B shows analogous behaviour to that in the unmodified protein broadening out of the spectrum below pH 5.

Thus, overall the cross-linking of Tyr 40 and Lys 35 has led to a considerable change in the pH dependence of resonances from Trp 71, Tyr 73 and Leu 45 and maybe Trp B (R18) over the pH range in which resonances of Trp A, Met B, His 33 and R9 of Tyr 40 in the native protein show selective broadening. Indeed, many of the latter peaks show the same changes in the modified protein as the pH is lowered, but resonances of the former residues become more like those seen in the native protein over the same pH change. The explanation of this phenomenon is not clear but conjecture is possible. The effects on the group of resonances involving Trp A, Met B, His 33 were considered most likely the result of a carboxyl group ionisation in section 4.2 and possibly the same group that is responsible

for maintaining His 33 in a protonated state. Resonance R9 of Tyr 40 was also suggested to be involved in what appeared as a local unfolding of part of the structure, and Tyr 40 has been shown to be spatially related to the residues involved by a number of experiments. We note that Trp 71, Tyr 73 and Leu 45 are also clustered around the ligand/lanthanide ion binding site and that the cross linking reagent incorporates a hydrophobic group into the structure. Consequently, it may be proposed that at lower pH (below pH 5) some local unfolding of the protein involving Met B, His 33 Trp A and to some extent Tyr 40 results in the additional ring being removed from the protein core and Trp 71, Tyr 73, Leu 45 are all relatively unperturbed compared with their environment in the native protein at the same pH. Then, as the pH is raised the rest of the protein loop folds into the main structure leading to perturbation of the resonances as noted, both restricting side chain mobility as revealed by resonance broadening and through additional secondary shifts of resonances as seen for L1 and L2 from the extra aromatic ring. It must be emphasised that this is conjecture and remains to be more clearly defined although it is in keeping with all the information gathered so far on the protein structure. Obviously, the results of adding ligand to the sample would be of considerable interest with this modification but this experiment and lanthanide ion probe studies have yet to be carried out. But it is noteworthy that this protein retains affinity for lysine-Sepharose columns.

5.3.4 Summary

It has been demonstrated that nitration of two tyrosine residues has little effect on the overall structure of the protein in solution and even cross-linking Tyr 40 and Lys 35 produces changes compatible with only perturbation of residues close to the site of the modification. The results obtained all fit into the framework of data constructed for the native protein and have in some cases strengthened it, for instance by

the effects on the Met B resonance confirming its spatial proximity to Tyr 40. In particular, the ability to cross link Tyr 40 with what is presumed to be a surface residue, Lys 35 confirms a conclusion previously suggested by the lanthanide ion probe experiments that Tyr 40 is more superficially situated in the structure. In addition, the relatively minor spectral perturbations of the tyrosine nitrations are completely consistent with the retention of ligand binding ability by these proteins. As just mentioned a study of the ligand binding of the cross linked protein would be of more interest. The histidine residues have been little considered in the discussion above, largely because the pH titrations were not sufficiently detailed for subtle changes to be detected. However, the resonances of His 3 (R17,R10) are, of the three residues, most easily followed and always appeared unperturbed by the modifications in complete agreement with the structural model being built up which indicates some separation in space of His 3 from the modification sites. We now go on to briefly consider the last aromatic residue modification that we have studied.

5.4 Tryptophan 71, Methionines 27 and 48 Oxidised

This protein, formed by the reaction of kringle 4 with hydrogen peroxide, contains an N-formylkynurenine side chain instead of Trp 71 as shown in Fig. 5.12 and both methionine residues are converted to methionine

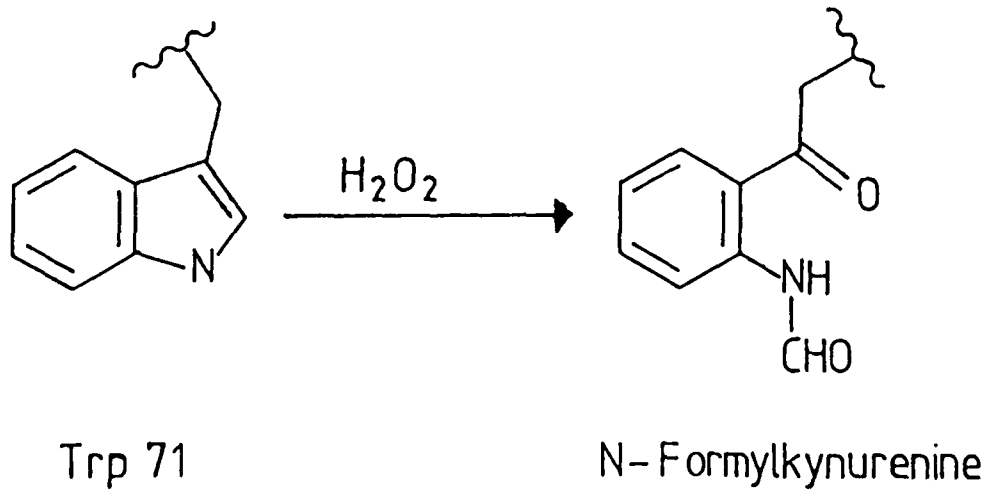

Fig. 5.12 Chemical structure of the modified tryptophan residue

sulphone side chains. The spectrum of the protein is shown in Fig. 5.13. In the alphatic region the spectrum is fairly similar to that of the native protein although, of course, the two methionine methyl proton resonances are no longer at the same chamical shifts. However, closer inspection of the resolution enhanced spectrum shows the peaks L1 and L2 to be "doubled" but in unequal amounts. Dr. Patthy has supplied us with two separate preparations of this modified protein and this spectral feature has been observed for both, although with the second sample the two peaks were approximately of equal intensity, the rest of the spectrum being otherwise very similar. It is very unlikely this represents only partial modification as Patthy reports a yield of modified protein of at least 80%. Cassels, (1979) selectively modified Trp 62 of lysozyme using N-bromo-succinimide which does not cleave the indole ring but introduces a chiral centre. The resulting spectrum included some peaks of half proton intensity which were attributed to different proton environments arising in the two diastereomers rather than two distinct conformations of a single configuration. However, no such chiral centre is introduced into the final product of hydrogen peroxide modification and in view of the different intensity ratios of the peaks in the two samples, neither explanation offered for the situation in lysozyme is applicable here. Thus, the reason for this feature remains elusive.

The aromatic region of the oxidised protein spectrum differs more markedly from that of the native protein. The second stage assignment of the Trp 71 resonances have already been discussed from independent evidence, but the resonances R23, R3 and R4 are absent in the modified protein spectrum in agreement with this. Llinás et al (1983) confirm the assignment through their selective conversion of Trp 71 to the 2-hydroxy-5-nitrobenzyl derivative.

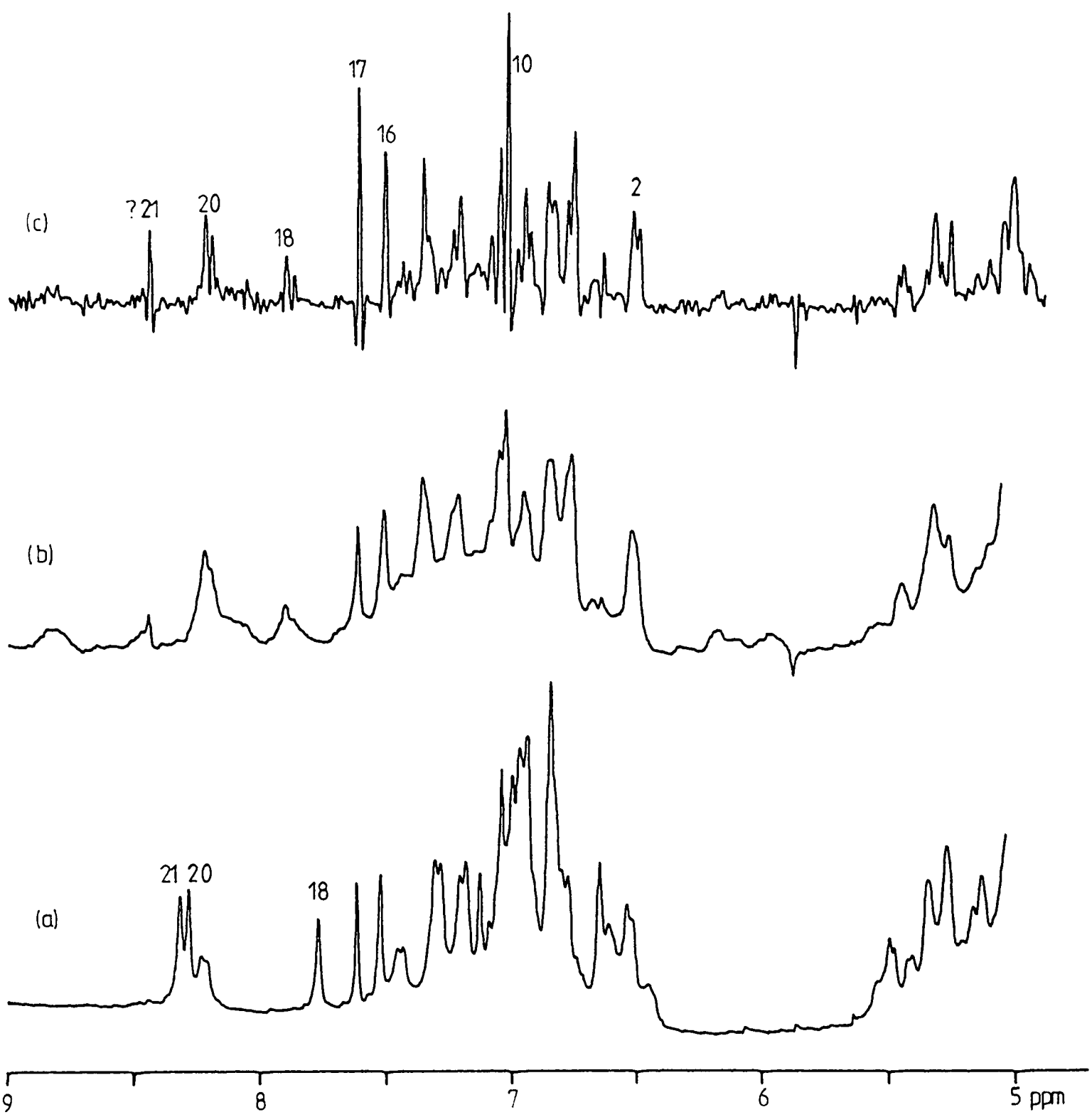

Fig. 5.13A Aromatic region of the spectrum; 37°C, pH 8.9 (a) Native kringle 4 (b) Trp 71, Mets 28, 47 oxidised kringle 4 (c) Resolution enhanced form of (b).

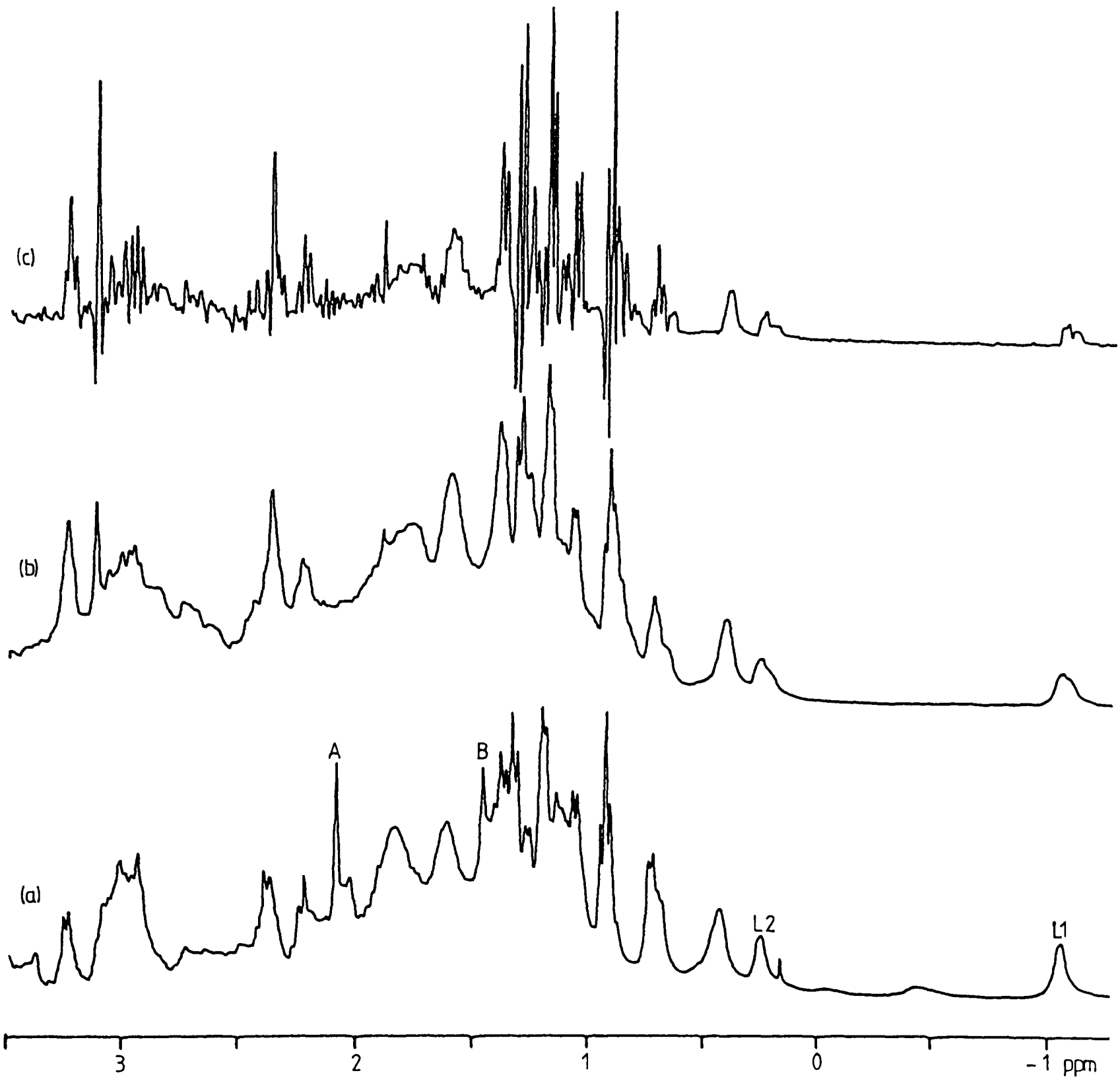

Fig. 5.13B Aliphatic region of the spectrum; 37°C, pH 8.9 (a) Native kringle 4 (b) Trp 71, Mets 28, 47 oxidised kringle 4 (c) Resolution enhanced form of (b).

Some resonances such as R2 of Tyr 2 and R17, R10 of His 3 are readily seen to be unperturbed by the modification, but others are not so easily identified. An extensive pH titration of one sample was performed and demonstrated the peak labelled R18 in Fig. 5.13A(c) to have a similar pH dependence to that of the Trp B C2 proton in the native protein, despite being downfield shifted. The tentative assignment of R21 (His 31) in the modified protein spectrum was made similarly. The resonance labelled R20 (His 33) broadened out at lower pH as seen for the native protein, and has a small upfield shift. Thus, both histidines previously shown to be close in space to Trp 71 are affected to varying extents by its modification. pH dependence above pH 8.8 revealed the resonances of Tyr 40 to be unperturbed, but those of Tyr 73 have not been definitely identified as yet, nor have the resonances of the modified residue.

The doubled peak phenomenon was also seen on the NH proton resonance of Trp A and presaturation of these peaks at 11.5ppm, shown in Fig. 5.14, gave comparable results to those demonstrated for the native protein. We note

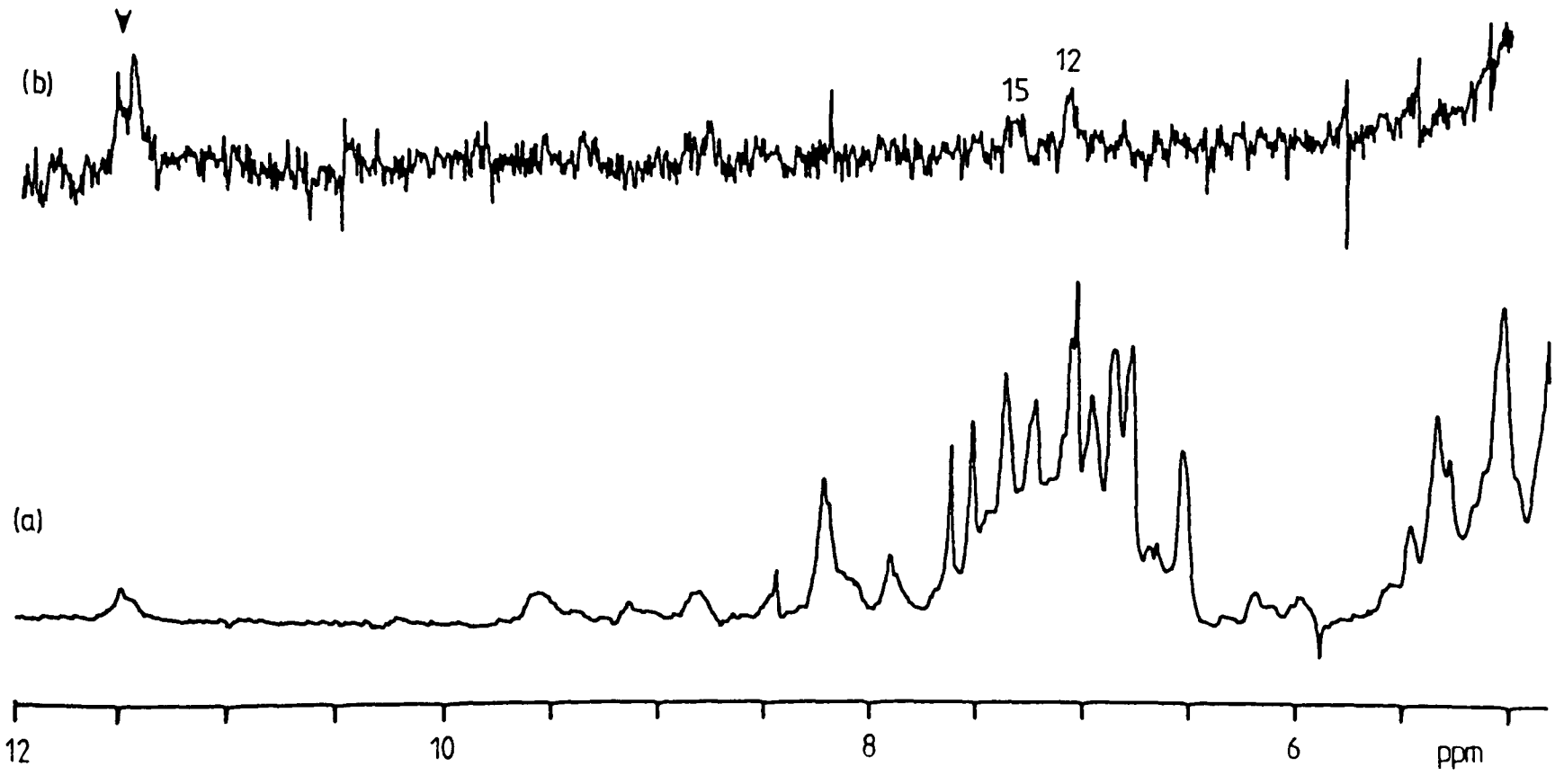

Fig. 5.14 NOE difference spectrum of the Trp 71, Mets 28, 47 oxidised kringle 4, 27°C, pH 8.9

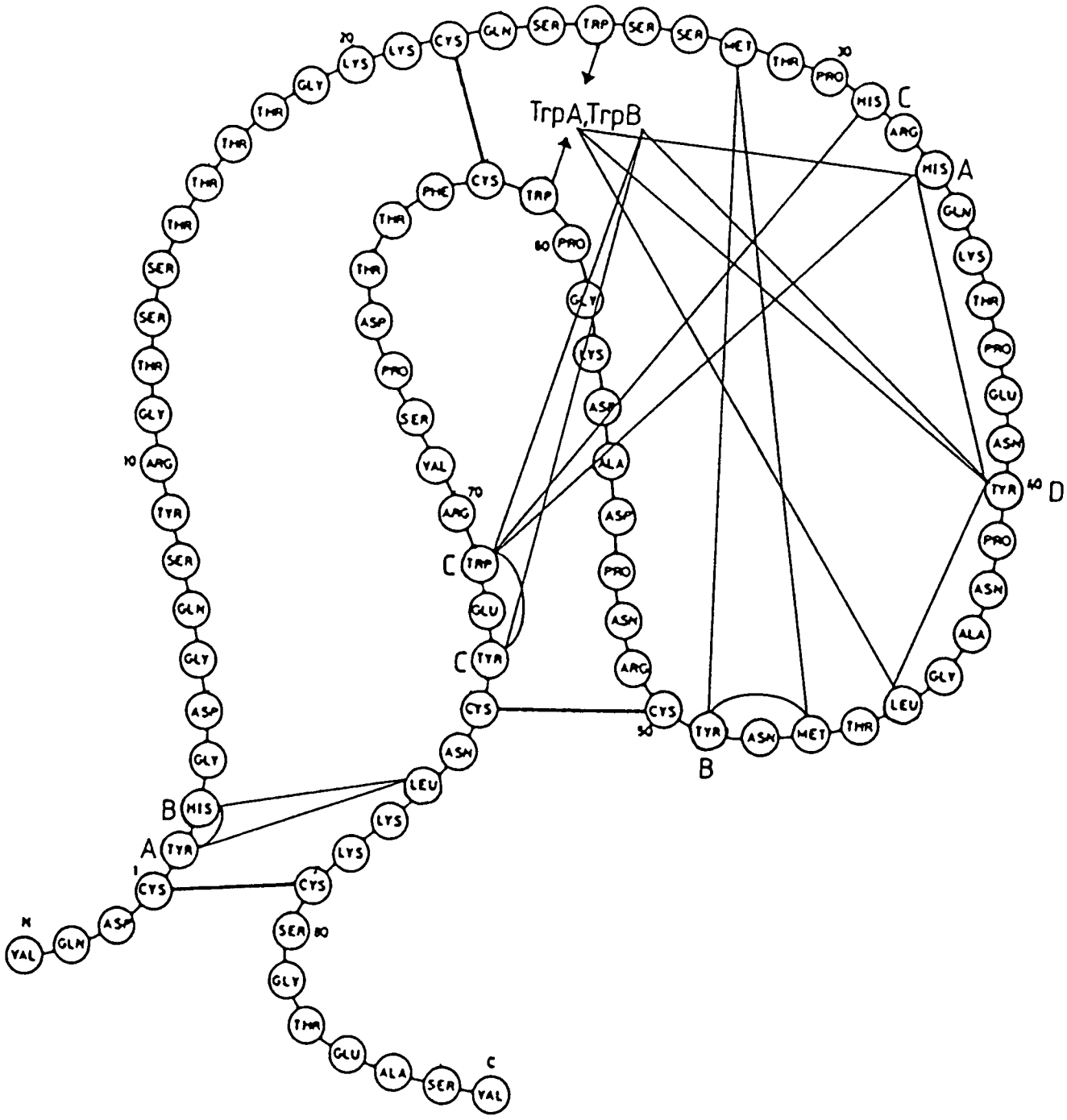

Fig. 4.7 Primary structure of kringle 4. Lines connect residues found to be close in space within the three dimensional structure (see text).

that the resonances clearly showing this feature L1, L2 of Leu 45 and the indole NH of Trp A have already been shown to be close in space, but were not thought to be immediately adjacent to Trp 71. However, Trp B is affected by the modification as shown by the perturbation of resonance R18 and indeed, close inspection of Fig. 5.13B(c) suggests R18 may actually be doubled. It may be then that Trp B mediates the effects of the Trp 71 modification on Trp A and Leu 45, as it also has been shown to be close to Trp 71 (see Fig. 4.7). Alternatively, these effects may be a consequence of the methionine residues having been modified.

Obviously, the effects of the hydrogen peroxide oxidation of kringle 4 need much more extensive investigation to be elucidated in more detail. Unfortunately, the small amounts of protein available and the relatively poor spectrum that it gives add to the difficulty of the task. This modified protein no longer has affinity for lysine-Sepharose consistent with the presence of Trp 71 in the ligand binding site as revealed by a number of experiments discussed previously. In addition, oxidation carried out in the presence of added 6 aminohexanoic acid resulted in considerable protection of the tryptophan residue , but both methionine residues were oxidised in the protein that retained affinity for lysine-Sepharose (Patthy, personal communication). While much of the protein structure is seen to be conserved in the modified protein there are some notable effects on resonances from His 31, His 33, Trp B in the immediate vicinity of Trp 71 as well as on Trp A and Leu 45 which are further from the modification site. Thus, at this stage it is not possible to say precisely how Trp 71 is involved in the ligand binding site. It is not clear whether the modification simply causes a local pertubation resulting in the loss of ligand affinity perhaps through some steric or electrostatic hindrance or whether the binding site structure is destabilised by the modified side chain resulting in an unfavourable conformational change destroying

the site. In connection with the latter possibility we note that the resonances between 5 and 5.5ppm arising from downfield shifted αCH protons show quite substantial changes in the modified protein spectrum indictaive of some alteration of β secondary structures in the protein. Further study is thus required.

It is interesting to note that in all studies Trps 25 and 61 (Trps A and B) are not modified. This may well be due to those residues being buried within the molecule and inaccessible to the modification reagents, and this agrees with the results already presented which also indicate this to be the case. We now go on to consider two selective modifications to Arginine residues.

5.5 Arginine Modifications

Specific modification of arginine residues with 1,2-cyclohexanedione has been developed by Patthy and Smith (1975) and the resulting structure is shown in Fig. 5.15. The product is unstable at alkaline pH in the

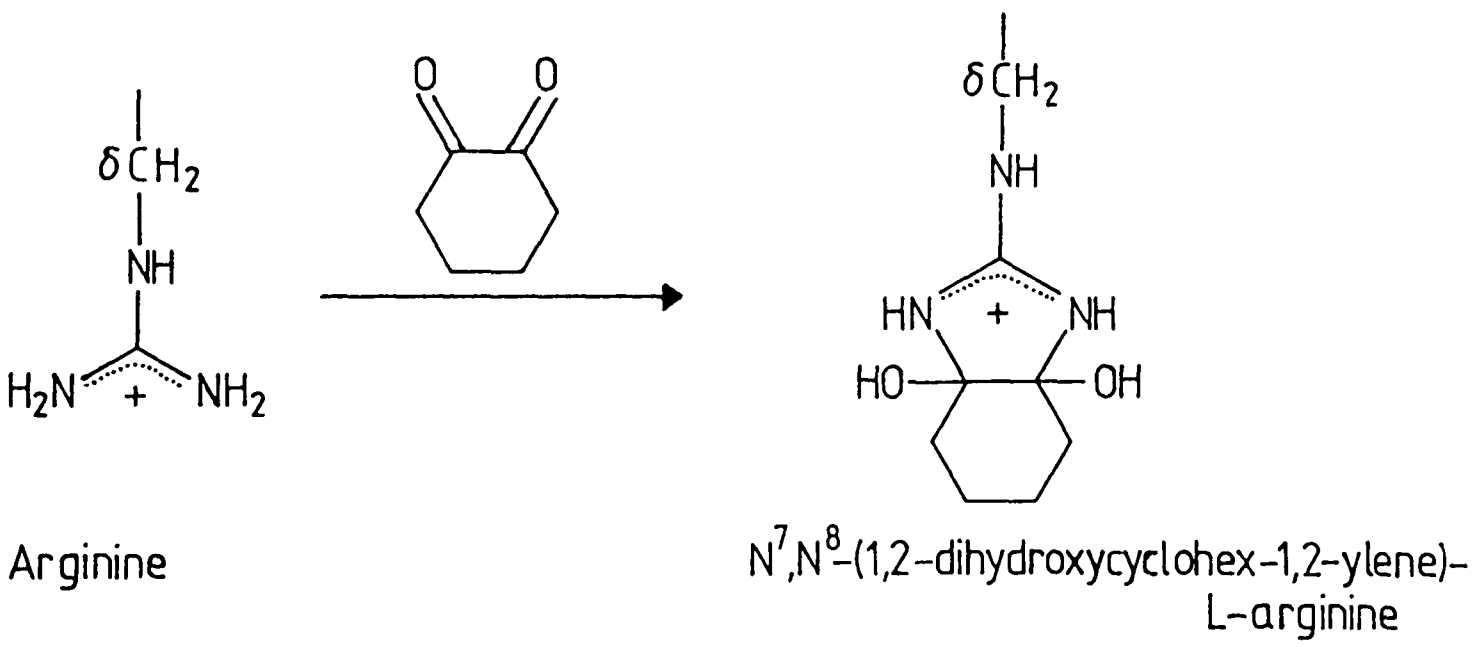

Fig. 5.15 Chemical structure of the modified arginine residues

absence of borate buffer but stable in acidic solution with no added buffer. There are four arginine residues in kringle 4 at position 10, 32, 51 and 70 but Patthy and coworkers have found only Arg 32 and Arg 70 to be susceptible to such modification. It is interesting that Arg 10 adjacent in the sequence to Tyr 9 has not been found to be readily modified, in view of the peculiar nature of Tyr 9 demonstrated by the lack of assigned resonances in the spectrum for this residue.

Spectra of the single and double arginine modified proteins are shown in Fig. 5.16 compared to the spectrum of the native protein at a similar pH and temperature. Arginines are positively charged at neutral pH and are frequently found as surface residues in X-ray crystallographic studies of proteins. The modification does not alter the charge on the residue and so it might be anticipated that these altered residues will have little effect on the tertiary fold of the kringle. Indeed, the great similarity of all the spectra in Fig. 5.16 confirms that this is the case. The aliphatic region shows the modified protein samples to contain more acetate impurity (1.93ppm) than in the native protein and a higher proportion of the Val 86 C terminus. A noteworthy feature is the lack of change of the downfield αCH proton resonances (Fig. 5.16A) in agreement with at most minor conformational changes resulting from the chemical modification. We now consider each protein in slightly more detail.

5.5.1 Arginine 32 modified

The spectrum obtained immediately after dissolving the protein in D_2O is shown in Fig. 5.17 and compared with that of the native protein although the pH of the two samples are very different. As was seen and commented on for the nitrated Tyrosine 40 protein in section 5.3, an additional labile proton resonance is seen around 10.3ppm as well as intensity at 6.2ppm which has also been seen for the native protein as shown in Fig. 3.30(a).

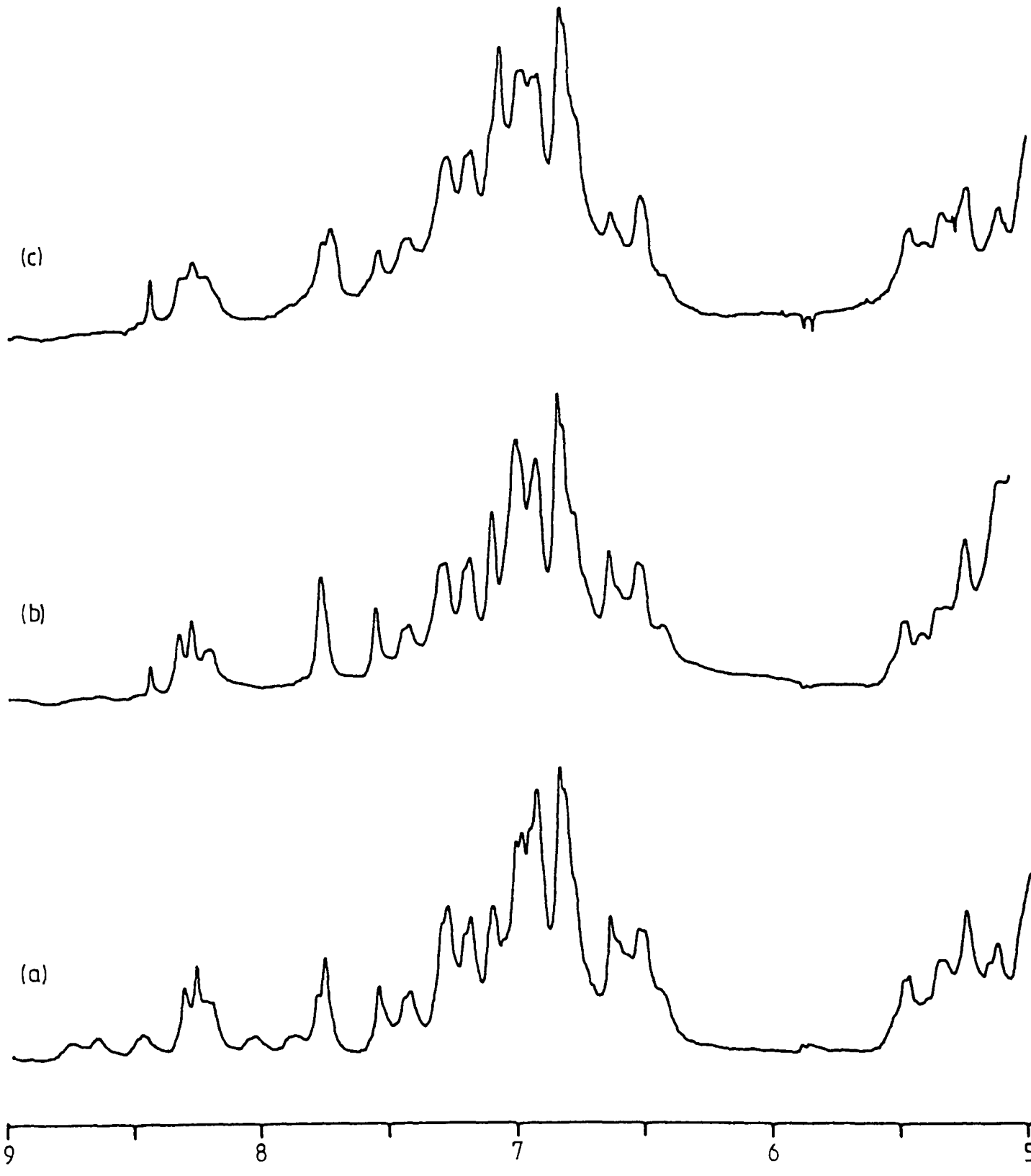

Fig. 5.16A Aromatic region of the spectrum; 37°C, pH 7.1 (a) Native kringle 4 with some unexchanged labile proton resonances present (b) Arg 32 modified kringle (c) Arg 32, 70 modified kringle.

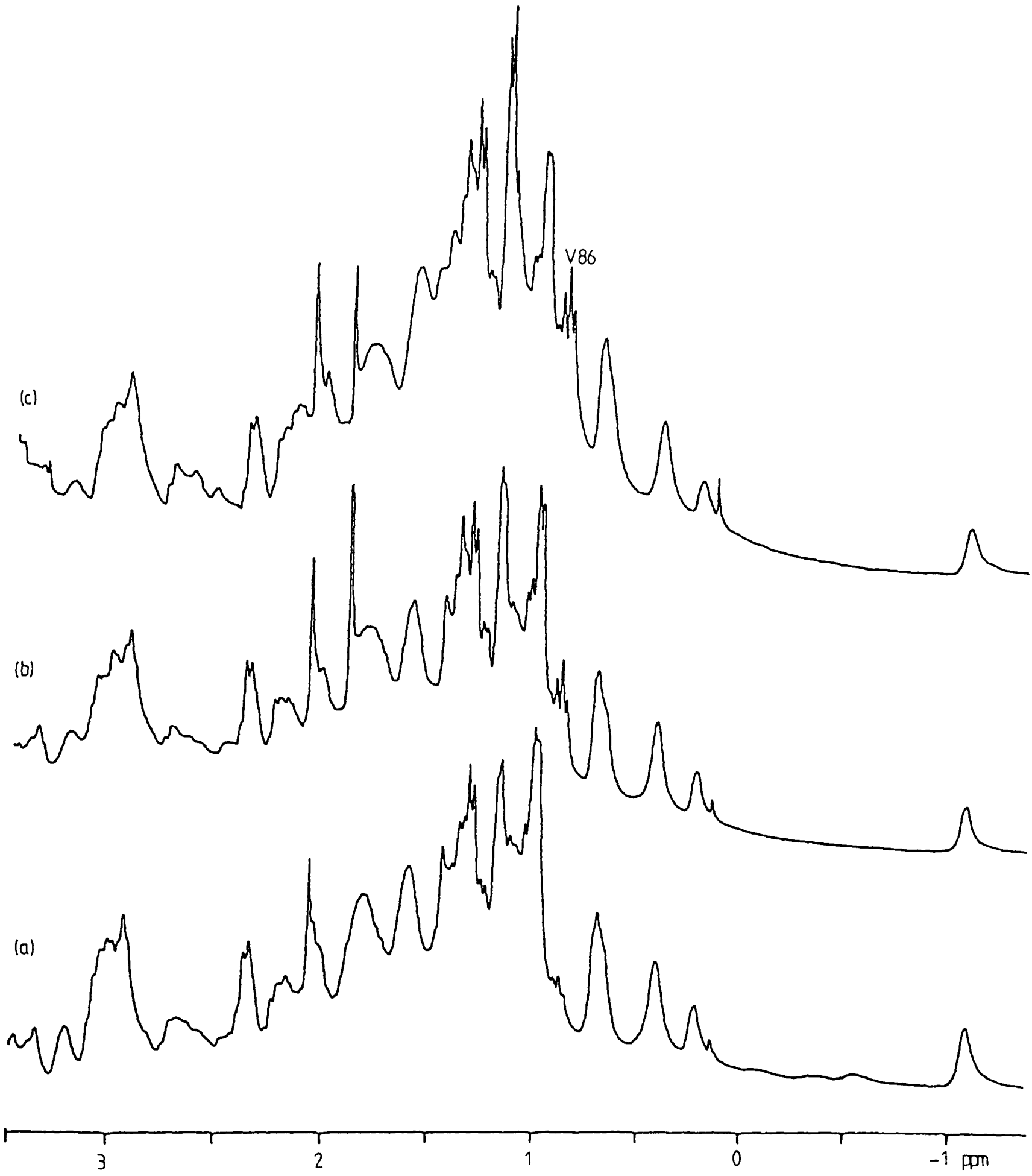

Fig. 5.16B Aliphatic region of the spectrum; 37°C, pH 7.1 (a) Native kringle 4 (b) Arg 32 modified kringle (c) Arg 32, 70 modified kringle.

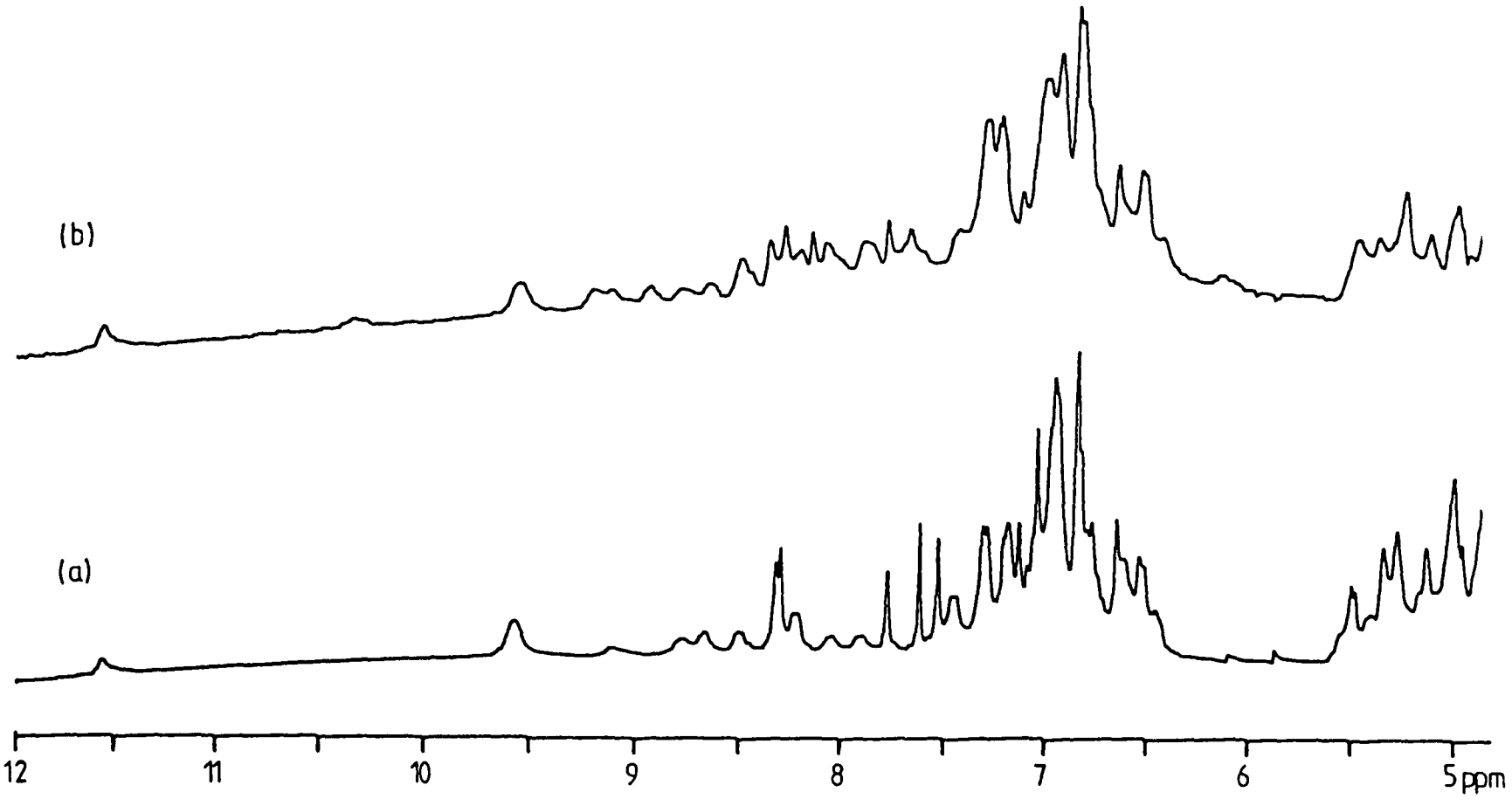

Fig. 5.17 Spectra obtained soon after dissolving in D_2O, 37°C (a) Native kringle 4, pH 9.36, (b) Arg 32 modified kringle 4, pH 6.14.

However, there was no subjective difference in the persistence of the labile proton resonances in this protein. Again the resonance at 10.3ppm exchanged too rapidly for a NOE experiment to be performed.

In view of Arg 32 lying between two histidine residues in the primary sequence, a careful pH titration was performed to detect any perturbation of their resonances. The spectra are shown in Fig. 5.18 which can be compared directly with Fig. 4.1A for the native protein. (The pH of the modified protein was not raised above pH 7.60 because of the instability of the chemical modification at alkaline pH). The two titrations are remarkably similar with perhaps the modified protein giving slightly better resolved spectra allowing the resonances to be followed more easily. Chemical shift versus pH curves for both proteins are also extremely alike and confirm

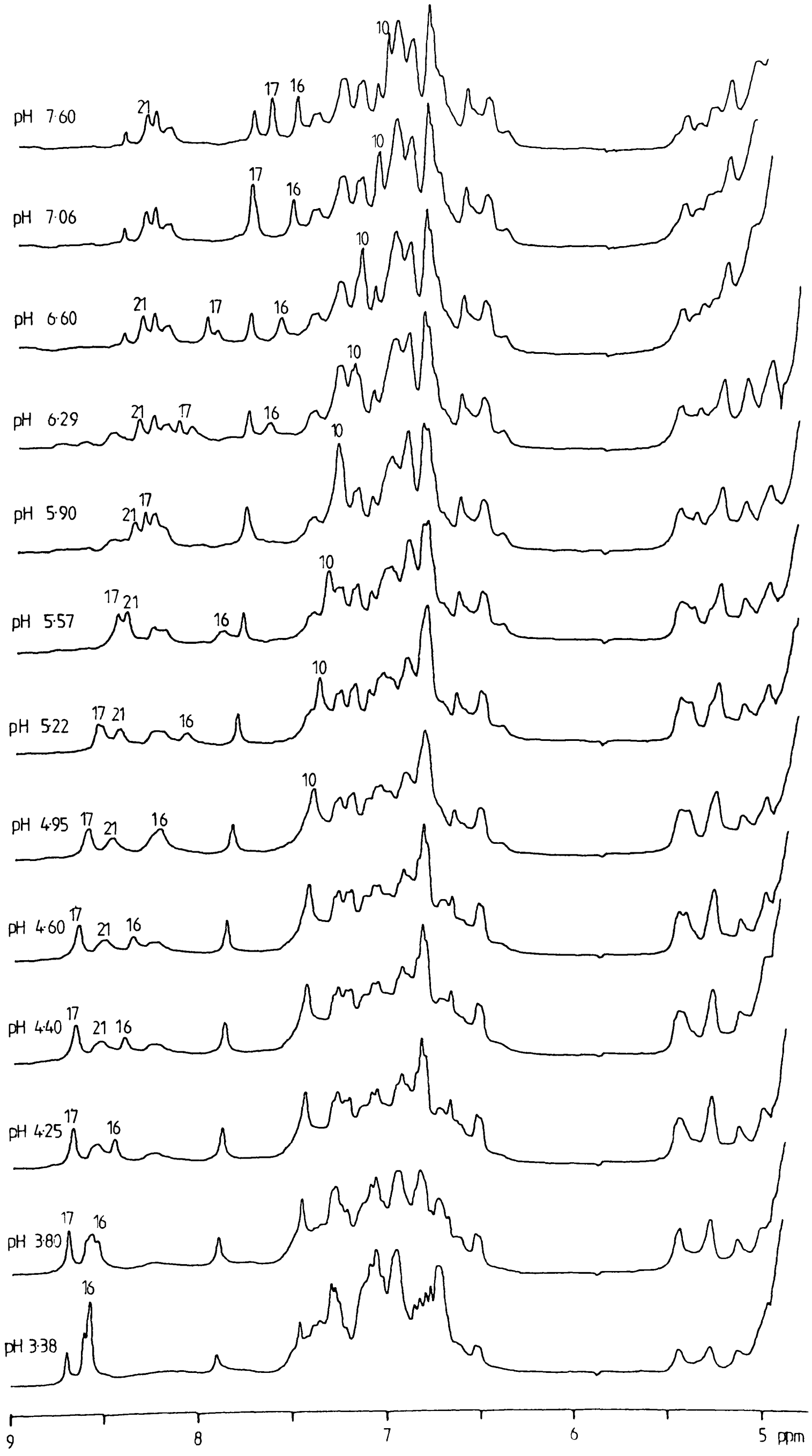

Fig. 5.18 Aromatic region of the pH titration of the Arg 32 modified kringle 4; 37°C, 100mM NaCl.

the more subtle effects noted for the native protein in section 4.2. Selected curves are shown in Fig. 5.19 superimposed on those of the unmodified protein. Small differences are noted on the curves of R16 and R21 of His 31, as well as a similar effect on the C2 proton peak of Trp B (R18) all three curves showing moves of about 0.1 pH units to higher pH over the range of their pH dependence. These small differences may have been regarded as an acceptable systematic experimental error in the pH measurement were it not for the fact that the curves of His 3 (R17,R10) are completely unchanged. This indicates that the effect is real and that the modification of Arg 32 is reflected in the pK_a of His 31 and also affects the pH dependence of R18. The latter effect is difficult to understand in that the ligand binding studies demonstrated the pH dependence of R18 to be independent of the ionisation of His 31 (section 4.4). It may be that Arg 32 has some interaction also with the carboxyl group involved in ligand binding and which influences R18. R20 of His 33, the other adjacent residue to the modified side chain, appears unperturbed in its behaviour although subtle effects on this resonance would be even harder to detect, and the other resonance, R7 of this residue cannot be followed satisfactorily at all. Thus, the assignment of resonances to His 31 and His 3 are certainly well supported by this modification which is seen to produce only very minor local perturbations, although the effect on R18 is curious.

The modified protein was further probed using praseodymium ions, some of the spectra being shown in Fig. 5.20. The protein concentration was not accurately known and so no metal ion to protein concentration ratios are given, although the spectra can be compared directly with those for the native protein given in Fig. 4.32. Curves of the induced shift against metal ion concentration are not included but Table 5.2 lists resonances of interest and the direction and relative magnitude of their praseodymium ion induced shifts. This data can be compared with shift curves

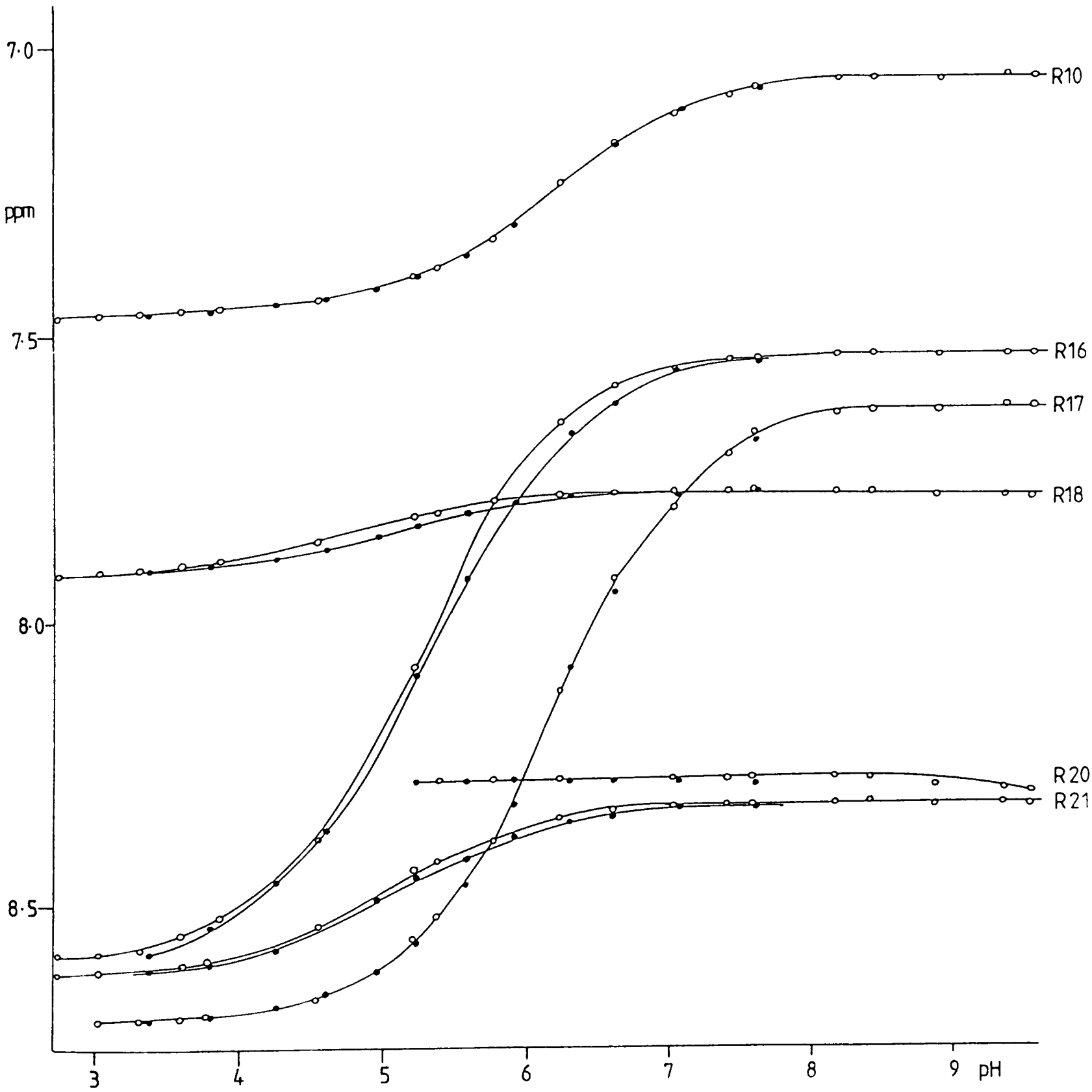

Fig. 5.19 Chemical shift versus pH curves; 37°C, 100mM NaCl
- ∘ Native kringle 4
- • Arg 32 modified kringle 4

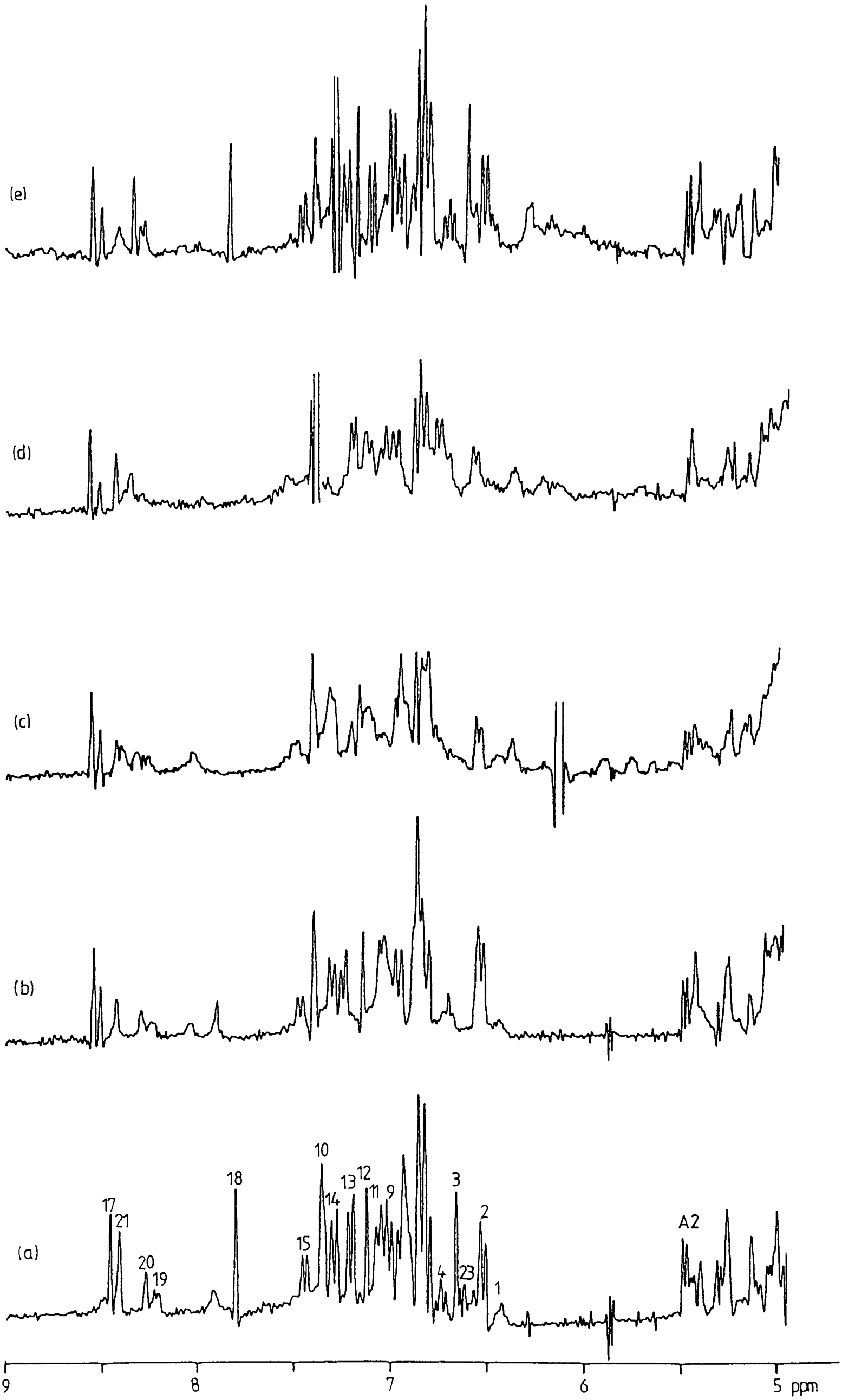

Fig. 5.20A Aromatic region of the resolution enhanced spectra of the praseodymium ion titration of the Arg 32 modified kringle 4; 37°C, pH 5.5. (a) No added metal ions (b)-(d) increasing Pr^{3+} concentration (e) 6 Aminohexanoic acid added to the sample of spectrum (d).

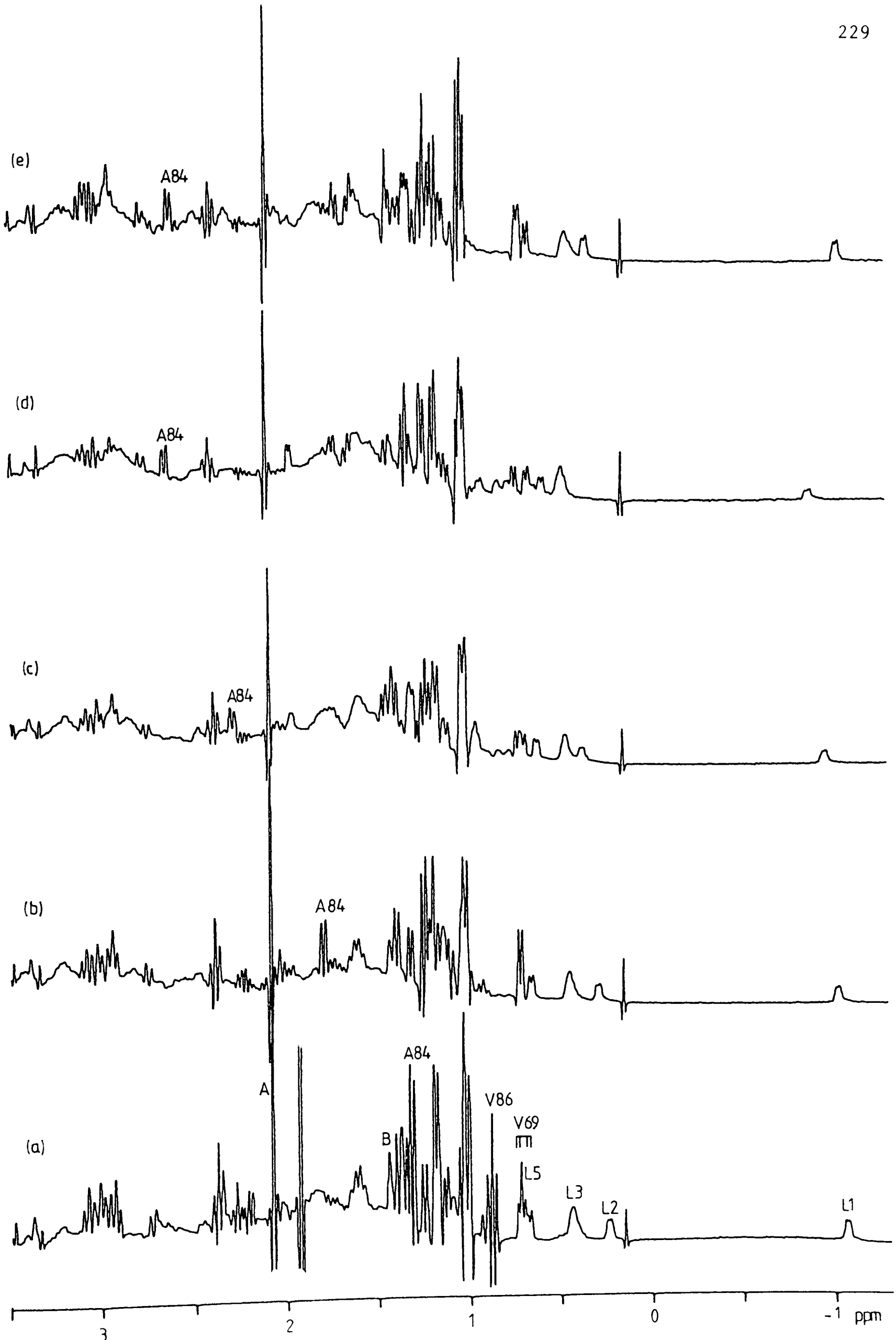

Fig. 5.20B Aliphatic region of the resolution enhanced spectra of the praseodymium ion titration of the Arg 32 modified kringle 4; 37°C, pH 5.5. (a) No added metal ions (b)-(d) increasing Pr^{3+} concentration (e) 6 Aminohexanoic acid added to the sample of spectrum (d).

Table 5.2 Summary of the resonance shifts induced by praseodymium ion binding to the Arg 32 modified kringle 4 at 37°C, pH 5.5.

SHIFT	DOWNFIELD	UPFIELD
Large	Trp B (R18) Ala 84 Val 86 (Acetate)	Trp 71 (R3,R23,R4,R11)
Medium	Leu 45 (L1,L2) Tyr 40 (R9,R13) Trp A (R1,R12,R15,R19)	Val 69 (L4,L5)
Small	Leu 76 (L3) Tyr 2 (R2,R5) His 3 (R17,R10) L5 Tyr 73 (R14,R6) His 33 (R20,R7)	Met B

Unaffected resonances include Met A, A2

for the native protein shown in Figs. 4.33 and 4.34. As would be expected from the discussion above, the results of lanthanide ion binding are practically identical to those obtained for the native protein. (Note the acetate impurity peak is shifted into the aromatic region of the spectrum in Fig. 5.20A(c)). The effects on R21 of His 31 are again unclear as additional unassigned intensity appears at a similar chemical shift, and as discussed the other resonances of this residue R16 is exchange broadened at the pH of this titration. However, the resonances of His 33 (R20,R7) show very similar behaviour to those of the native protein. Thus, no convincing differences in the effects of praseodymium binding are noted on the resonances from the two histidine residues either side of the modified residue in the amino acid sequence. Figure 5.20(e) shows the effects of adding 6 aminohexanoic acid to the protein containing bound lanthanide ions and as with the native protein the metal ion is displaced from the ligand binding site, resulting in restoration of much of the spectrum to its original form. The C terminal residues, though, remain shifted by bound metal ions that the ligand does not displace as discussed in section 4.5.

In summary, the effects of reacting cyclohexanedione with Arg 32 on the structure of the protein have been shown to be minimal. Very small changes were detected on resonances of His 31 and Trp B through their slightly altered pH dependence. Otherwise the results of experiments on this modified protein have served as complete confirmation of much data already considered for the native protein. We now consider the double arginine modification.

5.5.2 Arginines 32 and 70 modified

The spectrum from this protein was shown above in Fig. 5.16(c) and as commented was, like the single arginine modification, very similar to that of the native protein. Closer comparison does suggest that the

spectrum is slightly less well resolved. This may be due to some residual aggregation for on lowering the pH of the solution the protein was found to precipitate below pH 5.0. The poorer spectra at low pH and not being able to raise the pH above 7.8 because of the instability of the modified groups meant that no useful information has been obtained from either pH or lanthanide ion probe studies.

The insolubility at low pH is very curious because of the small additional change that the modification makes to the chemical structure of the protein and without altering the total charge. Furthermore, this protein no longer binds to lysine-Sepharose whereas the single arginine modified protein does. Thus, alteration of Arg 70 certainly has some important effects on the properties of the protein, but the spectrum indicates that this is not due to any sizeable conformational change resulting from the additional modification as may have occurred, for instance, if Arg 70 had been involved in a structurally important salt bridge. Arg 70 lies adjacent to Trp 71 in the sequence and the latter residue has been seen from chemical modification and lathanide ion studies to be an important residue in the ligand binding site. Trexler et al. (1982) have suggested that Arg 70 forms the ligand carboxyl group binding site. This may be the case or alternatively its modification may simply obstruct the ligand sterically. However, the decreased solubility of this protein in conjunction with no marked change in the protein structure strongly suggests Arg 70 to be a surface residue which when modified causes a subtle change promoting protein aggregation at pH below 5.0; modification of an internal residue in the absence of a large conformational change would not be expected to cause such a profound effect.

Thus, study of the arginine modified derivatives of kringle 4 supports the notion of Arg 32 and 70 being surface residues and accessible to chemical reagents, while allowing the possibility that the other two

residues at position 10 and 51 are either buried in the protein or otherwise unavailable for reaction with cyclohexanedione. We now go on to consider two chemical modifications of the protein with potential for more drastic effects on the structure since they involve cleavage of the peptide chain.

5.6 Met 47-Asn 48 Cleavage

Cyanogen bromide was used to bring about the cleavage and the spectrum of the modified protein is shown in Fig. 5.21 compared to that of the native protein. It is seen immediately that breaking the peptide chain has resulted in a dramatic change in the spectrum. Although one methionine side chain is modified in the procedure the spectrum shows the loss of both methionine methyl resonances. The methyl proton peaks of Leu 45 (L1,L2) are no longer present and the whole of the aromatic region of the spectrum bears very little resemblance to that of the native protein. The spectrum of the modified protein is approaching that expected for a random coil protein as evidenced for instance by the intensity at the random coil chemical shift value of the threonine methyl protons, a feature noted previously in the spectra of the denatured native protein. However, the spectrum is not identical to that of the denatured unmodified protein indicating some residual structure is present. For instance, some of the downfield shifted αCH proton resonances are still present and the aromatic intensity is not simply a superposition of the constituent resonances at their random coil positions. Obviously to detail the remaining structure would require extensive assignment studies and indeed the folded elements that are present need not be found in the native protein structure but may be completely new. Thus, this protein has been little investigated.

However, from the above discussion alone it is readily understood that this modification results in the loss of lysine-Sepharose affinity. The environment around the Leu 45 methyl groups, only two residues from the site of modification in the sequence, has been completely altered. This

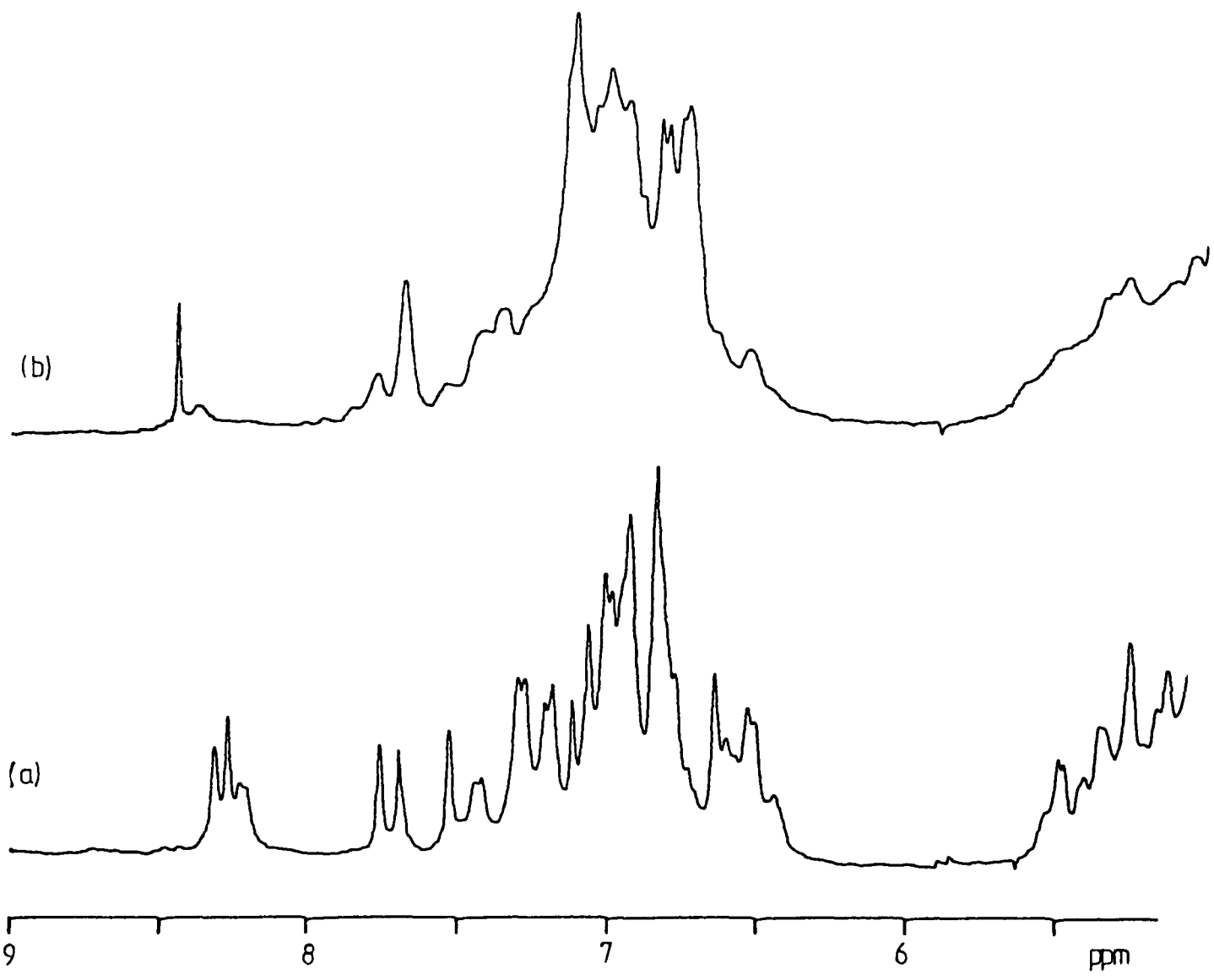

Fig. 5.21A Aromatic region of the spectrum; 37°C, pH 7.5. (a) Native kringle 4 (b) Met 47-Asn 48 cleaved kringle.

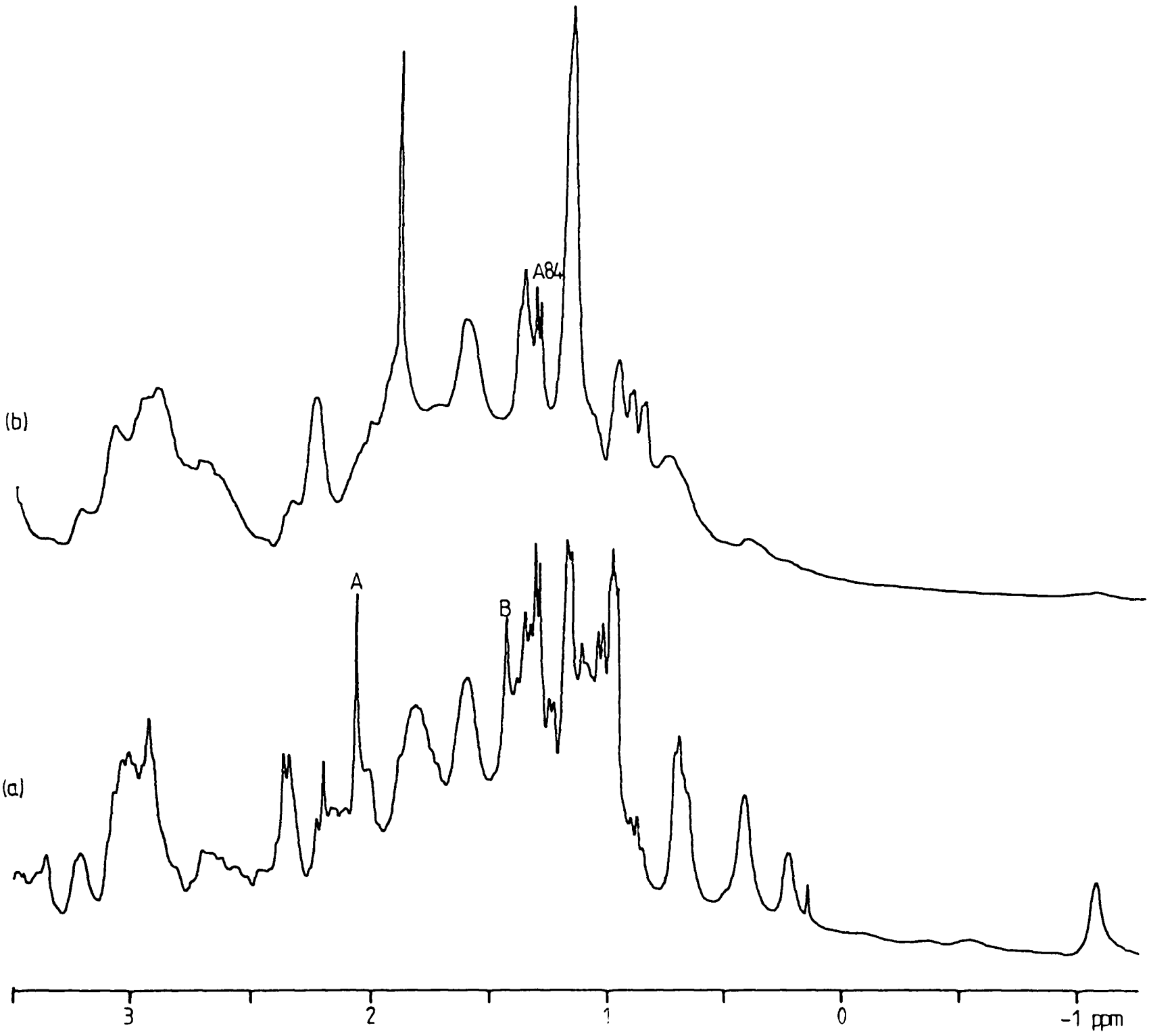

Fig. 5.21B Aliphatic region of the spectrum; 37°C, pH 7.5. (a) Native kringle 4 (b) Met 47-Asn 48 cleaved kringle.

residue has been shown to be near to the ligand amino group binding site, in the heart of the molecule, from the lanthanide ion probe studies and this alone provides very good evidence that the modification has resulted in the architecture of the ligand binding site being completely destroyed. This is in contrast to the modification involving Arg 70 and perhaps that of Trp 71 where the Leu 45 methyl resonances are little if at all perturbed and structural alterations are minimal. In the latter cases lysine-Sepharose affinity has been presumed to be lost through much more subtle effects of steric or electrostatic hindrance of the binding process.

It is interesting to note that of the two methionine residues in kringle 4, Met 47 is much more susceptible to cyanogen bromide cleavage than Met 28, although both residues lie on the same interdisulphide loop. Unfortunately though, this protein modification has not led to the second stage assignment of these residues being made. pH dependence studies of the native protein showed one methionine methyl peak, Met A, to fold into the structure at much lower pH than the other, but at the same time as many other resonances including those of Leu 45. The Met B resonance only appeared at its secondary shifted position around pH 5.5 accompanied by similar behaviour of the resonances of Trp A, His 33 and R9 of Tyr 40. It is tempting therefore to postulate Met A to be Met 47 from its similar pH dependence to Leu 45 and so Met B would be Met 28 with the speculation extended to suggest Trp A as Trp 25. The pH effects around 5.5 would then be understood as some exchange process involving residues 25 to 28 at least, with the effects on His 33, Tyr 70 mediated by their proximity to Trp A (?Trp 25). Trp B would then be assigned to Trp 61 in the sequence. There is little point in pursuing these suggested assignments for there is no evidence as yet to substantiate them, but they will form a useful hypothesis against which to test the results of future experiments.

Finally, a different type of protein cleavage is considered.

5.7 Cys 1-Cys 79 disulphide bond cleavage

This modification was achieved through selective reduction and carboxymethylation of the first disulphide linkage in the protein. The resulting spectrum has already been considered in section 4.2.10 when the second stage assignments of the tyrosine and histidine resonances were made. It was shown that the resonances of Tyr 2, His 3 and Leu 76 were markedly affected by the modification in accord with their position adjacent to this disulphide bond in the primary sequence. However, these effects could be distinguished because the remainder of the spectrum was remarkably unperturbed when compared with that of the native protein. This is in marked contrast to the effects of peptide chain cleavage at Met 47 considered in the previous section. However, although much of the structure is retained despite the disruption, the protein is, not surprisingly, less stable thermally as demonstrated by the spectra shown in Fig. 5.22. With only a 10°C increase in temperature to 47°C the spectrum indicates definite protein denaturation - the upfield shifted methyl resonances have almost disappeared as have the separate methionine methyl peaks and the aromatic region is almost completely that of a random coil protein. Such spectral changes are not observed for the native protein until the temperature is between 67 and 77°C (Fig. 3.31).

Further evidence for much of the protein structure remaining intact in the modified protein is provided by NOE experiments the results of some of these being included in Fig. 5.23. The NOE difference spectra of Figs. 5.23(b) and (c) can be compared directly with Figs. 3.26(b) and (c) for the native protein and are seen to be extremely similar. This confirms that the relative disposition of Trp B (R18) and Tyr 73 (R14,R6) are unaltered in the modified protein and forms a vital piece of evidence for the second stage assignment of resonances R14 and R6 to Tyr 73 discussed in section 4.2.10. Figure 5.23(d) confirms that the familiar result of the

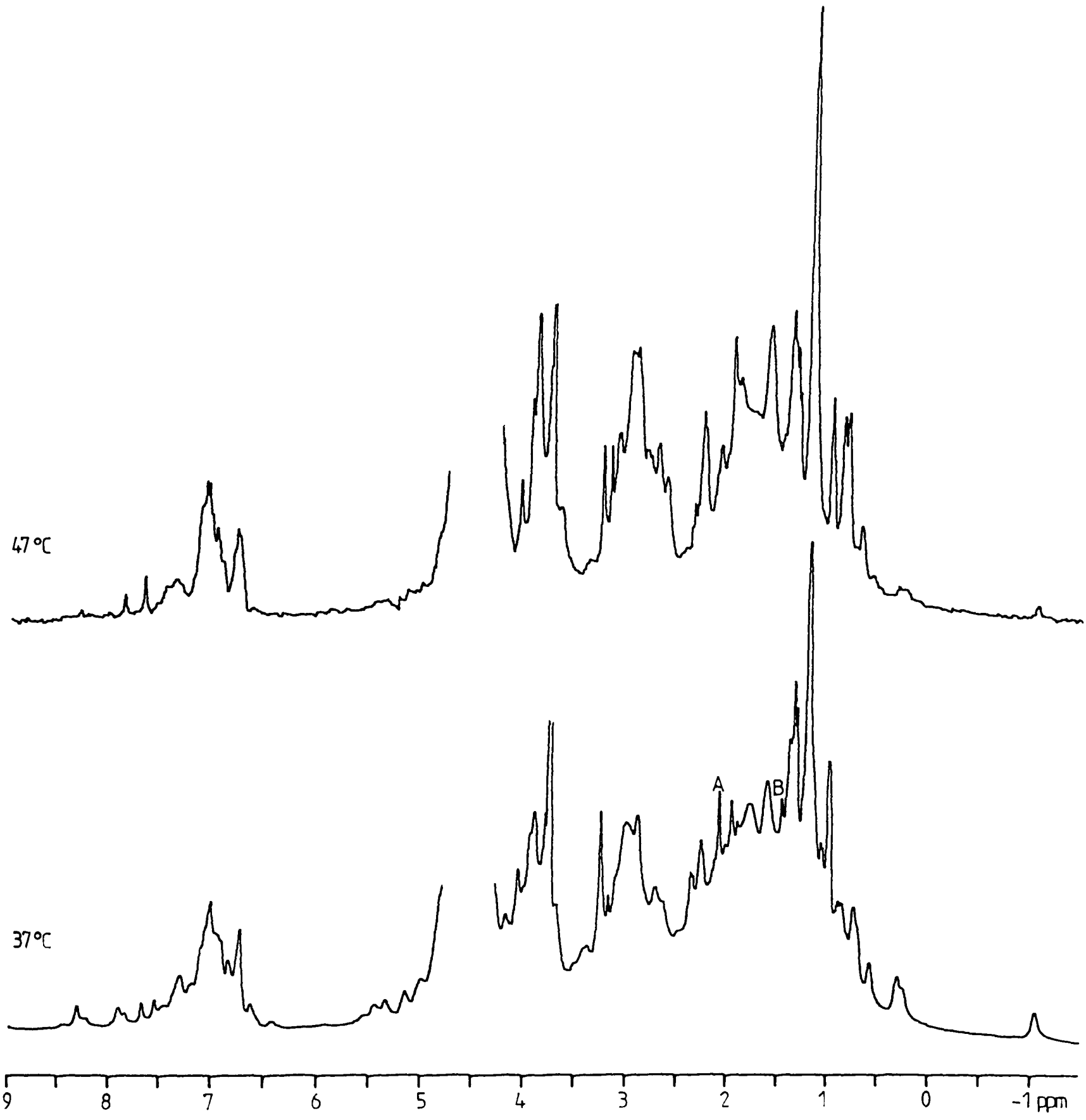

Fig. 5.22 Temperature dependence of the spectrum of the Cys 1-Cys 79 cleved kringle 4.

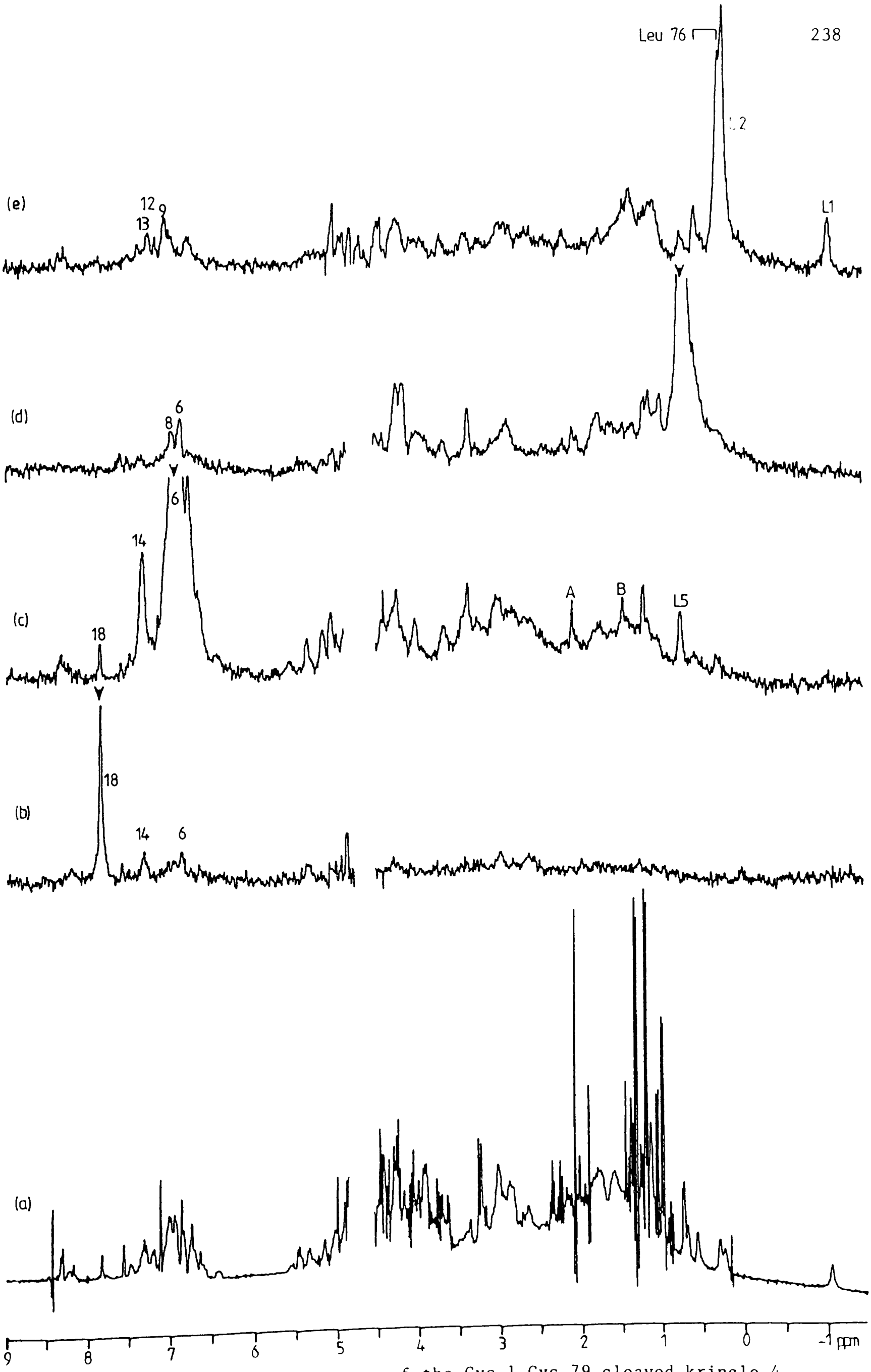

Fig. 5.23 NOE difference spectra of the Cys 1-Cys 79 cleaved kringle 4.
(a) Resolution enhanced spectrum.

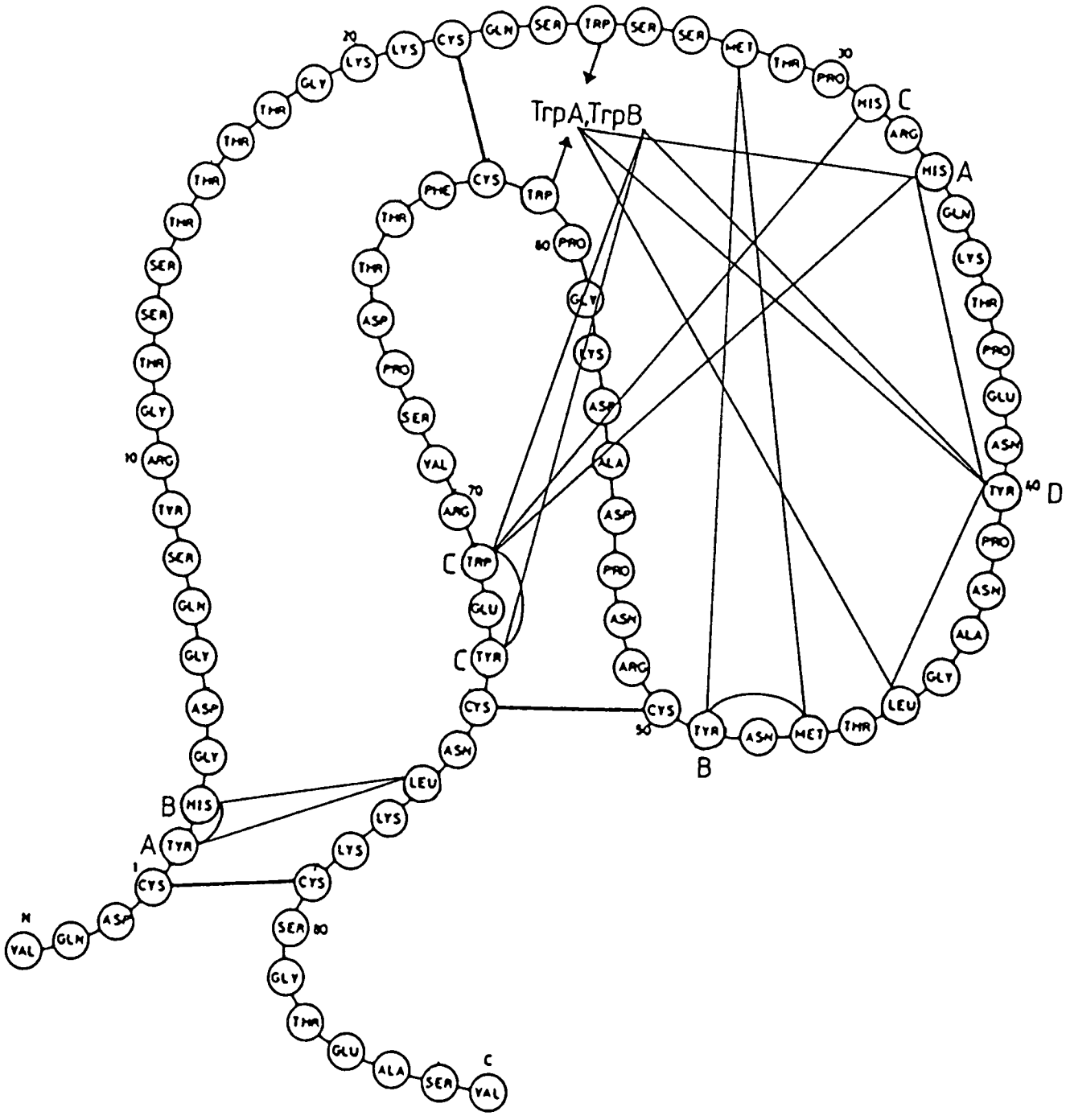

Fig. 4.7 Primary structure of kringle 4. Lines connect residues found to be close in space within the three dimensional structure (see text).

enhancement between L5 and resonances R6, R8 of Tyr 49 is unchanged. In Fig. 5.23(e) the pre-saturation pulse was centred on L2 and the usual enhancement of L1 was therefore obtained, but inevitably the adjacent methyl proton resonance was caught in the irradiation pulse bandwidth and demonstrates an enhancement of another three proton doublet peak. This confirms the assignment of the methyl group proton resonances of Leu 76 in the modified protein. In the same spectrum resonances R9, R13 of Tyr 40 and R12 of Trp A are also enhanced and this is very comparable to the analogous spectrum from the native protein shown in Fig. 3.24(c).

Thus, disruption of the first disulphide bond while causing a number of well defined changes in the spectrum leaves much of the remainder completely unchanged. This indicates that the structure of the protein involving the two short loops and the second long loop is very much intact although less thermally stable. Furthermore, despite the possibility of considerable structural change resulting from protein cleavage, observation of the spectrum of this particular protein would suggest the chances of it retaining affinity for lysine-Sepharose are high in view of the lack of perturbation of resonances from residues intimately related to the ligand binding site. Indeed, this is the case as was mentioned in section 5.2 and the cleaved protein not only binds to lysine-Sepharose but also to ligands in solution. Figure 5.24 shows the spectral effects of adding 6 amino-hexanoic acid to the protein and table 5.3 summarises the effects on resonances from residues of interest.

This table can be compared with the similar tables 4.3 and 4.4 for 6 aminohexanoic acid and AMBOC binding respectively to the native protein and the results will be seen to be extremely similar. One noticeable difference is perhaps the small shifts on the Leu 76 methyl proton resonances on ligand binding to the modified protein, but this is under-standable in that the protein structure has been destabilised by breaking

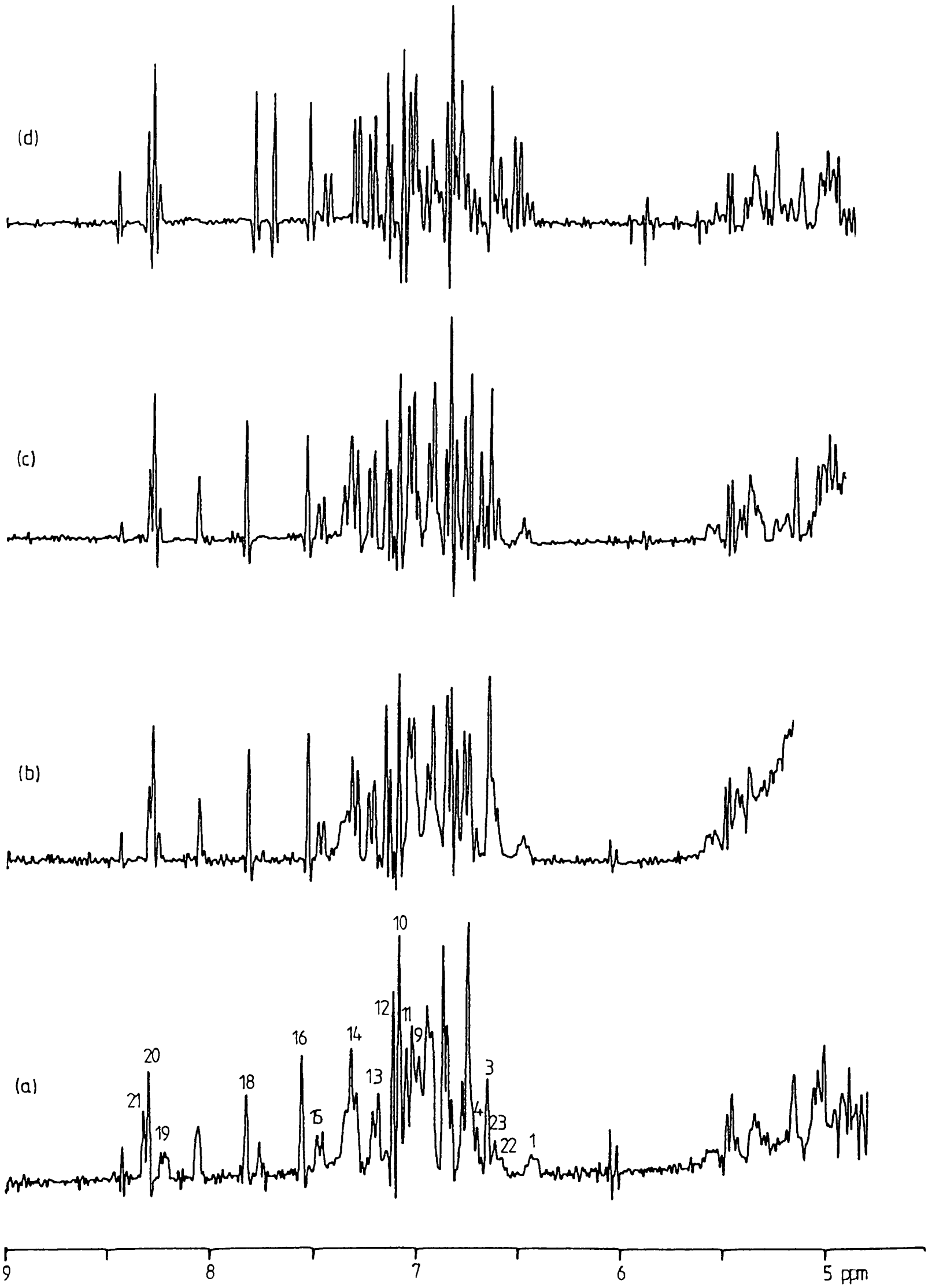

Fig. 5.24A Aromatic region of the spectrum; pH 7.4

$27^{o}C$ (a) Cys 1-Cys 79 cleaved kringle 4

(b) Cys 1-Cys 79 cleaved kringle in the presence of 6 amino-hexanoic acid.

$37^{o}C$ (c) same sample as (b)

(d) Native kringle 4.

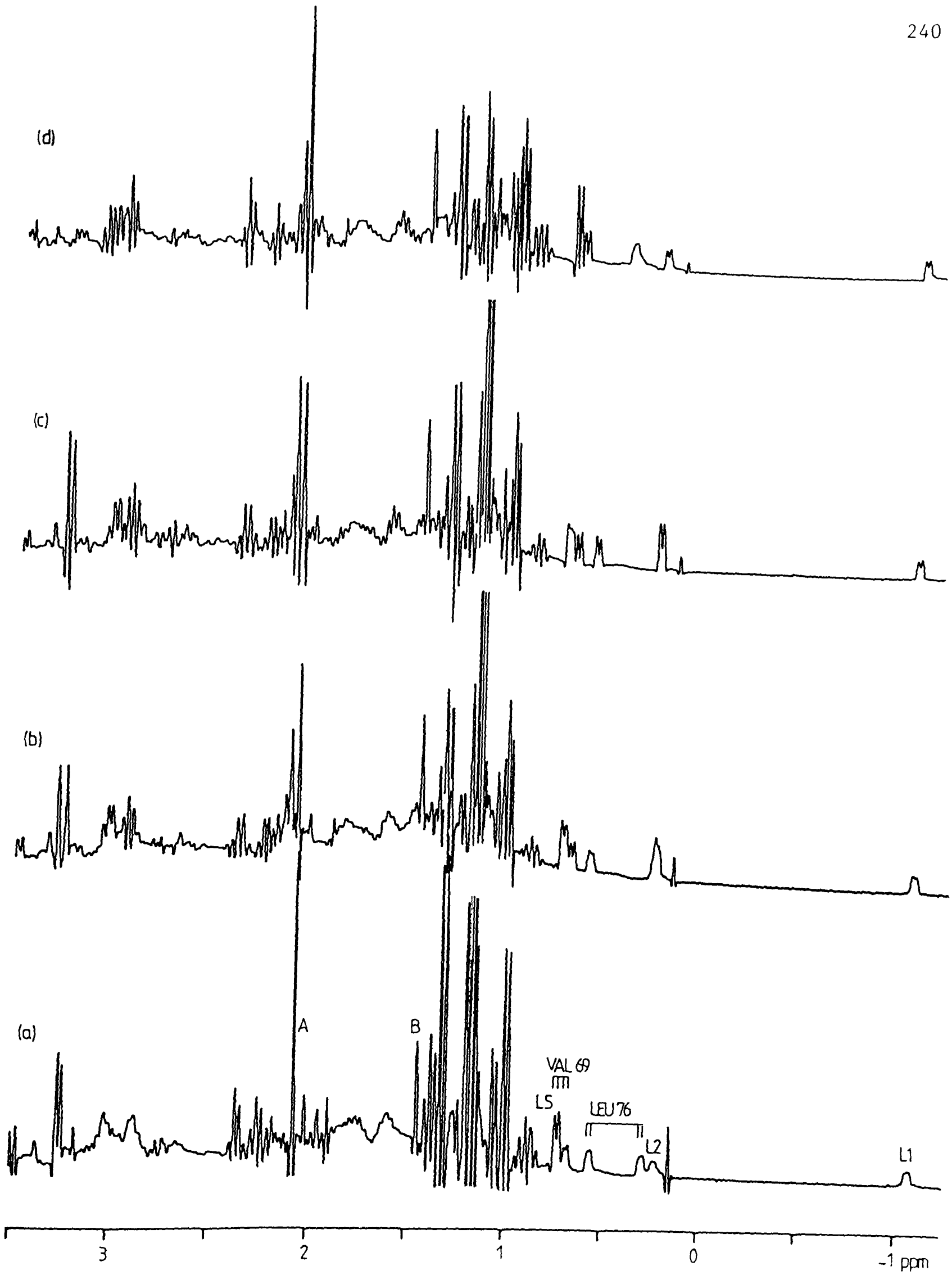

Fig. 5.24B Aliphatic region of the spectrum; pH 7.4

$27^{o}C$ (a) Cys 1-Cys 79 cleaved kringle 4
(b) Cys 1-Cys 79 cleaved kringle in the presence of 6 aminohexanoic acid.

$37^{o}C$ (c) Same sample as (b)
(d) Native kringle 4.

Table 5.3 Summary of the Assigned Resonances and Residues that are affected or not by the Binding of 6 Aminohexanoic Acid to the Cys 1 - Cys 79 cleaved Kringle 4.

	ALTERED	UNALTERED
AROMATICS	Trp A (R1,R12,R15,R19)	
	Trp B (R18,R22)	
	Trp 71 (R11)	
	His 31 (R21,R16)	His 3 (R10)
	His 33 (R20,R7)	
	Tyr 40 (R9,R13)	Tyr 73 (R14)
ALIPHATICS	Leu 45 (L1,L2)	
	Leu 76	
		L5
		Val 69
		Met A
		Met B

the disulphide bridge and would therefore be expected to show more flexibility to perturbations of its structure, even if these are only slight on ligand binding. However, comparison of the modified protein with the native spectrum at the same temperature and pH in Figures 5.24(c) and (d) shows that the ligand induced changes in the modified protein are also of comparable magnitude to those occurring in the native sample. This provides excellent confirmation for the notion that ligand binding causes minimal structural alteration and rather that the protein is folded in such a way as to provide a specifically constructed binding site. Previously we noted the large intensity at the threonine methyl proton random chemical shift value in the modified protein ("truncated" in Fig. 5.24) to be indicative of most of the length of the first long loop of the protein being free in solution; no longer intimately associated with the rest of the protein. (Five of the eleven threonine residues being located in this part of the molecule). Thus, this provides good support for the proposition that this loop of the protein between the first and second disulphide bridges has little or no part to play in the formation of the ligand binding site which was also suggested in section 5.2 from other protein modification studies.

The study of chemically modified derivatives of kringle 4 has thus provided information for resonance assignments as well as very useful data on the protein structure, its stability and aspects of the ligand binding site. This concludes the presentation and discussion of experimental data for kringle 4 of human plasminogen. However, before considering work on the kringle structure present in prothrombin fragment 2 we conclude this chapter by discussing the possibilities for model building and refining the structure in the light of the data that has been presented.

5.8 Model Building

Section 4.2 concluded with a preliminary structural model incorporating data presented upto that point and depicted in Fig. 4.7 which has been included in this chapter for reference. Succeding sections have confirmed and amplified much of the data summarised in Fig. 4.7 and the lanthanide ion studies were of particular importance with regard to defining the ligand binding site. The situation has now been attained for model building of the structure to be a viable proposition not requiring an excessive number of assumptions or theoretical computations based on sequence analysis. (The latter possibility will be discussed in the next section). In the first instance, the extent of the model building has been limited to inclusion of only the two short loops and the right hand long loop of the kringle sequence, incorporating the second and third disulphide bridges. The aim has been to find a configuration of the residues assigned in the spectrum that fits as much of the data previously described as possible. Thus, using the Nicholson molecular models the peptide backbone was constructed with the L form of the amino acid side chains concerned and the two disulphide bridges formed. The problem then was to find a satisfactory fold. Photographs of the model structure postulated at the time of writing are shown in Figures 5.25 and 5.29. It must be emphasised though, that it is not offered as a final definitive form but rather as a preliminary working hypothesis that can be altered to varying extents as demanded by further interpretation of data already obtained and in the light of future experiments. The reasoning behind the model structure being as shown will be described with the aid of the photographs.

As discussed already certain structural features that had been elucidated, immediately provided considerable constaints on further possible conformations. One such was the requirement of the proximity of Leu 45, Tyr 40 and Trp A, and here the first assumption was made namely

Key to the colours of the model atoms

White - peptide backbone

Purple - aromatic residues

Yellow - sulphur atoms

Red - carboxyl groups, hydroxyl groups

Blue - amino groups

Grey - methyl groups

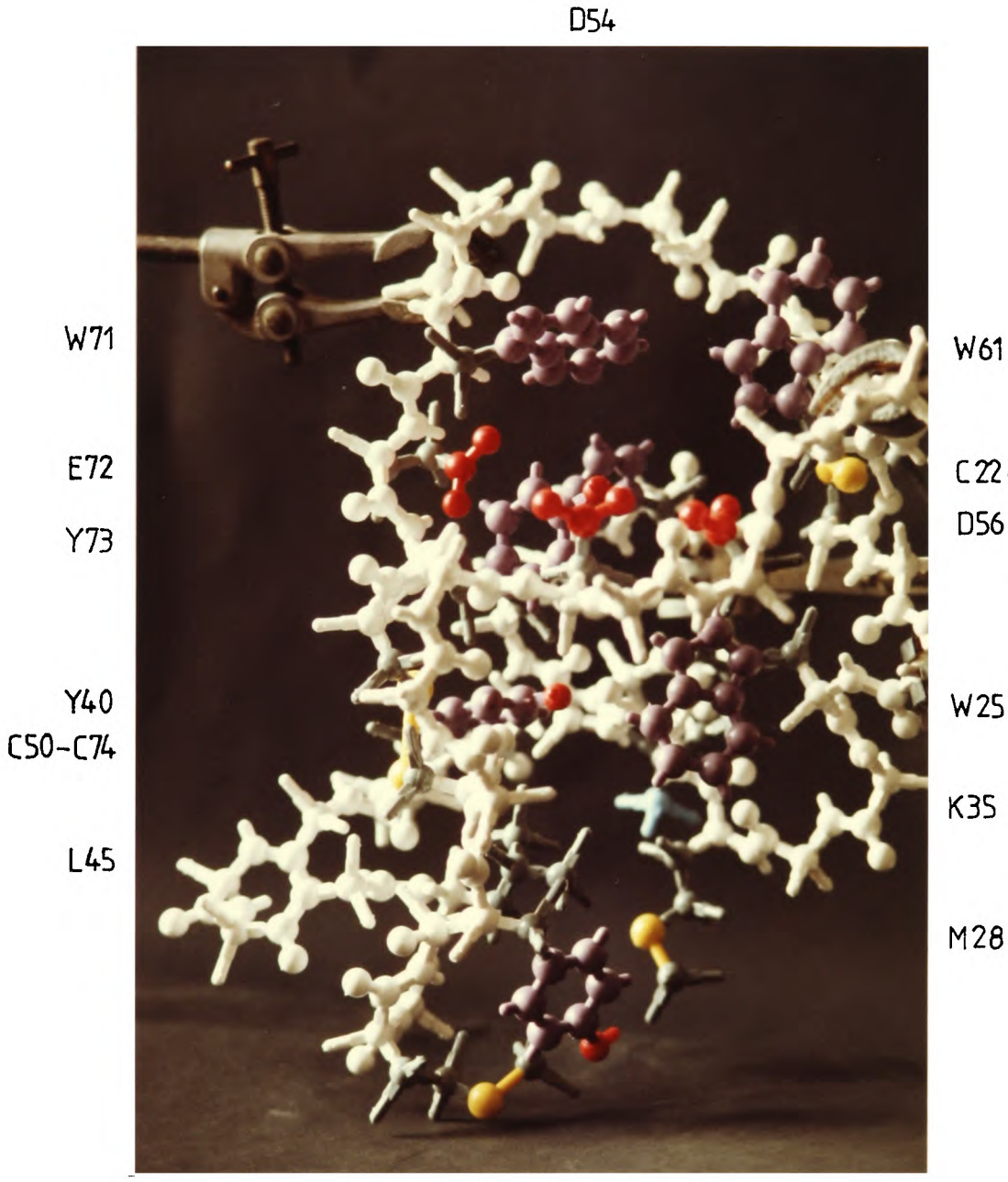

Fig. 5.25 Photograph of what is arbitrarily taken as the "front" of the molecule for reference of the other photographs. An enlarged copy was shown in Fig. 1.4.

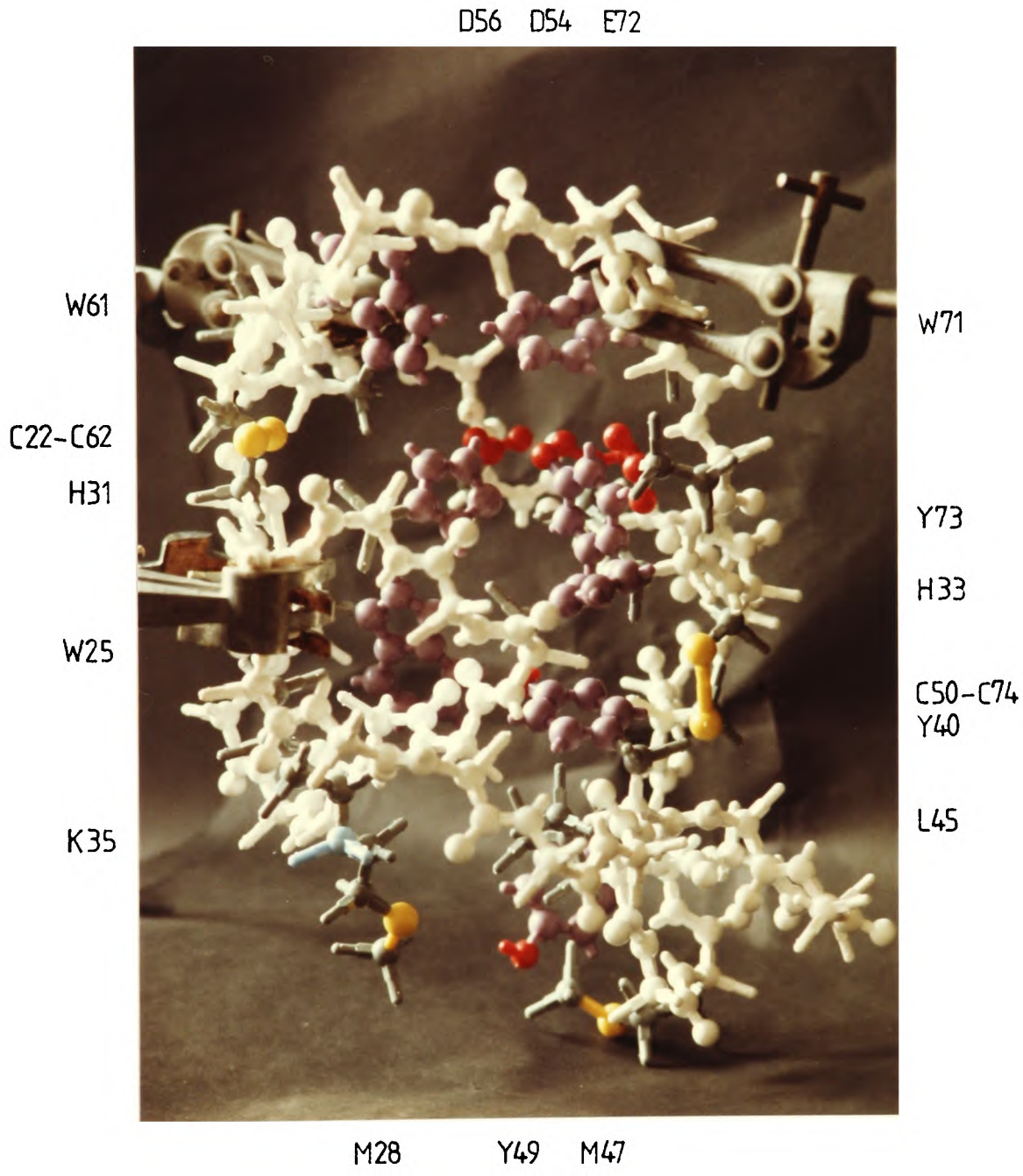

Fig. 5.26 The back of the molecule. An enlarged copy was shown in Fig. 1.5.

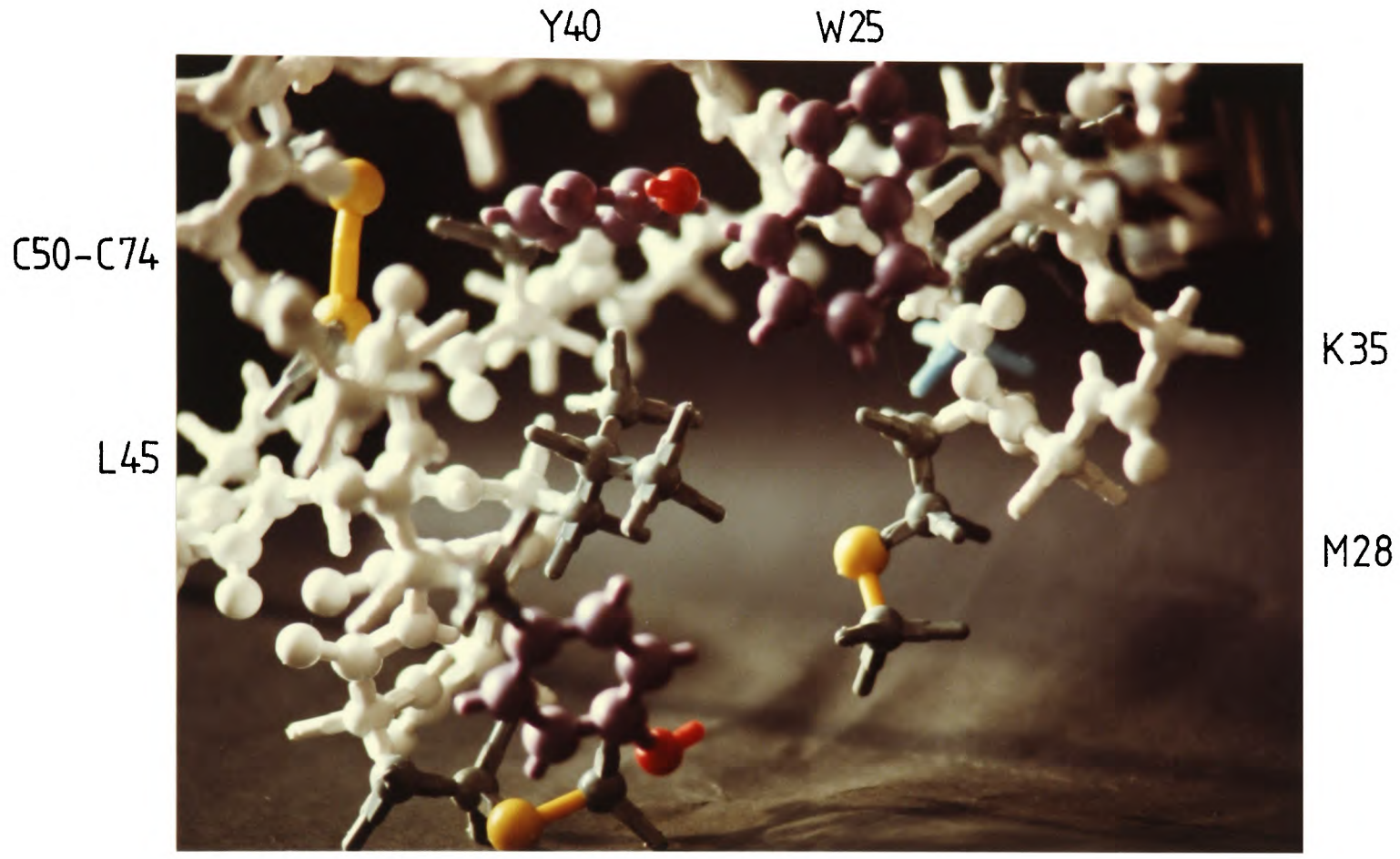

Fig. 5.27 Close-up of the bottom of the molecule from the front.

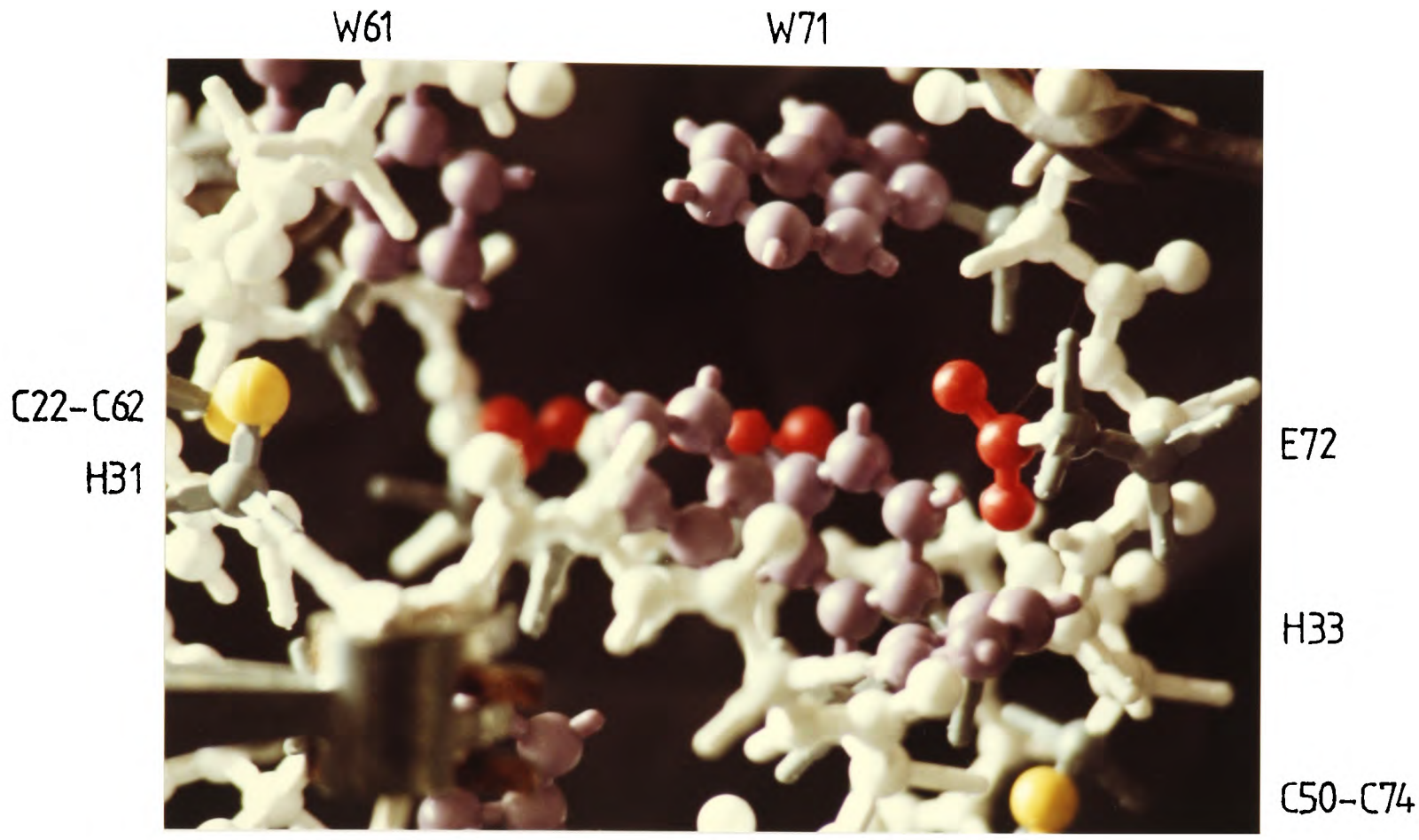

Fig. 5.28 Close-up of the middle of the molecule from the back.

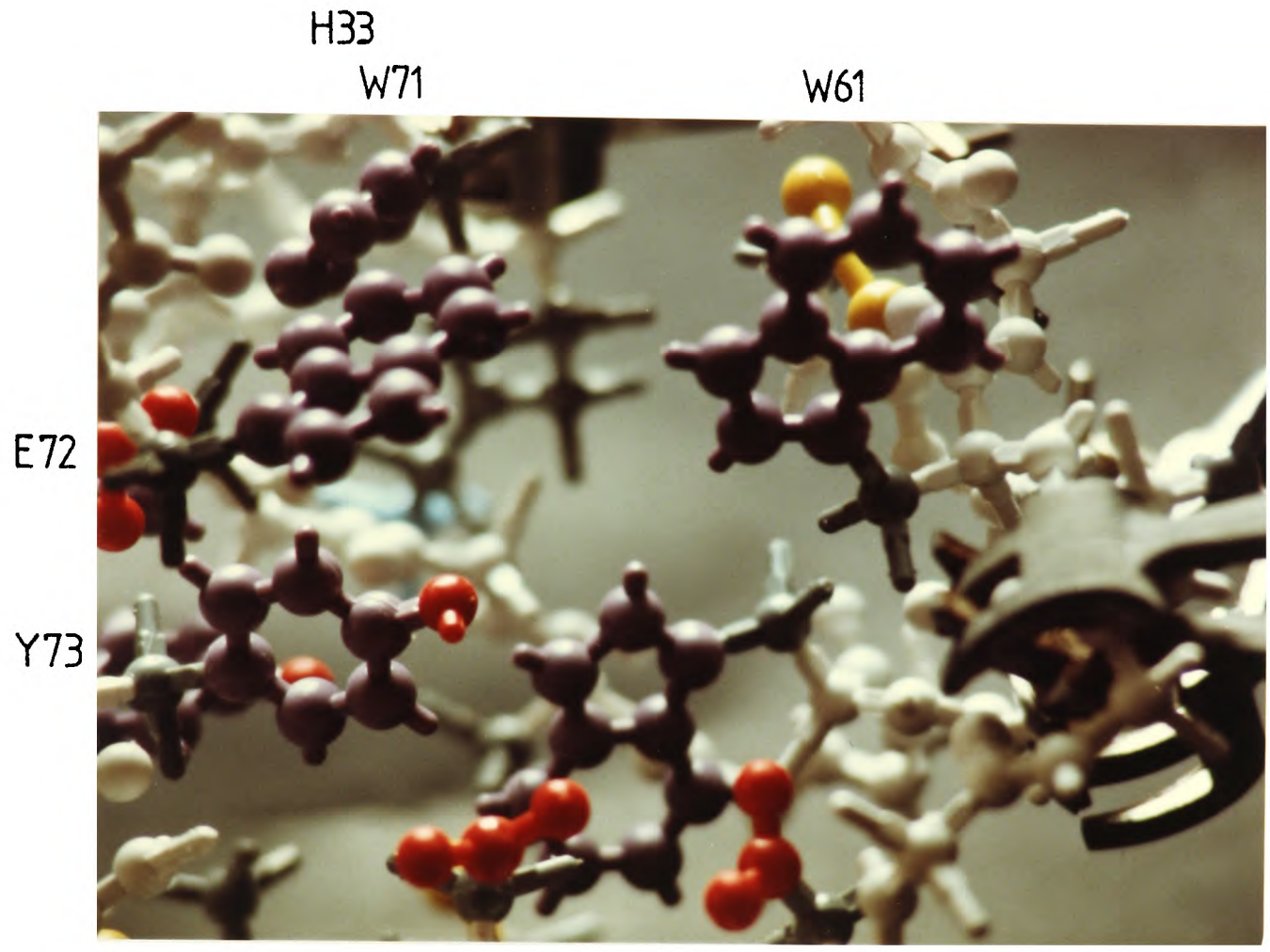

Fig. 5.29 Close-up of the middle of the molecule from the front and viewing from above into the centre of the molecule.

to assign Trp A to Trp 25 as has been suggested as reasonable on two occassions in the text. (From this Trp B being taken as Trp 61 follows). This required arrangement of residues as shown in close up in Fig. 5.27, and indeed it is not difficult to place the methyl groups of Leu 45 in satisfactory positions relative to the aromatic rings to account for the upfield secondary shifts and the differing NOE results described in Chapter 3. Rough proximity of Tyr 40 to Lys 35 (blue amino group) can also be seen in this photograph, the gap certainly being bridgeable by an aromatic ring as indicated by the formation of the Tyr 40 - Lys 35 crosslinked kringle 4 described in this chapter. Bearing that in mind, some of the effects described as a result of the modification such as the change in the Leu 45 resonances become understandable. Furthermore, Fig. 5.26 showing the back of the molecule, reveals the charged residue Lys 35 to be on the surface although this does not necessarily have to be the case, (and it must be remembered that one loop of the protein has not been included in the model). Finally, in Fig. 5.27 it is clearly seen that the two methionine residues and Tyr 49 are all clustered in space as suggested by the results of NOE experiments.

Considering now the histidine residues, these were required to be close in space to Trp 71. In addition His 33 had to interact with a carboxyl group and the second assumption made was that this was the carboxyl group of Glu 72. Data in support of this can be given as follows. The resonances of His 33 were relatively unperturbed by disruption of the Cys 1 - Cys 79 disulphide bridge and so only carboxyl groups after the second link in the sequence need be considered. Glu 38 was relatively unlikely in view of the required proximity of His 33 and Trp 71 and indeed in the model Glu 38 like Lys 35 would be on the surface. The only remaining possibilities were Asp 54, 56 and Glu 72. Asp 56 was dismissed as Trexler et al., (1982) found it could be readily modified and was

essential for ligand binding which was incompatible with the behaviour of a carboxyl group interacting with His 33 from the NMR effects observed on ligand binding. Then, out of Asp 54 and Glu 72 the latter was a more natural choice from the constraints of the model. This spatial disposition of the histidines around Trp 71 and the proximity of His 33 to Glu 72 are shown in the close up of Fig. 5.28 from the back of the molecule (His 33 is seen on edge view).

Finally, the ligand amino group binding site must be contained in this part of the molecule being modelled. Asp 56 has already been implicated and Asp 54 is seen in Fig. 5.29 to be very close in space. Furthermore, the results of the lanthanide ion binding studies served also to delineate the residues in close proximity - namely Trp 71 and Trp B (61), again as seen in Figures 5.29 and 5.25. One curious feature was demonstrated by the model. Tyr 73 and the C2 proton of Trp B (61) are linked by strong NOE's and this was recognised by the proximity of Tyr 73 to Trp 61 in the model. However, although the C2 proton resonance of Trp B is dramatically affected by paramagnetic lanthanide ion binding, the peaks of Tyr 73 receive minimal effects. The only explanation offered for this is that Tyr 73 may lie on the edge of the shift cone of the lanthanide ion as depicted in Fig. 4.35. Certainly such a cone can be envisaged for a metal ion bound to the Asp 54/56 region that would give shifts in opposite directions for Trp 61 on the one hand and Trp 71, Val 69 on the other. From Fig. 5.25 it is seen that the methionines and Tyr 49 are well removed from the lanthanide ion binding site, but with the possibility that Met B (? Met 28) is close to the second metal ion binding site, near the first disulphide bridge which is not included in the model.

Obviously, all the data of the previous three chapters could be discussed in the light of the implications of the model but this would be inappropriate at this stage. Much of it has already been included in the

discussion above, both in regard to the salient findings as well as some subtle effects. Furthermore, NMR studies of some proteins for which highly resolved X-ray crystal structures are available have not been found to agree on precisely every point. Nevertheless, this preliminary model can provide reasonable scenarios to explain some of the more detailed results such as the differential broadening of the Trp A, His 33, Met B and Tyr 40 resonances on lowering the pH, in terms of the relative loosening of part of the structure.

Data analysis using this model has not proceeded to any great extent as yet. For instance, the possible assignment of the threonine residue giving the methyl proton resonance at L5 has not been considered and other such predictions should follow. Observation of the strucure as a whole in Figures 5.25 and 5.26 confirms the protein to have a hydrophobic core with the majority of aromatic residues clustered in the centre and the ligand amino group binding site amongst them. This feature was not deliberately contrived but simply resulted out of the folding process described above, and having handled the unfolded molecular model, this would not have been an inevitable consequence of any arbitary folding process! However, clearly there is a substantial scope for refining the details of this proposed structure and some of the possibilities for doing this are now discussed.

5.9 Structural Refinement

One of the most obvious things to do would be to try and incorporate details of secondary protein structure into the model as predicted by various theoretical treatments and this has indeed been considered. Using computer programmes developed by Dr. M.J. Sternberg the methods of Chou and Fasman (1978) and Robson et al., (1978) for predicting protein secondary structure have been applied to the kringle 4 sequence. However, it was

found that both methods indicated minimal amounts of defined secondary strucural elements to be present. This conclusion was also obtained by Llinás et al., (1983). Some β turns are undoubtedly present but no attempt has been made to incorporate any into the model.

The prospects of fitting lanthanide ion shift and relaxation probe data to a model with effective axial symmetry were seen to be promising from the results presented in Chapter 4. This model immediately provides a basis for this procedure, although X-ray crystal structures usually supply the molecular framework for such studies (see Cassels, 1979 for instance for an example using lysozyme). Much of the NMR data that has been presented is of the detail obtained on proteins for which a good crystal structure is available. In these cases calculations can be performed to compare experimental with theoretically derived secondary shifts of resonances based on the crystal structure (Perkins, 1982). An extension of this procedure has been the use of experimentally derived secondary shifts to refine crystal structures as carried out on proteins carrying antibody combining sites (Leatherbarrow, 1983). However, we have been investigating the possibilty of obtaining detailed information on the relative orientation of aromatic rings solely from experimentally derived secondary shift values.

In conjunction with Dr. R. Leatherbarrow a computer programme has been devised to fit a set of secondary shifts using standard ring current calculation theory. The initial aim has been to fit the secondary shifts derived for Trp A and given in Table 3.2 as resulting from the influence of another tryptophan ring assumed to be Trp B. This is somewhat artificial in that most secondary shifts are found to arise from the effects of more than one other aromatic ring current in proteins where a good crystal structure is available. However, the largest effects usually predominate from only one ring and the aim of this study is to see how good a fit can

be achieved for what are some quite remarkable secondary shifts of tryptophan resonances. Initially the secondary shifts of the C4 - C7 protons of Trp A have been fitted and the programme has generated a considerable number of orientations of the Trp A ring relative to Trp B that give rise to theoretical secondary shifts within the experimental error of the actual values. Analysis of these solutions has not been pursued systematically as yet but a typical result is shown in Fig. 5.30. Using the coordinates of the relative orientation of the two rings in Fig. 5.30, the theoretical secondary shifts on the Trp B resonances due to proximity to Trp A have been calculated and both sets of data are shown in Table 5.4 compared to the experimental values. It can be seen that although the values calculated for Trp B are not such a good fit they are at least all of the right sign, and it must be stressed that this particular solution was chosen almost at random from a very large number of families of possible computer generated fits.

Precise details of the methods involved in this computer fitting programme have not been included as the procedure has not been used extensively as yet. However, such an approach demonstrates the possibility of being able to refine parts of the predicted structure to an accuracy comparable to that achieved by the best resolved X-ray crystal structure. Some reasons for initially chosing to investigate the interaction of Trp A and Trp B (Trps 25 and 61) are outlined in section 6.2.2, but it can be seen in Fig. 5.29 that the model structure will allow these two residues to approach quite closely and they have been implicated in the studies described so far, and from further data discussed in the next chapter, to be part of a conserved structural element of kringles. In actual fact the perspective of Fig. 5.29 is such that Trp 25 and Trp 61 appear closer than they are in the model, as can be seen from Fig. 5.25 for instance. However, a relative orientation of the two rings according to Fig. 5.30

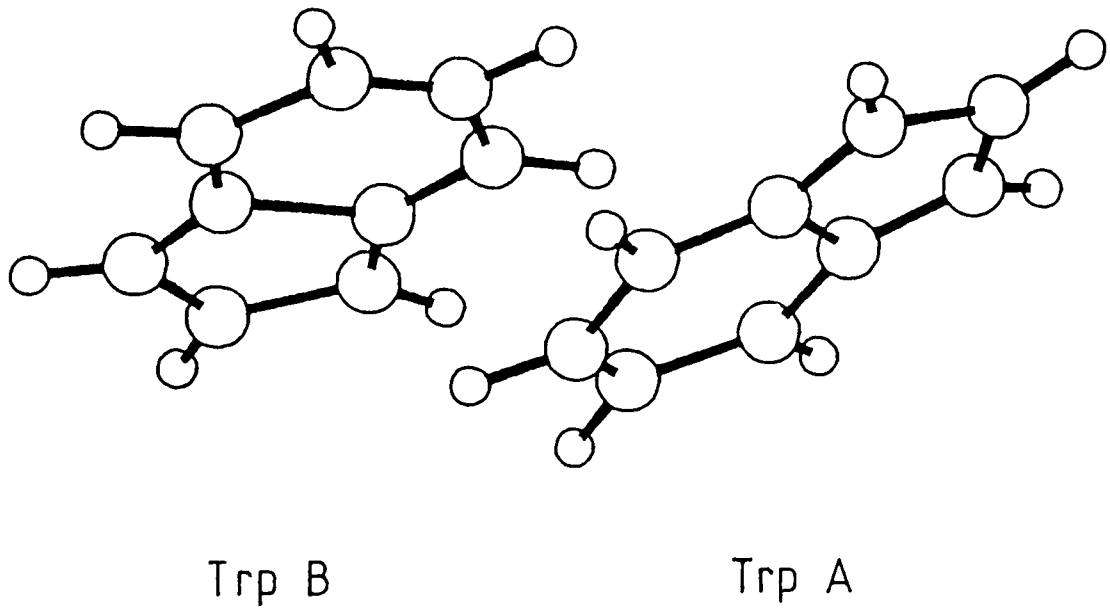

Fig. 5.30 Diagram to show the relative orientation of the two indole rings calculated as a fit of the experimental secondary shifts on Trp A due to proximity to Trp B (see text).

Table 5.4 Comparison of secondary shifts on indole ring resonances between experimental values and those for the computer calculated relative orientation of the Trp A and Trp B rings of kringle 4 shown in Fig. 5.30 (see text). (+ve is a downfield shift; -ve upfield).

		Indole Ring Proton Secondary Shifts - ppm			
		C4	C5	C6	C7
Trp A	Experimental	+0.57	-0.73	-2.29	-0.07
	Computer Fit	+0.32	-0.70	-2.42	-0.03
Trp B	Experimental	-0.69	-2.33	-0.67	-0.56
	Computer Fit	-2.8	-2.7	-0.14	-0.02

can be readily achieved without altering the model to any great extent.

All of this looks promising in terms of producing a useful and accurate model of a good part of the structure of kringle 4 solely from NMR data and without recourse to an X-ray crystal structure. Data for kringle 4 is used in the next chapter for comparison and aid in the analysis of spectral features of prothrombin fragment 2 which contains another kringle structure.

CHAPTER 6

NMR STUDIES OF PROTHROMBIN FRAGMENT 2

6.1 Introduction

As mentioned in Chapter 1, the blood clotting protein, prothrombin, contains two kringle structures in the non-enzymatic, "pro" part of the molecule. These can be prepared individually incorporated into parts of the molecule obtained by limited enzymatic cleavage. In this chapter the kringle contained in the portion designated Fragment 2 is considered. This protein consists of 118 residues which is 30 more residues than in the kringle 4 containing fragment of human plasminogen and the higher molecular weight partially accounts for the poorer NMR spectrum obtained for this protein when compared with that of kringle 4. The additional residues are roughly distributed either side of the kringle sequence within the molecule. The bovine protein will be considered in most detail and the amino acid sequence is shown in Fig. 6.1. The aim of this chapter is to consider aspects of the kringle strucure of fragment 2 as revealed through study of its NMR spectrum and to compare the findings with those discussed in the previous chapters for kringle 4. Consequently, only the experiments using fragment 2 relevant to this purpose, will be included in what follows.

Figure 6.2 shows the amino acids within the kringle structure that are common to both bovine fragment 2 and kringle 4. They amount to 31 of the total 79 residues and Fig. 1.3 showed that 18 of them are common to all the kringles sequenced so far. A number of altered residues are nevertheless of similar chemical nature, for instance Tyr 40, Tyr 49, Phe 63, Trp 71 in kringle 4 are Phe 39, Phe 49, Tyr 63 and Phe 71 in fragment 2. Table 6.1 lists the composition of fragment 2. Of particular note is the absence of methionine and histidine residues from the sequence. These side chains, giving rise to singlet resonances in the NMR spectrum, are usually readily

Fig. 6.1 Amino acid sequence of bovine prothrombin fragment 2. (Magnusson et al., 1975)

Table 6.1 Composition of Bovine Prothrombin Fragment 2.

Ala 10	Glu 11	Pro 9
Arg 8	Gly 12	Ser 3
Asn 5	Ile 1	Thr 5
Asp 13	Leu 9	Trp 2
Cys 6	Lys 2	Tyr 4
Gln 4	Phe 3	Val 5

Total number of residues is 118.

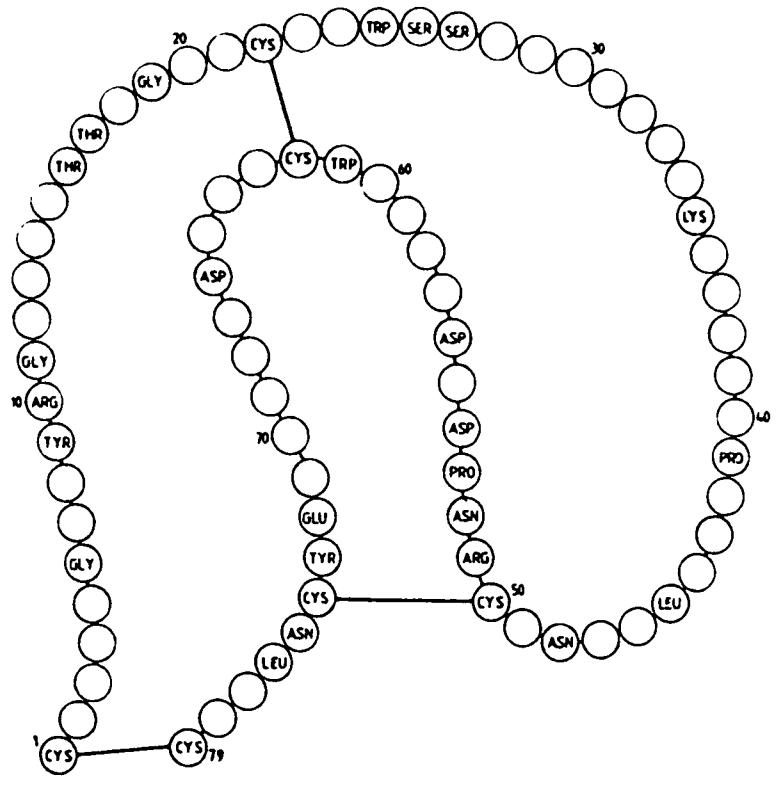

Fig. 6.2 Amino acids common to the sequences of kringle 4 of human plasminogen and of bovine prothrombin fragment 2.

identified as was seen for kringle 4, but no such useful reporter groups are available in the study of fragment 2.

The aliphatic region of the spectrum of bovine prothrombin fragment 2 was briefly considered in Fig. 3.19(c) when the upfield shifted methyl proton resonance, L1 was shown to be present and assigned on homology arguments to the Leu 45 common to all kringles. The complete spectrum of fragment 2 is shown in Fig. 6.3 obtained shortly after dissolving the protein in D_2O, and some hours later showing the loss of the labile proton resonances.

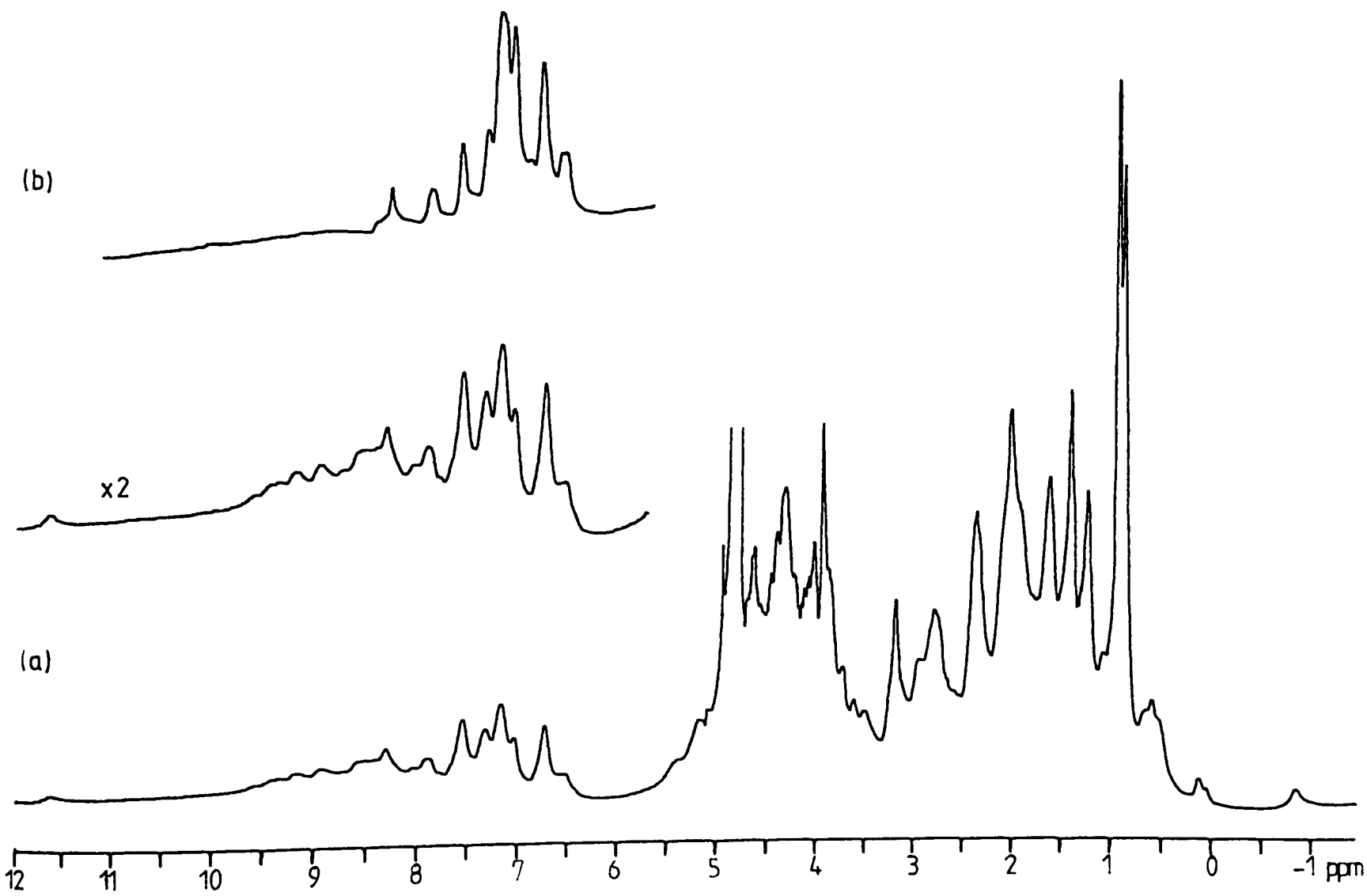

Fig. 6.3 Bovine prothrombin fragment 2; 27°C, pH 8.7 (a) shortly after dissolving in D_2O (b) similar sample some hours later.

Again no formal studies have been made of the labile proton exchange rates for solvent deuterons but practical experience suggests that they are comparable with those of native kringle 4. However, the presence of those resonances does indicate that certain parts of the molecule have restricted access to solvent molecules. This, along with the wide dispersion of resonances from the upfield shifted methyl proton peaks to the aromatic region with many secondary shifted resonances shows fragment 2, like kringle 4, to have a specific tertiary fold. It is tacitly assumed that the fold will primarily involve the residues of the kringle portion of fragment 2 with little structure expected for the extended extra kringle regions of the sequence. In actual fact this assumption makes little difference to the discussion which follows, but is probably the case especially for the C terminal end of the molecule which contains a very high proportion of charged, hydrophilic residues. Furthermore, the presence of the L1 resonance in the spectrum from Leu 45 and the labile proton resonance at 11.6 ppm assigned to Trp A in kringle 4 (shown below to be the case also for fragment 2) confirm that folded regions of the molecule do include residues contained within the kringle part of the protein.

As with all protein NMR studies significant progress requires assignments of resonances to individual protons within the molecule, and again the aromatic region of the spectrum will be concentrated upon. This is not just because there are fewer and more readily resolved resonances in this part of the spectrum, but also as the aromatic side chains are all found in the kringle region of the sequence and well distributed along its length, they act as monitors of the various parts of the structure. In addition, comparison of Fig. 6.4 showing the disposition of the aromatic residues in fragment 2 with the analogous diagram for kringle 4 (Fig. 3.2) reveals conserved aromatic residues at positions 9, 25, 61 and 73, with conservative substitutions at 39, 49, 63 and 71. The main differences

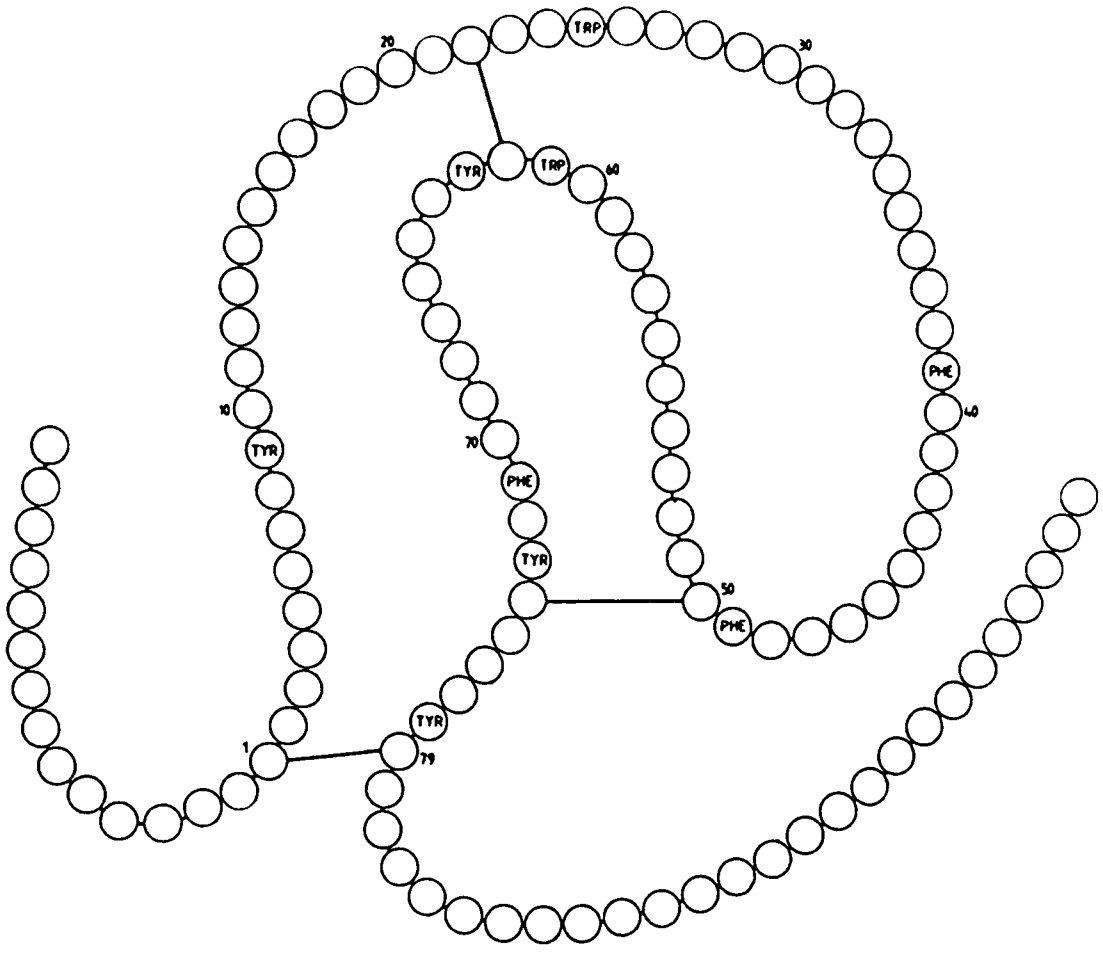

Fig. 6.4 Positions of the aromatic residues of bovine prothrombin fragment 2 in the amino acid sequence.

Table 6.2 Origin of the expected multiplets in the aromatic region of the NMR spectrum of bovine fragment 2.

RESIDUE	SINGLETS	DOUBLETS		TRIPLETS	
		One proton	Two proton	One proton	Two proton
2 Tryptophans	2	4		4	
3 Phenylalanine			3	3	3
4 Tyrosines			8		
TOTAL	2	4	11	7	3

Total Number of Protons is 41.

then being Tyr 78 in fragment 2 instead of Tyr 2 in kringle 4 and the lack of any histidine residues in the former protein. Thus, consideration solely of the aromatic residues of fragment 2 would be of considerable benefit in the intention of comparing the kringle structures of the two proteins.

6.2 Aromatic Region of the Spectrum

The process of assigning the resonances in the spectrum will be carried out in a similar way to that employed for the kringle 4 spectrum, and thus begins with consideration of the number and types of multiplets expected for the constituent residues. This is shown in Table 6.2 and assumes that the phenylalanine and tyrosine side chains are free to rotate about their Cβ - Cγ bonds. Multiplet selection spectra are shown in Fig. 6.5 and resonances are labelled but with no correlation to the numbering used for kringle 4 resonances. To avoid confusion, fragment 2 aromatic resonances will be referred to in the text with the prefix "R" coming after the number. Unfortunately, the higher molecular weight of fragment 2 leads to shorter relaxation times and poorer multiplet selection spectra than obtained for kringle 4 (Fig. 3.3). However, clearly resolved in Fig. 6.5(c) are the two trytophan singlets, 8R and 15R. 13R is seen to be a one proton triplet resonance and two proton triplet intensity occurs at 4R, 11R and 12R. Doublet proton intensity is indicated in Fig. 6.5(d) to be present at 1R, 4R, 6R and 9R, although the intensity at 1R is somewhat reduced for what would appear from the normal and resolution enhanced spectra to be a two proton doublet. In addition, 14R appears from the normal spectrum to be a one proton doublet resonance. The variable intensities of the doublet resonances in Fig. 6.5(d) arises from the aromatic residues having different local side chain mobilities in the protein structure. (The very sharp doublet peak between 4R and 5R is due

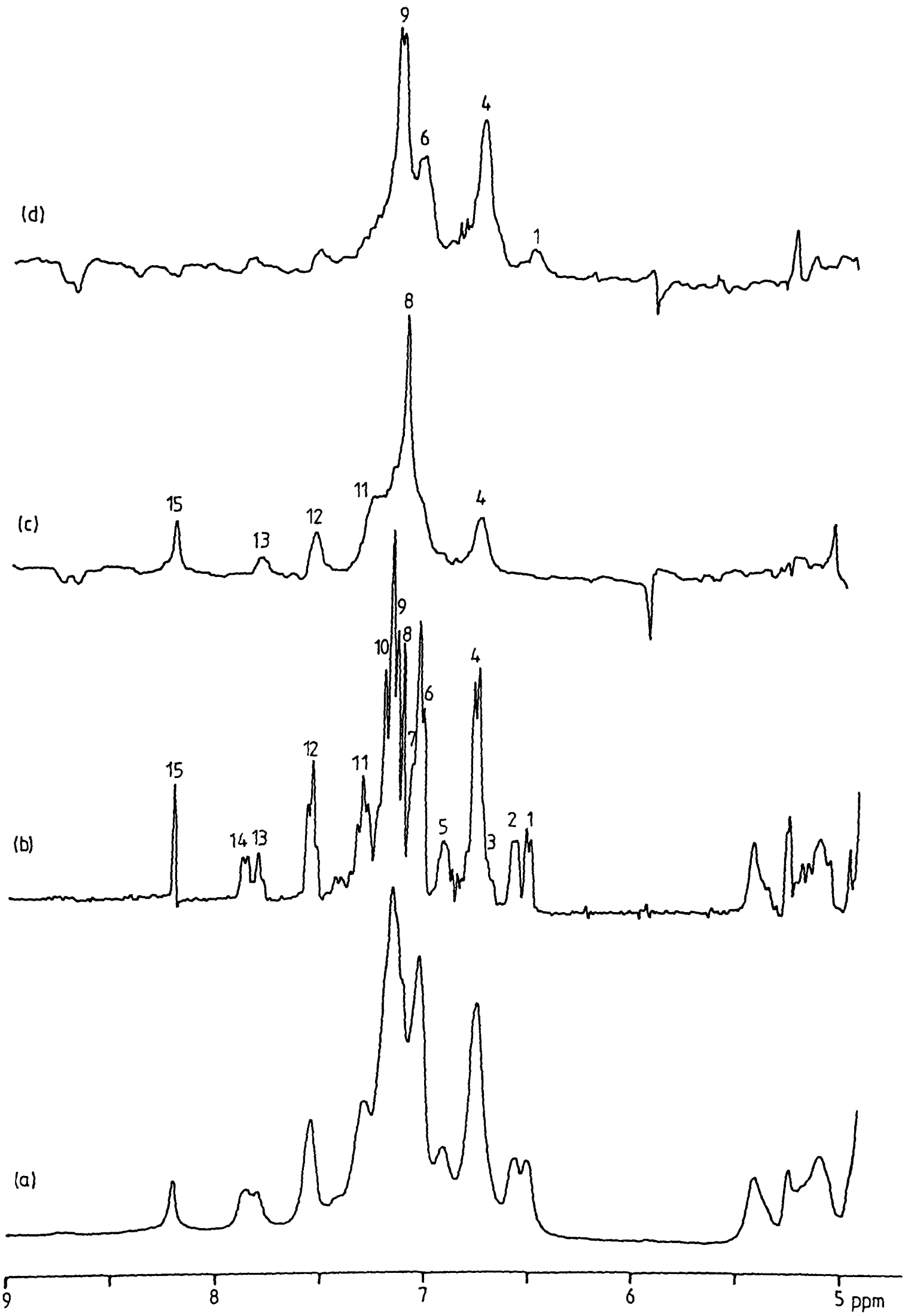

Fig. 6.5 Aromatic region of the spectrum of bovine fragment 2, 37°C, pH 8.7. (a) Normal (b) Resolution enhanced spectrum (c) Odd multiplet selection (d) Even multiplet selection.

to an impurity not seen in the rest of the spectra shown in this chapter).

The presence of unassigned phenylalanine intensity in the spectrum can cause confusion in the assignment of resonances to tyrosine and tryptophan side chains because as seen in Table 6.2, phenylalanine residues give rise to types of multiplet expected for both of the others. If the phenylalanine ring is immobilised then the possibility for confusion with tryptophan resonances is even greater and considerable care was taken to avoid this in the spectral assignment process of kringle 4. Thus, we begin the detailed assignment of the spectrum with the resonances of the three phenylalanine rings.

6.2.1 Phenylalanines

12R was seen in the last section to be a two proton triplet and Fig. 6.6(b) shows that a spin decoupling pulse sited at the one proton triplet peak 13R results in 12R collapsing to a doublet. Performing this experiment in reverse in Fig. 6.6(c) leads to 13R becoming a singlet resonance and the assignment of a pair of phenylalanine meta protons to 12R and the para proton to 13R, being made. Figure 6.6(c) also shows a spectral change around 9R and irradiating at this position results once again in 12R collapsing to a doublet, confirming the ortho protons resonance for this residue to be at 9R which is also compatible with the position of doublet proton intensity indicated in Fig. 6.5(d). Thus, the complete assignment of the aromatic proton intensity of one of the three phenylalanine residues of fragment 2 is elucidated.

Another well resolved two proton triplet resonance most likely assigned to phenylalanine meta protons was indicated above to be 11R. Figure 6.7(b) shows that a spin decoupling pulse at this position causes a significant spectral change at 6R and irradiating at the latter position

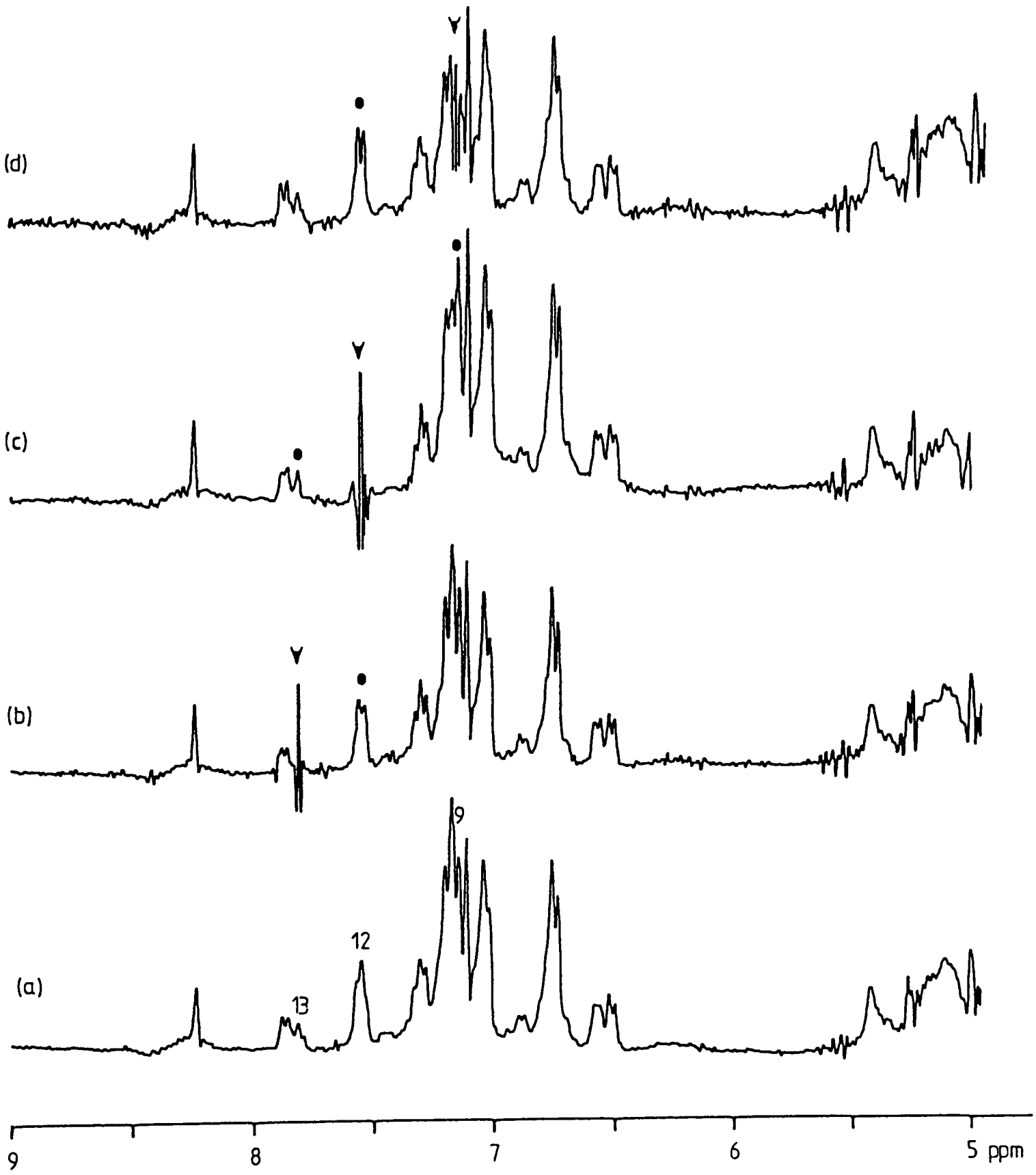

Fig. 6.6 Resolution enhanced spectra of bovine fragment 2; 37°C, pH 6.6. (a) Normal spectrum (b)-(d) Spin decoupling experiments.

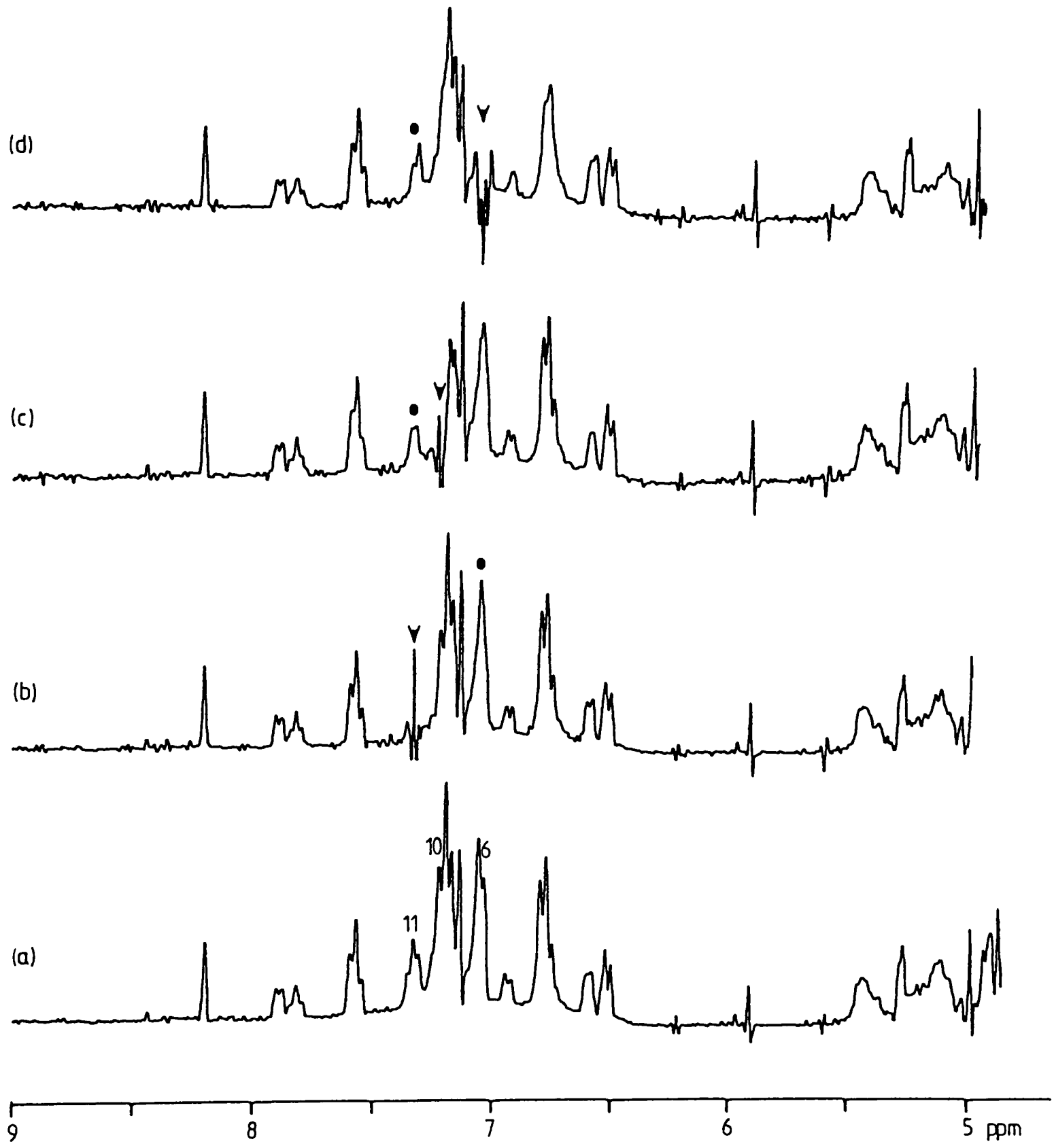

Fig. 6.7 Resolution enhanced spectra of bovine fragment 2; 37°C, pH 6.6. (a) Normal spectrum (b)-(d) Spin decoupling experiments.

(Fig. 6.7(d)) leads to a reciprocal change in 11R going from a triplet to a doublet resonance. Incidentally, the line shape of the doublet resonance in Fig. 6.7(d) indicates that the other resonance to which it is coupled has a very similar chemical shift just upfield and indeed irradiation on the edge of 10R in Fig. 6.7(c) causes 11R to once again collapse to a doublet peak. Thus, the resonances of a second phenylalanine residue are identified. The intensity at 6R is taken to be from the ortho protons, as again Fig. 6.5(d) indicates suitable doublet intensity at this position rather than on the edge of 10R which is therefore assigned as the one proton triplet resonance of the para proton.

Finally, the remaining two proton triplet indicated by the multiplet spectra to be at 4R is most likely to arise from the meta protons of the third phenylalanine side chain . However, unlike 11R and 12R, this resonance is not clearly seen to be a triplet in the ordinary spectrum since it is part of a composite peak of a number of overlapping resonances. A spin decoupling pulse sited on 4R led to collapse of the two proton doublet, 1R to a singlet as seen in Fig. 6.10(b) below, and for some time it was considered that the two resonances involved were from a tyrosine residue. However, NOE experiments indicated this was not the case as three strong resonances were apparant in the NOE difference spectrum obtained on the pre-irradiation of 1R. This result is typical of a phenylalanine side chain which usually give rise to all three sets of protons in the NOE experiment on irradiation of any one of them (Dalgarno, 1983). The assignment of the third phenylalanine resonance was therefore made using NOE difference spectra with simultaneous spin decoupling as shown in Fig. 6.8. The pre-saturation pulse was sited on 6R and clearly seen in Fig. 6.8(b), with the blank spin decoupling irradiation, is a triplet resonance at 4R. When the spin decoupling pulse was placed on the 1R doublet, as now expected, the 4R triplet collapsed to a doublet, shown in

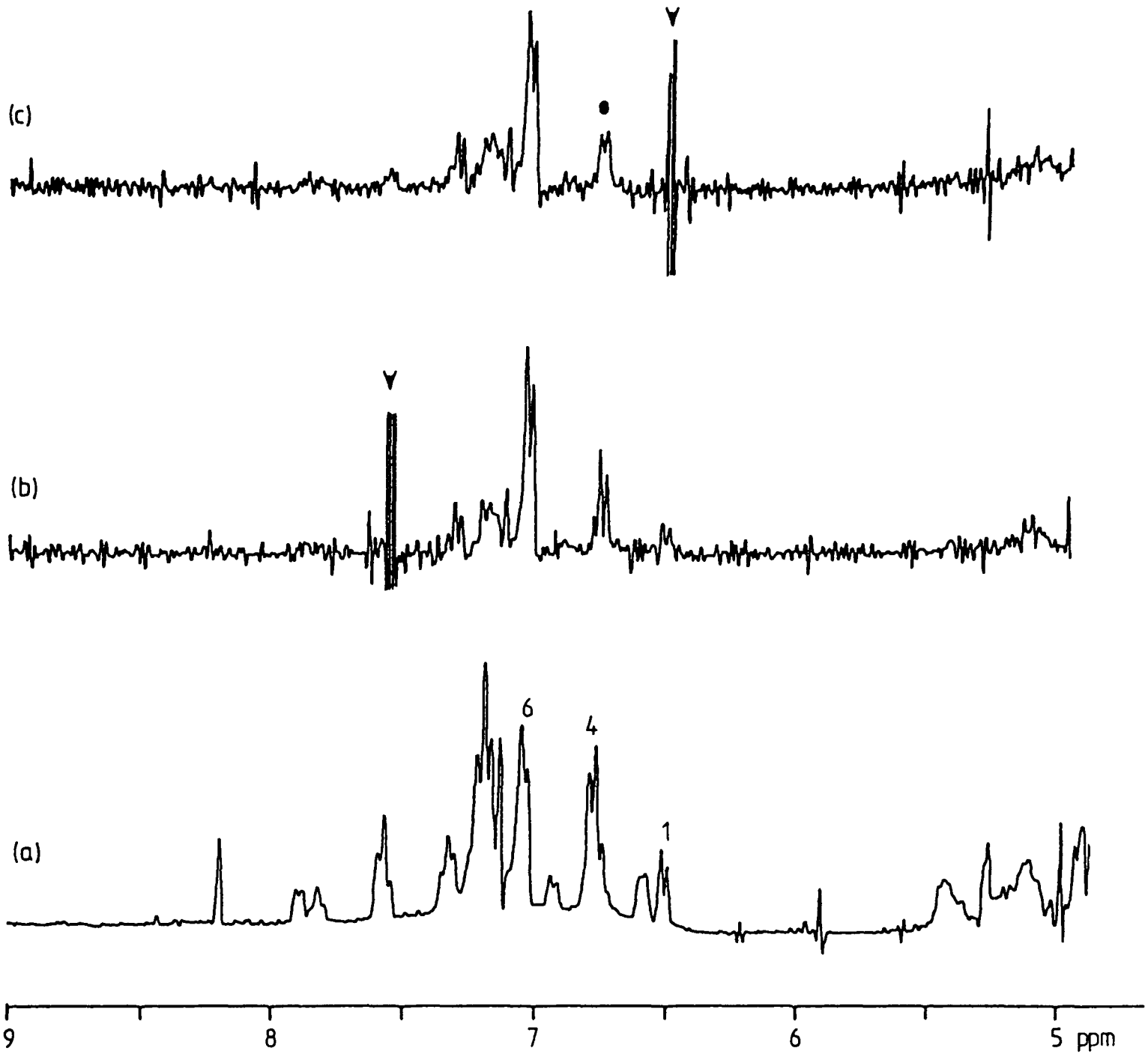

Fig. 6.8 Resolution enhanced spectra of bovine fragment 2; 37°C, pH 7.6. (a) Normal spectrum (b),(c) NOE difference spectra with irradiation at 7.04ppm and simultaneous spin decoupling pulses at the positions indicated.

Fig. 6.8(c). The NOE spectra were thus produced by irradiation of the para proton at 6R.

This completes the full assignment of the three phenylalanine side chain aromatic protons and the data is summarised in Fig. 6.9. (Discussion of possible second stage assignments of these residues will be delayed until the NOE data has been considered).

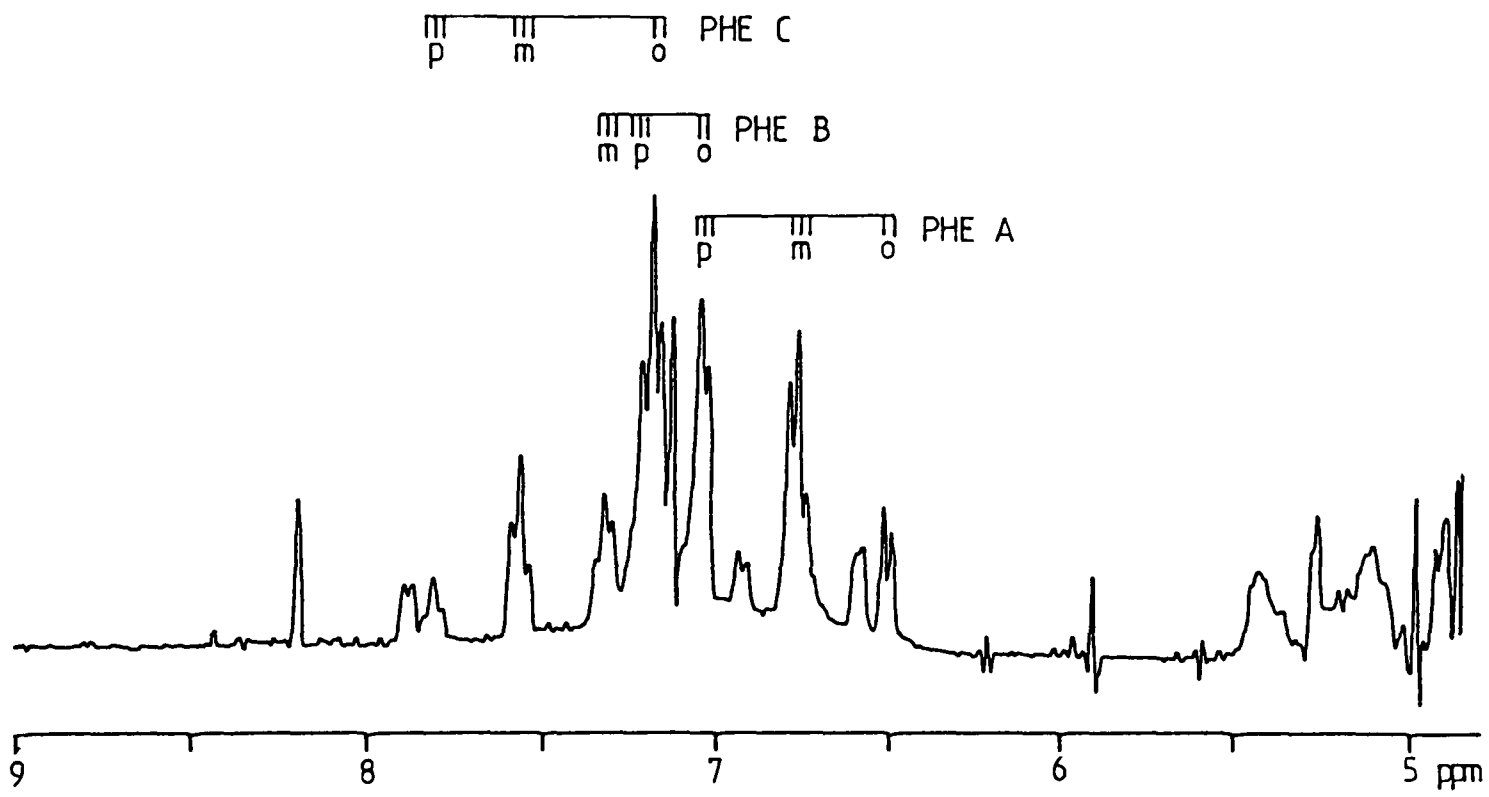

Fig. 6.9 Summary of the coupling patterns of three phenylalanine residues of fragment 2.

For the reasons discussed above this is a very useful situation to have reached as the remaining one proton resonances in the spectrum arise from tryptophan side chains with no possible confusion with resonances of immobilised phenylalanine rings. Similarly, all remaining two proton doublets are assigned to tyrosine residues. These statements assume that there are no immobilised tyrosine ring resonances visible in the spectrum and this possibility must be borne in mind during the assignment of the two tryptophan side chains considered next.

6.2.2 Tryptophans

There now remain two clearly resolved one proton doublet peaks in the spectrum, 14R and 5R. Figure 6.10(b) and (c) shows that these peaks are decoupled to singlets by irradiations at 3R and 7R respectively. However, as with kringle 4 numerous spin decoupling experiments alone and with simultaneous Overhauser irradiation failed to demonstrate any further coupling patterns. In addition the multiplet structure of the 3R and 7R resonances was not conclusively known. When it became possible to perform COSY experiments these problems were resolved and the contour plot of the COSY experiment for bovine fragment 2 is shown in Fig. 6.11. (Note, the same impurity as seen in the spectra of Fig.6.5 was present in this sample but its presence makes no difference to the results discussed here). Two sets of two cross peaks were demonstrated between the aromatic region (beyond 6 ppm) and the downfield shifted αCH region (upfield of 5.5 ppm). This is perhaps more convincingly demonstrated by the cross sections from the contour plot data which are shown in Fig. 6.12. The upfield peaks around 5.2 ppm by virtue of being coupled to two others are therefore triplets and as was demonstrated in COSY spectra of kringle 4, under the conditions of this experiment (that is with no additional delay), doublet-triplet cross peaks are more intense than triplet- triplet ones. Thus, it is seen from the fewer contours in Fig. 6.11 that 3R and 7R are triplet resonances and the required coupling patterns for the two tryptophan rings have been elucidated with no possible confusion with immobilised tyrosine ring intensity. The C2 proton resonances, singlets 8R and 15R now need to be linked to their correct set of resonances and it was noted in Fig. 6.3 that the labile proton resonance at 11.6 ppm was present in the spectrum just after dissolving the protein. An Overhauser experiment on this peak is shown in Fig. 6.13 and gives the familiar result of an enhanced singlet and doublet proton resonance in the difference spectrum confirming

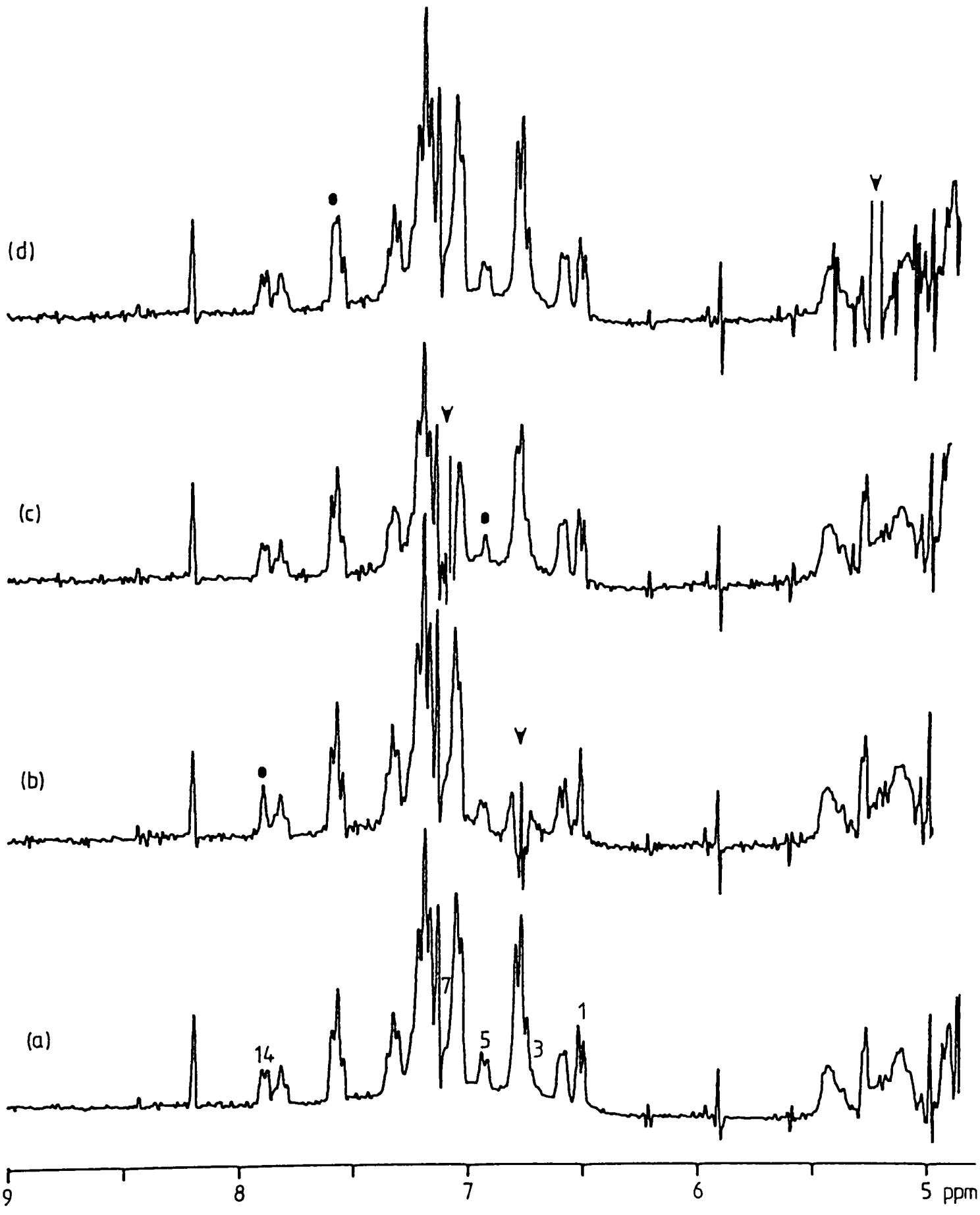

Fig. 6.10 Resolution enhanced spectra of bovine fragment 2; 37°C, pH 6.6. (a) Normal spectrum (b)-(d) Spin decoupling experiments.

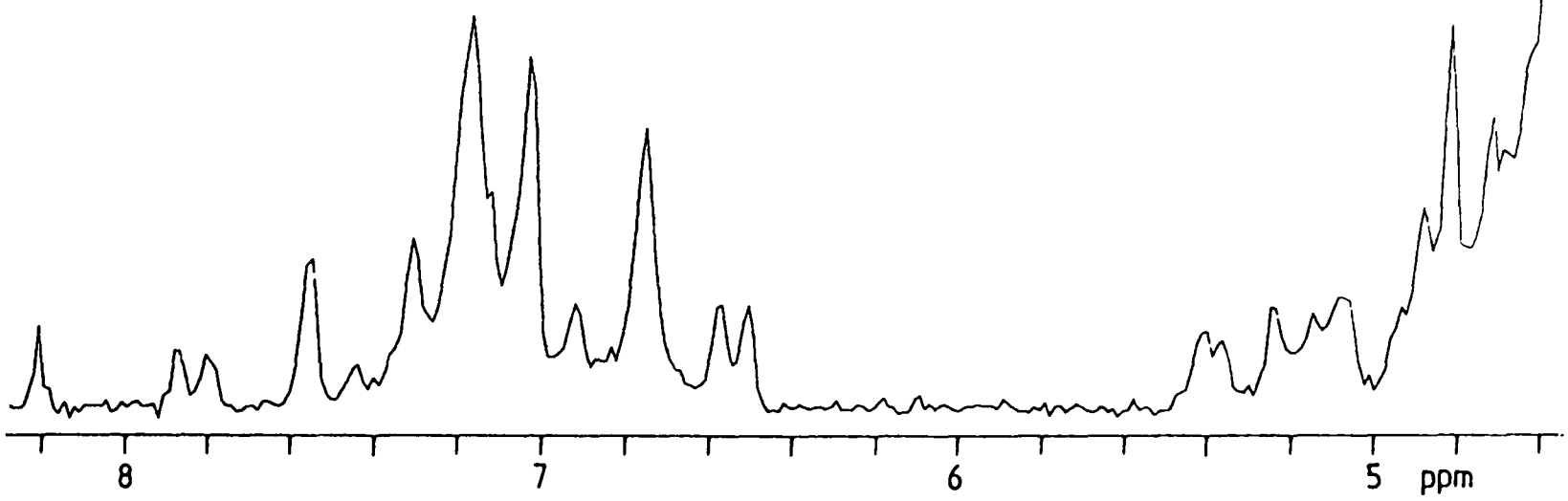

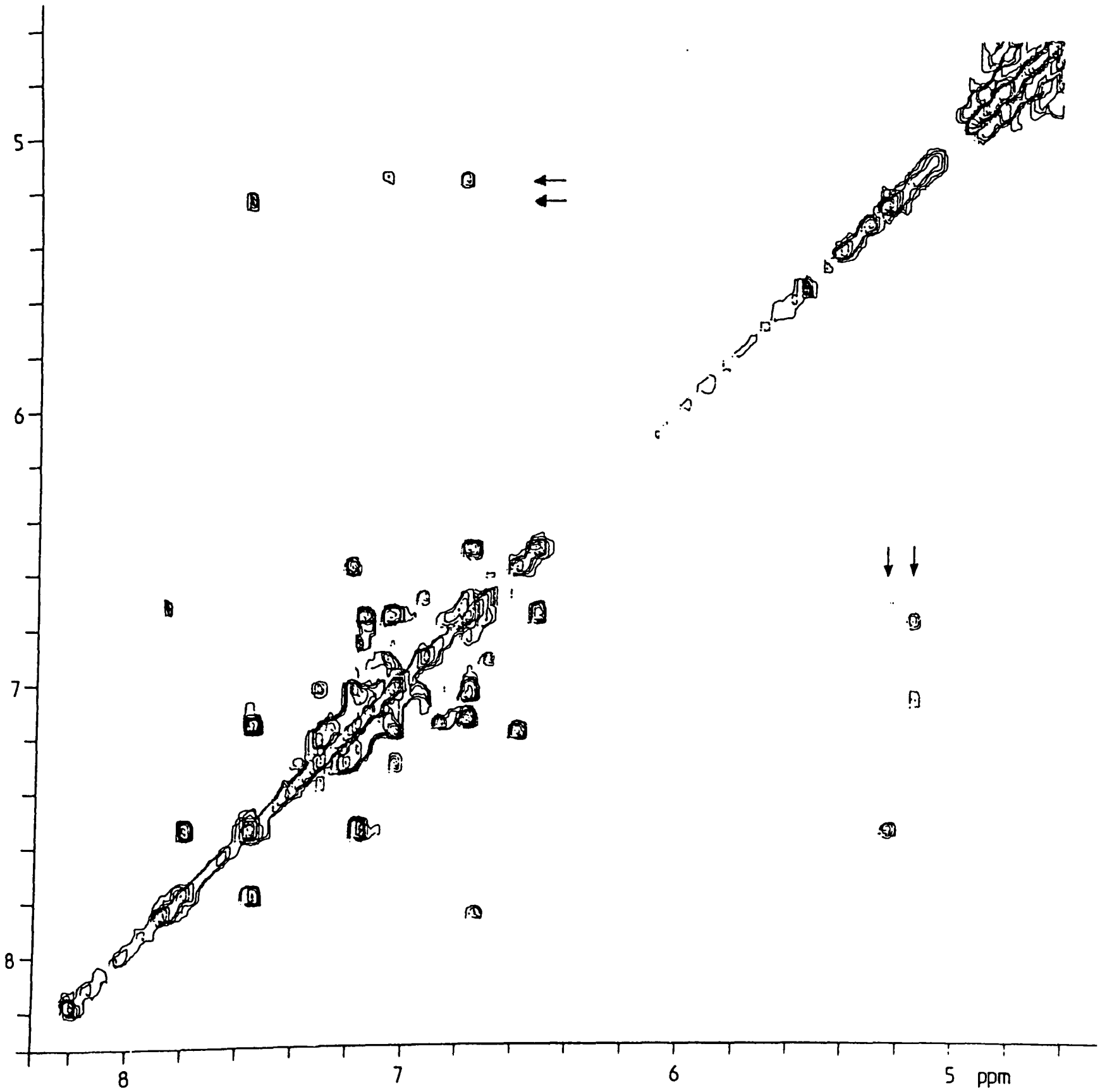

Fig. 6.11 Aromatic region of the 470MHz COSY experiment for bovine fragment 2; 37°C, pH 7.8.

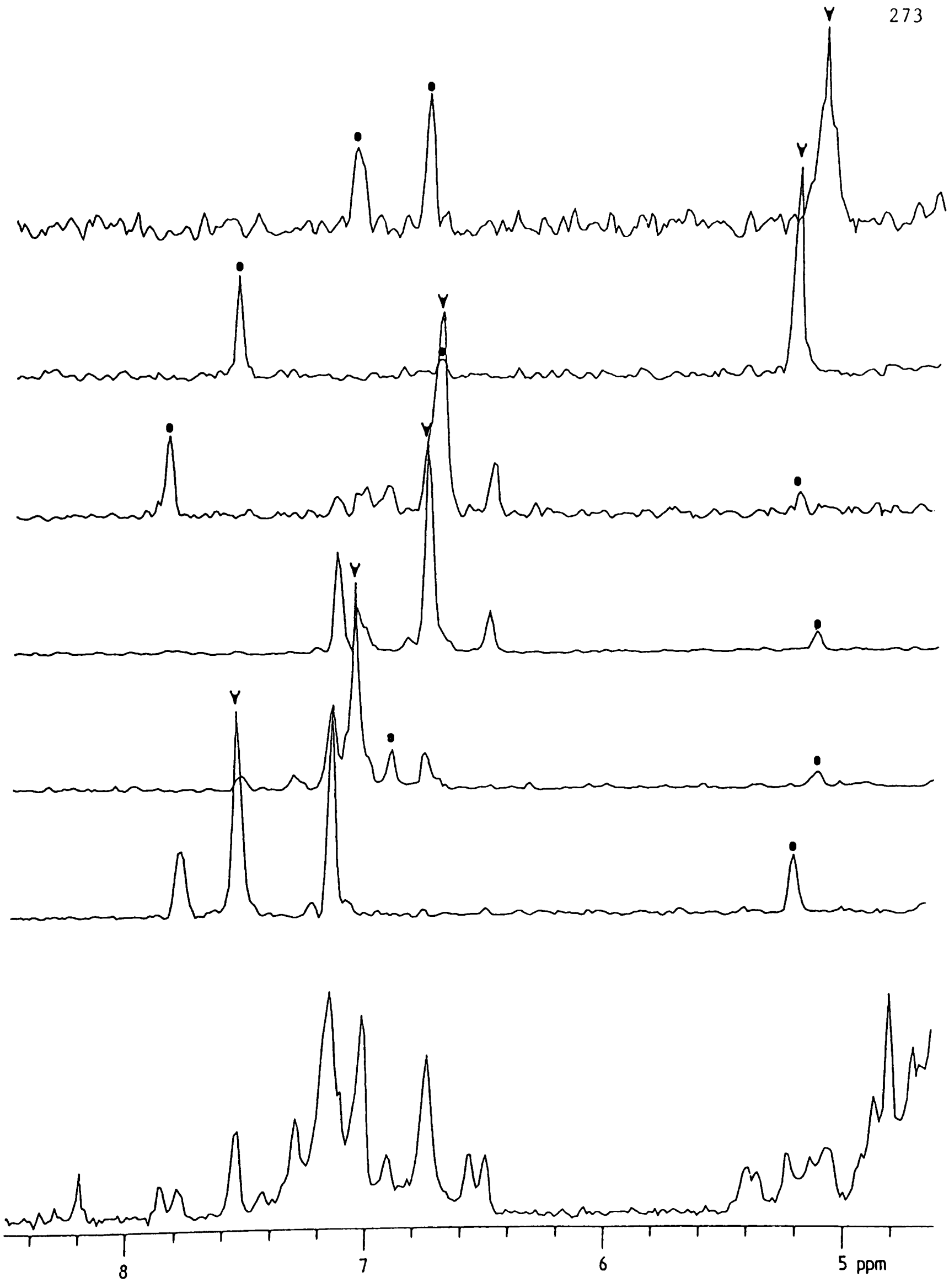

Fig. 6.12 Cross sections taken from the COSY experiment data that gave the contour plot of Fig. 6.11. The arrow head indicates in each cross section the intensity along the diagonal in the latter figure.

it as an indole ring NH proton resonance.

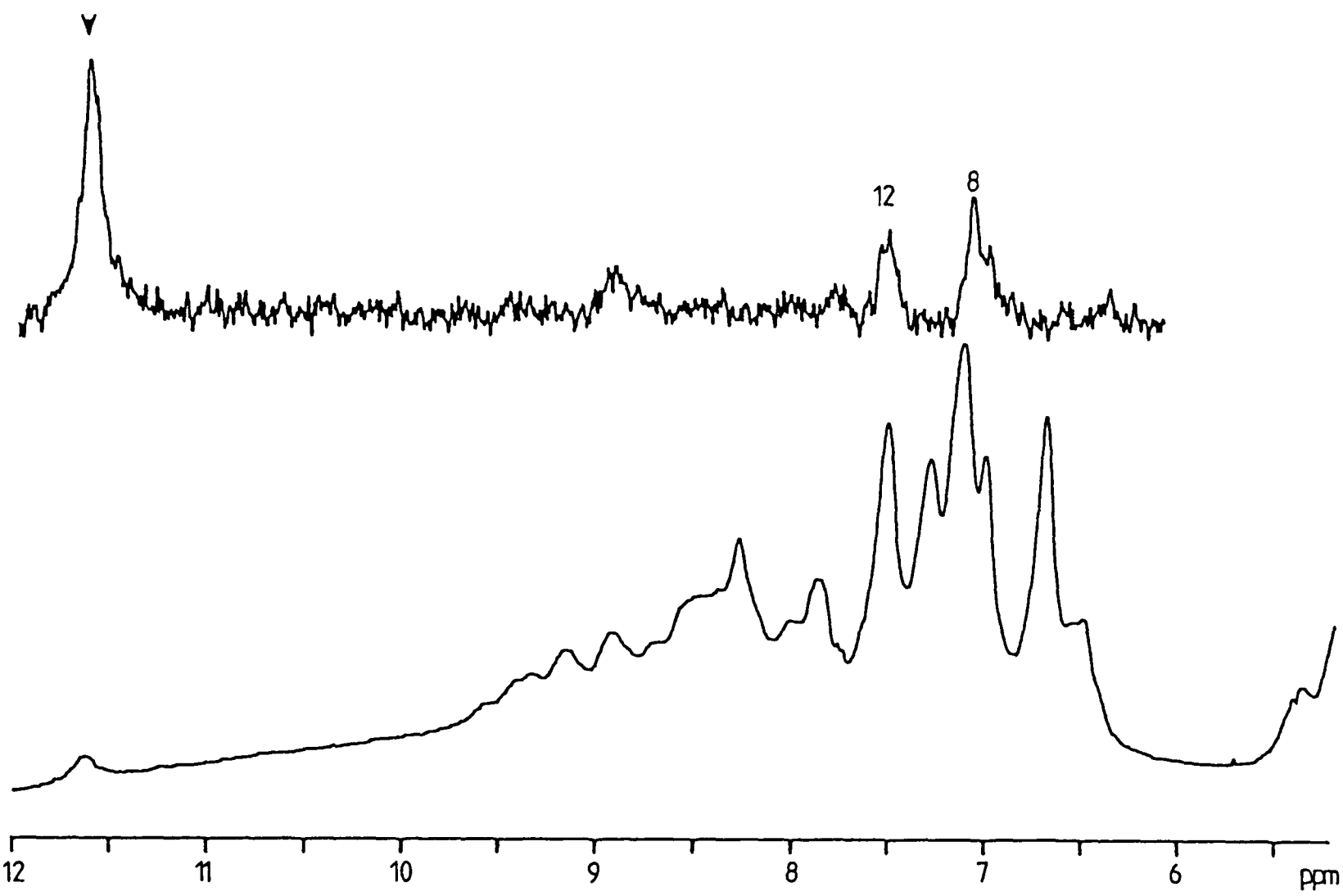

Fig. 6.13 27°C, pH 8.4 (a) normal spectrum of bovine fragment 2 (b) NOE difference spectrum.

As yet the NH proton resonance for the other tryptophan residue has not been identified. It can be seen that the phenylalanine coupling patterns are present in the COSY experiment contour plot of Fig. 6.11 and the first cross section of Fig. 6.12 shows the resonances of Phe C, as the diagonal peak includes not only the C7 proton resonance Trp A but also the meta proton peak of Phe C. Figure 6.10(d) shows the selective collapse of the C7 doublet to a singlet on irradiating the upfield shifted C6 triplet at 5.22 ppm.

The coupling schemes for the two tryptophan rings have been summarised in Fig. 6.14 and labelled similarly to two of the three such residues in

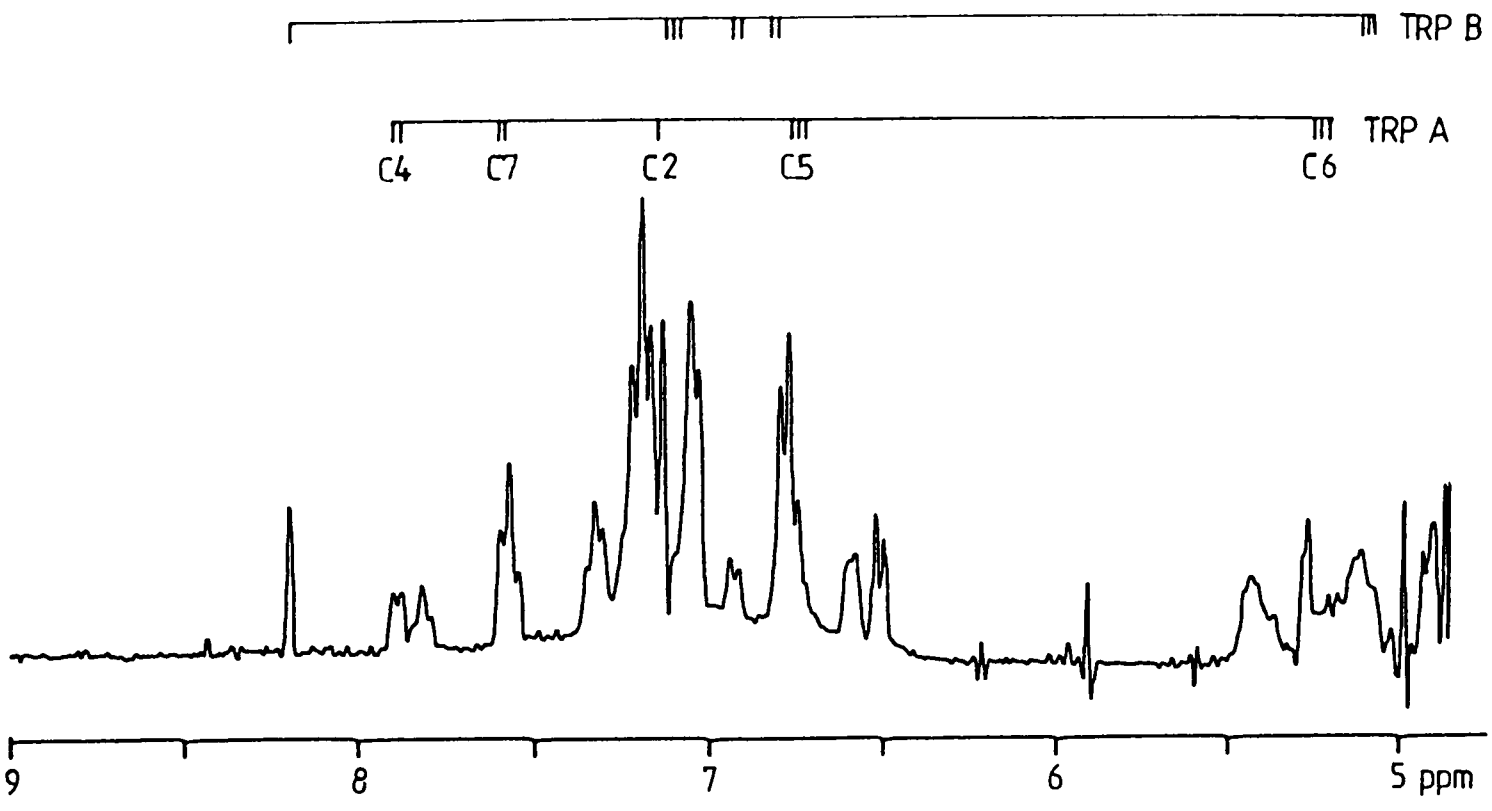

Fig. 6.14 Summary of the coupling patterns of the two tryptophan residues of bovine fragment 2.

the kringle 4 spectrum. This is not coincidental for the two residues in question are Trps 25 and 61, common to both protein sequences. A number of features of the resonances are strikingly similar in the two proteins - for instance the persistence of the Trp A NH proton and the presence of two remakably well upfield shifted triplet resonances. Comparison of the two diagrams Fig. 6.14 and Fig. 3.9 shows this more clearly and the chemical shifts are given in Table 6.3. (The specific assignment of the Trp B resonances around the indole ring for kringle 4 was made possible by the data obtained from the ligand bound protein (section 4.4). The values for the fragment 2 residue are given by analogy as they have not been conclusively demonstrated as such). The values for each protein are seen to be sufficiently similar to fully justify the assignment of the Trp C resonances in kringle 4 to the additional residue, Trp 71 as discussed in section 3.2. The remarkable secondary shifts of the resonances are common to both proteins and indicates that not only are the residues homologous in the two sequences, but must also have very similar environments

Table 6.3 Chemical shifts of the two homologous tryptophan residues Trps 25, 61 in human plasminogen kringle 4 and bovine prothrombin fragment 2; 37°C, pH 8. (See text).

		Chemical Shifts - ppm				
		C2	C4	C5	C6	C7
TRP A	Kringle 4	7.12	8.22	6.44	4.95	7.43
	Fragment 2	7.13	7.89	6.72	5.22	7.58
TRP B	Kringle 4	7.76	6.96	4.84	6.57	6.94
	Fragment 2	8.20	6.77	5.13	7.08	6.93

in the protein structures. Reference to Fig. 6.2 shows that apart from each other the aromatic residues that could be involved in this conserved structural element to give these secondary shifts include Tyr 9 and Tyr 73. However, the conservative changes of tyrosine for phenylalanine might also implicate these residues at positions 39/40, 49 and 63. The simplest option is that the two indole rings are in close proximity and cause secondary shifts of each other, and this is the basis of the initial computations discussed in section 5.9. Until that work yields more results or further data clarifies the situation it will not be known to what extent other residues are involved in producing those conserved spectral features. However, we do note that the resonances of Tyr 73 and the C2 proton resonance of Trp B were linked by a strong reciprocal Overhauser enhancement in kringle 4 indicating the two residues to be close in space and since Tyr 73 is conserved in both sequences, it may well contribute to the large downfield shift on the C2 resonance and possibly to other secondary shifts. Certainly, the NOE from the tryptophan C2 to tyrosine intensity is conserved in fragment 2 as will be shown below, but first the

tyrosine residue assignments must be considered.

6.2.3 Tyrosines

Bovine fragment 2 contains four tyrosine residues, and having completed the phenylalanine and tryptophan resonance assignments all remaining aromatic intensity arises from tyrosine protons. Figure 6.15 shows the assignment of two of the four tyrosines and spin decoupled spectra to substantiate them. The expected cross peaks for these coupled resonances are also visible in the COSY contour plot of Fig. 6.11. However, intensity from the remaining two side chains remains elusive.

The letters used to designate the tyrosines in Fig. 6.15 were chosen to avoid confusion with the kringle 4 designations. But, it will be recalled that the aromatic assignments of kringle 4 were missing intensity from two residues, namely Tyr 9 which is conserved in fragment 2 and Phe 63 which is Tyr 63 in fragment 2. Thus, it is very tempting especially in view of the discussion above on the similarity of the tryptophan resonances in the two spectra, to suggest that it is intensity from Tyr 9 and Tyr 63 in bovine fragment 2 that remains unaccounted for at present in the spectrum. This in turn implies that the resonances of Tyr E and F arise from tyrosines at positions 73, and 78 and this will be considered further in the light of some NOE data. A pH dependence study is not required to confirm the tyrosine assignments already made, for the reason mentioned above, but it would obviously be of benefit in investigating the spectrum for the unassigned intensity. A preliminary titration has been performed but no firm conclusions were reached and it will not be discussed further. (A much more limited study is described below and does not consider pH values sufficiently high for tyrosine side chain ionisation). However, an alternative approach is to simulate the spectrum as was done for kringle 4 in section 3.2.5.

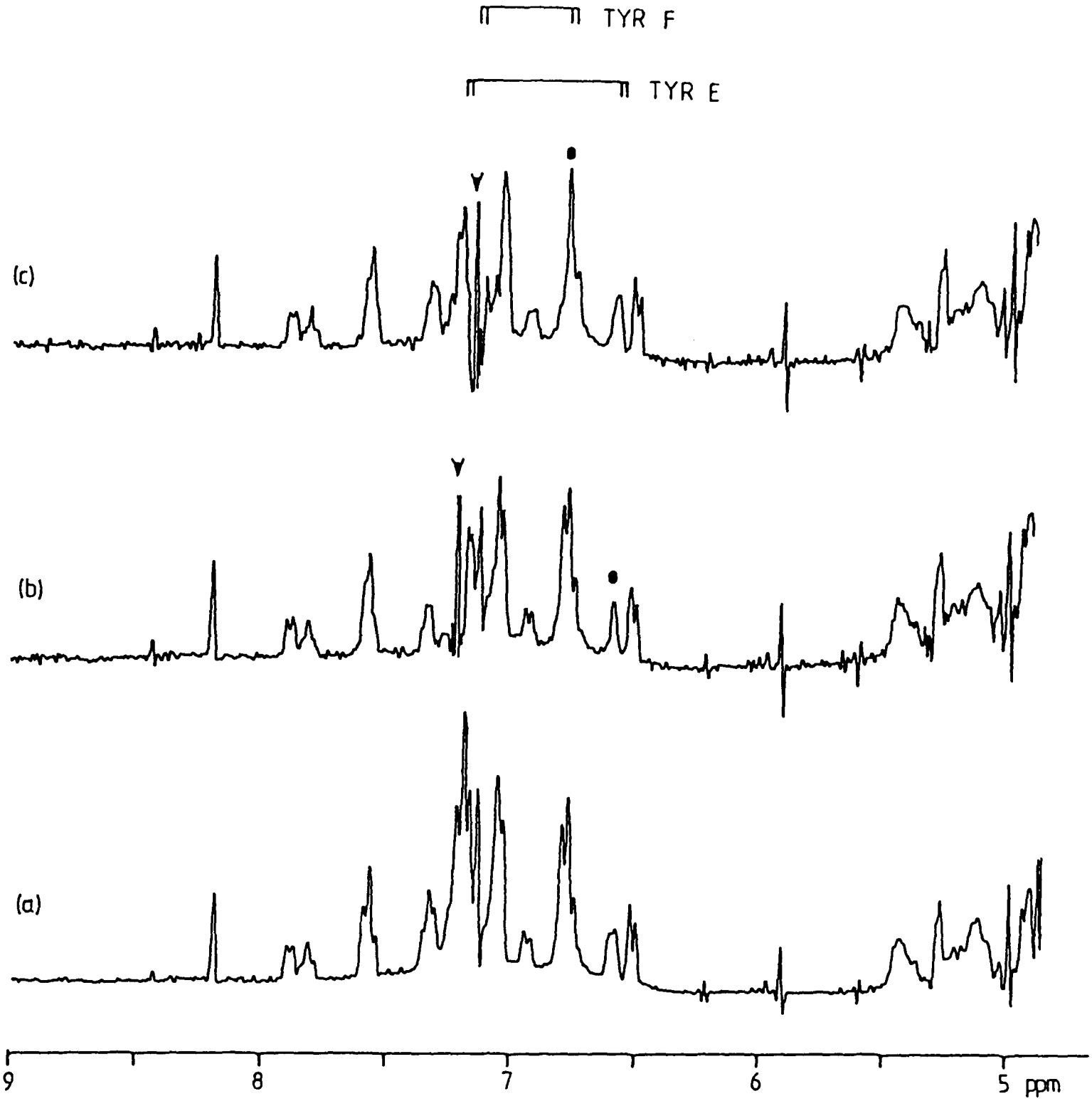

Fig. 6.15 Resolution enhanced spectra of bovine fragment 2; 37°C, pH 7.6. (a) Normal spectrum (b),(c) Spin decoupling experiments. The coupling patterns of two tyrosine residues are summarised.

6.2.4 Spectral Simulation

The simulated spectrum is given in Fig. 6.16(c) using data included in Appendix II. Only thirty three of the total expected fourty one protons have been included. As was found for kringle 4 the simulation is remarkably close to the real spectrum despite intensity from two side chains not being present in the simulated spectrum. However, comparing the intensities in the real and simulation reveals the largest difference to be in peaks 6R and 9R, each being compatible with a two proton deficit. No data has strongly suggested two,two proton resonances at these chemical shifts and indeed if one or both tyrosine rings that have not been assigned are immobilised then two proton peaks would not be expected in any case. Otherwise, the rest of the spectra match extremely well and leave no possibility of additional intensity. Structural details of fragment 2 are now considered through NOE experiments.

6.3 NOE Experiments

As for kringle 4, numerous NOE experiments have been performed under a variety of different solution and instrumental conditions. However, only those pertinent to our purposes here will be discussed and some are shown in Fig. 6.17.

Presaturation of resonance L1 of the conserved Leu 45 is seen in Fig. 6.17(b). Compared to kringle 4, L1 in fragment 2 is shifted downfield as is the L2 resonance revealed by the NOE, such that L2 is no longer clearly resolved and cannot be presaturated selectively without also irradiating other upfield shifted methyl proton resonances. Nevertheless, NOE experiments on L2 are in agreement with the conclusion obtained from that on L1. Thus, in Fig. 6.17(b) it is seen that the Trp A resonances 8R, 12R and 14R are selectively enhanced and this is exactly analogous for kringle 4 (Fig. 3.24(b)) which also showed selective enhancements of the

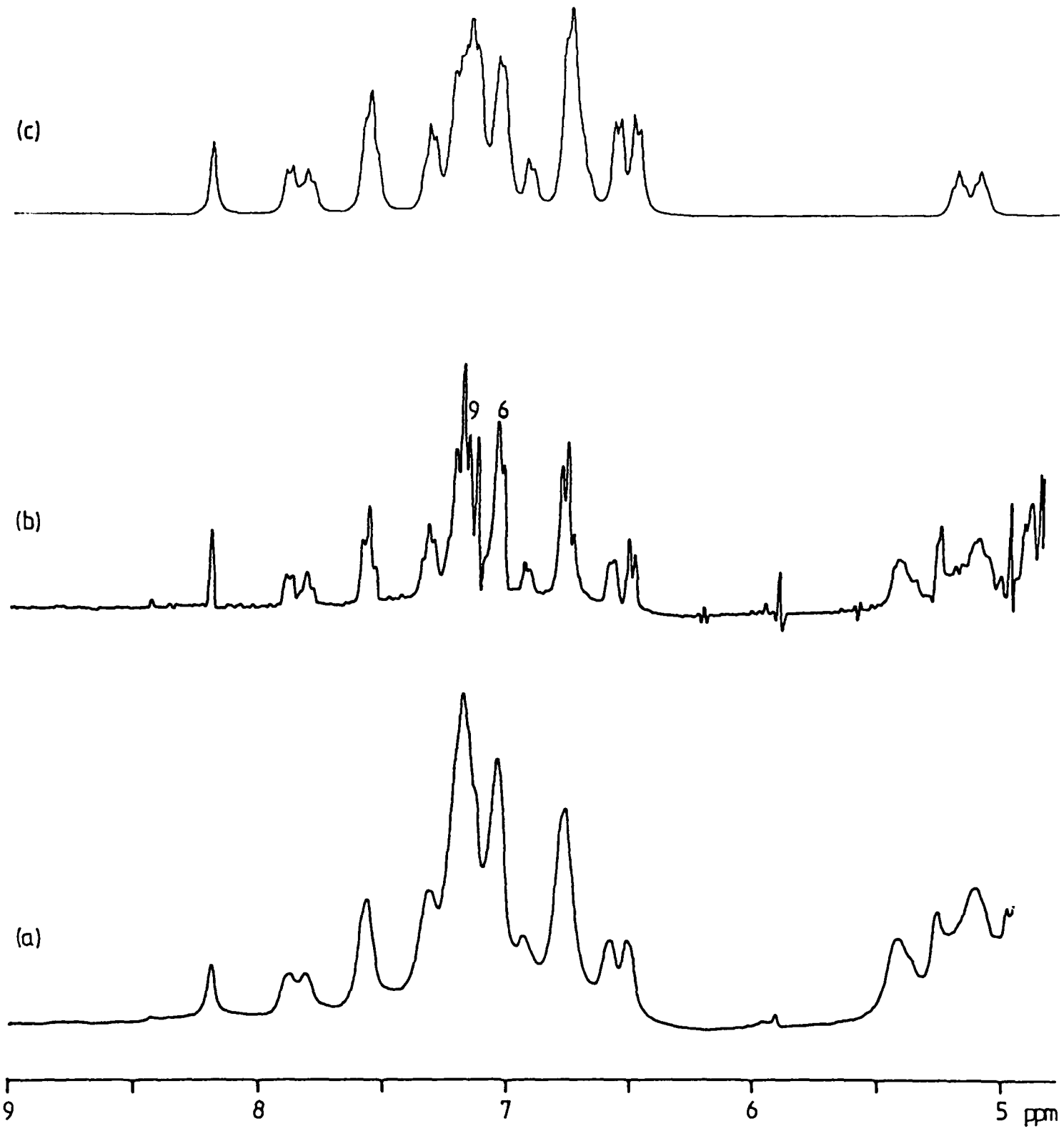

Fig. 6.16 (a) Normal (b) resolution enhanced spectrum of bovine fragment 2; 37°C, pH 7.6 (c) computer simulation of the aromatic region of the spectrum of bovine fragment 2 (see text).

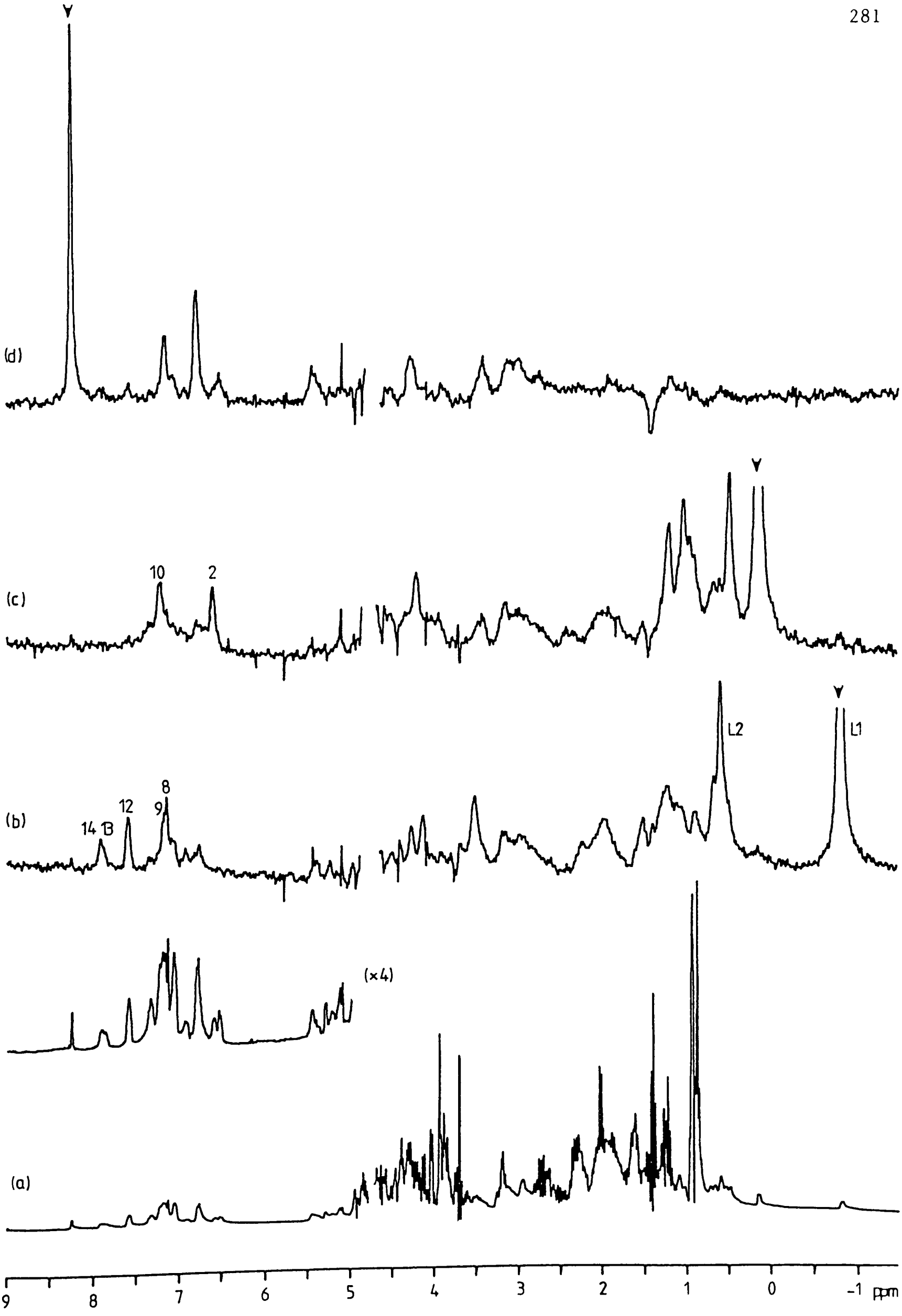

Fig. 6.17 27°C, pH 7.8 (a) Resolution enhanced spectrum of bovine fragment 2, (b)-(d) NOE difference spectra.

C2 and C7 proton resonances of Trp A. This confirms conclusively the statements already made that the methyl groups of the conserved residue Leu 45 are also in a highly conserved structural environment and it is worth reiterating that this is also the case for human prothrombin fragment 2 and bovine prothrombin fragment 1 as shown by their spectra in Fig. 3.19. In addition, the spectral similarities in the published data on kringle 1 of human plasminogen indicates this is also the case for that protein too (De Marco et al.,1982).Now, as well as the enhancements of Trp A resonances from L1, peaks 9R, 12R and 13R assigned to Phe C are also seen in the NOE difference spectrum. The corresponding additional peaks in the kringle 4 spectrum were from Tyr 40 protons. Thus, it is likely that Phe C corresponds to Phe 39 in the fragment 2 sequence. This is made more plausible by the other two phenylalanine residues being at positions 49 and 71. From the kringle 4 studies Tyr 49 was shown to be well removed from the ligand binding site and Leu 45, Trp A. Similarly, Trp 71 while part of the ligand binding site showed very different behaviour to Leu 45, Trp A, Tyr 40 in many experiments. In addition the resonances of both Tyr 40 in kringle 4 and Phe C in fragment 2 are downfield shifted. By a similar argument it is possible to assign Phe A to Phe 71 since the Phe A resonances, like those of Trp 71 in kringle 4, have marked secondary shifts. This then leaves Phe B assigned to Phe 49 and noticing that, without using the argument, the chemical shifts of Phe B in fragment 2 and Tyr 49 in kringle 4 are the closest, of all the assigned phenylalanine and tyrosine residues, to those of the random coil residues. However, it must be emphasised that the postulated second stage assignment of Phe A and B, at least, remain tentative.

Presaturation of another upfield shifted methyl proton resonance is shown in Fig. 6.17(c). Another methyl proton resonance is seen to be enhanced in the difference spectrum suggesting either a leucine or valine

side chain is irradiated but more importantly two aromatic resonances 2R, 10R are clearly visible and confirm the assignment of these resonances to a tyrosine residue, Tyr E. The aliphatic region has been much less extensively investigated than for kringle 4, but reference to Table 6.1 and Fig. 6.1 shows that not only does the sequence contain more leucine and valine residues than kringle 4, but there are also more of both amino acids within the actual kringle sequence. This makes assignment a much more complicated process and less progress has been made than with kringle 4.

The final spectrum in Fig. 6.17(d) shows the result of presaturation of the C2 proton resonance of Trp B. Clearly enhanced in the difference spectrum are two aromatic resonances entirely consistent with their assignment to a tyrosine residue, Tyr F. Furthermore, by direct comparison with the analogous result for kringle 4 (Fig. 3.26(b)) the second stage assignment of Tyr F can be made to the conserved Tyr 73. This, in conjunction with the discussion of the missing tyrosine intensity suggests that Tyr E is assigned to Tyr 78 but there is no evidence to support this.

Table 6.4 summarises the tentative second stage assignments of the aromatic residues considered, using the same postulated assignment of the tryptophan residues as discussed for kringle 4.

Table 6.4 Tentative second stage assignments in the aromatic region of the spectrum of bovine prothrombin fragment 2.

Phe A	Phe 71	Tyr E	Tyr 78
Phe B	Phe 49	Tyr F	Tyr 73
Phe C	Phe 39	Intensity from Tyr 9 and Tyr 63 has yet to be assigned.	
Trp A	Trp 25		
Trp B	Trp 61		

This is provided not so much as a synopsis of results but rather the

extrapolation of data from the better studied protein, kringle 4. Although the reasoning used above is not conclusive it is nevertheless not outrageous and Table 6.4 thus provides a stimulus to further work to confirm or refute the conclusions in it.

6.4 Temperature Dependence

This is shown in Fig. 6.18 which can be compared with similar spectra for kringle 4 in Fig. 3.31. One important practical difference between the thermal behaviour of the two proteins is that fragment 2 is reversibly denatured there being no apparent protein destruction in the process. This may be a genuine difference or alternatively may simply occur because fragment 2 is not raised to as high a temperature as kringle 4 in the experiment; for fragment 2 is denatured by $50^{o}C$ whereas the kringle 4 structure is still intact at $57^{o}C$. Nevertheless the process of denaturation is manifest in similar ways for the two proteins essentially via a slow / intermediate exchange process, the majority of shifted resonances broadening out rather than moving to their random coil positions with increasing temperature.

The most useful aspect of the temperature dependence study is the generation of a spectrum for the denatured, random coil protein, against which the native, folded protein spectrum can be compared. This reveals, as already discussed, that the aromatic resonances are quite dispersed. However, unlike the spectral changes for kringle 4 on thermal denaturation, the aliphatic region of the spectrum of fragment 2 appears much less perturbed by the process. The upfield shifted methyl group resonances disappear but rearrangements in the main aliphatic envelope are few. This is probably largely accounted for by the masking effect of the additional intensity of the extra kringle residues which if extended into the solvent will show very little spectral change on raising the temperature. The

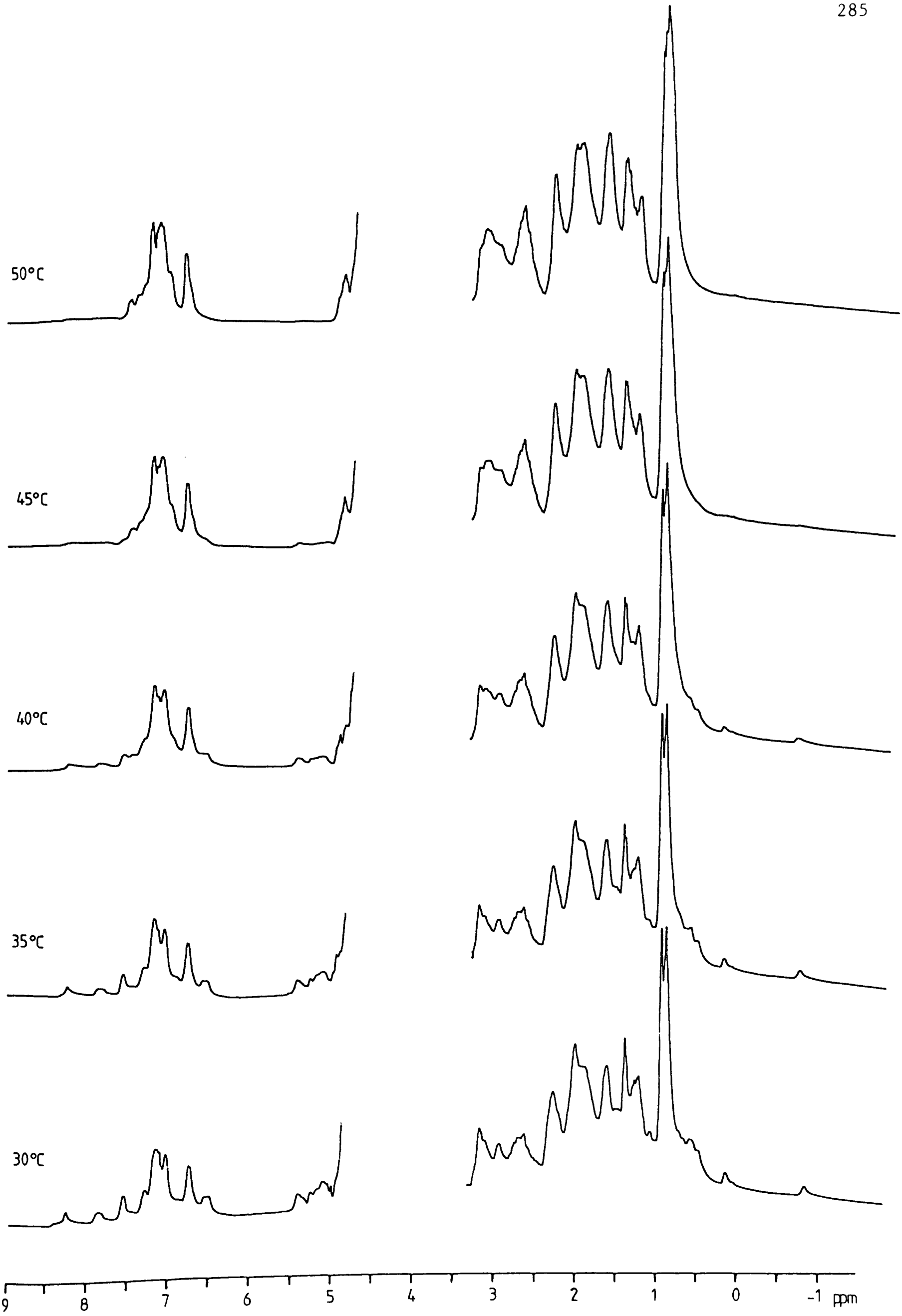

Fig. 6.18 Temperature dependence of the bovine fragment 2 spectrum; pH 7.8.

disappearance of the downfield shifted αCH proton intensity also confirms the presence of some β secondary structure within the intact molecule.

Finally a brief description of a limited pH dependence study of the spectrum is considered.

6.5 pH Dependence

Resolution enhanced spectra are shown in Fig. 6.19 between pH 4.3 and 7.3. At more acidic pH values the protein precipitates, conceivably as a result of an acid induced denaturation leading to an unstable structure. Kringle 4 was shown to be denatured by acid but remained soluble in its protonated form. Chemical shift versus pH curves are shown in Fig. 6.20 and demonstrate that despite there being no histidines in the sequence there is considerable movement of aromatic resonances over the pH range between 5 and 7. 15R, the C2 resonance of Trp B shows a pH dependence like that of R18 of kringle 4. In the latter protein this effect was distinguished from histidine ionisations and corroborated by the similar result being observed in fragment 2, although the pH dependence of 15R occurs at about one pH unit higher. The doublet resonance 5R assigned to the C7 proton of Trp B in Table 6.3 shows an even larger pH dependence over the same range. However, the C 7 doublet (R12) and C2 singlet (8R) resonances of Trp A also show shifts, albeit smaller. (This also clearly demonstrates that the Trp A C7 proton doublet lies underneath the meta proton peak of Phe C at higher pH as was also shown in the spin decoupling experiment of Fig. 6.10(d)). This provides further evidence of the notion that the indole rings of Trps A and B do interact. The triplet resonance 12R of Phe C also moves slightly during the titration, but the para proton resonance of the same residue, 13R is unaffected. Other composite peaks such as 4R also show some movement but the interpretation of which residues contribute to this is not clear. In the aliphatic region on the

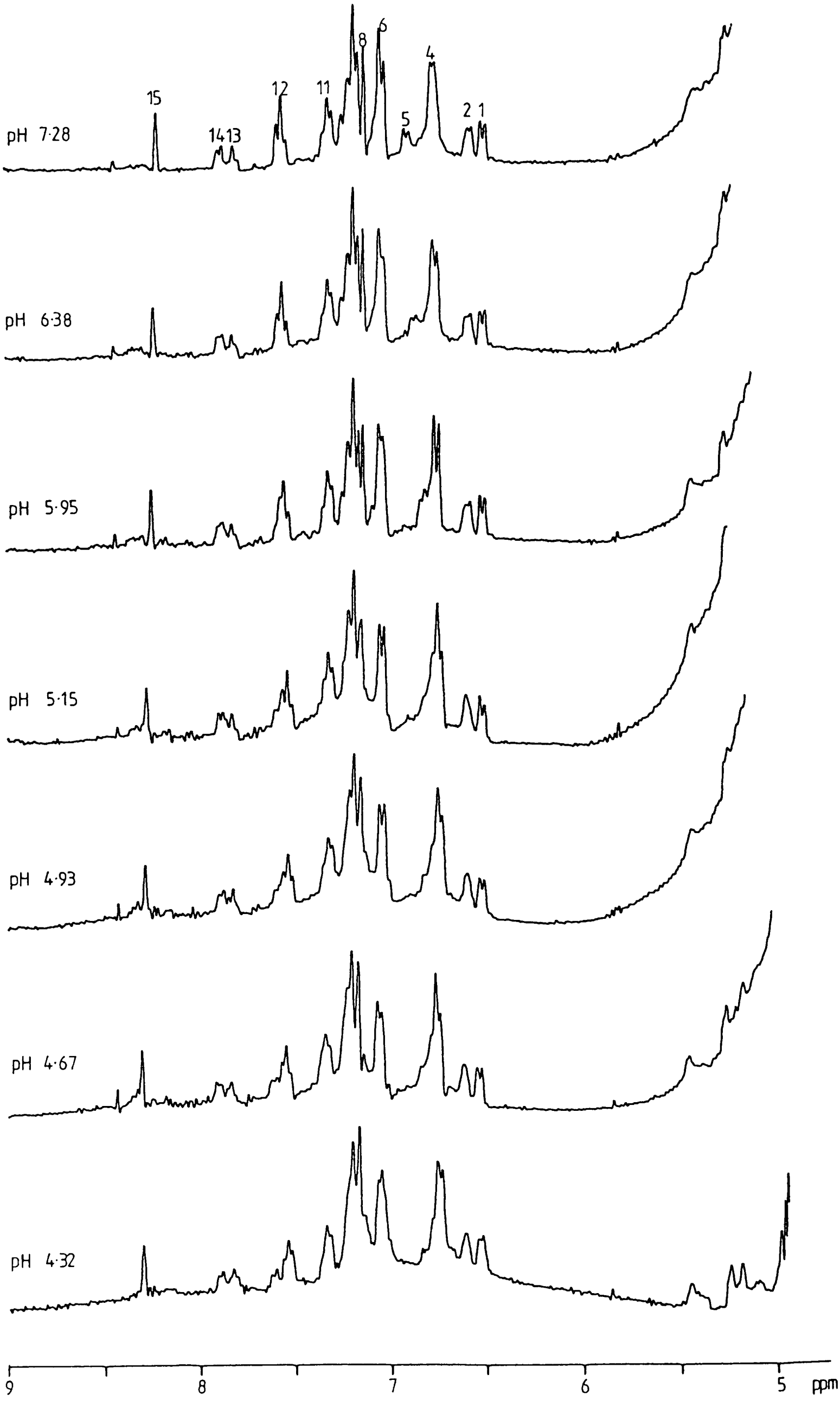

Fig. 6.19A Aromatic region of the pH dependence of bovine fragment 2; 37°C, 100mM NaCl.

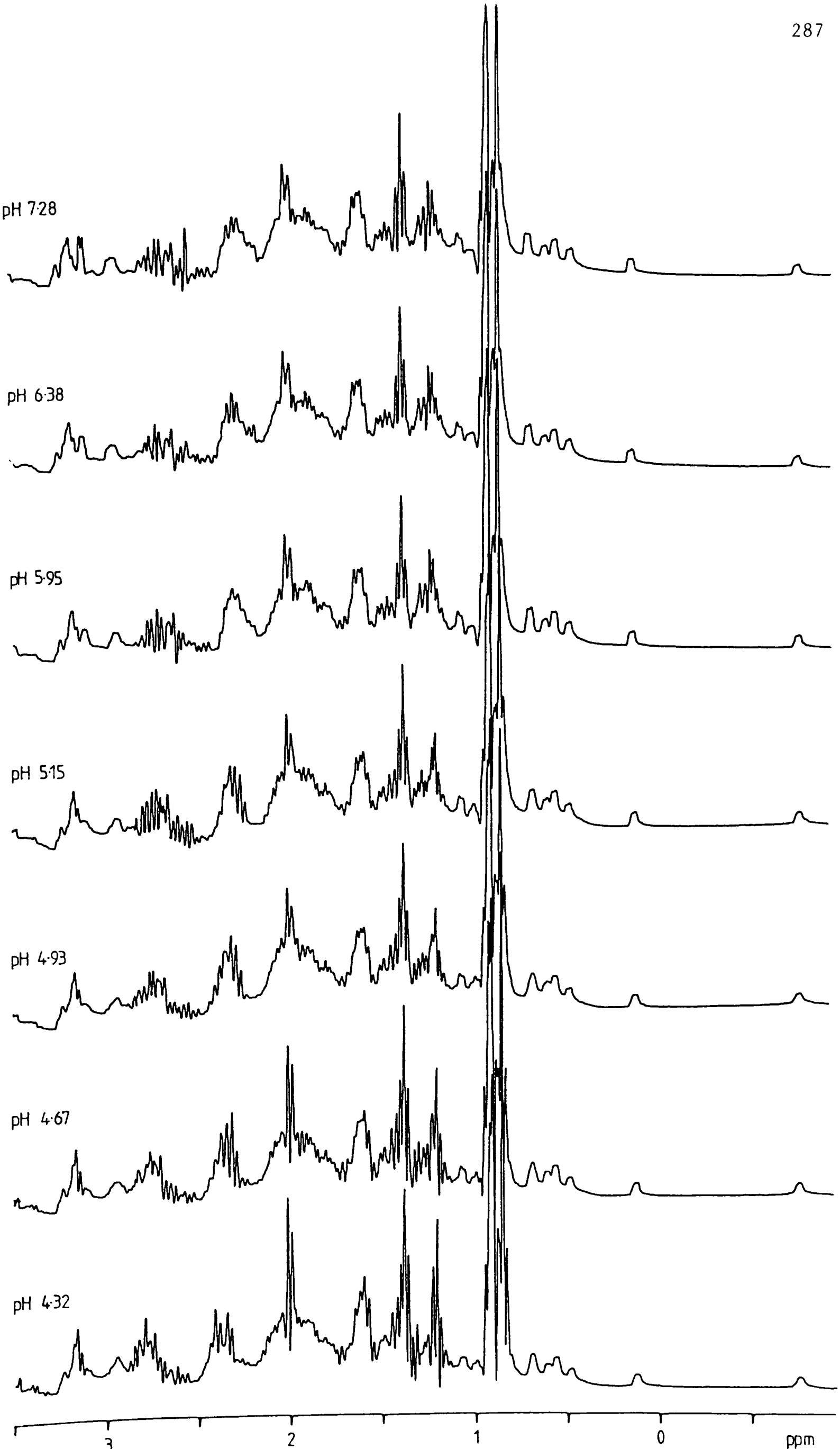

Fig. 6.19B Aliphatic region of the pH dependence of bovine fragment 2; 37°C, 100mM NaCl.

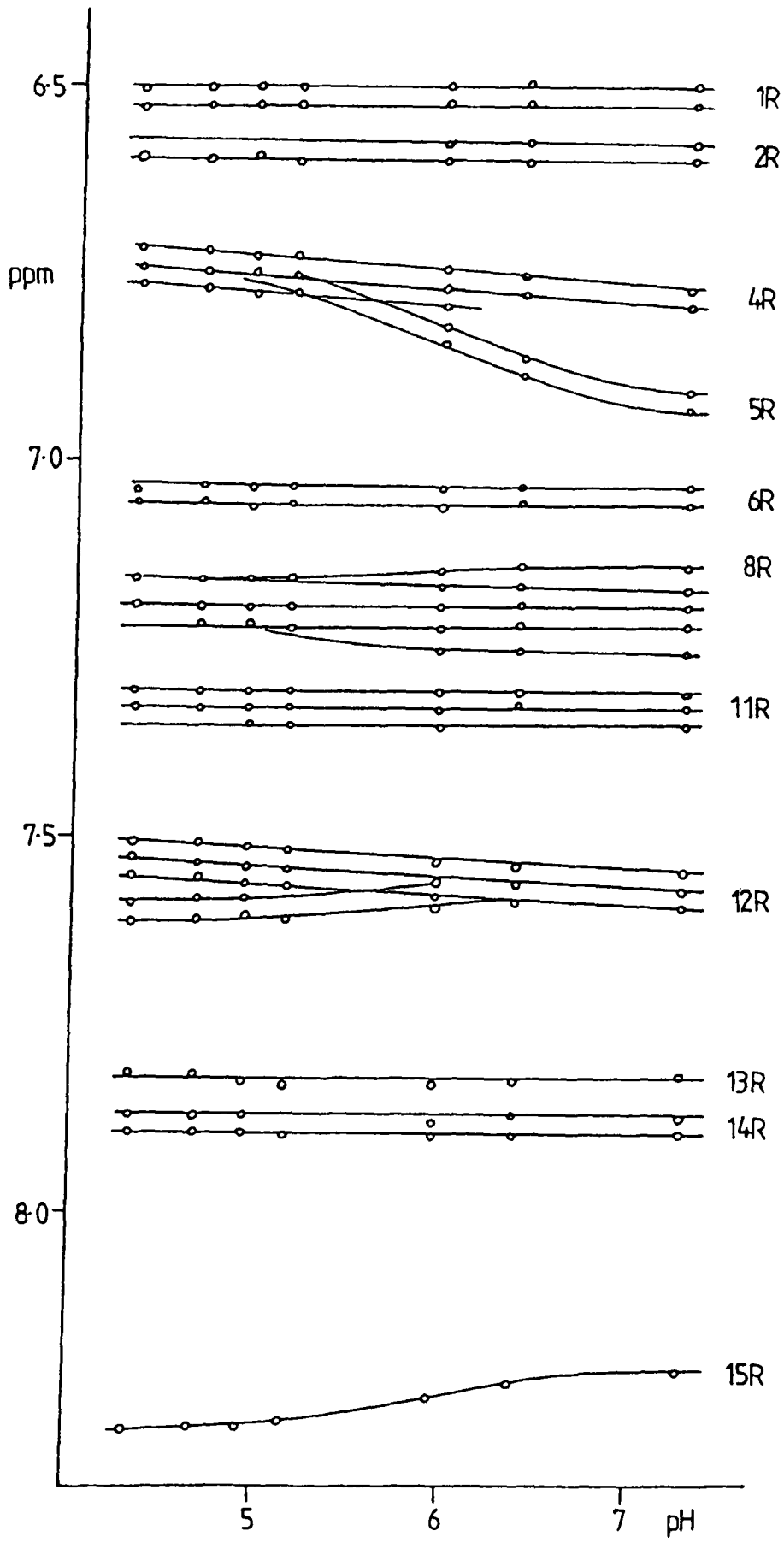

Fig. 6.20 Chemical shift versus pH curves for some aromatic resonances of bovine fragment 2; 37°C, 100mM NaCl.

other hand it is quite striking that despite the sizeable changes in aromatic resonance positions none of the upfield methyl proton resonances show any pH dependent shift whatsoever; not even L1 which might have been anticipated to be affected in view of the NOE from it to the C2, C7 protons of Trp A.

These pH dependent shifts must arise through a carboxyl group ionisation from an aspartate or glutamate side chain having a raised pKa. This suggests the residue is located in a relatively solvent inaccessible environment and the data is consistent with it being buried in the hydrophobic core of the protein for instance with Trp B in close proximity - note the lack of changes in the upfield shifted methyl proton resonances indicates that the ionisation does not cause any large conformational change. In view of the similar behaviour of the Trp B C2 proton resonance in kringle 4, a conserved acid residue is implicated and Fig. 6.2 shows that only Asp 54, 56, 66 and Glu 72 are prime candidates. However, these are just the acid groups considered to be so intimately related to the hydrophobic core of the molecule and involved in the ligand amino group binding site. As far as is known bovine fragment 2 has no specific ligand binding capability although this part of the prothrombin molecule is certainly involved in mediating a protein interaction as will be discussed in the next chapter. Nevertheless, although fragment 2 may possess the necessary structural element for binding the amino group of an ω-aminocarboxylic acid ligand, the kringle 4 modification studies have demonstrated that to be an insufficient requirement for ligand binding capability. Alteration of Arg 70 or Trp 71 in kringle 4 destroyed the binding ability without destroying the protein structure and it may well be the presence of the opposite charge with Glu 70 or the different size of Phe 71 in fragment 2 that prevents it from binding lysine analogues for instance. Further thoughts on the structure - function relationship of kringles will be

reserved for the next chapter, but the studies described herein make it plain that very subtle alterations in the protein sequence can alter the biological function of the protein substantially without changing the structure. This is but another example of a well known phenomenon classically illustrated by the single amino acid difference in the β haemoglobin chain resulting in sickle cell disease.

Human prothrombin fragment 2 will now be briefly considered.

6.6 Human Prothrombin Fragment 2

The complete sequence of this protein is given in Appendix III, but Fig. 6.21 shows the amino acids in the kringle part of the molecule which differ from those of the bovine protein. It is of particular note that all the aromatic residues are conserved with the addition of two histidine residues in the human protein sequence at positions 18 and 36. The presence of the latter amino acids made a pH dependence study of particular interest and this is considered first.

6.6.1 pH Dependence

Figure 6.22 shows the aromatic region of the spectrum at pH values between 4.7 and 9.6 and Fig. 6.23 gives the chemical shift versus pH curves for a few resonances. The histidine resonances are readily identified from their pH dependences, and chemical shifts and are summarised in Table 6.5

Table 6.5 Summary of the resonance assignments of the two histidine residues of human fragment 2.

	C2	C4
His 1	III	II
His 2	IV	I

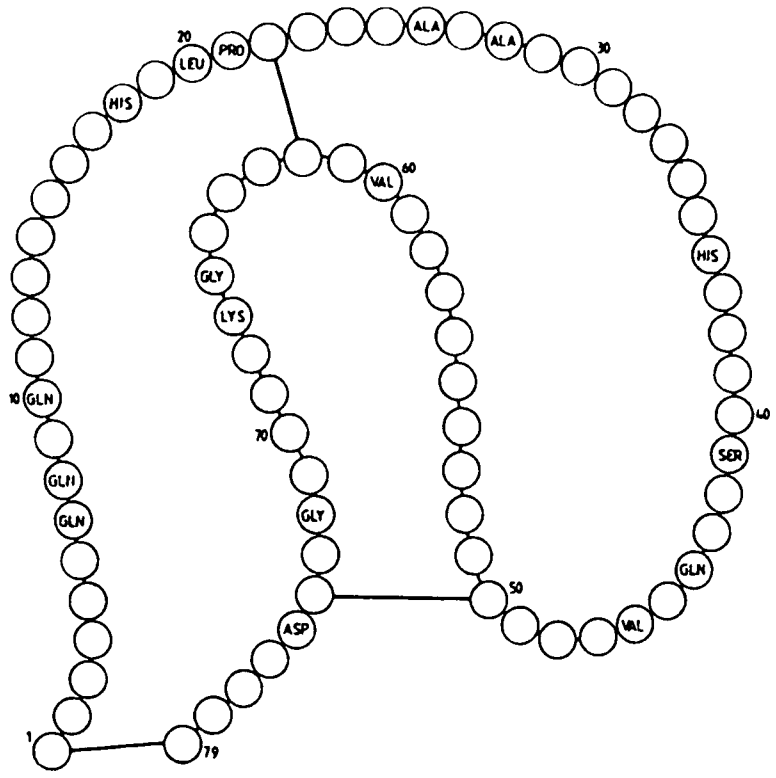

Fig. 6.21 Amino acids within the sequence of the kringle part of human prothrombin fragment 2 that differ from those of the bovine protein.

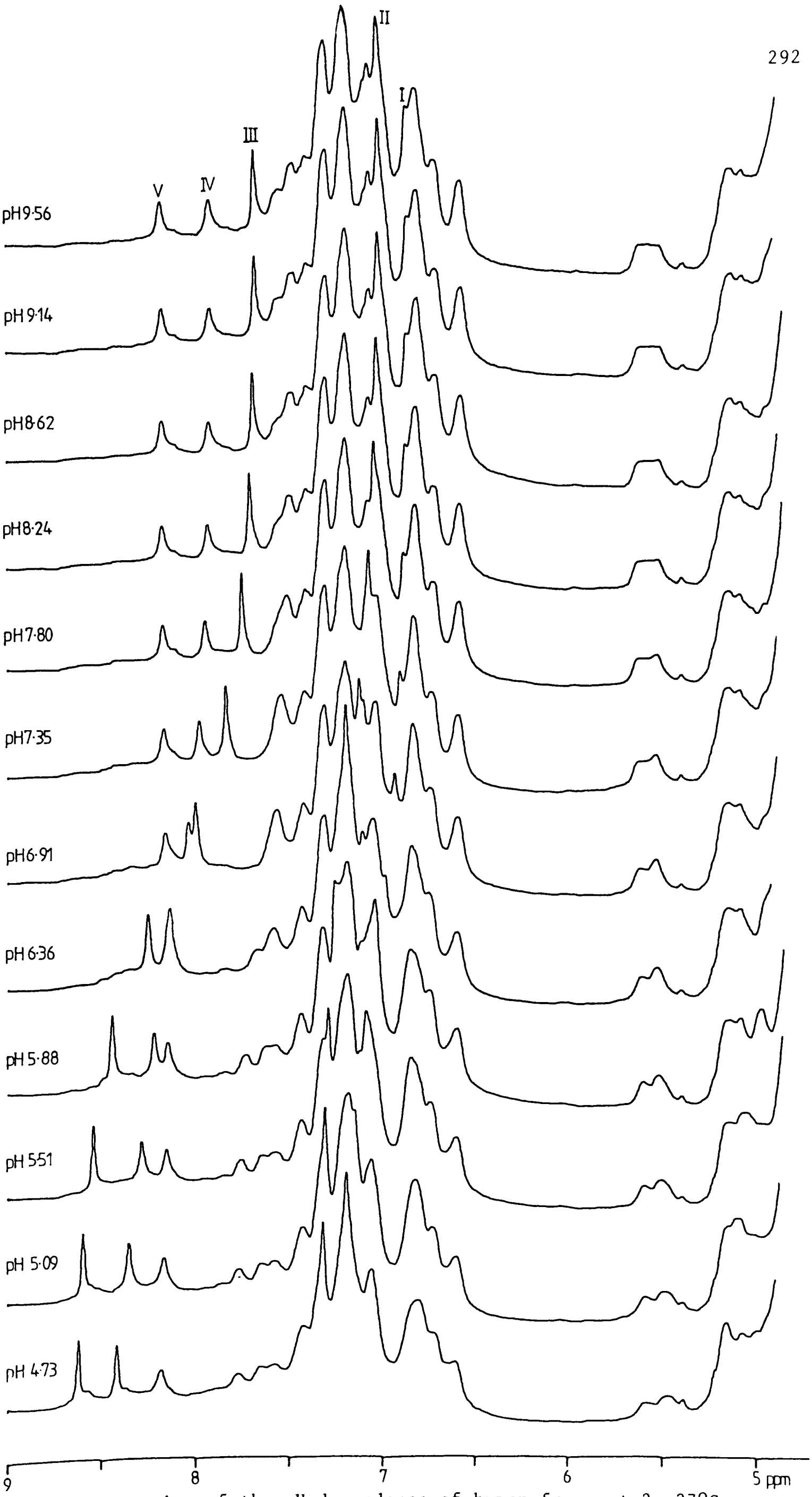

Fig. 6.22 Aromatic region of the pH dependence of human fragment 2; 37°C, 100mM NaCl.

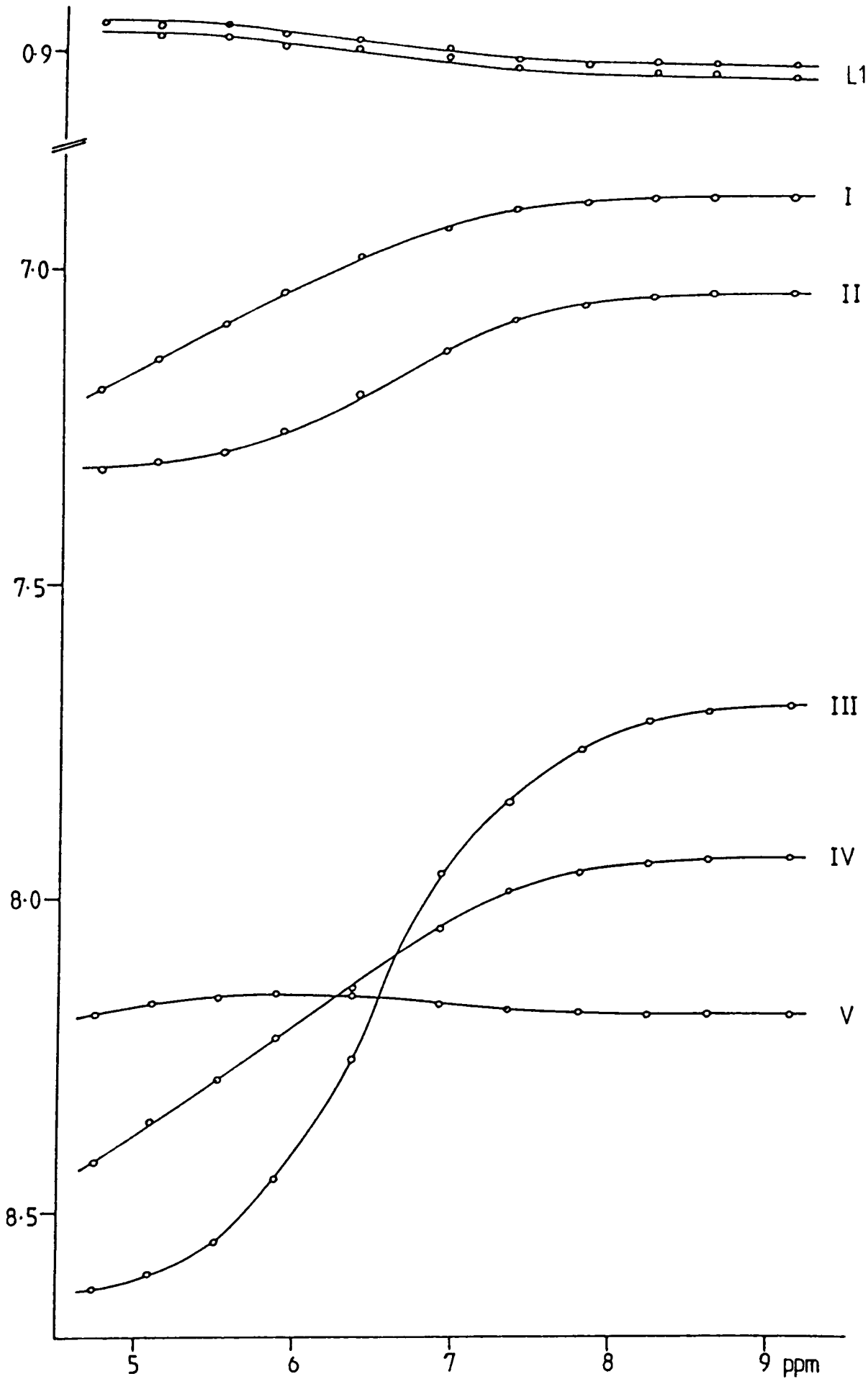

Fig. 6.23 Chemical shift versus pH curves for some of the resonances of human fragment 2; 37°C, 100mM NaCl.

His 1 shows a pKa of around 6.5 and its resonances are very close to those obtained for histidine in a tetrapeptide both in chemical shift values and their range over the pH dependence. This suggests that His 1 is situated in a solvent accessible environment. A striking feature of the pH titration of human fragment 2 is the marked pH dependence of the L1 resonance of Leu 45 as seen in Fig. 6.23 which shows a pKa very similar to His 1. The second stage assignment of the histidine residues has not been conclusively demonstrated at present. It was noted in kringle 4 that a number of results indicated Tyr 40 to be near to the protein surface or at least very accessible to the solvent, but more importantly it is situated close in space to Leu 45. Thus, it could be postulated that His 1 in human fragment 2 is His 36 in view of its pH behaviour and the effect on L1. This would then imply that His 2 be assigned to His 18 in the sequence. Figure 6.23 shows that His 2 does not have a simple pH dependence and should this assignment be vindicated it would form a useful reporter group for a part of the kringle molecule little studied so far.

Having identified the histidine singlets in the spectrum, the remaining aromatic singlets arise from the C2 protons of the two conserved tryptophan residues (Trps 25, 61). One such singlet is resonance V which also shows a pH dependence. This, in conjunction with its chemical shift, indicates its assignment to Trp B and this is confirmed by indentification of the Trp A, C2 resonance by the familiar NOE experiment on the indole NH peak at 11.6 ppm shown in Fig. 6.24. In addition, we note that Asp 66 and Glu 72 are no longer present in the sequence both being replaced by glycine residues in human fragment 2, although the Trp B C2 resonance still shows a pH dependence. This is then most likely a reflection of the ionisation of one or both of the two aspartate side chains at positions 54 and 56 as discussed in the previous chapter.

There are other marked pH dependences over the range studied, as

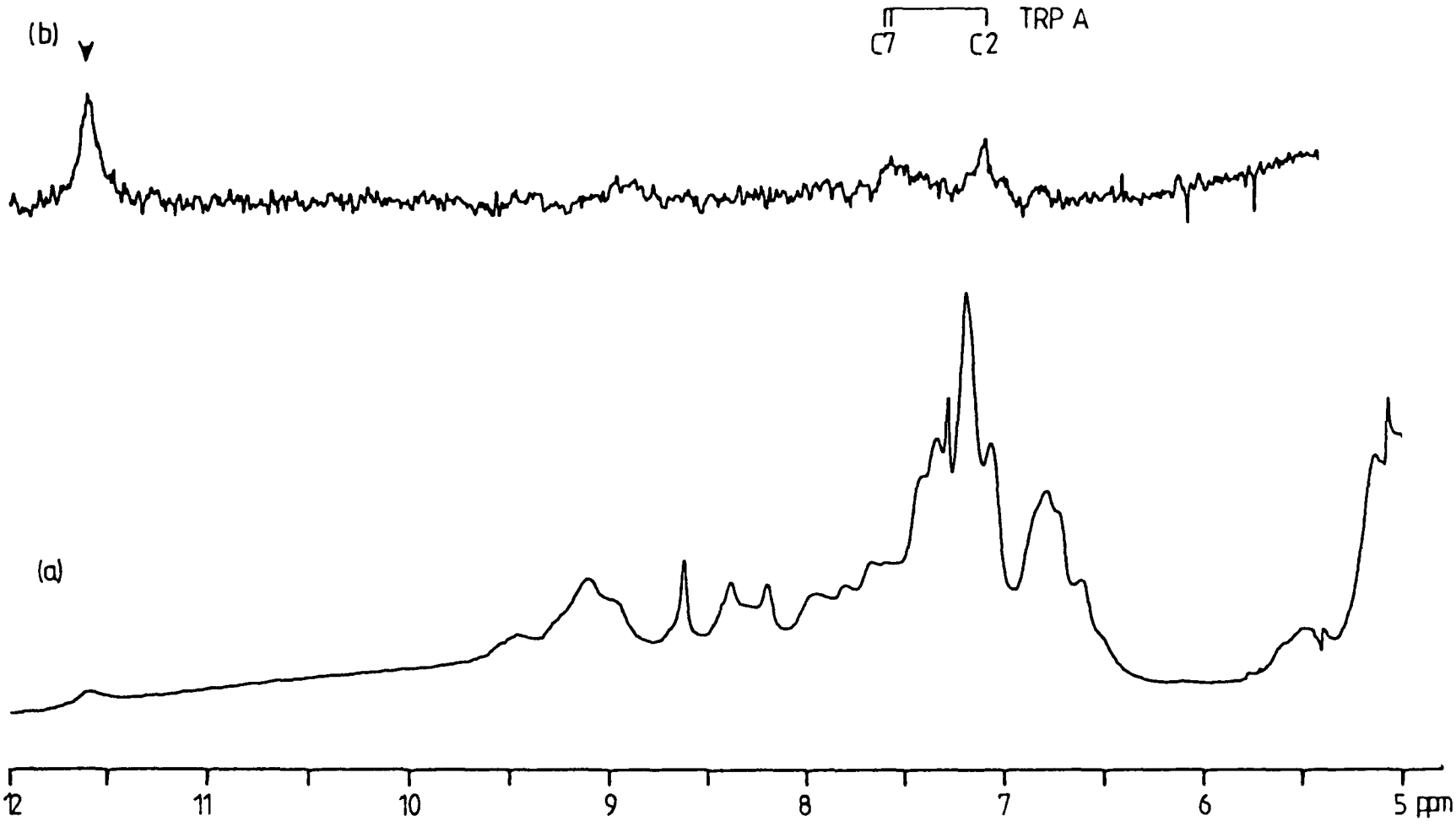

Fig.6.24 27°C, pH 8.3 (a) normal spectrum of human fragment 2 (b) NOE difference spectrum.

can be seen, for instance in Fig. 6.22 beginning around 7.7 ppm at the lowest pH spectrum. However, with no definite assignment of other aromatic resonances in the human fragment 2 spectrum as yet, these effects will not be discussed further. But it is noticeable that there is no alteration in the spectrum between pH 8.62 and 9.56, a pH change over which tyrosine residues might have been expected to begin to ionise.

6.6.2 Temperature Dependence

This is shown for human fragment 2 in Fig. 6.25. The usual form of the denaturation process of the kringle is seen in the slow / intermediate exchange of resonances. (Note the presence of impurities giving rise to sharp peaks at 0.03 and 1.32 ppm). This can be compared with the thermal denaturation of the bovine sample shown in Fig. 6.18 and very similar remarks apply in both cases, although we note that the human protein is slightly more stable thermally. Incidentally, the C2 proton resonance

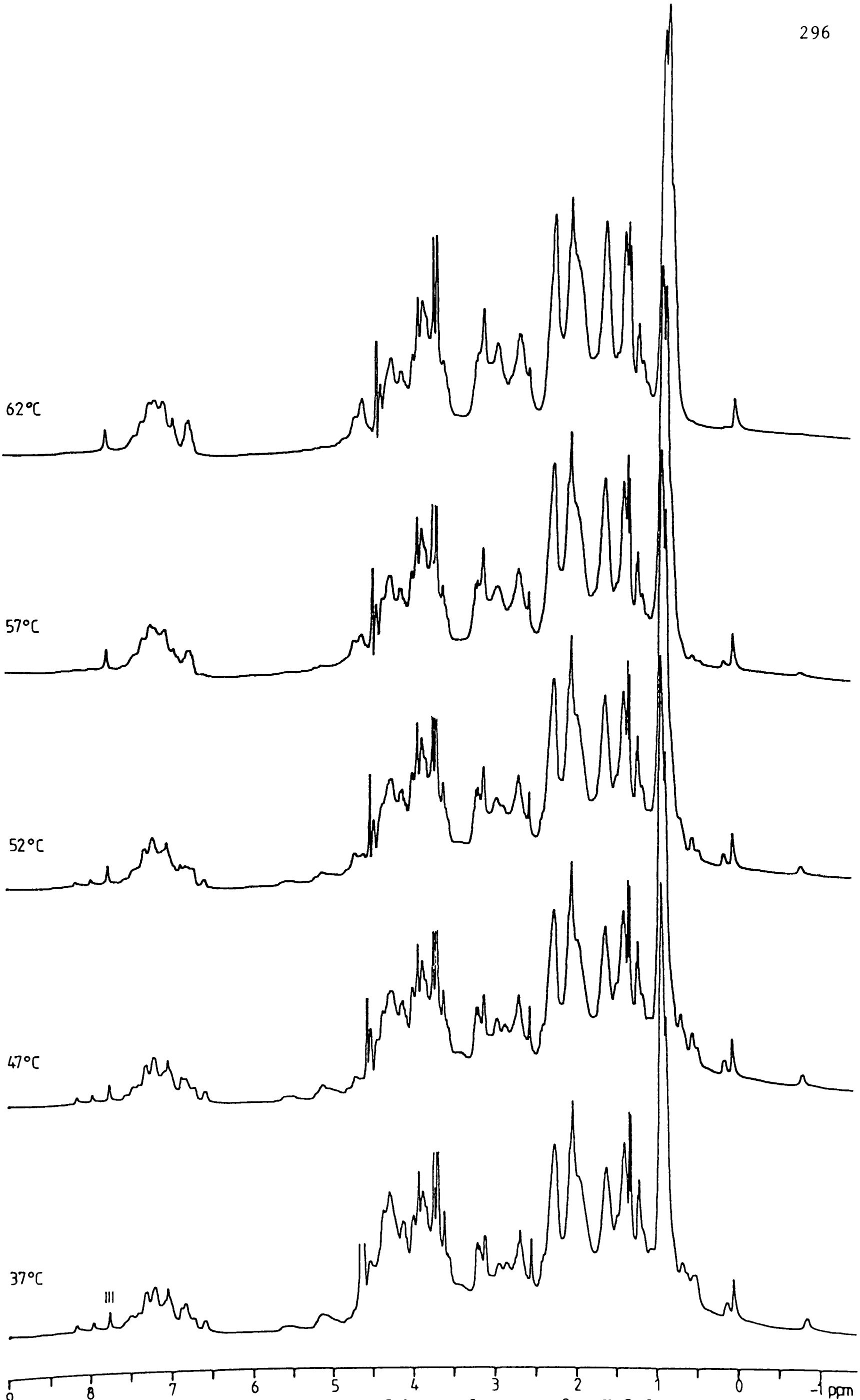

Fig. 6.25 Temperature dependence of human fragment 2; pH 8.3.

of His 1 (III) is seen to be unaffected by the denaturation process confirming it to have no secondary shift as indicated by its pH dependence.

6.6.3 Comparison of the Human and Bovine Spectra

The spectra of the human and bovine proteins are more formally compared in Fig. 6.26.

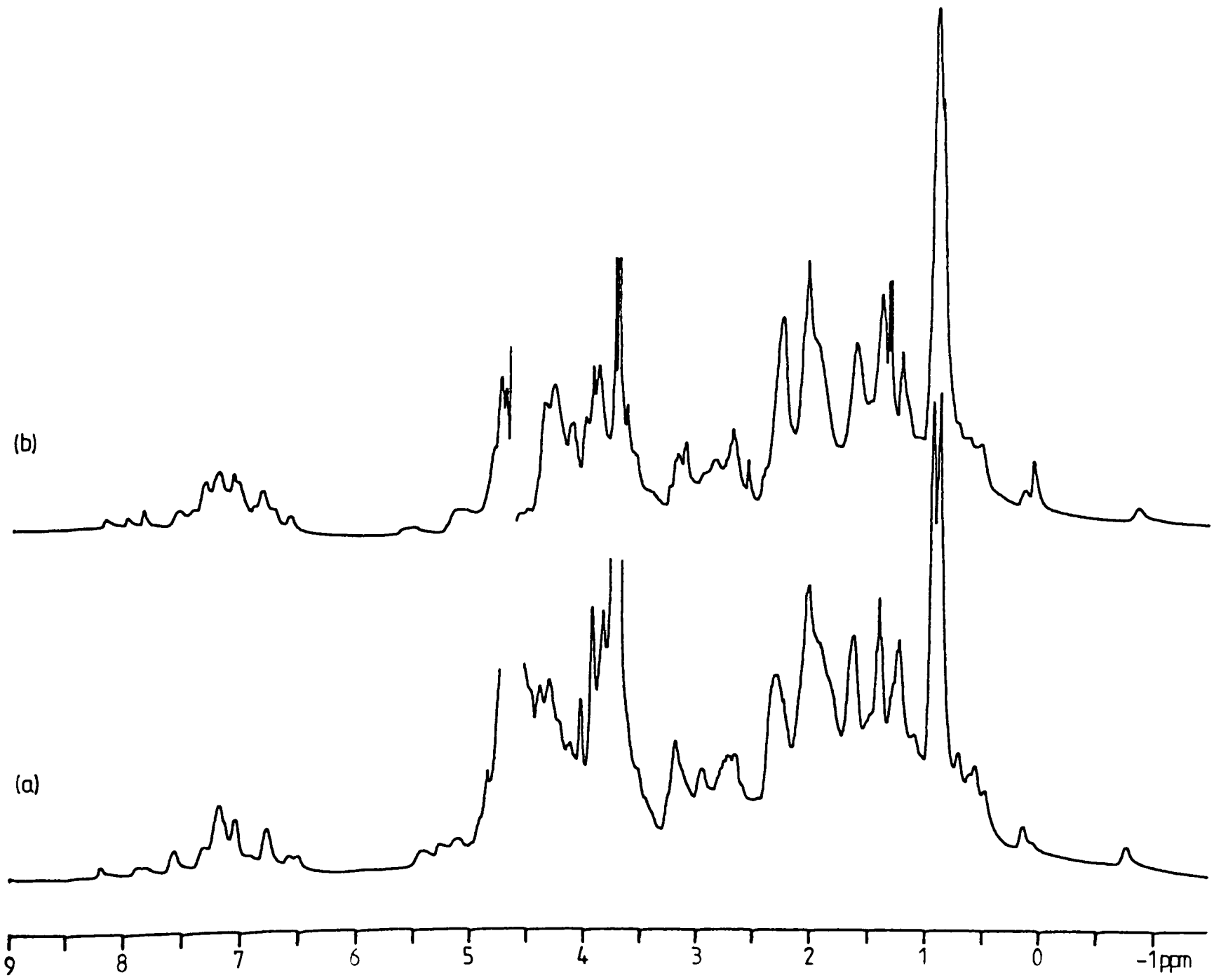

Fig. 6.26 37°C, pH 7.4 (a) bovine prothrombin fragment 2, (b) human prothrombin fragment 2.

The aliphatic regions of the spectra are fairly similar bearing in mind the different compositions but the aromatic regions appear much less comparable, despite having completely conserved aromatic residues with the addition of two histidine side chains in the human protein sequence. Figure 6.27 shows resolution enhanced forms of the aromatic regions of the spectra in Fig. 6.26. The C2 proton resonances of the two tryptophans are found at very similar chemical shifts in both spectra but other obvious similarities are few. Indeed, the human protein spectrum is less dispersed over the chemical shift range than the bovine, although Fig. 6.22 does show greater spread of resonances at low pH. Obviously more detailed comparisons of the two spectra must await further assignment of the aromatic region of the human fragment 2 spectrum. The kringle structure has been shown to be composed of a hydrophobic core of closely related aromatic residues and certainly the structural element involving Trp A and Leu 45 is present in human fragment 2 and Trp B is probably related to this and also conserved structurally. Differences in the positions of other resonances of the aromatic region of the spectra of the two proteins may then result from subtle juxtaposition of the interacting residues brought about by the altered composition. The temperature dependence of the aromatic region of the human protein (Fig. 6.25) clearly shows that many resonances do experience secondary shifts in accord with this. In addition, the differences in the αCH resonances between the two spectra confirms some alteration of secondary structure.

6.7 Summary

The kringle structure from another protein, prothrombin has been studied in this chapter and related to the findings already described for the plasminogen kringle. The aromatic region of the spectrum of bovine fragment 2 has been assigned with the exception of two residues,

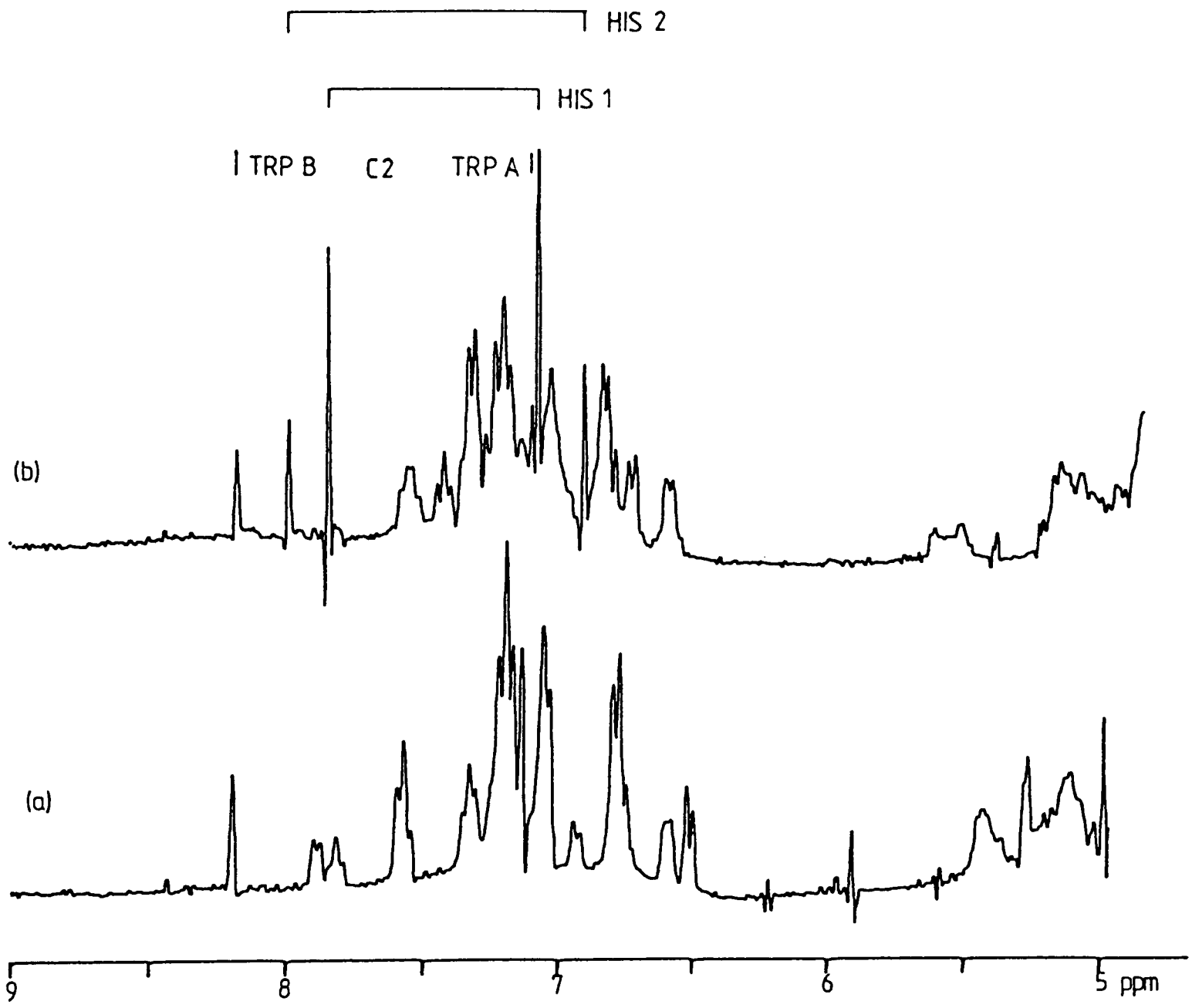

Fig. 6.27 Resolution enhanced spectra of the aromatic region; 37°C, pH 7.4 (a) Bovine fragment 2 (b) Human fragment 2, with a summary of assigned aromatic resonances.

as was also achieved for kringle 4. NOE experiments and a pH dependence study revealed a number of detailed features common to both proteins and indeed arguments were proffered from kringle 4 results, to suggest second stage assignments in the fragment 2 spectrum. Comparison of the bovine and human fragment 2 spectra perhaps showed more differences than might have been anticipated in view of all the aromatic residues being conserved. But, the structural element involving the tryptophan residues around the second disulphide bridge with the Leucine 45 residue, close to the third bridge was seen to be very well maintained in all three proteins. Likewise, pH dependence studies demonstrated effects on the C2 proton of Trp B in all the proteins. In kringle 4 this feature was shown to be caused by a carboxyl group ionisation and markedly affected by ligand binding. However, no specific ligand binding capability is known for prothrombin fragment 2 although, as to be considered in the next chapter, it is involved in mediating protein-protein interactions.

CHAPTER 7

BIOLOGICAL SIGNIFICANCE OF THE KRINGLE STRUCTURE

7.1 Introduction

It must be stressed at the outset that the biological roles of the kringle structure are not known in detail. In chapter 1, involvement in mediating protein - protein interactions was one function ascribed to certain kringles and this will be considered further below. It is worth reiterating that kringles have been found only in the non protease portion of serine protease zymogens involved in maintaining haemostasis and often present in more than one copy. Protein - protein interactions are an inevitable feature of enzyme cascade systems and their means of control, and a role for the "pro" parts of the protein in this might well have been anticipated, especially in view of the large proportion of the molecule that the contained kringles occupy (see Table 1.1). Furthermore, the multiple copies of a closely homologous sequence of residues immediately raises the possibility of them performing a similar specific function in much the same way as the presence of homologous residues in the protease portion of the molecules shows them all to be forms of the classical serine proteases. Thus, in this final chapter each kringle containing protein is considered in turn. Data from other sources is discussed as it relates to the possible function of the kringle within the molecule and considered in the light of the findings that have been presented in the previous four chapters.

7.2 Prothrombin

Prothrombin contains two kringles in the N terminal, non protease portion of the molecule and each of these can be studied separately

as a result of limited enzymic digestion (part of which at least occurs in vivo) as fragment 1 and 2 respectively.

7.2.1 Prothrombin Fragment 1

Fragment 1 contains the first kringle of prothrombin and the sequence of the bovine protein is shown in Fig. 7.1. It also carries two of the three asparagine linked oligosaccharide chains of the entire molecule on side chains within the kringle sequence (Magnusson et al., 1975). The function of the carbohydrate chains on proteins is not precisely known for most cases but possibilities include biological recognition and influencing protein folding and conformation (Berger et al., 1982). With regard to the former suggestion , it is known that the state of the carbohydrate chain can influence the rate of prothrombin turnover by recognition of the terminal carbohydrate residues (Nelsestuen and Suttie, 1971). However, the possibility of the sugar residues altering the conformation of the kringle part of the molecule is particularly interesting. From the spectrum of the aliphatic region of bovine prothrombin fragment 1 shown in Fig. 3.19(d) it can be seen that the structural element giving rise to the marked upfield shift of the Leu 45 methyl proton resonance remains; this has also been shown to incorporate one or both of the conserved Trps, 25 and 61, some distance away in the primary sequence. This suggests that at least part of the kringle structure is unaffected by the presence of the carbohydrate chains despite the fact that one of them is present on Asn 36. An attempt was made to remove the oligosaccharides from bovine fragment 1 in conjunction with Dr. J. Holloway, using anhydrous hydrogen flouride (Mort and Lamport, 1977). Unfortunately, too little product was obtained from a sizeable outlay of protein to be of any use for NMR studies and the procedure was not repeated.

Fragment 1, the first 157 residues of bovine prothrombin, includes

Fig. 7.1 Amino acid sequence of bovine prothrombin fragment 1 (Magnusson et al., 1975). CHO indicates attached carbohydrate chains.

not only the first kringle but also the ten γ carboxyglutamic acid residues in the N terminal portion that are formedin a post translational vitamin K dependent modification (Stenflo and Suttie, 1977). These residues are responsible for binding the prothrombin molecule to phospholipid surfaces in the presence of calcium, and in vitro studies show the rate of activation of prothrombin to be considerably enhanced by this interaction (Suttie and Jackson, 1977). (Indeed, the rat poison warfarin, also used clinically as an anti-thrombotic, produces its results by preventing the vitamin K dependent modification of several blood clotting proteins including prothrombin from occurring and thus leading to fatal haemorrhage in rats). There have been numerous studies of calcium binding to fragment 1, which carries all the high affinity sites of prothrombin, and the binding is found to be positively co-operative (Bajaj et al., 1975). But it was also found that the presence of γ carboxylated glutamate residues alone is not sufficient for co-operativity, as shown in experiments that demonstrate that intact disulphide bridges in fragment 1 and, by inference, specific protein tertiary structure are also necessary for co-operative calcium binding (Henriksen and Jackson, 1975). Although, fragment 1 contains two disulphide bridges outside those of its kringle portion, this and other features of calcium binding and fragment 1 structure do raise the possibility of a role for the first kringle of prothrombin in the important metal ion binding process.

Indeed, as mentioned in Chapter 1 the original aim had been to study the effects of metal ion binding to fragment 1 using NMR spectroscopy and combined with lanthanide ion probe studies. Fragment 1 has a higher molecular weight (22,500) and in particular the aromatic region of the spectrum is less well resolved than for the proteins discussed above. Many experiments were performed and included both calcium and magnesium ion titrations. Although addition of calcium ions caused protein

aggregation at the concentrations used in the NMR studies, the spectral changes observed during the titration were minimal. This led, with other results, to the conclusion that there was no significant change in the tertiary structure of fragment 1 on the binding of calcium ions as revealed by NMR (Esnouf et al., 1979). This was at variance with the results of studies using other physical methods (Nelsestuen et al., 1981) which indicated quite substantial structural alterations to occur on the addition of calcium ions. However, with the insight subsequently gained into the structure of the kringle portion of the molecule this discrepancy can be understood.

From the previous discussion it is very likely that even with the attached carbohydrate chains the kringle portion of the molecule is still a tightly folded globular structure. However, the N terminal part of the protein contains many charged residues including twenty carboxyl groups from the ten γ carboxyglutamic acid residues, and may well be expected to have a very extended conformation in solution. That such a situation does pertain has been strongly indicated by the results obtained from X-ray crystallographic studies (Aschaffenburg et al., 1983). A photograph of the electron density map obtained to 6 Å resolution is shown in Fig. 7.2, and it can be seen that two distinct regions are demonstrated. An extended portion is considered to be the N terminal region and a compact globular part taken to be the kringle region of the molecule. Unfortunately the protein backbone cannot be accurately discerned, as yet, for comparison with our model presented in section 5.8 for kringle 4 of human plasminogen. However, the picture of a globular protein fold is in complete agreement with our NMR studies. The discrepancy over the preliminary results of calcium binding as studied by NMR compared with other methods are then understood, in that calcium ion addition could cause quite large changes in the conformation of the extended part of the molecule but which would

Fig. 7.2 Photograph of the balsa wood model of bovine prothrombin fragment 1 from X-ray crystal data to 6Å resolution. The model was constructed by Dr M.P. Esnouf.

not necessarily alter the NMR spectrum of the whole protein to any great extent at all.

Thus, the prospects of further comparison of better resolved crystal structures and the results of NMR studies look extremely promising, and much remains to be learnt about the significance of the kringle structure in fragment 1 of prothrombin. A little more is known about this aspect of the kringle contained in fragment 2.

7.2.2 Prothrombin Fragment 2

The biological activation of prothrombin has been shown to involve not only phospholid surfaces and calcium but also activated factor X and active factor V; the last two being proteins involved slightly earlier in the blood clotting cascade (Esnouf, 1977). Such an activation complex requires several protein-protein interactions and indeed, for instance, active factor V has been shown to bind to prothrombin (Esmon et al., 1973). Ong (1979) demonstrated that factor V bound specifically to the fragment 2 portion (residues 157 - 274) of prothrombin containing the second kringle and therefore also the two conserved tryptophan residues. Cleavage of bovine prothrombin fragment 2 at these tryptophans and subsequent reduction and carboxymethylation results in three peptides. Binding studies with each peptide showed that factor V bound to the middle of the three peptides and limited chymotryptic digest indicated the strongest affinity to active factor V to reside in a dodecapeptide comprising Ser 34 to Leu 45 as numbered in Fig. 6.1 and situated on the right hand outer loop of the kringle. This part of the molecule was demonstrated from the chemically modified proteins to be essential for preserving the ω-aminocarboxylic acid binding site of kringle 4. In addition it was also suggested in the last chapter that fragment 2 may process the strucural elements required for binding the amino group of ω-aminocarboxylic acids but various other

differences in the sequence, compared to kringle 4, result in this not being the case. As yet no specific ligands or binding peptides are known for fragment 2, but the data discussed above do confirm the fragment 2 kringle to be very much involved in mediating protein-protein interactions vital to the biological function of prothrombin. The five kringles of plasminogen are now considered.

7.3 Plasminogen

Plasmin, the serine protease derived from plasminogen, has a broad specificity very similar to that of trypsin, yet its intravascular action is primarily directed toward a single protein, fibrin. Wiman and Collen (1978) have proposed a model to account for this restricted activity. In essence plasminogen and its activators are bound to fibrin during clot formation and any plasmin released into the surrounding medium is rapidly inactivated by the fast acting plasmin inhibitor, α_2-antiplasmin. These protein interactions are apparently mediated by the ω-aminocarboxylic acid binding sites (referred to as lysine binding sites) of plasminogen since they have been shown to coincide with the fibrin binding sites of plasminogen (Wiman and Wallen, 1977; Thorsen et al.,1981) and with those essential for binding the rapid acting α_2-antiplasmin (Wiman et al., 1979). It has been known for over 20 years that the amino acids such as 6-aminohexanoic acid have antifibrinolytic properties (Okamoto et al., 1959) and indeed agents such as tranexamic acid are used in the medical management of patients who have had a subarachnoid haemorrhage, although clinical trials have been reported to be contradictory on their usefulness (Warlow, 1983). Their mode of action probably includes inhibition of the binding of plasminogen to fibrin (Thorsen, 1975).

Native human plasminogen (termed Glu-plasminogen from its N-terminal residue contains one strong (K_d 9μM) and possibly four or five weak (K_d 5mM)

6-aminohexanoic acid binding sites (Markus et al., 1978a). Glu-plasminogen is readily proteolytically cleaved, by plasmin for instance, with the loss of seventy-six residues from the N terminus giving rise to Lys-plasminogen and now the high affinity binding site is somewhat weaker (K_d 35μM) and at the expense of one of the weak sites, a new site of intermediate affinity for 6 aminohexanoic acid (K_d 260μM) appears; the remaining low affinity sites are essentially unchanged (Markus et al., 1978b). The same pattern of high, intermediate and low affinity ω-aminocarboxylic acid binding sites was detected using tranexamic acid in the binding assay, the only difference being that each binding site showed about an order of magnitude higher affinity for tranexamic acid than for 6-aminohexanoic acid (Markus et al., 1979). Thus it is seen that plasminogen contains about five independent ω-aminocarboxylic acid binding sites of similar ligand specificity.

However, although plasminogen contains five kringles, studies on fragments of the protein revealed that only isolated kringles 1 and 4 each contain a single high affinity site for 6-aminohexanoic acid (K_d16 and 36μM respectively); kringle 1+2+3 carries a strong and weak site, whereas no ligand binding could be demonstrated in a fragment bearing kringle 5 alone (Lerch et al., 1980b). Thus, these kringles account for three of the suggested five ω-aminocarboxylic acid binding sites in intact plasminogen. This discrepancy in the number of binding sites detectable in the constituent fragments may well be due to the fragmentation itself.

Váli and Patthy (1982) have shown it is only the high affinity binding sites that provide a suitably low K_d value to mediate dectable binding to lysine-Sepharose columns, and indeed all plasminogen forms and fragments which bind to lysine-Sepharose harbour a high affinity ω-aminocarboxylic acid binding site. They, also demonstrated by chemical modification that the single high affinity site present in intact plasminogen is the one contained in kringle 1 and that the one on kringle 4 is masked and only

partially revealed, forming an intermediate affinity site, in Lys-plasminogen. Thus this indicates that it is the kringle 1 part of the molecule that mediates fibrin and α_2-antiplasmin binding through its high affinity lysine binding site. Thorsen and coworkers (1981), studying binding of plasminogen and fragments to fibrin in the presence of ω-aminocarboxylic acids and α_2-antiplasmin, have confirmed much of the above. (However, they did raise the possibility that rather than direct binding via the high affinity lysine binding site, there was the alternative possibility of binding through a different place specific for fibrin, and that the ω-aminocarboxylic acid when bound to the high affinity lysine binding site acted as an allosteric effector to change the conformation of the fibrin binding site). In particular, they found that the fibrin binding of kringle 4 was relatively weak compared to that of kringle 1+2+3, and they confirmed the finding of Wiman et al., (1979) that an important binding site for α_2-antiplasmin is located on kringle 1+2+3. They also found that the fragment containing kringle 5 alone (comprising kringle 5 and the catalytic part of the molecule known as "miniplasminogen", residues 442 - 790) bound to fibrin more strongly than any of the other fragments, despite data from the same laboratory showing this fragment to have no available lysine binding site. Several possible explanations can be proposed for this that are consistent with other findings and kringle 5 will be considered in a little more detail below.

Thorsen and coworkers (1981) also confirmed that the presence of residues 1 - 76 in Glu-plasminogen decreases the extent of fibrin binding when compared to Lys-plasminogen. When native Glu-plasminogen is converted to Lys-plasminogen there are large changes in the relative position of entire domains leading to a much looser conformation (Vuk-Pavlovic et al., 1979) and, as discussed above, a partial unmasking of the kringle 4 binding site. Now a very similar general loosening of the plasminogen molecule

has been indicated to occur in native Glu-plasminogen, from studies on saturating the lysine binding sites with ω-aminocarboxylic acid resulting in the sedimentation coefficient decreasing, the molecular weight as determined by gel filtration rising, and the intrinsic flourescence increasing (Markus et al., 1979, Wallen and Wiman, 1972 , Violand et al., 1978).

Váli and Patthy (1982) have proposed a model for the role of kringle 4 in controlling the conformation of plasminogen to account for these results. They suggest that in intact Glu-plasminogen, kringle 4 is involved in interactions with certain regions of plasminogen, which include the N terminal activation peptide and directly or indirectly some segments of kringle 1+2+3. The intramolecular interactions compete for the lysine binding site of kringle 4 and therefore it appears as one of the weak sites for small ligands and the interactions protect the binding site from chemical modification. Conversion to Lys-plasminogen with the concomittant conformational change results in the loss of the compact structure of Glu-plasminogen and some of the interaction competing for the kringle 4 binding site, as reflected in an increase in the affinity of the site for small ligands. In Lys-plasminogen though, the kringle 1+2+3 region still interacts with the kringle 4 part and indeed, it has been found that even Lys-plasminogen undergoes a definite conformational change in the presence of ligands (Markus et al., 1979) it is only in the isolated kringle 4 that the binding site has comparable ligand affinity to that of the high affinity binding sites of plasminogen or kringle 1.

This model, as the authors point out, assumes that the binding site in kringle 4 is fully formed even in Glu-plasminogen and changes in its affinity reflect changes in its accessibility rather than stepwise evolution of the binding site. A number of points can be made to support this notion and that the kringle has a stable autonomous structure:

(i) Studies of various ω-aminocarboxylic acids have revealed the binding site to have very strict structural requirements in the ligands. This was discussed in chapter 4, but in particular the sharp cut off in the optimum length of the ligand indicates a rigid binding site since in the case of a more flexible site a much less sharp distance requirement would be expected. This conclusion was amply demonstrated by the results of the ligand binding and chemical modification studies presented in the previous chapters.

(ii) Winn et al., (1980) have shown that kringle 1+2+3, kringle 4, Glu- and Lys-plasminogen all display an identical ligand specificity spectrum. Neither the optimal ligand length nor the strictness of the length requirement differs in the different plasminogen forms and fragments. The results already presented demonstrated that bovine fragment 2 and kringle 4 - kringles from two different proteins - have similar structures well supporting the postulate of closely conserved structures in the various kringle sequences.

(iii) Although conversion of Glu- to Lys plasminogen leads to a dramatic conformational change manifest in several physiochemical parameters discussed above, the far ultraviolet circular dichoism spectra do not reveal any significant change in the polypeptide backbone (Sjöholm et al., 1973), in addition, circular polarisation of luminescence spectra of Glu-plasminogen with and without ligand present are indistinguishable and this was interpreted to mean that the gross conformational change of plasminogen is due to changes in spatial relationship of entire domains, but little change within the domains (Vuk-Pavlovic et al., 1979). These domains can probably be identified with the kringles. Again ligand binding to kringle 4 was shown in Chapter 4 to cause only small local perturbations in the spatial arrangement of side chains and certainly no gross

conformational change in the kringle structure, in complete support of the idea of the kringles being independent structures strung like beads on a chain in plasminogen. This is further suggested by (iv).

(iv) The flexibility of the interkringle regions is evident from the sensitivity of these regions to proteases, since freedom of movement of peptide chains is a precondition for susceptibility to limited proteolysis in native proteins (Neurath, 1975). The peptide chains connecting kringle 3 to kringle 4 and kringle 4 to kringle 5 are selectively attacked by elastase and the same regions are also the sites for limited proteolysis by thermolysin and subtilisin (Sottrup-Jensen et al., 1978), emphasising that the primary factor that decides the susceptibility of these regions to the different proteases is the flexibility of these probably random peptide structures. It seems likely therefore that the intervening peptide segments serve as hinges for the large movements of the kringles relative to each other.

With reference to the last point it is worthy of note that proteolytic cleavage of prothrombin by thrombin and factor Xa also takes place in the interkringle regions (Suttie and Jackson, 1977).

Hollerman et al., (1975) have shown that plasminogen will also bind to p-aminobenzamidine substituted Sepharose and provided evidence that the binding sites for ω-aminocarboxylic acids and benzamidine are independent since lysine cannot elute plasminogen from p-aminobenzamidine Sepharose and vice versa. Markwardt et al., (1968) have reported that benzamidines are potent competitive inhibitors of plasmin when either the amidase or fibrinolytic activity of the enzyme is assayed and suggested that these compounds are bound in the specificity pocket of the enzyme, in analogy with the binding of these inhibitors to trypsin (Maries-Guia and Shaw, 1965)

and other trypsin-like proteases (Geratz and Tidwell, 1978). However, Hollerman and coworkers showed that the benzamidine binding site is not identical with the primary specificity site of the enzyme as plasmin inactivated by other serine protease inhibitors still showed affinity for p-aminobenzamidine-Sepharose. Varadi and Patthy (1981) have demonstrated that apart from the primary specificity there is a second benzamidine binding site in the catalytic chain in accord with results for several trypsin-like proteases (Geratz and Tidwell, 1978). In addition, they also showed that a further benzamidine binding site is carried by the kringle 5 portion. This raises the possibility that this domain may also participate in the interactions of plasminogenwith fibrin that was mentioned above.

The summary of data on the functions of kringles so far, has confirmed the expectation of their involvement in the protein-protein interactions of zymogens that contain non protease portions comprising half the molecule or more, and for which activation in protein complexes is an integral part of their biological role. The NMR studies of kringles described in this thesis confirm these entities to have specific globular protein folds that can be modified very simply to alter their biological function. They have been demonstrated to have consistently conserved structural elements despite being present in different proteins but related by conserved residues in the sequence. The ligand binding studies of kringle 4 have demonstrated its structure to be folded to bind an ε amino group, ideally suited to interaction with the lysine residue of another protein, and it is conceivable that subtle variations on the theme could result in other kringles making excellent units for mediating the recognition and binding of other proteins. The postulate of a regulatory role for kringle 4 in the plasminogen molecule by virtue of its lysine binding site is particularly intriguing.

It is clear that much is to be revealed on the functions of kringles

and many details are still to be elucidated. However, the knowledge already gained makes possible some understanding of the possible roles of the kringles in plasminogen activators briefly considered below and about which much less is known.

7.4 Plasminogen Activators

Tissue plasminogen activator is known to bind tightly to fibrin and the possibilty of binding to plasminogen rather than fibrin was ruled out by Thorsen et al., (1972). Furthermore, the activation of plasminogen by tissue plasminogen activator is enhanced in the presence of fibrin but it is a relatively poor plasminogen activator in the absence of fibrin (Wallen, 1978). These protein interactions obviously result in the fibrinolytic activity being concentrated at the precise location that it is required - the fibrin clot - and adds support to the proposed model of Wiman and Collen (1978) which suggests that fibrin mediates its own subsequent destruction. Furthermore, the efficient activation of plasminogen only occurring when the activator is fibrin bound means the powerful protease plasmin is localised to its required site of action and indiscriminate activity in the plasma is minimised as well as being prevented by the α_2-antiplasmin inhibitor. The previous discussion strongly suggests a vital role for the two kringles of the tissue plasminogen activator in mediating the protein-protein interactions fundamental to its action. In addition, by analogy with the findings for plasminogen it is possible that one of the kringles may also be involved in intramolecular interactions, which via fibrin binding, may help to control the catalytic activity of the molecule.

Urokinase, on the other hand, shows only very weak binding to fibrin (Thorsen et al., 1972). In accord with this finding, studies comparing tissue plasminogen activator with urokinase, revealed that the latter caused

extensive activation of the fibrinolytic system as evidenced by depletion of plasminogen, α_2-antiplasmin and fibrinogen, whereas the former resulted in only moderate activation of the fibrinolytic system but nevertheless causing extensive fibrinolysis and only very limited fibrinogenolysis (Matsuo et al., 1981). Thus, it could be suggested that any fibrin binding capability invested in the kringles of tissue plasminogen activator has been substantially lost in the single kringle of urokinase or alternatively the latter is more specifically designed to interact with plasminogen in a similar fashion to α_2-antiplasmin, in either case the kringle of urokinase would be expected to play a part but it is not so clear what this may be.

It is noteworthy that urokinase has been used clinically as a thrombolytic agent but is found to cause systemic activation of plasminogen with consumption of α_2-antiplasmin and fibrinogen breakdown as unwanted side effects (Collen and Verstraete, 1979). This was also found to be the case for streptokinase, a bacterial enzyme, that is also used as a thrombolytic agent. However, clinical use of tissue-type plasminogen activator has demonstrated its thrombolytic efficacy without any signs of systemic activation of the fibrinolytic system that lead to haemostatic breakdown and bleeding (Weimar et al., 1981). Matsuo and coworkers (1981) also demonstrated that in vitro the tissue plasminogen activator has a lower threshold activity and a progressive effect in time which urokinase did not display. Thus, it is suggested to be a superior thrombolytic agent compared to urokinase. Unfortunately, until recently it has only been available in extremely small amounts.

Plasminogen activator production is a feature of several human tumours and they produce more activator than the normal tissues confirming a a correlation between neoplasia and plasminogen activator production (Nagy et al., 1977). Human melanoma cells have been used as a source of tissue-type plasminogen activator and of its messenger RNA for bacterial cloning

(Rijken and Collen, 1981, Pennica et al., 1983). Interestingly, many other human tumours produce a urokinase type plasminogen activator, for instance in ovarian carcinoma (Åstedt and Holmberg, 1976) and in patients with malignant ovarian tumours, fibrinogen-fibrin degradation products in the blood are a common finding, with extremely large amounts being constantly found in ascitic fluid. This indicates the activator to be highly active in vivo in such patients, but the role played by it in the survival, growth and spread of the cancer remains to be elucidated. With regard to the spread of cancer - the feature characteristic of malignancy - the possibility of kringle mediated protein-protein interactions contributing to the action of the secreted plasminogen activators suggests the design of chemical inhibitors, such as tranexamic acid in the fibrinolytic system, may eventually be of theraputic benefit.

7.5 Conclusion and Prospects for Future Study

This chapter has shown the kringle structure to be an important biological entity, very much involved in the recognition and binding of other proteins involved in multi protein complexes. This thesis has demonstrated it to be a tightly folded globular protein entirely consistent with it behaving as an autonomous structural unit within the protein as suggested by a number of other studies. Kringle 4 of human plasminogen has been seen to have a fold giving rise to a specific ligand binding site. Chemical modifications and comparison with prothrombin fragment 2 has shown this property to be very susceptible to minor sequence alterations without concomittant gross structural changes whatsoever. Thus, the concept of the kringle as a highly adaptable unit for the provision of highly specific binding sites is promulgated and this coincides with much of what is known of its biological function.

This thesis provides a foundation for further study of kringle structure

and function. Prospects for refining the solution structure of a good deal of the kringle 4 molecule to considerable detail were discussed in section 5.9 and shown to be very promising. Information on the structure of kringle 4 has already been shown to be very relevent to the study of that of prothrombin fragment 2 and will provide much further insight into the kringle portion of prothrombin fragment 1. Dr. Patthy has already supplied us with kringle 5 of human plasminogen which may well prove to be as fascinating a protein as kringle 4. In addition, kringle 5 contains a benzamidine site as discussed above which promises to make a valuable and interesting contrast to ω-aminocarboxylic acid binding studies being pursued on kringle 4.

Overall, the power of NMR as a technique for the investigation of protein structure in solution has been clearly seen. In turn the kringle has been seen to be a protein ideally suited to study by NMR. The prospect of producing a structure using NMR, approaching that of X-ray crystallographic analysis in detail, has been demonstrated to be a practical proposition in the not too distant future.

APPENDIX I

THE SEQUENCES OF TWELVE KRINGLES

Table A.I.1 lists the amino acid compositions of each kringle and also gives the single-letter code for the amino acids. Using this code Table A.I.2 shows the sequences of the following kringles:

BF1	Bovine Prothrombin Fragment One	Magnusson et al., (1975)
BF2	Bovine Prothrombin Fragment Two	
HF1	Human Prothrombin Fragment One	Walz et al., (1977)
HF2	Human Prothrombin Fragment Two	
PK1		
PK2		
PK3	Human Plasminogen Kringles	Sottrup-Jenson et al., (1978)
PK4		
PK5		
PA1	Human Tissue-Type Plasminogen Kringles	Pennica et al., (1983)
PA2		
HU1	Human Urokinase Kringle	Günzler et al., (1982)

Sequence numbering has been based for historical reasons on the prothrombin kringle as archetype and deletions and insertions in the other sequences have been accommodated by aligning them to achieve maximum homology.

Table A.I.1

Compositions

Residue	Code	BF1	HF1	BF2	HF2	PK1	PK2	PK3	PK4	PK5	PA1	PA2	HU1
Ala	A	2	3	8	8	1	2	3	2	4	7	6	4
Arg	R	8	7	6	3	5	5	5	4	6	6	4	7
Asn	N	5	5	5	4	5	6	8	5	5	5	6	5
Asp	D	2	3	7	6	6	5	2	4	4	4	3	4
Cys	C	6	6	6	6	6	7	7	6	6	6	6	6
Gln	Q	1	3	3	6	2	2	3	3	3	2	2	5
Glu	E	6	5	6	3	5	4	5	2	3	4	2	2
Gly	G	7	6	6	8	6	4	5	6	9	7	8	7
His	H	2	2	-	2	2	3	5	3	2	1	2	5
Ile	I	3	4	-	-	2	3	1	-	1	2	2	-
Leu	L	3	3	5	6	2	4	2	2	2	3	7	7
Lys	K	1	1	2	3	6	7	4	6	4	4	4	3
Met	M	1	-	-	-	1	2	-	2	1	-	2	2
Phe	F	1	1	3	3	1	2	-	1	2	2	1	1
Pro	P	7	7	5	4	8	7	6	6	8	5	5	5
Ser	S	7	7	5	3	6	6	4	7	1	10	7	3
Thr	T	7	9	2	2	8	3	8	10	9	4	4	4
Trp	W	2	2	2	2	2	3	3	3	2	3	3	2
Tyr	Y	3	3	4	4	5	3	3	5	5	6	5	5
Val	V	5	2	4	6	-	-	4	1	3	1	3	5
		79	79	79	79	79	78	78	78	80	82	82	82

Table A.I.2

The Amino Acid Sequences of Twelve Kringles

	1								10								20								30
BF1	C	A	E	G	V	G	M	N	Y	R	G	*N	V	S	V	T	R	S	G	I	E	C	Q	L	W	R	S	R	Y	P
HF1	C	A	E	G	L	G	T	N	Y	R	G	*N	V	S	I	T	R	S	G	I	E	C	Q	L	W	R	S	R	Y	P
BF2	C	V	P	D	R	G	R	E	Y	R	G	R	L	A	V	T	T	S	G	S	R	C	L	A	W	S	S	E	Q	A
HF2	C	V	P	D	R	G	Q	Q	Y	Q	G	R	L	A	V	T	T	H	G	L	P	C	L	A	W	A	S	A	Q	A
PK1	C	K	T	G	D	G	K	N	Y	R	G	T	M	S	K	T	K	N	G	I	T	C	Q	K	W	S	S	T	S	P
PK2	C	M	H	C	S	G	E	N	Y	D	G	K	I	S	K	T	M	S	G	L	E	C	Q	A	W	D	S	Q	S	P
PK3	C	L	K	G	T	G	E	N	Y	R	G	N	V	A	V	T	V	S	G	H	T	C	Q	H	W	S	A	Q	T	P
PK4	C	Y	H	G	D	G	Q	S	Y	R	G	T	S	S	T	T	T	T	G	K	K	C	Q	S	W	S	S	M	T	P
PK5	C	M	F	G	D	G	K	G	Y	R	G	K	R	A	T	T	V	T	G	T	P	C	Q	D	W	A	A	Q	E	P
PA1	C	Y	E	D	Q	G	I	S	Y	R	G	T	W	S	T	A	E	S	G	A	E	C	T	N	W	*N	S	SAL		A
PA2	C	Y	F	G	*N	G	S	A	Y	R	G	T	H	S	L	T	E	S	G	A	S	C	L	P	W	N	S	MIL		I
HU1	C	Y	E	G	N	G	H	F	Y	R	G	K	A	S	T	D	T	M	G	R	P	C	L	P	W	N	S	ATV		L

	31								40								50								60
BF1	H	K	P	E	I	*N	S	T	T	H	P	G	A	D	L	R	E	N	F	C	R	N	P	D	G	S	I	T	G	P
HF1	H	K	P	E	I	*N	S	T	T	H	P	G	A	D	L	Q	E	N	F	C	R	N	P	D	S	S	I	T	G	P
BF2	K	A	L	S	K	D	Q	D	F	N	P	A	V	P	L	A	E	N	F	C	R	N	P	D	G	D	E	E	G	A
HF2	K	A	L	S	K	H	Q	D	F	N	S	A	V	Q	L	V	E	N	F	C	R	N	P	D	G	D	E	E	G	V
PK1	H	R	P	R	F	S	P	A	T	H	P	S	E	G	L	E	E	N	Y	C	R	N	P	D	N	D	P	Q	G	P
PK2	H	A	H	G	Y	I	P	S	K	F	P	N	K	N	L	K	K	N	Y	C	R	N	P	D	R	E	L	R	-	P
PK3	H	T	H	N	R	T	P	E	N	E	P	C	K	N	L	D	E	N	Y	C	R	N	P	D	G	K	R	A	-	P
PK4	H	R	H	Q	K	T	P	E	N	Y	P	N	A	G	L	T	M	N	Y	C	R	N	P	D	A	D	K	G	-	P
PK5	H	R	H	S	IFT		P	E	T	N	P	R	A	G	L	E	K	N	Y	C	R	N	P	D	G	N	V	G	G	P
PA1	Q	K	PYS		G	R	R	P	D	A	I	R	L	G	L	G	NHN		Y	C	R	N	P	D	R	D	S	K	-	P
PA2	G	K	VYT		A	Q	*N	P	S	A	Q	A	L	G	L	G	KHN		Y	C	R	N	P	D	G	D	A	K	-	P
HU1	Q	Q	TYH		A	H	R	S	D	A	L	Q	L	G	L	G	KHN		Y	C	R	N	P	D	N	R	R	R	-	P

	61								70								79
BF1	W	C	Y	T	T	S	P	T	L	R	R	E	E	C	S	V	P	V	C
HF1	W	C	Y	T	T	D	P	T	A	R	R	Q	E	C	S	T	P	V	C
BF2	W	C	Y	V	A	D	Q	P	G	D	F	E	Y	C	N	L	N	Y	C
HF2	W	C	Y	V	A	G	K	P	G	D	F	G	Y	C	D	L	N	Y	C
PK1	W	C	Y	T	T	D	P	E	K	R	Y	D	Y	C	D	I	L	E	C
PK2	W	C	F	T	T	D	P	N	K	R	W	E	L	C	D	I	P	R	C
PK3	W	C	H	T	T	N	S	Q	V	R	W	E	Y	C	K	I	P	S	C
PK4	W	C	F	T	T	D	P	S	V	R	W	E	Y	C	N	L	K	K	C
PK5	W	C	Y	T	T	N	P	R	K	L	Y	T	Y	C	D	V	P	Q	C
PA1	W	C	Y	V	F	K	A	G	K	Y	SSE		F	C	S	T	P	A	C
PA2	W	C	H	V	L	K	N	RRL		T	W	E	Y	C	D	V	P	S	C
HU1	W	C	Y	VQV		G	L	K	P	L	V	Q	E	C	M	V	H	D	C

* Indicates site of attachment of the carbohydrate chains.

APPENDIX II

PARAMETERS USED IN SPECTRAL SIMULATIONS

NTCSIM was the spectral simulation used in the Nicolet NTCFT-1180 programme. A linewidth of 6Hz was used for all kringle 4 resonances but increased to 8Hz for the bovine fragment 2 spectrum. In generating the individual spectra, the programme demands a threshold line intensity and this was set to 0.05 for phenylalanines and 0.1 for tryptophans in order to limit the number of spectral lines generated. It was otherwise set to zero. A coupling constant of 7.8Hz was used throughout. In the data below the multiplets are indicated: s - singlet, d - doublet, t - triplet with a subscript for 2 proton intensity. The following spectra were simulated:

Aromatic Region of Kringle 4; 37°C, pH 7.5 (Fig. 3.16(b))

Trp A	4.951(b)	6.441(t)	7.125(s)	7.435(d)	8.215(d)
Trp B	4.841(t)	6.575(t)	6.941(d)	6.964(d)	7.765(s)
Trp C	5.090(t)	6.620(d)	6.645(s)	6.731(t)	7.075(d)
Tyr A	6.516(d_2)	6.785(d_2)			
Tyr B	6.835(d_2)	6.946(d_2)			
Tyr C	6.892(d_2)	7.285(d_2)			
Tyr D	7.005(d_2)	7.205(d_2)			
His A	6.845(s)	8.270(s)			
His B	7.060(s)	7.675(s)			
His C	7.530(s)	8.320(s)			

Aromatic Region of Kringle 4 in the Presence of 6 Aminohexanoic Acid; 37°C pH 8.4 (Fig. 4.15(b)).

Trp A	4.944(t)	6.474(t)	7.144(s)	7.435(d)	8.244(d)
Trp B	4.926(t)	6.604(t)	6.773(d)	7.010(d)	7.785(s)
Trp C	5.020(t)	6.618(d)	6.643(s)	6.731(t)	7.131(d)
Tyr A	6.513(d_2)	6.789(d_2)			
Tyr B	6.843(d_2)	6.941(d_2)			
Tyr C	6.803(d_2)	7.294(d_2)			
Tyr D	7.011(d_2)	7.213(d_2)			
His A	6.892(s)	8.264(s)			
His B	7.037(s)	7.620(s)			
His C	7.515(s)	8.293(s)			

Aromatic Region of Bovine Fragment 2; 37°C, pH 7.6 (Fig. 6.16(c))

Trp A	5.217(t)	6.717(t)	7.131(s)	7.584(d)	7.890(d)
Trp B	5.127(t)	6.775(d)	6.926(d)	7.075(t)	8.199(s)
Phe A	6.507(d_2)	6.761(t_2)	7.037(t)		
Phe B	7.047(d_2)	7.229(t_1)	7.327(t_2)		
Phe C	7.177(d_2)	7.567(t_2)	7.818(t_2)		
Tyr A	6.585(d_2)	7.223(d_2)			
Tyr B	6.783(d_2)	7.154(d_2)			

APPENDIX III

AMINO ACID SEQUENCE OF HUMAN PROTHROMBIN FRAGMENT 2

(Walz et al., 1977)

REFERENCES

AGUIAR, A.B.V.P.de (1980). PMR studies of some molecules of biological interest using inorganic probes. D.PHIL THESIS, OXFORD.

ASCHAFFENBURG, R., BLAKE, C.C.F., BURRIDGE, J.M., ESNOUF, M.P. (1977) Preliminary X-ray investigation of fragment 1 of bovine prothrombin. J.MOL. BIOL., 114, 575-579.

ASCHAFFENBURG,R., BLAKE, C.C.F., BURRIDGE, J.M., ESNOUF, M.P. (1983). Data to be published.

ÅSTEDT, B., HOLMBERG, L. (1976). Immunological identity of urokinase and ovarian carcinoma plasminogen activator released in tissue culture. NATURE, 261, 595-596.

BAJAJ, S.P., BUTKOWSKI, R.J., MANN, K.G. (1975). Prothrombin fragments, Ca^{2+} binding and activation kinetics. J.BIOL.CHEM., 250, 2150-2156.

BERGER, E.G., BUDDECKE, E., KAMERLING, J.P., KOBATA, A., PAULSON, J.C., VLIEGENTHART, J.F.G. (1982) Structure, biosynthesis and functions of glycoprotein glycans. EXPERIENTIA, 38, 1129-1258.

BLAKE, C.C.F., GRACE, D.E.P., JOHNSON, L.N., PERKINS, S.J., PHILLIPS, D.C., CASSELS, R.C., DOBSON, C.M., POULSEN, F.M., WILLIAMS, R.J.P. (1978) Physical and chemical properties of lysozyme. MOLECULAR INTERACTIONS AND ACTIVITY IN PROTEINS. CIBA FOUNDATION SYMPOSIUM 60 (New series) EXCERPTA MEDICA, 137-185.

BLEANEY, B., DOBSON, C.M., LEVINE, B.A., MARTIN, R.B., WILLIAMS, R.J.P., XAVIER, A.V. (1972) Origin of lanthanide NMR shifts and their uses. CHEM. COMM., 791-793.

BRAUN, W., BOSCH, C., BROWN, L.R., GO, N., WÜTHRICH, K. (1981). Combined use of proton-proton Overhauser enhancements and distance geometry algorithm for deteremination of polypeptide conformations. Application to micelle bound glucagon. BIOCHIM.BIOPHYS.ACTA, 667, 377-396.

BREWER, H.B., RONAN, R. (1970). Bovine parathyroid hormone: Amino acid sequence. PROC.NATL.ACAD.SCI, 67, 1862-1869.

BUNDI, A., WÜTHRICH, K. (1979) ^{1}H NMR parameters of the common amino acid residues measured in aqueous solutions of the linear tetrapeptides H-Gly-Gly-X-L-Ala-OH. BIOPOLYMERS, 18, 285-297.

CAMPBELL, I.D. (1977) An NMR view of protein structure. NMR IN BIOLOGY (Eds. DWEK, R.A., CAMPBELL, I.D., RICHARDS, R.E., WILLIAMS, R.J.P.) ACADEMIC PRESS, 33-49.

CAMPBELL, I.D., DOBSON, C.M., WILLIAMS, R.J.P. (1975) Nuclear magnetic resonance studies on the structure of lysozyme in solution. PROC.R.SOC.LOND. 345, 41-59.

CAMPBELL, I.D., DOBSON, C.M., WILLIAMS, R.J.P., WRIGHT, P.E. (1975) Pulse methods for the simplification of protein NMR spectra. FEBS. LETT. 57, 96-99.

CANTERS, G.W., HILL, H.A.O., KITCHEN, N.A., ADMAN, E.T. (1983) Assignment of the PMR spectrum of azurin. EUR.J.BIOCHEM., in press.

CASS, A.E.G.,HILL, H.A.O., SMITH, B.E., BANNISTER, J.V., BANNISTER, W.H. (1977) Investigation of the structure of bovine erythrocyte superoxide dismutase by ^{1}H NMR. BIOCHEM., 16, 3061-3066.

CASS, A.E.G., HILL, H.A.O. (1980). Copper proteins and copper enzymes. BIOLOGICAL ROLES OF COPPER, CIBA FOUNDATION SYMPOSIUM 79, 71-91.

CASSELS, R. (1979) Investigations of protein structure-Lysozme in the crystalline and solution states. D.PHIL THESIS, OXFORD.

CASSELS, R., DOBSON, C.M., POULSEN, F.M., WILLIAMS, R.J.P. (1978) Study of the tryptophan residues of lysozyme using ^{1}H NMR. EUR.J.BIOCHEM., 92, 81-97.

CASTELLINO, F.J., PLOPLIS, V.A., POWELL, J.R., STRICKLAND, D.K. (1981). The existence of independent domain structures in Lys77-plasminogen. J.BIOL.CHEM. 256, 4778-4782.

CHOU, P.Y., FASMAN, G. (1978) Prediction of the secondary structure of proteins from their amino acid sequence. ADV.IN.ENZYMOLOGY, 47, 45-148.

COLLEN, D., VERSTRAETE, M. (1979) α_2-antiplasmin consumption and fibrinogen breakdown during thrombolytic therapy. THROMB.RES., 14, 631-639.

CRIPPEN, G.M., OPPENHEIMER, N.J., CONNOLLY, M.L. (1981) Distance geometry analysis of the NMR evidence on the solution conformation of bleomycin. INT. J.PEPT.PROT.RES., 17, 156-169.

DALGARNO, D.C. (1983) Calcium binding proteins. D.PHIL.THESIS, OXFORD.

DALGARNO, D.C., LEVINE, B.A., WILLIAMS, R.J.P. (1983) Structural information from NMR secondary chemical shifts of peptide αCH protons in proteins. BIOSCIENCE REPORTS, 3, 443-452.

DAYHOFF, M.O., ECK, R.V., PARK, C.M. (1972) A model of evolutionary change in proteins. ATLAS OF PROTEIN SEQUENCE AND STRUCTURE (Ed. DAYHOFF, M.O.), 5, 89-99.

DELEPIERRE, M., DOBSON, C.M., POULSEN, F.M. (1982) Studies of sheet structure in lysozyme by ^{1}H NMR. Assignments and analysis of spin-spin coupling constants. BIOCHEM., 21, 4756-4761.

DE MARCO, A., HOCHSCHWENDER, S.M., LAURSEN, R.A., LLINAS, M. (1982) Human Plasminogen. Proton NMR studies on Kringle 1. J.BIOL.CHEM., 257, 12716-12721.

DEUTSCH, D.G., MERTZ, E.T. (1970) Plasminogen: Purification from human plasma by affinity chromatography. SCIENCE, 70, 1095-1096.

DOBSON, C.M. (1975) The conformation of lysozyme in solution. D.PHIL.THESIS, OXFORD.

DOBSON, C.M., LEVINE, B.A. (1976) Lanthanide ions as NMR probes of the conformations of molecules in solution. NEW TECHNIQUES IN BIOPHYSICS AND CELL BIOLOGY, (Eds. PAIN, R.H., SMITH, B.J.) 3, 19-79.

DOBSON, C.M., WILLIAMS, R.J.P. (1977) NMR studies of the interaction of lanthanide cations with lysozyme. METAL-LIGAND INTERACTIONS IN ORGANIC CHEMISTRY AND BIOCHEMISTRY (Eds. PULLMAN, B., GOLDBLUM, N.), 255-281.

DOWER, S.K., WAIN-HOBSON, S., GETTINS, P., GIVOL, D., JACKSON, W., ROLAND, C., PERKINS, S.J., SUNDERLAND, C.A., SUTTON, B.J., WRIGHT, C.E., DWEK, R.A. (1977) The combining site of the dinitrophenyl-binding immunoglobulin A myeloma protein MOPC 315. BIOCHEM.J. 165, 207-225.

DUBS, A., WAGNER, G., WÜTHRICH, K. (1979) Individual assignments of amide proton resonances in the proton NMR spectrum of the basic pancreatic trypsin inhibitor. BIOCHIM.BIOPHYS.ACTA., 577, 177-194.

DWEK, R.A. (1973) Nuclear magnetic resonance in biochemistry. CLARENDON PRESS, OXFORD.

DWEK, R.A., KNOTT, J.C.A., MARSH, D., McLAUGHLIN, A.C., PRESS, E.M., PRICE, N.C., WHITE, A.I. (1975) Structural studies on the combining site of the myeloma protein MOPC 315. EUR.J.BIOCHEM., 53, 25-39.

ESMON, C.T., OWEN, W.G., DUIGUID, D.L., JACKSON, C.M. (1973) The action of thrombin on blood clotting factor V: Conversion of factor V to a prothrombin binding protein. BIOCHIM.BIOPHYS.ACTA., 310, 289-294.

ESNOUF, M.P. (1977) The biochemistry of blood coagulation. BRIT.MED.BULL., 33, 213-218.

ESNOUF, M.P., ISRAEL, E.A., PLUCK, N.D., WILLIAMS, R.J.P. (1979) Solution studies of bovine prothrombin fragments using high resolution NMR. THROMB. HAEM. 42, 95 (Abstract).

ESNOUF, M.P., ISRAEL, E.A., PLUCK, N.D., WILLIAMS, R.J.P. (1980a) The study of bovine prothrombin fragments by high resolution NMR spectroscopy. REGULATION OF COAGULATION (Eds. MANN, K.G., TAYLOR, F.B.), ELSEVIER.

ESNOUF, M.P., ISRAEL, E.A., PLUCK, N.D., WILLIAMS, R.J.P. (1980b) High resolution NMR of bovine prothrombin fragments. PROTIDES OF THE BIOLOGICAL FLUIDS, 28, 261-264.

GERATZ, J.D., TIDWELL, R.R. (1978) Current concepts on action of synthetic thrombin inhibitors. HAEMOSTASIS. 7, 170-176.

GUNZLER, W.A., STEFFENS, G.J., OTTING, F., KIM, S-M.A., FRANKUS, E., FLOHE, L., (1982) The primary structure of high molecular mass urokinase from human urine. HOPPE-SEYLER'S Z.PHYSIOL.CHEM., 363, 1155-1165.

HENRIKSEN, R.A., JACKSON, C.M. (1975) Cooperative calcium binding by the phospholipid binding region of bovine prothrombin: A requirement for intact disulphide bridges. ARCH.BIOCHEM.BIOPHYS., 170, 149-159.

HOCHSCHWENDER, S.M., LAURSEN, R.A. (1981) The lysine binding sites of human plasminogen. Evidence for a critical tryptophan in the binding site of kringle 4. J.BIOL.CHEM., 256, 11172-11176.

HOCHSCHWENDER, S.M., LAURSEN, R.A., DE MARCO, A., LLINAS, M. (1983) 600MHz ^{1}H NMR studies of the kringle 4 fragment of human plasminogen. ARCH.BIOCHEM. BIOPHYS., 223, 58-67.

HOLLEMAN, W.H., ANDERS, W.W., WEISS, L.J. (1975) The relationship between the lysine and the p-aminobenzamidine binding sites on human plasminogen. THROMB.RES., 7, 683-693.

INAGAKI, F., TAMIYA, N,. WILLIAMS, R.J.P. (1981) Structural differnces betweeen erabutoxins in aqueous solution and in crystalline states. EUR.J. BIOCHEM., 118, 618-625.

JARDETZKY, O., ROBERTS, G.C.K. (1981) NMR in biology. ACADEMIC PRESS.

JOHNSON, C.E., BOVEY,F.A. (1958) Calculation of nuclear magnetic resonance spectra of aromatic hydrocarbons. J.CHEM.PHYS. 29, 1012-1014.

KING, G., WRIGHT, P.E. (1982) A 2D NMR method for assignment of imidazole ring protons of histidine residues in proteins. BIOCEM.BIOPHYS.RES.COMM., 106, 559-565.

KUMAR, A., WAGNER, G., ERNST, R.R., WÜTHRICH, K. (1981) Buildup rates of the NOE measured by 2 dimensional proton NMR spectroscopy: Implications for studies of protein conformation. J.AMER.CHEM.SOC. 103, 3654-3658.

KUROSKY, A., BARNETT, D.R., LEE, T-H., TOUCHSTONE, B., HAY, R.E., ARNOTT,M.S., BOWMAN, B.H., FITCH, W.M. (1980) Covalent structure of human haptoglobin: A serine protease homologue. PROC.NATL.ACAD.SCI., 77, 3388-3392.

LEATHERBARROW, R. (1983) Structural studies on DNP binding antibodies. D.PHIL.THESIS, OXFORD.

LERCH, P.G., RICKLI, E.E. (1980) Studies on the chemical nature of lysine-binding sites and on their location in human plasminogen. BIOCHM.BIOPHYS.ACTA. 625, 374-378.

LERCH, P.G., RICKLI, E.E., LERGIER, W., GILLESSEN, D. (1980b) Localisation of individual lysine-binding regions in human plasminogen and investigations on their complex-forming properties. EUR.J.BIOCHEM. 107, 7-13.

LEVINE, B.A., MERCOLA, D., THORNTON, J.M., COFFMAN, D. (1977) Calcium binding by troponin C. A proton magnetic resonance study. J.MOL.BIOL., 115, 743-760.

LLINAS, M., DE MARCO, A., HOCHSCHWENDER, S.M., LAURSEN, R.A. (1983) A ^{1}H NMR study of isolated domains from human plasminogen. Structural homology between kringles 1 and 4. EUR.J.BIOCHEM, in press.

McDONALD, C.C., PHILLIPS, W.D. (1970) PMR spectroscopy of proteins. FINE STRUCTURE OF PROTEINS AND NUCLEIC ACIDS (Eds. FASMAN, G.D., TIMASHEFF, S.N.), IV, NEW YORK.

MAGNUSSON, S., PETERSEN, T.E., SOTTRUP-JENSEN, L., CLAEYS, H. (1975) Complete primary structure of prothrombin. PROTEASES AND BIOLOGICAL CONTROL (Eds. REICH, E., RIFKIN, D.B., SHAW, E.) COLD SPRING HARBOR, NEW YORK. 123-149.

MARIES-GUIA, M., SHAW, E. (1965) Studies on the active centre of trypsin. The binding of amidines and guanidines as models of the substrate side chain. J.BIOL.CHEM., 240, 1579-1585.

MARKLEY, J.L. (1975) Observation of histidine residues in proteins by means of NMR spectroscopy. ACC.CHEM.RES., 8, 70-80.

MARKUS, G., DEPASQUALE, J.L., WISSLER, F.C. (1978a) Qualitative determination of the binding of ϵ-aminocaproic acid to native plasminogen. J.BIOL.CHEM., 253, 727-732.

MARKUS, G., EVERS, J.L., HOBIKA, G.H. (1978b) Comparison of some properties of native (Glu) and modified (Lys) plasminogen. J.BIOL.CHEM.,253, 733-739.

MARKUS, G., PRIORE, R.L., WISSLER, F.C. (1979) the binding of tranexamic acid to native (Glu) and modified (Lys) human plasminogen and its effect on conformation. J.BIOL.CHEM., 254, 1211-1216.

MARKWARDT, F., LANDMANN, H., WALSMANN, P. (1968) Comparative studies on the inhibition of trypsin, plasmin and thrombin by derivatives of benzylamine and benzamidine. EUR.J.BIOCHEM., 6, 502-506.

MARTELL, A. (1958) Stability constants of metal ion complexes. THE CHEMICAL SOCIETY, LONDON.

MATSUO, O., RIJKEN, D.C., COLLEN, D. (1981) Comparison of the relative fibrinogenolytic, fibrinolytic and thrombolytic properties of tissue plasminogen activator and urokinase in vitro. THROMBOSIS.HAEMOSTASIS. 45, 225-229.

MATSUSHIMA, A., TAKIUCHI, H., SAITO, Y., INADA, Y. (1980) Significance of tryptophan residues in the D-domain of the fibrin molecule in fibrin polymer formation. BIOCHIM.BIOPHYS.ACTA., 625, 230-236.

MEANS, G.E., FEENEY, R.E. (1971) Chemical modification of proteins. SAN FRANCISCO.

MOORE, G.R. (1978) The structure and function of cytochrome c. D.PHIL THESIS, OXFORD.

MORT, A.J., LAMPORT, D.T.A. (1977) Anhydrous hydrogen fluoride deglycosylates glycoproteins. ANAL.BIOCHEM., 82, 289-309.

NAGY, B., BAN, J., BRDAR, B. (1977) Fibrinolysis associated with human neoplasia: Plasminogen activator production by human tumours. INT.J.CANCER. 19, 614-620.

NELSESTUEN, G.L., SUTTIE, J.W. (1971) Properties of asialo and agalycoprothrombi BIOCHEM.BIOPHYS.RES.COMM., 198-203.

NELSESTUEN, G.L., RESNICK, R.M., WEI, G.J., PLETCHER, C.H., BLOOMFIELD, V.A., (1981) Metal ion interactions with bovine prothrombin fragment 1. Stoichiometry, self-association, conformational change. BIOCHEM., 20, 351-358.

NEURATH, H. (1975) Limited proteolysis and zymogen activation. PROTEASES AND BIOLOGICAL CONTROL (Eds. REICH, E., RIFKIN, D.B., SHAW, E.) 51-64, COLD SPRING HARBOUR, NEW YORK.

OKAMOTO, S., NAKAJIMA, T., OKAMOTO, U., WATANABE, H., IGUCHI, Y., IGAWA, T., CHING, C.C., HAYASHI, T. (1959) A suppressing effect of ϵ-aminocaproic acid on the bleeding of dogs, produced with the activation of plasmin in the circulatory blood. KEIO.J.MED., 8, 247-256.

OLSSON, G., ANDERSEN, L., LINDQVIST, O., SJOLIN, L., MAGNUSSON, S., PETERSEN, T.E., SOTTRUP-JENSEN, L. (1982) A low resolution model of fragment 1 from bovine prothrombin. FEBS.LETT., 154, 317-322.

ONG, T.C. (1979) The biochemistry of blood coagulation. D.PHIL.THESIS, OXFORD.

PATTHY, L., SMITH, E.L. (1975) Reversible modification of arginine residues. J.BIOL.CHEM., 250, 557-564.

PENNICA, D., HOLMES, W.E., KOHR, W.J., HARKINS, R.N., VEHAR, G.A., WARD, C.A., BENNETT, W.F., YELVERTON, E., SEEBURG, P.H., HEYNEKER, H.L., GOEDDEL, D.V. (1983) Cloning and expression of human tissue-type plasminogen activator cDNA in E COLI. NATURE, 301, 214-221.

PERKINS, S.J. (1982) Application of ring current calculations to the proton NMR of proteins and transfer RNA. BIOL.MAG.RES., 4, 193-335.

PLETCHER, C.H., BOUHOUTSOS-BROWN, E.F., BRYANT, R.G., NELSESTUEN, G.L. (1981) Effects of temperature and pH on prothrombin fragment 1 conformation as determined by NMR. BIOCHEM, 20, 6149-6155.

POULSEN, F.M., HOCH, J.C., DOBSON, C.M. (1980) A structural study of the hydrophobic box region of lysozyme in solution using nuclear Overhauser effects. BIOCHEM., 19, 2597-2607.

RIJKEN, D.C., COLLEN, D. (1981) Purification and characterisation of the plasminogen activator secreted by human melanoma cells in culture. J.BIOL. CHEM., 256, 7035-7041.

ROBSON, B., GARNIER, J., OSGUTHORPE, D.J. (1978) Analysis of simple methods for predicting the secondary structure of proteins. J.MOL.BIOL. 120, 97-120.

SIGEL, H., MARTIN, R.B. (1982) Coordinating properties of the amide bond. Stability and structure of metal complexes of peptides and related ligands. CHEM.REV., 82, 385-426.

SJOHOLM, I., WIMAN, B., WALLEN, P. (1973) Studies on the conformational changes of plasminogen induced during activation to plasmin and by 6-amino hexanoic acid. EUR.J.BIOCHEM., 39, 471-479.

SOKOLOVSKY, M., RIORDAN, J.F., VALLEE, B.L. (1966) Tetranitromethane. A reagent for the nitration of tyrosyl residues in proteins. BIOCHEM., 5, 3582-3589.

SOTTRUP-JENSEN, L., CLAEYS, H., ZAJDEL, M., PETERSEN, T.E., MAGNUSSON, S. (1978) The primary structure of human plasminogen. PROGRESS IN CHEMICAL FIBRINOLYSIS AND THROMBOSIS (Eds. DAVIDSON, J.F., ROWAN, R.M., SAMAMA, M.M., DESNOYERS, P.C.), 3, 191-209.

SPANDE, T.F., WITKOP, B., DEGANI, Y., PATCHORNIK, A. (1970) Selective cleavage and modification of peptides and proteins. ADV.PROT.CHEM. 24, 98-206.

STENFLO, J., SUTTIE, J.W. (1977) Vitamin K dependent formation of γ-carboxy-glutamic acid. ANN.REV.BIOCHEM., 46, 157-172.

SUDMEIER, J.L., EVELHOCH, J.L., JONSSON, N.B-H. (1980) Dependence of NMR lineshape analysis upon chemical rates and mechanisms: Implications for enzyme histidine titrations. J.MAG.RES., 40, 377-390.

SUTTIE, J.W., JACKSON, C.M. (1977) Prothrombin structure, activation and biosynthesis. PHYSIOL.REV., 57, 1-70.

TANFORD, C. (1968) Protein denaturation. ADV.PROT.CHEM., 23, 121-282.

TAYLOR, S.E. (1982) Carbon acidity of histidine and its use in structural studies of proteins. LIFE CHEMISTRY REPORTS, 1, 69-104.

THORSEN, S., GLAS-GREENWALT, P., ASTRUP, T. (1972) Differences in the binding to fibrin of urokinase and tissue plasminogen activator. THROMB.DIATH. HAEM., 28, 65-74.

THORSEN, S. (1975) Differences in the binding to fibrin of native plasminogen and plasminogen modified by proteolytic degradation. BIOCHIM.BIOPHYS.ACTA., 393, 55-65.

THORSEN, S., CLEMMENSEN, I., SOTTRUP-JENSEN,L., MAGNUSSON, S. (1981) Fibrin binding of native fragments of known primary structure from human plasminogen. PROTIDES OF BIOLOGICAL FLUIDS. (Ed. PEETERS, E.), 28, 365-369.

TREXLER, M., VALI, Z., PATTHY, L. (1982) Structure of the ω-aminocarboxylic acid binding sites of human plasminogen. J.BIOL.CHEM., 257, 7401-7406.

VALI, Z., PATTHY, L. (1982) Location of the intermediate and high affinity ω-aminocarboxylic acid binding sites in human plasminogen. J.BIOL.CHEM., 257, 2104-2110.

VAN GEET, A.L. (1968) Calibration of the methanol and glycolNMR thermometers with a static thermistor probe. ANAL.CHEM., 40, 2227-2229.

VARADI, A., PATTHY, L. (1981) Kringle 5 of human plasminogen carries a benzamidine-binding site. BIOCHEM.BIOPHYS.RES.COMM., 103, 97-102.

VAUGHAN, J.D., MUGHRABI, Z., WU, E.C. (1970) The kinetics of deuteration of imidazole. J.ORG.CHEM., 35, 1141-1145.

VIOLAND, B.N., BYRNE, R., CASTELLINO, F.J. (1978) The effect of ω-amino acids on human plasminogen structure and activation. J.BIOL.CHEM., 253, 5395-5401.

VUK-PAVLOVIC, S., GAFNI, A. (1979) 6 Aminohexanoic Acid-plasminogen interactions studied by fluorescence. BIOCHEM.BIOPHYS.RES.COMM. 91, 971-975.

WAGNER, G., WÜTHRICH, K., TSCHESCHE, H. (1978) A ^{1}H NMR study of the conformation and the molecular dynamics of the glycoprotein cow-colostrum trypsin inhibitor. EUR.J.BIOCHEM., 86, 67-76.

WAGNER, G., WÜTHRICH, K., TSCHESCHE, H. (1978) A ^{1}H NMR study of the solution conformation of the isoinhibitor K from Helix Pomatia. EUR.J.BIOCHEM., 89, 367-377.

WAGNER, G., KUMAR, A., WÜTHRICH, K. (1981) Systematic application of 2D PMR techniques for studies of proteins. Combined use of correlated and NOE spectroscopy for the sequential assignments of backbone resonances and elucidation of the polypeptide secondary structures. EUR.J.BIOCHEM., 114, 375-384.

WAGNER, G., WÜTHRICH, K. (1982) Sequential resonance asssignments in ^{1}H NMR spectra. Basic pancreatic trypsin inhibitor. J.MOL.BIOL., 155, 347-366.

WALLEN, P. (1978) Chemistry of plasminogen and plasminogen activation. PROGRESS IN CHEMICAL FIBRINOLYSIS AND THROMBOLYSIS (Eds. DAVIDSON, J.F., ROWAN, R.M., SAMAMA, M.M., DESNOYERS, P.C.), 3, 167-181.

WALLEN, P., WIMAN, B. (1972) Characterisation of human plasminogen. BIOCHIM. BIOPHYS.ACTA., 257, 122-134.

WALZ, D.A., HEWETT-EMMETT, D., SEEGERS, W.H. (1977) Amino acid sequence of human prothrombin fragments 1 and 2. PROC.NATL.ACAD.SCI., 74, 1969-1972.

WARLOW, C.P. (1983) Intracranial aneurysms. OXFORD TEXTBOOK OF MEDICINE (Eds. WEATHERALL, D.J., LEDINGHAM, J.G.G., WARRELL, D.A.),OXFORD. 21.74.

WEIMAR, W., VAN SEYEN, A.J., STIBBE, J., BILLIAU, A., DESOMER,P., COLLEN, D. (1981) Specific lysis of an iliofemoral thrombus by administration of extrinsic (tissue-type) plasminogen activator. LANCET, ii, 1018-1020.

WIDER, G., LEE, K.H., WÜTHRICH, K. (1982) Sequential resonance assignments in protein ^{1}H NMR spectra. Glucagon bound to perdeuterated dodecylphosphocholine micelles. J.MOL.BIOL., 155, 367-388.

WILLIAMS, G.W. (1983) Electrostatic interactions between cytochrome c and metal complexes. D.PHIL.THESIS, OXFORD.

WIMAN, B., COLLEN, D. (1978) Molecular mechanism of physiological fibrinolysis. NATURE, 272, 549-550.

WIMAN, B., WALLEN, P. (1977) The specific interaction between plasminogen and fibrin. A physiological role of the lysine binding site in plasminogen. THROMB.RES., 10, 213-222.

WIMAN, B., LIJNEN, H.R., COLLEN, D. (1979) On the specific interaction between the lysine binding sites in plasmin and the complementary sites in α_2-antiplasmin and in fibrinogen. BIOCHIM.BIOPHYS.ACTA., 579, 142-154.

WINN, E.S., HU, S-P., HOCHSCHWENDER, S.M., LAURSEN, R.A. (1980) Studies on the lysine-binding sites of human plasminogen - the effect of ligand structure on the binding of lysine analogues to plasminogen. EUR.J.BIOCHEM, 104, 579-586.

WÜTHRICH, K. (1976) NMR in biological research: Peptides and proteins. NORTH HOLLAND, AMSTERDAM.

WÜTHRICH, K., WAGNER, G. (1979) NMR of labile protons in the basic pancreatic trypsin inhibitor. J.MOL.BIOL., 130, 1-18.

WÜTHRICH, K., WIDER, G., WAGNER, G., BRAUN, W. (1982) Sequential resonance assignments as a basis for determination of spatial protein structures by high resolution proton nuclear magnetic resonance. J.MOL.BIOL., 155, 311-319.